AFFDL-TR-78-186

AD A067997

LEVEL Ⅱ

LOWER COST BY SUBSTITUTING STEEL FOR TITANIUM

D.E. Parker, G.V. Bennett, R.P. Robelloto
Rockwell International Corporation
Los Angeles Division
Los Angeles, California 90009

November 1978

Technical Report AFFDL-TR-78-186

Final Report for Period August 1975 - October 1978

D D C

MAY 1 1979

RECEIVED

A

Approved for public release; distribution unlimited

AIR FORCE FLIGHT DYNAMICS LABORATORY
AIR FORCE WRIGHT AERONAUTICAL LABORATORIES
AIR FORCE SYSTEM COMMAND
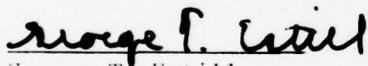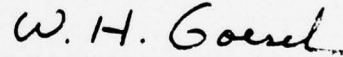WRIGHT-PATTERSON AIR FORCE BASE, OHIO 45433
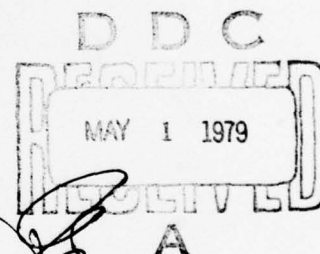
79 04 24 021

NOTICE

When Government drawings, specifications, or other data are used for any purpose other than in connect-on with a definitely related Government procurement operation, the United States Government thereby incurs no responsibility nor any obligation whatsoever; and the fact that the government may have formulated, furnished, or in any way supplied the said drawings, specifications, or other data, is not to be regarded by implication or otherwise as in any manner licensing the holder or any other person or corporation, or conveying any rights or permission to manufacture, use, or sell any patented invention that may in any way be related thereto.

This technical report has been reviewed and is approved for publication.
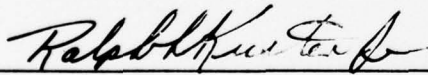
George T. Estill
Project Engineer

William H. Goesch
Act. Program Manager
AMS Program Office
Structural Mechanics Division

FOR THE COMMANDER

Ralph L. Kuster, Jr., Colonel, USAF
Chief, Structural Mechanics Division

"If your address has changed, if you wish to be removed from our mailing list, or if the address is no longer employed by your organization, please notify AFFDL/FBB, W-PAFB, OH 45433 to help us maintain a current mailing list."

Copies of this report should not be returned unless return is required by security considerations, contractual obligations, or notice on a specific document.

REPORT DOCUMENTATION PAGE	READ INSTRUCTIONS BEFORE COMPLETING FORM

1. REPORT NUMBER	2. GOVT ACCESSION NO.	3. RECIPIENT'S CATALOG NUMBER
AFFDL-TR-78-186		

4. TITLE (and Subtitle)	5. TYPE OF REPORT & PERIOD COVERED
Lower Cost by Substituting Steel for Titanium	Final Report, August 1975 to October 1978
	6. PERFORMING ORG. REPORT NUMBER
	NA-78-415

7. AUTHOR(s)	8. CONTRACT OR GRANT NUMBER(s)
D. E. Parker, G. V. Bennett, R. P. Robelloto	F33615-75-C-3109

9. PERFORMING ORGANIZATION NAME AND ADDRESS	10. PROGRAM ELEMENT, PROJECT, TASK AREA & WORK UNIT NUMBERS
Rockwell International, Los Angeles Div 815 Lapham Street El Segundo, CA 90245	

11. CONTROLLING OFFICE NAME AND ADDRESS	12. REPORT DATE
Air Force Flight Dynamics Laboratory (FBS) Air Force Systems Command Wright-Patterson Air Force Base, Ohio 45433	November 1978
	13. NUMBER OF PAGES

14. MONITORING AGENCY NAME & ADDRESS(if different from Controlling Office)	15. SECURITY CLASS. (of this report)
Air Force Flight Dynamics Laboratory (FBS) Air Force Systems Command Wright-Patterson Air Force Base, Ohio 45433	Unclassified
	15a. DECLASSIFICATION DOWNGRADING SCHEDULE

16. DISTRIBUTION STATEMENT (of this Report)

Approved for public release; distribution unlimited

447 p.

17. DISTRIBUTION STATEMENT (of the abstract entered in Block 20, if different from Report)

18. SUPPLEMENTARY NOTES

19. KEY WORDS (Continue on reverse side if necessary and identify by block number)

fracture toughness, stress corrosion, machinability, damage, tolerance, material properties, heat treatment, titanium substitute AF1410 steel, cost/weight reduction

20. ABSTRACT (Continue on reverse side if necessary and identify by block number)

This program was part of an overall program to develop a high-strength steel, designated AF1410, which compares favorably with titanium in strength/weight efficiency and fatigue characteristics and yet can be produced at a significant reduction in cost. The Rockwell portion of the overall program consisted of selecting existing candidate designs, developing steel substitute designs, and comparing their estimated cost with their titanium counterparts.

DD FORM 1 JAN 73 1473 EDITION OF 1 NOV 65 IS OBSOLETE

20.   ABSTRACT (Continued)

It also consisted of development of heat-treat processes to optimize machinability and of a comprehensive materials test program. Finally, the program included the machining of a full-scale test article from a forging provided by the Air Force from another portion of the program, and the fatigue, damage tolerance, and static residual strength testing of the full-scale article. In addition, validation of the production cost reduction was a prime objective.

During testing, cracks developed which were subsequently analyzed as being the result of excessive deflections. An in-test repair was accomplished, and the testing was successfully completed.

FOREWORD

This report summarizes the work accomplished on Air Force contract F33615-75-C-3109, "Lower Cost by Substituting Steel for Titanium," during the period of 27 August 1975 to 1 October 1978.

The program was jointly sponsored by the Air Force Flight Dynamics Laboratory and Air Force Material Laboratory, Air Force Systems Command, Wright-Patterson Air Force Base, Ohio. Mr. George Estill, AFFDL, and Mr. W. Harris, AFML, were the Air Force project engineers.

Performance of the contract was under the direction of the Rockwell International Los Angeles Division, 815 Lapham Street, El Segundo, CA 90245. Mr. C. Routh was program manager during phases I and II of the program. Following Mr. Routh's retirement, Mr. D. Parker was appointed program manager. Mr. G. Bennett, in addition to his supporting activities in Materials and Processes, performed the project engineering function. Mr. R. Robelotto was responsible for the machinability/heat-treatment studies. Major Rockwell participants in the program were:

D. Brubaker	Weld Repair of Test Component
J. Harrington	Weld Repair of Test Component
R. Lorenz	Machinability/Heat-Treat Studies
G. Martin	Mechanical Properties Data & Design Allowables
T. Matoi	Stress Analysis
S. Rangel	Structural Test Conductor
J. Stolpestad	Damage-Tolerance Analysis

Rockwell wishes to acknowledge the cooperation of both H. Black of Universal Cyclops, and W. Kuhlman, of Alcoa, in providing the forging and supporting data in a timely manner.

iii

TABLE OF CONTENTS

v

LIST OF ILLUSTRATIONS

x

xi

xii

LIST OF TABLES

Section I

INTRODUCTION

AF1410, a new high-strength, high-toughness steel, has been developed by the Air Force as a low-cost substitute for annealed Ti-6Al-4V (Reference 1). The steel is readily weldable after heat treatment, exhibits a minimum K_{1_c} of 130 ksi$\sqrt{\text{in}}$. at 230 ksi yield strength, and on a strength/density basis, demonstrates properties equal or slightly superior to annealed Ti-6Al-4V. To demonstrate the cost-saving potential of this alloy for airframe construction, the Air Force Flight Dynamics Laboratory initiated contract F33615-75-C-3109 with the Los Angeles Division of Rockwell International to select a typical titanium fitting, design an AF1410 substitute part, and demonstrate the structural integrity and cost-saving potential of the AF1410 fitting.

The program, which was assigned the acronym of LOCOSST (LOwer COst by Substituting Steel for Titanium), was conducted in five phases:

Phase I: Preliminary Design

Phase II: Detail Design and Development Test Program

Phase III: Fabrication of Test Component

Phase IV: Component Test

Phase V: Technology Transfer

Included in the study was the development of mechanical property design values, heat-treatment and machinability improvement studies, fabrication of the AF1410 test component, cost comparisons with titanium, and a full-scale spectrum fatigue test of the AF1410 fitting to demonstrate its structural integrity.

This is the final report on the program, and contains detailed data and results obtained in phases III and IV. Results of the phase II effort, which are contained in Reference 2, are summarized herein to assist the reader in conceiving the full scope of the program.

Section II

PHASE I - PRELIMINARY DESIGN

A 15-month preliminary design study was conducted representing phase I of the program to validate AF1410 steel. During this phase of the program, a screening of existing titanium fitting candidates and selection of three for the preliminary study was accomplished. A cost baseline for each was established which included actual costs for the first part, where available, and projected to a 300-unit cumulative average cost for production comparison.

Many innovative substitute designs were proposed from which new design concepts using AF1410 steel were selected through a cost and risk grading process. The selected design concepts were developed into scale layouts and analyzed for aircraft loads, fracture mechanics, weight, manufacturing feasibility, and cost.

A development test plan was prepared for conducting a comprehensive test program to establish AF1410 material allowables, fracture toughness, and fatigue characteristics and to verify the fracture mechanics analysis results during phase II.

OBJECTIVES

The primary objective of phase I was to lay a foundation on which the other phases could be built. In order to do this, several other objectives were established, as follows:

1. Select three candidate fittings of 6Al-4V titanium from the current list of B-1 structure which are subjected to high load intensity and fatigue cycles.

2. Establish cost baselines for each candidate item based on actual cost, where available, for the first B-1 part and on estimated production cost projected to a 300-unit cumulative average cost.

3. Develop innovative substitute designs of each candidate item using AF1410 steel and exploring the use of welding as a cost and weight advantage.

4. Estimate single- and 300-unit cumulative average costs of AF1410 substitute designs for direct comparison with the titanium baseline costs. A cost saving objective of 30 percent on production values was established.

2

5. Prepare a comprehensive development test plan for a subsequent testing program which will establish AF1410 steel basic design allowables, fatigue and fracture mechanics characteristics, weld data, and the effects of manufacturing processes on these data. Additionally, an optimum premachining heat treatment was to be developed in phase I.

6. Prepare a preliminary manufacturing plan for subsequent fabrication of full-scale components for static and fatigue testing.

7. Culminate the results of the phase I effort into a preliminary design report documenting all data obtained from studies and tests performed during this first 15-month phase.

A task/event flow diagram is shown in Figure 1, which identifies the significant tasks and their relationship to each other.

CANDIDATE ITEM SELECTION

A search throughout the B-1 A/C-1 and DVT-2 airframe was conducted to find titanium fittings or assemblies that would meet the following requirements:

1. Must have reasonably high load intensity

2. Should be a forging, hogged-out machine part, or diffusion-bonded assembly

3. Fabrication should be possible in steel by current methods and available equipment

4. Must have a potential for cost reduction, both by simplification of design and material cost

5. Preferably subject to a substantial fatigue spectrum to demonstrate fracture mechanics qualities in steel

6. Costs of fabrication and testing must be commensurate with the available AF budget

A total of 13 parts were found that appeared to meet the aforementioned conditions:

L1100029	Fitting - shear, pivot pin, outboard
L1100030	Fitting - shear, inboard pivot pin, assy of
L1100036	Retainer, bearing - lower outboard lug, wing pivot
L2100033	Support, bearing - main box, horiz stab, assy of

PHASE I – PRELIMINARY DESIGN
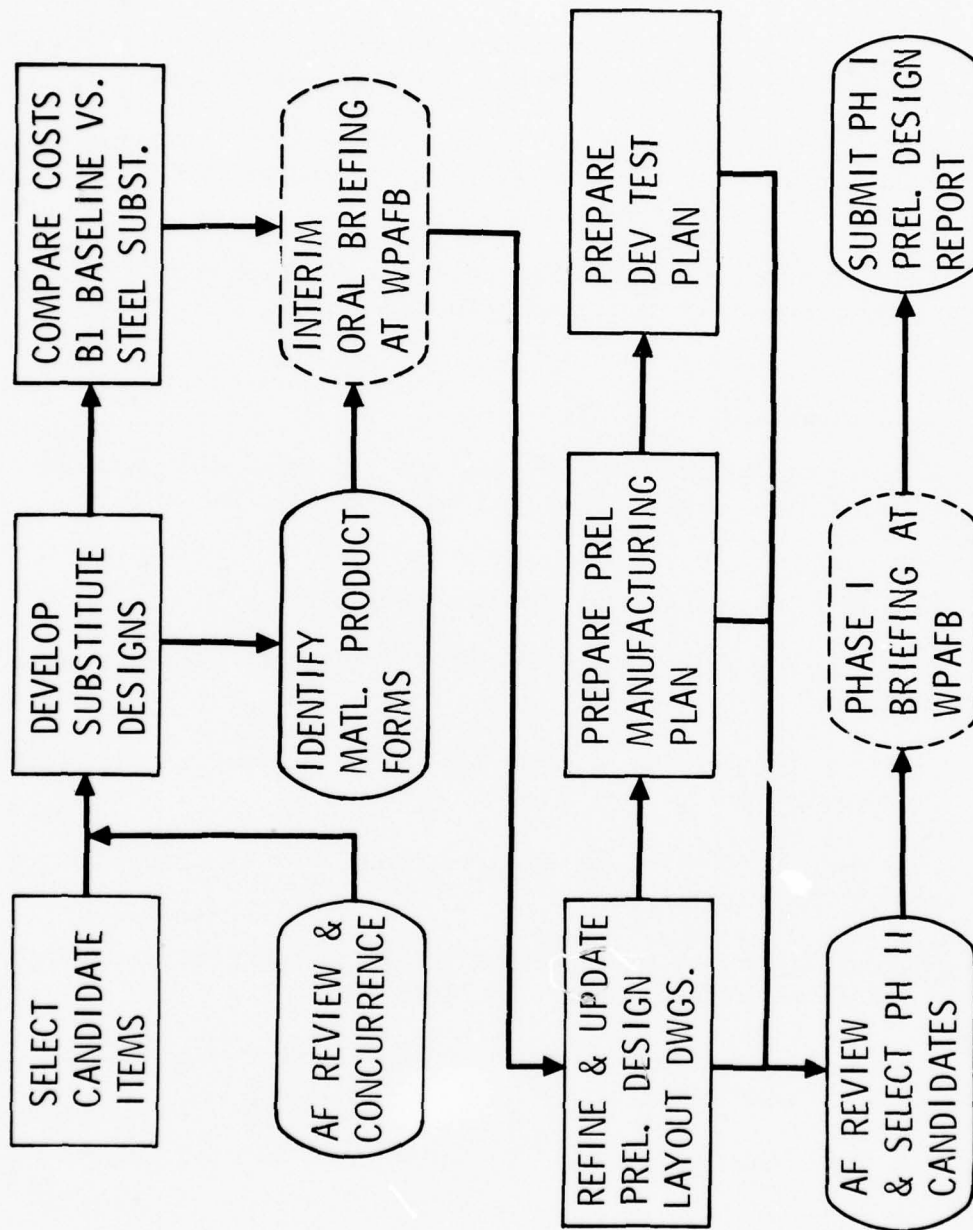
Figure 1. Task/event flow diagram.

4

L3003015	Rib - Wing center section closeout
L3004251	Beam, support - nacelles Y_f 1256 and Y_f 1244
L3007214	Fitting - wing sweep actuator, inboard attach
L3007251	Fitting, support - drag brace, MLG, assy of
L3202364	Fitting, nacelle center beam - Y_n 336.25 - canted
L3200402	Frame, nacelle - upper station 265.250, firewall
L3200403	Fitting - nacelle bulkhead, Y_n 265.250 canted lower center
L3200444	Fitting, nacelle - center beam Y_n 293.650 canted upper, assy of
L6310010	Arm, swing - weapons bay door

Part L3004251 is only one frame of the L3004250 nacelle support beam assembly which was chosen in its place. Joint AF/Rockwell meetings were conducted to select three parts from this list of 13 candidates.

Comparisons of cost, load, and fatigue data of the parts resulted in the selection of three that best met the requirements within the scope of the program:

1. L1100030, wing pivot inboard shear fitting

2. L3004250, nacelle support beam assembly

3. L3007214, wing sweep actuator inboard attach fitting

SUBSTITUTE DESIGN CONCEPTS AND SELECTION PROCESS

Engineering design developed as many design concepts in the form of sketches as could be conceived of the three selected candidate items, substituting AF1410 steel for the 6A1-4V titanium material currently used. The resulting effort produced 19 concepts for the nacelle support beam assembly, 14 for the wing sweep actuator inboard attach fitting, and six for the wing pivot inboard shear fitting. These were evaluated, and the number was selectively narrowed down to nine (three concepts on each candidate item). Additional refinement and trade data were developed on each. To select a preferred concept of the three, a cost/risk grading factor chart was then established that provided a system of grading for four cost factors and four risk factors (Figures 2 and 3). Cost factors were tooling, machining or forming, welding, and material loss. Risk factors were structural integrity in static and fatigue, weight increase as compared to the B-1, and fabrication risks. A meeting was held to select the best concept based on evaluation data presented and best judgment of each representative. The results were included on the chart for overall review. Functions represented were engineering design, stress, fatigue and fracture mechanics, materials and producibility, and manufacturing engineering. Grading was on the basis of numbered levels of cost or risk, from 1 (low) to 10 (high).

COST FACTORS

CONCEPT	TOOLING VALUE	TOOLING REMARKS	MACHINING/FORMING VALUE	MACHINING/FORMING REMARKS	WELDING VALUE	WELDING REMARKS	MATL. LOSS (BUY-FLY WT) VALUE	MATL. LOSS REMARKS	(TOT)
L110030 SHEAR FTG.									
A EXTR. PLATE - FORMED/MACH.	4	REQUIRES EXTRUSION DIES & HOT SIZING DIES FOR FORMING	6	REQUIRES HOT FORMING, ROUGH MACH & FINISH MACH. & TO CLOSE TOLERANCE	4	WELD ON LUG PLATES & STRAIGHTEN	5	ALL SURF. MACH. TO REMOVE SCALE. ROUGH & FINISH MACH. REQD AFTER FORMING	19
E ROLL FORG. RINGS - WELDED	4	SHAPED ROLLERS REQD FOR ROLL FORGINGS. ASSY. WELD TOOLING ALSO REQD.	5	MACH 3 WEBS AT A TIME WILL REDUCE COST OVER CONCEPT A	5	WELD JOIN 2 RING FORGINGS & WELD 3 SEP. LUG PLATES, FOR 3 PARTS.	4	MINIMAL MATL. REMOVED BY ROUGH & FINISH MACH.	18
F FORGED NEAR NET - MACH.	7	REQUIRES BLOCKER & FINISH FORGING DIES. TOOLING ALSO REQD FOR 3D MACH	7	REQUIRES SINGLE PART MACH PLUS 3D MILLING OF OUTER SURFACE & LUGS	0	NO WELDING REQD.	8	LARGE MATL. LOSS IN SCALE REMOVAL PLUS ROUGH & FINISH MACH. & SLOT MACH OF LUGS.	22
L3004250 NACELLE BEAM.									
1A FLAT WEB WELDED ASSY.	1	MINIMUM FORM TOOLING REQD. ASSEMBLY WELD FIXTURES REQD.	2	REQUIRES TAPER MILLING & FORMING FRAME CAPS. OTHERWISE ONLY CUT & TRIM.	7	EXTENSIVE BITS & PIECES ASSY WELDING OF FRAMES AND BEAM ASSY.	2	MATL LOSS IN CAP TAPERS PLUS CUT & TRIM BY NEST & GAIN ON SD SHEET.	13
2 SINE WAVE WEB WELDED ASSY	9	EXTENSIVE HOT FORM TOOLS FOR WEBS PLUS COMPLEX WELD FIXTURE & CONTROL SYS. REQD.	2	SAME AS 1A EXCEPT WEB STIFF REQD BUT WEB MAY REQUIRE CHEM MILLING	7	SAME AS 1A EXCEPT LESS SINE WAVE WEB TO CAP WELDS	2	SAME AS CONCEPT 1A	20
7 1 PC. FORG. - MECH. ATT. PLATES	8	HIGH COST BLOCKER & FINISH FORGING DIES REQD. 3D MACH CONTROL TAPES REQD.	8	FORGED FRAMES REQUIRE EXTENSIVE 3D MACH. REQUIRING MANY SET-UP & FINISH MACH	5	ASSY WELDING OF LINK ATTACH FITTGS OTHERWISE MECH ATTACHED ASSY	8	LARGE MATL LOSS FROM REQD POCKET MACHINING & MACH ALL SURFACES.	29
7C 2 PC FORG. - WELD SPLICE & MECH. ATTACHED PLATES	8	SAME AS 7 EXCEPT SMALLER DIES & DOUBLE NUMBER REQUIRES FRAME WELD FIXTURE	8	SAME AS 7 BUT SMALLER PARTS FOR ROUGH MACH & DOUBLE NO. PLUS WELD PREP.	5	SAME AS 7 EXCEPT WELD JOINT IN FRAMES.	8	SAME AS CONCEPT 7	29
L3007214 ACTUATOR FTG.									
B BITS 1 & 2 - WELDED BEAM TYPE	1	MIN. TOOLING REQD. ASSY WELD FIXTURE ONLY.	2	SIMPLE SLAB MILLING OF LUG PLATES PLUS CUT, TRIM & DRILLING REQD	6	LARGE NO. BITS & PIECES WELDED ASSY. DIFFICULT WELD ACCESS	3	LOW MATL LOSS IN LUG PLATES & BITS & PIECES CUT & TRIM FROM STA SHT.	12
C MACH. FORG. - BEAM TRUSS	7	BLOCKER & FINISH FORGING DIES PLUS HOLDING FIXTURE & TAPE CONTROL FOR MACH REQD.	7	EXTENSIVE MACH OF DIE FORGING, DEEP POCKETING & SEVERAL SET-UPS REQD.	0	NO WELDING INVOLVED	7	HIGH LOSS OF MATL FROM DEEP POCKET MILLING & FINISH MACH. ALL SURFACES.	21
N 2 MACH LUG PLATES - TRUSS WELDED ASSY	1	SIMILAR TOOLING TO CONCEPT B LESS PARTS.	4	SLAB MILLING & LIGHT POCKETING OF LUG PLATES & BLADE REQD. CUT, TRIM & DRILL OTHER PTS	4	2 LUG PLATES, WELDED TO BLADE + SEVERAL SMALL BITS & PIECES IN WELD ASSY.	3	LOW MATL LOSS IN LUG PLATES & BLADE. MIN LOSS FROM CUT & TRIM	12

Figure 2. Cost factor grading chart.

RISK FACTORS

CONCEPT	STRUCTURAL INTEGRITY - STATIC		STRUCTURAL INTEGRITY - FATIGUE		MEET B-1 BASELINE WEIGHT		FABRICATION PROBLEMS	
	VALUE	REMARKS	VALUE	REMARKS	VALUE	REMARKS	VALUE	REMARKS
L110030 SHEAR FTG.						(B-1 BASELINE WT = 48.7#)		
A EXTR. PLATE FORMED/MACH.	1	VERY LOW RISK IN ATTAINING FULL STATIC STRENGTH	4	MODERATE RISK IN LTG. WELDS & LUGS	9	INITIAL SIZING = 58.7" SOME WT REDUCTION POSSIBLE BY ADDING LTG HOLES	6	MOD. HIGH RISK DUE TO EXTR. SIZE-APPR. 2.75×17.5 & FORMING & WARPAGE
E ROLL FORG. RINGS - WELDED	1	LTG. WELDS NOT CRITICALLY LOADED	4	MODERATE RISK IN RING & LUG WELDS	9		5	MODERATE RISK IN WELDING DUE TO WARPAGE
F FORGED NEAR NET - MACH.	1	LOW RISK - STRENGTH IS DETERMINATE - LUGS INTEGRAL	2	LOW RISK DUE TO INTEGRALLY MACHINED LUGS	9		4	LOW RISK - REQUIRES PROFILE TAPE CONTROL OF OUTER SURFACE WEB.
L300A250 NACELLE BEAM						(B-1 BASELINE WT = 26.9#)		
1A FLAT WEB WELDED ASSY.	2	LOW RISK CONVENTIONAL BEAM CONSTRUCTION - WELDS SIZED TO REQUTS.	6	2 POINTS FOR GEOMETRIC STRESS CONCENTRATIONS OF BASIC DESIGNS	2	EST WT = 28S.3# CAN REDUCE BY REFINED DESIGN OF LOAD END	7	HIGH RISK DUE TO EXTENSIVE WELDING WARPAGE & CRACKS
2 SINE WAVE WEB; WELDED ASSY.	3	MODERATE RISK DUE TO SECONDARY BUCKLING ACTION IN CORRUGATIONS	6	4 POINTS ASSIGNED FOR HIGH DEGREE OF WELDING	1	EST. WT = 26.5# WEB THIN MAY INCREASE AT WELDS TO CAPS	8	VERY HIGH RISK CONST. DUE TO FORMING SINE WAVE WEB IN HEAVY STEEL
7 1 PC FORG. - MECH ATTACH PLATES	0	NO RISK - SAME CONFIG AS TO BASELINE WHICH HAS BEEN SUBSTANTIATED BY TEST	5	3 POINTS FOR BASIC DESIGN & 1 POINT FOR MECHANICAL ATTACHMENTS	4	EST WT = 36.7#	2	LOW RISK - SIMILAR TO TITANIUM BASELINE
7C 2 PC FORG - WELD SPLICE & MECH. ATTACHED PLATES	3	MODERATE RISK IN SPLICE WELD & MECH FASTENER COMBINATION	6	2 POINTS FOR BASIC DESIGN 4 POINTS FOR WELD JOINTS & MECH ATTACHED PLATES	4	EST WT = 31.7#	3	MODERATELY LOW RISK - ABILITY TO CONTROL QUALITY WELD SPLICE.
L300721C ACTUATOR FTG.						(B-1 BASELINE WT = 17.8#)		
B BITS & PCS - WELDED BEAM TYPE	2	RELATIVELY LOW RISK - WELD QUALITY CONTROL MAY BE DIFFICULT - ACCESS	6	2 POINTS FOR BASIC DESIGN 4 POINTS FOR WELDING COMPLEXITIES & JOINTS.	5	APPROX. EQUIV TO BASELINE (NOT SIZED)	6	MODERATELY HIGH RISK DUE TO MULTIPLE PART ASSY. WELDS & WARPAGE
C MACH. FORG. - BEAM TRUSS	0	NO RISK - CONVENTIONAL FORGED CONFIGURATION	2	2 POINTS FOR RELATIVELY CLEAN DESIGN - NO WELDS	1	EST. WT = 16.7#	4	MODERATELY LOW RISK COMPLEX MACHINING & POCKET MILLING
N 2 MACH. LUG PLATES - TRUSS WELDED ASSY.	1	VERY LOW RISK DESIGN STATICALLY DETERMINATE TRUSS CONCEPT	4	2 POINTS FOR BASIC DESIGN 2 POINTS FOR LIMITED WELDS	3	EST WT = 17.0#	5	MEDIUM RISK IN WELD ACCESS AND ASSEMBLY WARPAGE

Figure 5. Risk factor grading chart.

DESIGN LAYOUTS AND ANALYSES

After the selection of substitute design concepts which showed greatest possibility of cost savings was made, each design was layed out to scale and sized in accordance with the same load and stiffness requirements as the baseline part. This permitted detail stress, weight, and fracture mechanics analyses to be made.

SHEAR FITTING

Layout drawing 3109-100000B, Figure 4, was designed to replace the existing titanium part without change to interfacing structure. Attaching bolts and bearing blocks are reduced in length to match the thinner steel fitting. A relocation of the strut attach hole can be accommodated by a simple adjustment of the strut length. System mounting bracket holes have not been changed.

The substitute design is cylindrical in shape and is included within one-third of a cylinder. Two rolled ring forgings are butt welded together to form the required cylinder which can be lathe turned inside and out. Strut lugs and mounting brackets are welded in place, and final cleanup machining is done after welding. The cylinder assembly is then cut into three segments, and the edges finished and holes drilled and broached.

ACTUATOR ATTACH FITTING

Layout drawing 3109-100001D, Figure 5, was designed as a welded truss assembly of 11 separate parts. The primary load-carrying lugs and truss members are each machined as one piece from thick plate. The base is sculptured from a separate plate and joined to the lug members at both ends. The design of these parts permits arbor gang milling and shallow end milling. The remaining parts require only a minimum of trim and surface machining for welding fitup. Lug bushings are included as a part of the fitting assembly.

The interface structure will require minor changes in the base attaching hole locations on YF 932.00 bulkhead and in the attachment to XF 114.916 rib near the fitting lugs.

Layout drawing 3109-100003A, wing sweep actuator inboard attach fitting (forged) (Figure 6), is a machined forging concept which was conceived to improve the low-cost saving which resulted from the welded truss design. It includes a more direct load path for the lug loads and more closely simulates the baseline design. All welding is eliminated, resulting in a significant increase in cost saving.

.58
REF

.167

.300

1.140

L1100073 REF

.036

1.31

.53
30°
(BEFORE MACHINING
THICKNESS = 1.00)
OR FLASH WELD

5.868

1.504

.70

7.562 +.000/-.000 R

2.00

1.50 DIA LIGHTENING HOLES
8 PLACES

L1100073 REF

VIEW A-A
UNWRAPPED VIEW OF DATUM A SURFACE

L1100073 REF

.036

.125 R

10.080 R
9.813 R
8.313 R

8.515 ±.005 R

-A-

-B-

8.250 ±.005 R

.100 R

13° 30'

25° 00'

.78

.13

1.31

3.50 R

3.50 R

.23 TYP
2 PLACES

7.36 ±.10   .50

8.008

1.16

OUTLINE
OF B1 EXISTING
TITANIUM PART

.120 R
2 PL

.75 R

C

11.503

INSPECTION
HOLE

.220
BEFORE WELDING

.74

3.50 R

3.50 R

.10

1.16 ±.03

15.868

1.504 ±.001

.40 × 45°
2 PL

.573

1.58

TD
.220

2.32

.70

.80

9.00 R

.25 TYP
2 PL

REMOVE .035 BEFORE WELD

7.562 +.002
     -.000 R

.75 R

REMOVE .063 BEFORE WELD

1.38 R

1.125 ±.010
FINAL MACHINING

.22

TD
.2375

3.10

.375 STOCK SIZE

TD
.220

7.362 +.002
     -.000 R

C

1.0621 ±.0011 DIA
2 HOLES IN LINE

VIEW C-C

.25 × 45°
CHAMFER

.5

.67

9.902

SECT B-B

.22
REF

.67 REF

FULL R

SECT D-D

.280 BEFORE
FINAL MACHINING

XF 124.99

Z, 27.54

35° 35' 59.532"
TAN 1.7159261

.58

.8

.035 PAD
LWR SURF

A

.50 R

45°

.10

52° 45'

53° 30'

3° 50'

15° 40'

24° 10'

9.902 REF

VIEW LOOK

-005

WELD ARE

.25

-111 WELDED RING ASSY

1.00 REF

16.46

SECT E-E ROTATED CW 93°

2

CODE IDENT   FRAME

3109-100000 C

Figure 4. Wing pivot inboard shear fitting.

L9900618-009 AL ALY SPLICE PLATE (REDESIGNED)

.20

5.00
−8   3.25   .40   −9   −11
.30 2 PL   L10
3.25   4.62   3.20

E ← → E SYM

F   F

DOWN

FWD ←

SECT **D-D**
LOOKING OUTBD
FASTENERS ARE TITANIUM LOCKBOLTS
DIA SHOWN IN 1/32 INCH

SEE L9300618

(ADD)
SPLICE FITTING
7075-T7351 AL ALY

−8
INBD
FWD ←   −9

SECT **F-F**
LOOKING DOWN

−8
.090   .19   .070   −9   −11
.19   .125

INBD
FWD ←   SECT **E-E**
LOOKING DOWN

Xₚ 194.7026
Yₚ 923.9307
Zₚ 12.3861

Xₚ 211.0207
Yₚ 380.9377
Zₚ 11.5012

SECT G-G

21 2 RCS

45° 4 PLCS

45° 2 RCS

-B- 4.500 +.0016/-.0000 2 HOLES IN LINE
-A- 4.1250 +.0006/-.0000 2 HOLES IN LINE

XF 122.75

1°30'41.95"

XF 114.916

XF 114.728

.188 REF

3.00 R TRUE

.26

-6

7

.38

2.90

6.00 R

9.10

BUSHINGS & SPOTFACES NOT SHOWN

35.90

29.734

.125

XF 114.916

6.067 +.008/-.010

3.625 +.008/-.003

1.028 ±.015

3.324

⊥ A .005

1.182

1.028 ±.015

⊥ B .005

12

.42 (-12)

XF 122.75
YF 917.00 } REF
ZF 14.7479

4.38 R

₵ HOLES

0°21'40.36"
(0.3612111°)

5.26 DIA 4 PL

5.63 DIA SPOTFACE .25 FILLET R 2 PL

13

.57 (-19)

CBK 90° X 4.750 DIA 4 PL

.120

3.417 +.030/-.000

.120

40

7

3.00 R

4

3

10.66

.70 REF

.45

55°

19.868

₵.42 KIPS ULT

.92 KIPS ULT

.₵ BUR SPOTFACE .25 FILLET R 2 PL

2.00 R

3.812

6.367

14.35

7.00 R

8

6

1

2

9

2.00 R

B

B

.125 REF

.19 R

11

.70

XF 114.916

Y 952.00

G

G

L3003005

.25

5

1.00

.40

VIEW LOOKING DOWN

.19 R

.25

.100

3.00

.50

.25

.30

-1

5.549268°

XF 122.7500
YF 917.0000
ZF 14.7479

₵ ACTR WING FWD POS

35.51715°

₵ ACTR WING AFT POS

FWD

OUTBD

VIEW LOOKING DOWN
SCALE = 1/10

.19 R

.20

1.20

.35

.50

.50

2.12

2.32

SECT B-B

XF 114.916

XF 107.08

XF 9

1°50'49"

.125

.50 R 8 PL

.40

3/8

3/8

19 R REF

3/4

1.00

1.00

3/8

1 3/4

3/4

4.00 R 2 PL

ZF 14.748

ZF 14.804

.40

.150 R 4 PL

L3007215-011
WING CARRY-THRU CLOSEOUT RIB

XF 122.75

VIEW LOOKING FWD

FRAME
3109 100001 C 1

13 12 11 10 9 8 7

WEIGHT table:

WEIGHT	BASELINE	AF1410	SAVING LBS	REDUCTION %
FITTING ASSY	176.3	150.8	25.5	-.5
FITTING	172.2	47.7	24.5	
BUSHINGS	4.1	3.1	1.0	
INSTL ITEMS				
FASTENERS	26.8	18.2	8.6	
PIN	27.5	24.4	3.1	
TOTAL	230.6	193.4	37.2	16.1
TOTAL A/V		74.4		

NOTES~
1. ALL MATERIAL AF1410 STEEL PER SPEC LB0160-184
2. WELD LENGTH = 180 INCHES (15 FEET) PER FITTING
3. WELD SYMBOLS IN ACCORDANCE WITH AWS A2.0-68

Parts list:

DASH NO	NAME	STOCK SIZE	ZONE
13	BUSHING	1.00 X 5.3 X 10.6	11E
12	BUSHING	3/4 X 5.3 X 10.6	11F
11	ATTACH PLATE	.125 X 4.1 X 6.4	8D
10	SUPPORT	1/2 X 2.8 X 6.6	5G
9	ATTACH PLATE	.19 X 5.0 X 9.3	8D
8	ATTACH PLATE	.19 X 4.7 X 6.8	8E
7	SUPPORT	1/2 X 3.5 X 4.2	9G
6	WEB	1/2 X 4.7 X 28.4	8E
5	BASE	1.25 X 12.0 X 44.3	8C
4	STIFFENER	1/2 X 3.0 X 10.7	12D
3	STIFFENER	1/2 X 3.0 X 10.7	11D
2	LUG	1.50 X 18.2 X 45.5	8E
1	LUG	1.50 X 18.2 X 45.5	8E

VIEW LOOKING DOWN

VIEW LOOKING FWD

SECT C-C

SECT A-A

L3007240-003

Figure 5. Wing sweep actuator inboard attach fitting

11

		REVISIONS		
ZONE	LTR	DESCRIPTION	DATE	APPROVED
	B	REDRAWN	4/19/76	D. Munger
	C	ADDED WELD SYMBOLS ADDED WEIGHT OF WELD FILLETS (+1.50 lbs) REVISED WT TABLE.	8/12/76	D. Munger
	D	REVISED WELD SYMBOLS FOR -10 & -7. SECONDARY WAS PRIMARY ADDED SECT. G-G & WELD SYM REMOVED FROM MAIN VIEW.	8-9-76	D. Munger

WEIGHT	BASELINE	AF1410	SAVING LBS	REDUCTION %
FITTING ASSY	176.3	150.8	25.5	14.5
FITTING	172.2	47.7	2.45	
BUSHINGS	4.1	3.1	1.0	
INSTL ITEMS				
FASTENERS	26.9	18.2	8.6	
PIN	27.5	24.4	3.1	
TOTAL	230.6	193.4	37.2	16.1
TOTAL A/V			74.4	

NOTES~
1. ALL MATERIAL AF1410 STEEL PER SPEC LB0160-184
2. WELD LENGTH = 180 INCHES (15 FEET) PER FITTING
3. WELD SYMBOLS IN ACCORDANCE WITH AWS A2.0-68

3109-100001 D

SECT A-A

.65 REF

Y = 932.00

.04

.65 REF

Y = 932.00

DASH NO	NAME	STOCK SIZE	ZONE	
13	BUSHING	1.00 X 5.3 X 10.6	11E	} MATERIAL WAS PH 13-8 Mo CRES BAR
12	BUSHING	3/4 X 5.3 X 10.6	11F	
11	ATTACH PLATE	.125 X 4.1 X 6.4	8D	
10	SUPPORT	3/8 X 2.8 X 6.6	5G	
9	ATTACH PLATE	.19 X 5.0 X 9.3	8D	
8	ATTACH PLATE	.19 X 4.7 X 6.5	8E	
7	SUPPORT	1/2 X 3.5 X 4.2	9G	
6	WEB	3/8 X 4.7 X 28.4	8E	
5	BASE	1.25 X 12.0 X 44.3	8C	
4	STIFFENER	1/2 X 3.0 X 10.7	12.D	
3	STIFFENER	1/2 X 3.0 X 10.7	11D	
2	LUG	1.50 X 18.2 X 45.5	8E	
1	LUG	1.50 X 18.2 X 45.5	8E	

3109-100001 D 11

DRN BY	D. Munger	16-4-76	FITTING ATTACH, INBD WING SWEEP ACTUATOR (LAYOUT)
CHK BY			
ENGR		11-4-76	

DO NOT SCALE PRINT

	SIZE	CODE IDENT NO.	DWG. NO.
	J	43999	3109-100001
	SCALE 1/2		SHEET 1 OF 1

Figure 5. Wing sweep actuator inboard attach fitting (welded assembly).

11

SECT **C-C** c/7
4 PL

LUGS ARE SHOWN BEFORE SPOTFACING
AND INSTL OF BUSHINGS

VIEW LOOKING AFT

VIEW LOOKING DOWN

SECT **B-B** D/9

FRAME

3109-100003 A 1

EW LOOKING AFT

.25R TYP
24 PL

3.75

.50

L3002560-009

⅜ DIA TI
HI-LOKS
8 PL

D 2.90

5.80

D E/3

¼ DIA TI HI-LOKS
58 PL

L3002561-007

SECT **A - A** F/9
LOOKING OUTBD
ROTATED CCW 1°50'41.95"

Yₑ 909.50

Yₑ 932.00

DOWN

FWD

Xₑ 114.916

SECT **D - D** G/2
LOOKING DOWN

INBD

FWD

15.16

C

8.55

.52 REF

2.00

.75R
5 PL EACH SIDE

TD=.210
.200

TD=.270

.50R
REF

TD=.320

.250

TD=.400

.125

.250

.50R
REF

TD=.400

6.06

.75R
REF

.250
27.00

.250

.250

32.66

35.86

38.58

.400

.400

42.25

C G/11

ING DOWN

27.00

35.20

TAN PT
OF 1.00R

6.04

.75

1.00

1.00

3.44

5/16

6.88

.75

3.02

1.00

1.00

Zₑ 14.748

1.00R
REF

1.00R
4 PL

1.75R
2 PL

Xₑ 95.45

Xₑ 84.00

3109-100

WEIGHT	BASELINE AF1410	SAVINGS LBS	REDUCTION %
FITTING ASSY	173.8	50.15	25.95	14.38
FITTING	.72.2	47.85	24.35	
BUSHINGS	4.1	3.1	1.00	
INSTL ITEMS				
FASTENERS	26.8	21.87	4.93	
PIN	27.5	24.4	3.1	
TOTAL	230.0	197.2	33.38	14.49
TOTAL A/V			66.76	

3. SEE SH 3 FOR DIE FORGING

2. SEE SH 2 FOR HAND FORGING

1. MACHINE -1 FROM FORGING. MATERIAL FOR FORGING -2 & -3 BUSHING
   BE AF1410 STEEL PER SPEC LB0160-194.

NOTES~

FITTING ATTA
SWEEP ACTUAT
(LAYOUT)

J 43999 31

SCALE 1/2

Figure 6. Wing sweep actuator inboard attach fitti

13

REVISIONS

ZONE	LTR	DESCRIPTION	DATE	APPROVED
C9	A	1.31 DIM WAS 1.38	7/14/76	
C5 C9		ADDED 3.96 DIM , S 2.81 REF		
B11		.50R WAS .25R 2 PL		
		ADDED .2.00 F 50.20 DIMS		
		ADDED SHT 3 DIE FORGING		

$D_{E/3}$

Y_F 932.00

X_F 114.916

3109-100003 A

WEIGHT	BASELINE	AF 1410	SAVING LBS	REDUCTION %
FITTING ASSY	175.8	150.45	25.35	14.38
FITTING	172.2	147.25	24.95	
BUSHINGS	4.1	3.1	1.00	
INSTL ITEMS				
FASTENERS	26.8	21.87	4.93	
PIN	27.5	24.4	3.1	
TOTAL	230.6	197.2	33.38	14.49
TOTAL A/V			66.76	

SH 3 FOR DIE FORGING   3

SH 2 FOR HAND FORGING

E -1 FROM FORGING. MATERIAL FOR FORGING -2 & -3 BUSHINGS SHALL
1410 STEEL PER SPEC LB0160-184.

FITTING ATTACH ... WING
SWEEP ACTUATOR (FORGING)
(LAYOUT)

J | 43999 | 3109-100003

sweep actuator inboard attach fitting (forging).

13

NACELLE SUPPORT BEAM

Layout drawing 3109-100002C, Figure 7, is a welded box beam concept made up of numerous bits and pieces welded into two main frame assemblies. These are then tied together with upper and lower cap close-out sheets and internal link attach fittings. It is designed to interface with existing structure with only attaching bolt grip length changes and a slight lengthening of the diagonal stabilizing strut.

Machining is held to a minimum by using standard sheet and plate gages requiring only edge fitup trim where possible. Simple machine taping of the heavy caps is required. Cap weight is slightly higher than the baseline cap weight due to their being designed by using stiffeners. The ratio of the E value of titanium to that of steel is 0.57, whereas the density ratio is only 0.56.

WEIGHT ANALYSIS

Detail weight calculations were obtained from the B-1 records for each of the titanium candidate items. These were established as baseline weights (Table 1).

A complete breakdown of weights on each of the substitute designs was calculated and compared with the corresponding baseline weights (Table 2). Weight savings as a percent of baseline weight were:

- 3109-100000 shear fitting - 4.0 percent

- 3109-100001 actuator fitting - 14.5 percent

- 3109-100002 nacelle support beam - 12.6 percent

- 3109-100003 actuator fitting (forging) - 14.4 percent

PRELIMINARY ANALYSIS - FATIGUE AND FRACTURE MECHANICS

Each of the three candidate fittings for the LOCOSST study was subjected to fatigue and fracture mechanics analyses to assure that the predicted life under the design spectrum loading would meet the fatigue design requirements of MIL-A-8866A and the damage tolerance requirements of MIL-A-83444 per the LOCOSST program Statement of Work, Paragraph 4.2.1. Simply stated, the fatigue requirement is to ensure that the design will not initiate a fatigue crack in four lifetimes of predicted service usage, and the fracture mechanics (crack growth) requirement is to ensure that an undetected flaw in the material will not grow to critical size within two design service lifetimes.

5.75   5.75

-3   -4

-5   -6

6.32   5.52

30R
4 PL

-9   -8

17.31   -7   10

E

1.50R
4 PL

60°
4 PL

-35   -36

-25   -26

-47   -48

VIEW **L-L**

-13   -53

-40   -32

-44   -43

-48   -47

VIEW **J-J**

-16

-20

PT A.   -20

PT A.

FRAME
3109-100002 D

SECT **F-F**

SECT **H-H**

SECT **G-G**

SECT **E-E**

WELD BEFORE INSTL -17 & -21

TYP FOR -61/-2, -18/-1

MELT THRU WELD 2 PL

LD111-0026-0304 4 REQD
LD111-0026-0305 4 REQD
LD153-0027-1005 8 REQD
M: 76L3 8 REQD

LD111-0026-0405 10 REQD
LD111-0026-0106 10 REQD
LD111-0026-0407 8 REQD
LD153-0027-1004 38 REQD
MS21076L4 38 REQD

LD111-0026-0412
MS21076L4
LD153-0027-1004
6 REQD

97,283 LB ULT LD
COND 360313

TRACE -F-

10   9   8   7   6   5

(II) BEAM ASSY

6.00 R

PT A

PT B

CUTOUT
.080

SEE L3009260
AL ALY

-G-

-F-

-D-

CSK HOLES
LDIII-0028-0403 BOLT
MS21076L4 NUTPLATE
22 REQD

(I) BEAM ASSY

6.00 R

Xf 76.984
Xf 76.975

Yp 1250.00

Yf 1253.00

Xf 75.984
7 REQD

Xf 75.430

FUS ATTACH
FT FOR STRUT
VIEW LOOKING UP

.38 x 45°
3 FL

Xf 75.264

66,333 LB ULT LD
COND 360312

LDIII-0026-0408
6 REQD

LDIII-0026-0410
4 REQD

-G-   -D-

10.14

-40   2.07 REF   .145 REF   .080   -39

.45 R

-42

-1

WELD

-17

1.00 REF   1.00 REF   .080

10.00

SECT B-B

-18

-41

-62

-63

-47

-54.527

TD .160

TD .160

TD .160

TD .160

TD .160

TD .160

TD .160

TD .160

F

C

C

B

B

H

E

E

G

G

33.72

6.00 R

TYP FOR -45/-46,
-49/-50/-51/-52

VIEW LOOKING
FWD

OUTBD   UP

BASELINE LOC

4.00 R

8.18   21.13

6.00 R

2.00

1.75 REF   2.00 REF   1.00

WELD

WELD

VIEW LOOKING UP

2.50

K

K

L

Yf 1253.0

SEE L300484
AL ALY

10   9   8   7   6   5

Figure 7. Nacelle support beam assembly.

17

TABLE 1

BASELINE WEIGHTS

Drawing No.	Title	Weight
L1100030-011	Wing Pivot Inboard Shear Fitting	48.70
L1100030-005	Fitting	48.64
L1100063-003	Bushing	0.06
L3007214-011	Fitting Wing Sweep Actuator, Inboard Attach Fitting	176.3
L3007214-005	Fitting	172.20
L1200234-005	Bushing - Outer	1.96
L1200235-003	Bushing - Inner	2.14
L3004250-001	Nacelle Support Beam Assembly	367.92
L3004250	Dash Items	2.46
		1.30
		6.52
		19.21
		10.16
L3004251-001	Beam	161.16
L3004251-008	Beam	154.76
L3004257-001	Support	4.90
L3004258-001	Support	4.87
L3004259-001	Support	1.34
L3005237-001	Bracket	0.70
L3005239-001	Bracket	0.54

TABLE 2

WEIGHT BREAKDOWN - AF1410 DESIGNS

3109-100000C   Wing Pivot Inboard Shear Fitting

Machined body	43.08 lb
-007 lugs	2.27 lb
-009, -013, -015, -017 brackets	0.64 lb
Welds	0.71 lb
Total	46.70 lb

B-1 titanium baseline part	48.64 lb
Fitting weight difference	+1.94 lb

Installation and assembly parts weight reduction due to reduced lug thicknesses and bolt grip lengths.

L1100063-003 bushing	-0.012 lb
L1100073-017 bushing	-0.497 lb
L1100073-009 bushing	-0.129 lb
5/8 dia bolt	-0.120 lb
7/8 dia bolt	-0.357 lb
Total	-1.115 lb

Net weight savings = 1.115 + 1.94 = 3.055 lb
Net weight savings per airplane 2 x 3.055 = 6.11 lb

3109-100002 D Nacelle Support Beam Assembly

I	Aft beam assembly	146.605 lb
II	FWD beam assembly	142.597 lb
IV	Fitting assembly	2.535 lb
III	Major assembly parts	19.867 lb
		311.404 lb
	Fasteners	+1.843 lb
	Weld	+8.129 lb
	Total	321.376 lb

B-1 titanium baseline assembly weight	367.92 lb
Beam assembly weight difference	46.54 lb

TABLE 2

WEIGHT BREAKDOWN - AF1410 DESIGNS (Concl)

Installation bolts weight reduction due to reduced grip lengths
    5/8 dia bolts   -0.09 lb
    1.00 dia bolts   -0.37 lb
            Total   -0.46 lb

Net weight savings 46.54 +0.46 = 47.00 lb
Total weight savings per airplane 94.00 lb

3109-100003 A Wing Sweep Actuator Inboard Attach Fitting

-1 fitting   147.85 lb
-2 & -3 bushings   3.10 lb
            Total   150.95 lb

B-1 titanium baseline assembly   176.30 lb
Fitting assembly weight difference   25.35 lb

Installation bolts and actuator attach pin weight reduction
due to reduced grip lengths, bolt sizes (6 places) and lug
thicknesses.

    L1200241-007 Pin   -3.10 lb
               Bolts   -4.93 lb
            Total   -8.03 lb

Net weight savings 25.35 + 8.03 = 33.38 lb
Total weight savings per airplane 2 x 33.38 = 66.76 lb

21

The fatigue damage and fatigue life prediction analyses were done using Miner's linear cumulative damage rule. The fatigue analyses were done in parametric form for a matrix of limit design stress levels and effective stress concentration factors. From a set of parametric fatigue life curves, the maximum allowable operating stress can be determined from the intersection of the life requirement and the stress concentration factor of the section being analyzed. Additionally, the fatigue allowable stress can be compared to two-thirds of the material ultimate tensile strength to assess the impact of fatigue in relation to the static stress requirements.

The emphasis of the damage tolerance analysis is in the calculation of subcritical flaw growth. Per MIL-A-83444, the life requirement must be obtained between the specified initial flaw size and the critical flaw size defined by limit or maximum spectrum load. The assumed initial flaw size is determined by the assumed location of the flaw, and the life requirement to the critical length is a function of the assumed inspectability level of the structure. For all analyses done in this phase, it was assumed that the structure would be classified as "in-service noninspectable," requiring the capability of sustaining two design service lifetimes of slow crack growth before failure.

The analytical crack growth prediction methodology which was employed to calculate subcritical flaw growth is based on the principles of linear elastic fracture mechanics. Rockwell computer program, EFFGRO, was used for performing the crack growth predictions. EFFGRO uses a specialized integration routine where an initial crack size, a_i, is chosen and the crack growth rate, da/dN, is integrated to yield the relationship between "a" and "N" for the given stress spectrum. Crack growth parametric studies were made at several limit design stress levels, starting with the appropriate initial crack size as defined by MIL-A-83444. A more detailed description of the analysis approach is included with the discussion of each of the three fittings.

Material Properties Used in Analysis

The fatigue S/N data used for the preliminary analysis phase were generated by the Advanced Metallic Air Vehicle Structure Program and are reported in AFFDL-TR-74-17 as 10-Nickel (HY180) steel with a design ultimate strength of 190 ksi. Per agreement between the customer and Rockwell, it was determined that for the LOCOSST program preliminary design effort, these fatigue data would be used but would be increased by the ratio of the ultimate strengths of AF1410 (230 ksi) and HY180 (190 ksi).

The da/dN crack growth rate properties for the dry-air and sump tank water environments were taken from NA-75-555, Volume IV, "Material Properties, B-1 Outer Wing Pivot Structure Study."

The sump water environment data are from HY180 steel tests conducted by General Dynamics and reported in AFFDL-TR-74-17. The dry-air data are from 10-nickel modified steel tests conducted by General Dynamics. These data were used for the preliminary analysis phase of this program; however, the final analysis conducted in phase II used the fatigue, crack growth, and toughness properties of AF1410 as determined by the LOCOSST Program material properties development tests.

Wing Sweep Actuator Attach Fitting

The fatigue life analysis on the wing sweep actuator fitting was made in parametric form for a matrix of maximum design limit stress levels and geometric stress concentration factors. Each of the parametric stress lines plotted in Figure 8 represents a flight-by-flight analysis to the net section operating stress spectrum for a realistic selection of stress concentration factors likely to occur in the fitting. The figure shows that the four-lifetime requirement can be met at a severe combination of 140-ksi limit stress and $K_T = 5$. Such a combination of high stress and high concentration factor does not exist on this fitting. For specific points of reference, the actuator attach lug has a geometric $K_T = 2.7$, together with an average net section limit stress of 63 ksi in the actuator holding position and 70-ksi limit while in the operating position. The diagonal flange has an operating limit stress of 130 ksi, but the K_T factor is low (<2); the boltholes in the flange have a $K_T = 4+$, but the operating tension stress is less than 100 ksi. Each of these points would predict a fatigue life well in excess of the requirement.

The crack growth analysis was done for one specific location, the attach lug net section, and in parametric form for three general areas, including two combinations of hole diameters and flange thicknesses typical of the flange attaching to the fuselage station 932 bulkhead. Figure 9 shows the predicted crack growth rate of an assumed 0.05R initial corner flaw in the net section of the lug hole for two assumed stress distributions (gradients) leading away from the edge of the hole. Both show the assumed flaw capable of sustaining the two-lifetime requirement of MIL-A-83444.

Figure 10 shows the predicted crack growth rate of an assumed 0.125R initial corner flaw in the diagonal flange for the flight-by-flight operating spectrum with limit load stress levels of 120, 130, and 140 ksi. All show the assumed flaw capable of sustaining two lifetimes of growth without failure. From the static stress analysis, the maximum tension stress in this flange is 195 ksi at ultimate load, which is equivalent to 130 ksi limit for both the forging and welded truss concepts. Thus, the range of crack growth stresses studied is acceptable. All of the crack growth analyses on the sweep fitting used the crack growth rate properties for a sump tank water environment. This is knowingly an overconservative assumption, but it is the only aggressive environment for which properties were available.

- PARAMETRIC FATIGUE LIFE ANALYSIS
- WING SWEEP ACTUATOR ATTACH FITTING
- AF1410 STEEL - F_{Tu} = 230 KSI
- FLIGHT-BY-FLIGHT FATIGUE SPECTRUM

σ_{LIMIT} = 100 KSI

σ_{LIMIT} = 110 KSI

σ_{LIMIT} = 120 KSI

σ_{LIMIT} = 130 KSI

σ_{LIMIT} = 140 KSI

FATIGUE
LIFE
REQUIREMENT

STRESS CONCENTRATION FACTOR, K_T

AIRCRAFT LIVES
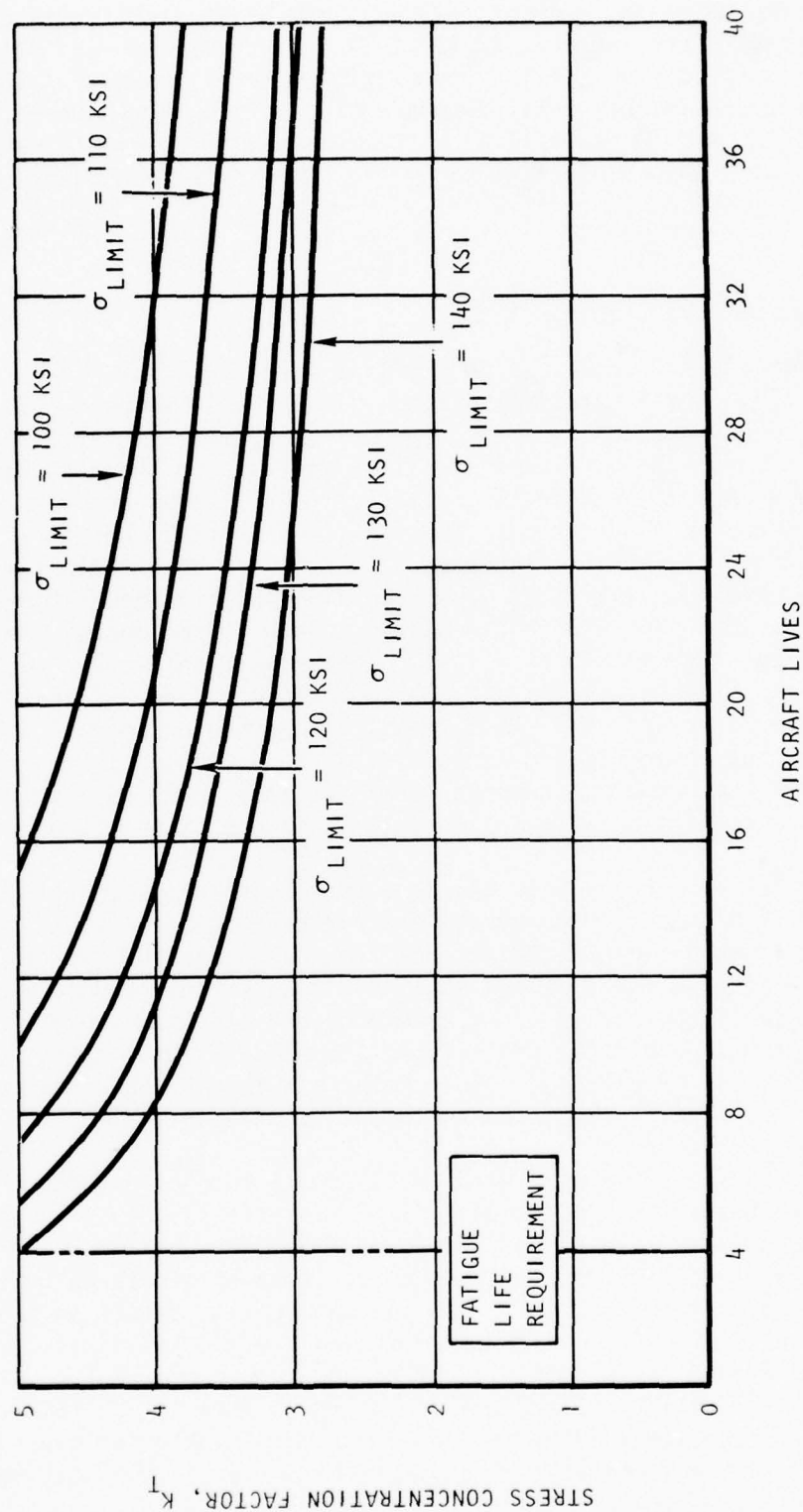
Figure 8. LOCOSST preliminary fatigue analysis.

24
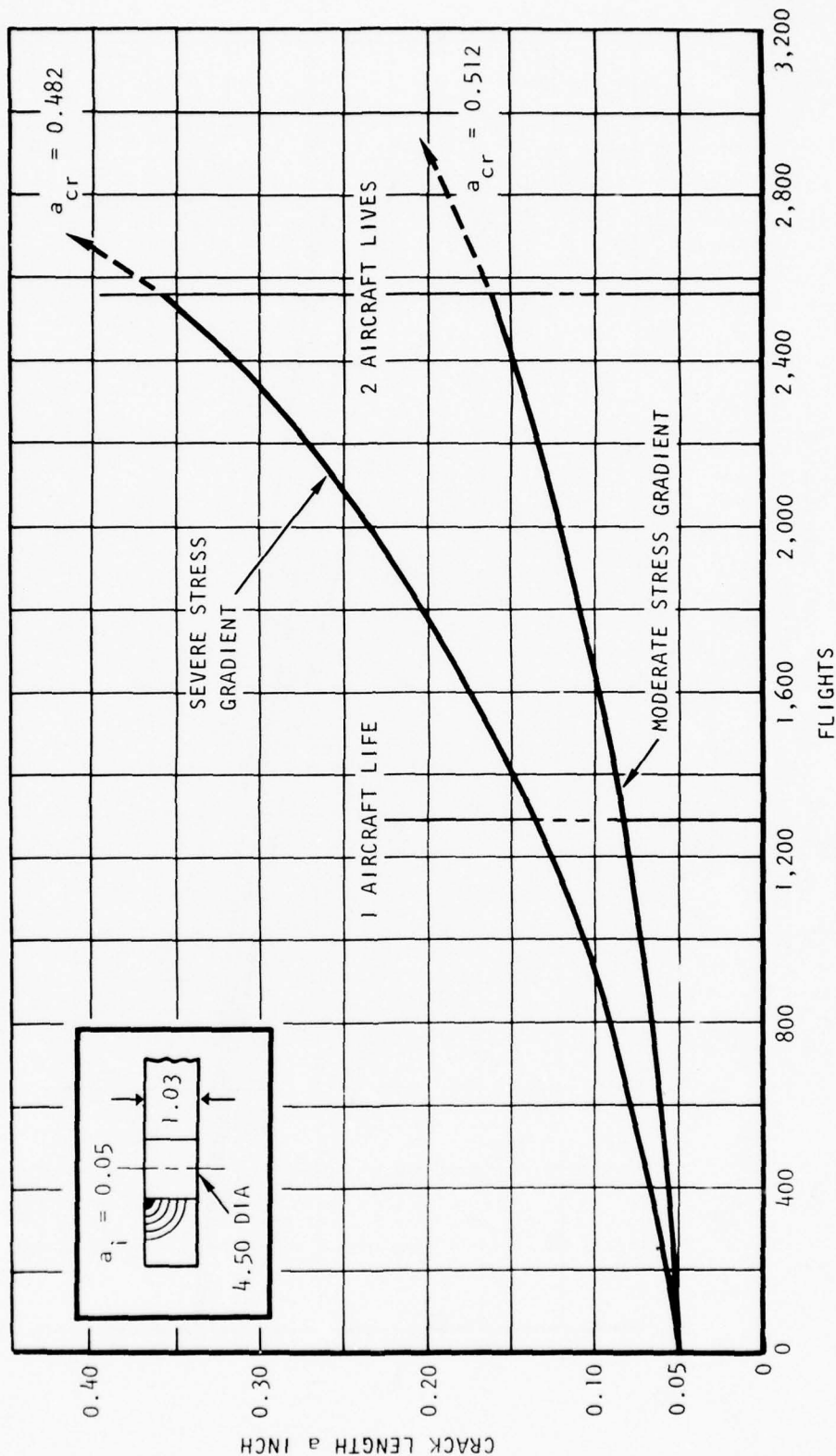
Figure 9. LOCOSST preliminary crack growth analysis.

25

- WING SWEEP ACTUATOR ATTACH FITTING
- PARAMETRIC CRACK GROWTH ANAYLSIS
- AF1410 STEEL – SUMP TANK WATER ENVIRONMENT
- FLIGHT-BY-FLIGHT FATIGUE SPECTRUM
- CORNER-CRACKED DIAGONAL FLANGE

$a_i = 0.125$
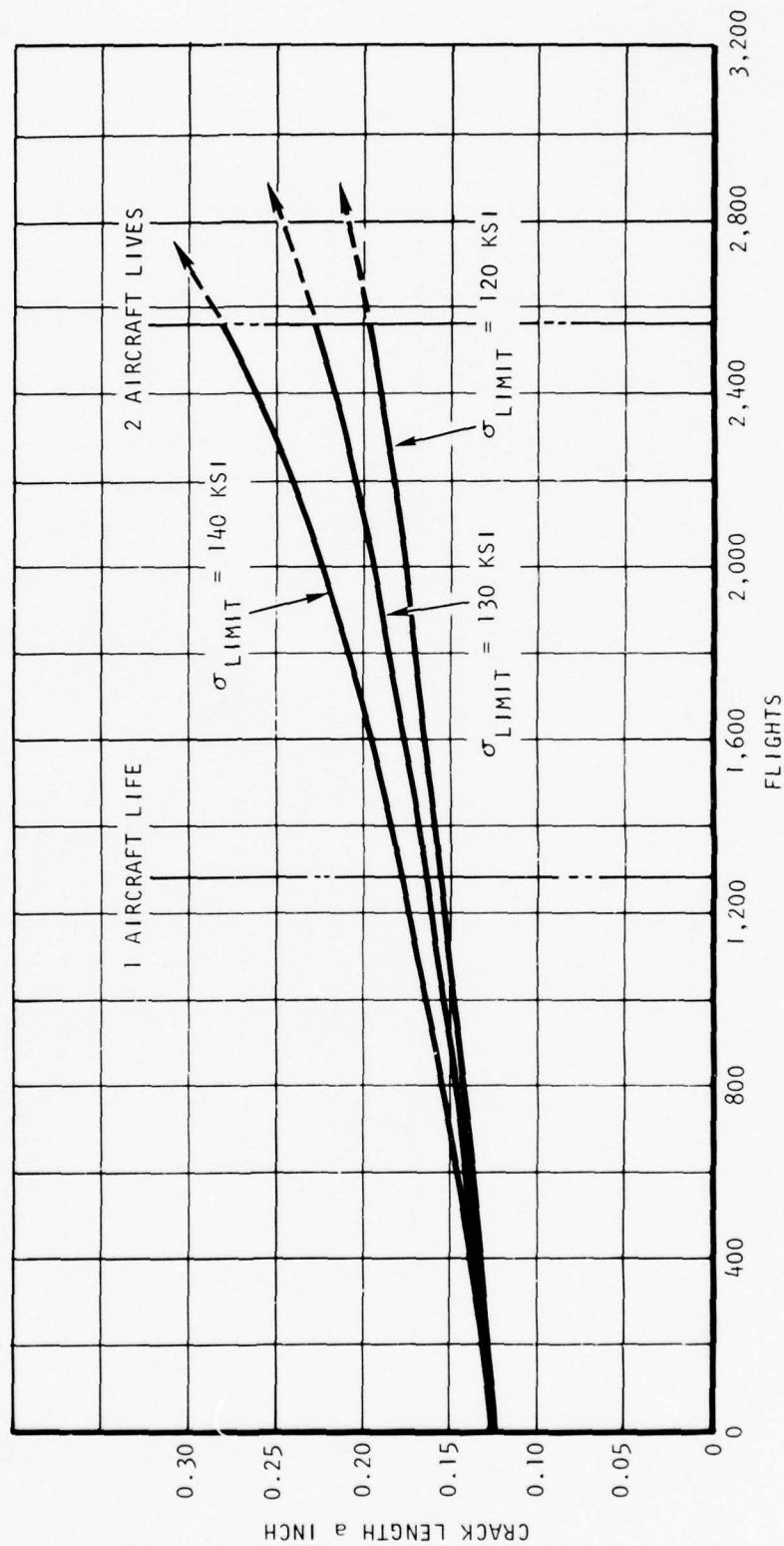
Figure 10. LOCOSST preliminary crack growth analysis.

Figures 11 and 12 show the predicted growth rates of assumed 0.005R initial corner flaws in 3/4- and 1-inch-diameter boltholes in the flange which attaches to the station 932 bulkhead. For each diameter, the analysis was made in the flange thickness appropriate to the hole. The analyses were made to the flight-by-flight operating stress spectrum at limit stress levels of 120, 130, and 140 ksi. Each of the figures shows the capability to sustain two lifetimes of slow crack growth without failure at a limit stress of 120 ksi on the flange gross area. This is acceptable since static net stress limitations at ultimate load prevent the limit gross area flange stress from ever exceeding 110 ksi. Thus, all boltholes meet the crack growth requirement.

Wing Pivot Inboard Shear Fitting

The only critical section in fatigue or crack growth on the pivot shear fitting is the actuator attach lug hole. This lug has an outside radius of 1.38 inches, a thickness of 0.2375 inch, and a pin diameter hole of 1.062 inches. The geometric stress concentration factor, K_T, based on these dimensions, is 3.25 at the edge of the hole. Using a quality factor of 1.2, the effective stress concentration factor used for the fatigue analysis was 1.2 X 3.25 = 3.90. An analysis to the operating spectrum stress on the lug net section produces a fatigue life well in excess of the required four lifetimes.

A crack growth analysis was made on this same net section assuming an initial corner flaw of 0.05-inch radius at the edge of the lug hole. Crack growth rate properties used in this analysis were for a low-humidity air environment. The life of the assumed initial flaw under the operating stress spectrum was marginally equal to the two-lifetime requirement of MIL-A-83444. A plot of the predicted crack growth rate is shown in Figure 13. All other sections on the body of this fitting have less severe stress concentration factors and are not critical in fatigue or fracture.

Nacelle Support Beam

The nacelle support beam on the B-1 is designed to a stiffness criteria requiring a substantially larger bending section than is needed to react the static airload conditions. The excessive placement of material in the beam flanges to meet the stiffness requirement causes a low operating stress spectrum which, in turn, results in a predicted high fatigue life and slow crack

- WING SWEEP ACTUATOR ATTACH FITTING
- PARAMETRIC CRACK GROWTH ANALYSIS
- FLIGHT-BY-FLIGHT FATIGUE SPECTRUM
- AF1410 STEEL - SUMP TANK WATER ENVIRONMENT
- CORNER-CRACKED 3/4 INCH DIA HOLE

t = 0.25 a_i = 0.005
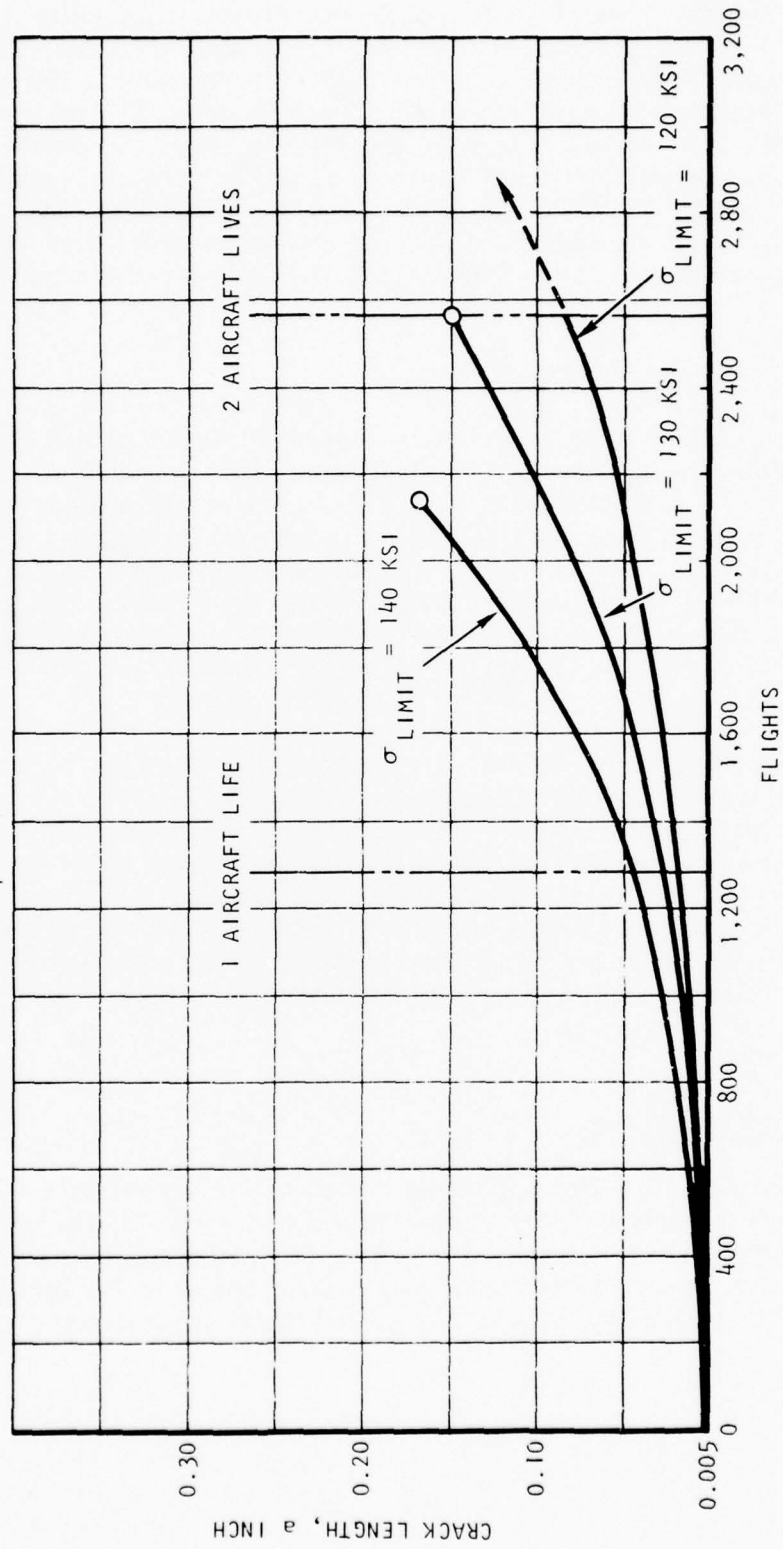
Figure 11. LOCOSST preliminary crack growth analysis

28
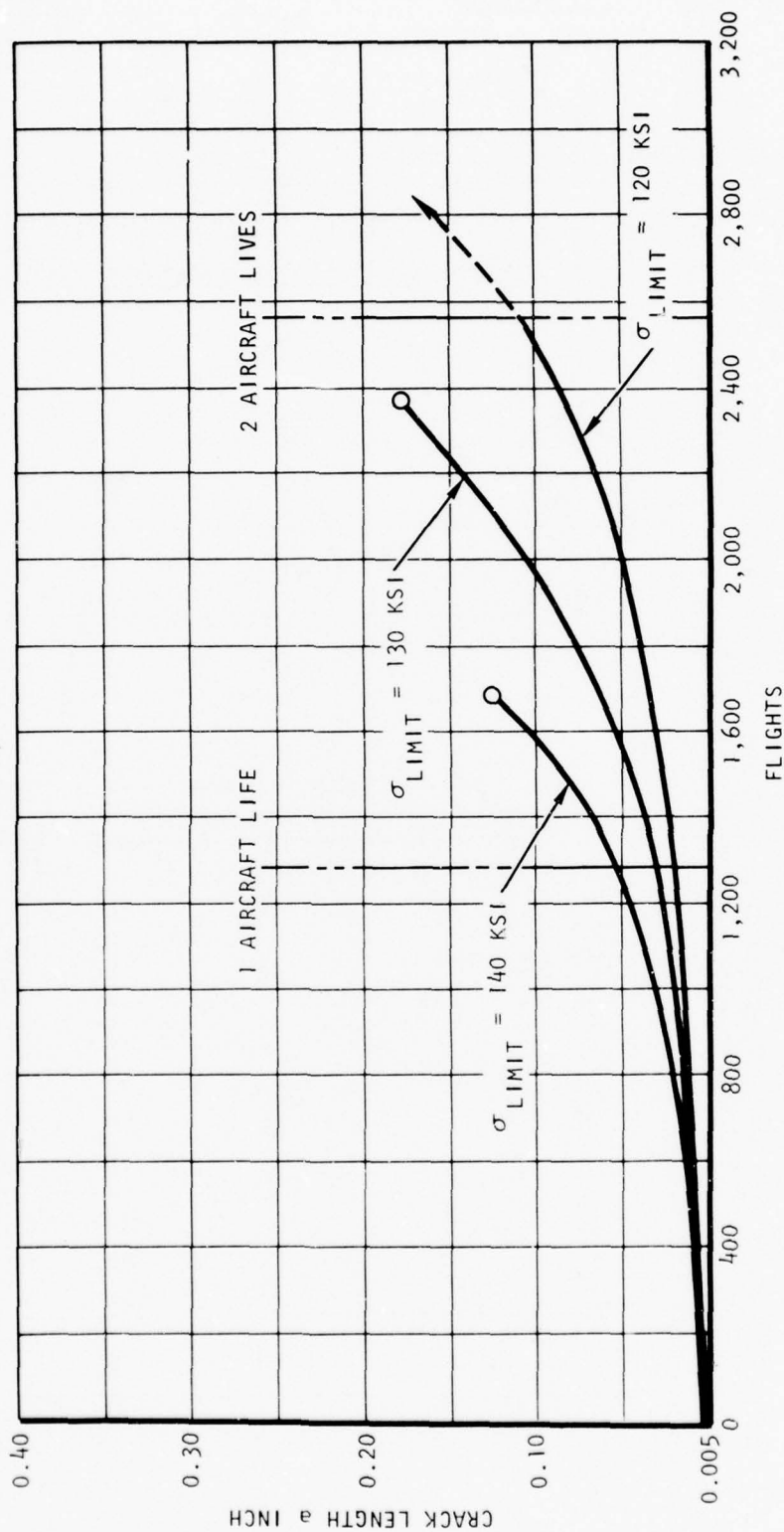
Figure 12. LOCOSST preliminary crack growth analysis.

29

- WING PIVOT INBOARD SHEAR FITTING
- FLIGHT-BY-FLIGHT SPECTRUM ANALYSIS
  OF CORNER CRACK IN ACTUATOR ATTACH LUG HOLE
- AF1410 STEEL – LOW-HUMIDITY AIR ENVIRONMENT
- INITIAL CRACK OF 0.05R IN A 1.062 IN. DIA LUG HOLE
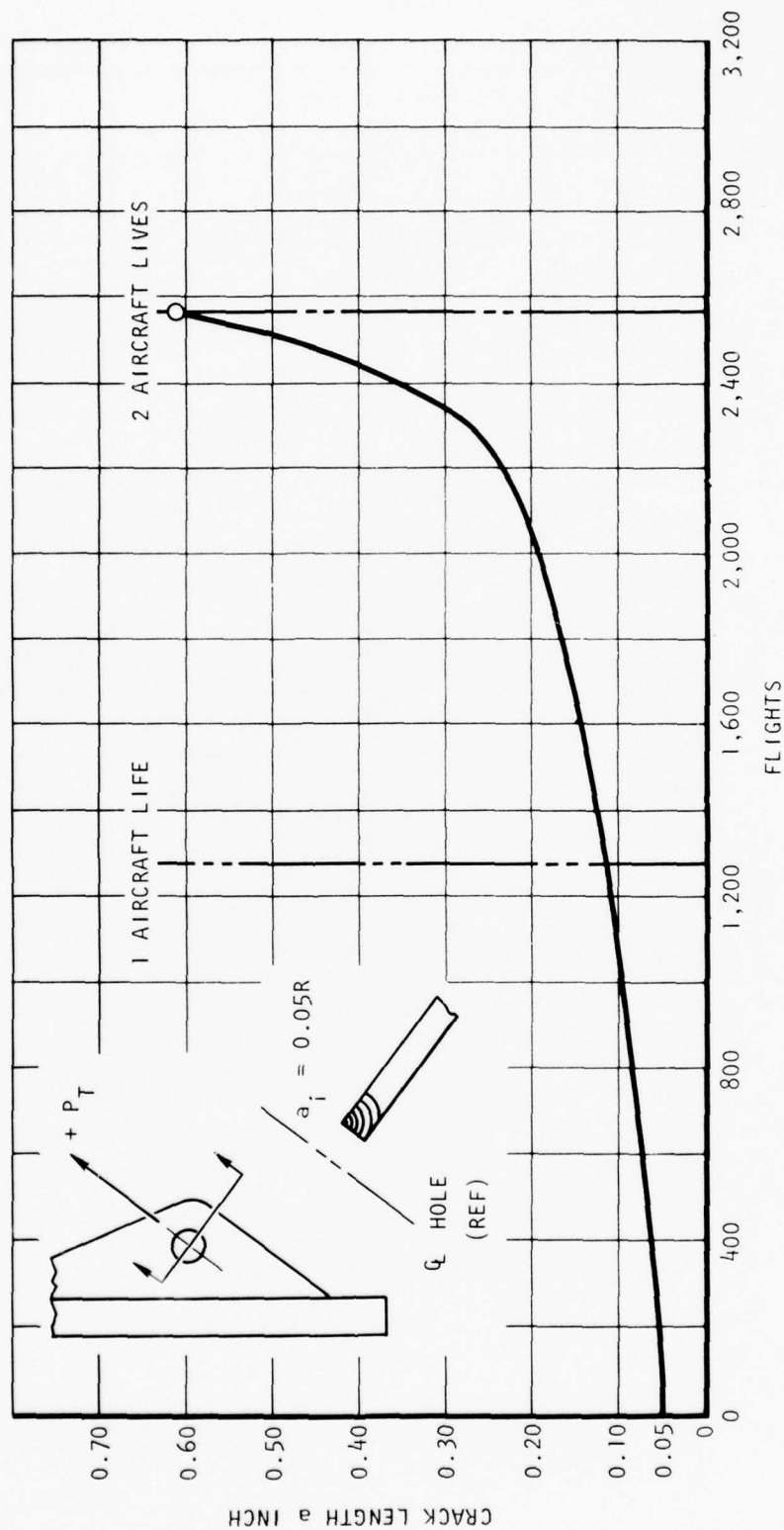
Figure 13. LOCOSST preliminary crack growth analysis.

growth rates in the most highly stressed region of the beam flanges. The upper flange of the beam was analyzed for fatigue and crack life at three sections, XF 96, XF 111.87, and XF 124. The predicted fatigue lives were grossly in excess of the requirement. To demonstrate the crack growth requirement, corner cracks with an initial size of 0.125-inch radius per MIL-A-83444 were assumed in the flange corners. The analysis conservatively assumed an aggressive sump tank water environment. Plots of the predicted crack growth rates in the operating flight-by-flight stress spectrum are shown in Figure 14. All three sections have a crack life in excess of two aircraft lifetimes, thus meeting the in-service noninspectable life requirement of MIL-A-83444.

Summary

The three fitting designs are sized by either the static load or stiffness requirements and are not additionally impacted by the fatigue and fracture mechanics requirements as defined by specifications MIL-A-8866A and MIL-A-83444. As shown by the parametric fatigue and fracture analyses of the wing sweep actuator attach fitting, the highest possible design stresses in AF1410 steel will support the fatigue and fracture life requirements. The nacelle support beam, designed to a stiffness requirement, has a sufficiently low operating stress spectrum to ensure a cyclic life greatly in excess of the requirements. The fatigue life of the wing pivot shear fitting is well in excess of requirements, while the crack life of the actuator attach lug is marginally acceptable by a conservative analysis approach.

TEST PLAN FOR THE FRACTURE MECHANICS ANALYSIS VERIFICATION PROGRAM

A series of fracture mechanics analysis verification tests were conducted as part of the phase II materials test program. The purpose of this type of testing is to generate crack growth data from flaw configurations typical of those which develop in aircraft structure, with the intent of using these data to support and verify the development of analytical prediction methodology in AF1410 steel. The specimen configurations shown in Figure 15 were tested to either a constant-amplitude cyclic load or to a generalized spectrum of loads simulating the loading of an element in the B-1 lower wing skin. A listing of the parameters pertinent to each of the tests is shown in Table 3.

The initial analytical predictions of the test coupon crack growth curves were made using da/dN vs ΔK crack growth rate properties generated from compact tension-type specimens of AF1410 steel in the phase II material properties program. Conventional fracture mechanics stress intensity formulae together with appropriate surface, width, and stress gradient factors were used in predicting the growth curves of the test cracks. A comparison of these predictions and the actual test growth curves was made, and the

Figure 14. LOCOSST preliminary crack growth analysis.

- NACELLE SUPPORT BEAM
- FLIGHT-BY-FLIGHT SPECTRUM ANALYSIS OF
  CORNER CRACK IN BEAM UPPER FLANGE
- AF1410 STEEL - SUMP TANK WATER ENVIRONMENT
- INITIAL CRACK OF 0.125R AT X_F96, X_F111 & X_F124 UPPER FLANGE

$a_i = 0.125R$

CRACK LENGTH a INCH

FLIGHTS

1 AIRCRAFT LIFE

2 AIRCRAFT LIVES

X_F96

X_F124

X_F111.87

32

TYPE I PART-THROUGH CRACK

P/N 3109-100004-11

$a_i = 0.05$

$a/2c_i = 1/2$

TOTAL 7 TESTS & 2 SPARES

TYPE II CORNER CRACKED OPEN HOLE

P/N 3109-100004-21 & 23

$a_i = 0.05$ IN

W = 4 IN & 8 IN

HOLE DIA = 1/2 IN
CONVENTIONAL REAMED

TOTAL 8 TESTS & 2 SPARES

TYPE III THROUGH CRACK

P/N 3109-100004-31

$2a_i = 0.50$ IN

TOTAL 6 TESTS & 2 SPARES

TYPE IV BOLTED JOINT WITH CORNER CRACKED HOLE

P/N 3109-100005-1

CLOSE-TOLERANCE 5/8 DIA
LOADED BOLT

$a_i = 0.05$ IN

TOTAL 4 TESTS & 1 SPARE

Figure 15. Fracture mechanics analysis verification test program test specimen configurations.

TABLE 3

SPECIMEN LIST - FRACTURE MECHANICS ANALYSIS VERIFICATION TESTS

TEST NO.	PART NO.	CONFIGURATION	TYPE LOAD	ENVIRON.	MAX STRESS
11	3109-100004-11	Part-thru crack	Const amplit	Lab air	75 ksi
12		Part-thru crack	Const amplit	Lab air	150 ksi
13		Part-thru crack	Const amplit	Sump water	75 ksi
14		Part-thru crack	Const amplit	Sump water	150 ksi
15		Part-thru crack	Spectrum	Lab air	120 ksi
16		Part-thru crack	Spectrum	Lab air	150 ksi
17	3109-100004-11	Part-thru crack	Spectrum	Sump water	120 ksi
18	Spare	TBD	TBD	TBD	TBD
19	Spare	TBD	TBD	TBD	TBD
21	3109-100004-23	Cracked hole	Const amplit	Lab air	100 ksi
22	3109-100004-21	Cracked hole	Const amplit	Lab air	100 ksi
23	3109-100004-21	Cracked hole	Const amplit	Lab air	+100 ksi
24	3109-100004-21	Cracked hole	Const amplit	Sump water	100 ksi
25	3109-100004-23	Cracked hole	Spectrum	Lab air	100 ksi
26	3109-100004-21	Cracked hole	Spectrum	Lab air	100 ksi
27	3109-100004-21	Cracked hole	Spectrum	Lab air	125 ksi
28	3109-100004-21	Cracked hole	Spectrum	Sump water	100 ksi
29	Spare	TBD	TBD	TBD	TBD
30	Spare	TBD	TBD	TBD	TBD
31	3109-100004-31	Through crack	Const amplit	Lab air	100 ksi
32		Through crack	Const amplit	Lab air	+100 ksi
33		Through crack	Const amplit	Sump water	100 ksi
34		Through crack	Spectrum	Lab air	100 ksi
35		Through crack	Spectrum	Lab air	75 ksi
36	3109-100004-31	Through crack	Spectrum	Sump water	100 ksi
37	Spare	TBD	TBD	TBD	TBD
38	Spare	TBD	TBD	TBD	TBD
41	3109-100005-11	Cracked hole	Const amplit	Lab air	100 ksi
42		Cracked hole	Const amplit	Lab air	120 ksi
43		Cracked hole	Spectrum	Lab air	100 ksi
44	3109-100005-11	Cracked hole	Spectrum	Lab air	120 ksi
45	Spare	TBD	TBD	TBD	TBD

Tests 18, 19, 29, 30, 37, 38, and 45 are undesignated spares, disposition to be determined (TBD)

level of empirical correction factors required to provide agreement between test and analysis was determined. The Rockwell-developed B-1 computer program EFFGRO, crack propagation analysis by the Vroman model, was used for the crack growth rate predictions.

STRUCTURAL ANALYSIS

The preliminary stress analysis was conducted using baseline loads from the B-1 Stress analysis. These loads were the values quoted for the baseline titanium parts used on the B-1. Stress checks were made on the following substitute designs:

1. Inboard wing pivot shear fitting, 3109-100000 (machined forging, welded lugs)

2. Inboard wing sweep actuator fitting - two versions:

    a. Truss design, 3109-100001 (welded, machined)

    b. Stiffened web, 3109-100003 (machined forging)

3. Nacelle support beam, 3109-100002 (multipiece welded)

In addition, during the candidate design concept selection phase, preliminary sizing and analysis checks were conducted on the various concepts to obtain comparable strength and/or stiffness equivalent structural components.

Conventional stress analysis procedures per Reference 3 were used.

Structural Analysis Properties - AF1410 Steel

The basis structural design properties used for preliminary analysis are summarized in Table 4 for the AF1410 steel material. The compressive stress-strain curve shown in Figure 16 was used to generate the stiffness (modulus), buckling, column, and crippling curves shown in Figure 17 through 24, using a Ramberg-Osgood curve fit routine to account for the material stress-strain nonlinearity. The basic methods for developing the structural analysis curves were obtained from Reference 4.

Inboard Shear Fitting - Pivot Pin - AF1410 Version

The inboard shear fitting (Figures 4 and 25) was analyzed on a preliminary basis using the structural analysis curves and material properties provided under "Structural Analysis Properties" (Table 4 and Figures 16 through 24). The applied design loads are those obtained from the B-1 Stress analysis and used for the titanium baseline part.

35

TABLE 4

MATERIAL PROPERTIES - AF1410 STEEL

For preliminary design subsequent to 1-14-76, the following properties were used: (Air Force and LAAD concurrence at Program Review 13 and 14 January 1976)

Heat-Treated Condition	Parent Metal	Welds Loaded in Shear or Transverse
F_{tu} (ksi)	230	196
F_{ty} (ksi)	215	183
F_{cy} (ksi)	226	192
F_{su} (ksi)	147	125
F_{bru} (ksi)	331 (e/D = 1.5)	
	446 (e/D = 2.0)	
F_{bry} (ksi)	301 (e/D = 1.5)	
	357 (e/D = 2.0)	
e (percent)	10	
E 10^6 psi	28.0	28.0
E_c 10^6 psi	28.0	28.0
G 10^6 psi	10.6	10.6
μ (in/in.)	0.32	0.32
w (pci)	0.285	0.285
K_{Ic} (ksi $\sqrt{in.}$)	130	

36
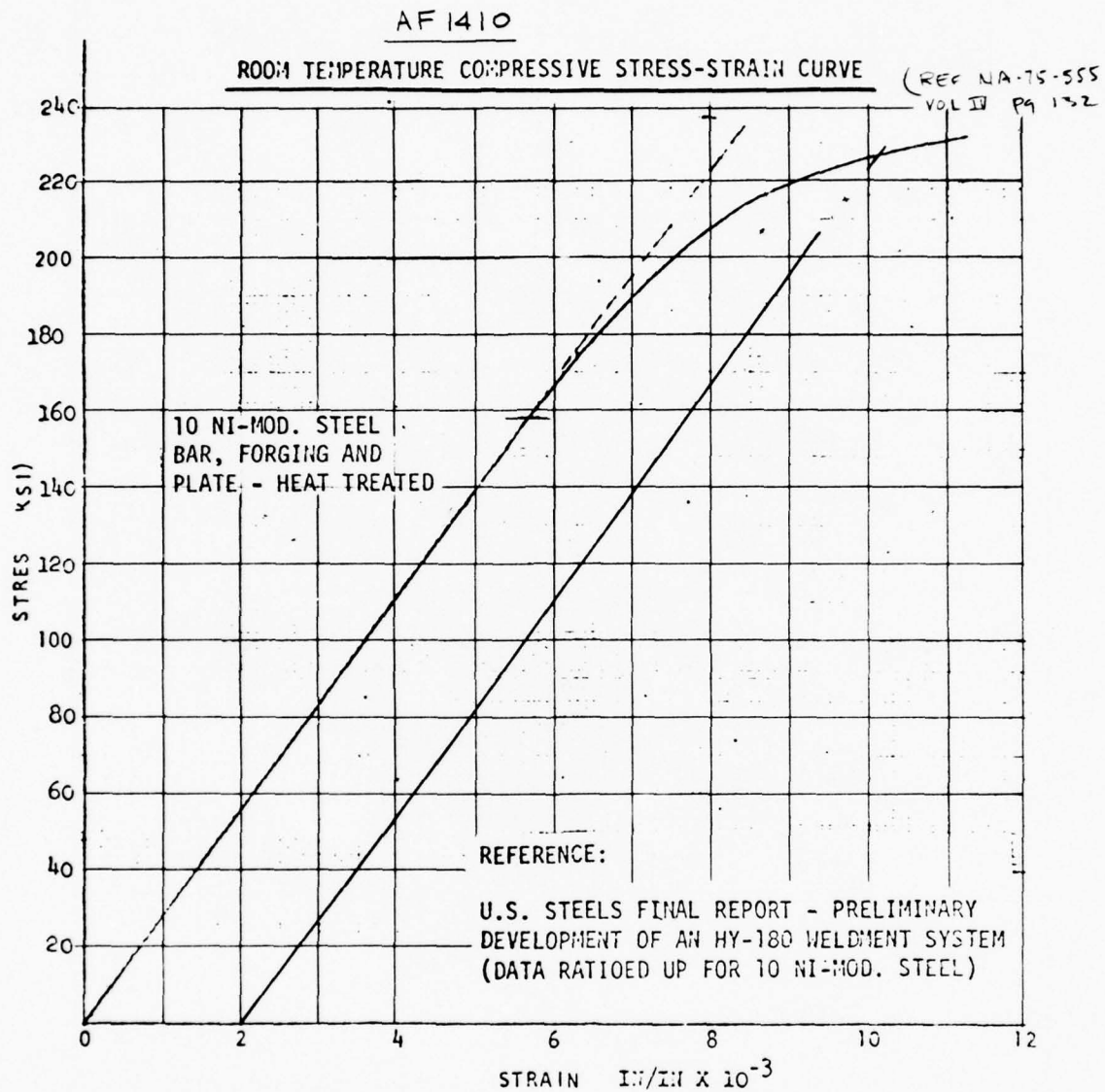
Figure 16. AF1410 steel - room temperature compressive strain-strain curve.

TANGENT AND SECANT MODULUS CURVES
AF1410 ALLOY STEEL BAR,FORGINGS,AND PLATE HEAT TREATED TO 230 KSI
  PRELIMINARY DESIGN PROPERTIES
    TEMPERATURE= RT   FCY=226 KSI   E=28 MSI   FSU-147 KSI   N=16.5
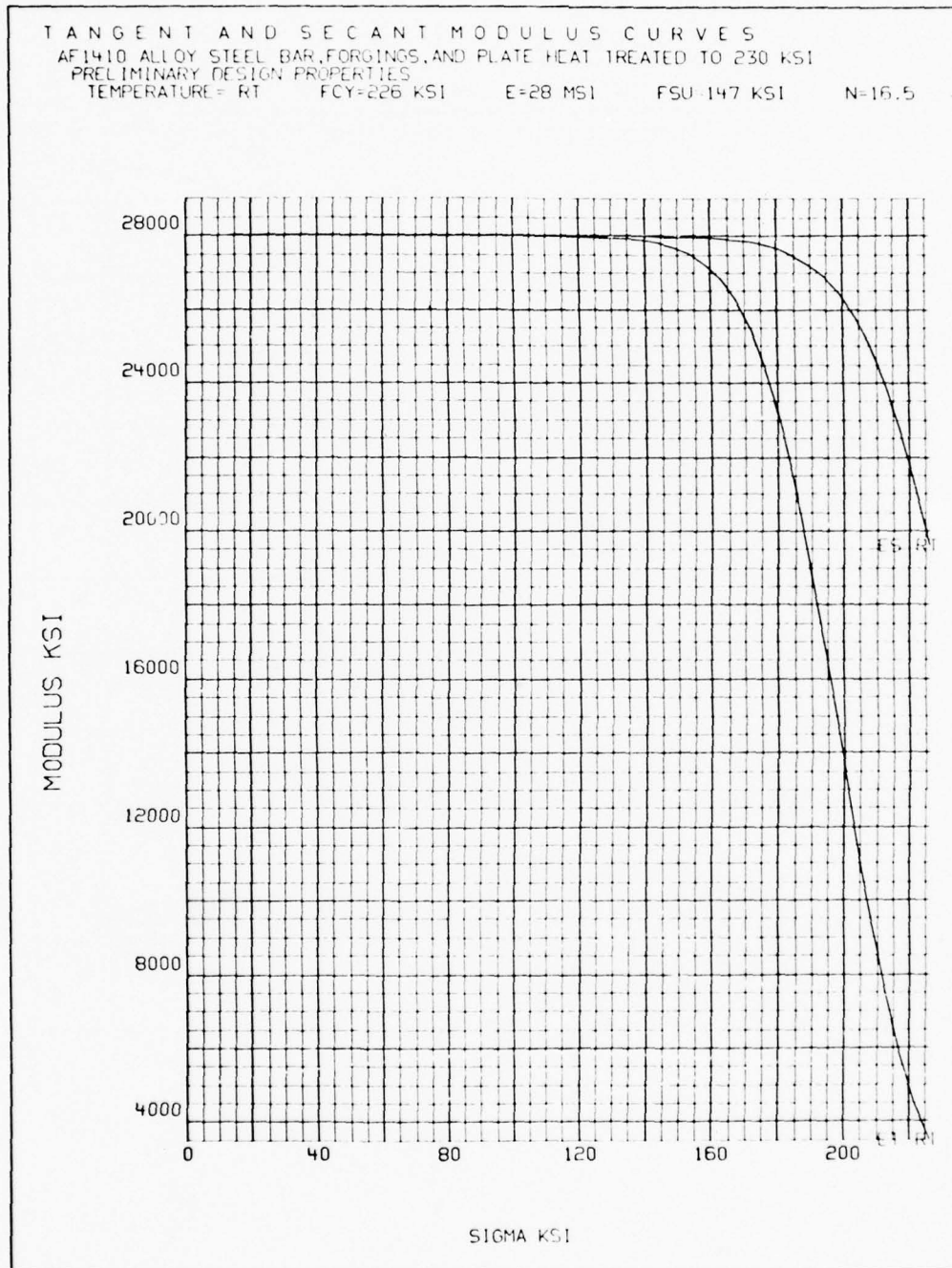
AF1410 ALLOY STEEL

Figure 17. Tangent and secant modulus curves.

PLASTICITY CORRECTION IN COMPRESSION
AF1410 ALLOY STEEL BAR,FORGINGS,AND PLATE HEAT TREATED TO 230 KSI
PRELIMINARY DESIGN PROPERTIES
TEMPERATURE= RT   FCY=226 KSI   E=28 MSI   FSU=147 KSI   N=16.5
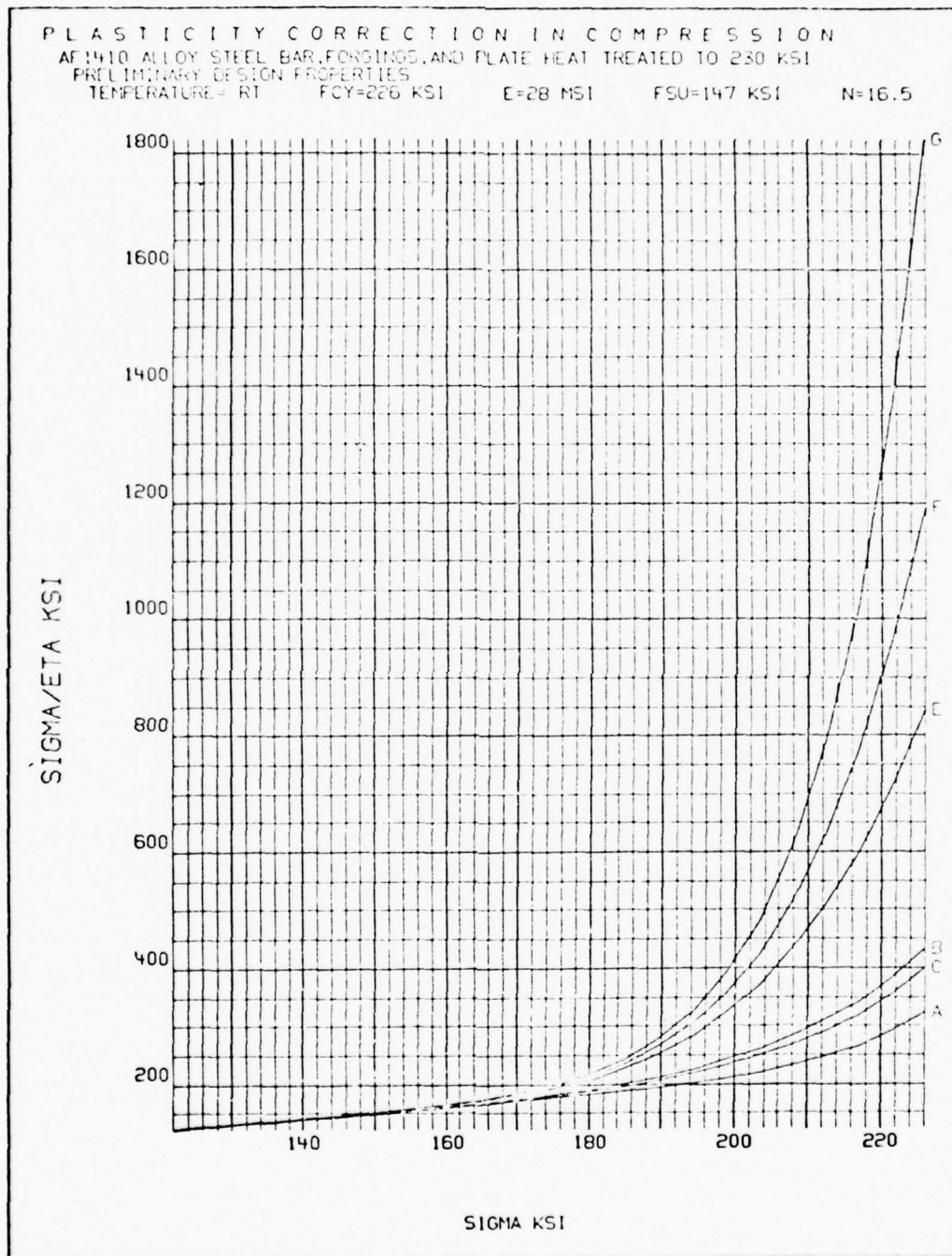
AF1410 ALLOY STEEL

Figure 18. Plasticity correction in compression.

39

PLASTICITY CORRECTION IN SHEAR
AF1410 ALLOY STEEL BAR,FORGINGS,AND PLATE HEAT TREATED TO 230 KSI
PRELIMINARY DESIGN PROPERTIES
TEMPERATURE= RT   FCY=226 KSI   E=28 MSI   FSU=147 KSI   N-16.5
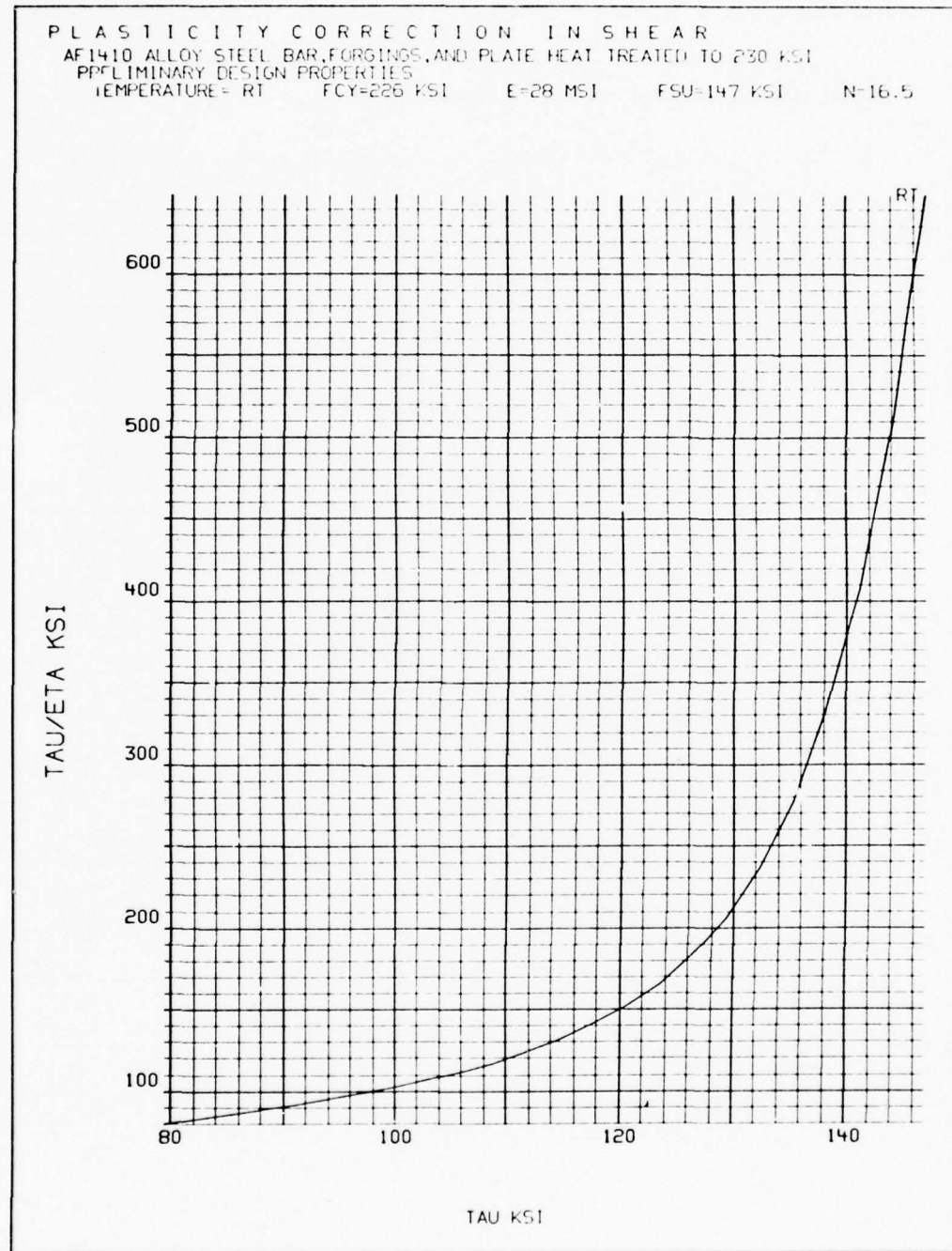
AF1410 ALLOY STEEL

Figure 19.   Plasticity correction in shear.

40

COMPRESSION BUCKLING STRESS
AF1410 ALLOY STEEL BAR,FORGINGS,AND PLATE HEAT TREATED TO 230 KSI
PRELIMINARY DESIGN PROPERTIES
TEMPERATURE= RT   FCY=226 KSI   E=28 MSI   FSU=147 KSI   N=16.5
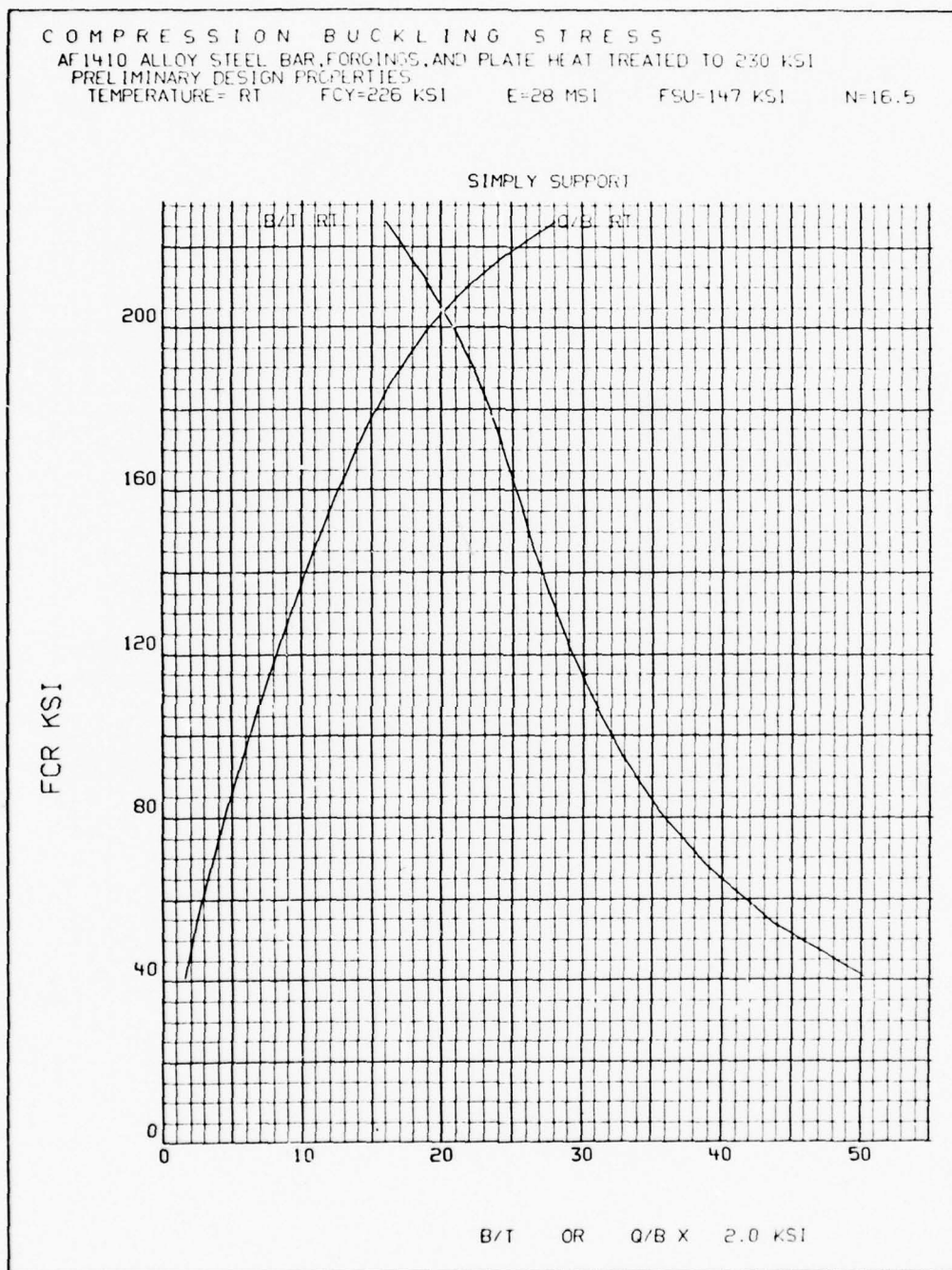
AF1410 ALLOY STEEL

Figure 20.   Compression buckling stress.

41

ALLOWABLE COLUMN STRESSES
AF1410 ALLOY STEEL BAR,FORGINGS,AND PLATE HEAT TREATED TO 230 KSI
PRELIMINARY DESIGN PROPERTIES
TEMPERATURE= RT   FCY=226 KSI   E=28 MSI   FSU=147 KSI   N=16.5
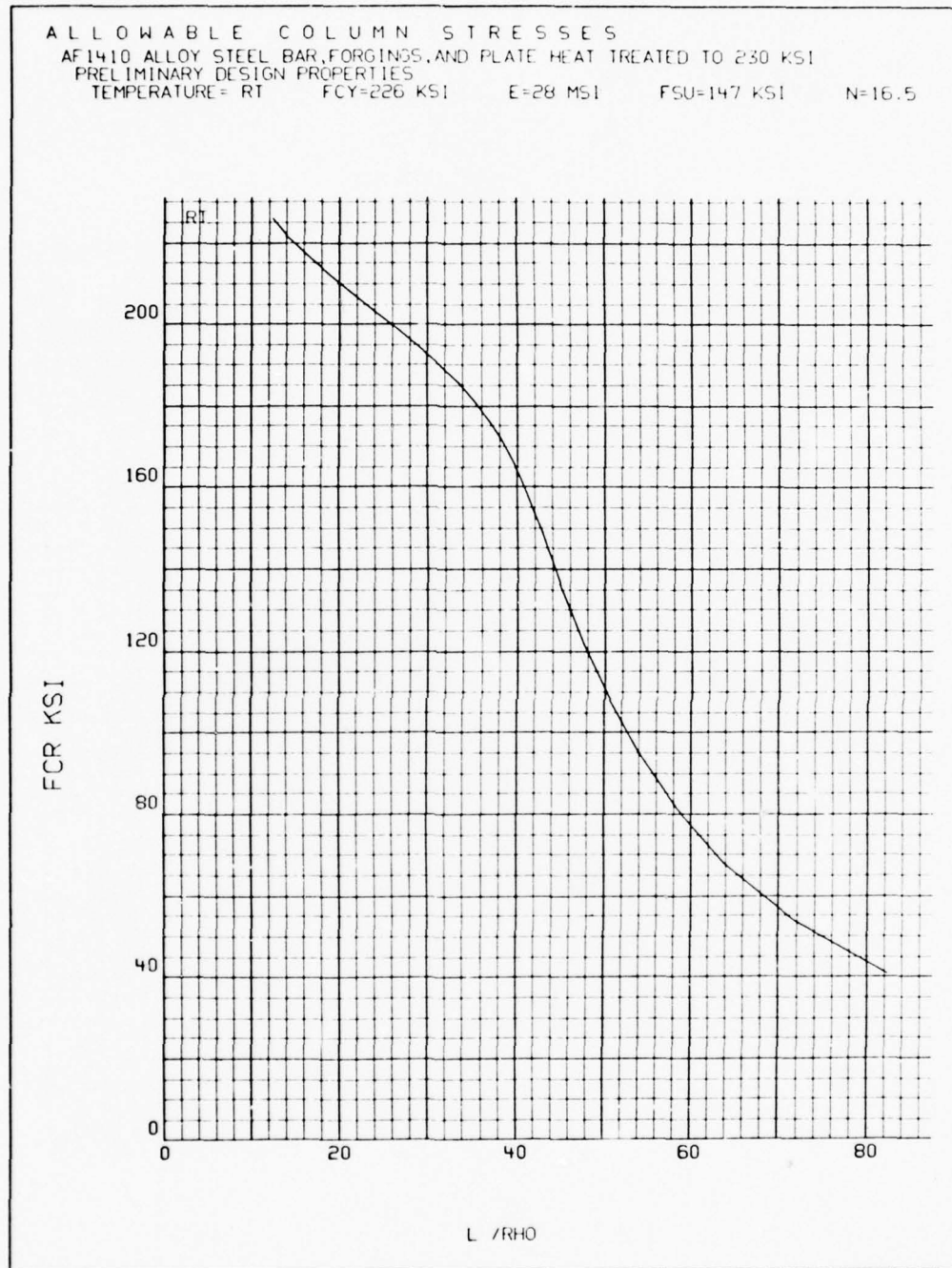
AF1410 ALLOY STEEL

Figure 21. Allowable column stresses.

42
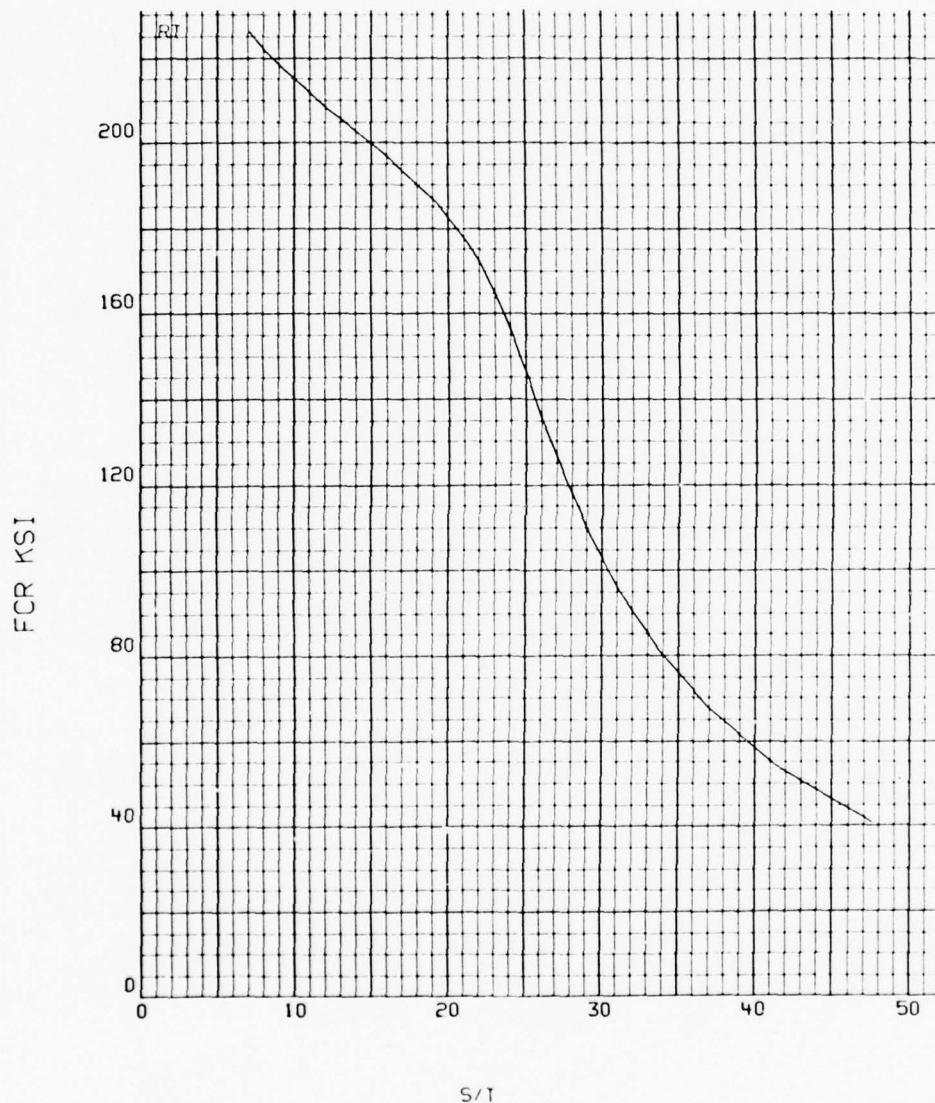
Figure 22.   Interrivet buckling.

SHEAR BUCKLING STRESS
AF1410 ALLOY STEEL BAR,FORGINGS,AND PLATE HEAT TREATED TO 230 KSI
PRELIMINARY DESIGN PROPERTIES
TEMPERATURE= RT   FCY=226 KSI   E=28 MSI   FSU=147 KSI   N=16.5

B/T   OR   Q/B X   5.0 KSI
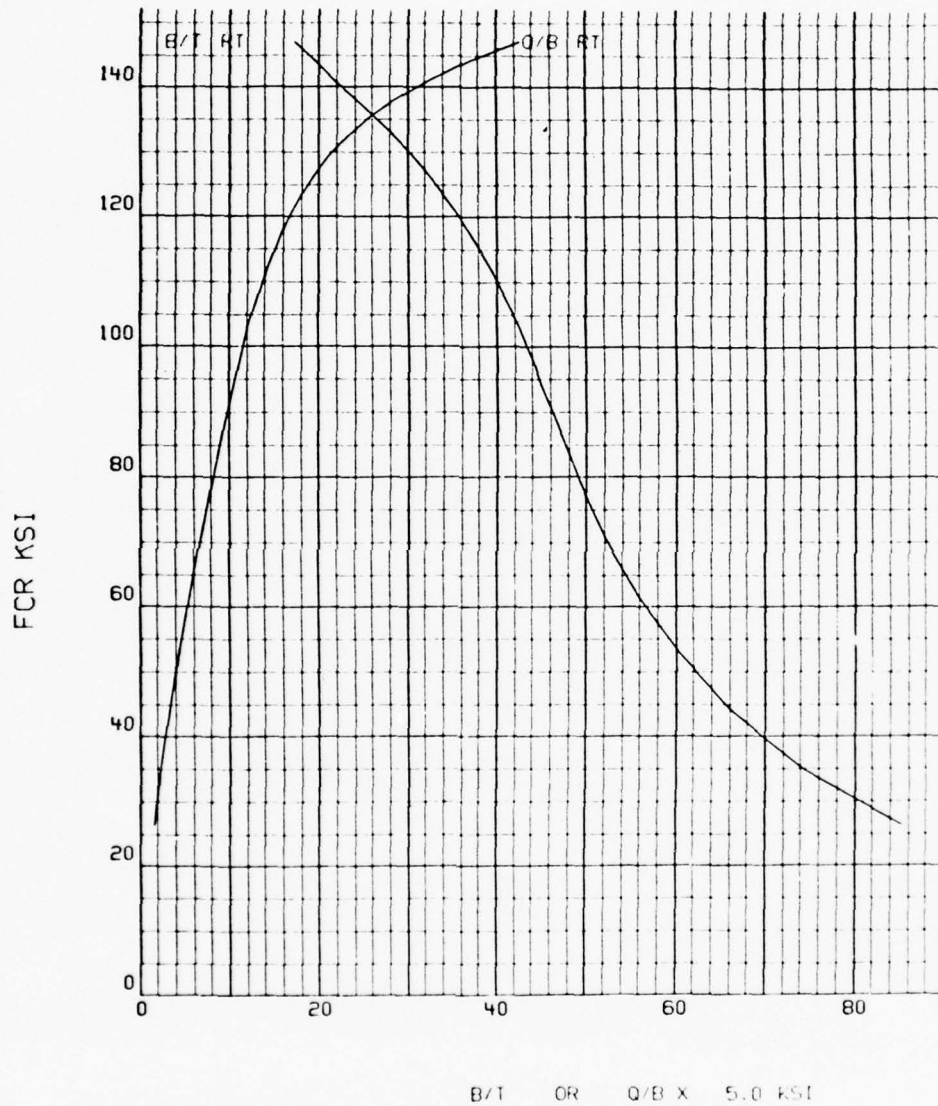
AF1410 ALLOY STEEL

Figure 23. Shear buckling stress.

44
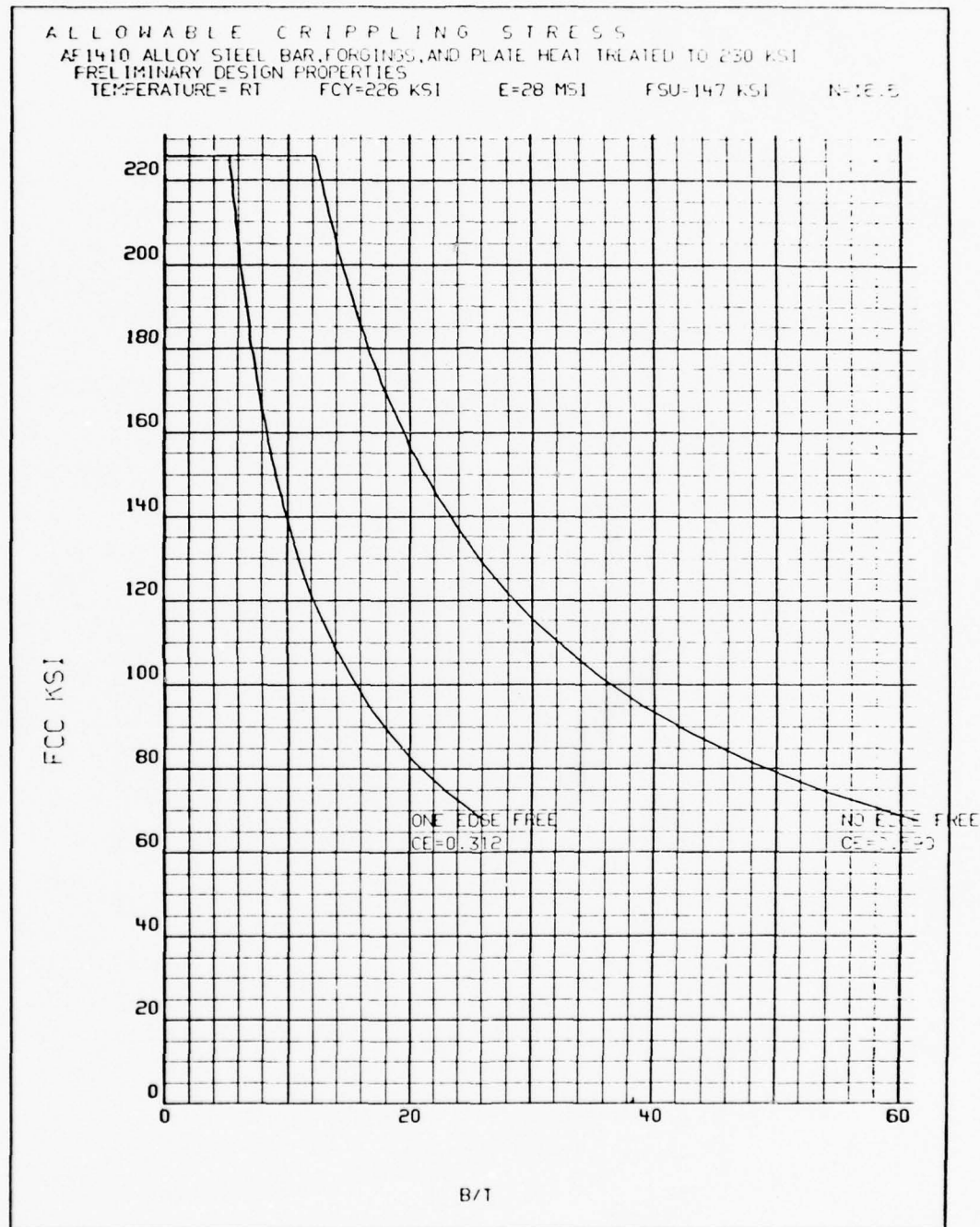
Figure 24. Allowable crippling stress.
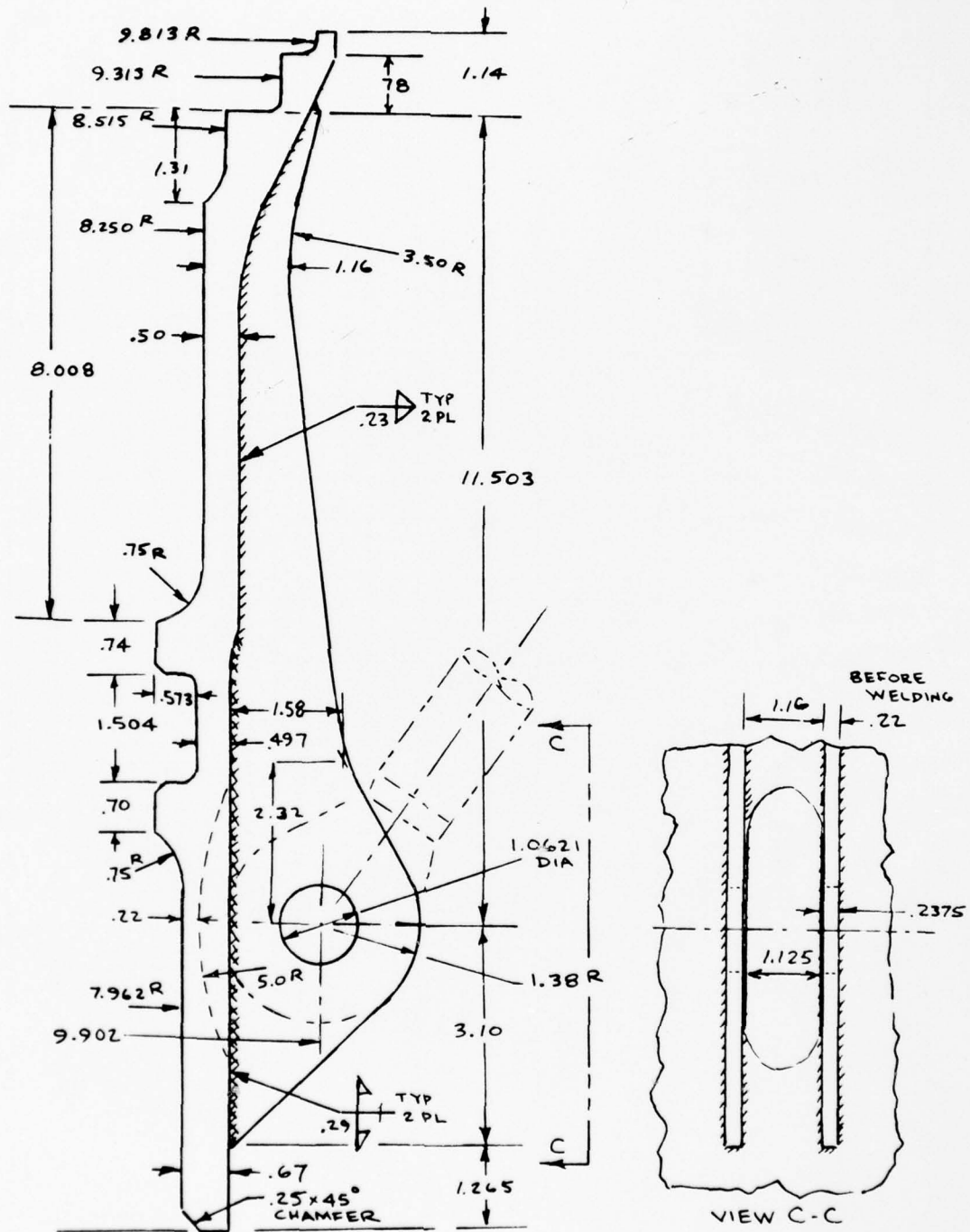
Figure 25. Inboard shear fitting geometry.

46

A summary of critical margins of safety is presented in Table 5 in which margins less than +0.50 are listed.

The critical conditions for the shear strut attachment lugs are the terrain-following and low-level penetration mission segment loads for lug tension and compression respectively (conditions 1A and 1B). The critical condition for the fitting sections (conditions 2A or 2B) is the case where the upper or lower outboard wing pivot lug fails and an induced thrust load, either up or down, on the fitting occurs.

The preliminary stress analysis of the shear fitting checked the shear strut attachment lugs for tension and compression strut loads with compression bearing being the critical mode. Stress checks of cross sections at various locations along the fitting wall were made for the effect of combined axial and bending stresses using assumed effective width sections. The effects of curved fitting wall cross sections in terms of locating bending eccentricities were accounted for. No negative margins were identified for this preliminary analysis.

Inboard Wing Sweep Actuator Support Fitting

The inboard wing sweep actuator support fitting was stress analyzed for two different versions:

1. Truss design - Machined, welded (Figures 5 and 26)

2. Stiffened web design - Machined forging (Figures 6 and 27)

The preliminary analysis for both versions used the structural analysis curves and AF1410 steel material properties under "Structural Analysis Properties." The applied design loads were the same as those used in the B-1 Stress analysis for the titanium baseline component. Conventional stress analysis techniques were used per References 3 and 4.

A summary of margins of safety are presented in Tables 6 and 7 in which margins less than +0.50 are listed. Analysis details are provided in Appendix B.

The critical loads and conditions (Figure 26) have been identified as an actuator tension load (condition 1) and a compressive load (condition 2) of approximately 70 percent of the tension load magnitude. The support fitting serves to transfer the outer wing sweep loads into the wing carry-through structure via the YF932 bulkhead and ribs at XF 121 and XF 84.

47

TABLE 5

SUMMARY - CRITICAL MARGINS OF SAFETY (MS +0.50) INBOARD SHEAR FITTING

Item	Description	Load Conditions	Margins of Safety
Lug analysis	Maximum bearing check	Condition ①B low-level penetration	+ 0.51 (bearing)
Section D-D without lugs	Check of region above shear strut attach point (rect section)	Condition ②B P_u acting	+ 0.15 (axial + bend)
Section D-D with lugs	Same check as above except consider lugs as part of section	Condition ②B	+ 0.04 (axial + bend)
Section D-D with lugs	Section checked as a curved section	Condition ②B	+ 0.03 (axial + bend)
Section B-B	Section above shear strut attach point curved section	Condition ②A P_L acting	+ 0.19 (lug crippling)
Section F-F	Section 2.9 below section B-B curved section	Condition ②A	+ 0.014 (crippling)
Section K-K	Section through shear strut attach point	Condition ②A	+ 0.27 (axial + bend)
Section C-C	Section below shear strut attach point curved section	Condition ②A	+ 0.24 (axial + bend)

Rockwell International

| PREPARED BY: TM | INBD SWEEP ACTUATOR | REPORT NO. |
| DATE: | SUPPORT FITTING. TRUSS DESIGN | MODEL NO. |

TRUSS LOADS	COND I	COND II
DIAGONAL TRUSS MEM. $\overline{AB}$	914^k (TEN)	(636^k)(COMP)
CHORDWISE TRUSS MEM. $\overline{AC}$	-856^k (COMP)	(596^k) (TEN)
SPANWISE TRUSS MEM. $\overline{BC}$ *	-617^k (COMP)	(430^k) (TEN)

* VARIES ~ VALUES SHOWN FOR X_F 93.
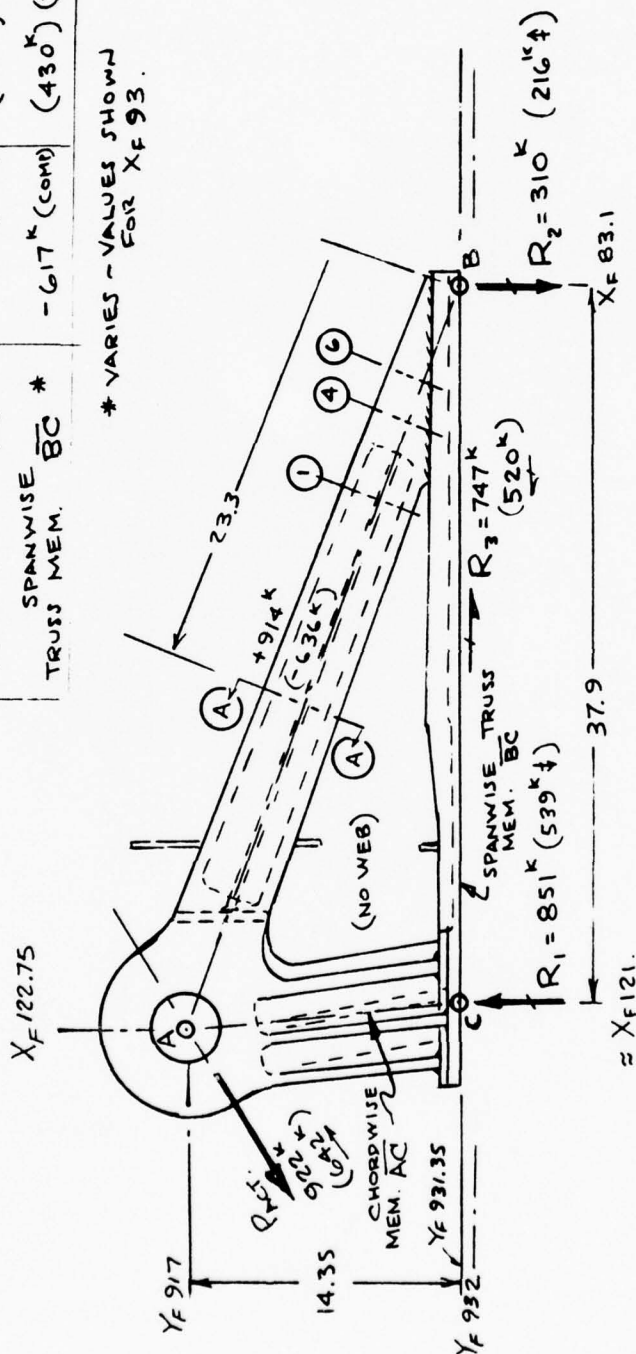
LOADS

COND I ~ P_{ACT} = 922^k
COND II ~ P_{ACT} = (-642^k)

ULTIMATE

X_F 122.75

Y_F 917

14.35

Y_F 931.35

Y_F 932

P_{ACT} 922^k + (642^k)

CHORDWISE MEM. $\overline{AC}$

A

(NO WEB)

23.3

+914^k

(-636^k)

A

A

① ④ ⑥

B

R_2 = 310^k (216^{ik}↑)

X_F 83.1

R_3 = 747^k (520^k)

37.9

¢ SPANWISE TRUSS MEM. $\overline{BC}$

R_1 = 851^k (539^k↓)

C

X_F 121.

≈ X_F 121.

Figure 26. Summary loads and geometry inboard sweep support fitting.

49

LOCOSST
INBOARD WING SWEEP
ACTUATOR FITTING
MACHINED FORGING
DWG # 3109-100003

STIFFENED WEB
DESIGN

ULTIMATE

CONDITION	P ACT	R₁	R₂	R₃
I	+972ᵏ	860ᵏ ↑	320ᵏ ↑	741ᵏ →
II	-642ᵏ	600ᵏ ↓	223ᵏ →	520ᵏ ↓
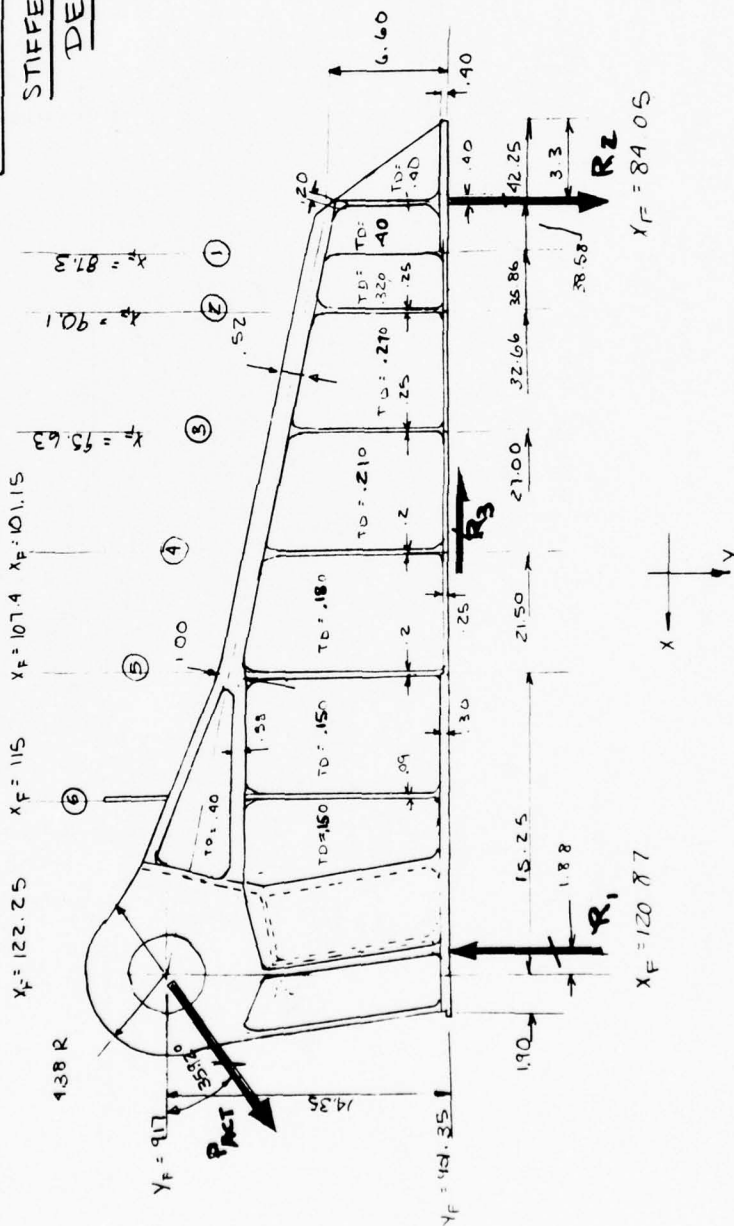
LOADS & DIMENSIONAL THICKNESS SUMMARY

Figure 27. Loads and dimensional thickness summary.

50

TABLE 6

SUMMARY - CRITICAL MARGINS OF SAFETY (MS 0.50) INBOARD SWEEP ACTUATOR
FITTING - TRUSS DESIGN

Item	Description	Load Conditions	Margins of Safety
Attach	Fasteners along lower truss member	Condition I	+ 0.19 (bolt tension & shear)
Attach	Fasteners at X_F 121 region	Conditon II	+ 0.11 (bolt tension & shear)
Section A-A	Diagonal truss AB member - comp	Condition II	+ 0.47 (column stab)
Section A-A	Diagonal truss web	Condition II	+ 0.02 (crippling)
Section A-A	Diagonal truss - tension	Condition I	+ 0.17 (tension)
Section ①①	Diagonal truss section	Condition I	+ 0.07 (tension & bend)
Section ①①	Diagonal truss section	Condition II	+ 0.09 (crippling)
Section ④④	Diagonal truss section	Condition I	- 0.01 (tension)
Section ⑥⑥	Diagonal truss section	Condition I	+ 0.30 (tension)
X_F 93	Lower truss mem section	Condition I	+ 0.05 (crippling)
X_F 93	Lower truss mem section	Condition I	+ 0.015 (comp & bend)

TABLE 6

SUMMARY - CRITICAL MARGINS OF SAFETY (MS 0.50) INBOARD SWEEP ACTUATOR
FITTING - TRUSS DESIGN (Concl)

Item	Description	Load Conditions	Margins of Safety
X_F 96	Lower truss mem section	Condition I	+ 0.07 (crippling)
X_F 96	Lower truss mem section	Condition I	+ 0.02 (comp & bend)
X_F 102	Lower truss BC member section	Condition I	+ 0.01 (column)
Y_F 923	Member AC section	Condition I	+ 0.37 (crippling)
X_F 121	Member AC compression	Condition I	+ 0.39 (column)
Y_F 917	Lug analysis actuator attach	Condition I	+ 0.36 (shear-out)
Y_F 917	Lug analysis actuator attach	Condition I	+ 0.11 (bend)
X_F 83	Weld-mem BC to mem AB	Condition I	+ 0.31 (shear & tension)

TABLE 7

SUMMARY - CRITICAL MARGINS OF SAFETY (MS   0.50) INBOARD SWEEP ACTUATOR
FITTING - STIFFENED WEB DESIGN - MACHINED FORGING

Item	Description	Load Conditions	Margin of Safety
Fastener check	Fasteners at X_F 84.05	P_{ACT} = 922K Condition I Case B	+ 0.46 (attach shear & tension)
X_F 84.05	Web check	Condition I	+ 0.10 (shear)
X_F 87.3	Web check	Condition I	+ 0.05 (shear & buckling)
X_F 90.1	Upper flange	Condition I	+ 0.18 (tension)
X_F 95.63	Web check	Condition I	+ 0.05 (shear buckling)
X_F 95.63	Upper cap	Condition I	+ 0.20 (tension)
X_F 95.63	Lower cap	Condition I case B	+ 0.43 (inter-rivet buckling)
X_F 101.15	Web check	Condition I	+ 0.07 (shear - buckling)
X_F 101.15	Upper cap	Condition I	+ 0.19 (tension)
X_F 101.15	Lower cap	Condition I case B	+ 0.26 (inter rivet buckling)

53

TABLE 7

SUMMARY - CRITICAL MARGINS OF SAFETY (MS 0.50) INBOARD SWEEP ACTUATOR
FITTING - STIFFENED WEB DESIGN - MACHINED FORGING (Concl)

Item	Description	Load Conditions	Margin of Safety
X_F 107.4	Web check	Condition I	+ 0.08 (shear-buckling)
X_F 107.4	Upper cap	Condition I	+ 0.24 (tension)
X_F 107.4	Lower cap	Condition I case A	+ 0.10 (inter-rivet buckling)
Section X_F 115.0	Web check	Condition I	+ 0.03 (shear buckling)
X_F 115.0	Lower cap	Condition I case A	+ 0.45 (inter-rivet buckling)
Y_F 923.35	Section check of forging under pin attachment	Condition I	+ 0.05 (crippling)
Lug X_F 122.75	Lug analysis (shear-out)	Condition I $P_{ACT} = 922K$	+ 0.16 (shear-out)
Lug X_F 122.75	Lug analysis (shear bearing)	Condition I	+ 0.40 (shear bearing)
Lug X_F 122.75	Lug analysis (shear bearing) neglect bushing	Condition I	+ 0.29 (conserv-shear bearing)
Lug X_F 122.75	Transverse shear-bearing	Condition I	+ 0.45 (transverse, shear bearing)

The preliminary stress analysis of the wing sweep actuator support fitting-truss version (Appendix B) checked the fastener attachment to the YF 932 bulkhead substructure for shear and tension; the diagonal truss member, the spanwise lower truss member, and chordwise truss member for axial tension and/or compression. The actuator attachment lug region was checked with the maximum actuator tension load. Typical weld joint regions were checked for combined shear and tension. No significant negative margins were identified.

The stress analysis of the machined forging-stiffened web design (Appendix B) checked the fitting attachments to the substructure for shear and tension, the webs for shear buckling, and the caps for axial tension and/or compression. The actuator attachment lug region was checked for the maximum actuator load case of 922K tension. No negative margins were identified in the preliminary analysis.

Nacelle Support Beam

The preliminary stress analysis was performed on the built-up welded design version of the nacelle support beam (Figures 7 and 28), using AF1410 steel material. The material properties and allowable structural analysis curves provided under "Structural Analysis Properties" were used with conventional stress analysis methods per References 3 and 4.

A summary of margins of safety are presented in Table 8, in which margins less than +0.50 are listed. Analysis details are provided in Appendix C.

The critical loads and conditions (Figure 28) for the nacelle support beam are B-1 designated conditions 360313 and 360312 for down bending, vertical shear, and drag strut loading. Load condition 360392 is critical for upbending, but the moment at the fuselage attachment region is only 27 percent of the downbending case, so that in general the downbending condition governs for all of the structure. The link loads were provided for the total box beam assembly. The box beam assembly has the lower surface cover omitted outboard of XF 125; therefore, the fore and aft acting link loads which induce torsional loads were transferred by means of differential bending into the side beams. The internal loads which were developed in the beam caps and shears in the webs accounted for this incremental effect. The baseline nacelle support beam was designed for stiffness as well as strength requirements so that the AF1410 steel design incorporated equivalent stiffness (EA) cap areas to provide equivalent beam flexural rigidities. In terms of cap areas, this translated into the fact that the steel cap areas could be 57 percent of the baseline titanium areas.

The preliminary stress analysis of the nacelle support beam checked the webs at critical locations to insure that web buckling under shear loads did not occur prior to limit load application. In addition, a lug analysis was

PREPARED BY: TM NACELLE SUPPORT REPORT NO.

DATE 11-1-75 BEAM ASSEMBLY MODEL NO.

DWG 3103-...

LOADS

LOADS SHOWN FOR COMPLETE
BEAM ASSEMBLY (₵ AT Y_F 1250)

(SIDE VIEW)

X_F 75.98

X_F 85.66

X_F 96.9

X_F 124.9

X_F 130.511

X_F 111.87

X_F 139.535

X_F 158.084

MAX P_C = 282.1^k
COND 360312

MAX V = 66.3^k
COND 360312

MAX M = 6,399 IN-KIP

OUTBD +X

P_4^X P_6^X

FRP

P = 224^k

+ P_2^Z

P_5^Z P_6^Z

+ Z
DOWN
ACTING
LOAD

COND 360392
V = -29.6^k
M = -1732 IN-KIP

X_F 14.66

P_6 DRAG STRUT

Y_F 1256
Y_F 1250
Y_F 1244

+2 +4 +5 6

P_2^Y P_4^Y P_5^Y P_Y^6

+y
FWD

(VIEW - LOOKING UP)

LINK & STRUT LOADS (KIPS)   ULTIMATE
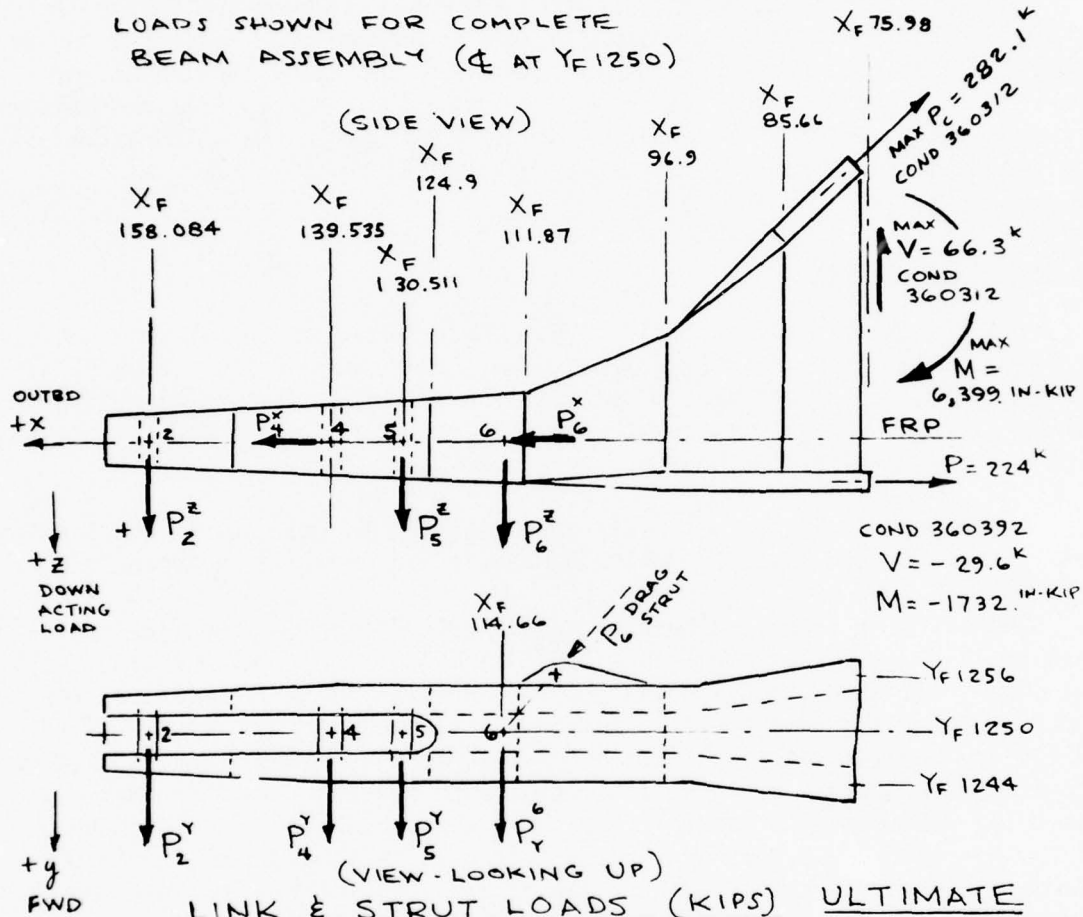
COND	P_2^Y	P_2^Z	P_4^X	P_4^Y	P_5^Y	P_5^Z	P_6^X	P_6^Y	P_6^Z
360312							46.61	40.21	
360313	-9.77	97.89	-39.83	1.98	3.22	-32.24	11.46	13.29	-0.78
360315			-37.14			-34.12			
360316			18.73						
360392		-72.83				43.25			
161422						99.26			

Figure 28. Nacelle support beam assembly.

TABLE 8

SUMMARY - CRITICAL MARGINS OF SAFETY NACELLE SUPPORT BEAM (MS < 0.50)

Item	Description	Load conditions	Margin of safety
X_F 97 - X_F 86	Web shear check	360313 ultimate q_{avg} = 9.5 K/in.	+ 0.38 (web buckling)
X_F 136-149	Web check	360313 ultimate q = 9.5 K/in.	+ 0.47 (ultimate shear)
Lug X_F 115	Lug analysis drag strut attach	360312 ultimate P = 61.6 K	+ 0.48 (shear-out)
X_F 136	Upper cap	360312	- 0.04 (tension)
X_F 136	Lower cap	360312	+ 0.57 (compression)

made using the drag strut load acting in the tension direction. No significant negative margins were identified for this preliminary study. A more detailed check would be in order in the event this component design is selected for further development.

COST ANALYSIS

BASELINE COSTS - TITANIUM CANDIDATE ITEMS

Ground Rules

In order to determine accurate comparative cost values, a cost baseline was established for the three titanium candidate items selected from the B-1 structure. Certain ground rules were laid down for establishing the values to be used. These are:

1. Actual costs shall be used where available.

2. Part costs for B-1 DVT-2 test item were applicable.

3. Both first- and 300-unit cumulative average costs are to be established.

4. First-unit costs, both actual and estimated, shall be adjusted to current 1975 values.

5. 300-unit cumulative average projected costs shall be adjusted to 1981 values (midpoint of planned B-1 production).

6. Costs are to include only primary direct acquisition costs items, i.e., material, fabrication, and tooling.

7. Standard B-1 production factors and learning curves shall be used.

8. Major cost drivers are to be identified on 300-unit cumulative average costs.

First-Unit Costs

Actual costs were obtained on the wing pivot inboard shear fitting for material and fabrication, however, tooling costs were estimated. Die forgings were designed considerably oversize for initial parts to assure sufficient material for possible changes, and thus reflect a higher cost than an optimized design.

58

The wing sweep actuator inboard attach fitting was machined from a diffusion-bonded assembly. Since the costs of this process at the time incurred are not considered representative of production, the costs were estimated as a machined die forging.

The nacelle support beam assembly actual costs were obtained for all material, hardware, fabrication and assembly, and tooling after the DVT-2 parts were completed. All costs obtained were factored to a common base to reflect current 1975 values.

300-Unit Cumulative Average Costs

The first-unit costs formed the base from which projections to 300 units were made. Standard B-1 cost factors and learning curves were used. Prices were adjusted for inflationary changes to mid-1981, which was the approximate midpoint of the planned B-1 production period.

Disciplines involved in the baseline costs and estimates include B-1 Material Procurement, Manufacturing Operations Proposals and Estimating, and Systems Operations and Cost. Refer to Table 9 for established baseline costs.

ESTIMATED COSTS - AF1410 STEEL DESIGNS

Ground Rules

Ground rules 3 through 8 for baseline costs also apply to estimated costs of the steel substitute designs. In addition, the estimated costs are based on design layout drawings as follows:

1. 3109-100000C, Wing Pivot Inboard Shear Fitting

2. 3109-100001D, Wing Sweep Actuator Attach Fitting (Weldment)

3. 3109-100002D, Nacelle Support Beam Assembly

4. 3109-100003A, Wing Sweep Actuator Attach Fitting (Forging)

(See Figures 4 through 7.)

Methodology

The preceding drawing items 1 and 4 involve ring roll and press forgings, respectively. Present estimates were made by in-house forging specialists. As die forging drawings were completed, actual procurement bids were

TABLE 9

BASELINE COSTS

	First Unit	300 Unit Cumulative Average
Item 1 - Shear Fitting		
Material	$ 9,568	$ 7,784
Fabrication	5,974	743
Tooling	56,270	260
Total	$ 71,812	$ 8,787
Item 2 - Actuator Fitting		
Material	$ 11,713	$ 9,530
Fabrication	17,672	3,468
Tooling	124,018	611
Total	$ 153,403	$ 13,609
Item 3 - Nacelle Beam		
Material	$ 23,480	$ 19,315
Fabrication	37,820	4,629
Tooling	230,423	1,076
Total	$ 291,723	$ 25,020

obtained and used. Items 1, 2, and 3 all involve weldments. Item 1 is unique, in that two roll forged rings are welded together, turn machined, assembled to lugs and brackets by welding, then separated into three segments to form three identical parts. Costs were estimated for manufacturing disciplines involved, on the basis of this fabrication procedure.

Item 2 is a new concept of design from the baseline parts. Costs involve material in rolled plate form coupled with considerable machining and weld preparation, and approximately 180 inches of fillet and butt welding. The welding alone, including setup time for this part, averages $17.82 per running inch of joint. Prorated weld tooling costs increase this to almost $19.00 per inch.

Item 3 is also a new design concept from the baseline. This assembly, like item 2, is a weldment consisting of rolled sheet and plate. Material costs are low on this concept; however, machining and assembly welding costs are high. Material costs were compiled from the drawing list of material sizes. Costs were based on sufficient oversize to allow for finishing to the weld preparation requirements of the assembly.

Item 4 is a redesign of the item 2 concept and is based on a machined die forging. This concept was developed in an attempt to improve the cost saving, which turned out to be less than expected on the welded concept. This forged concept is a complete new design from the baseline titanium forging. New load paths and revised distribution of reaction loads were included in this innovative design. Although material costs are higher than for the weldment design, this is more than overcome by machining costs being substantially lower than the combined machining and welding costs of the welded design.

The Research and Development Operations Analysis group compiled all cost estimates obtained from various sources and applied standard learning curve and procurement factors for final values (Table 10).

Cost Comparison

With baseline costs established and first- and 300-unit costs estimated, a direct comparison of AF1410 steel design costs can be made with the titanium baseline costs and savings as a percent of baseline costs predicted. The following are the results of this comparison:

First-unit costs	Titanium	AF1410	Savings (%)
Shear fitting	$ 71,812	$ 47,007	34.5
Actuator fitting (welded)	153,403	137,506	10.4
Actuator fitting (forged)	153,403	152,989	0.3
Nacelle beam	291,723	263,511	9.7

TABLE 10

ESTIMATED COSTS - AF1410 STEEL DESIGNS

	First Unit	300 Unit Cumulative Average	Percent
Item 1 - 3109-100000 Shear Fitting			
Material	$ 1,244	$ 1,012	30.8
Machining	10,437	1,350	41.1
Welding	4,692	732	22.3
Tooling	30,634	192	5.8
Total	$ 47,007	$ 3,286	100
Item 2 - 3109-100001 Actuator Fitting (Welded)			
Material	$ 4,769	$ 3,880	31.6
Machining - preweld	19,564	3,741	30.4
- postweld	4,731	918	7.5
Welding	19,853	3,207	26.1
Tooling	88,589	546	4.4
Total	$ 137,506	$ 12,292	100
Item 3 - 3109-100002 Nacelle Support Beam			
Material	$ 4,222	$ 3,435	19.3
Machining - preweld	50,770	6,499	36.5
- postweld	10,543	1,387	7.8
Welding	25,506	4,165	23.4
Assy fab	12,433	1,298	7.3
Tooling	160,037	1,005	5.7
Total	$ 263,511	$ 17,789	100
Item 4 - 3109-100003 Actuator Fitting (Forged)			
Material	$ 6,359	$ 5,174	50.4
Machining	22,612	4,488	43.7
Tooling	124,018	612	5.9
Total	$ 152,989	$ 10,274	100

300-unit cumulative average	Titanium	AF1410	Savings (%)
Shear fitting	$ 8,787	$ 3,286	62.6
Actuator fitting (welded)	13,609	12,292	9.7
Actuator fitting (forged)	13,609	10,274	24.5
Nacelle beam	25,020	17,789	28.9

The saving of 62.6 percent shown for the production shear fitting is high due to the baseline cost being projected from an actual first-unit cost which resulted from an extremely oversize forging resulting from procurement prior to final design. This figure will reduce significantly when a production redesign is introduced.

Major Cost Elements

As shown in Table 10, the major cost elements in acquisition cost for production are those associated with fabrication. High first-unit costs in each case are in tooling, since no prorating is considered. However, fabrication costs are next highest. These costs under the production case run only 13 to 20 percent of first-unit costs. Overall production costs vary from 1.1 to 7 percent of first-unit costs. This reduction is due largely to prorated tooling costs.

An important discovery was made in the case of the 3109-100001 actuator fitting (welded concept) versus the 3109-100003 actuator fitting (forged concept). Where a substantial amount of machining is involved in conjunction with welding, the fabrication costs run considerably higher than on the completely machined forging concept.

EFFECTS OF WEIGHT SAVING ON COST

Weight saving, where possible, is an important factor in cost saving. This results not so much in acquisition costs, but substantially in life cycle costs. In the case of the B-1, the value of a pound of weight saved results in a saving of $110 (1976 $) in these life cycle costs. This results from savings in: (1) B-1 fuel consumed during training missions, and (2) the tanker support required. On the actuator fitting, a total weight saving on left and right sides amounts to 66.8 pounds. A B-1 order of 240 aircraft over 10 years of service would save over $1.76 million.

MANUFACTURING PLAN AND DEVELOPMENT TEST PLAN

MANUFACTURING PLAN

A complete manufacturing plan for the production of two test components was prepared and submitted to the customer as report NA-76-846. This plan included the tooling concepts, manufacturing methods, and control provisions to be used in the fabrication of either the wing pivot shear fitting or the wing sweep actuator attach fitting. Both were included since selection of one for fabrication and test was made subsequent to drafting of the manufacturing plan.

Verification of estimated fabrication costs was made by recording machining rates, tool wear, and other direct costs during the production of the selected part.

DEVELOPMENT TEST PLAN

A detailed development test plan was also prepared and submitted to the customer for approval. This plan outlined the objectives and purpose for conducting a comprehensive test program on AF1410 mechanical properties and fatigue characteristics. It included detail information on numbers and conditions of tests to be run for both weld and parent metal mechanical properties and the effects of manufacturing processes such as grinding, shot peening, and plating. It also included fatigue, fracture toughness, and fracture mechanics crack growth tests.

A machinability/heat-treat program plan to develop a premachining heat treatment to permit good low-cost rough machining was included as part of the development test plan. In addition to treatments to improve the machinability, the plan included evaluation and selection of heat treatment procedures to attain the best combination of material properties.

Section III

PHASE II DETAIL DESIGN AND DEVELOPMENT TEST

Phase II consisted of a 9-month period during which the development test program and detail design and drawing release of the two selected candidate items was accomplished.

This phase of the program was fully reported in Reference 2 and will only be summarized herein. Should additional detail be desired it can be obtained from Reference 2

The development test portion of this phase was started with the receival and preparation of the first shipment of rolled plate AF1410 steel. It was layed out, sectioned into specimen size blocks, and heat treated.

Parent metal material property tests for tension, compression, shear, and bearing values were done. The effects of grinding, shot peening, plating, and welding were determined on tensile values. A series of fatigue and crack growth tests was also conducted on the basic material as well as for manufacturing process effects. A number of dog-bone-type specimens were tested for fracture mechanics analysis verification.

Butt fusion weld data were obtained through K_{1c} Charpy V-notch and fatigue tests. Special specimens were designed for fillet-weld tension across the welds and for fatigue.

Tests were also conducted to develop an optimum final product heat-treatment which is compatible with a premachining heat treatment selected during phase I, and will develop the required mechanical properties of the material. Machining tests were conducted on AF1410 material specimens subjected to this heat treatment during phase III of the program.

Detail design drawings were developed of the two candidate items for component test. All preliminary analyses of stress, fatigue, damage tolerance, weight, and cost were refined and updated to reflect the final designs. Drawings were released to manufacturing for use in preliminary planning and tool design. The wing sweep actuator inboard attach fitting was selected for fabrication and test.

Tools to be used in machining and heat treatment of the selected part were designed. These included holding fixtures, tracer pattern, heat-treat fixture, and match drill jig for attach holes. A complete manufacturing plan was developed for producing either candidate test part. (Refer to report NA-76-846.)

OBJECTIVES

The planned objectives of this portion of the program were:

1. Prepare specimens and conduct a thorough development test program on representative production heats of AF1410 steel. Tests included mechanical properties of parent metal and of butt and fillet welds. They also included manufacturing process effects, stress corrosion, and fatigue.

2. Conduct fracture mechanics analysis verification tests to substantiate analytical methods of predicting lifetimes using established growth rates and prescribed flaws.

3. Conduct heat-treat tests to select a heat-treatment which is compatible with premachining heat treatments selected for easier machining and which will result in the required mechanical properties of the material.

4. Refine the preliminary designs of both candidate parts and update the analyses on each for strength, fatigue, damage tolerance, weight, and cost.

5. Prepare and release to manufacturing detail drawings of each candidate part.

6. Select one of the two candidate parts for fabrication and component test for static and fatigue strength.

7. Design all tools required for machining the selected part from a furnished die forging.

8. Prepare a complete detail design report and submit to the customer, and prepare and present an oral briefing at Wright-Patterson Air Force Base, Ohio, in April 1977.

A task/event flow diagram is shown in Figure 29 which shows the sequence of significant events and their interrelationship.
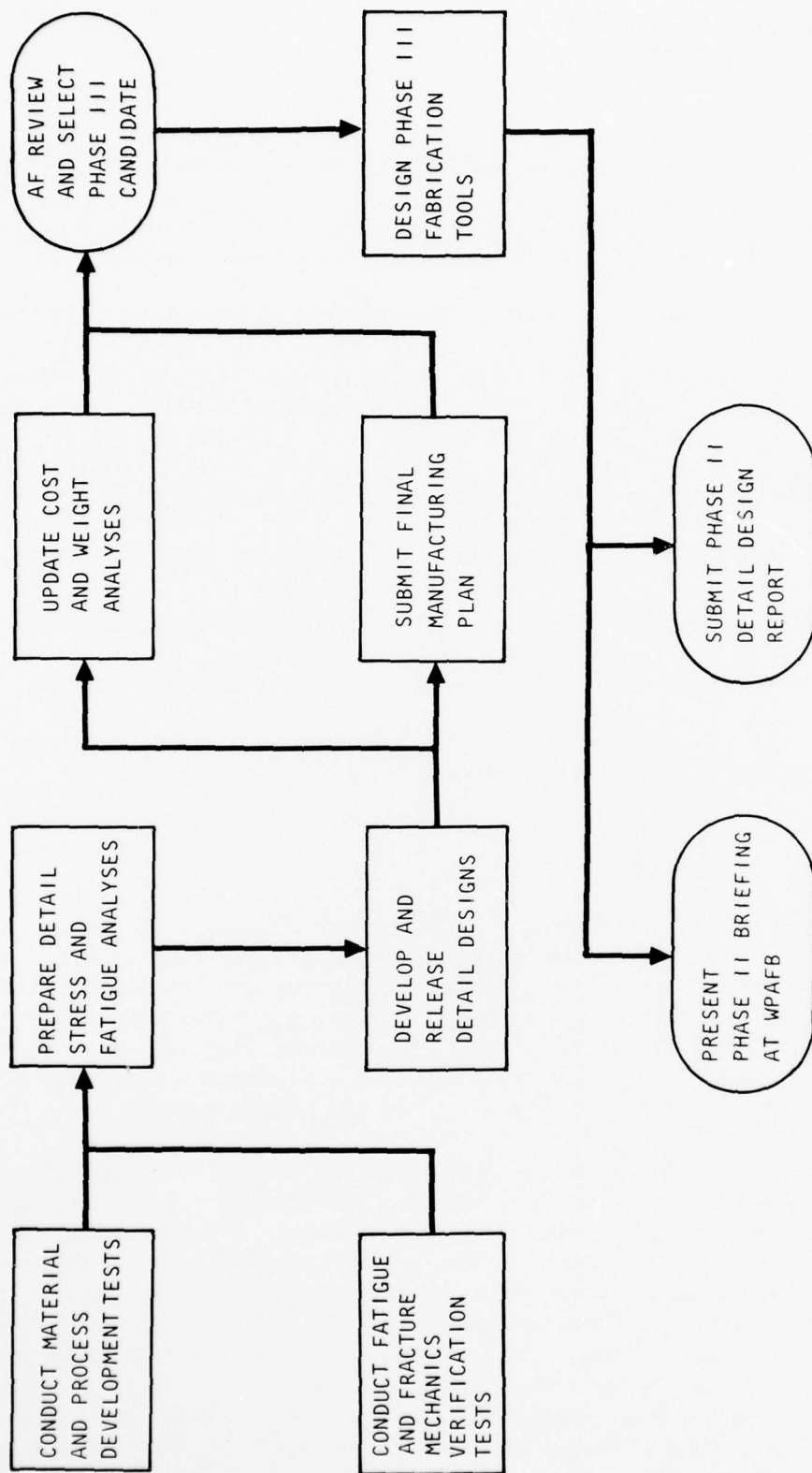
Figure 29. Task/event flow diagram phase II - detail design and development test.

DETAIL DESIGN OF CANDIDATES

INTRODUCTION

The two candidate preliminary layout designs selected for phase II detail design were:

- 3109-100000, fitting - shear, wing pivot inboard (layout)

- 3109-100003, fitting - attach, inboard wing sweep actuator (layout)

These layouts were used as a basis for design refinement and preparation of working drawings during phase II. The detail drawings developed from these layouts are:

- 3109-100010 fitting - shear, inboard pivot pin, wing (forging)

- 3109-100006 fitting - inboard attach, wing sweep actuator, assembly of

- 3109-100008 bushing, outer - attach fitting, wing sweep actuator

- 3109-100009 bushing, inner - attach fitting, wing sweep actuator

These detail drawings were released to manufacturing for tool design and fabrication of one of the fittings during phase III.

DETAIL DESIGN

During the last part of phase I, preliminary design, a change was made in the concept of the wing sweep actuator attach fitting from a welded truss assembly to a machined die forging design. This was done to improve the low cost-saving, which resulted in comparing the cost of the welded assembly with the baseline cost, which was based on a titanium die forging. A considerable improvement was made. This change resulted in a production cost saving of 24.5 percent, as compared to 9.7 percent for the welded assembly.

A change was also made in the design concept of the wing pivot shear fitting from a welded assembly to a machined die forging. This resulted from a new production cost comparison using recent quotes on the baseline titanium part rather than the actual costs of the B-1 DVT part. The high cost of an oversize forging on the DVT part produced a distorted baseline value. Quotes were obtained from the same vendor on a steel die forging similar to the B-1 part. A new comparison showed a marked reduction in cost saving from 62.6 percent to around 30 percent. However, a comparison with the steel-welded design showed a much greater reduction. A new drawing was prepared of the steel die forging design and is used as the basis for a final cost saving on this candidate part.

68

On 1 February 1977, selection of the actuator attach fitting was made for fabrication and test. Final detail design incorporated all requirements for tooling, fracture mechanics, and fabrication.

COST ANALYSIS

Wing Pivot Shear Fitting

The preliminary cost analysis on the wing pivot shear fitting was based on a design involving two ring forgings welded together, end-to-end, to make one ring assembly from which three parts could be made by cutting it into three 120-degree segments after lathe turning and weld attaching several lugs for strut attachment and equipment mounting. The cost of this design was compared to a baseline titanium part cost resulting from actual part cost of the B-1 DVT part. This comparison yielded a predicted cost saving of 62.6 percent.

This value has been considered invalid due to the extremely oversized forging purchased for initial B-1 parts. During the detail design phase of the steel substitute part, a new cost estimate was made for a production baseline part based on actual quotes on an optimized titanium forging. This new cost, when compared to the steel substitute design cost, resulted in a reduction of cost saving far below the 30-percent level.

A quote was obtained on a substitute steel die forging from the same forging vendor supplying the titanium quote. A new cost estimate based on this design and compared to the new titanium part cost resulted in a predicted cost saving in the 30- to 40-percent range.

A new detail design of the wing pivot shear fitting was completed based on a completely machined die forging. A cost analysis based on actual detail drawings showed a potential cost saving of 42.1 percent. A sequence of cost analyses leading up to this final figure is shown in Table 11 starting with the initial analysis and baseline developed in phase 1. Changes affecting each subsequent analysis are:

- Analysis 2 - Revised baseline costs for a production size forging weighing 114 pounds.

- Analysis 3 - Changed substitute design to die forging.

- Analysis 4 - Revised steel rough machining cost to the same as titanium based on new premachining heat-treat data. Also increased steel forging weight.

TABLE 11

COST ANALYSIS AND COMPARATIVE SAVINGS WING PIVOT INBOARD SHEAR FITTING;

1975 DOLLARS

	Baseline		Substitute	
	Ti die forging (DVT)		AF1410 steel ring forging	
	500/48.6		Weldment 135.5/48.0	
	First unit	300 U cum ave	First unit	300 U cum ave
Weight - B/F lb				
Analysis No. 1 (From Phase 1)				
Material	$ 9,568	$7,784	$ 1,244	$1,012
Fabrication	5,974	743	15,129	2,082
Tooling	56,270	260	30,634	192
Total	$71,812	$8,787	$47,007	$5,286
Savings			54.5%	62.6%
	Ti die forging (prod)		AF1410 steel ring forging	
	114/48.6		Weldment 135.5/48.0	
Weight - B/F lb				
Analysis No. 2 (11-26-76)				
Material		$2,387		$1,012
Fabrication		536		2,082
Tooling		211		192
Total		$3,134		$3,286
Savings				4.62%

TABLE 11

COST ANALYSIS AND COMPARATIVE SAVINGS WING PIVOT INBOARD SHEAR FITTING· (CONT)

1975 DOLLARS

	Baseline		Substitute	
	Ti die forging (prod)		AF1410 steel die forging	
	114/48.6		104.65/48.0	
	First unit	300 U cum ave	First unit	300 U cum ave
Weight - B/F lb				
Analysis No. 3 (12-16-76)				
Material		$1,641		$ 803
Fabrication		502		686
Tooling		284		224
Total		$2,427		$1,715
Savings				29.41%
Weight - B/F lb	114/48.6		(Rough machining cost equivalent to Ti) 120/48.0	
Analysis No. 4 (1-7-77)				
Material		$1,775		$ 875
Fabrication		532		646
Tooling		211		151
Total		$2,518		$1,672
Savings				33.59%

71

TABLE 11

COST ANALYSIS AND COMPARATIVE SAVINGS WING PIVOT INBOARD SHEAR FITTING (CONCL)

1975 DOLLARS

	Baseline		Substitute	
	Ti die forging (prod)		AF1410 steel die forging	
	114/48.6		120/48.0	
	First unit	300 U cum ave	First unit	300 U cum ave
Weight - B/F lbs				
Analysis No. 5 (1-7-77)				
Material		$2,328		$1,722
Fabrication		685		832
Tooling		250		178
Total		$3,263		$2,732
Savings				16.27%
Analysis No. 6 (2-16-77) (Rev 3-31-77)			Forging raw material at $3.25/lb	
Material	$ 3,054	$2,485	$ 1,815	$1,476
Fabrication	5,447	1,025	6,656	1,244
Tooling	44,679	257	32,970	184
Total	$53,180	$3,767	$41,421	$2,904
Savings			22.1%	22.9%

72

- Analysis 5 - Revised forging costs on both baseline and substitute in accordance with vendors quotes and updated costs to 1977 dollars.

- Analysis 6 - Reduced baseline for final vendor quotes. Reduced substitute forging quotes based on cost of raw material per AFFDL/FBS data obtained from Universal-Cyclops Steel Co.

First unit costs were developed for only the final analysis (6) since all intermediate analyses were exercises in developing the final cost.

Wing Sweep Actuator Fitting

The baseline cost of the wing sweep actuator fitting was established in phase I, and is shown in Table 12. The preliminary design cost comparison, based on machined die forgings on both the baseline part and the substitute part, showed a saving of 24.5 percent. This was based on an estimated buy/fly weight ratio of 4:1 and an estimated forging cost of $8.00 per pound.

A forging drawing was prepared in phase II and a calculated weight obtained. In addition, the cost of rough machining was reduced from 24 percent higher than titanium to equal to titanium. A revised analysis and cost comparison, analysis 2, as shown in Table 12, was made based on these changes and an actual vendor quote on the die forging. This comparison showed a savings of 28.34 percent for production. First unit costs were not obtained for this intermediate analysis.

An estimated cost of $3.25 per pound for forging ingot material was obtained from Universal-Cyclops through AFFDL/FBS. This value was provided to the forging vendor who then revised the forging quote accordingly. The final cost figures are shown as analysis 3 in Table 12 and result in a cost saving of 22.1 percent. A comparison of first unit cost shows 1.4 percent saving of the baseline first unit cost.

Weight Analysis

A final weight calculation was made on the released detail designs of the two candidate parts. Baseline weights, as reported in NA-76-860, "Preliminary Design Report," page 19, are shown for comparison along with the new substitute design weights in Table 13. Weight breakdowns on each of the substitute detail designs are shown in Table 14.

Although weight saving was not a primary goal in this program, significant savings can be made by efficient design and through weight reduction of installation parts such as bolts, pins, and bushings due to shorter lengths required for thinner higher strength material. Reduced fixed weight in an aircraft results in considerable savings in operational costs.

73

TABLE 12

COST ANALYSIS AND COMPARATIVE SAVINGS WING SWEEP ACTUATOR ATTACH FITTING

1975 DOLLARS

	Baseline		Substitute	
	Ti die forging		AF1410 steel die forging	
	537/172.2		591/147.85	
Weight - B/F lb	First unit	300 U cum ave	First unit	300 U cum ave
Analysis No. 1 (From Phase 1)				
Material	$ 11,713	$ 9,530	$ 6,359	$ 5,174
Fabrication	17,672	3,468	22,612	4,488
Tooling	124,018	611	124,018	612
Total	$155,403	$13,609	$152,989	$10,274
Savings			0.3%	24.5%
Analysis No. 2				
Material		$ 9,530		$ 5,174
Fabrication		3,468		3,966
Tooling		611		612
Total		$15,609		$ 9,752
Savings				28.34%

74
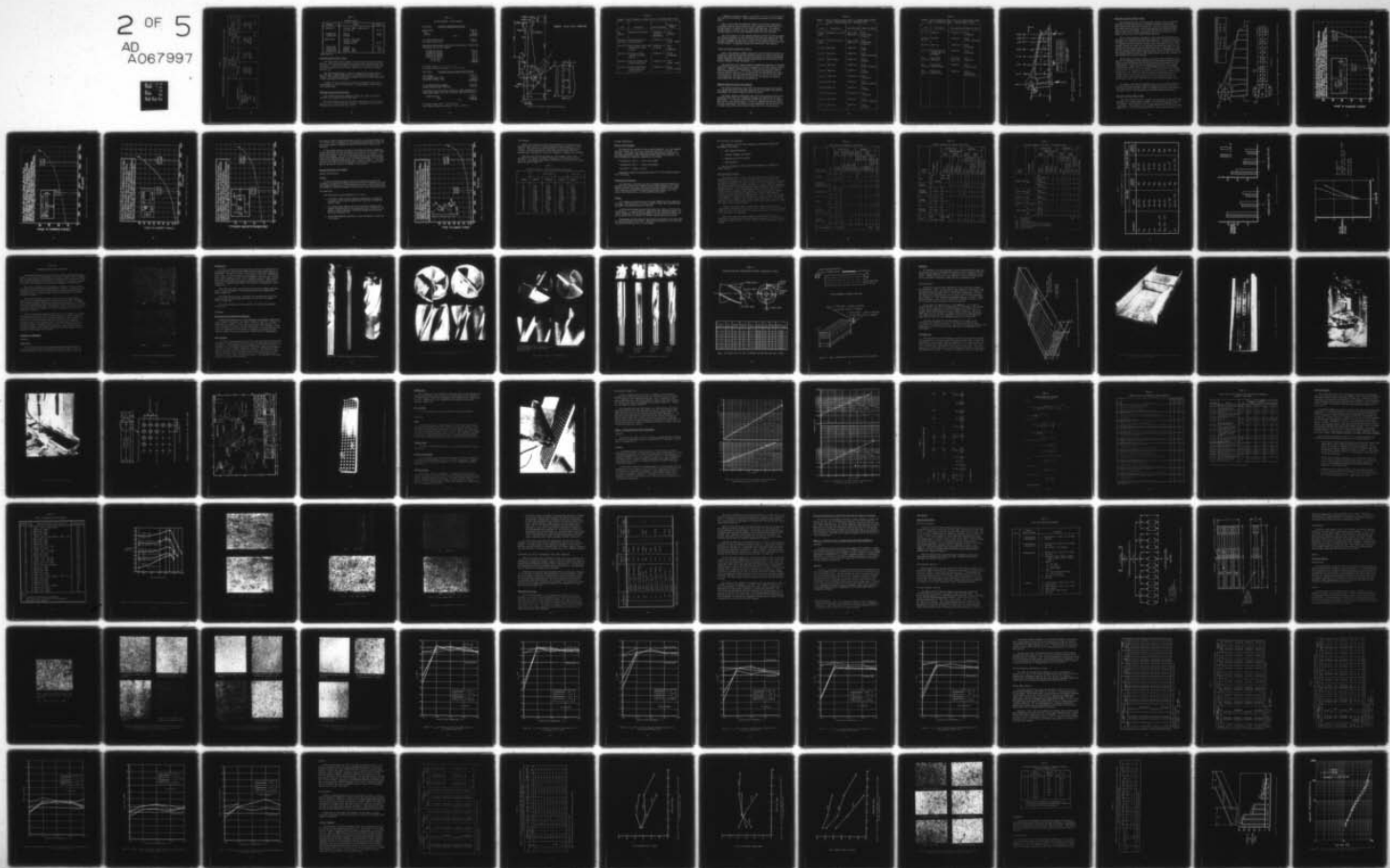
TABLE 12

COST ANALYSIS AND COMPARATIVE SAVINGS WING SWEEP ACTUATOR ATTACH FITTING (CONCL)
1975 DOLLARS

	Baseline		Substitute	
	Ti die forging		AF1410 steel die forging	
Weight-B/F lb	537/172.2		591/147.85	
	First unit	300 U cum ave	First Unit	300 U cum ave
Analysis No. 3 Rev 3-31-77				
Material	$ 14,385	$11,703	$ 8,952	$ 7,284
Fabrication	23,319	4,577	26,367	5,234
Tooling	138,779	712	138,779	712
Total	$176,483	$16,992	$174,098	$13,230
Savings			1.47%	22.1%

75

TABLE 13

BASELINE WEIGHTS

Drawing	Title	Weight
L1100030-011	Fitting - shear, inboard pivot pin, assy of	48.70
L1100030-005	Fitting	48.64
L1100063-003	Bushing	0.06
L3007214-001	Fitting - wing sweep Actuator, inboard Attach, assy of	176.30
L3007214-005	Fitting	172.20
L1200234-005	Bushing - outer	1.96
L1200235-003	Bushing - inner	2.14

STRESS ANALYSIS

Wing Pivot Inboard Shear Fitting

The inboard shear fitting (Figure 30) was analyzed using the structural analysis curves and material properties provided under "Structural Analysis Properties." (Table 4 and Figures 16 through 24). The applied design loads are those obtained from the B-1 Stress analysis and used for the titanium baseline part.

The shear fitting design is based on a machined die forging concept so that the design strength reductions for as-welded structure need not be imposed. The previous design had the diagonal shear strut attach lugs welded to the curved walls of the fitting.

A summary of critical margins of safety is presented in Table 15, in which margins less than +0.50 are listed. Typical analyses are provided in the following pages.

Wing Sweep Inboard Actuator Fitting

The stiffened web design (machined forging) was chosen as the final candidate for validation of the AF1410 steel.

The applied design loads were the same as those used in the B-1 Stress analysis for the titanium baseline component. Conventional stress analysis techniques were used per References 3 and 4.

TABLE 14

WEIGHT BREAKDOWN - AF1410 DESIGNS

3109-100010   Wing Pivot Inboard Shear Fitting

Machined body		43.08 lb
lugs		2.61 lb
brackets		.36 lb
	Total	46.05 lb

B-1 titanium baseline part	48.64 lb
Substitute weight saving	2.59 lb

Installation and assembly parts weight reduction due to reduced lug thicknesses and bolt grip lengths.

L1100048-003 bushing	0.003 lb
L1100063-003 bushing	.004 lb
L1100073-017 bushing	.475 lb
L1100073-009 bushing	.137 lb
5/8 dia bolts	.129 lb
7/8 dia bolts	.362 lb
	1.110 lb

Net weight savings = 1.11 + 2.59 = 3.70 lb
Net weight savings per airplane 2 x 3.70 = 7.40 lb

3109-100006   Wing Sweep Actuator Inboard Attach Fitting

-003 fitting	153.47 lb
3109-100008 bushing, outer	1.83 lb
3109-100009 bushing, inner	2.40 lb
	157.70 lb

B-1 titanium baseline assembly	176.30 lb
Fitting assembly weight difference	18.60 lb

Installation bolts and actuator attach pin weight reduction due to reduced grip lengths, bolt sizes (6 places) and lug thicknesses

L1200241-007 pin		-3.10 lb
bolts		-4.84 lb
	Total	-7.94 lb

Net weight savings 18.60 + 7.94 = 26.54 lb
Total weight savings per airplane 2 x 26.54 = 53.08 lb

77
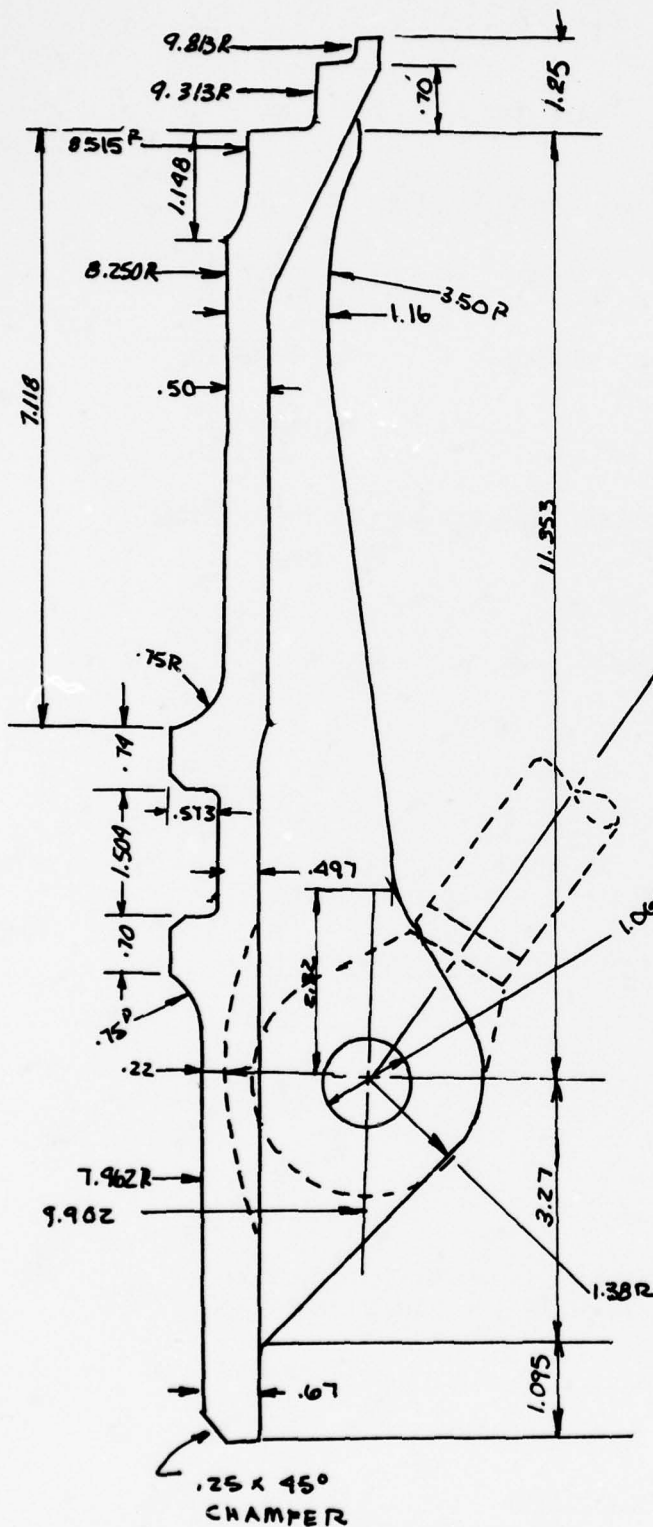
MATERIAL: AF1410 STEEL (LB0160-184)
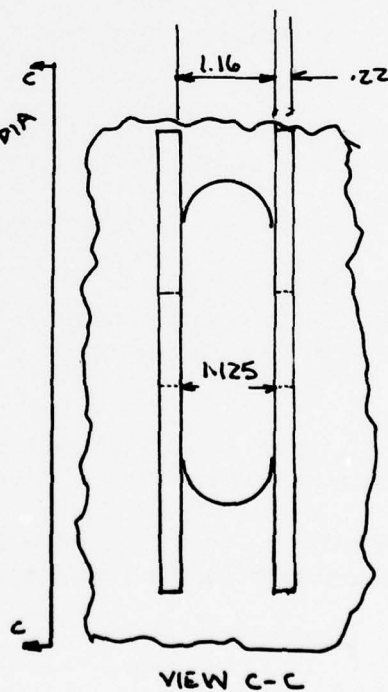
Figure 30. Wing pivot inboard shear fitting.

VIEW C-C

TABLE 15

SUMMARY - CRITICAL MARGINS OF SAFETY (MS $<$ +0.50) INBOARD SHEAR FITTING

Item	Description	Load conditions	Margins of safety
Lug analysis	Maximum bearing check	Condition 1-B low-level penetration	+0.31 (bearing)
Section D-D with lugs	Section checked as a curved section	Condition 2-B	+0.03 (axial + bend)
Section B-B	Section above shear strut attach point curved section	Condition 2-A P_L acting	+0.19 (lug crippling)
Section F-F	Section 2.9 below section B-B curved section	Condition 2-A	+0.014 (crippling)
Section K-K	Section through shear strut attach point	Condition 2-A	+0.27 (axial + bend)
Section C-C	Section below shear strut attach point curved section	Condition 2-A	+0.24 (axial + bend)

A summary of margins of safety is presented in Table 16 in which margins less than +0.50 are listed. Typical analyses are provided in the following pages.

The critical loads and conditions (Figure 31) have been identified as an actuator tension load (condition 1) and a compressive load (condition 2) of approximately 70 percent of the tension load magnitude. The support fitting serves to transfer the outer wing sweep loads into the wing carry-through structure via the YF932 bulkhead and ribs at XF121 and XF84.

The stress analysis of the machined forging-stiffened web design checked the fitting attachments to the substructure for shear and tension, the webs for shear buckling, and the caps for axial tension and/or compression. The actuator attachment lug region was checked for the maximum actuator load case of 922K tension. No negative margins were identified in the analysis.

FATIGUE AND FRACTURE MECHANICS ANALYSIS

Each of the candidate LOCOSST fittings for the final analysis phase was subjected to fatigue and fracture mechanics analyses to assure that the predicted life under the design spectrum loading would meet design requirements of MIL-A-8866A and the damage tolerance requirements of MIL-A-83444 per the program Statement of Work, Paragraph 4.2.1.

The analytical crack growth prediction methodology employed to calculate subcritical flaw growth is based on the principles of linear elastic fracture mechanics. Rockwell computer program, EFFGRO, was used for performing the crack growth predictions. EFFGRO uses a specialized integration routine where an initial crack size, a_i, is chosen and the crack growth rate, da/dN, is integrated to yield the relationship between "a" and "N" for the given stress spectrum. The influence of stresses in the compression region on crack growth rate are taken into consideration.

Material Properties Used in the Analysis

The fatigue stress/cycle life (S/N) data and the fatigue crack growth rate (da/dN) data used in the final analysis were generated by the material development test program conducted during this phase.

The Walker equation coefficients used in the crack growth analyses were determined from a best fit straightline through the da/dN versus ∆K crack growth data. A 3.5-percent salt water solution was selected as the environment for the crack growth analyses. This is a somewhat conservative choice of design environment, but seems to be more appropriate for the service life of these fittings than either ambient laboratory air or sump tank water.

TABLE 16

SUMMARY - CRITICAL MARGINS OF SAFETY (MS < 0.50) INBOARD SWEEP ACTUATOR
FITTING - STIFFENED WEB DESIGN - MACHINED FORGING

Item	Description	Load conditions	Margin of safety
Fastener check	Fasteners at X_F 84.05	P_{ACT} = 922K Condition 1-B	+0.46 (attach shear & tension)
Fastener check	Fasteners at X_F 121	P_{ACT} = -672K Condition 2-A	+0.08 (attach shear & tension)
X_F 84.05	Web check	Condition 1	+0.10 (shear)
X_F 87.3	Web check	Condition 1	+0.05 (shear & buckling)
X_F 90.1	Upper flange	Condition 1	+0.18 (tension)
X_F 95.63	Web check	Condition 1	+0.05 (shear & buckling)
X_F 95.63	Upper cap	Condition 1	+0.20 (tension)
X_F 95.63	Lower cap	Condition 1-B	+0.30 (crippling)
X_F 101.15	Web check	Condition 1	+0.07 (shear & buckling)
X_F 101.15	Upper cap	Condition 1	+0.21 (tension)
X_F 101.15	Lower cap	Condition 1-B	+0.17 (crippling)
X_F 107.4	Web check	Condition 1	+0.08 (shear & buckling)
X_F 107.4	Upper cap	Condition 1	+0.24 (tension)

TABLE 16

SUMMARY - CRITICAL MARGINS OF SAFETY (MS < 0.50) INBOARD SWEEP ACTUATOR
FITTING - STIFFENED WEB DESIGN - MACHINED FORGING (CONCL)

Item	Description	Load conditions	Margin of safety
X_F 107.4	Lower cap	Condition 1-A	+0.01 (crippling)
Section X_F 115.0	Web check	Condition 1	+0.03 (shear & buckling)
X_F 115.0	Lower cap	Condition 1-A	+0.10 (crippling)
Y_F 923.35	Section check of forging under pin attachment	Condition 1	+0.42 (crippling)
Lug X_F 122.75	Lug analysis (shear-out)	Condition 1 P_{ACT} = 922K	+0.16 (shear-out)
Lug X_F 122.75	Lug analysis (shear bearing)	Condition 1	+0.40 (shear bearing)
Lug X_F 122.75	Transverse shear-bearing	Condition 1	+0.45 (transverse, shear bearing)

Figure 31. Loads and dimensional thickness summary wing sweep actuator fitting.
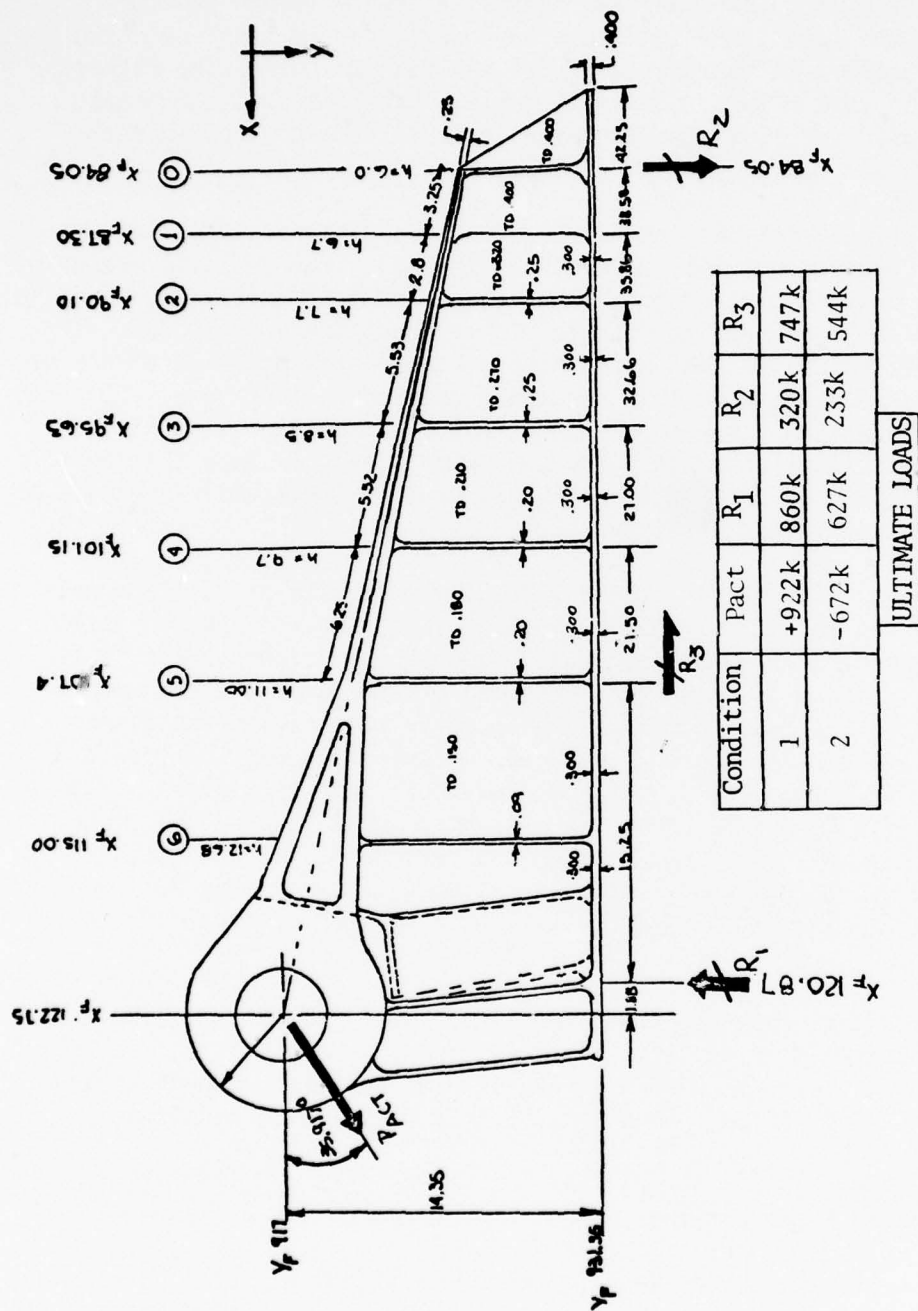
Material: AF1410 Steel (LBO 160-184)
Ref: Dwg 3109-100006)

83

Wing Sweep Actuator Attach Fitting

Four specific sections of the wing sweep actuator attach fitting were analyzed for durability (fatigue) and damage tolerance (crack growth). These sections are identified in Figure 32. The cross sections selected were those identified in the static stress analysis as having the highest stress levels in that member. Stress transfer functions from the static analysis were used to relate the actuator loads to the stresses in each member for each step of the design fatigue spectrum.

For the fatigue analyses, geometric stress concentration factors were determined by conventional fatigue analysis methods. For specific points of reference, the actuator attach lug, point three, has a geometric K_t equal to 2.7 together with an average net section limit load stress of 70 ksi. The diagonal flange, point two, has a relatively high operating limit stress of 130 ksi, but the K_t factor on this unnotched section is less than 1.5. The boltholes in the attach flange, point one, have a K_t of approximately four, but the operating limit load net section tension stress is less than 80 ksi. The fatigue analyses of each of these points predict lives well in excess of the required four aircraft lifetimes.

For the damage tolerance analyses, crack growth rate predictions were made for the operating stress spectra and with the required assumed initial flaw size per specification MIL-A-83444 to qualify the structure as "slow crack growth." Figure 33 shows the predicted growth rate of an assumed 0.005R initial corner flaw in a 3/4-inch-diameter bolthole in the flange which attaches to the station 932 bulkhead. Figure 34 shows the predicted growth rate of an assumed 0.125R initial corner flaw in the diagonal flange at station X_f 90. Figure 35 shows the predicted crack growth rate of an assumed 0.05R initial corner flaw in the net section of the lug hole. Figure 36 shows the predicted growth rate of an assumed initial 0.125R part-through crack in the 0.300-inch-thick wall of the lug support frame.

All figures show that the predicted crack lives to critical length are in excess of the two aircraft lifetimes required to qualify structure as "slow crack growth" per MIL-A-83444. All fatigue and crack growth analyses were done to the B-1 395,000-pound gross weight operational spectrum.

Wing Pivot Inboard Shear Fitting

The only critical section in fatigue or crack growth on the pivot shear fitting is the actuator attach lug hole. This lug has an outside radius of 1.38 inches, a local thickness of 0.32 inch, and a pin diameter hole of 1.062 inches. The geometric stress concentration factor, K_t, based on these dimensions, is 3.25 at the edge of the hole. Using a quality factor of 1.2,

84

LOAD DIRECTION	LIMIT LOAD	MAXIMUM SPECTRUM LOAD
P_1	615,000 LB	305,000 LB
P_2	448,000 LB	280,000 LB

SECTION A-A
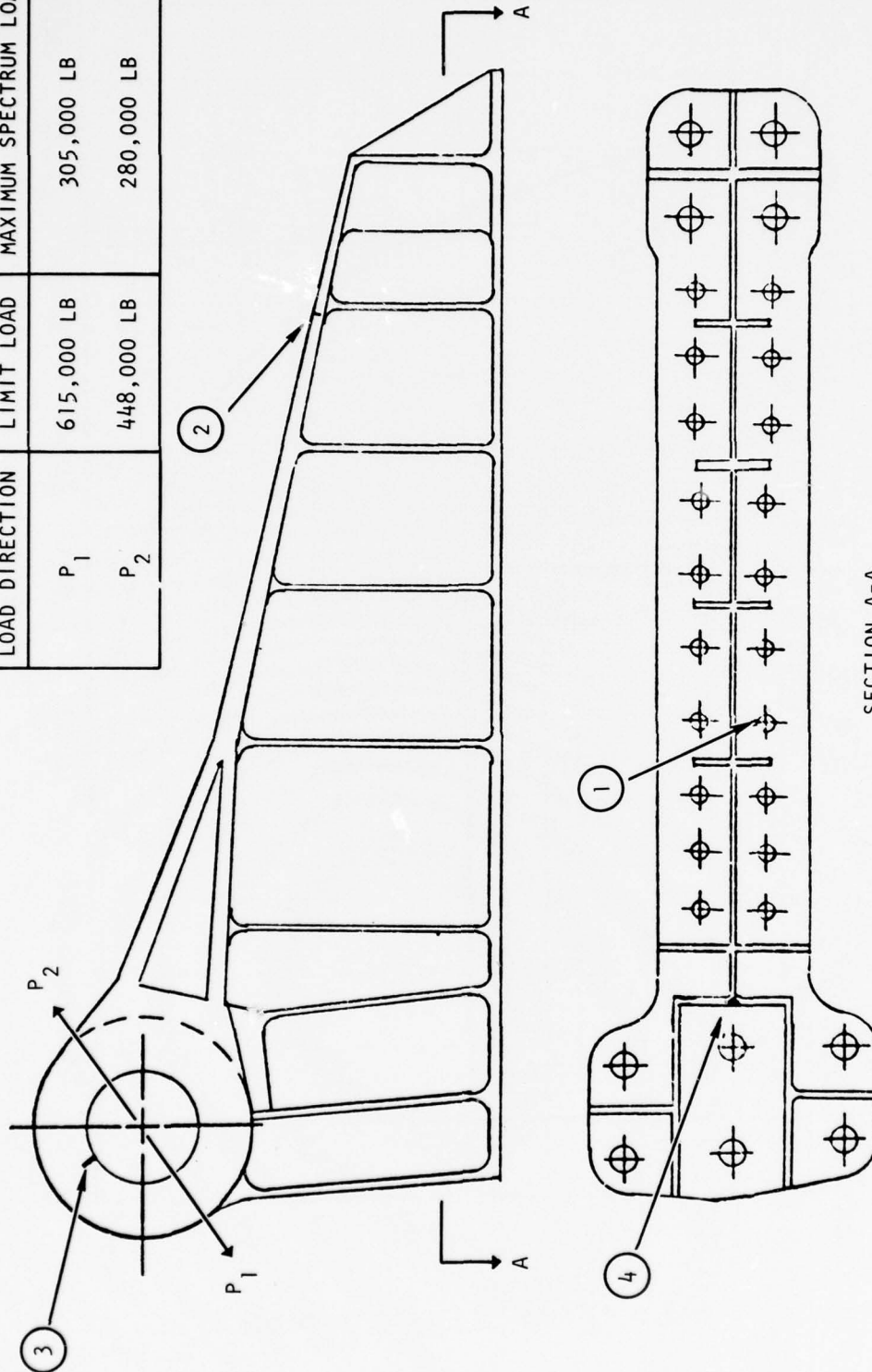
Figure 32. Areas of fatigue and damage tolerance analysis - wing sweep actuator attach fitting.

85
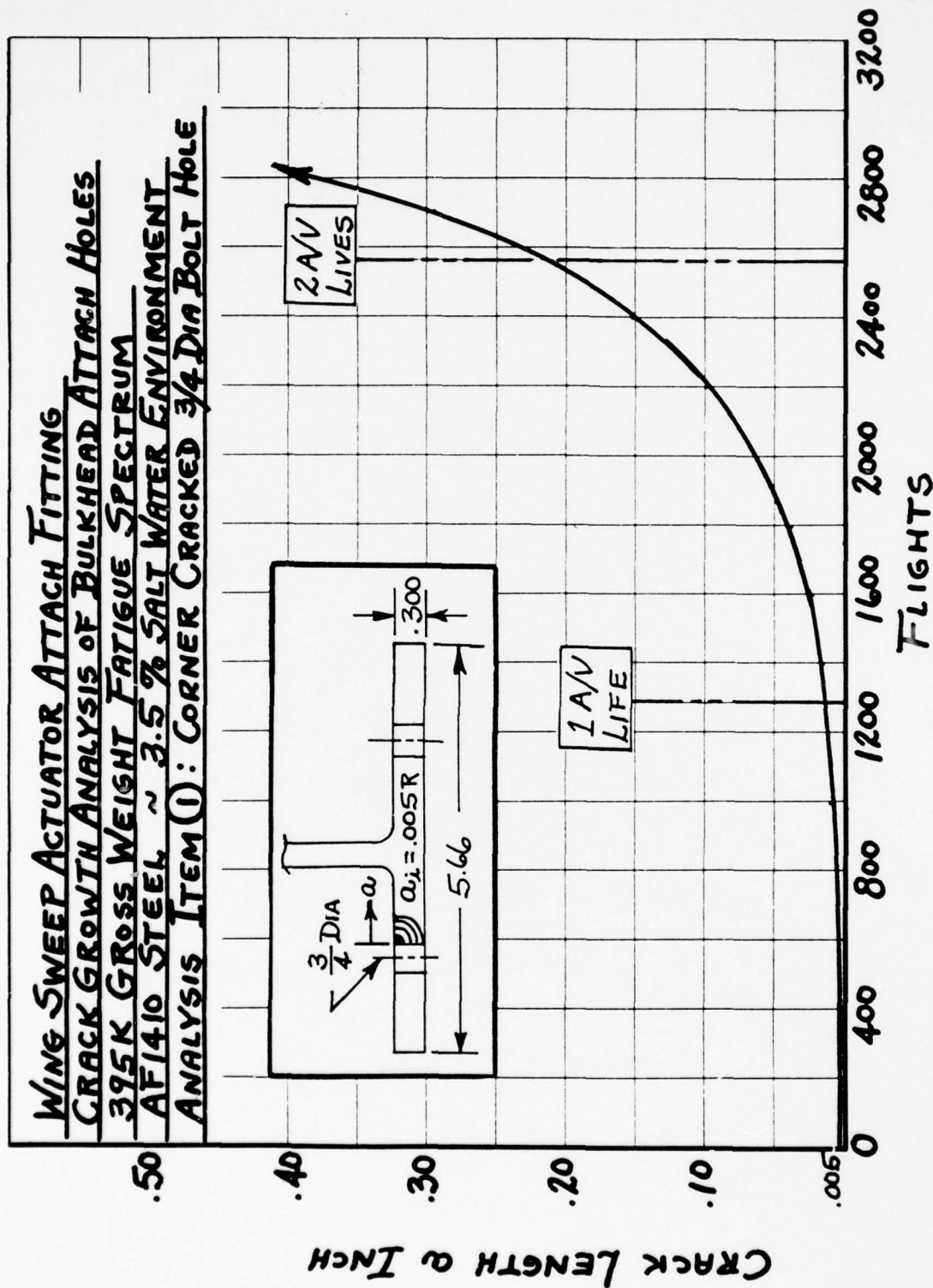
Figure 33. Wing sweep actuator fitting - item 1 crack growth analysis.
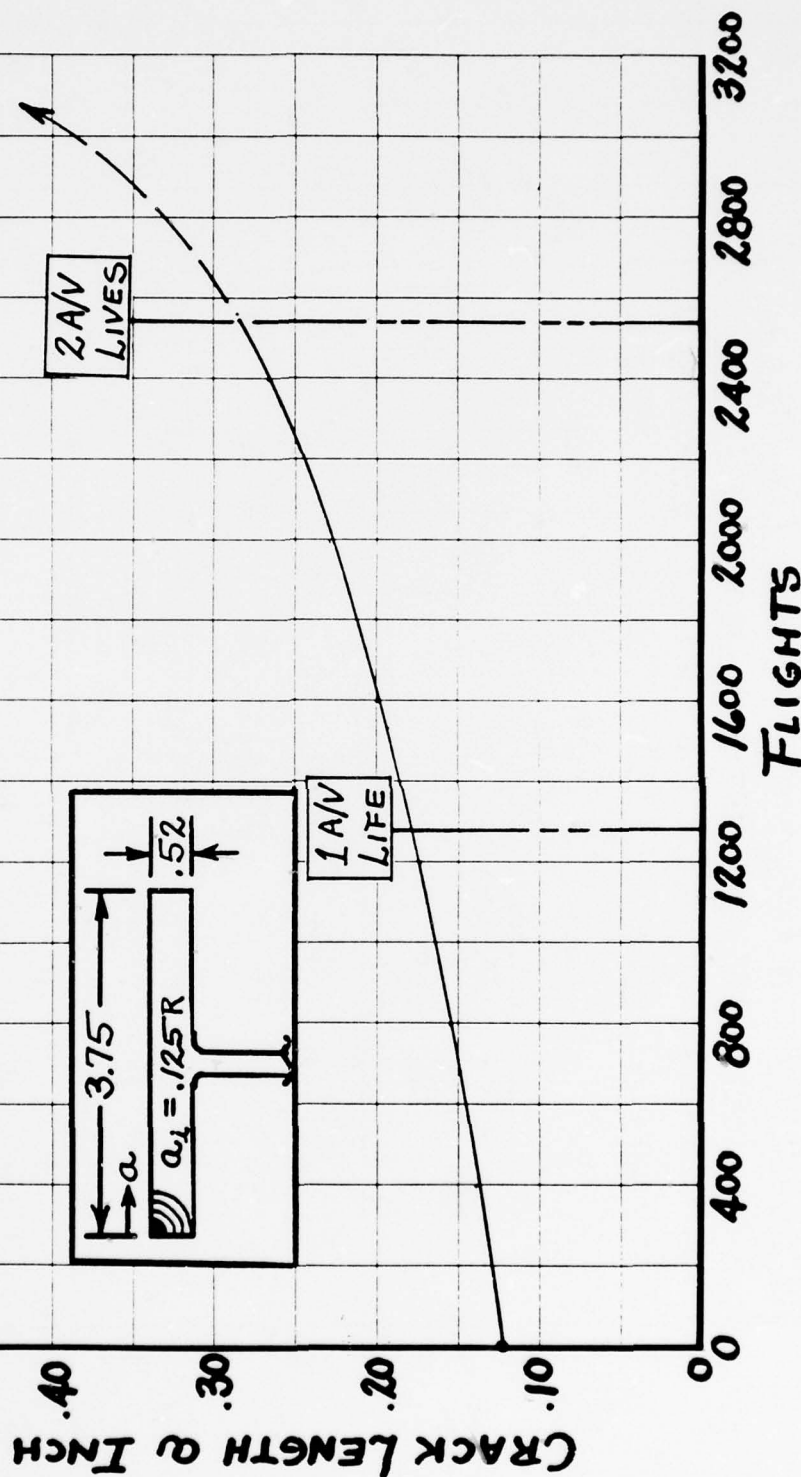
Figure 34. Wing sweep actuator fitting - item 2 crack growth analysis.

87
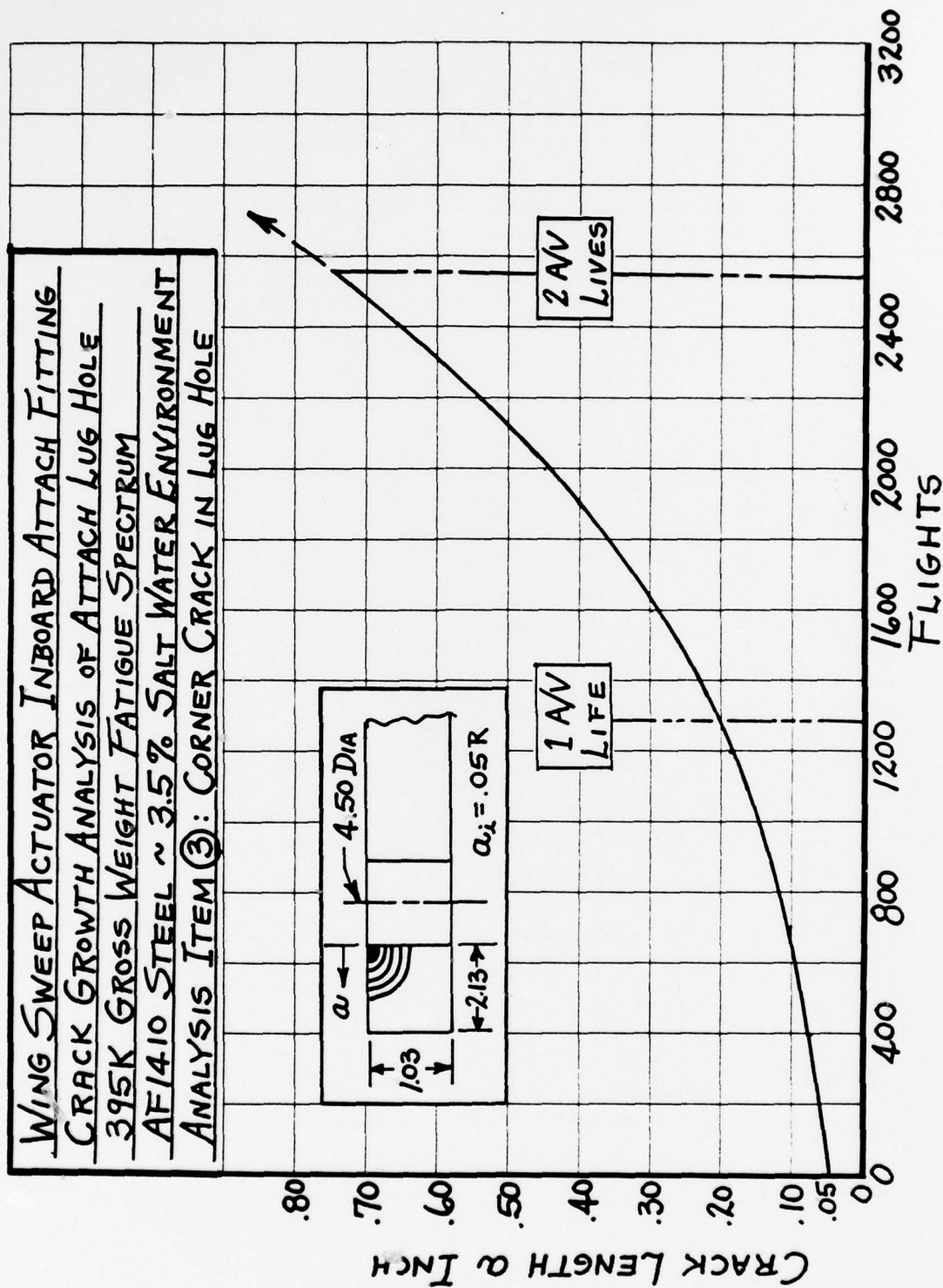
Figure 35. Wing sweep actuator fitting - item 3 crack growth analysis.

88
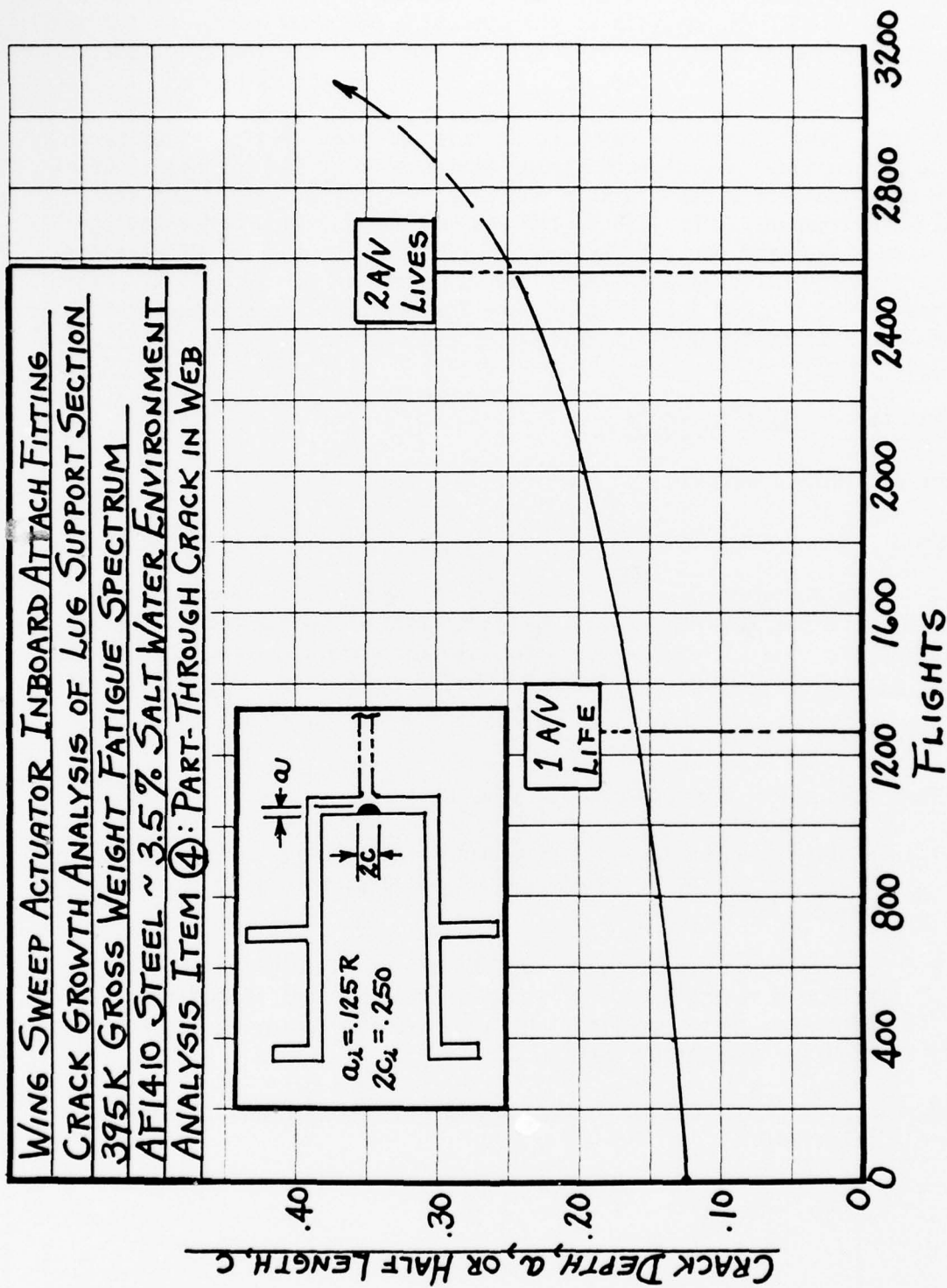
Figure 36. Wing sweep actuator fitting - item 4 crack growth analysis.

89

the effective stress concentration factor used for the fatigue analysis was 1.2 x 3.25 = 3.90. An analysis to the operating spectrum stress on the lug net section produces a fatigue life well in excess of the required four lifetimes.

A crack growth analysis was made on this same net section assuming an initial corner flaw of 0.05-inch radius at the edge of the lug hole. Crack growth rate properties used in this analysis were for a 3.5-percent salt solution environment. The life of the assumed initial flaw under the operating stress spectrum exceeds the two lifetime requirements of MIL-A-83444. A plot of the predicted crack growth rate is shown in Figure 37. All other sections on the body of this fitting have less severe stress concentration factors and are not critical in fatigue or crack growth.

MATERIAL PROPERTIES TEST PROGRAM

PURPOSE AND OBJECTIVES

Purpose

A series of material property tests were conducted to provide the essential data required for detail design of full-scale components for static and fatigue testing later in the program and for more accurately predicting serviceability, fabrication methods, and production costs using AF1410 steel.

Test Objectives

Test objectives for this program were as follows:

1. To provide a check of basic mechanical properties of production size heats of the material against those previously obtained on subscale heats.

2. To provide a more complete set of data on basic properties and fatigue characteristics of the parent metal and, in addition, the effects on these properties of selected manufacturing processes which are ordinarily used.

3. To provide mechanical properties, static and dynamic, of butt and fillet welds.
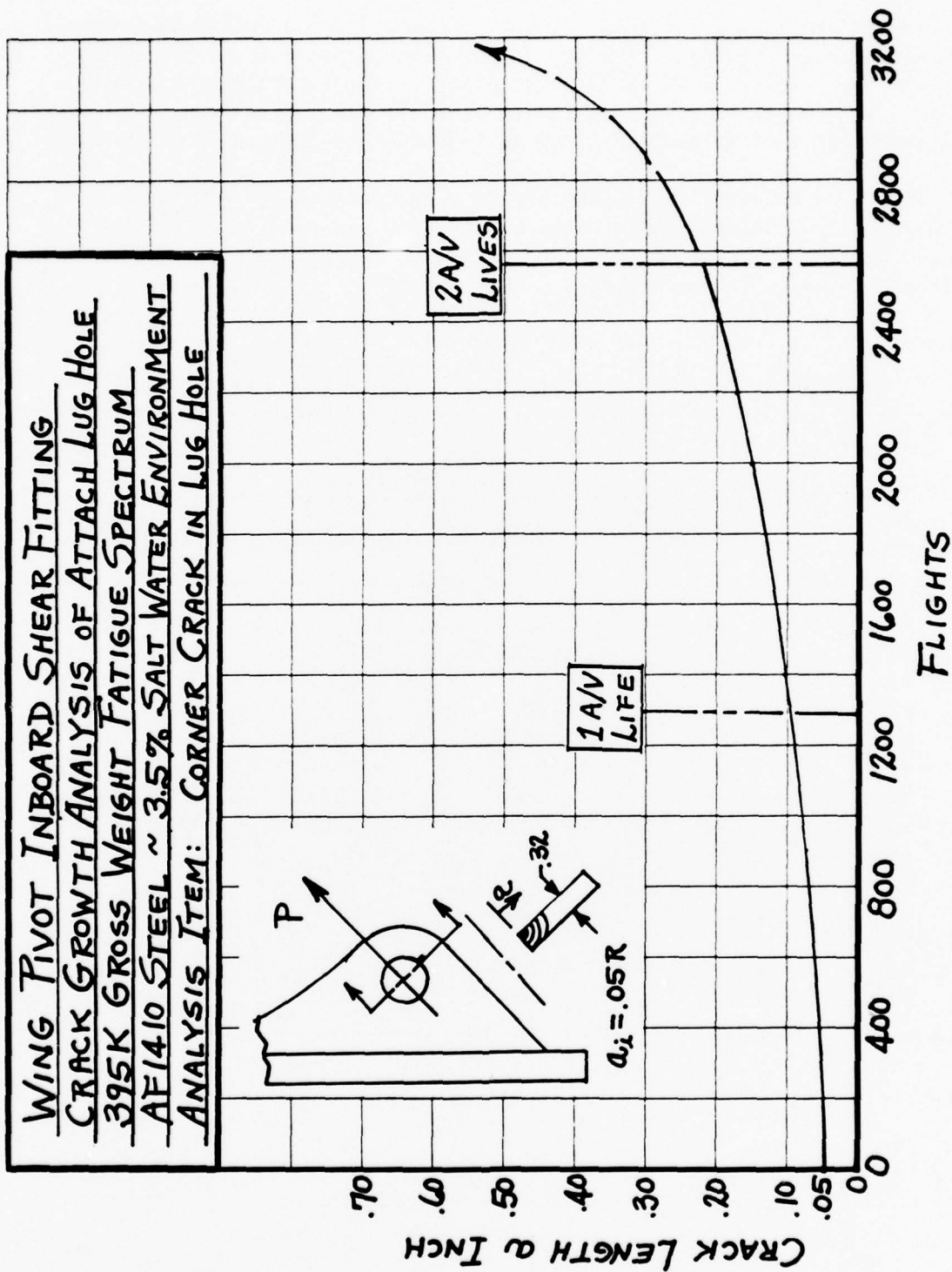
Figure 37. Wing pivot inboard shear fitting - lug hole crack growth analysis.

TEST MATERIAL

AF1410 steel used for all tests was produced by the Universal-Cyclops Specialty Steel Division of Cyclops Corporation under separate Air Force contract. The material was hot-rolled plate in varying thicknesses up to 2 inches. Material received was rolled from VIM-VAR ingots from three separate heats identified by Cyclops as L-3616K13, L-3614K18, and L-3550K20.

Weld wire used for weld specimens is 0.062-diameter AF1410 steel. It was made by U.S. Welding in Tarzana, California, and identified as heat TLA 260.6. The chemical compositions of this weld wire and the rolled plate heats are given in Table 17.

TABLE 17

CHEMICAL ANALYSIS - AF1410 STEEL PLATE AND WELD WIRE

| Element | Plate heat no. | | | Weld wire |
	L3550K20	L3614K18	L3616K13	TLA2606
C	0.16	0.16	0.17	0.15
Mn	0.07	0.076	0.06	<0.05
Si	0.03	0.03	0.04	<0.01
S	0.002	0.002	0.001	0.005
P	0.005	0.004	0.004	<0.001
Cr	2.06	1.99	1.91	1.90
N_2	0.001	0.0005	0.0002	0.0004
O_2	0.0006	0.0007	0.0003	0.0052
Ni	10.14	10.22	10.10	9.82
Mo	1.02	1.04	0.97	1.00
Co	13.91	13.92	13.98	13.76
Fe	Bal	Bal	Bal	Bal
Al	0.001	0.003	0.003	0.025
Ti	0.004	0.004	0.004	<0.01

SPECIMEN FABRICATION

Material Heat Treatment

The material was received in the as-rolled condition. For the nonwelded specimens, blanks were fully heat treated and aged before machining. For specimens to be welded, the blanks were double-austenitized, machined for weld edge preparation, manual GTAW-welded, aged, then finish machined. All heat treatment was conducted in ambient air as follows:

- Austenitize 1,650° F - 1 hour, water-quench

- Austenitize 1,500° F - 1 hour, water-quench

- Age 950° F - 5 hours, air-cool

Temperature control was maintained within ±25° F for austenitizing and ±10° F for aging.

Machining and Processing

All machining of specimens was done by regular production methods and machines using cutting tools normally used for high-strength steel. Sharp notches for start of fatigue cracks were machined by electrical discharge. After machining, specimens for manufacturing process effects tests were given a prescribed process by normal manufacturing methods.

Welding

All welding was performed using the manual GTAW process with argon gas shielding. Butt weld joints utilized a double-U groove edge preparation and were made using multiple passes as required.

Fillet welds were made using no edge groove for corner or partial penetration welds. A J-type groove was employed for full penetration welds. All fillet welding was with the minimum number of passes required to achieve the desired fillet size as specified in Rockwell Specification ST0107LA0019.

Radiographic and dye-penetrant inspection was performed on all butt welds and full-penetration fillet welds. The partial penetration fillet welds were dye-penetrant-inspected only (no radiography).

TEST CATEGORIES AND PROCEDURES

Four categories of tests were performed on AF1410 steel during the development test program:

1. Basic material properties

2. Fracture toughness and fatigue

3. Manufacturing process effects

4. Weld properties

The tests conducted in each of the four categories are defined in Tables 18 and 19.

Material Property Results

The detailed results of this portion of the program were previously published in Reference 2. Little or no anisotropy was observed for all the properties measured, and scatter of data within any one group of replicate specimens was generally less than 2 percent. The static properties derived for design allowables are summarized in Table 20 together with the allowables used for Ti-6Al-4V in the recrystallized annealed condition (heat-treated for maximum toughness). On a strength/density basis, AF1410 is superior to Ti-6Al-4V in all properties except bearing. Since few designs are bearing-critical, the static properties suggest AF1410 could be substituted for Ti-6Al-4V without incurring a weight penalty; in fact, a small weight savings is attainable. A summary of the fatigue data is shown in Figure 38 compared to recrystallized annealed Ti-6Al-4V on an equal-weight basis. Designs with more severe stress concentrations would incur a small weight penalty if AF1410 were used in place of the titanium.

Fatigue crack-growth rates of AF1410 and titanium (Figure 39) show significantly lower growth rates for the steel. However, for a slowly growing crack, one with a rate less than 10^{-6} inches per load cycle, the growth rates of the two alloys are comparable.

Hence, the static and dynamic properties obtained in the program demonstrate that AF1410 could be substituted for annealed Ti-6Al-4V without incurring a weight penalty. In fact, a weight savings should result for most designs.

TABLE 18

STATIC MECHANICAL PROPERTIES TEST MATRIX

Type of Test	Temp	Parent metal Basic prop. No. of spec & grain dir*	Manufacturing process effect Grinding	Grind + shot peen	Plating	Hydrogen embrittle	Weldments Butt welds 0.500 thick Weld	HAZ	Fillet welds Corner pen. 0.200 thick	0.375 thick	Full pen. 0.0375 thick Asym	Sym	Total specimens
Tension	-65° F	3L + 2T					14						19
	RT	7L + 4T	2	2	6		14		5	5	5	5	55
	265° F	5L + 3T											8
Sustained notch tension	RT					10							10
Compression	-65° F	3L + 2T											5
	RT	3L + 3T											6
	265° F	3L + 2T											5
Shear	-65° F	3L + 2T											5
	RT	3L + 2T											5
	265° F	3L + 2T											5
Bearing ED = 1.5 dia	-65° F	1L + 1T											2
	RF	1L + 1T											2
	265° F	1L + 1T											2
Bearing ED = 2 dia	-65° F	3L + 2T											5
	RT	3L + 2T											5
	265° F	3L + 2T											5

*L = Longitudinal, T = Transverse   Total   144

95

TABLE 19

FRACTURE TOUGHNESS AND FATIGUE TESTS MATRIX

Type of test	Environment or stress ratio R	Parent metal				Weldments						Total specimens
		Basic prop.	Manufacturing process effects			Butt welds		Fillet welds				
						0.500 thick		Corner pen		Full pen		
										0.375 thick		
		No. of spec & grain dir*	Grinding	Grind + shot peen	Plating	Weld	HAZ	0.200 thick	0.375 thick	Asym	Sym	
K_{1c}	-65° F	1RW + 1WR				2	2					6
	RT	2RW + 2WR				2	2					8
	RT - repair					1						1
Charpy	RT					12	12					24
Fatigue unnotched	R = +0.5	6T				11						17
	R = +0.05	8T + 4L	5	5	18	22		8	8	8	9	95
	R = -1.0	6T				11						17
Fatigue K_t = 3.0	R = +0.5	6T										6
	R = +0.05	8T + 4L										12
	R = -1.0	6T										6
Fatigue K_t = 5.0	R = +0.5	6T										6
	R = +0.05	8T + 4L										12
	R = -1.0	6T										6
K_{1scc} RT	STW	7WR + 4RW										11
	3.5% NaCl	5RW				5	5					15

TABLE 19

FRACTURE TOUGHNESS AND FATIGUE TESTS MATRIX (CONCL)

Type of test	Environment or stress ratio R	No. of spec & grain dir*	Grinding	Grind + shot peen	Plating	Weld	HAZ	0.200 thick	0.375 thick	Asym	Sym	Total specimens
		Basic prop.	**Manufacturing process effects**			**Butt welds 0.500 thick**		**Corner pen**		**Full pen 0.375 thick**		
da/dN 0.08R	RT LHA	1WR at 60 cpm										1
		2WR at 1,800 cpm				2	2					6
		1RW at 1,800 cpm										1
da/dN 0.08R	-65° F LHA	1WR at 1,800 cpm										1
da/dN 0.3R	RT LHA	1WR at 1,800 cpm										1
da/dN 0.3R	RT 3.5% NaCl	1WR at 60 cpm										1
da/dN 0.08R	RT 3.5% NaCl	2WR at 60 cpm				1						3
	RT STW	1RW at 60 cpm										1

*L   = longitudinal
T   = transverse
LHA = low humidity air
RW = crack prop normal to roll direction
WR = crack prop parallel to roll direction
STW = sump tank water

Total   257

TABLE 20

AF1410 PROPERTIES COMPARED TO Ti-6Al-4V

PROPERTY	AF 1410		Ti-6AL-4V ANN.	
	VALUE	$\dfrac{\text{VALUE}}{\text{DENSITY}}$	VALUE	$\dfrac{\text{VALUE}}{\text{DENSITY}}$
Ftu	235 KSI	839	130 KSI	812
Fty	220 KSI	786	120 KSI	750
Fcy	231 KSI	825	126 KSI	787
Fsu	139 KSI	496	79 KSI	494
Fbru (e/D = 2.0)	438 KSI	1564	256 KSI	1600
Fbry (e/D = 2.0)	324 KSI	1157	208 KSI	1300
E	28×10^6	100	16×10^6	100
KIc	130 KSI $\sqrt{\text{IN.}}$	464	70 KSI $\sqrt{\text{IN.}}$	437

98
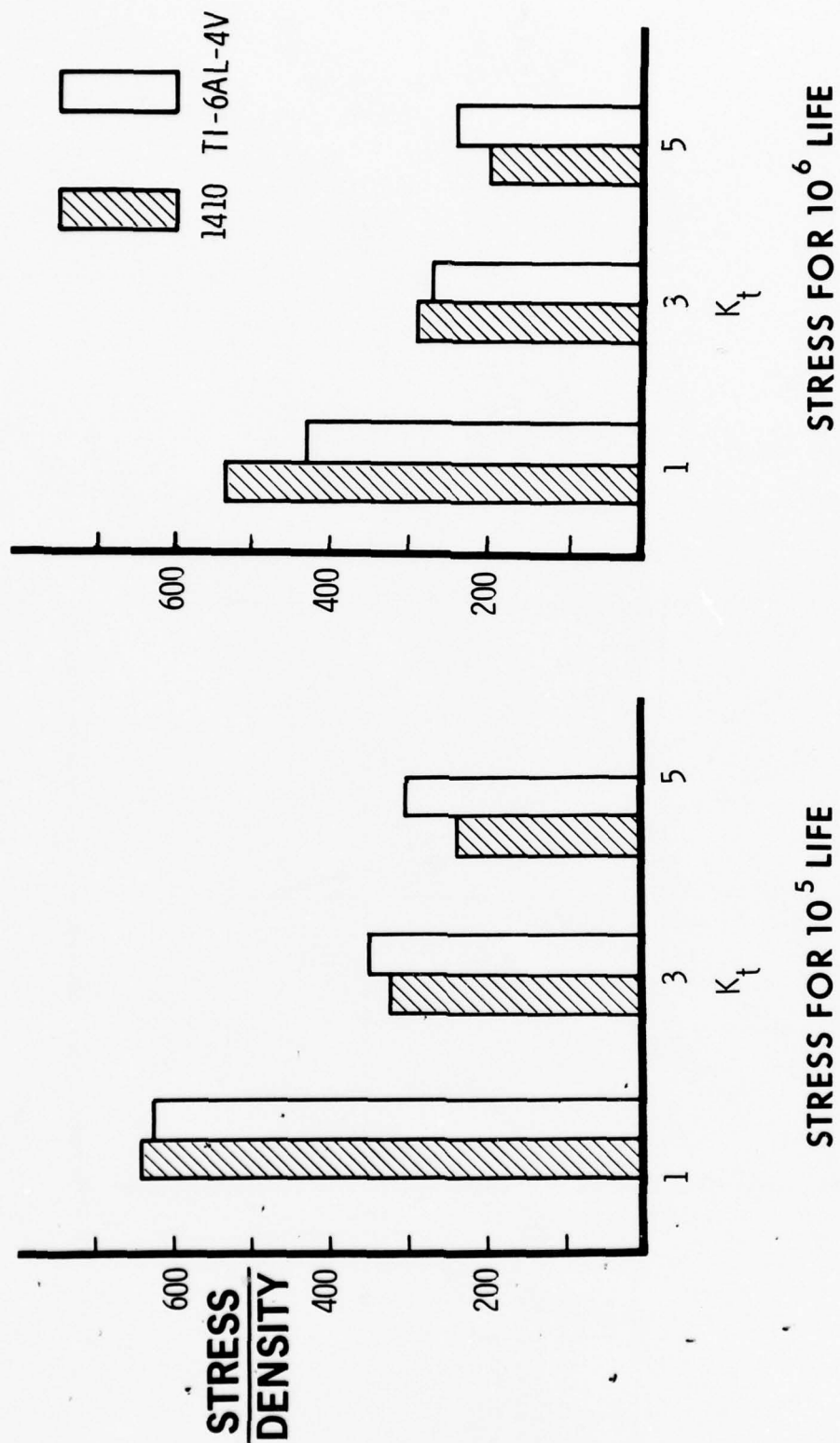
Figure 38. Fatigue comparison, plate.

da/dn
MICROINCH/
CYCLE
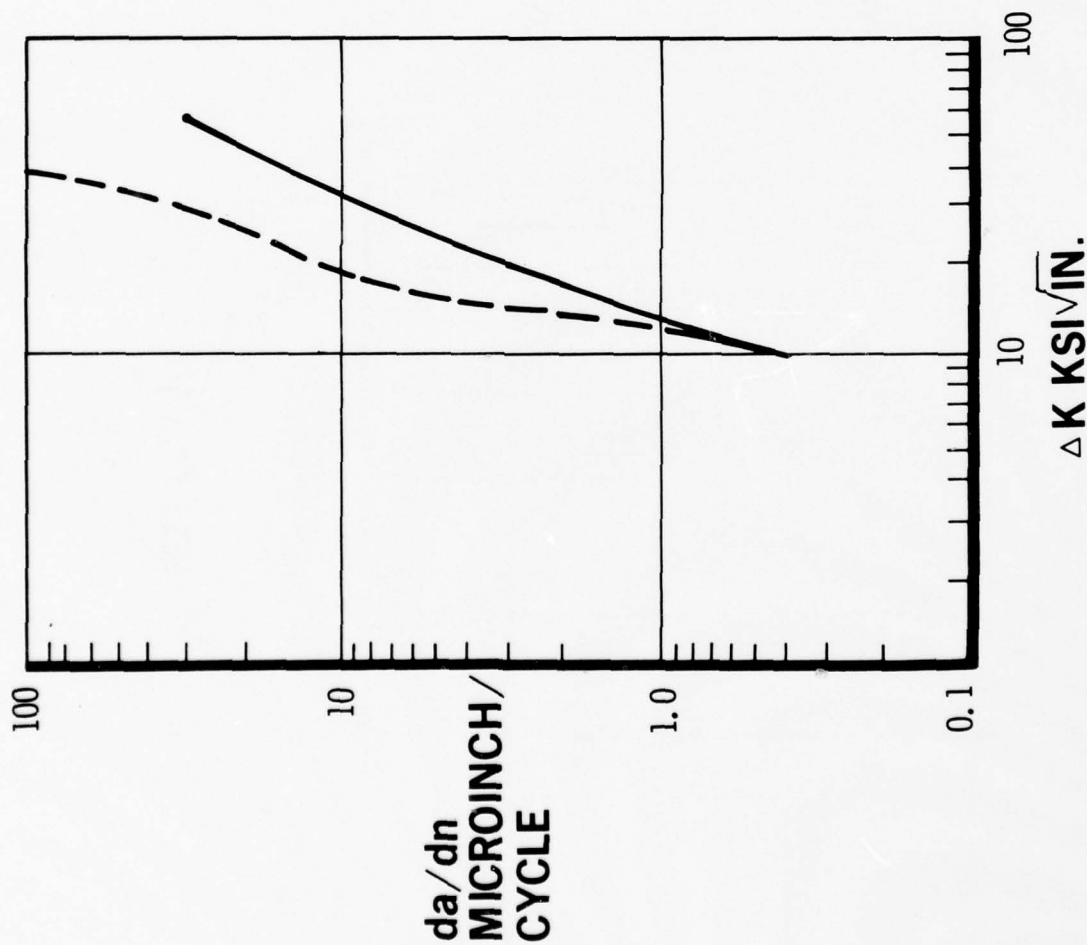
RW DIRECTION
R = 0.08
TITANIUM PLATE 1-1/2 IN. THICK
AF 1410 1-1/4 IN. THICK

——— AF 1410
— — — Ti-6AL-4V

ΔK **KSI$\sqrt{IN}$.**

Figure 39. Comparison of AF1410 with recrystallization annealed Ti-6Al-4V.

Section IV

MACHINABILITY/HEAT-TREAT EVALUATION

The machinability/heat-treat activity was actually accomplished during phases I, II, and III of the program. It was felt, however, that to separate the data would reduce the clarity and effectiveness of the evaluation. Therefore, machinability/heat-treat activity is presented as a separate, complete discussion. This portion of the program was conducted in three phases.

Phase I was concerned with investigating a variety of heat treatments with potential for improving the machinability of AF1410. Evaluation of the machinability of the various conditions were based upon metallurgical and end milling studies. Two heat-treat conditions were selected for further evaluation in phase II.

The objectives of phase II were (1) to verify that subjecting the material to the premachining heat treatment(s) would not impair subsequent heat-treatment response, weldability, and mechanical properties, (2) establish heat-treat procedures which would minimize quench distortion, (3) verify aging time-temperature parameter relationships, and (4) finalize selection of the premachining heat treatment for extensive machinability studies to be conducted in phase III.

Phase III was mainly devoted to machining tests on material in both the premachining and full-hard, heat-treatment conditions. Heavy (rough) cuts were made in testing material in the premachining heat-treat condition, whereas light cuts were used for material in the full-hard condition. End milling cuts were of the slotting type for both heat-treat conditions. Drilling, reaming, and chemical-milling tests were performed on the full-hard material only. Machining data was analyzed using a modified form of the Taylor equation after results indicated the standard equation did not adequately describe the tool life data.

MATERIALS AND PROCEDURES

MATERIALS

AF1410 Steel

The AF1410 steel used in this program was obtained from Universal Cyclops, and had the chemical compositions previously shown in Table 17. The microstructure of the as-received plate stock is shown in Figure 40.
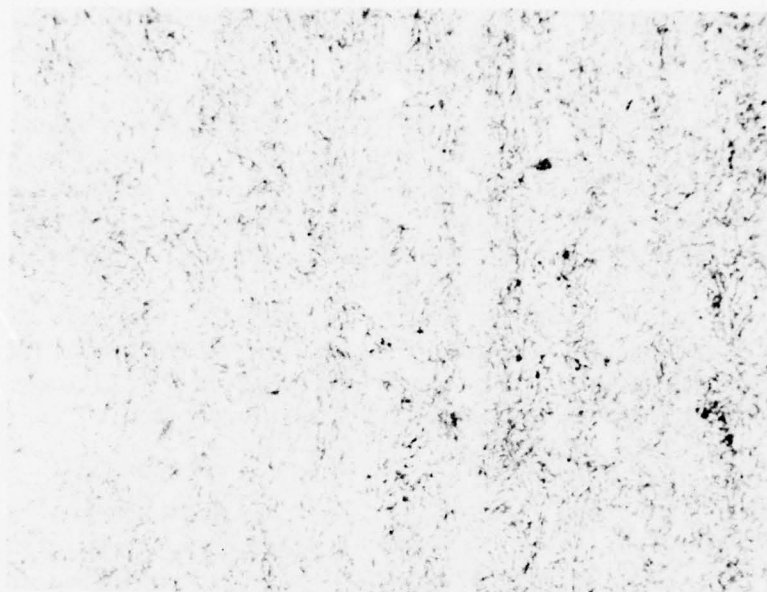
250X   NITAL ETCH

1,000X   NITAL ETCH

Figure 40. As-received AF1410 plate microstructure.

Cutting Tools

All drills, reamers, and end mill cutters used in this program were of standard geometries obtained from commercially available stock (Figures 41 through 44). The end mill cutters used in phase I were Cobalt high-speed steel (CHSS), 3/4-inch in diameter, as described in Table 21. The end mill cutters used in phase III were 1 inch in diameter, with four and six flutes and of Cobalt high-speed steel, C5, C6, and WA107 carbides. Upon receipt, a 0.060-inch corner radius was ground on the end mill cutters prior to use (Figure 42). Complete cutter details are listed in the appropriate tables in phase III.

The drills were 23/64-inch-diameter twist drills of Cobalt high-speed steel, C2, and C5 carbides. The as-received drills had standard split points (Figure 43).

The reamers were 3/8 inch in diameter with straight and spiral flute geometries, and of Cobalt high-speed steel, or with C2 or C5 carbide inserts (Figure 44).

All of the cutting tools were inspected to establish tool geometry prior to use.

PROCEDURES

Preparation of Test Blanks for Machining

AF1410 steel plates were cut into machining test blanks by means of an abrasive wheel. The phase I test blank is shown in Figure 45. In phase III eighty-four test blanks, 4 inches wide by 18 inches long, were cut from 1-1/8-inch plate for the drilling and reaming tests; and 16 blanks, 6 inches wide by 18 inches long, were cut from 2-inch plate for the end milling tests. After heat treatment, the test blanks were machined to provide flat and parallel surfaces free of any mill scale or other types of contamination.

Heat Treatment

The AF1410 steel speciments used in this study were heat treated in both laboratory and manufacturing heat-treat facilities depending on specimen size and quantity. The premachining heat treatments were carried out in an air atmosphere since subsequent preparation by machining could be relied upon to clean up any oxidized and/or decarburized surfaces. Full-hard heat treatments of specimens for finish machining tests were carried out in an endothermic atmosphere (with a dew point of 68° F) to preclude the need for cleanup of oxidized and/or decarburized surfaces. The procedures were implemented in accordance with MIL-H-6875.

DRILL

REAMER

END MILL

Figure 41. Typical cutting tools used for machining tests.

104
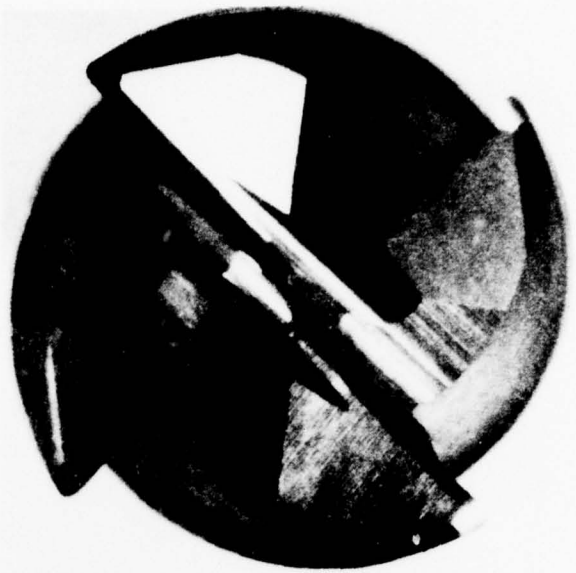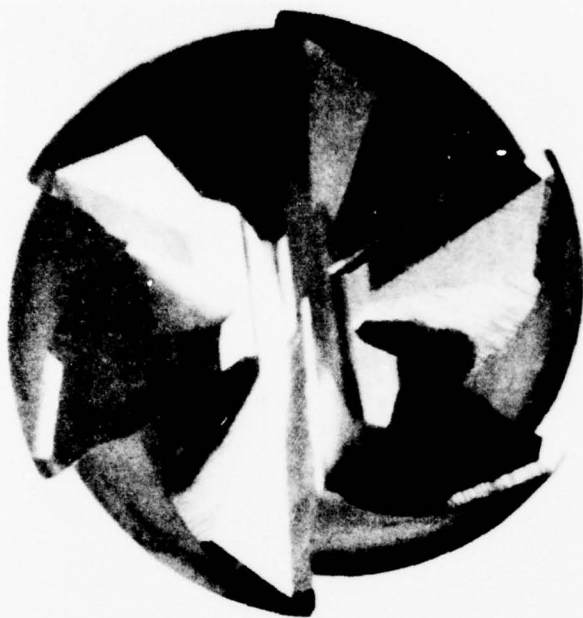
6 flutes   4 flutes

Figure 42. Typical 1-inch-diameter cobalt HSS M-42 end mills with
0.060-inch corner radius.
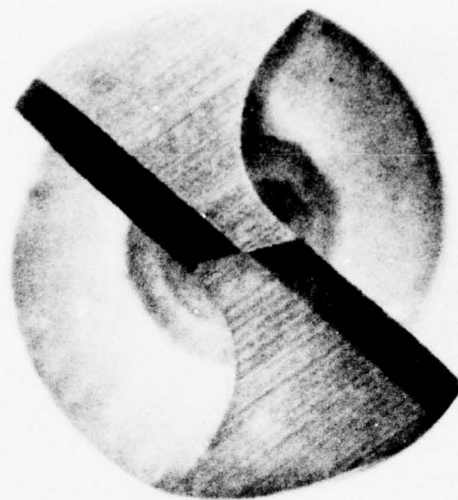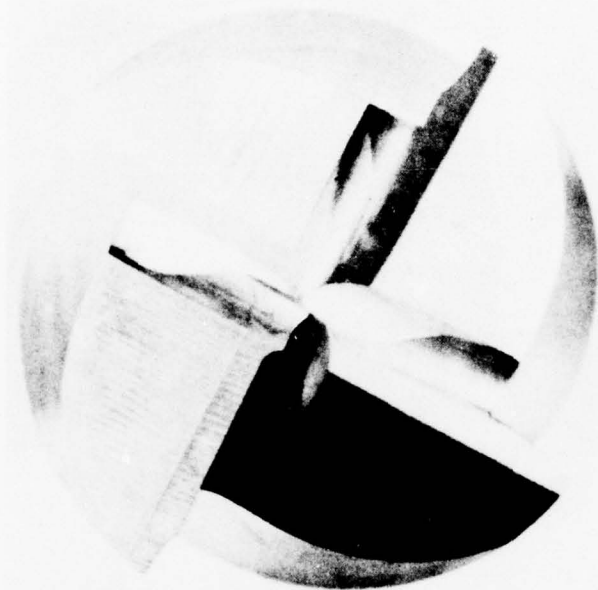
1-inch-diameter end mill, four flutes, as-received (0.060 1-inch radius ground prior to tests)

23/64-inch-diameter drill

Figure 43. Typical C-5 carbide tools.
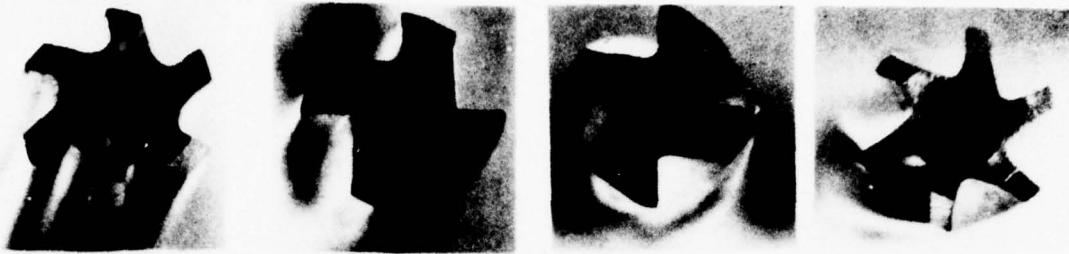
106

CHSS-M42   C-5 carbide   C-5 carbide   CHSS-M42
6 flutes   4 flutes   4 flutes   6 flutes
straight   straight   spiral   spiral

Figure 44. Typical 3/8-inch-diameter reamers.

TABLE 21

COBALT HSS END MILL CUTTERS USED FOR PHASE I MACHINABILITY TESTS
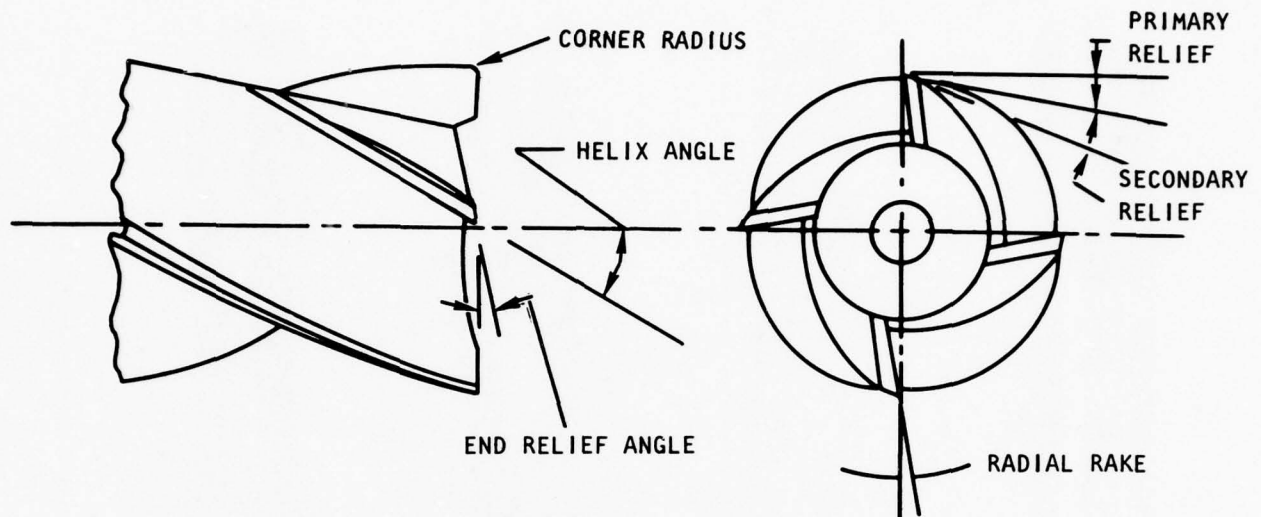
Cutter Serial No.	No. Flutes	Primary Relief	Secondary Relief	End Relief	Corner Radius	Helix Angle	Radial Rake	Concentricity OD to Shank
1	4	9	17	7	0.055	30	10	0.0003
2	4	10	21	7	0.055	30	10	0.0003
3	4	10	18	7	0.060	30	10	0.0002
4	4	9	20	7	0.055	30	10	0.0001
5	4	10	20	7	0.055	30	10	0.0004
6	4	9	20	7	0.055	30	10	0.0004
7	4	10	17	7	0.055	30	10	0.0004
8	4	10	21	7	0.058	30	10	0.0002
9	4	10	21	7	0.055	30	10	0.0005
10	4	10	18	7	0.055	30	10	0.0002

NOTE: All cutters were 3/4-inch in diameter and from the same heat of CHSS.

108

CUTTER ROTATION DIRECTION

3/4 IN. DIAMETER CUTTER ← FEED DIRECTION

CUT WIDTH EACH
CUTTER PASS
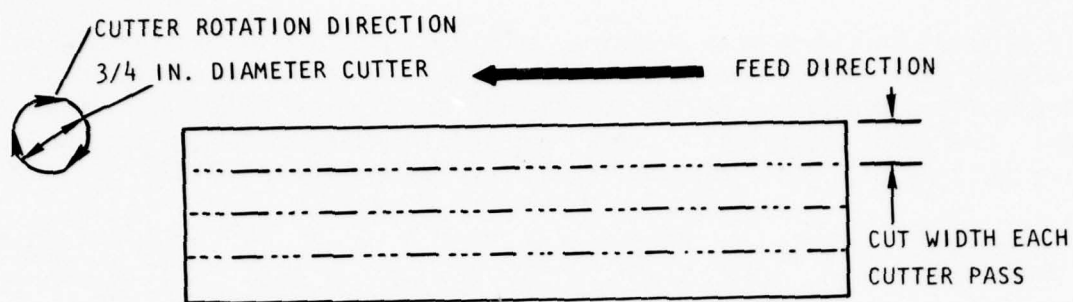
CUTTING SEQUENCE IN DOWN CUTTING MODE

1st TEST PHASE - 4 PASSES 0.300-DEEP
× 0.516 WIDE (4.445 IN.^{3} REMOVED)

2nd TEST PHASE - 4 PASSES 0.300 DEEP
× 0.516 WIDE (4.445 IN.^{3} REMOVED)

1st CUT

| 1 | 2 | 3 | 4 |
| 5 | 6 | 7 | 8 |

7 3/16

2 1/16
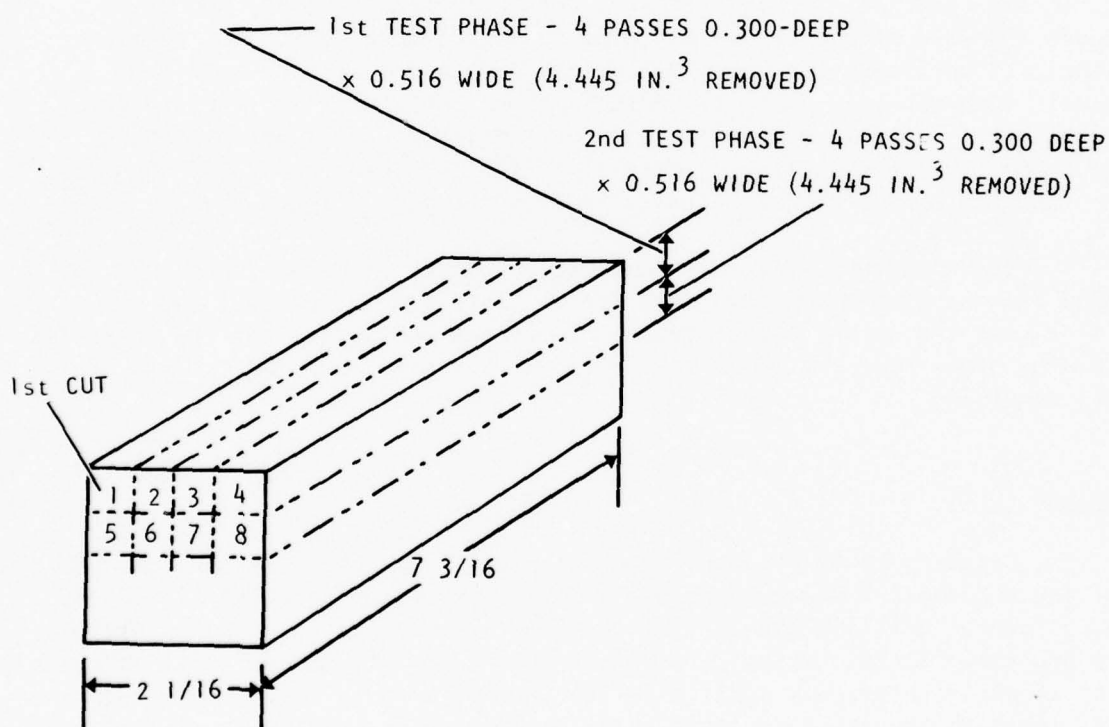
Figure 45. Phase I machinability test specimen and testing sequence.

109

Machining

All machining tests were performed in the Engineering Machine Shop, and all cutting tools were resharpened and inspected in the Production Tool and Cutter Grinding department at the Los Angeles Division of Rockwell International. Standard shop practices were employed. Cutting fluid application was in the form of a spray mist during all of the machining tests.

End Milling Tests

The end milling tests were performed on a No. 2 vertical Cincinnati Milling Machine. Type-4 cutting fluid, Texaco soluble oil HW, mixed 1 part with 40 parts of water, was used for the rough machining cuts in phase III; and Quaker Chemical Microcut 567-73, mixed 1 part with 25 parts of water, was used for the rough machining cuts in phase I and the finish machining cuts in phase III. The sequence of rough machining cuts is shown in Figure 45 for the phase I tests, and in Figure 46 for the phase III tests. All end milling was done in the down (climb) milling mode.

In the phase III machining tests, cuts numbered 1, 8, 15, and 22 (Figure 46) were slot cuts, 1-inch wide and 0.375-inch deep. The remainder of the cuts were semislot cuts, 0.375-inch deep and 0.75-inch wide. A typical rough machined phase III part is shown in Figure 47. The finish machining test cuts were made in a manner similar to the rough machining cuts except that the cuts were nominally 0.725-inch wide and 0.050-inch deep, and the center rib was eliminated from the part (Figure 48).

The feeds and speeds for the end milling tests in phase I were 0.0032 IPT and 39 SFM for the first set of tests, and 0.0026 IPT and 46.5 SFM for the second set of tests. The feeds and speeds for the phase III machining tests were varied on an individual basis to accommodate data requirements.

Drilling Tests

The drilling tests were performed on a positive feed Cleerman 25D, 5HP drilling machine, as shown in Figure 49 using the setup shown in Figure 50. The pattern of drilling the 23/64-inch-diameter holes is shown in Figure 51. Type-4 cutting fluid, Quaker Chemical Micro Cut No. 26, mixed 1 part with 13 to 15 parts water, was applied in the form of a spray mist. Tests were made with both the standard split point configuration and the SK drill point configuration (Figure 52). A typical test specimen is shown in Figure 53.

110
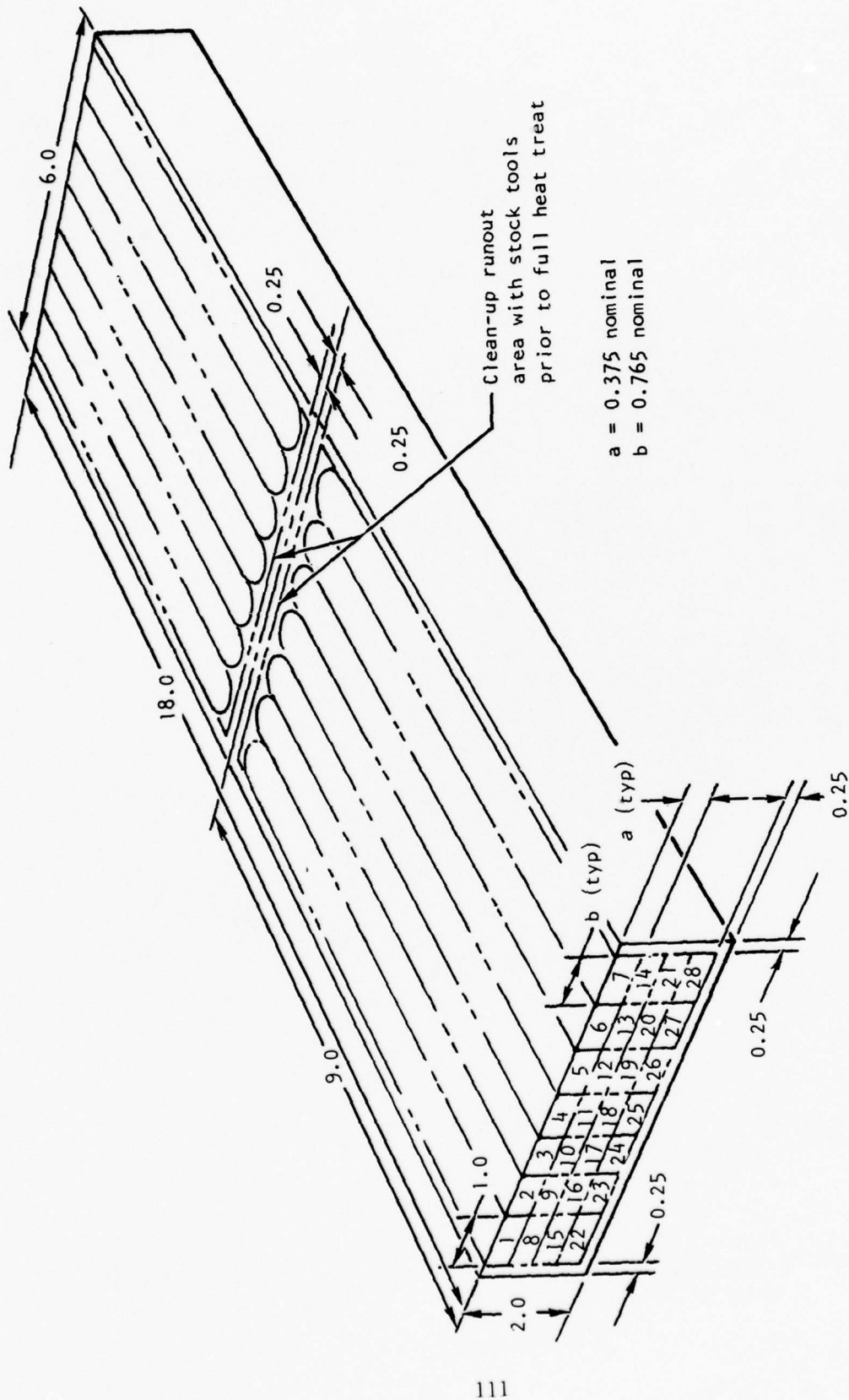
Figure 46. Sequence of cuts for phase III rough machining of end mill test blanks.

Clean-up runout
area with stock tools
prior to full heat treat

a = 0.375 nominal
b = 0.765 nominal
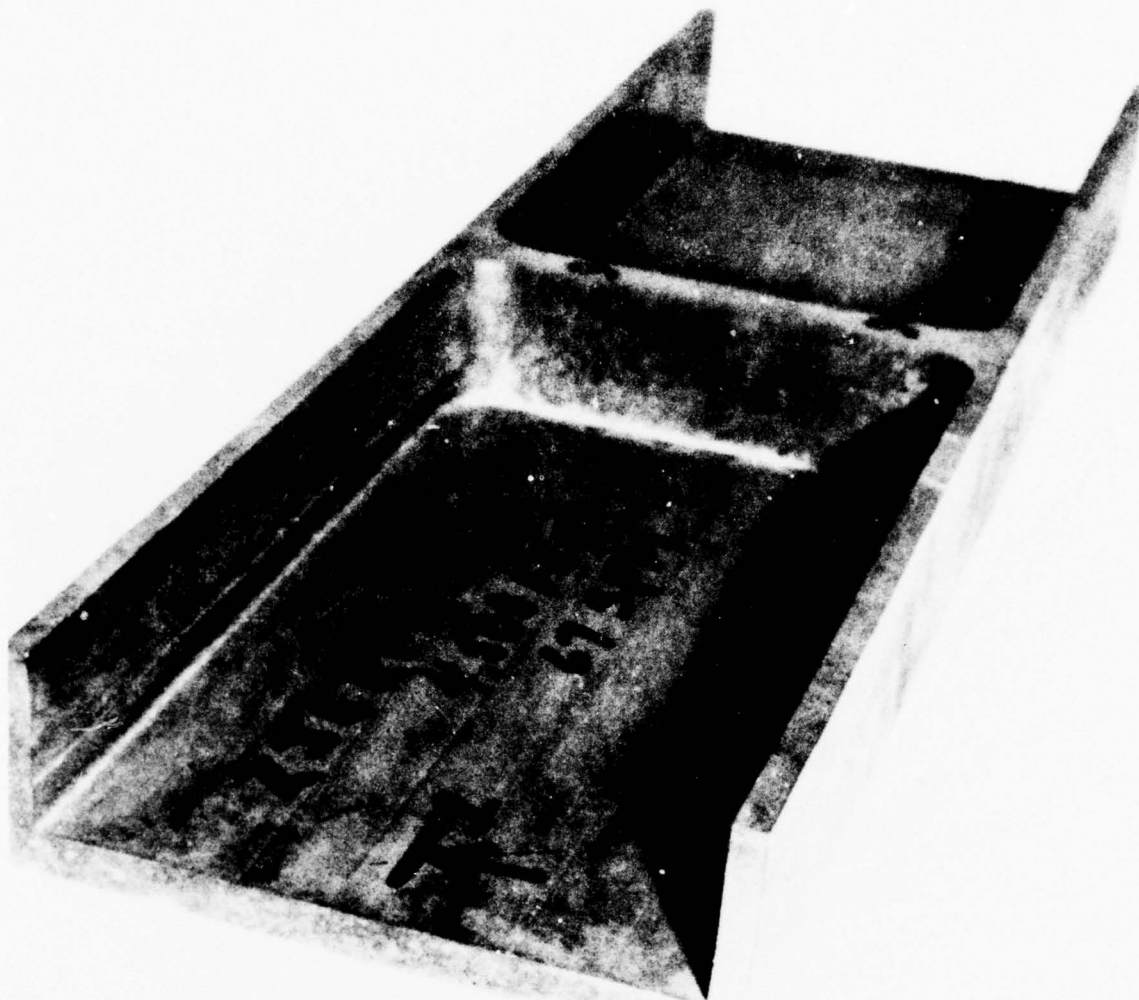
Figure 47. Typical Phase III open-ended, pocketed part after rough machining and final heat treating.

2 x 6 x 18 end milling specimen

Figure 48. Typical full-hard AF1410 machining test specimens.
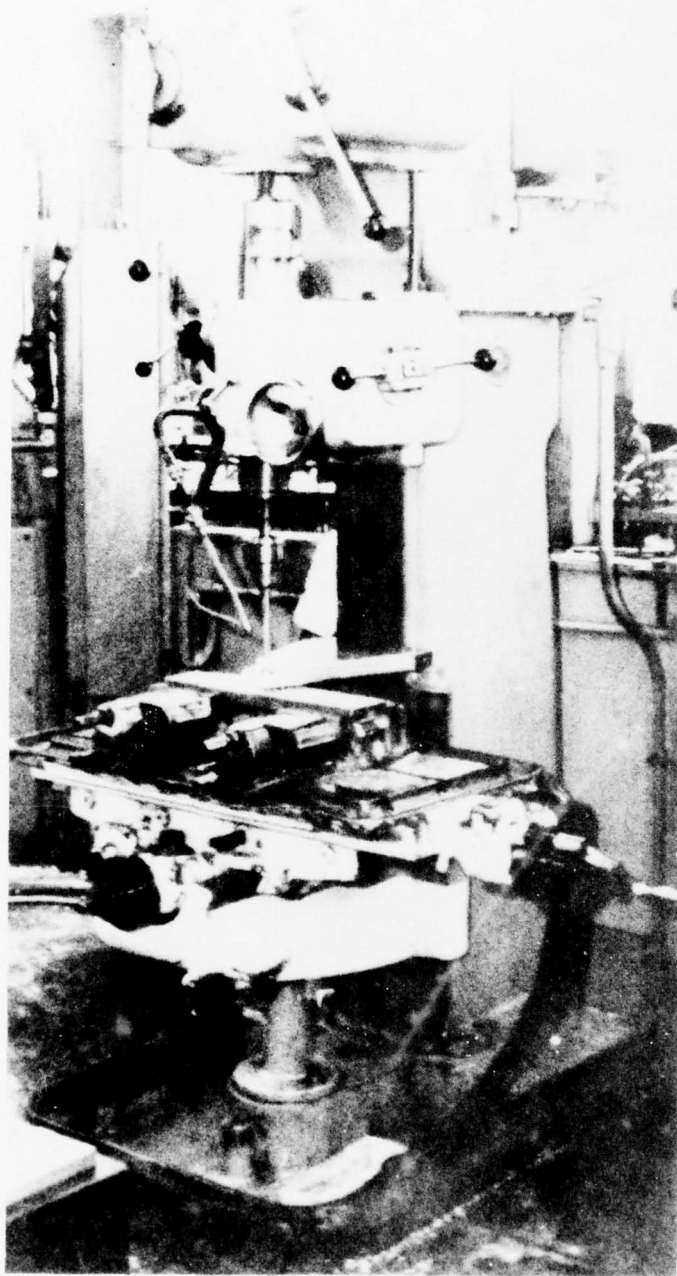
Figure 49. Cleereman 25D, 5-hp, drilling machine (set up for reaming tests).

114
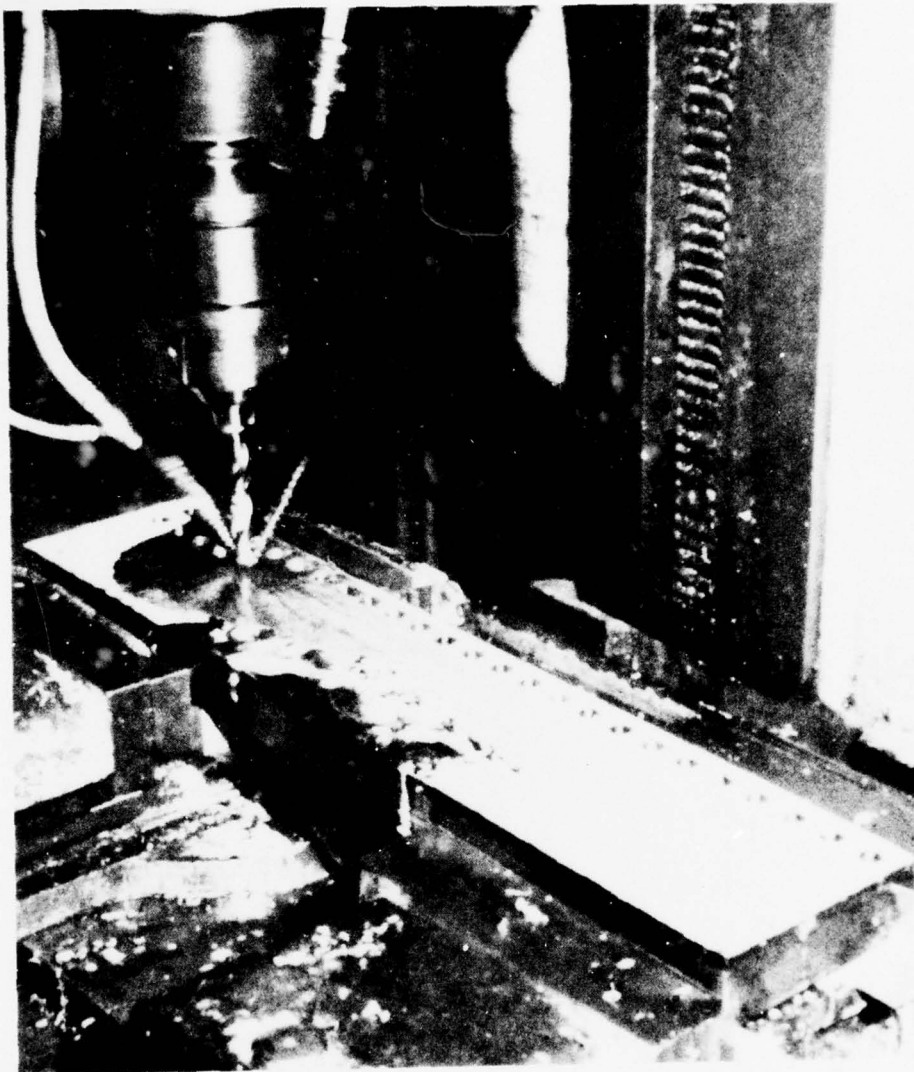
Figure 50. Drilling test set-up.

115
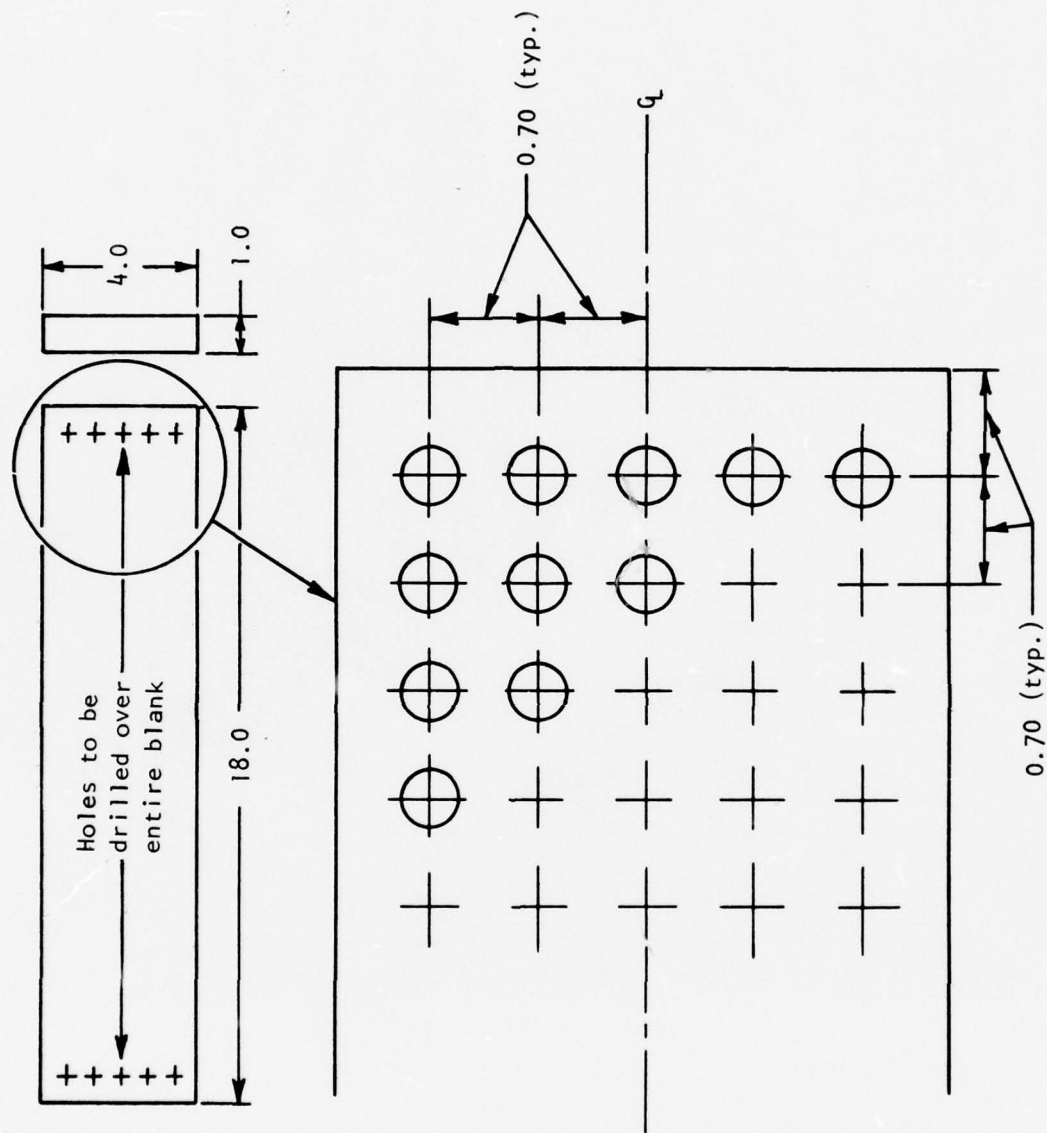
Figure 51. Hole pattern for drill and reamer test blanks.

116

Figure 52. SK drill point configuration.

117
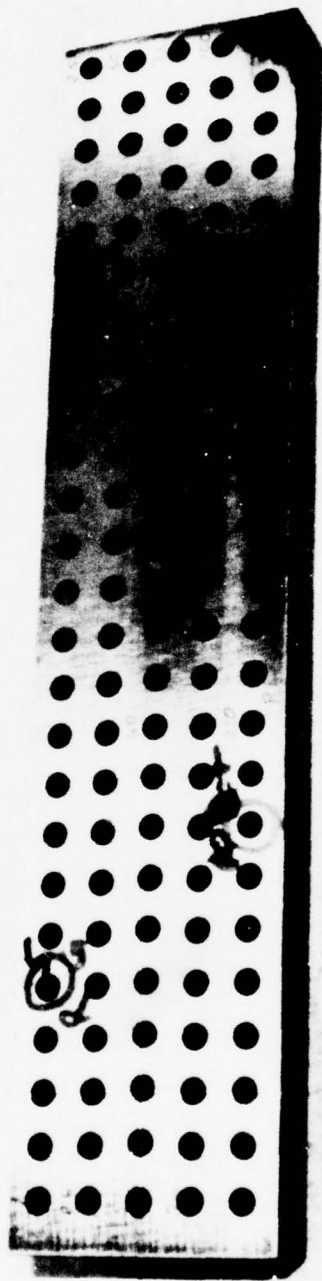
Figure 53. 1- x 4- x 18-inch drilling and reaming specimen.

118

Reaming Tests

The reaming tests were performed on the same positive feed Cleerman 25D, 5HP drilling machine as the drilling tests (Figure 49) with the addition of a bushing fixture (Figure 54) to maintain axial alignment of the reamer with the hole. Reaming tests were conducted on the completed drilling test specimens (Figure 53).

Tool Grinding

All tool grinding was done by standard tool grinding procedures.

INSPECTION

Tools

All cutting tools were inspected and all final cutting tool landwear measurements were made by means of a Stocker and Yale tool analyzer. Prior to making the final landwear measurements (near a landwear of 0.008 inch, the selected end point for these tests), at least four estimates of landwear were made by visual observation during the test. This involved visual comparison with a known tool dimension, such as the landwidth of the primary cutting edge for the end mill cutters and the margin width for the drills.

Surface Finish

The finish of the machined surfaces was measured by means of a brush profilometer.

Mechanical Properties

Tensile, charpy impact, and fracture toughness tests were performed in accordance with ASTM Standards E8, E23, and E399, respectively. Hardness measurements were made on the Rockwell C scale in accordance with ASTM Standard E18.

Chemical Milling

AF1410 steel plate was submitted to a commercial chemical milling company, Aerochem Inc, Orange, California, for chemical milling tests using various standard proprietary solutions. The rates of metal removal by the various solutions were measured in terms of etching depth in 30 to 40 minutes, and the chemically milled surfaces were examined at a magnification of 20X for roughness and pitting.
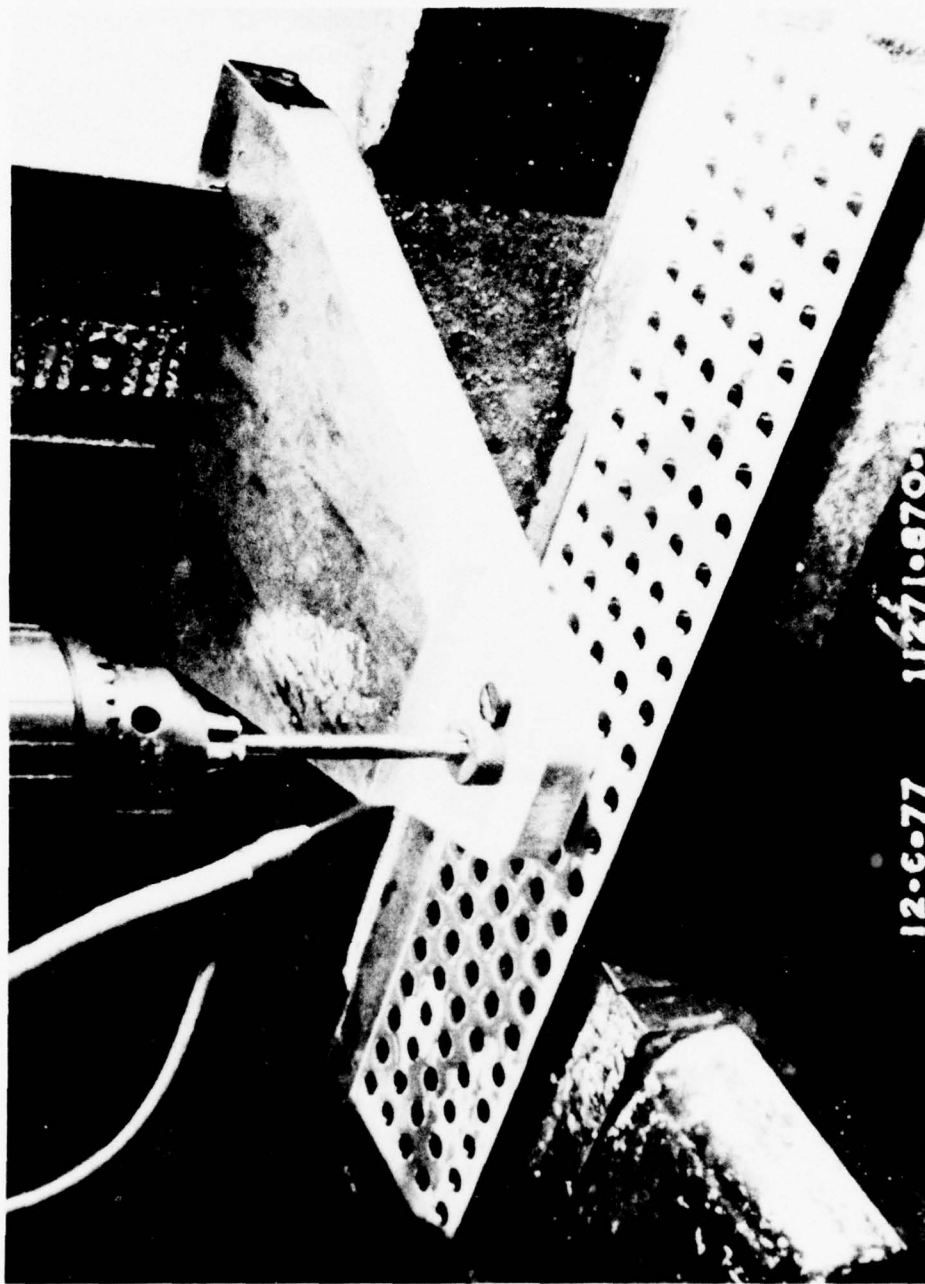
Figure 54. Reaming test with bushing to assure axial alignment.

120

DATA ANALYSIS (PHASE III)

A close estimate of the tool life at a landwear of 0.008 inch was obtained from a least-square regression of a straight line on a data plot of the logarithm of the landwear versus tool life. In making the least-square regression fits, the visual landwear estimates were given a weight of 1 and the tool analyzer measurements were given a weight of 4. Typical fits are shown in Figures 55 and 56.

After obtaining the tool life values for 0.008-inch wear, the Taylor equation constants were then substituted in the cost and optimum cutting speed equations derived on the basis of the Taylor equation (Tables 22 and 23) to allow calculation of optimum cutting speeds (Reference 5). The definition of symbols and the values used for the various constants are given in Tables 24 and 25. Because of incorrect predictions of optimum cutting speed values, the Taylor equation was modified on an empirical basis to yield more realistic predictions for the end milling of AF1410 steel with Cobalt high-speed steel cutters.

PHASE I - PREMACHINING HEAT TREAT DEVELOPMENT

OBJECTIVE

The objective of phase I was to establish a premachining heat treatment for AF1410 steel that would improve its machinability to approach or exceed that of titanium 6Al-4V.

APPROACH

The approach taken to attain the phase I objective was to develop metallurgical structures in the hardness range of 30 to 40 Rockwell C, having a maximum conglomeration of carbides, and/or reduced fracture toughness by limited enlargement of the prior austenitic grain size. The conglomeration of carbides reduces fracture toughness promoting chip breaking, thereby reducing the force required to separate the metal, a primary requirement for good machinability.

A wide range of austenitizing temperatures were investigated; most temperatures were in the range of 1,250° to 1,375° F, and were sufficiently low to minimize the dissolution of carbides; a high temperature of 1,625° F was selected to promote limited austenitic grain growth without causing permanent degradation of toughness. Subsequent to these austenitizing treatments, aging treatments were used to attain the desired hardness levels and carbide distributions.

121
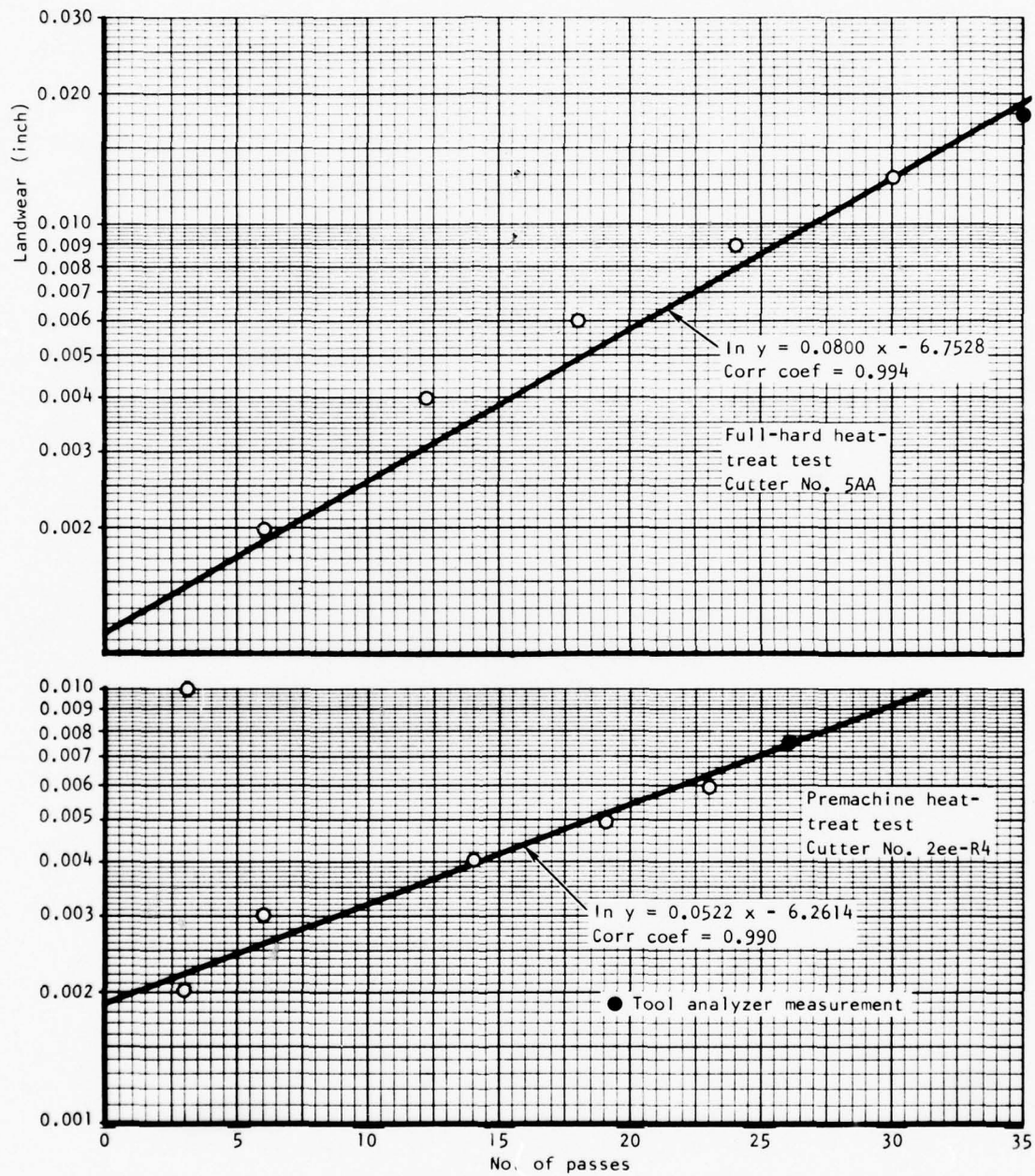
Figure 55. Typical fits of least-square semilog equation to landwear measurements on end mill cutters.

122
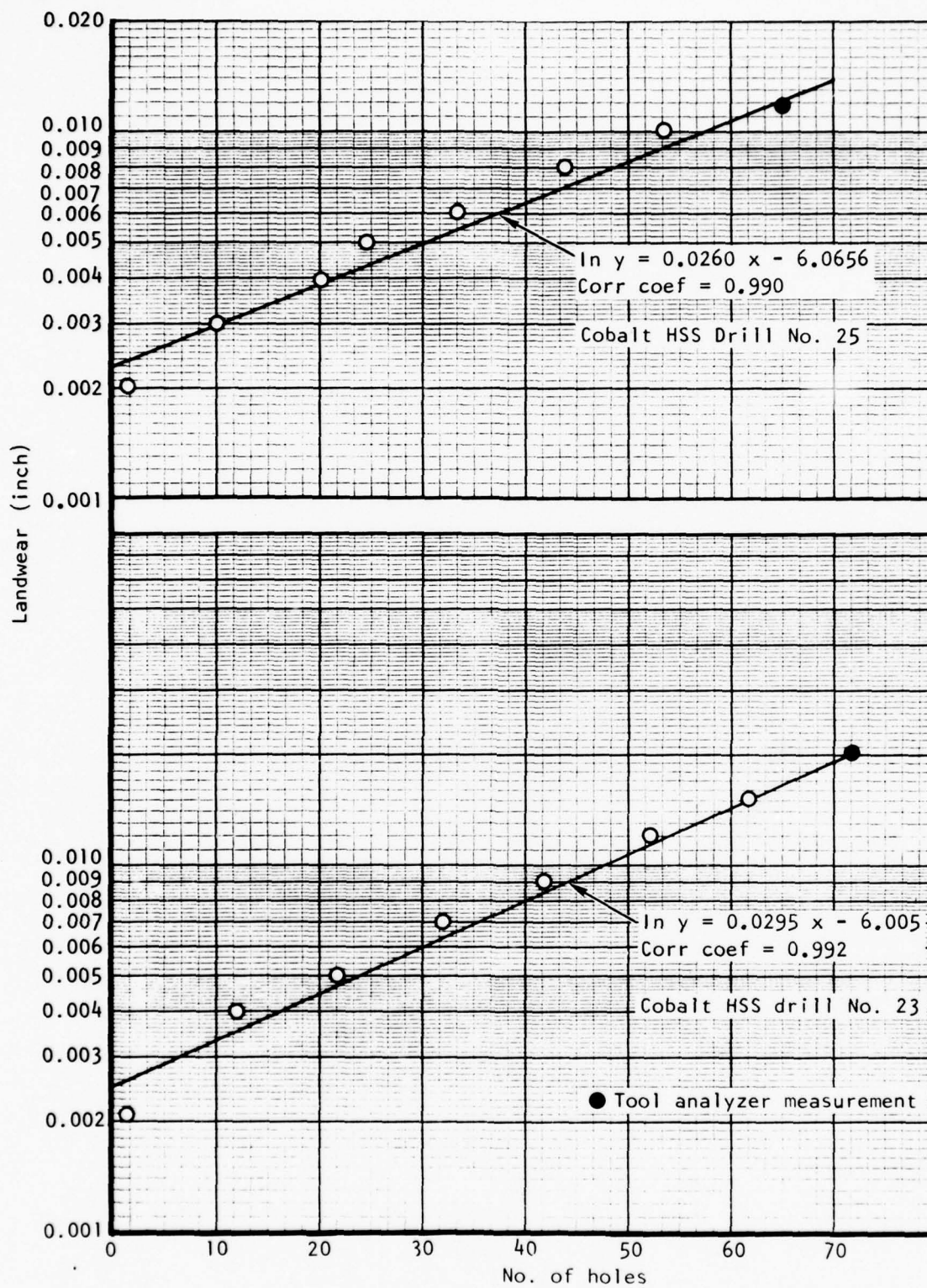
Figure 56. Typical fits of least-square semilog equation to landwear measurements on drills.

123

TABLE 22

GENERALIZED MACHINING COST EQUATIONS

Milling

$$C = M\left[\frac{D(L+e)}{3.82Zf_t v} + \frac{R}{r} + t_i + \frac{Lt_d}{2T_t} + \frac{L}{2T_t}\left(\frac{C_p}{(k_1+1)}\right) + Gt_s + \frac{Gt_b}{k_2} + \frac{ZC_c}{k_3} + C_w + Gt_p\right]$$

Drilling or reaming

$$C = M\left[\frac{D(L+e)}{3.82f_r v} + \frac{R}{r} + t_i + \frac{Lt_d}{T_t} + \frac{L}{T_t}\left(\frac{C_p}{(k_1+1)}\right) + Gt_s + Gt_p\right]$$

Tapping

$$C = M\left[\frac{mD(L+e)}{1.91v} + \frac{R}{r} + t_i + \frac{Lt_d}{T_t} + \frac{L}{T_t}\left(\frac{C_p}{(k_1+1)}\right) + Gt_s + Gt_p\right]$$

Labels (left to right): $\frac{S}{Min}$, Feeding time, Rapid traverse time, Load & unload time, Setup time, Cutter Index time, Dull tool replacement time, Tool depreciation cost, Tool resharpening cost, Rebrazing or blade reset cost, Insert or blade cost, Grinding wheel cost, Tool presetting cost

From reference 5

124

TABLE 23

OPTIMIZED MACHINING EQUATIONS

Optimized Cutting Speed Equations

For milling

$$v_{min.\ cost} = \left[\frac{nMD(L+e)}{3.82f_t L \left(Mt_d + \frac{C_p}{k_1+1} + Gt_s + \frac{Gt_b}{k_2} + \frac{ZC_s}{k_3} + C_w + Gt_p \right)} \right]^{\frac{n}{n+1}} (S_t)^{\frac{1}{n+1}}$$

$$v_{max.\ prod.} = \left[\frac{nD(L+e)}{3.82f_t L t_d} \right]^{\frac{n}{n+1}} (S_t)^{\frac{1}{n+1}}$$

For drilling or reaming

$$v_{min.\ cost} = \left[\frac{nMD(L+e)}{3.82f_r L \left(Mt_d + \frac{C_p}{k_1+1} + Gt_s + Gt_p \right)} \right]^{\frac{n}{n+1}} (S_t)^{\frac{1}{n+1}}$$

$$v_{max.\ prod.} = \left[\frac{nD(L+e)}{3.82f_r L t_d} \right]^{\frac{n}{n+1}} (S_t)^{\frac{1}{n+1}}$$

Optimized Tool Life Equations

For milling, drilling, reaming, or tapping

$$T_t\ min.\ cost = \left[\frac{S_t}{v_{min.\ cost}} \right]^{\frac{1}{n}}$$

$$T_t\ max.\ prod. = \left[\frac{S_t}{v_{max.\ prod.}} \right]^{\frac{1}{n}}$$

Equations for Operation Time per piece and production rate

Milling

$$t_m = \frac{D(L+e)}{3.82f_t v} + \frac{R}{r} t_i + \frac{Lt_d}{2T_t}$$

Drilling and reaming

$$t_m = \frac{D(L+e)}{3.82f_r v} + \frac{R}{r} t_i + \frac{Lt_d}{T_t}$$

Equation for production rate

$$P = \frac{60}{\left(\Sigma t_m + t_L + \frac{t_o}{N_L} \right)}$$

From reference 5

125

TABLE 24

SYMBOLS FOR COST AND PRODUCTION RATE EQUATIONS

Symbol	Definition	Mill	Drill and Ream	Center Drill
			Applies to Operation	
C	Cost for machining one workpiece; $/workpiece			
C_c	Cost of each insert or inserted blade; $/blade		No	No
C_p	Purchase cost of tool or cutter; $/cutter			
C_w	Cost of grinding wheel for resharpening tool or cutter; $/cutter		No	No
d	Depth of cut; in.		No	No
D	Dia of work in turning, of tool in milling, drilling, reaming, tapping; in.			
e	Extra travel at feedrate (f_r or f_t) including approach, overtravel, and all positioning moves; in.			
f_r	Feed per revolution; in./rev	No		
f_t	Feed per tooth; in./tooth		No	No
G	Labor + overhead in tool reconditioning department; $/min			
K_1	Number of times lathe tool, milling cutter, drill, reamer, or tap is resharpened before being discarded			
K_2	Number of times lathe tool or milling cutter is resharpened before inserts or blades are rebrazed or reset		No	No
K_3	Number of times blades (or inserts) are resharpened (or indexed) before blades (or inserts) are discarded			
L	Length of workpiece in turning and milling or sum of length of all holes of same diameter in drilling, reaming, tapping; in.			
m	Number of threads per inch	No	No	No
M	Labor + overhead cost on lathe, milling machine or drilling machine; $/min			
n	Tool life exponent in Taylor's equation			No
N_L	Number of workpieces in lot			
P	Production rate per 60 min hour; workpieces/hr			
r	Rapid traverse rate; in/min			
R	Total rapid traverse distance for a tool or cutter on one part; in.			
S	Reference cutting speed for a tool life of $T = 1$ min; ft/min	No	No	No
S_t	Reference cutting for a tool life of $T_t = 1$ in; ft/min			No
t_h	Time to rebraze lathe tool or cutter teeth or reset blades; min		No	No
t_d	Time to replace dull cutter in tool changer storage unit; min			
t_j	Time to index from one type cutter to another between operations (automatic or manual); min			
t_L	Time to load and unload workpiece; min			
t_m	Time (average) to complete one operation; min			
t_o	Time to setup machine tool for operation; min			
t_p	Time to preset tools away from machine (in toolroom); min			
t_s	Time to resharpen lathe tool, milling cutter, drill, reamer or tap; min/tool			
T	Tool life measured in minutes to dull a lathe tool; min	No	No	No
T_h	Number of holes per resharpening	No	No	
T_t	Tool life measured in inches travel of work or tool to dull a drill, reamer, tap, or one milling cutter tooth; in.			No
u_c	Number of holes center drilled or chamfered in workpiece	No	No	
v	Cutting speed; ft/min			
w	Width of cut; in.		No	No
z	Number of teeth in milling cutter or number of flutes in a tap		No	No

From reference 5

126

TABLE 25

VALUES USED IN COST EQUATION FOR CALCULATION OF MACHINING COSTS OF TEST PARTS

No.	Symbol	Definition	Units	Rough End Milling	Finish End Milling	Drilling	Reaming
					Values		
1	Cp	Purchase cost of tool or cutter	$/cutter	22.00	22.00	6.00	6.00
2	c_w	Cost of grinding wheel for re-sharpening tool or cutter	$/cutter	0.0416	.0416	.0416	.0416
3	D	Diameter of tool	Inch	1.000	1.000	23/64	3/8
4	e	Extra travel at feed rate including approach, over-travel and all positioning moves	Inch	126	31.5	25	25
5	f_t	Feed per *	Inch/*	.001 to .005	.001 to .005	.001 to .003	.0015 to .0045
6	G	Labor + overhead in tool re-conditioning department	$/minute	0.2165	.2165	.2165	.2165
7	k_1	Number of times milling cutter. drill or reamer is resharpened before being discarded		10	10	10	20
8	L	Length of workpiece in milling or sum of length of all holes of same diameter in drilling or reaming	Inch	490	119	137.5	137.5
9	M	Labor + overhead cost on machine	$/minute	0.40	0.40	0.40	0.40
10	t_d	Time to replace dull tool in tool changer storage unit	Minutes	2	2	2	2
11	t_p	Time to preset tools away from machine (in tool room)	Minutes	10	10	10	10
12	t_s	Time to resharpen tool	Minutes/tool	30	30	12	18
13	R	Total rapid traverse distance	Inches/part	616	150	250	250
14	r	Rapid traverse rate	Inches/minute	100	100	200	200
15	t_i	Time to index from one type cutter to another between operations	Minutes	0	0	0	0
16	t_t	Tool life in distance of work travel to dull tool	Inches	Per tool life equation		Per	data

*Per tooth for end milling; per revolution for drilling or reaming.

127

Heat-Treat Studies

The various heat-treat cycles investigated in developing premachining heat-treat schedules and the resulting hardness values are listed in Table 26. The Rockwell hardness data are plotted in Figure 57 as a function of aging temperature with austenitizing temperature as a parameter. The high hardness values obtained with most aging conditions after austenitizing at 1,375° and 1,625° F prompted evaluation of austenitizing temperatures between 1,250° and 1,375° F.

As-quenched hardness was found to increase with increasing austenitizing temperature to a maximum of 48 R_c for the 1,625° F austenitizing treatment (specimen 4E). Air cooling compared to water quenching after 16 hours at 1,250° F (specimen G versus 5A) resulted in an increase in R_c hardness of five points. A slight increase in hardness (1.6 R_c) for air-cooled specimens was also obtained on reducing the 1,250° F soak time from 16 hours (specimen G) to 8 hours (specimen F). There was a fairly substantial increase in hardness (4.5 R_c) as a result of the subzero treatment given to the 1,250° F, 24-hour, water-quenched specimen (5B) when compared to the 1,250° F, 16-hour, water-quenched specimen (5A) without the subzero treatment. The subzero treatment applied to the 1,375° F, 16-hour, water-quenched specimen (5D) resulted in only a slight increase in hardness (1.6 R_c), compared to that of the 1,375°, 8-hour, water-quenched specimen (5C) without the subzero treatment.

These results are explained on the basis of carbide conglomeration/dissolution and reverted austenite effects in the following manner:

1. The increase in water-quenched hardness with increasing austenitizing temperature is due to increased dissolution of carbides. This effect can be seen by comparing Figures 58, 59, and 60. The high density of carbides in specimen 5B (1,250° F) indicates much less dissolution of carbides than in specimen 4E (1,625° F). The carbide density in specimen 5D (1,375° F) is intermediate to the densities in specimens 5B and 4E.

2. The increase in hardness obtained by air cooling from 1,250° and 1,300° F austenitizing temperatures (specimens 1F, G, and 3H) compared to water quenching is attributed to partial aging of the freshly formed martensite during the slow cooling from the M_s temperature to room temperature.

3. The decrease in as-quenched hardness with increased soak time at 1,250° F (specimens G and 1F) is attributed to conglomeration of the undissolved carbide particles. This effect would be too subtle to be seen metallographically at a magnification of 1,000x.

128

TABLE 26

PHASE I MACHINABILITY HEAT TREATMENTS

Specimen No.	Material Condition (Heat L3550 K20)	Rc Hardness***
5A	1,250F - 16 hr - water quench	31.9
1A	Same as 5A + 600F**	36.6
2A	Same as 5A + 750F	37.6
3A*	Same as 5A + 850F	38.4
4A*	Same as 5A + 950F	36.2
5B	1,250F - 24 hr - water quench + -100F - 1 hr	36.4
1B	Same as 5B + 600F	38.0
2B	Same as 5B + 750F	39.1
3B	Same as 5B + 850F	39.2
4B*	Same as 5B + 950F	36.0
1F*	1,250F - 8 hr - air cool	38.7
2F*	Same as 1F + 850F	39.6
G	1,250F - 16 hr - air cool	37.1
3H	1,300F - 8 hr - air cool	40.1
1H	Same as 3H + 850F	42.4
2H	Same as 3H + 950F	38.9
5H	1,300F - 2 hr - air cool	40.8
6H	1,300F - 4 hr - air cool	40.3
7H	1,300F - 6 hr - air cool	40.3
4H*	Same as 6H + 850F - 24 hr	37
5C	1,375F - 8 hr + water quench	43.3
1C	Same as 5C + 600F	44.7
2C	Same as 5C + 750F	46.2
3C	Same as 5C + 850F	46.4
4C*	Same as 5C + 950F	40.4
6C*	Same as 5C + 1050F	38.5
5D	1,375 - 16 hr - water quench + -100F - 1 hr	44.9
1D	Same as 5D + 600F	45.0
2D	Same as 5D + 750F	47.3
3D	Same as 5D + 850F	46.3
4D	Same as 5D + 950F	40.1
4E	1,625F - 2 hr - water quench	48
3E	Same as 4E + 850F	51
1E	Same as 4E + 1,050F	43
2E*	Same as 4E + 1,150F	39.3

Notes:

   *Selected for machinability evaluation
  **All aging times 5 hours unless stated otherwise
 ***Average of four readings

129
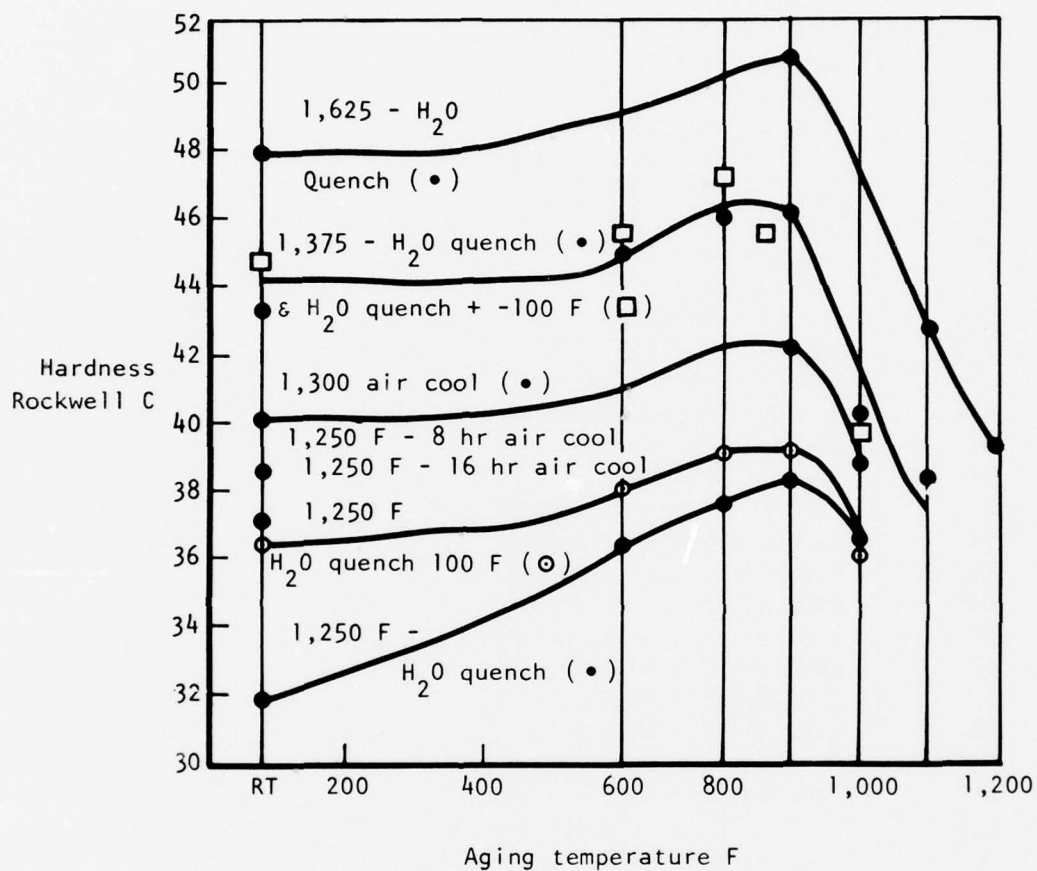
Figure 57. Aging response curves with austenitizing treatments as a parameter.

130
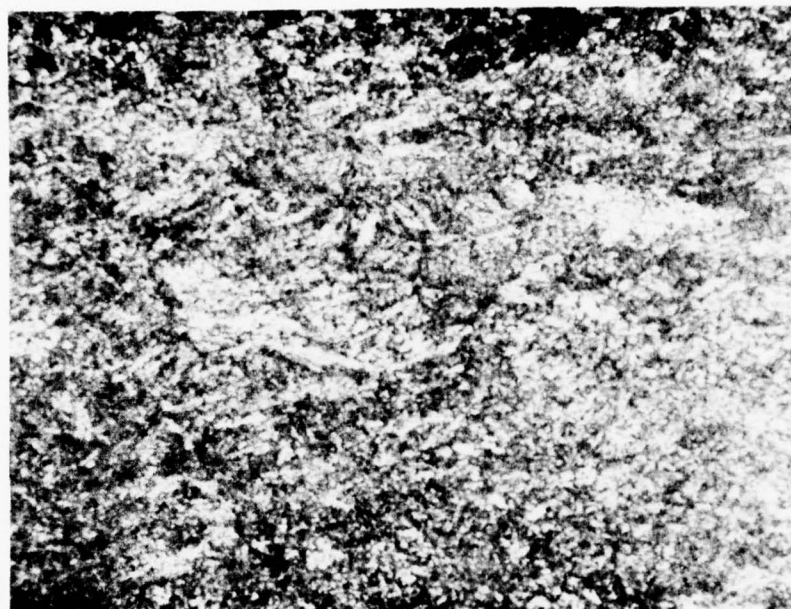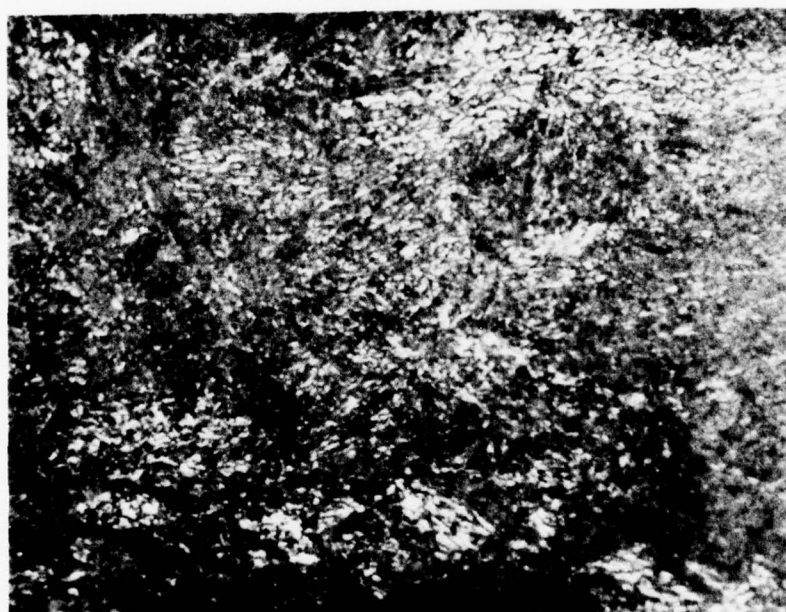
250X   NITAL ETCH

1,000X   NITAL ETCH

1,250 F - 24 HR - WATER QUENCH + -100 F - 1 HR

Figure 58. Microstructure of specimen 5B.

250X   NITAL ETCH

1,000X   PICKRAL ETCH

1,625 F - 2 HR - WATER QUENCH

Figure 59. Microstructure of specimen 4E.

132
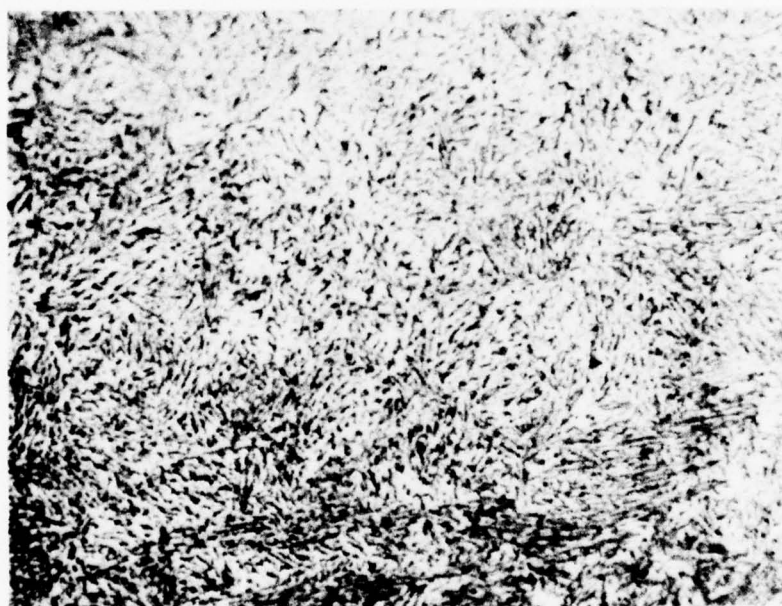
250X   NITAL ETCH

1,000X   NITAL ETCH

1,375 F - 16 HR - WATER QUENCH + -100 F - 1 HR

Figure 60. Microstructure of specimen 5D.

155

4. The larger increase in hardness resulting from the subzero treatment of the 1,250° F austenitized specimen (5B) compared to the water-quenched-only specimen (5A) is probably because of transformation of some retained austenite that had been sufficiently enriched with nickel by partitioning to lower the M_S below room temperature but above -100° F. The increase in hardness resulting from subzero treatments of the 1,350° F austenitized specimen (5D) compared to the water-quenched-only specimen (5C) is similarly attributed to transformation of retained austenite. With the higher austenitizing temperature, however, less nickel partitioning occurs so that there is less retained austenite that can undergo transformation during subzero treatment, and a smaller hardness increase is observed.

The 1,300° F heat-treat tests on specimens 4H, 5H, 6H, and 7H were conducted to establish the effect of austenitizing soak time on as-quenched hardness. The data indicate a small decrease in hardness (1/2 R_C point) when the austenitizing time is increased from 2 to 4 hours, whereas increasing the soak time from 4 to 8 hours has no further effect on as-quenched hardness.

PRELIMINARY SELECTION OF MACHINABILITY HEAT-TREAT CONDITIONS

Based on the metallurgical evaluation, eight heat-treat conditions were selected for machinability testing. The selections were made on the basis of metallographic appearance, Rockwell hardness, and the reported achievement of minimum material toughness on aging at 850° F (Reference 6). Two additional heat treatments were established and evaluated on the basis of the machining results obtained on the eight initial specimens.

Differences in microstructure resulting from the various heat treatments of the specimens selected for the machinability tests are primarily evident in the as-quenched condition, and provide only a coarse selection criteria. The microstructures become more similar with increased aging times because of increased carbide precipitation. The only exception to this pattern occurred with the 1,625° F austenitizing treatment. The maximum and minimum hardness values obtained from the 10 conditions were Rockwell C 40.4 and 36, respectively (Table 27).

Machinability Testing

Two sets of machining tests were conducted in phase I. They were designed to screen the relative machinability of test specimens that had been subjected to the selected thermal treatments. The type of tool, tool material, tool geometry, edge condition, cutting rates, depth and mode of cut, progression of cuts, and volume of material removed were held constant during each set of tests. The amounts of landwear on the cutter periphery and corner radius primary angles were measured and used as criteria for ranking the various heat treatments.

134

TABLE 27

MACHINABILITY RANKING

Test No. *	Specimen No.		Specimen R/C Hardness	1st Test Landwear	Ranking	2nd Test Total Landwear	Final Ranking
1	3A	1,250 F - 16 hr, water quench, age 850 F - 5 hr	38.4	0.003	1	0.00475	2
2	4A	1,250 F - 16 hr, water quench, age 950 F - 5 hr	36.2	0.00425	7		
3	4B	1,250 F - 24 hr, water quench, -100 F - 1 hr, age 950 F - 5 hr	36.0	0.00375	5		
4	1F	1,250F - 8 hr, air cool	38.7	0.00325	2	0.0045	1
5	2H	1,300 F - 8 hr, air cool, age 950 F - 5 hr	39.6	0.0035	4	0.006	4
6	4C	1,375 F - 8 hr, water quench, age 950 F - 5 hr	40.4	0.0045	8		
7	6C	1,375 F - 8 hr, water quench, age 1,050 F - 5 hr	38.5	0.00325	3	0.00525	3
8	2E	1,625 F - 2 hr, water quench, age 1,150 F - 5 hr	39.3	0.00375	6		
9	2F**	1,250 F - 8 hr, air cool, age 850 F - 5 hr	37.1			0.00525	3
10	4H**	1,300 F - 4 hr, air cool, age 850 F - 24 hr	37.0			0.00475	2

*End mill serial number.
**Added subsequent to first 8 tests, but same total volume of material removed

135

The results obtained on testing the machinability of AF1410 steel, after being subjected to the various premachining heat treatments, are presented in Table 27. Specimens 2F and 4H were included to determine whether aging at 850° F would add to the improvement in machinability observed for the F and H austenitizing conditions.

Table 21 lists the various tool geometry features that were checked and recorded on each end-mill cutter prior to testing. The average primary cutting angle was 9.7 ±0.48 degrees. The average indicator reading between the cutter shank and outside diameter at the primary cutting edge was 0.0003 ±0.00012 inch. Secondary relief angles had the greatest variation. The observed variations in cutter geometry were considered to be within normal tolerance and too small to influence machinability rankings.

Eight heat treatments were evaluated in the first set of machining tests to obtain the order of ranking presented in Table 27. There was a 50-percent difference in tool wear for the specimen in the heat-treat condition giving the most wear (specimen 4C - 0.0045-inch wear), compared with the specimen which had the least wear (specimen 3A - 0.003-inch wear). Specimens 1F and 6C followed specimen 3A very closely in ranking, with 0.00325-inch tool wear. Specimen 2H was fourth in order, with a tool wear of 0.0035-inch.

The top ranking of specimen 3A, which had been aged at 850° F, indicated a possibility of further improvement in the machinability of the 1,250° and 1,300° F air-cooled specimens if they were aged at 850° F. The 1,300° F air-cooled and 5-hour, 850° F aged specimen (1H) hardness was 42.4 R_c, which was considered to be too hard for good machinability; therefore, specimens 4H (aged 24 hours at 850° F, R_c 37) and 2F (aged 850° F, 5 hours - R_c 37.1) were included in the second set of phase I machinability screening test studies to provide six conditions (1F, 3A, 6C, 2H, 2F, and 4H) for further testing. This testing used the cutters used in the first set of tests without resharpening for specimens 1F, 3A, 6C, and 2H. New cutters were used for specimens 2F and 2H. The total volume of metal removed from each of the specimens was the same.

The results of the second set of specimens are also presented in Table 27. A change from first set rankings is evident. The ranking of specimen 1F is first with specimens 3A and 4H second, with about 5 percent greater wear. Machinability of these three conditions is essentially equivalent. The spread in total wear between the best condition (1F) and the poorest of the six (2H) was 33 percent (0.0015 inch). The best machining condition had a hardness of 38.7 R_c. All of the heat-treat conditions tested showed substantial improvement in machinability compared to either the as-received or full-hard material, as observed in the basic program.

136

Selection of Machinability Heat-Treat Conditions for Phase II Evaluation

On the basis of machinability and ease of heat treating, by either the mill or the user, the 1F condition was selected as the first choice for continuation into phase II. The second condition selected was the 4H condition. This choice was made over the 3A condition, which indicated equivalent machinability, because less distortion would result from air cooling, and also because the 4H condition would be a viable alternate in case retained reverted austenite* prevented proper full heat-treat response of material in the 1F condition. Hereafter the 1F and 4H treatment will be referred to as F and H respectively.

PHASE II - SELECTION OF PRE- AND POST-MACHINE-HEAT-TREAT COMBINATION

OBJECTIVE

The objective of this portion of the program was to establish a conventional quench and temper heat treatment for AF1410 steel which (1) is compatible with the premachining heat treatments selected in phase I to give maximum improvement in machinability, (2) permits adequate control of finished part dimensions, (3) results in satisfactory toughness properties in the 230 and 250 ksi ultimate strength heat-treat range, and (4) results in acceptable weldment mechanical properties.

APPROACH

A total of 54 specimens 1-inch thick were given various combinations of pre- and postmachining heat treatments, and then tested to determine tensile and Charpy impact values. The test results were used to evaluate the effect of the pre-machining heat treatments on the response of various subsequent postmachining heat treatments. On the basis of this evaluation, a final combination of pre- and postmachining heat treatments was selected, and refinement of the postmachining aging temperature was undertaken. The effect of the selected heat treatments on distortion and weldments was also evaluated. Subsequent heat-treat studies and toughness tests were performed on 2-inch-thick material when it appeared that air cooling would result in satisfactory response.

---

*Snide (Reference 6) states that austenite formed at 1,250° F completely transforms on quenching to room temperature, whereas Little and Machmeier (Reference 1) state that there will be 4 to 6 percent retained austenite on quenching from a 5-hour 1,250° F aging treatment.

EXPERIMENTAL

Specimen Preparation

Heat-Treat Response

A total of 55 AF1410 steel blocks were machined to a size of 1 by 2 by 6 inches from as-received stock that had been final rolled and air cooled from 1,570° F. Twenty-seven of these blocks were then subjected to the Type F and 27 to the Type H premachining heat treatments, (numbers 1 and 2 of Table 28). Of the 27 blocks in each group, 10 were postmachine heat-treated with air cooling, 10 with oil quenching, and seven with water quenching from austenitizing temperatures of 1,450°, 1,500°, 1,600°, and 1,650° F. Selected blocks were further cooled to -100° F to promote additional transformation of austenite to martensite. All of the blocks were aged at 950° F for 5 hours. The postmachining heat treatments used are summarized in Table 28 and Figure 61. The 55th block was given the standard AF1410 heat treatment (number 4 of Table 28) without being subjected to the premachining heat treatment for comparison purposes.

Each heat-treated block was machined and sectioned to obtain three, round tensile specimens per ASTM E8 and three, standard Charpy impact specimens per ASTM E23 (Figure 62).

Aging Response Specimens

Three, round tensile specimens and three, Charpy impact specimens were machined per ASTM E8 and ASTM E23, respectively, from each of 11 AF1410 blocks, 1 by 2 by 6 inches. These blocks had been given the "F" premachining heat treatment followed by a postmachining heat treatment (1,650° F for 1 hour, air cooled, austenitized at 1,525° F for 4 hours, oil quenched, -100° F for 1 hour, age) with variations in aging temperature (925° to 975° F) and time. Also for one set of specimens, the 1,650° F normalizing step was eliminated to evaluate if this would significantly affect mechanical properties.

Fracture Toughness Specimen

Two compact tension fracture toughness specimens were machined per ASTM E399 from each of three 2-inch thick blocks of AF1410 steel. The blocks had been given the "F" premachining heat treatment, and then subjected to the selected postmachining heat treatment (1,650° F for 1 hour, air cooled, austenitized at 1,525° F for 1 hour, quench, -100° F for 1 hour, age +950° F for 5 hours). Two of the specimens were air cooled, two were oil quenched and two were water quenched from the 1,525° F austenitizing temperature to establish the effect of cooling rate on fracture toughness. These blocks had been given the standard AF1410 heat treatment as a part of

TABLE 28

AF1410 HEAT TREATMENT PROCEDURES

No.	Type of Heat Treatment	Procedure
1	F premachining (per phase I)	1. Austenitize at 1,250° F for 8 hours 2. Air-cool
2	H premachining (per phase I)	1. Austenitize at 1,300° F for 4 hours 2. Air-cool 3. Age at 850° F for 24 hours
3	Postmachining	1. Austenitize at 1,650° F for 1 hour 2. Air-cool 3. Austenitize for 1 hour at either 1,450°, 1,500°, 1,550°, 1,600° or 1,650° F 4. Either: a. Air cool b. Oil quench c. Water quench 5. Either: a. No refrigerated cooling b. Cool to -100° F 6. Age 950° F for 5 hours 7. Air-cool
4	Standard	1. Austenitize at 1,650° F for 1 hour 2. Water quench 3. Austenitize at 1,500° F for 1 hour 4. Water quench 5. Age at 950° F for 5 hours 6. Air cool

PREMACHINE:
HEAT TREATMENTS

"F"   "H"

MACHINE

AUSTENITIZE AT 1650°F, FOR 1 HOUR, AIR COOL

AUSTENITIZE

1450°F   1500°F   1550°F   1600°F   1650°F

AC   OQ   WQ   AC   OQ   WQ   AC   OQ   WQ   AC   OQ   WQ   AC   OQ   WQ

+   +   0   +   +   0   +   +   0   +   +   0   +   +   0
0   0   0   0   0   0   0   0   0   0

AGE 950°F FOR 5 HOURS

AIR COOL

Legend

AC = Air Cooled
OQ = Oil Quenched
WQ = Water Quenched
0 = No Refrigerated Cool
+ = -100°F Cool
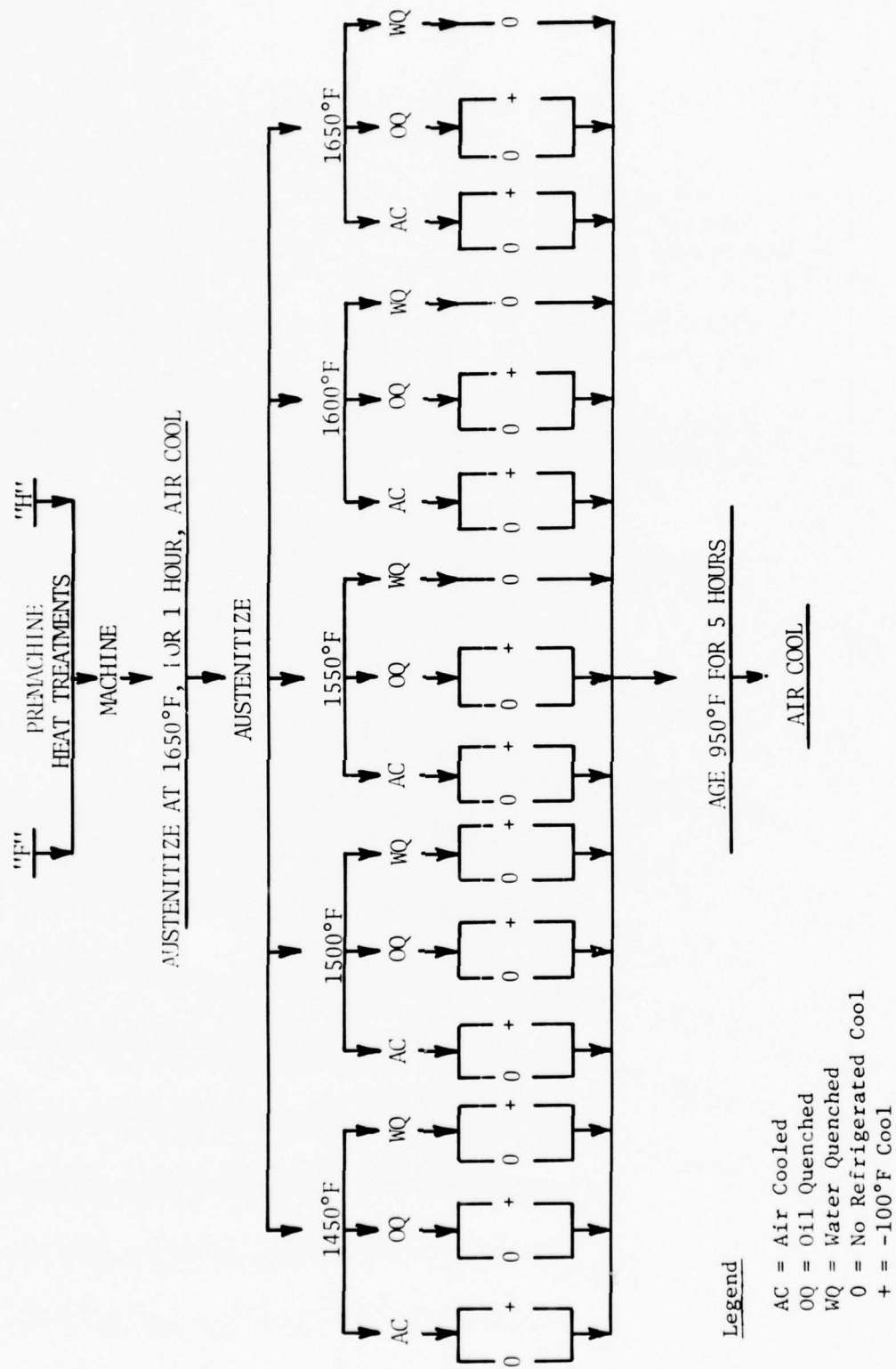
Figure 61. Flow chart showing the various heat-treatment sequences evaluated.

140
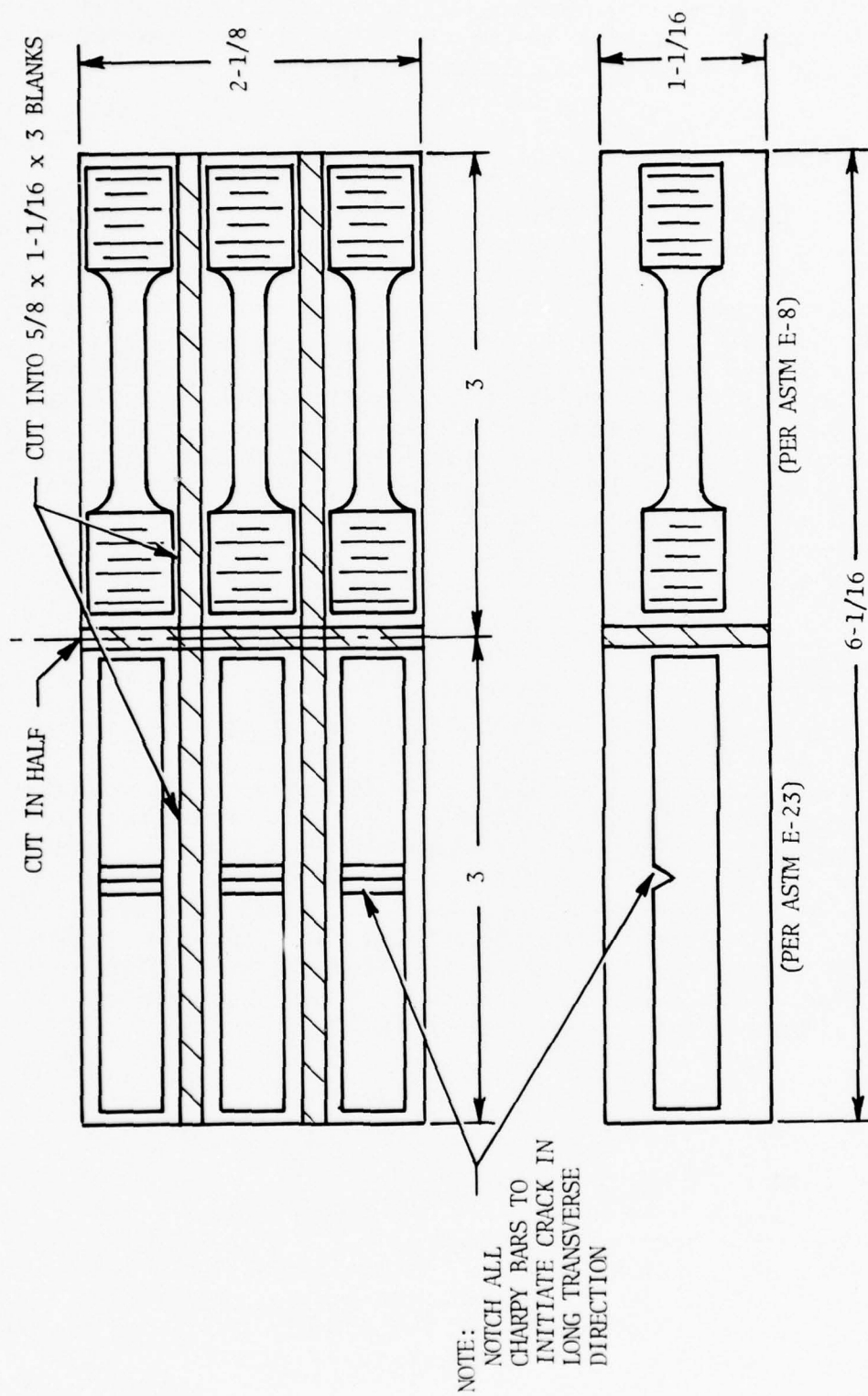
Figure 62. Sectioning and machined of AF1410 specimens for mechanical testing.

141

the basic program prior to being directed to this effort. Therefore, a seventh fracture toughness specimen was machined as a control specimen from stock that had not been subjected to the standard AF1410 heat treatments. It was heat treated along with the oil-quenched specimens.

Weld Specimens

Two AF1410 steel plates, 5/8 by 6 by 18 inches, each with a centrally located "K" weld along the 18-inch direction, were prepared. The "K" joint has one face of the joint prepared with a double bevel and the other has a square butt configuration. This was used to obtain a heat-affected zone having uniform structure through the plate thickness for impact testing. One plate, labeled AW, was welded in the premachine heat-treat condition, after which it was given the complete final heat treatment. The other plate, labeled BW, was given the premachined heat treat, normalized, austenitized, subzero treated, welded, and then aged only. Both plates were sectioned to give transweld blanks for machining into round tensile and Charpy impact test specimens containing the weld in the test sections.

RESULTS

Heat Treat Response

Microstructure

The microstructure of AF1410 steel in the full-hard condition obtained with the standard heat treatment is shown in Figure 63. At the magnification (250X) shown, there is no apparent difference between this microstructure and that obtained when the material in the premachining heat-treat conditions is subjected to the various austenitizing temperatures and cooling rates listed in Figure 61. Typical photomicrographs of these microstructures are shown in Figures 64 through 66. The similarity in microstructure persists when examined at higher magnifications with both light and electron microscopes, as noted in subsequent Metallurgical Evaluation.

Tensile

The peak tensile yield strength values, Tables 29 through 31, and Figures 67 through 72, occur in the 1,550° F austenitizing range and exhibit an increasing trend with increasing cooling rate (i.e., from air cooling to oil quenching to water-quenching, the tensile yield strength increases from 223 to 229 to 231 ksi, respectively). These values were obtained by cooling to -100° F to provide an increase of from 3 to 8 ksi in tensile yield strength of specimens austenitized at 1,500° to 1,650° F.

142
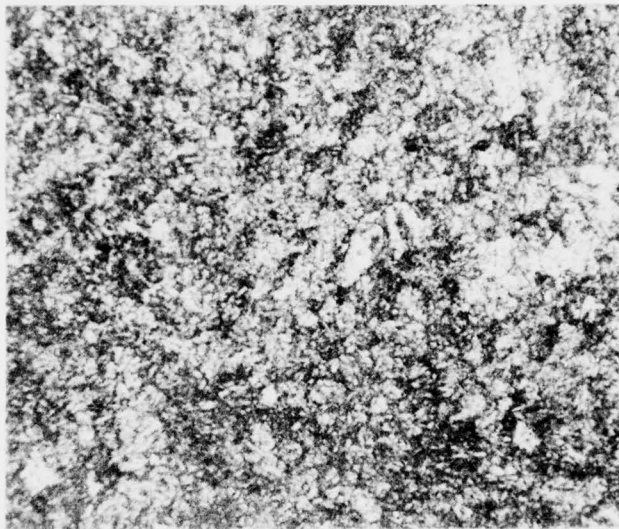
Doubly austenitized: 1,650° F for 1 hour,
water quenched; 1,500° F for 1 hour, water
quenched.

Aged: 950° F for 5 hours. (250X)

Figure 63. AF1410 steel after standard full-hard heat treatment.
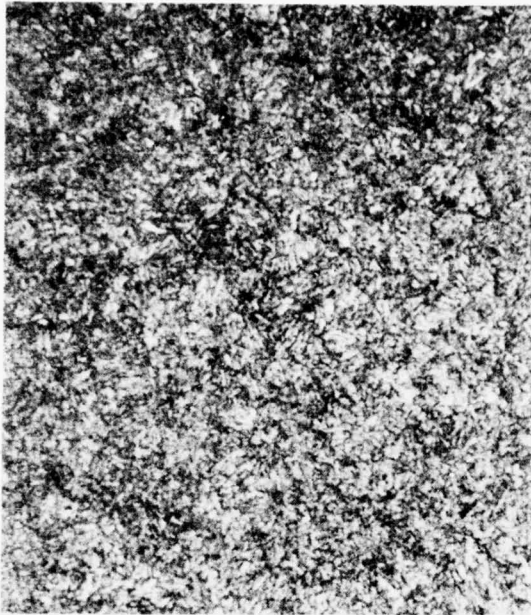
Austenitized at 1,500° F, and air quenched.
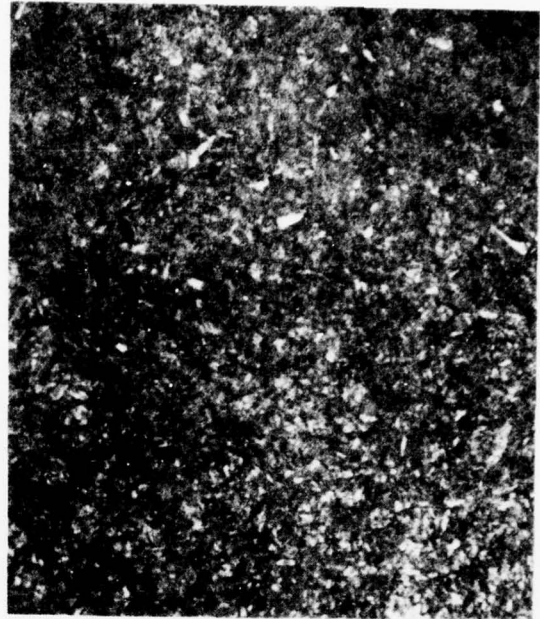
Austenitized at 1,500° F, air quenched, and cooled to -100° F.
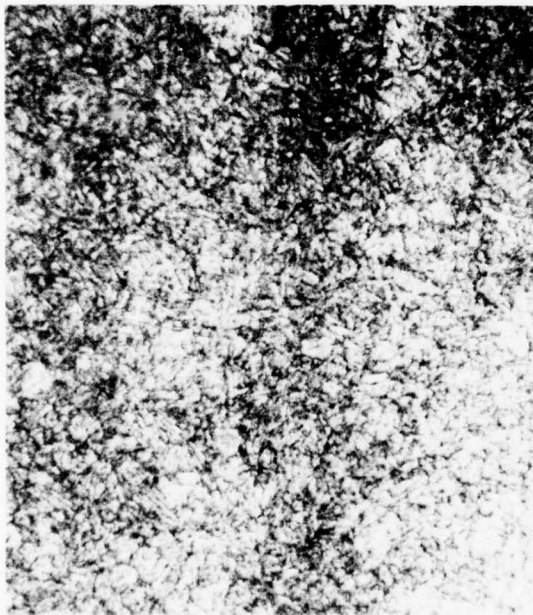
Austenitized at 1,550° F, and air quenched.

Austenitized at 1,550° F, air quenched, and cooled to -100° F.

Figure 64. AF1410 steel variously fully heat treated using air cooling after being subjected to the "F" premachining heat treat (250X). (All specimens aged at 950° F for 5 hours.)

144
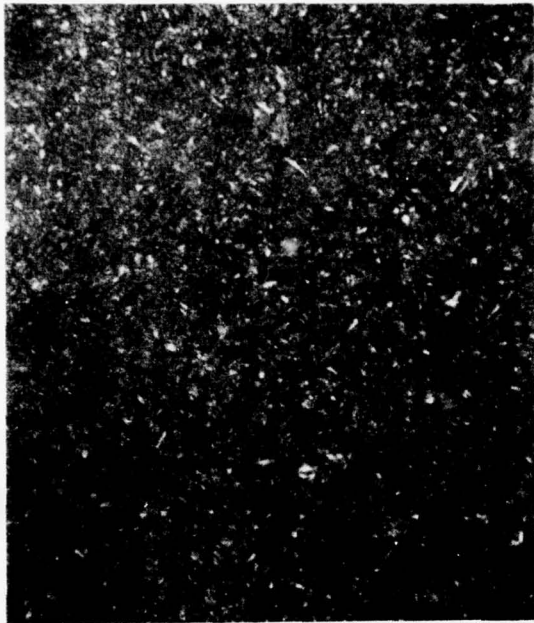
Austenitized at 1,500° F, and oil quenched.
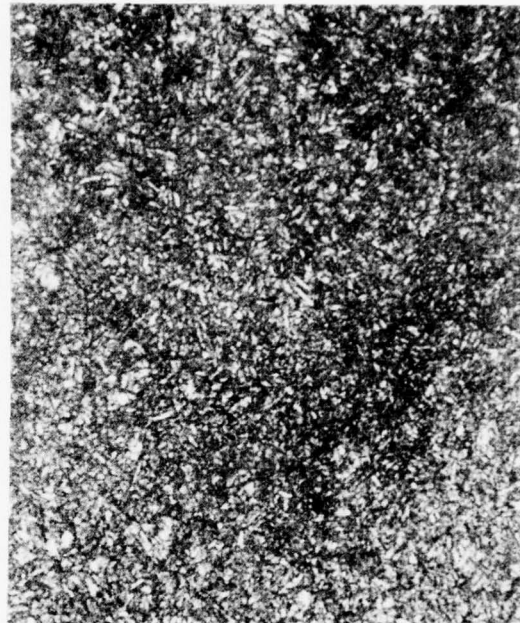
Austenitized at 1,500° F, oil quenched and cooled to -100° F.
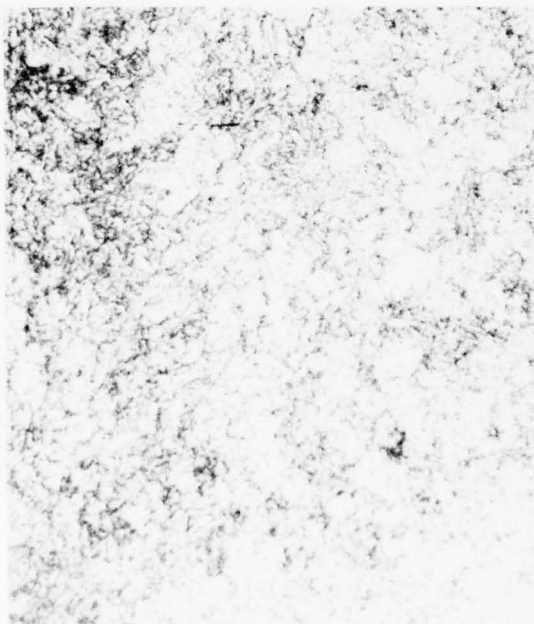
Austenitized at 1,550° F, and oil quenched.
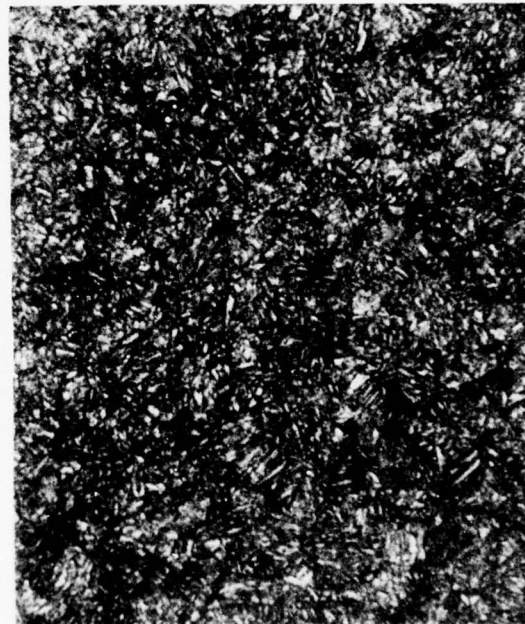
Austenitized at 1,550° F, oil quenched and cooled to -100° F.

Figure 65. AF1410 steel variously fully heat treated using oil quenching after being subjected to the "F" premachining heat treat (250X). (All specimens aged at 950° F for 5 hours.)

145
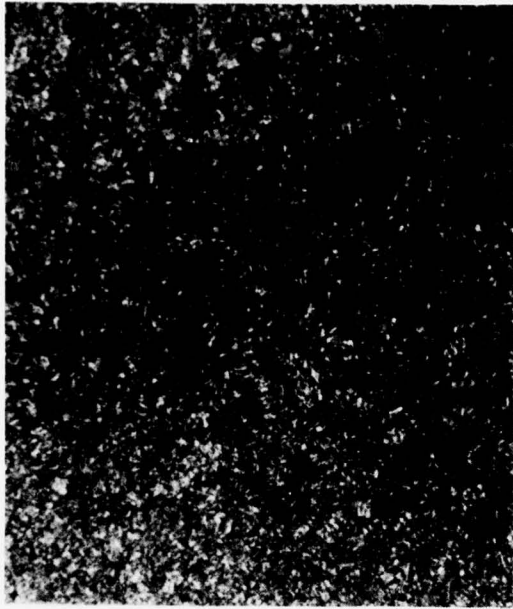
Austenitized at 1,500° F, and water quenched.
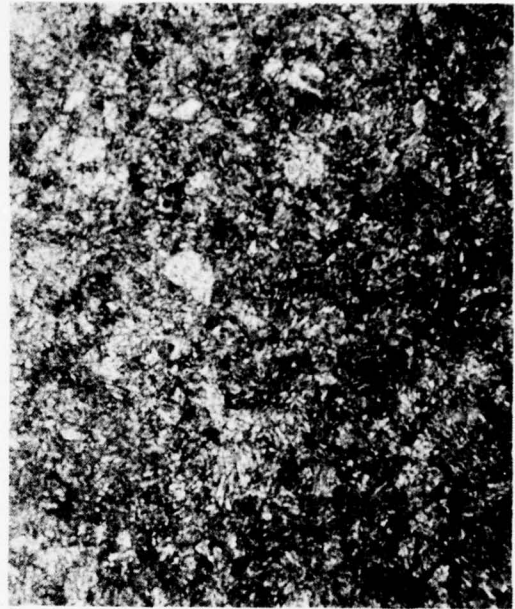
Austenitized at 1,500° F, water quenched and cooled to -100° F.
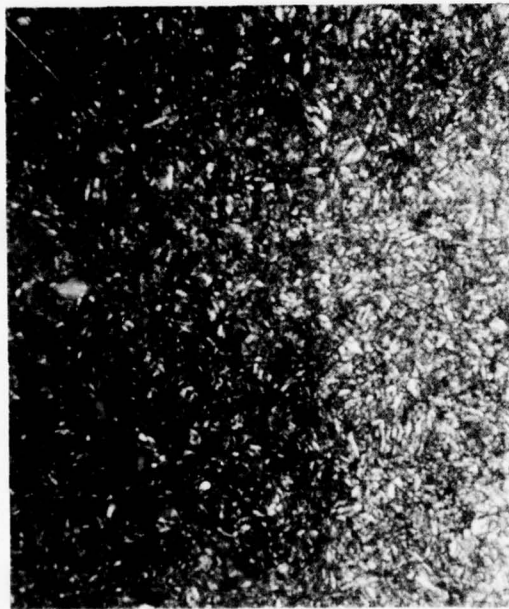
Austenitized at 1,550° F, and water quenched.

Figure 66. AF1410 steel variously fully heat treated with water quenching after being subjected to "F" premachining heat treat (250X). (All specimens aged at 950° F for 5 hours.)

116
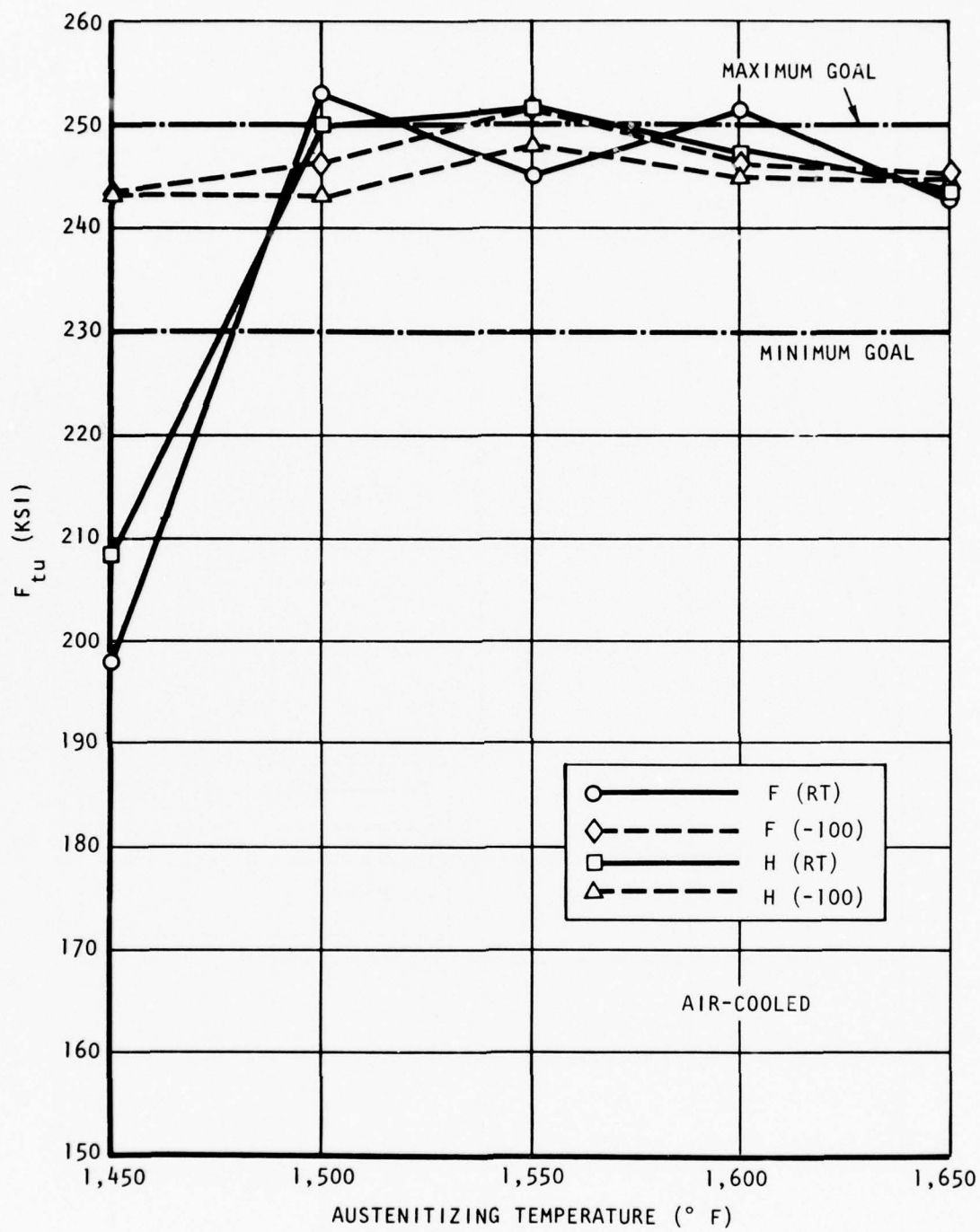
Figure 67. F_{tu} austenitizing and cooling temperature for air-cooled AF1410 steel.
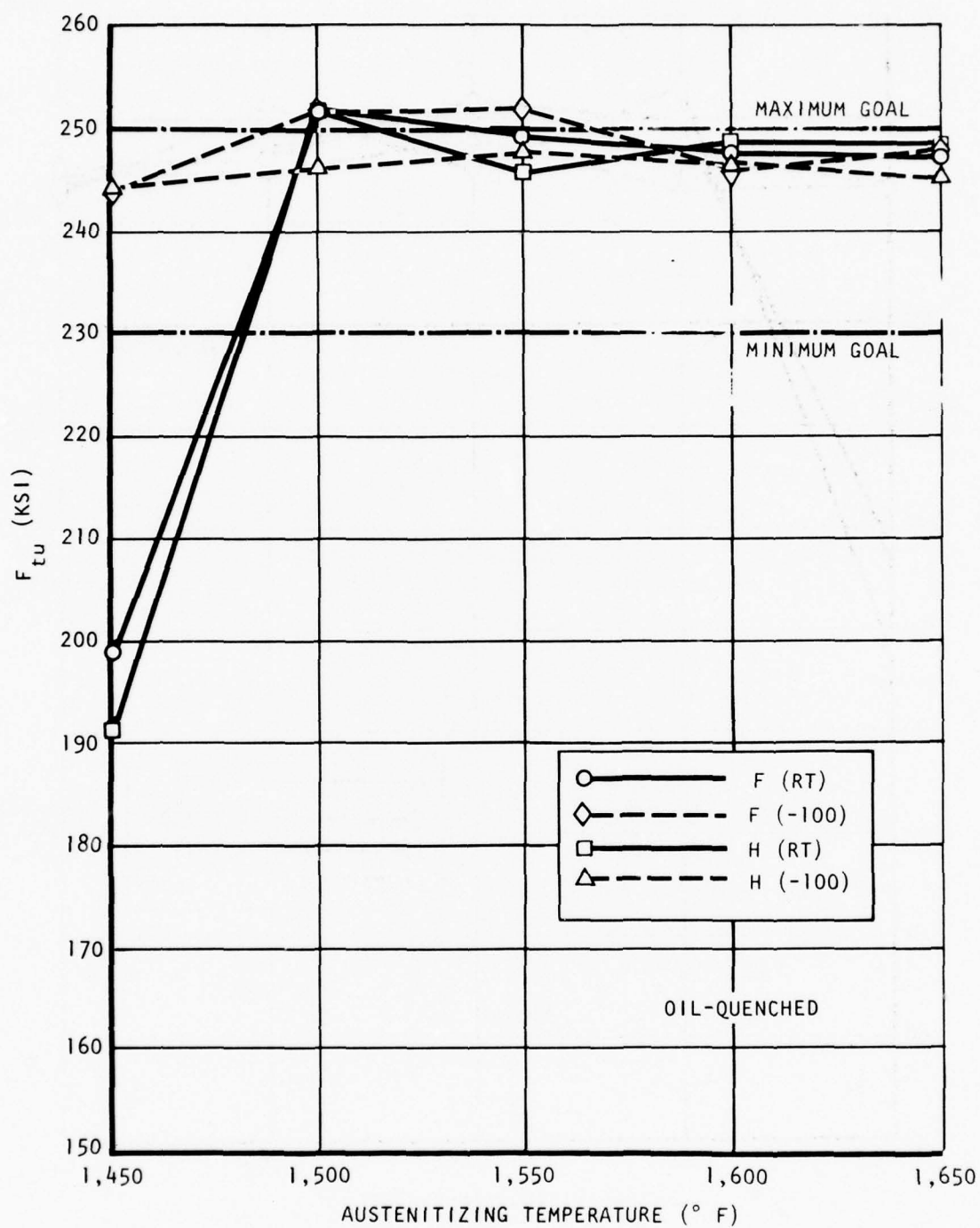
Figure 68. F_{tu} versus austenitizing and cooling temperature for oil-quenched AF1410 steel.

148
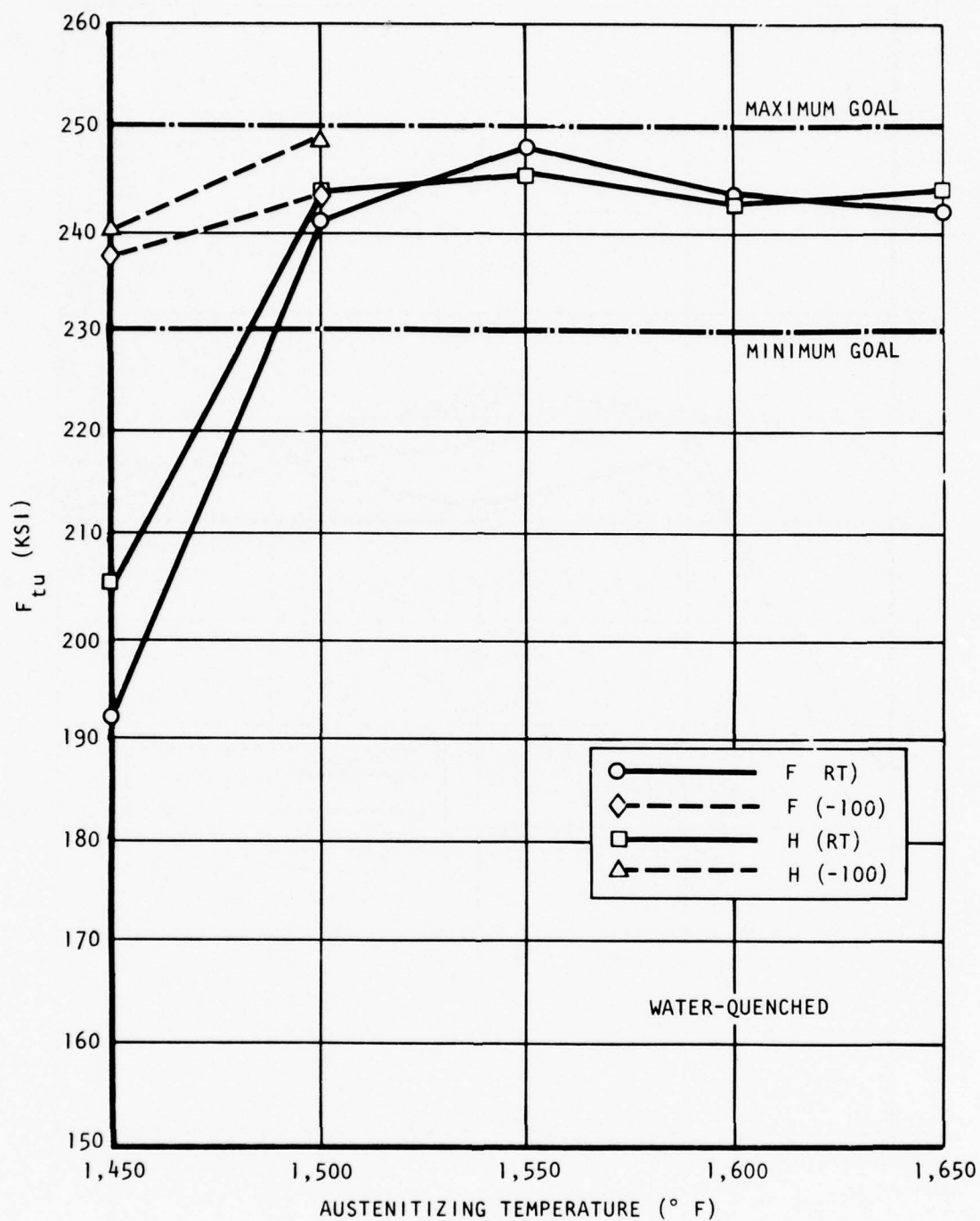
Figure 69. F_{tu} versus austenitizing and cooling temperature for water-quenched AF1410 steel.

149
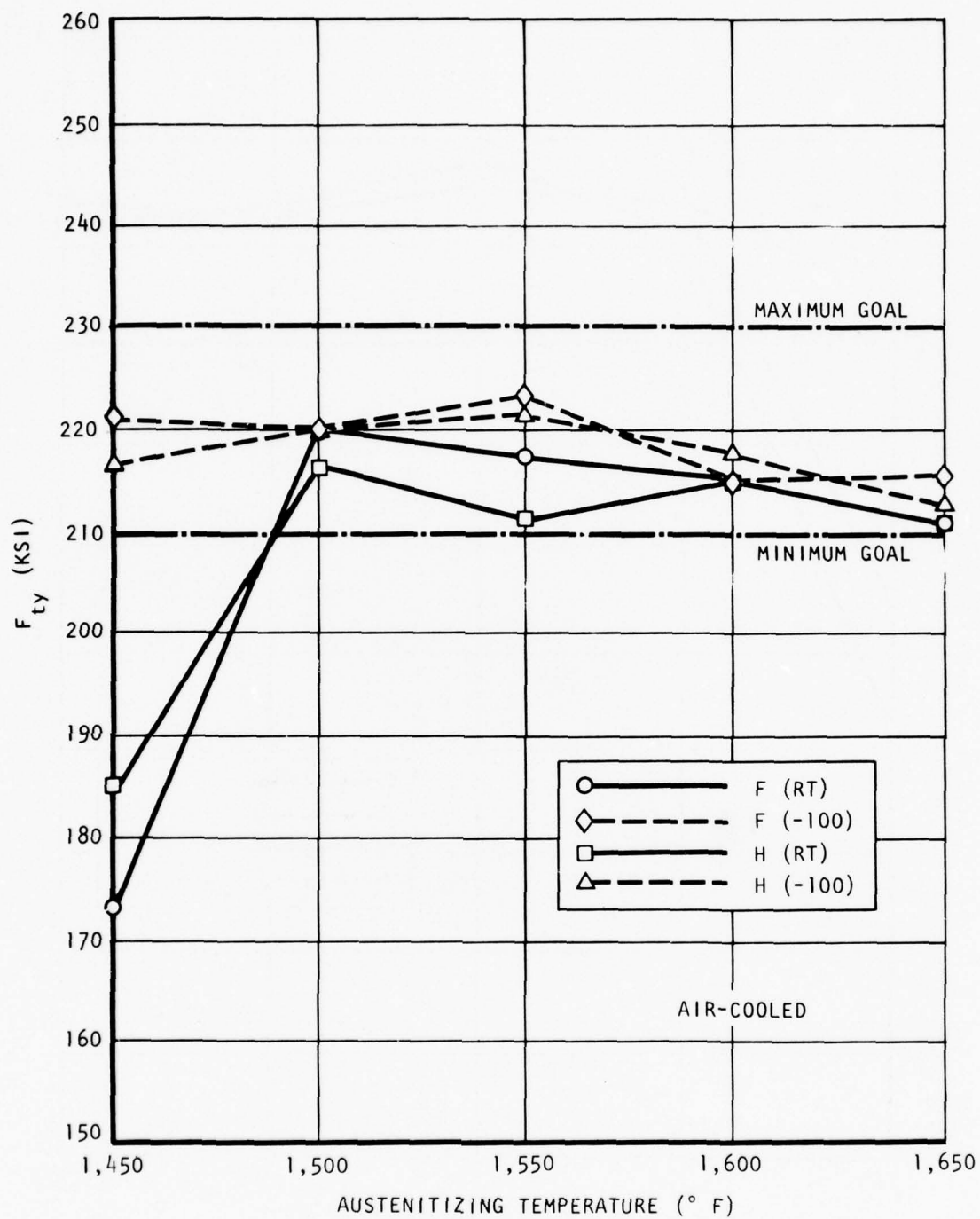
Figure 70. F_{ty} versus austenitizing and cooling temperature for air-cooled AF1410 steel.
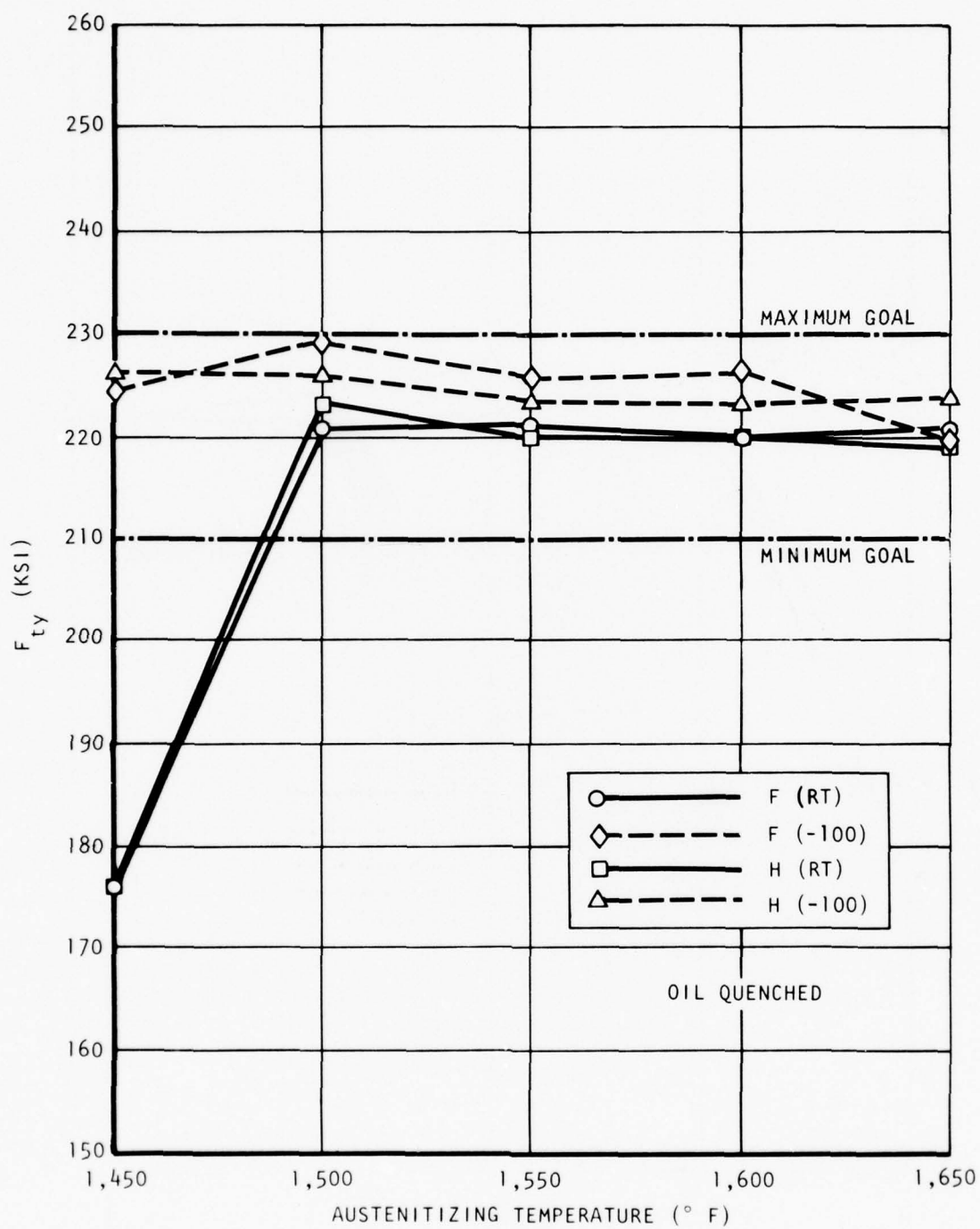
Figure 71. F_{ty} versus austenitizing and cooling temperature for oil-quenched AF1410 steel.

151
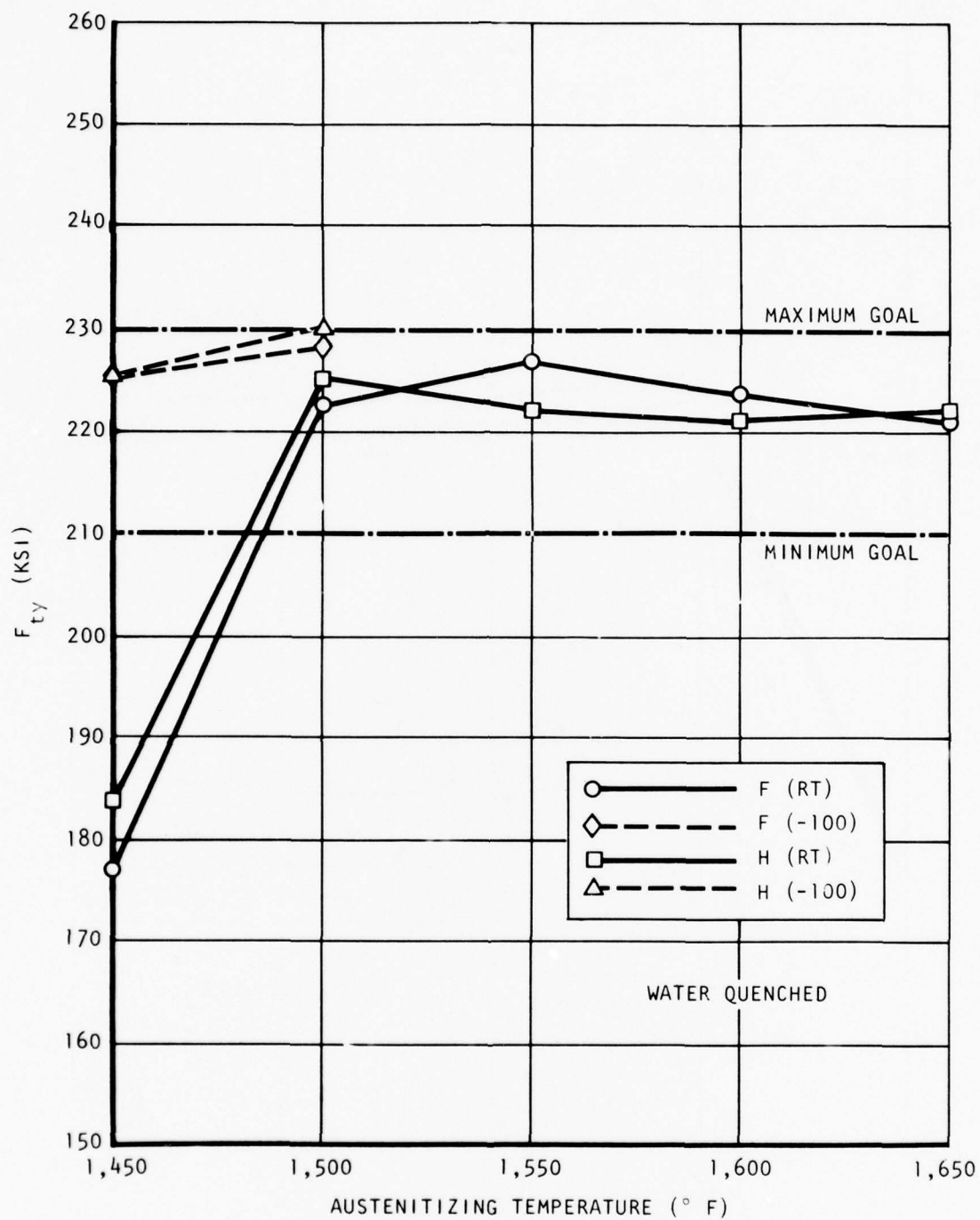
Figure 72. F_{ty} versus austenitizing and cooling temperature for water-quenched AF1410 steel.

152

The tensile ultimate strength is not strongly affected by the cooling rate. Peak values of about 252 ksi are observed with either air-cooled or oil-quenched specimens austenitized in the temperature range of 1,500° to 1,550° F with or without cooling to -100° F. Values for the water-quenched specimens peak in the 1,500° to 1,550° F temperature range at a value just below 250 ksi.

Specimens given the "F" premachining heat treatment had peak tensile ultimate and yield values from 1 to 6 ksi higher than those having the "H" premachining heat treatment. Thus, from the standpoint of maximizing tensile yield and ultimate strength values, the optimum heat-treat combination is the "F" pre-machining heat treatment followed by a postmachining heat treatment in which austenitizing is accomplished at 1,500° to 1,550° F.

Tensile Elongation and Reduction in Area

The values for elongation and reduction in area are presented in Tables 29, 30, and 31. The overall average values in the 1,500° to 1,650° F austenitizing temperature range are 16.1 +0.7 and 68.5 +1.9 percent, respectively. The small deviations show that the heat treatment combinations tested had little influence on elongation and reduction in area.

Charpy Impact Strength

The Charpy impact results are also presented in Tables 29, 30, and 31 and are shown graphically in Figures 73, 74, and 75. The minimum goal was 40 foot-pounds. These results show the air-cooled and oil-quenched specimens to have peak values in the 1,500° to 1,550° F austenitizing temperature range of near 54 foot-pounds, while the water-quenched peak value of 60 foot-pounds occurs at an austenitizing temperature of 1,600° F. In all cases, the peak value occurred when the material was in the "H" premachining heat-treatment condition. The "F" premachining heat treatment yielded peak Charpy impact values that were approximately 5 foot-pounds less than those obtained with the "H" premachining heat treatment.

Cooling to -100° F had little effect on the Charpy impact values except when austenitizing was done at 1,450° F where peak tensile ultimate strength and tensile yield strength values are not achieved. In the case of austenitizing at 1,450° F, subsequent cooling to -100° F caused the tensile ultimate strength, tensile yield strength, and Charpy impact values to increase on the order of 25 percent.

153

TABLE 29

MECHANICAL PROPERTIES OF AF1410 SPECIMENS HEAT TREATED WITH AIR COOLING*

| Spec | Heat Treat | | F_{ty} (ksi) | | F_{tu} (ksi) | | Elong (%) | | RA (%) | | CHARPY (ft-lb) | |
	Aust	Cooled	$\overline{X}$**	σ	$\overline{X}$**	σ	$\overline{X}$**	σ	$\overline{X}$**	σ	$\overline{X}$**	σ
F-1[1]	1,450	RT	173.3	1.5	198.3	1.2	16.0	0.0	47.0	5.2	32.7	0.8
F-7	1,500	RT	220.3	1.5	252.7	1.2	15.3	0.6	67.7	0.6	46.8	0.9
F-13	1,550	RT	216.7	1.2	245.3	1.5	16.3	0.6	69.0	2.0	47.3	1.7
F-17	1,600	RT	214.7	2.9	250.7	0.6	16.7	0.6	67.3	1.2	47.0	1.0
F-22	1,650	RT	210.7	3.1	243.3	1.6	16.3	0.6	67.0	0.0	41.0	1.0
F-2	1,450	-100	220.7	1.5	243.7	0.6	16.7	0.6	66.3	1.5	42.8	0.7
F-8	1,500	-100	219.0	3.0	246.0	1.0	16.7	0.6	68.7	1.2	45.5	0.5
F-14	1,550	-100	223.3	1.5	251.3	1.5	16.3	0.6	69.0	1.0	47.8	0.9
F-18	1,600	-100	215.0	1.7	245.7	1.2	15.7	0.6	68.3	1.2	49.3	5.3
F-23	1,650	-100	214.7	1.5	245.0	1.0	15.3	0.6	67.7	1.2	41.3	0.7
H-1[2]	1,450	RT	185.3	1.8	208.0	1.0	14.3	0.6	55.7	3.2	32.5	1.0
H-7	1,500	RT	216.3	4.6	250.7	1.2	15.7	0.6	69.3	0.6	49.8	5.4
H-15	1,550	RT	216.7	1.2	245.3	1.5	16.3	0.6	69.0	2.0	47.3	1.7
H-17	1,600	RT	215.3	3.5	246.7	1.5	15.7	1.2	69.0	0.0	49.9	1.7
H-22	1,650	RT	211.0	1.7	243.7	0.6	17.0	0.0	68.7	0.6	43.0	3.0
H-2	1,450	-100	216.0	2.7	243.0	1.0	16.0	0.0	69.3	2.1	47.8	1.8
H-8	1,500	-100	219.7	2.1	243.0	1.7	15.7	0.6	60.7	1.5	54.5	1.7
H-14	1,550	-100	220.7	3.2	248.3	1.2	16.0	0.0	68.0	2.0	49.2	2.2
H-18	1,600	-100	216.7	2.1	244.7	1.2	16.7	0.6	68.7	1.5	47.5	4.8
H-23	1,650	-100	212.0	2.0	244.5	1.5	16.7	0.6	69.0	0.0	52.5	2.6

*All specimens aged at 950° F for 5 hours (after air-cool) then air-cooled.
**Average value of 3 tests
(1) F = 1250° F - 8 hr - air cooled
(2) H = 1300° F - 4 hr - aged 840° F - 24 hr

154

TABLE 30

MECHANICAL PROPERTIES OF AF1410 SPECIMENS HEAT TREATED WITH OIL QUENCHING*

SPEC NO.	HEAT TREAT AUST TEMP (° F)	HEAT TREAT COOLED TO	F_{ty} (ksi) $\bar{X}$**	F_{ty} (ksi) σ	F_{tu} (ksi) $\bar{X}$**	F_{tu} (ksi) σ	ELONG. (%) $\bar{X}$**	ELONG. (%) σ	R.A. (%) $\bar{X}$**	R.A. (%) σ	CHARPY (ft-lb) $\bar{X}$**	CHARPY (ft-lb) σ
(1)												
F-3	1450	RT	176.0	1.0	199.0	0.0	15.0	0.0	52.3	1.6	34.0	0.5
F-9	1500	RT	221.0	3.5	252.3	1.3	16.0	0.0	69.0	1.0	44.0	1.7
F-15	1550	RT	220.7	2.6	249.3	1.2	15.7	0.7	69.0	1.0	44.7	3.8
F-19	1600	kT	220.0	2.6	247.7	2.2	16.0	0.0	69.3	0.8	41.8	9.5
F-24	1650	RT	219.7	2.1	247.7	2.0	15.0	0.0	68.3	0.8	48.5	2.2
F-4	1450	-100	224.7	1.9	243.7	2.2	15.0	1.0	68.0	0.0	41.5	1.0
F-10	1500	-100	229.3	4.3	251.7	1.7	16.0	0.0	69.0	1.0	44.2	0.3
F-16	1550	-100	225.3	2.5	242.0	1.0	16.0	0.0	69.0	0.0	45.0	1.5
F-20	1600	-100	226.0	3.6	246.3	2.4	15.7	0.7	69.0	0.0	43.2	1.5
F-25	1650	-100	218.7	1.6	248.3	1.2	15.7	0.7	67.3	1.3	44.8	4.5
(2)												
H-6	1450	RT	176.0	1.0	192.3	1.2	17.7	0.6	61.0	1.7	41.5	3.0
H-9	1500	RT	223.0	2.6	242.0	1.0	17.7	0.6	69.0	0.0	48.5	0.9
H-15	1550	RT	220.0	1.0	246.0	1.7	16.3	1.2	69.3	0.6	51.0	0.9
H-19	1600	RT	219.7	3.1	249.0	2.6	16.7	0.6	60.7	1.5	49.8	1.4
H-24	1650	RT	218.7	2.1	248.3	2.1	15.7	0.6	68.0	1.0	45.8	2.6
H-4	1450	-100	226.3	3.1	244.7	2.1	15.0	0.0	69.7	0.6	47.2	1.0
H-10	1500	-100	225.7	0.6	246.3	0.6	16.0	1.0	68.7	0.6	48.8	3.8
H-16	1550	-100	223.0	2.6	248.3	2.1	15.7	0.6	69.7	0.6	52.7	2.2
H-20	1600	-100	223.3	2.5	247.3	0.6	16.7	0.6	68.3	0.6	44.3	1.1
H-25	1650	-100	223.5	3.5	247.7	1.5	15.7	0.6	68.7	0.6	47.2	2.0

*All specimens aged at 950° F for 5 hours (after oil quench) then air-cooled.
**Average value of 3 tests
(1) F = 1250° F - 8 hr - air cooled
(2) H = 1300° F - 4 hr - aged 840° F - 24 hr

155

TABLE 31

MECHANICAL PROPERTIES OF AF1410 SPECIMENS HEAT TREATED WITH WATER QUENCHING*

SPEC NO.	HEAT TREAT AUST TEMP (°F)	COOLED TO	F_{ty} (ksi) $\overline{X}$**	σ	F_{tu} (ksi) $\overline{X}$**	σ	ELONG (%) $\overline{X}$**	σ	RA (%) $\overline{X}$**	σ	CHARPY (ft-lb) $\overline{X}$**	σ
(1)												
F-6	1450	RT	177.0	1.0	192.7	1.5	15.0	0.0	58.0	2.6	38.7	2.5
F-11	1500	RT	222.7	2.1	240.7	1.6	16.0	0.0	70.3	0.8	49.2	2.3
F-27	1550	RT	226.7	2.1	248.0	1.0	15.3	0.6	69.0	1.0	44.5	3.0
F-21	1600	RT	223.7	1.9	243.3	1.6	15.7	0.7	69.7	1.0	48.2	2.0
F-26	1650	RT	220.5	2.1	241.7	1.7	15.7	0.7	68.7	1.0	46.5	0.5
F-5	1450	-100	225.7	1.6	237.0	2.6	15.0	0.0	69.3	0.8	43.7	1.2
F-12	1500	-100	228.3	1.6	242.7	2.6	15.0	0.0	70.0	0.0	54.7	3.3
(2)												
H-3	1450	RT	184.0	1.0	205.0	1.7	14.3	0.6	56.3	2.1	33.7	1.6
H-11	1500	RT	225.3	1.5	243.3	2.1	15.0	0.0	69.0	1.0	50.3	4.0
H-27	1550	RT	222.0	1.0	245.0	1.7	16.0	0.0	68.7	0.6	55.2	1.0
H-21	1600	RT	221.0	1.7	242.0	2.6	17.3	0.6	70.3	0.6	60.8	3.1
H-26	1650	RT	222.0	1.7	243.3	4.9	17.7	0.6	69.7	1.5	52.7	2.0
H-5	1450	-100	226.0	2.6	240.0	2.6	15.0	0.0	70.7	0.6	51.0	1.8
H-12	1500	-100	230.7	2.3	248.7	3.1	16.0	0.0	69.0	1.0	53.8	0.9
PM + STD***	1500	RT	228.0	1.7	247.7	0.6	15.3	0.6	70.7	1.2	60.0	4.4
F + STD	1500	RT	227.0	0.0	250.3	1.2	16.0	0.0	69.0	1.0	48.0	1.7
H + STD	1500	RT	227.7	0.6	251.0	1.7	16.3	0.6	68.3	1.2	46.5	0.5

*All specimens aged at 950° F for 5 hours (after water quench) then air-cooled.

**Average Value of 3 Tests

***Std - Water quenched from 1650° F

(1) F = 1250° F - 8 hr - air cooled

(2) H = 1300° F - 4 hr - aged 850° F - 24 hr

156
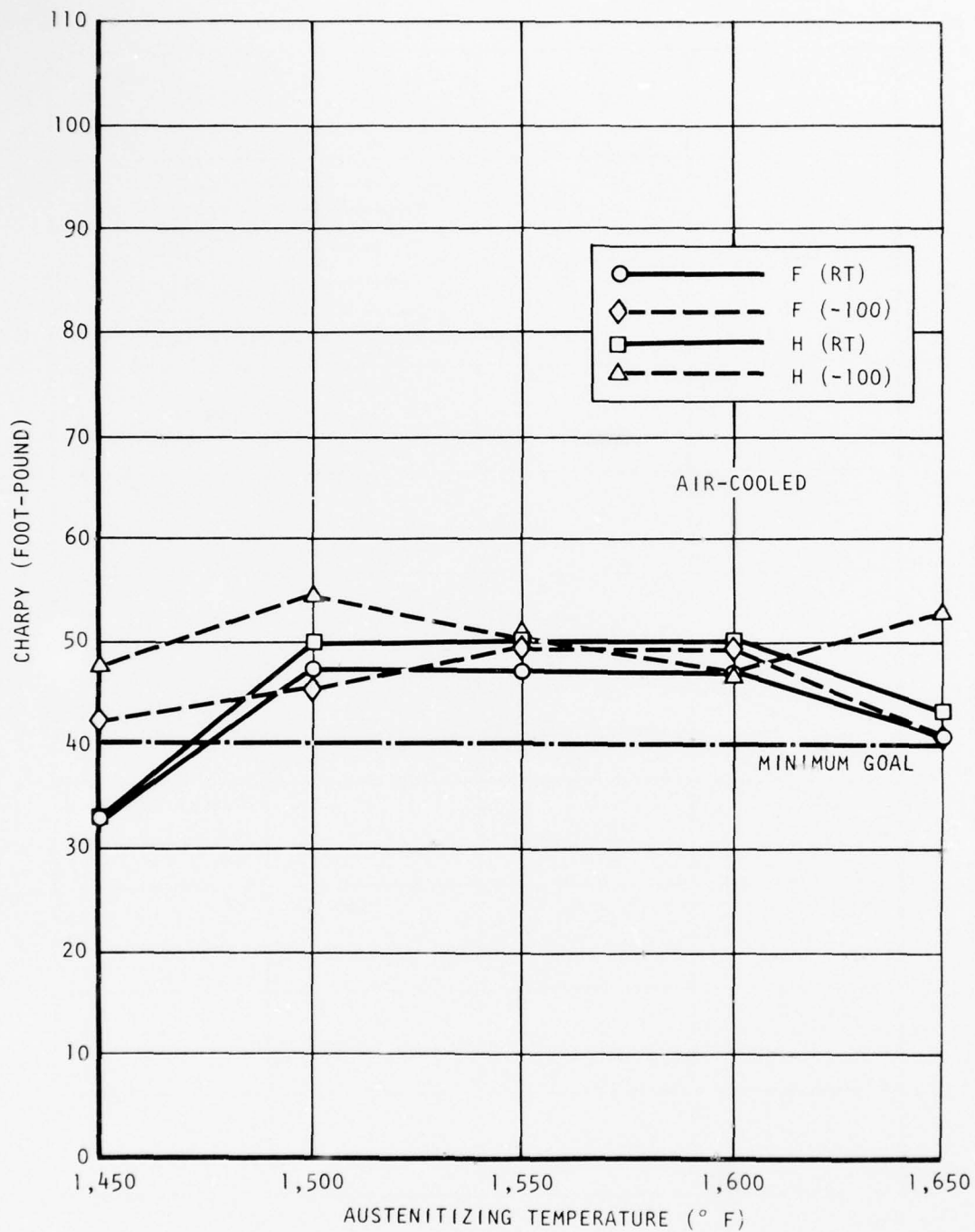
Figure 73. Charpy impact value versus austenitizing and cooling temperature for air-cooled AF1410 steel.

157
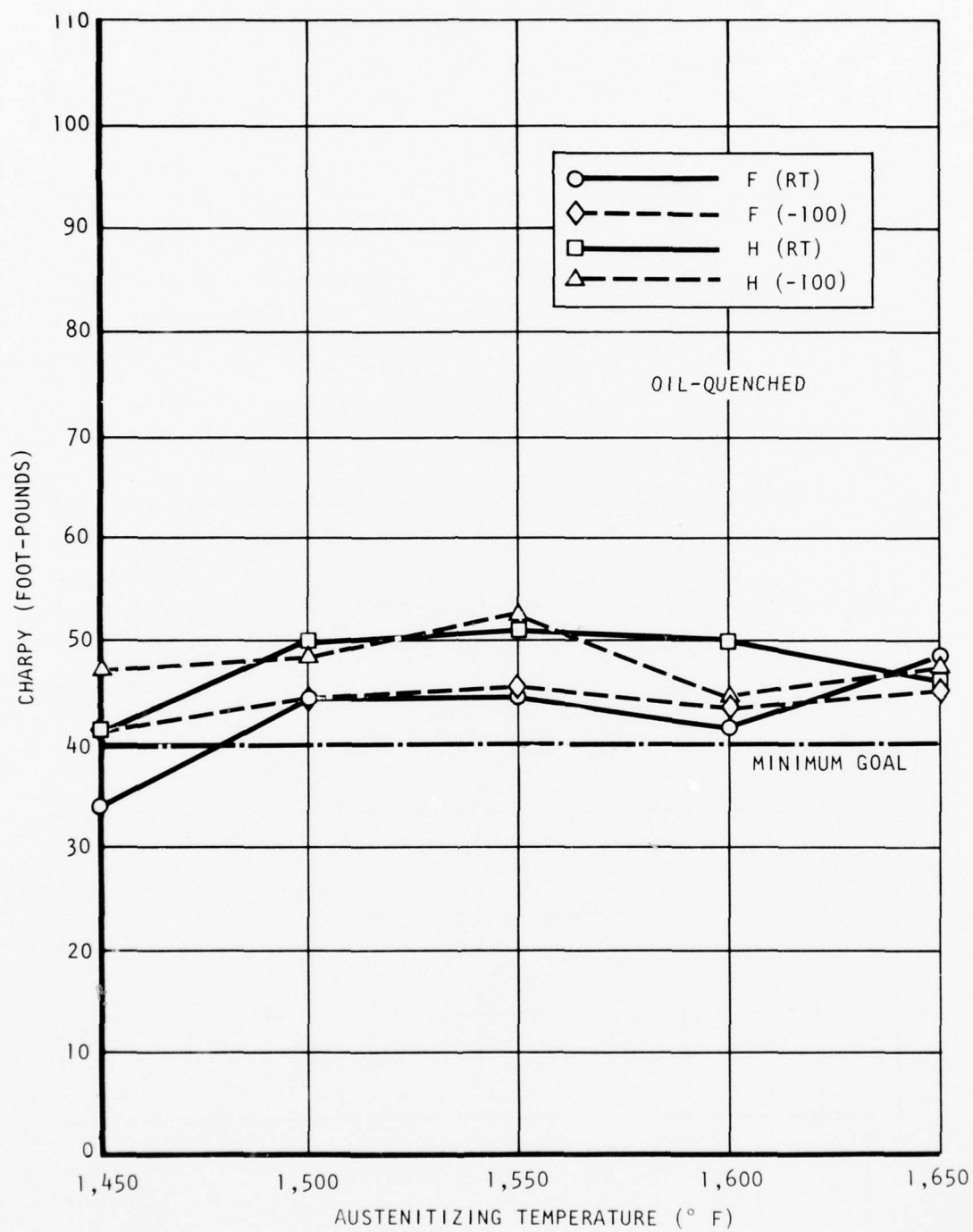
Figure 74. Charpy impact value versus austenitizing and cooling temperature for oil-quenched AF1410 steel.

158
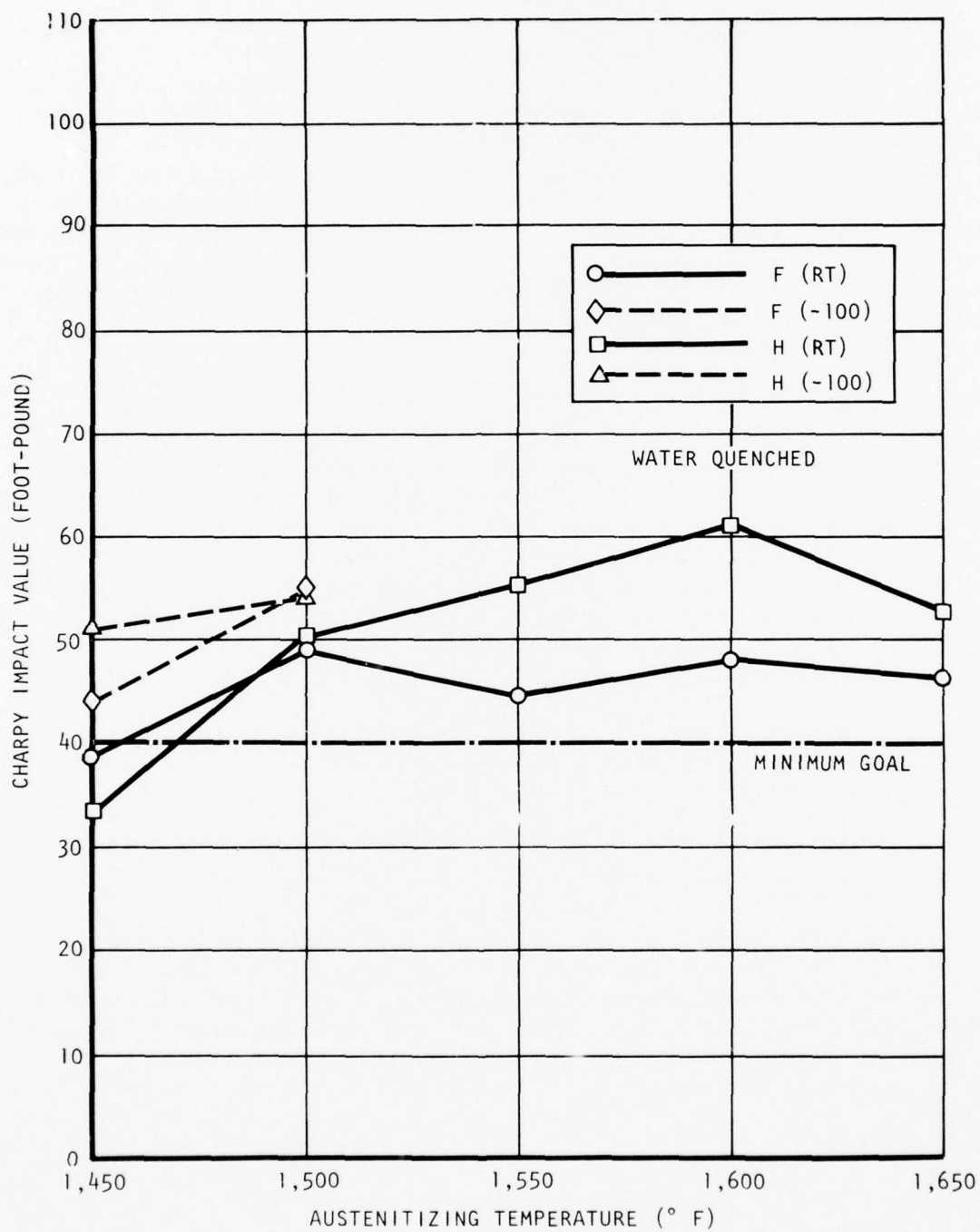
Figure 75. Charpy impact value versus austenitizing and cooling temperature water-quenched AF1410 steel.

Hardness

Hardness measurements were made on polished and etched sections. The results, presented in Table 32, show a hardness range of 40.7 to 50.8 R_C. Specimens austenitized in the temperature range of 1,500° to 1,650° F had hardness values in the range of 48.2 to 50.8 Rc, regardless of the quenching medium or subzero treatment. Specimens austenitized at 1,450° F and not given the subzero treatment had hardness values in the range of 40.7 to 43.8 R_C, regardless of the quenching medium. If given the subzero treatment, the hardness values for the 1,450° F austenitized specimens increased to the 48.2 to 50.8 R_C range. Apparently, the additional martensite transformation that occurs during the subzero treatment of the 1,450° F austenitized specimens is sufficient to bring the hardness level up to that of the specimens austenitized at 1,500° F and above.

Aging Response

Results of aging optimization tests are presented in Table 33, and are shown in Figures 76 through 78. Figure 79 shows the microstructure obtained for each condition. These results indicate the optimum aging temperature and time to be 925° F and 5 hours, respectively. However, 950° F and 5 hours are recommended for production at this time to allow for variations in temperature control and heat-to-heat material variations. Additional studies using the 925° F aging temperature should be included in future programs in order to establish the practicality of using this aging temperature in production.

Elimination of the normalizing treatment did not affect resulting properties indicating the possibility that this step may be eliminated, upon further verification.

Fracture Toughness

The results of the fracture toughness tests are presented in Table 34. The average fracture toughness values are 158.7, 140.2, and 146.6 ksi $\sqrt{in.}$ for the air, oil, and water-quenched specimens, respectively. The value of 140.2 ksi $\sqrt{in.}$ is sufficiently close to the oil-quenched control specimen value of 136.8 ksi $\sqrt{in.}$ to indicate that the full heat treatment of the two-inch-thick blocks prior to being given the premachining heat treatment did not affect the fracture toughness. The significantly higher fracture toughness of the air-cooled specimens suggested that air cooling should be considered as well as oil quenching for the postmachining heat treatment; especially since air cooling produces less distortion than oil quenching. The mechanical properties obtained on tensile testing, as shown in Table 35, indicate that there is only a slight loss of yield strength with air cooling. Charpy impact test results, listed in Table 35, also indicate improved toughness in the air-cooled, two-inch-thick blocks.

160

TABLE 52

HARDNESS TEST RESULTS ON AF1410 STEEL SPECIMENS VARIOUSLY HEAT TREATED

| Heat-Treat Variations | | Air Cooled | | | Oil Quenched | | | Water Quenched | | |
Aust Temp (°F)	Cooled to	Spec Ident	Hardness (R_C) X	σ	Spec Ident	Hardness (R_C) X	σ	Spec Ident	Hardness (R_C) X	σ
1,450	RT	F-1	42.6	0.5	F-3	42.1	0.8	F-6	42.4	0.4
1,500	RT	F-7	50.8	0.2	F-9	50.7	0.6	F-11	48.8	0.4
1,550	RT	F-13	49.7	0.5	F-15	49.9	0.2	F-27	48.4	0.4
1,600	RT	F-17	49.4	0.3	F-19	48.8	0.6	F-21	49.6	0.3
1,650	RT	F-22	48.4	0.6	F-24	48.4	1.0	F-26	48.6	0.4
1,450	-100	F-2	48.3	0.2	F-4	49.4	0.4	F-5	48.9	0.3
1,500	-100	F-8	49.3	0.3	F-10	50.0	1.4	F-12	49.3	0.9
1,550	-100	F-11	50.4	0.4	F-16	49.1	0.9	-	-	-
1,600	-100	F-18	48.3	0.9	F-20	49.6	1.0	-	-	-
1,650	-100	F-23	48.7	0.4	F-25	49.4	0.4	-	-	-
1,450	RT	H-1	43.8	0.3	H-6	40.7	0.3	H-3	43.5	0.7
1,500	RT	H-7	50.4	0.6	H-9	50.5	0.4	H-11	48.8	0.5
1,550	RT	H-13	49.1	0.3	H-15	48.6	0.7	H-27	48.6	0.6
1,600	RT	H-17	49.0	0.6	H-19	48.4	0.4	H-21	48.2	0.5
1,650	RT	H-22	48.5	0.5	H-24	48.7	0.5	H-26	48.7	0.5
1,450	-100	H-2	49.4	0.2	H-4	48.8	0.4	H-5	48.9	0.2
1,500	-100	H-8	49.7	0.2	H-10	49.5	0.4	H-12	48.8	0.2
1,550	-100	H-14	49.5	0.2	H-16	49.5	0.6	-	-	-
1,600	-100	H-18	48.8	0.4	H-20	48.7	0.4	-	-	-
1,650	-100	H-23	48.6	0.5	H-25	48.3	0.6	-	-	-
								PM + STD	49.4	0.5

*All specimens aged at 950° F for 5 hours and then air cooled.
**Average value of four tests.

161

TABLE 33

RESULTS OF MECHANICAL TESTING OF AF1410 STEEL SPECIMENS MACHINED FROM 1-INCH-THICK BLOCKS HEAT TREATED USING VARIOUS AGING TIMES AND TEMPERATURES

Spec no.	Aging treat		Fty (ksi)		Ftu (ksi)		Elong (%)		RA (%)		Charpy (ft-lb)	
	Temp (°F)	Time (hours)	X̄	δ	X̄	δ	X̄	δ	X̄	δ	X̄	δ
NN-2[1]	950	5	222.7	3.1	250.0	1.0	15.7	0.6	69.3	1.2	50.0	3.3
T-1	925	2	223.7	2.1	263.3	1.5	15.7	.6	66.3	0.6	34.3	2.8
T-2	925	5	228.7	2.5	257.7	0.6	15.7	.6	63.7	.6	47.2	2.4
T-3	925	10	225.0	1.0	252.7	1.2	16.0	.0	69.0	.0	46.0	3.5
T-4	950	2	222.7	1.2	259.0	1.0	16.0	.0	67.7	.6	40.3	0.8
T-5	950	5	217.7	0.6	245.3	.6	16.0	.0	70.0	.0	45.2	1.0
T-6 TS	950	10	219.3	.6	238.3	1.5	16.0	.0	70.0	.0	49.4	1.7
T-7 STS	950	15	206.7	1.5	224.0	5.5	16.0	.0	70.0	.0	48.0	2.6
T-8	975	2	221.7	3.2	247.3	2.3	15.7	.6	69.7	.6	49.8	.8
T-9 TS	975	5	215.3	3.0	233.7	1.2	16.0	.0	69.7	1.2	43.0	1.3
T-10 STS	975	10	204.0	2.6	214.3	1.5	16.0	.0	69.3	.6	27.7	1.5

[1] Not normalized at 1,650° F for 1 hour.

NOTE: All values are averages of test results from three specimens.

162
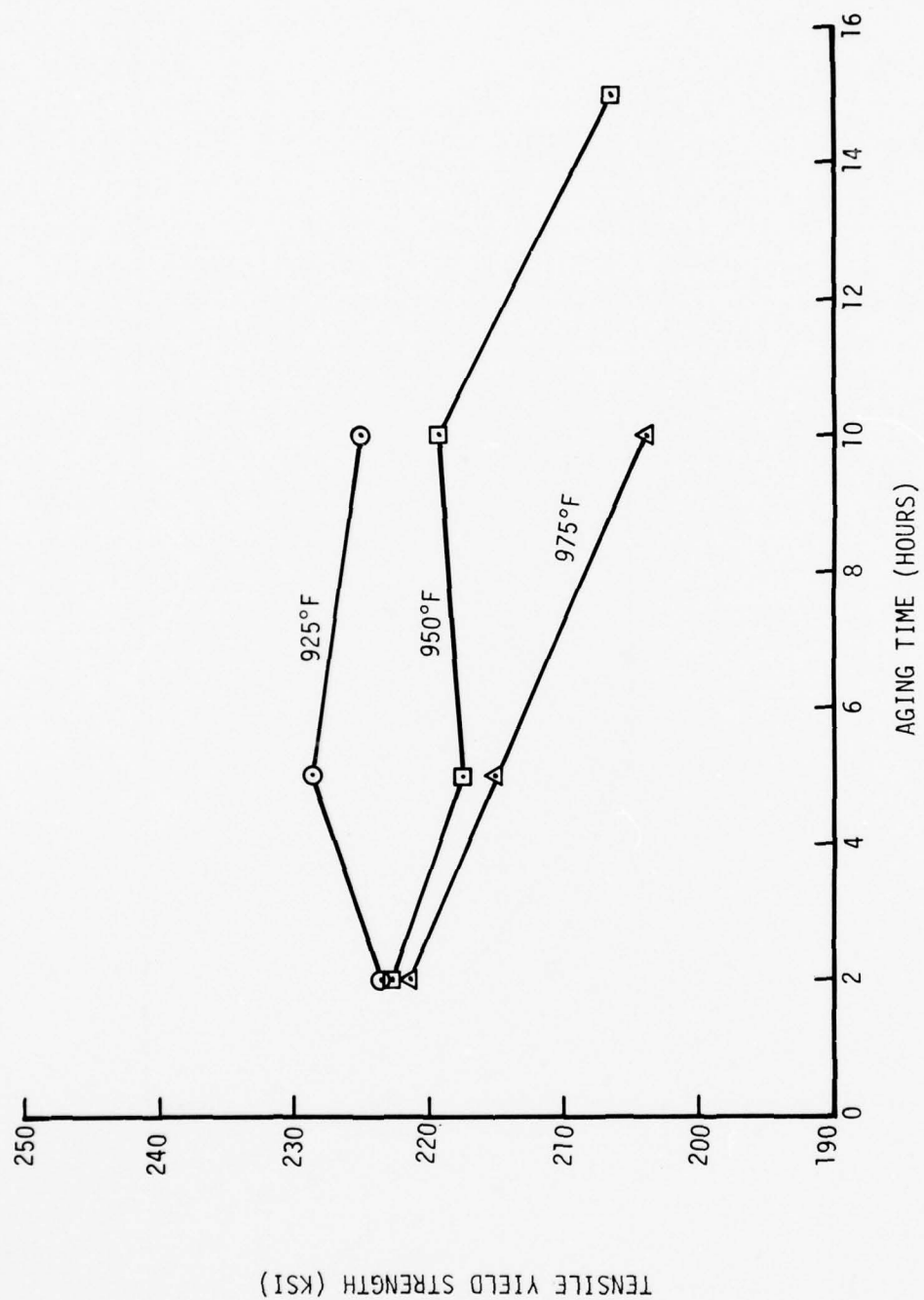
Figure 76. Effect of aging time and temperature on tensile yield strength of heat-treated AF1410 steel.

163
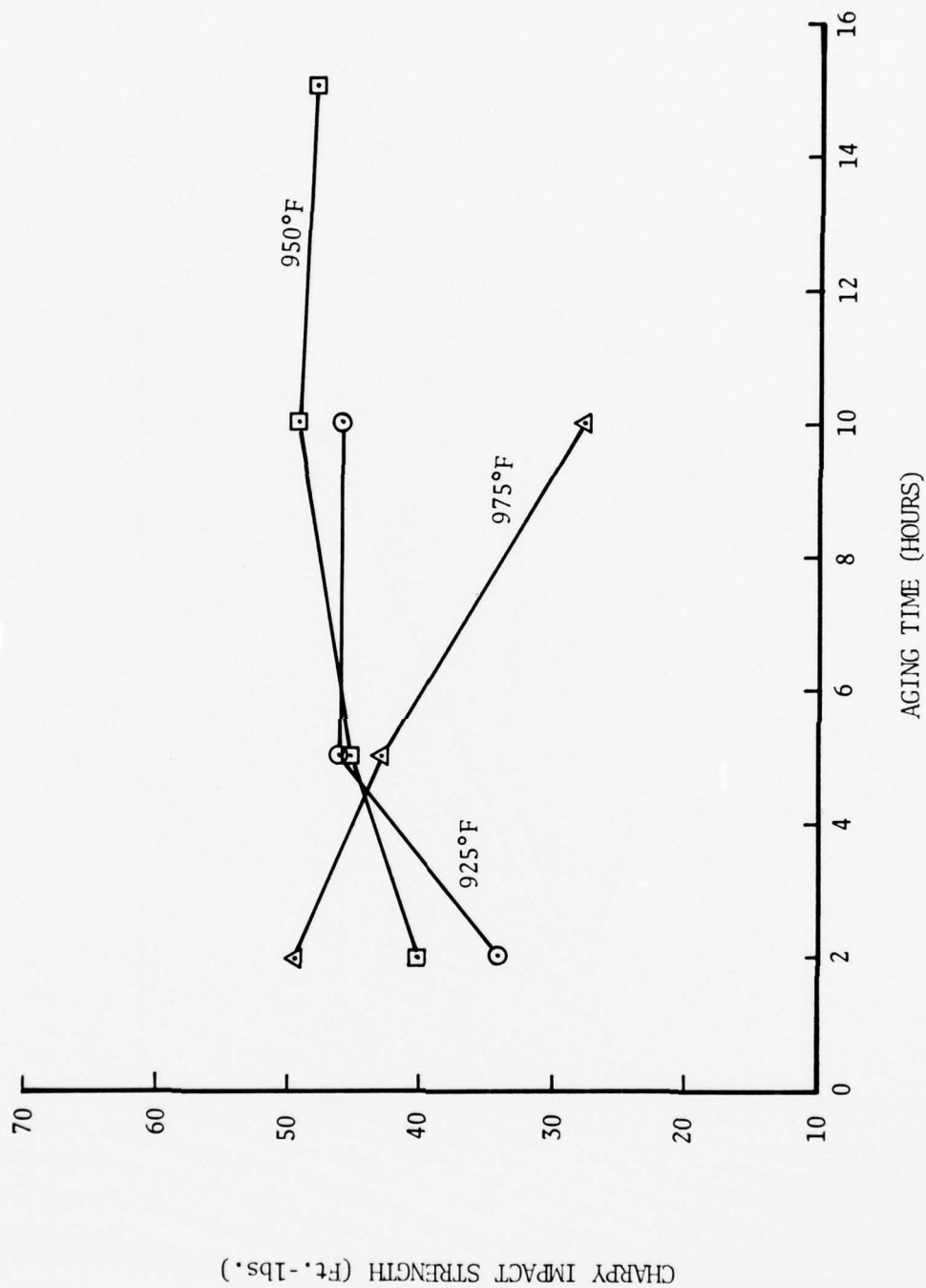
Figure 77. Effect of aging time and temperature on charpy impact values of heat treated AF1410 steel.

164
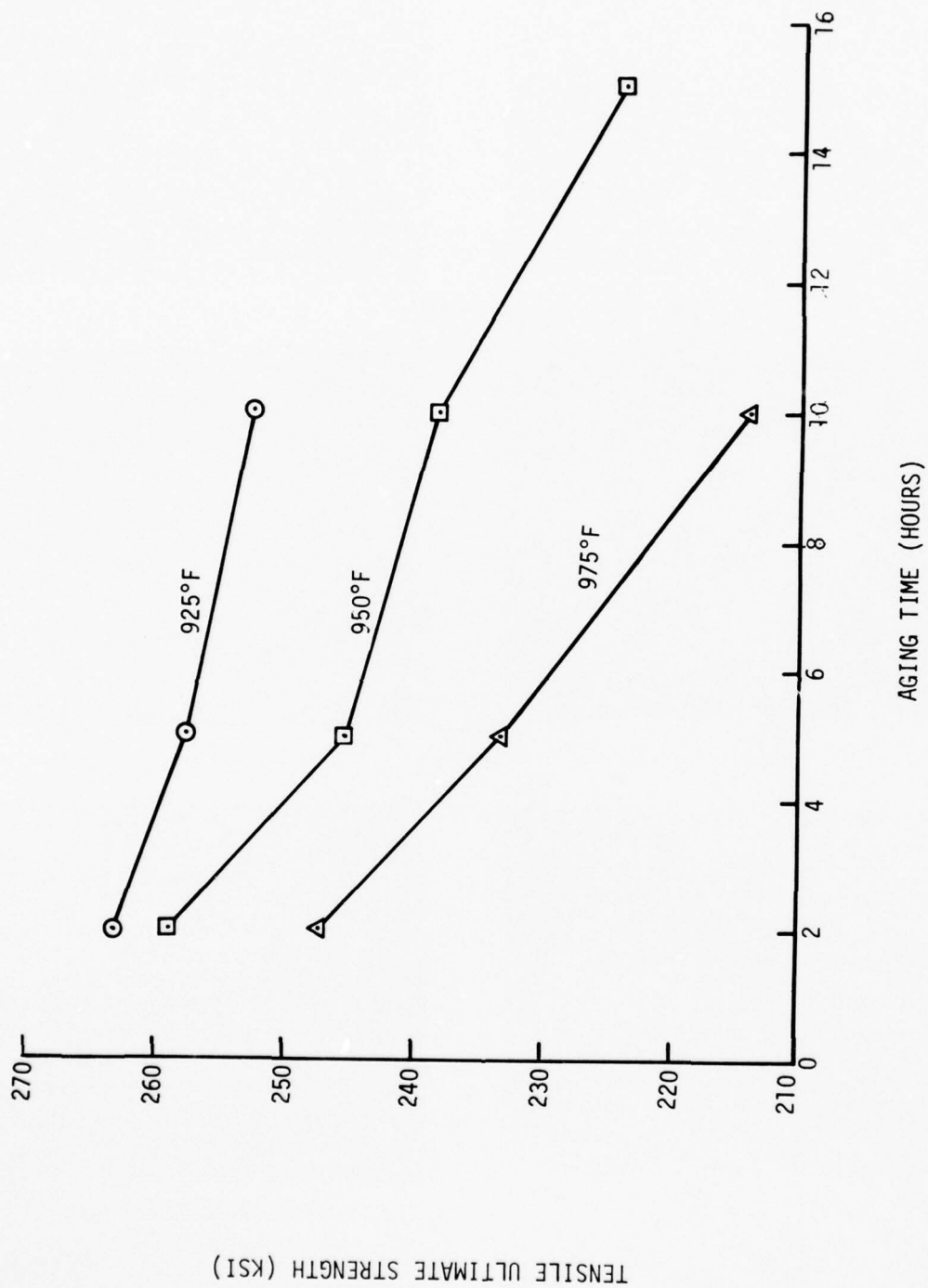
Figure 78. Effect of aging time and temperature on ultimate tensile strength of heat-treated AF1410 steel.

165
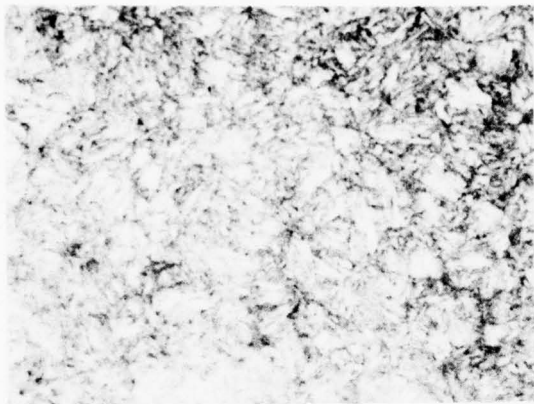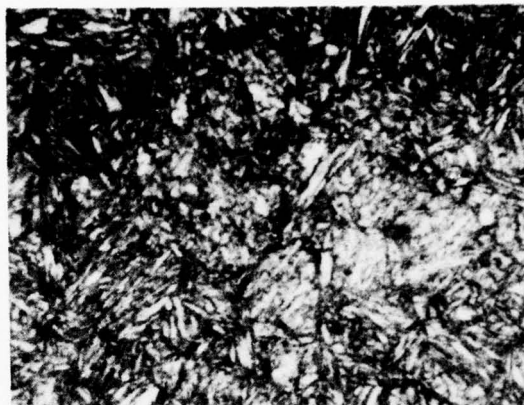
925° F for 2 hours

925° F for 10 hours
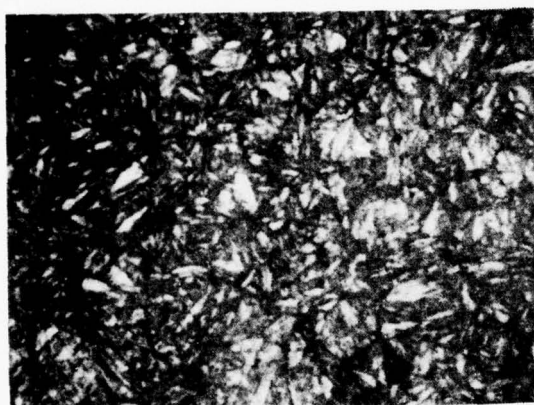
950° F for 5 hours

950° F for 15 hours
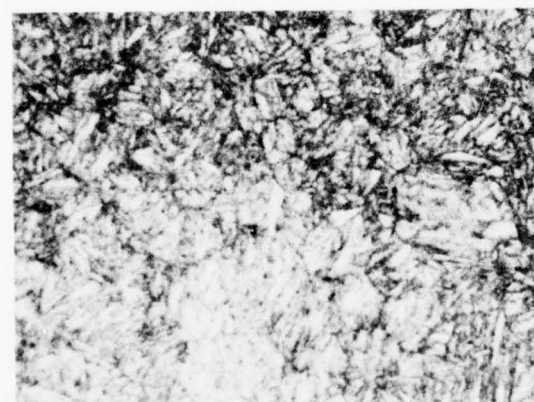
975° F for 2 hours

975° F for 10 hours

Figure 79.   Appearance of microstructures in full-hard (oil quenched)
AF1410 aged at various temperatures and times (500X).

TABLE 34

FRACTURE TOUGHNESS TEST RESULTS ON VARIOUSLY QUENCHED
AF1410 HEAT TREATED STEEL

No.	Specimen identification	Quenching medium	K_{IC} (ksi in.)
1	WR 4[1]	Air	154.9
2	WR 5[1]	Air	162.5
3	WR 9[1]	Oil	138.6
4	WR 10[1]	Oil	141.9
5	WR 14[1]	Water	148.6
6	WR 15[1]	Water	144.6
7	WR 16 (control)	Oil	136.8

[1] Subjected to full-hard heat treatment prior to being given the machinable heat treatment, followed by a second full-hard heat treatment.

DISTORTION

The results of measurements to quantify the amount of distortion on heat treating are shown in Figure 80. As would be expected, oil quenching resulted in significantly more distortion than air quenching. Measurements on water-quenched parts were not obtained. However, there is little question that water quenching would produce significantly more distortion than oil quenching.

CRACK GROWTH RATE

The results of da/dn testing of specimens subjected to the air-cooled and oil-quenched versions of the postmachine heat treatment are presented graphically in Figure 81 along with previous results obtained on a standard AF1410 heat-treated (water-quenched) specimen. All specimens were 1 inch thick, of the compact tension type, and tested in the WR direction (crack

TABLE 35

RESULTS OF MECHANICAL TESTING OF AF1410 STEEL SPECIMENS MACHINED FROM 2-INCH-THICK BLOCKS HEAT TREATED USING VARIOUS QUENCHING MEDIA

No.	Quenching medium	F_{ty} (ksi)		F_{tu} (ksi)		Elong (%)		RA (%)		Charpy (ft-lb)	
		$\overline{X}$	δ	$\overline{X}$	δ	$\overline{X}$	δ	$\overline{X}$	δ	$\overline{X}$	δ
1	Air	213.7	2.5	244.0	0.0	16.0	0.0	69.3	0.6	51.0	0.9
2	Oil	224.3	2.1	253.7	1.5	16.0	.0	68.7	.6	48.3	2.4
5	Water	228.0	2.0	248.3	2.1	15.7	.6	69.7	.6	48.0	2.6

NOTE: All values are averages of test results from three specimens

168
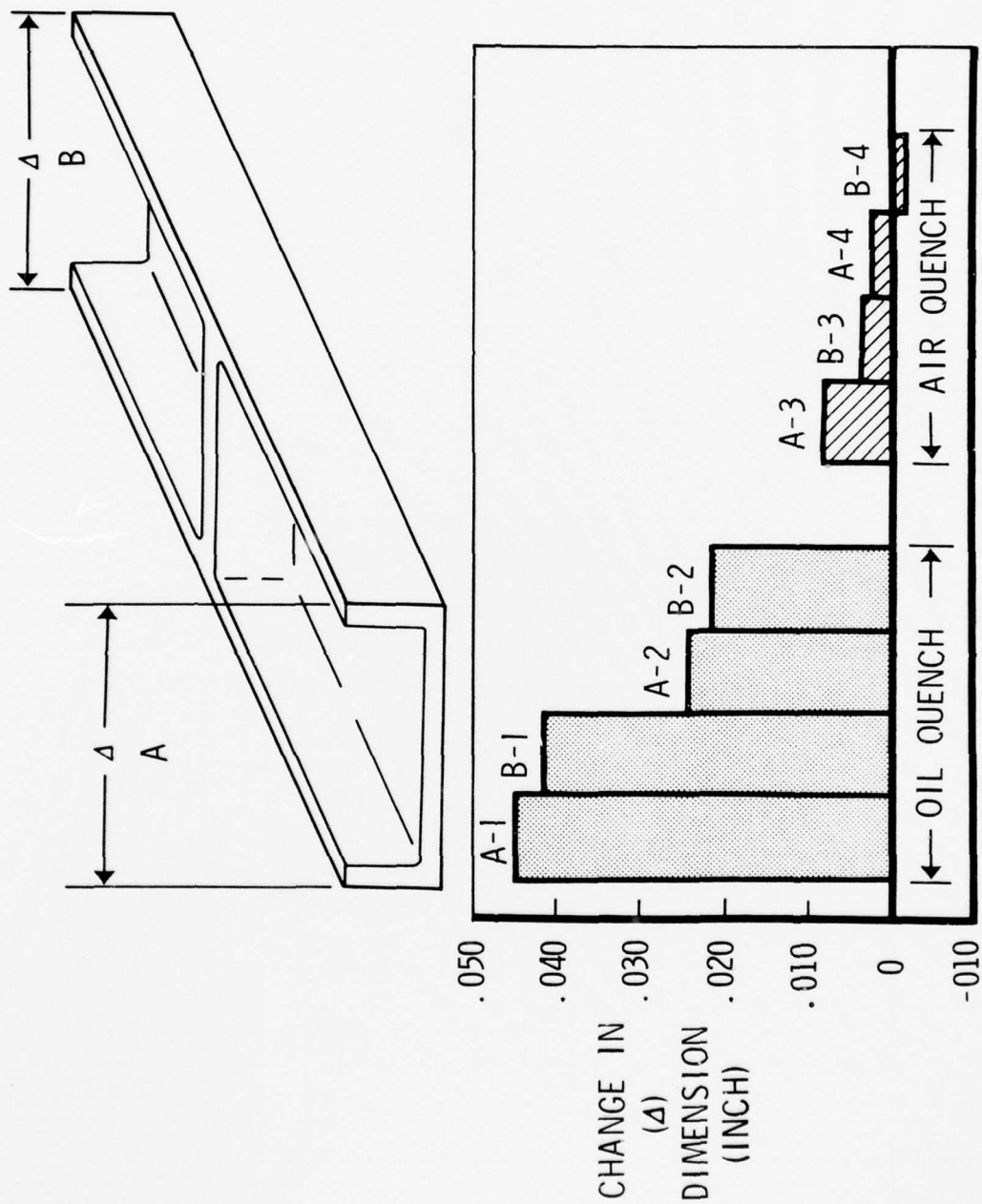
Figure 80. Effect of cooling rate on distortion of open ended pockets.
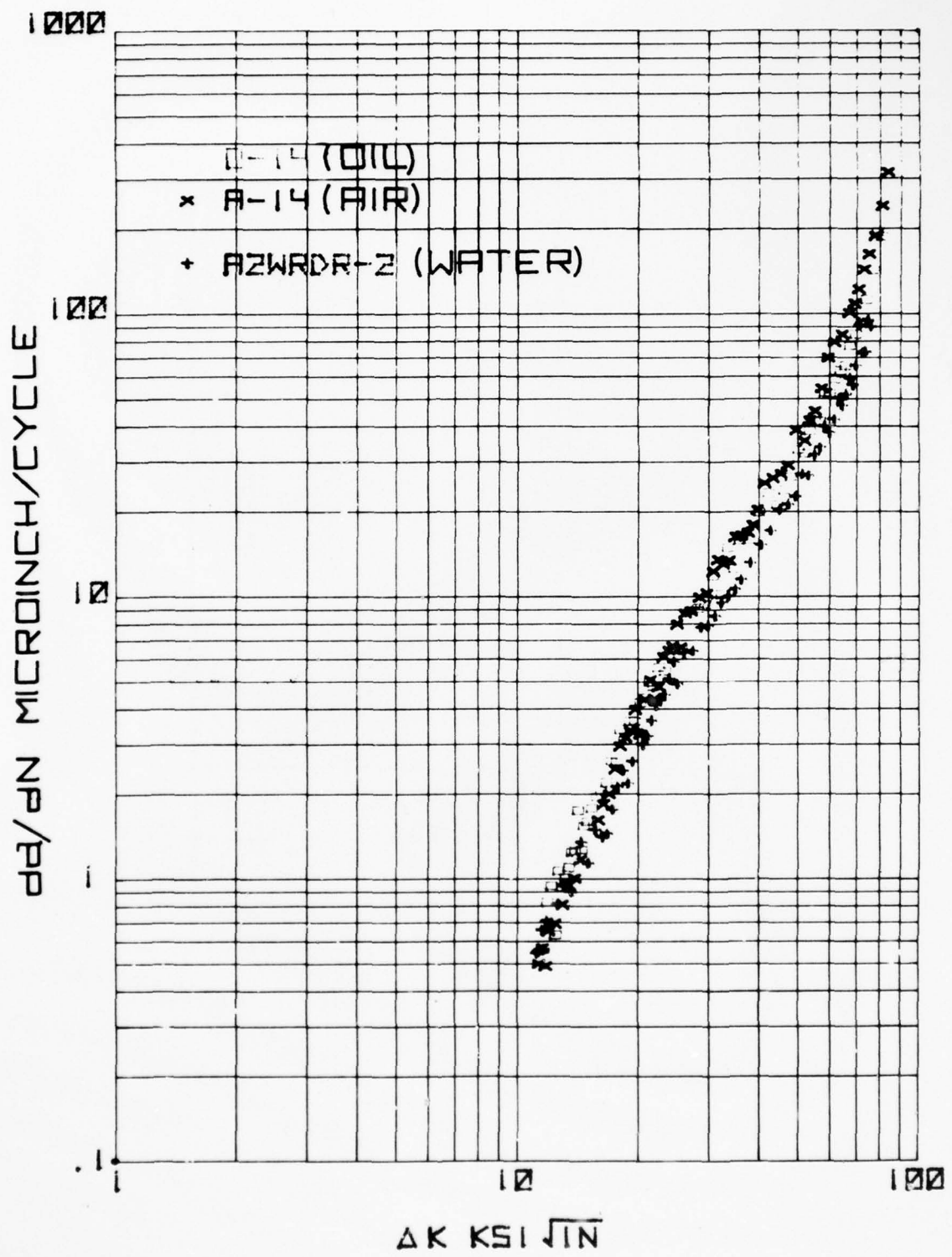
Figure 81. Effect of oil, air, and water quenching during heat treatment on rate of crack growth in AF1410 steel.

parallel to the rolling direction). The crack growth rate curves are practically identical for all three of the variously quenched specimens. Thus, the effects of quenching medium are insignificant relative to da/dn characteristics.

FATIGUE LIFE

The fatigue test results obtained on AF1410 specimens heat treated by austenitizing at 1,525° F and air cooling are listed in Table 36 and shown graphically in Figure 82, along with the results obtained on standard heat-treated (water-quenched) specimens. The results are very similar.

It is concluded that the use of air cooling during postmachining heat treatment for thicknesses up to 2 inches has no detrimental effect (except for a possible minor reduction in yield strength) on the mechanical proper-ties of AF1410, and provides a major benefit in reduced distortion on heat treating rough machined parts. Another benefit is an increase in fracture toughness from 146.6 ksi √in. for the standard heat treatment (water quenched to 158.7 ksi √in. for the air-cooled version of heat treatment. Specimens subjected to the oil-quench version of heat treatment had an average fracture toughness value of 140.2 ksi √in., which is low compared to the air- or water-quenched specimen data.

WELD PROPERTIES

The results obtained on testing weld specimens are presented in Table 37. Failure locations and microstructures are shown in Figures 83 through 86. BW designates specimens heat treated (except for aging) prior to welding, and AW designates specimens heat treated after welding.

The tensile test results show the ultimate and yield strengths of the welds in both the AW and BW plates to be about 90 percent of the parent metal. The elongation values are 75 percent of the parent metal values, primarily as a result of yielding being limited to the weld length. Since the weld length was significantly less than the 1-inch gage length, it follows that the actual elongations of these specimens would be significantly higher than the values reported in Table 37 if the gage length were reduced to include only the weld. The reduction-in-area values are also probably affected by parent material restraint on the weld deformation.

The Charpy impact test values show the impact strength of the welds and the heat-affected zones of the AW and BW specimens to be equal to or higher than the parent metal values.

The photomicrographs show the typical weld metal failures which occurred on testing tensile specimens, and the various notch (failure) locations in the

171

TABLE 36

ROOM TEMPERATURE AXIAL FATIGUE TEST RESULTS FOR AIR QUENCHED
AF1410 ALLOY STEEL (2-INCH-THICK PLATE STOCK) UNIVERSAL
CYCLOPS HEAT NO. L-3530 K20

Specimen identification	Specimen direction	Stress concentration	R factor	Stress ksi	% Ftu	Cycles to failure
1	Transverse	$K_t = 1.0$	+0.05	173.5	72.8	50,000
2				148.7	62.4	10×10^7 NF
3				198.2	83.2	23,000
4				155.0	65.1	221,000
5				161.6	67.6	92,000
6				151.0	63.4	10×10^7 NF
7				158.0	66.3	69,000
8				153.5	64.4	57,000
2^1				210.6	88.4	10,000
6^1				185.0	77.7	40,000

[1] Rerun specimen

NOTE: Transverse Ftu = 238.2 ksi

172

Axial Tension - Tension Fatigue Test Results for AF1410 Alloy Steel
3/4 Inch Thick Plate Stock - Universal Cyclops Heat No. L3614 K 18

Specimen Direction	- Transverse
R Factor	- R = +0.05
K_t Factor	- K_t = 1.0
Test Temperature	- Room Temperature
T-Thread Failure	- No Failure ⟶

Ftu = 238.2 - ⊙ Air Quenched (2" Thick)
Ftu = 247.8 - ☐ Water Quenched (3/4" Thick)

/Re-run
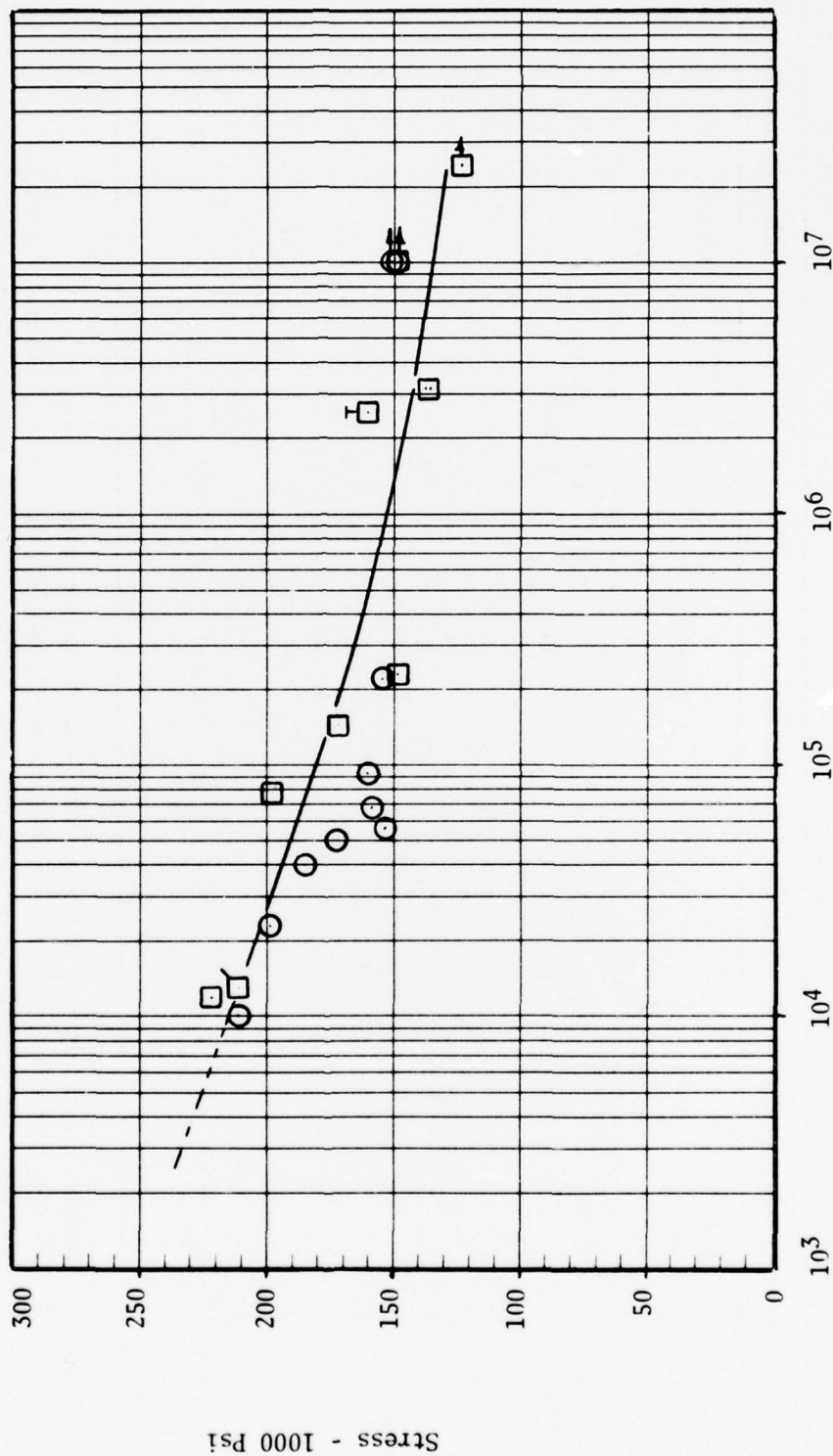
Figure 82.   Effect of air and water quenching on fatigue response of AF1410 steel.

173

TABLE 37

MECHANICAL PROPERTIES OF AF1410 STEEL SPECIMENS JOINED IN THE TEST SECTION BY WELDING

Identification	Number of tests	Tensile test results								Number of tests	Charpy test results	
		Fty (ksi) $\overline{X}$	δ	Ftu (ksi) $\overline{X}$	δ	Elongation (%) $\overline{X}$	δ	RA (%) $\overline{X}$	δ		Impact strength (ft-lb) $\overline{X}$	δ
AW Weld	4	210.9 (92.8)	2.1	219.7 (89.0)	1.3	12.0 (75.0)	0.4	64.6 (93.6)	0.6	12	43.67 (97.9)	4.29
AW HAZ	-	-	-	-	-	-	-	-	-	5	48.2 (108.1)	3.33
BW Weld	5	204.6 (90.0)	1.9	221.0 (89.5)	1.0	12.3 (76.9)	1.5	57.6 (83.5)	6.1	6	54.8 (122.9)	2.7
BW HAZ	-	-	-	-	-	-	-	-	-	11	49.4 (110.8)	4.3
Parent Metal	6	227.3	3.4	246.9	1.4	16.0	0.0	69.0	0.5	6	44.6	0.9

NOTES: 1. Numbers in parenthesis are percentages of parent metal values.
2. AW specimens were premachine heat treated, welded, and then full heat treated.
3. BW specimens were austenitized, subzero treated, welded, and then aged.
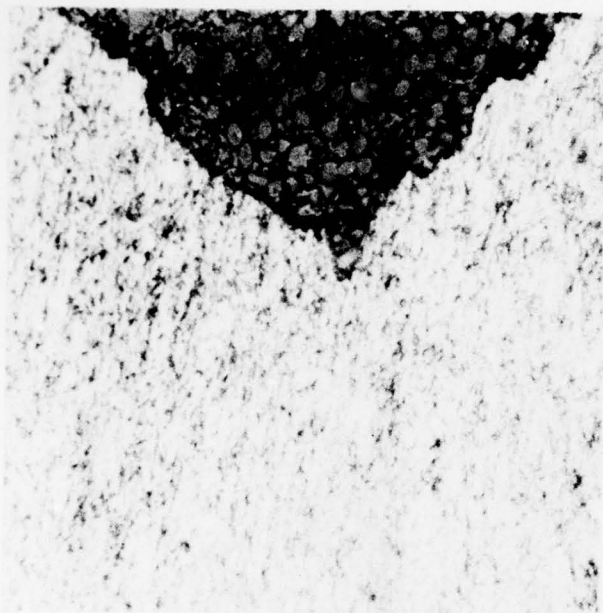
Weld region (250X)
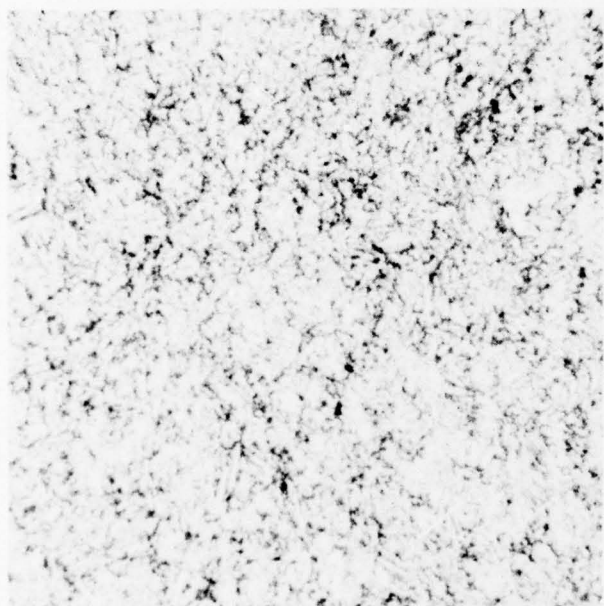
Parent metal region (250X)
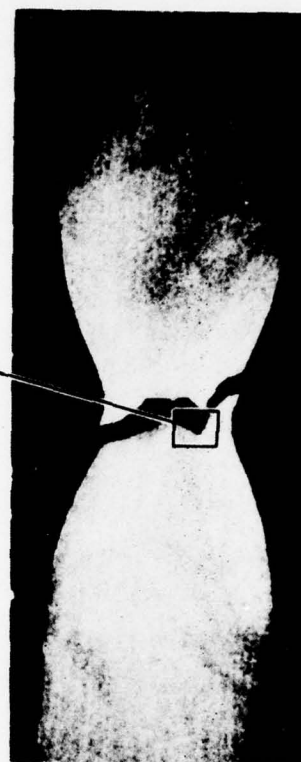
Longitudinal section (6X)

Figure 83. Microstructure of an "AW" fractured specimen
heat-treated after welding.

175

Weld metal in K-joint (250X)
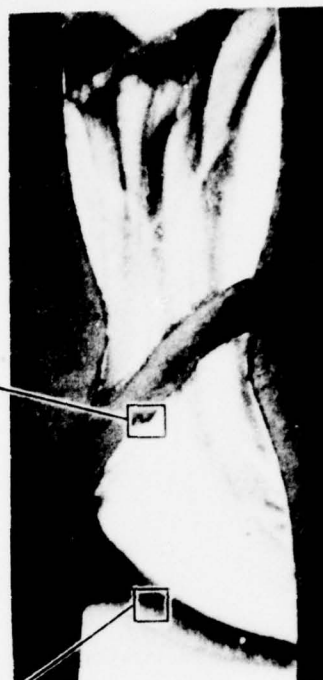
Longitudinal section (6X)
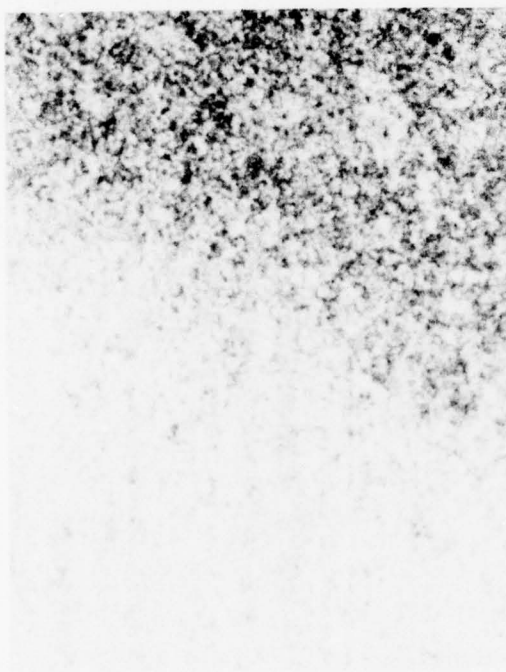
Heat-affected zone (250X)
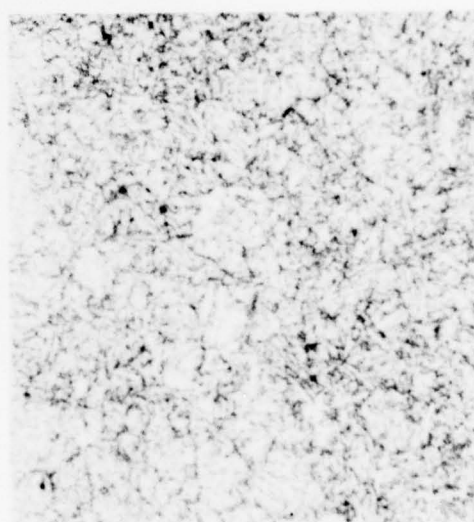
Reverted austenite
(eyebrow region)

Parent metal (250X)

Figure 84.   Microstructure of a "BW" fractured tensile specimen
solution treated and postweld aged.

176
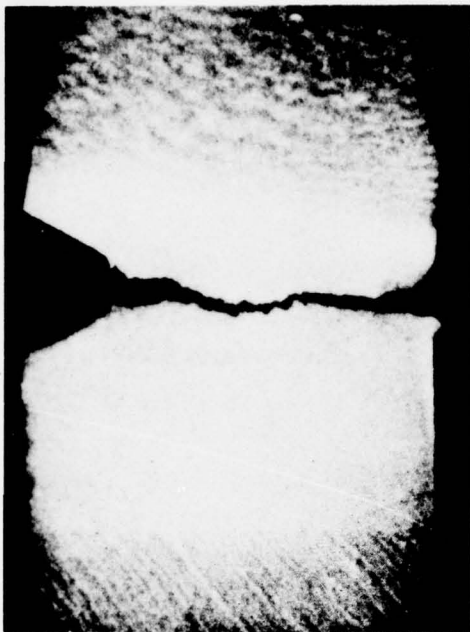
Fracture in weld

Fracture in weld
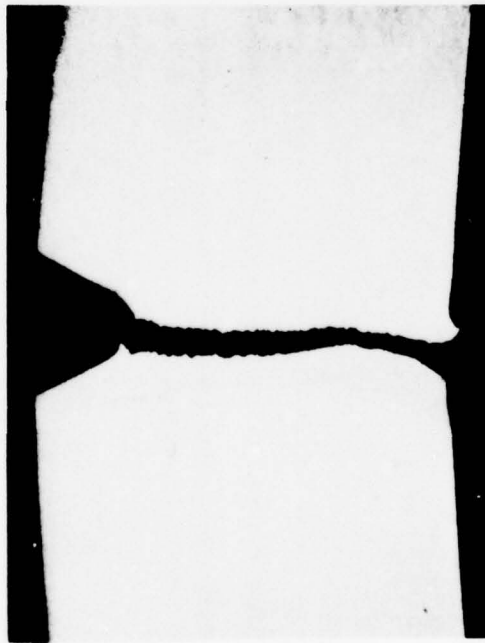
Fracture in haz

Figure 85. Longitudinal sections through "AW" fractured charpy impact specimens heat treated after welding.
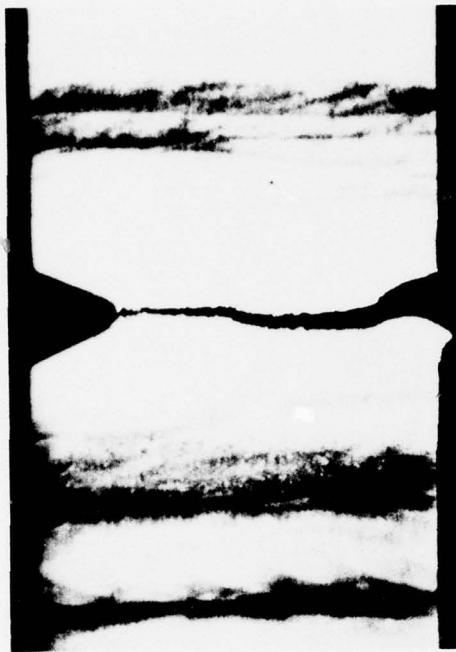
Fracture in weld

Fracture in haz near weld

Fracture in eyebrow region of haz

Figure 86. Longitudinal sections through "BW" fractured charpy impact specimens solution treated and postweld aged (6X).

Charpy Impact specimens. A comparison of the microstructures of specimens heat-treated after welding (Figures 83 and 85) with the microstructures of specimens austenitized, welded, and postweld aged (Figures 84 and 86) indicates a significant change in microstructure due to postweld heat treating. The eyebrow regions of reverted austenite have been completely eliminated by the postweld heat treatment, and the weld microstructure has been nearly eliminated, making it difficult to discern the weld metal from the base material. The structural differences seen in the weld and aged heat affected zones did not affect the Charpy impact strength as demonstrated by the low standard deviation (o) of the as-welded, heat-affected zone impact strength values.

These results show that although there are significant differences in microstructure as a result of different welding/heat-treat sequences, these differences are not reflected in the tensile and impact strengths.

METALLURGICAL ANALYSIS

To supplement the data developed in mechanical testing, a detailed metallurgical analysis of representative test specimens was performed. This analysis included: (1) standard light microscopy to evaluate general microstructure, (2) transmission electron microscopy to determine martensite morphology, location of retained austenite, and carbide distribution, (3) quantitative X-ray diffraction (Reference 7) to determine volume fraction of retained austenite, and (4) scanning electron microscopy to characterize the fracture faces of Charpy and tensile specimens. The specimens selected for this effort and their heat-treat history are listed in Table 38.

Micrographic Evaluation

Optical micrographs (500X) of cross sections from specimens F12, F10, F8, 1C, 7C, 2C, pmHT, "F", and T10 are shown in Figures 87, 88, and 89. There are no apparent differences in the microstructures except in the case of specimens "F" and T10 (Figure 89). This indicates that AF1410 microstructure is insensitive to cooling rate for both 1- and 2-inch-thick material. The microstructure of the "F" specimen has a very dense carbide distribution, possibly with some sphereoidization, which probably contributes to the excellent machinability of AF1410 in this condition. The overaged condition of T-10 has a low-density carbide distribution compared to all of the other microstructures.

Transmission electron micrographs of the specimens show that the retained austenite lies primarily at the martensite plate boundaries. A uniform distribution of fine carbides is generally observed with some

179

TABLE 38

HEAT-TREAT HISTORY OF METALLURGICAL ANALYSIS SPECIMENS

Specimen Code	Thickness (inches)	Heat Treat
F12	1	F + 1,650° F/1 hr/ac/1,500° F/1 Hr/WQ/ - 100° F/2 hr/950° F/5 hr/ac
F10	1	F + 1,650° F/1 hr/ac/1,500° F/1 hr/OQ/ - 100° F/2 hr/950° F/5 hr/ac
F8	1	F + 1,650° F/1 hr/ac/1,500° F/1 hr/ac/ - 100° F/2 hr/950° F/5 hr/ac
1C	2	F + 1,650° F/1 hr/ac/1,525° F/4 hr/WQ/ - 100° F/1 hr/950° F/5 hr/ac
7C	2	F + 1,650° F/1 hr/ac/1,525° F/4 hr/OQ/ - 100° F/1 hr/950° F/5 hr/ac
2C	2	F + 1,650° F/1 hr/ac/1,525° F/4 hr/ac/ - 100° F/1 hr/950° F/5 hr/ac
PMHT	1	1,650° F/1 hr/ac/1,500° F/1 hr/ac/950° F/5 hr/ac·
F	1	1,250° F/8 hr/ac
T10	1	F + 1,650° F/1 hr/ac/1,525° F/4 hr/OQ/ - 100° F/1 hr/950° F/5 hr/ac
F6	1	F + 1,650° F/1 hr/ac/1,450° F/1 hr/WQ/950° F/5 hr/ac
F19	1	F + 1,650° F/1 hr/ac/1,600° F/1 hr/OQ/950° F/5 hr/ac

NOTES: WQ = water quench, OQ = oil quench, ac = air cool.
F = 1,250° F - 8 hr - air cool
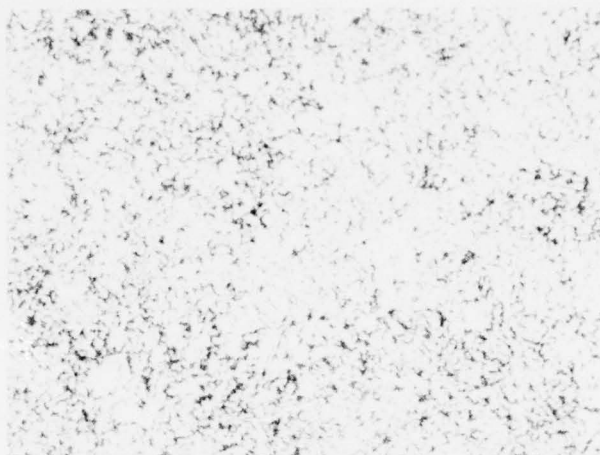
(F12) Water quenched from 1,500° F
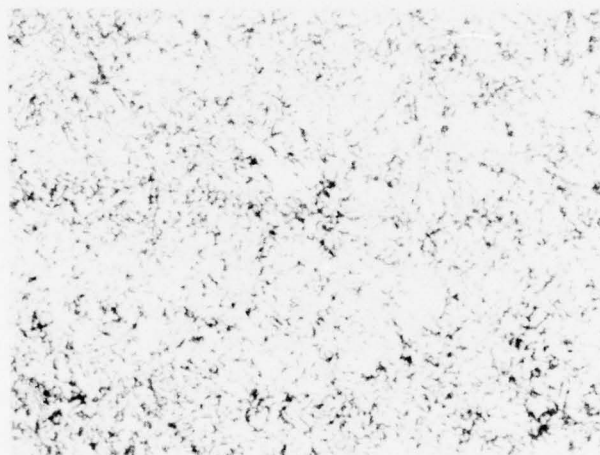
(F10) Oil quenched from 1,500° F
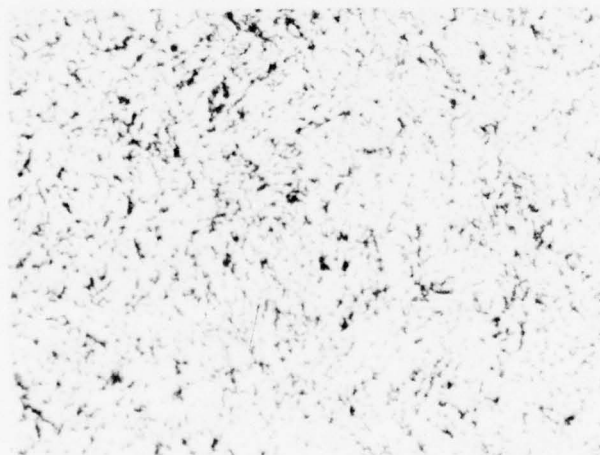
(F8) Air cooled from 1,500° F

Figure 87. Optical micrographs of (a) F12, (b) F10 and (c) F8 (500x).
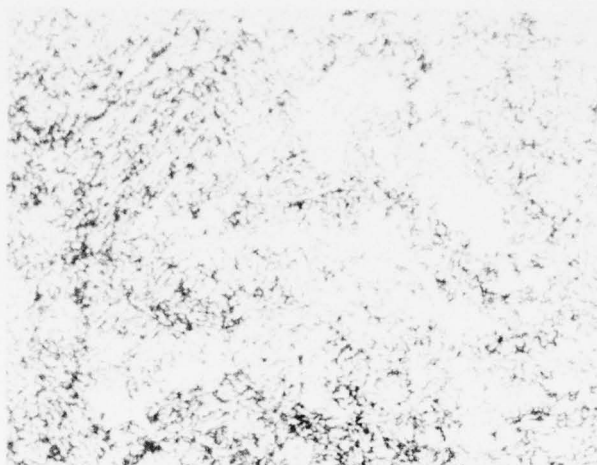
(1C) Water quenched from 1,525° F
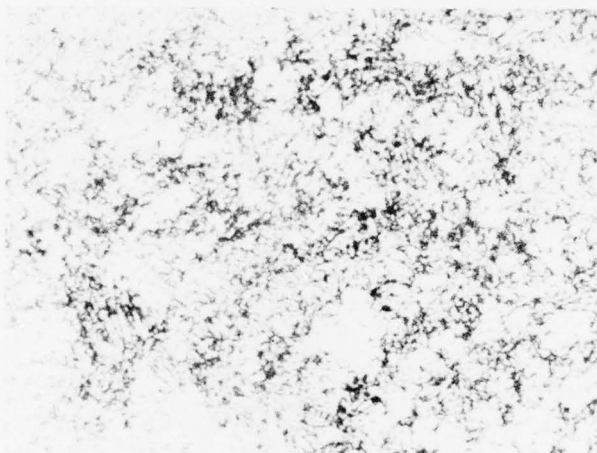
(7C) Oil quenched from 1,525° F
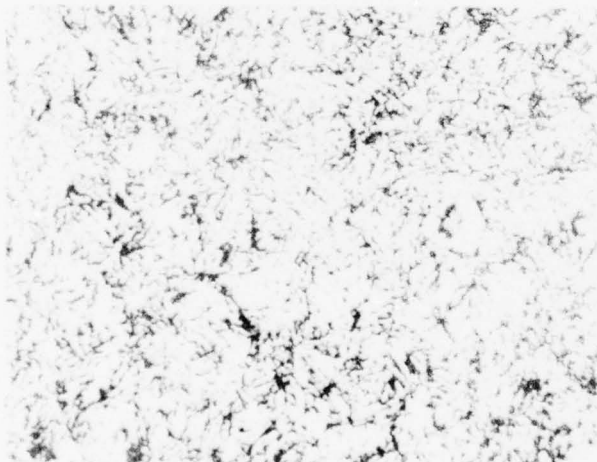
(2C) Air cooled from 1,525 °F

Figure 88. Optical micrographs of (a) 1c, (b) 7c, and (c) 2c. (500x).

182
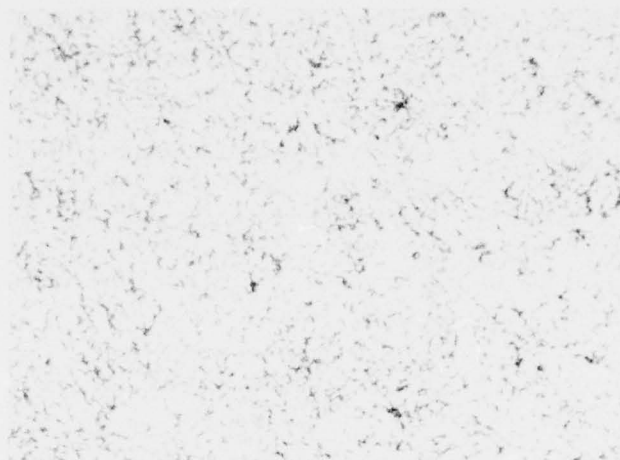
(PMHT) Standard heat treatment
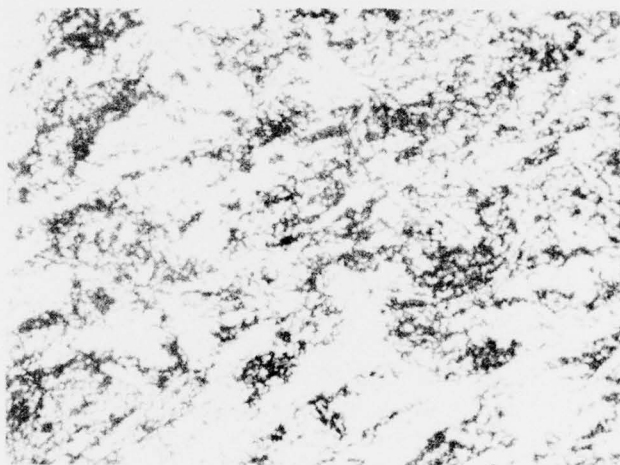
("F") Premachining heat treatment
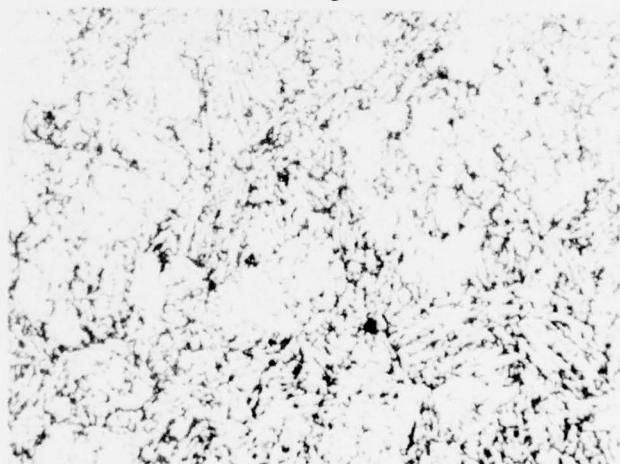
(T10) Aged at 975° F for 10 hours.

Figure 89. Optical micrographs of (a) PMHT, (b) "F" premachining
heat treatment (c) T10. (500x)

evidence of precipitation along crystallographic directions. There is no significant variation in carbide morphology because of quenching medium or material thickness. The blocky form of austenite in the "F" specimen, which had been given the 1,250° F, 8-hour premaching heat treatment, is consistent with reverted austenite. The microstructure is overtempered martensite and reverted austenite resulting from nickel partitioning. The microstructure of speciment T10 indicated a coarse martensitic structure with reverted austenite at the lath boundaries and a uniform distribution of fine carbides. The microstructure is essentially the same after full heat treatment regardless of whether the material was previously in the "F" condition. Typical transmission electron micrographs are shown in Figures 90 and 91.

Fractography

Scanning electron micrographs of selected tensile and Charpy bars are shown in Figures 92 - 100. (Note: Figure 94 is an energy dispersive X-ray spectographic analysis performed on tensile specimen F-6-2). The tensile fractures for specimens F-6, F-10, and PMHT were standard cup- and cone-type fractures exhibiting dimpled rupture in the center surrounded by a circumferential shear band (see Figures 92 and 93). The X-ray analysis (Figure 94) showed no difference in composition between the hole (location 5, Figure 92) and the matrix of the tensile specimen. Prior to this analysis, it had been thought that the hole may have been because of local structural morphology, such as carbides or high nickel austenite (reverted).

The "F" tensile specimens exhibited cup and cone fractures with large axial cracks extending along the specimen diameters (Figures 95 and 96). The tensile test results for the specimens are:

F_{ty} (ksi)	F_{tu} (ksi)	Elong (%)	RA (%)
124	126	17	62
121	176	16	59

The tensile specimen, T-10, also had a cup and cone fracture but contained radial cracks in the central portion of the fracture (Figures 97, 98, 99, and 100). Detailed SEM examination showed no association of the radial cracks (or "tensile splitting") with microstructure. The presence of shear dimples adjacent to the cracks (see micrograph 305 005 of Figure 99) suggests that an extreme triaxial stress state developed in this specimen during testing, causing the observed tensile splitting.

184

Figure 90. Bright field transmission electron micrograph of 1-inch-thick,
air-quenched AF1410 steel plate, specimen F-8 (35,000X).

185

Figure 91.   Dark field transmission electron micrograph of 1-inch-thick,
air-quenched AF1410 steel plate, specimen F-8 (55,000X).

186

Numbers show locations of
micrographs of Figure 93

Figure 92.   Scanning electron micrographs of fracture surface
of tensile bar F-6-2.

187

Location 2

Location 3

Location 4

Location 5

Figure 93. Scanning electron micrographs of fracture surface of tensile bar F-6-2.

188

291-005

Hole region = dots

Matrix region = Bars

Figure 94. Comparison of energy dispersed X-ray spectra of "hole" and matrix regions for fracture surface of tensile bar F-6-2.

189

Numbers show locations of
micrographs of Figure 96
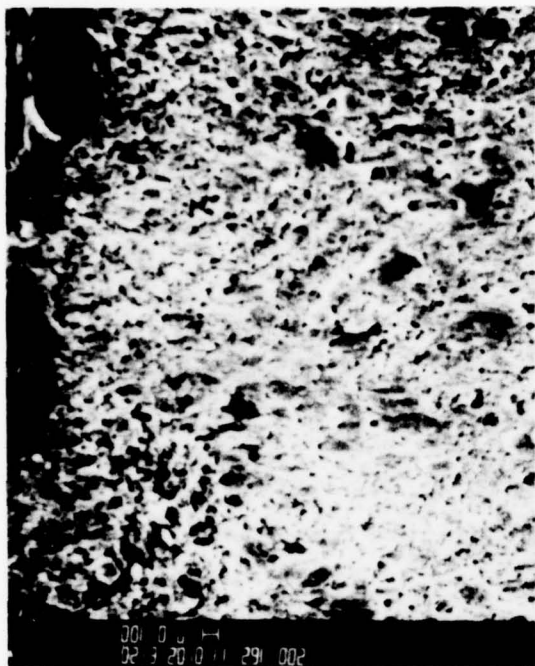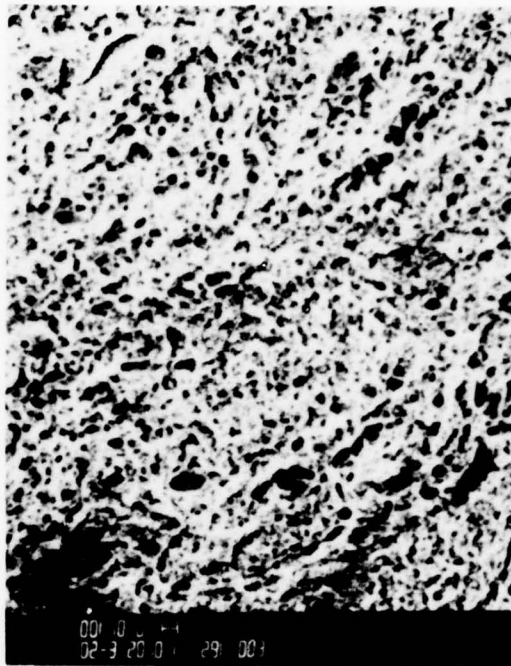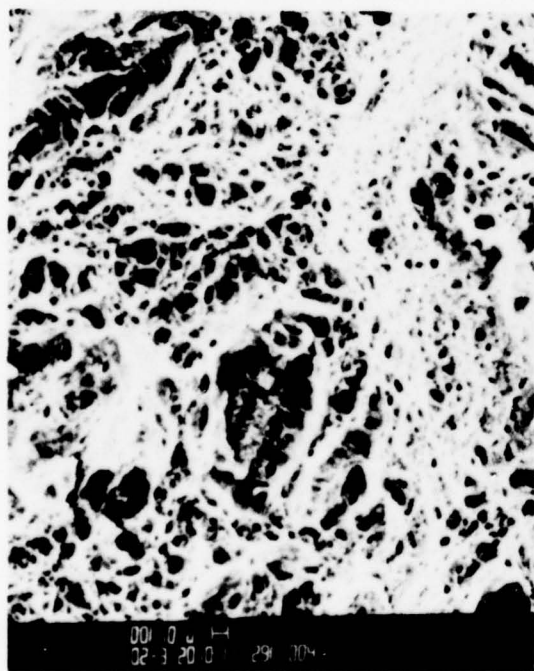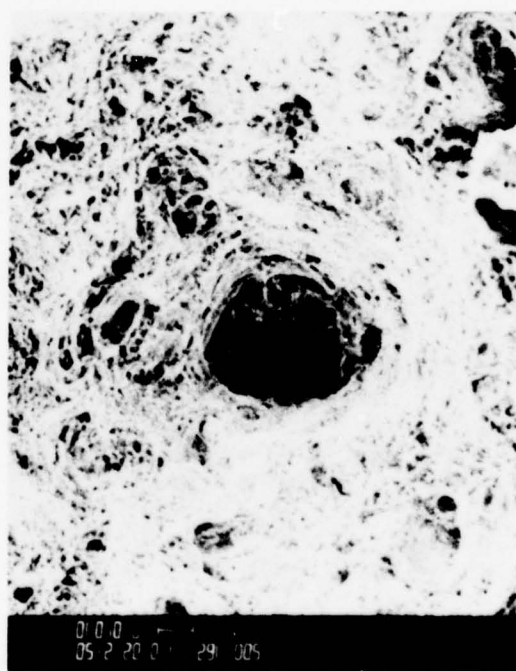
Figure 95.   Scanning electron micrograph of fracture surface of
tensile bar F.

190
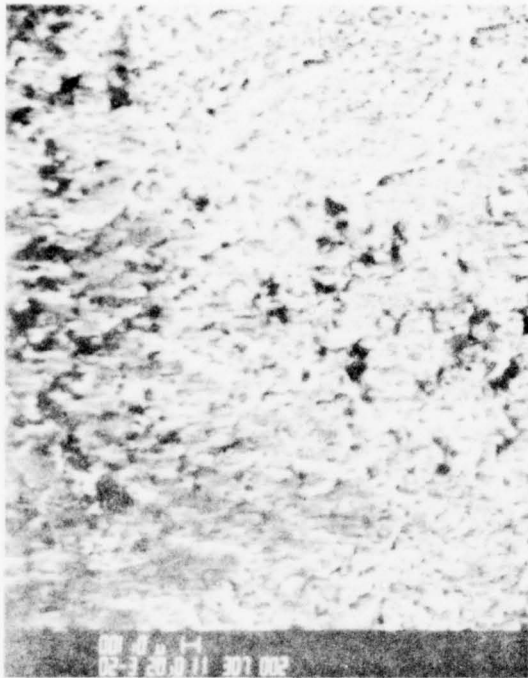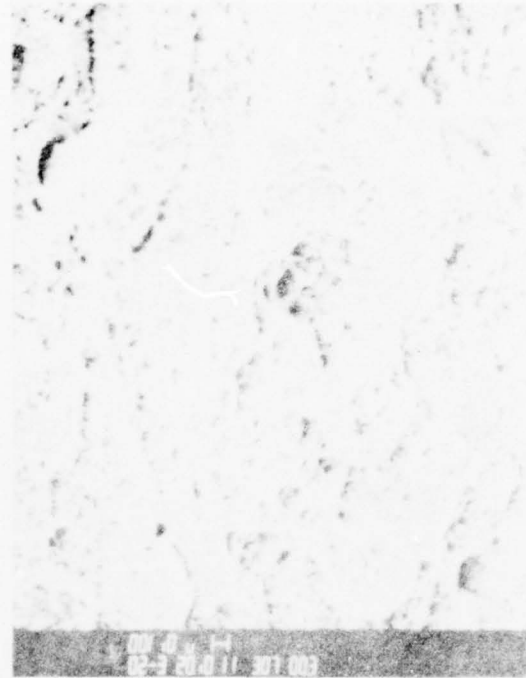
Location 2

Location 3

Location 4

Figure 96.   Scanning electron micrographs of fracture surface of
tensile bar F.

191

Figure 97. Scanning electron micrograph of fracture surface of tensile bar T-10.

192

Numbers show locations of
micrographs of Figures 99 and 100

Figure 98. Scanning electron micrograph of region of fracture surface
of tensile bar T-10.

193
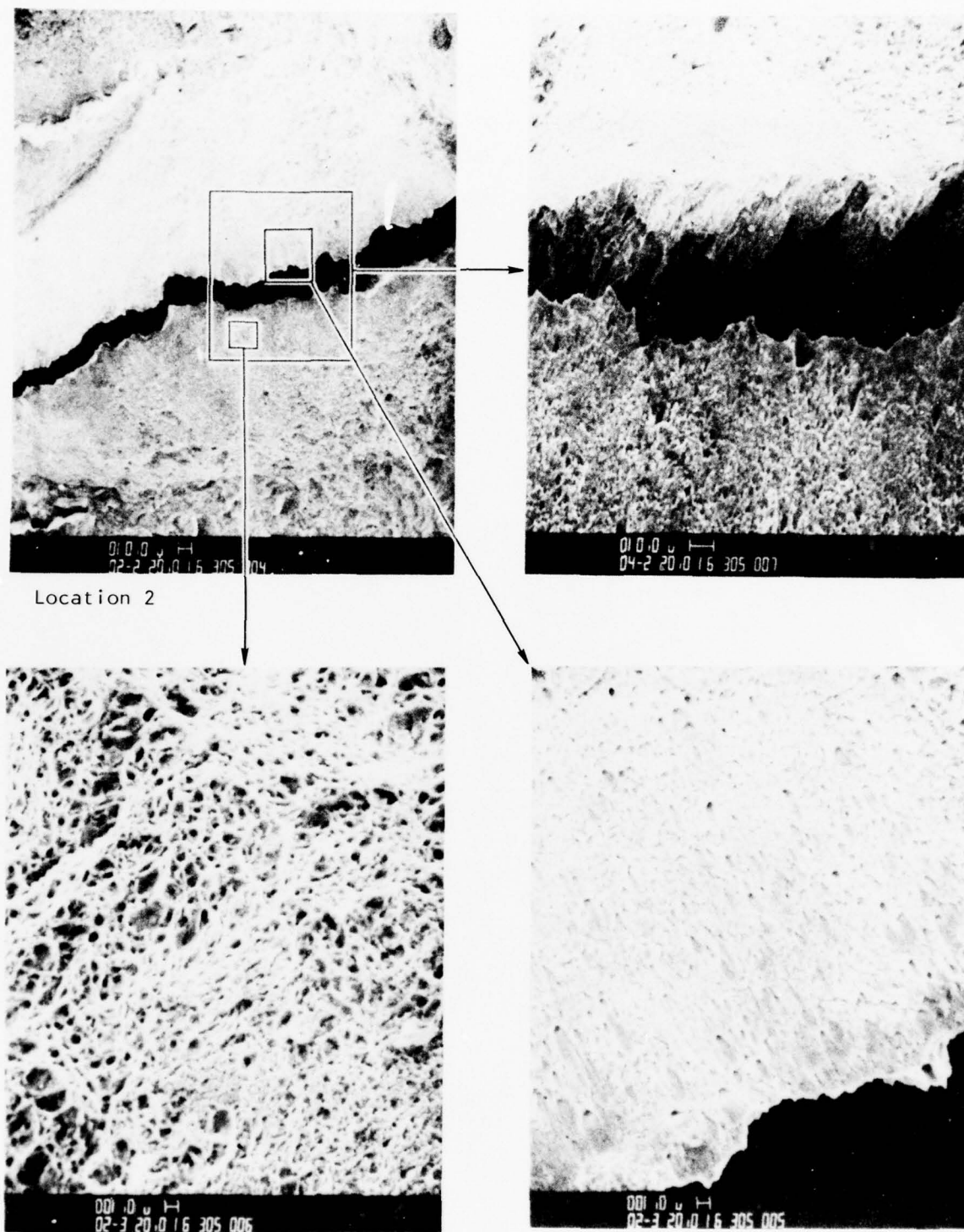
Location 2

Figure 99. Scanning electron micrograph at a "split" region in fracture surface of tensile bar T-10.
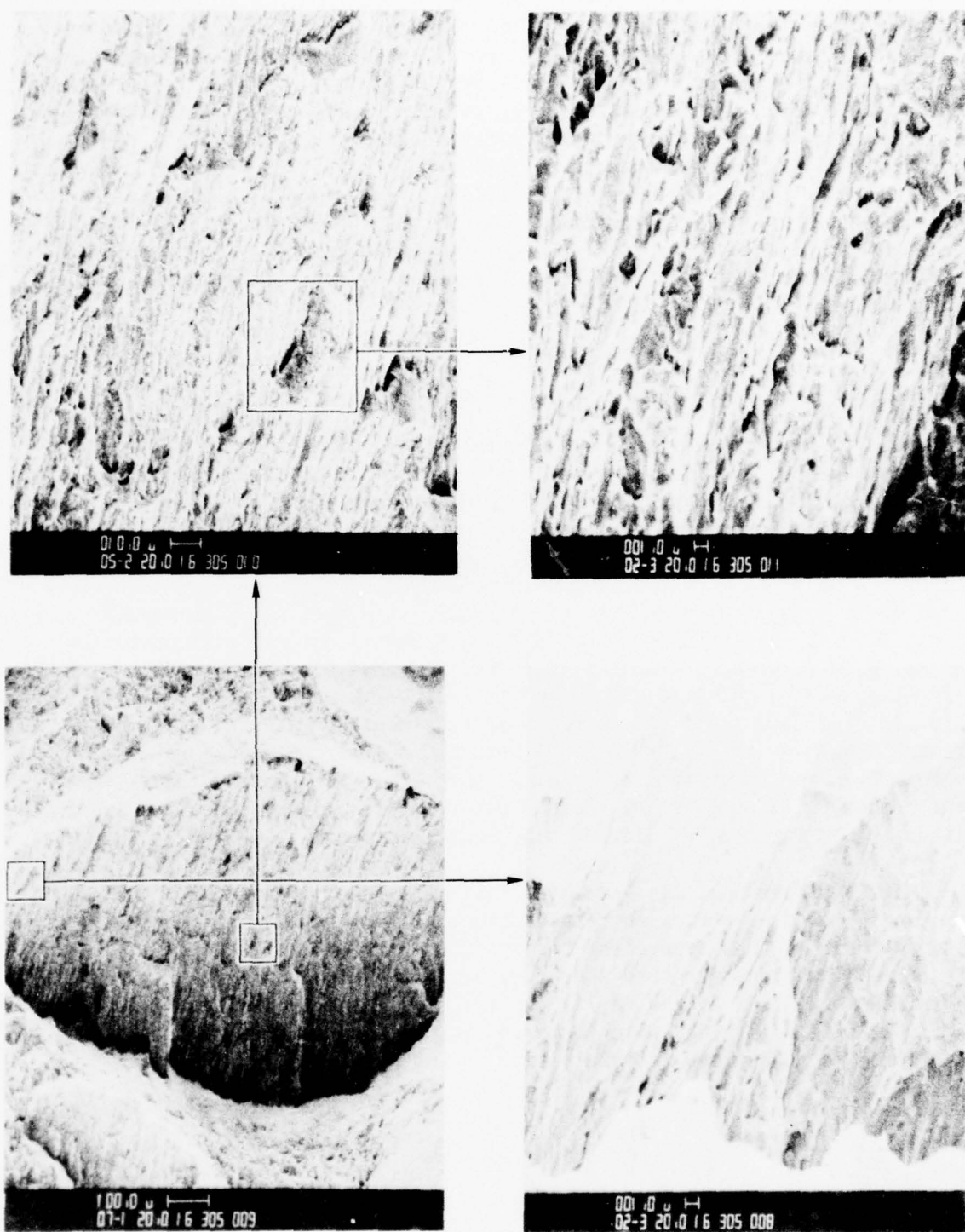
Location I

Figure 100. Scanning electron micrographs of fracture surface of tensile bar T-10.

195

The Charpy bars F-6, F-19, and PMHT (Figures 101 and 102) exhibited very similar fractures with a small shear zone at the leading edge of the fracture and ductile rupture developing as the crack progressed. All four specimens exhibited a series of parallel markings at low magnification, which higher magnification showed to be secondary cracking (e.g., Figure 102:302 003). By contrast, the low impact strength (Figure 103), (28 ft-1b) specimen T-10 exhibited very little secondary cracking and crack propagation was predominantly intergranular (Figure 104:306 003, 306 005). The higher impact resistance of the PMHT specimen (60 feet per pound) probably resulted from the initial fracture shear zone being steeply inclined to the macroscopic crack plane.

Austenite Determination

Results of the X-ray diffraction analysis to determine the volume fraction of austenite are listed in Table 39. A summary of these results and data developed at AFML on samples from this program are listed in Table 40. For 1- and 2-inch-thick material, the effect of section thickness and cooling rate on the volume fraction of retained austenite does not appear to be significant. (The value for the oil-quenched, 1-inch specimen appears to be anomalously high). When the material is held at higher aging temperatures (e.g., T10-975° F, 10 hours and F-1250° F, 8 hours), nickle will partition resulting in reverted austenite. Evidence for this effect is the high volume percentages (4.30 and 6.18) of austenite in the T10 and "F" specimens. The data also indicates that subsequent heat treatment of material given either premachining heat treat ("H" or "F") returned the percentage of reverted austenite to the same level as material only given the standard heat treatment. This verifies that full-hard, heat-treat response was not impaired by either the "H" or the "F" premachining heat treatment.

Metallurgical analysis indicates that although approximately 6 volume percent of reverted austenite results from the "F" premachining heat treat, no impairment of subsequent heat treat occurs. The similarity of microstructure of various quenched specimens is in agreement with results that, in thickness up to 2 inches, AF1410 is relatively insensitive to cooling rate. Tensile splitting, which occurred in overaged tensile specimens, is attributed to an extreme triaxial state during testing.

HEAT TREAT SELECTION

On the basis of obtaining the maximum improvement in machinability commensurate with cost and the retention of (1) satisfactory tensile ultimate and yield strengths, (2) satisfactory fatigue, da/dn crack rate growth, and impact properties, (3) good weldability, and (4) freedom from distortion,

Numbers show location of
micrographs of Figure 102

Figure 101. Scanning electron micrograph of fracture surface of charpy bar F-6.

197
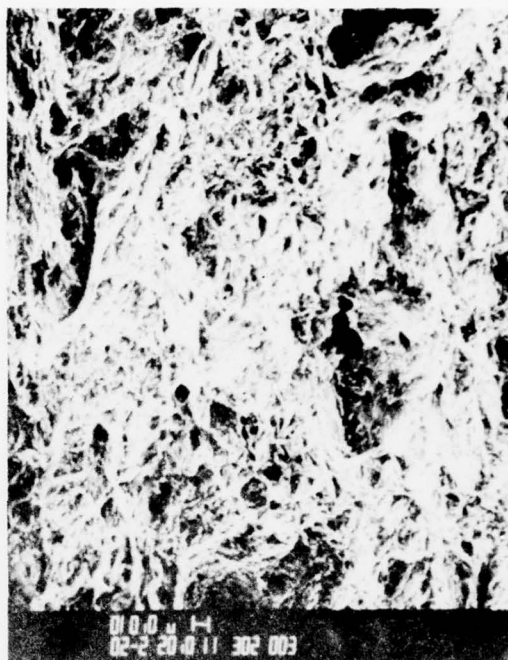
Location 2
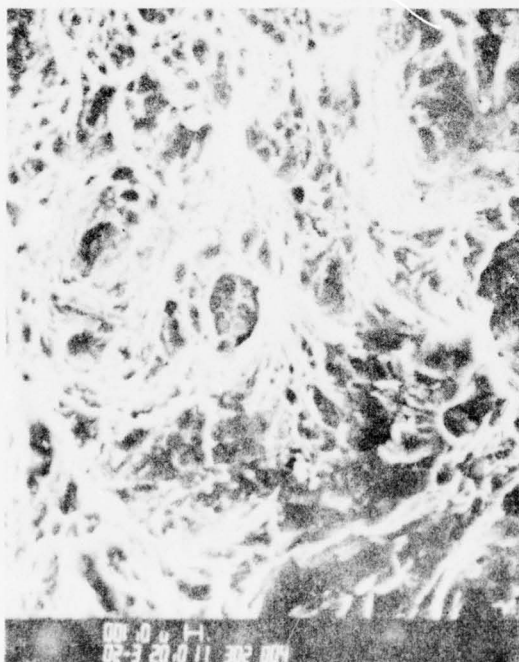
Location 3
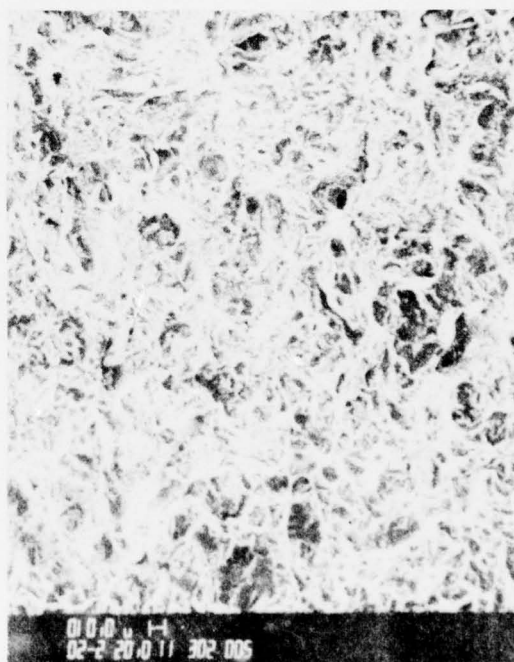
Location 4

Location 5

Figure 102. Scanning electron micrographs of fracture surface of charpy bar F-6.
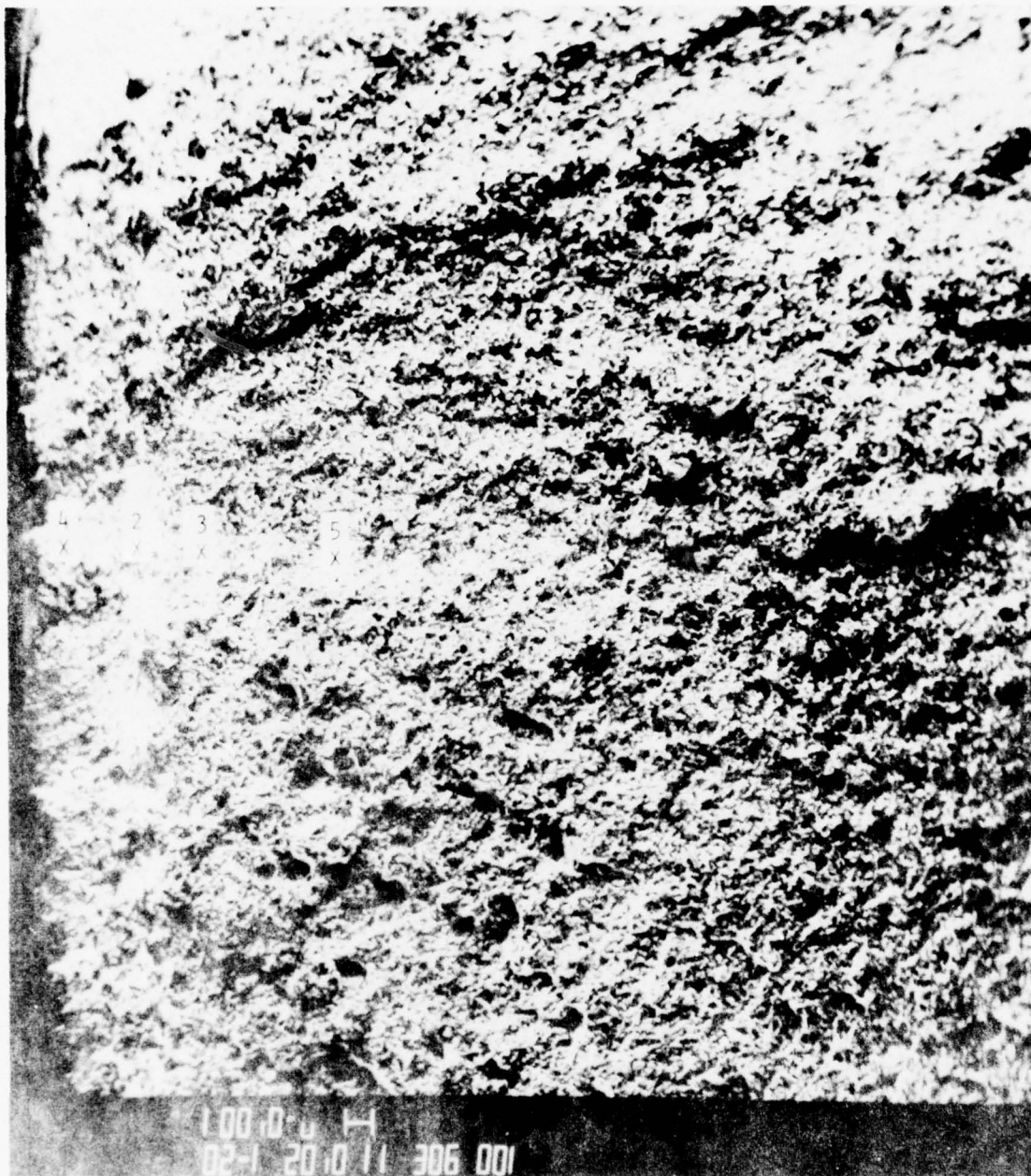
Numbers show locations of
micrographs of Figure 104

Figure 103. Scanning electron micrograph of fracture surface of
charpy bar T-10.
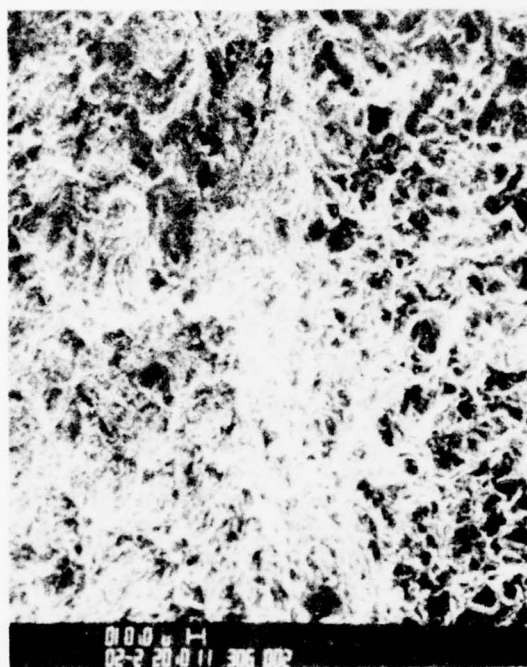
Location 2
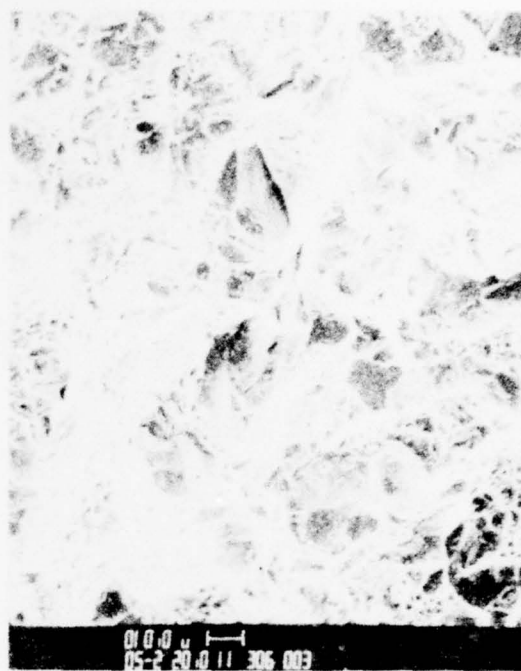
Location 3
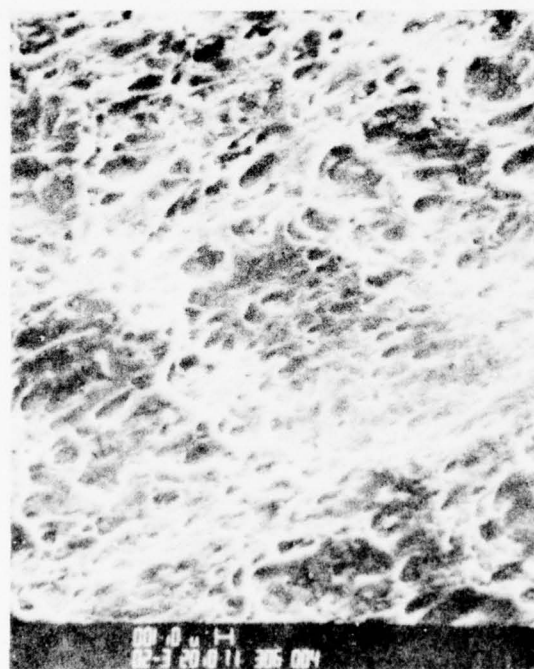
Location 4

Location 5

Figure 104. Scanning electron micrographs of fracture surface of charpy bar T-10.

200

TABLE 39

RETAINED AUSTENITE CONTENT OF VARIOUSLY HEAT-TREATED AF1410 STEEL SPECIMENS

| Specimen | Phase | Area | | V_γ^1 |
		Calculated	Ratio	(percent)
F8	α	596.32		
F8	γ	35.08	17.00	2.31
F10	α	686.50		
F10	γ	82.34	8.34	4.60
F12	α	600.79		
F12	γ	23.02	26.10	1.52
2C	α	654.75		
2C	γ	40.26	16.26	2.41
7C	α	705.72		
7C	γ	35.04	20.14	1.96
1C	α	654.25		
1C	γ	44.86	14.38	2.72
T10	α	718.00		
T10	γ	80.28	8.944	4.30
PMHT	α	600.6		
PMHT	γ	41.62	14.43	2.71
"F"	α	673.92		
"F"	γ	110.48	6.10	6.18

[1] $V_\gamma = \dfrac{1}{1+2.49(R)}$

201

TABLE 40

SUMMARY OF RETAINED AUSTENITE CONTENTS

Austenitizing temp (°F)	time (hrs)	Thickness (inches)	Retained austenite (volume percent)			Remarks
			Air cool	Oil quench	Water Quench	
1,525	4	1	-	-	4.30	Overaged, 975° F - 10 hr
1,500	1	1	2.31	4.60^1	1.52	Cooling rate evaluation
1,525	4	2	2.41	1.96	2.72	Cooling rate evaluation
1,500	1	1	-	-	2.71	Std heat treatment
1,500	1	1	-	-	[0]	Prior "F" heat treat + std ht
1,500	1	1	-	-	[2.14]	Prior "H" heat treat + std ht
1,300	4	1	[7.46]	-	-	"H" heat treat
1,250	8	1	6.18, [5.06]	-	-	"F" heat treat

[1] Anamolous result

NOTES: 1. The values in brackets are AFML data.

2. Std ht (-) standard heat treat

the recommended heat-treatment combination of AF1410 steel to obtain
maximum machinability for sections through 2 inches thick is as follows:

Premachining Heat Treatment

1. Austenitize at 1,250° F for 8 hours

2. Air Cool

Postmachining Heat Treatment

1. Austenitize at 1,650° F for 1 hour (if not previously performed)

2. Air Cool

3. Austenitize at 1,525° ±25° F for 1 hour

4. Air Cool

5. -100° F for 1 hour

6. Age 950° ±10° F for 5 hours

An austenitizing temperature of 1,525° ±25° F has been selected over the
standard 1,500° F treatment because of the lower properties indicated at
1,450° F. It is not now known exactly at what point below 1,500° F an
unsatisfactory heat-treat response will occur. Consequently, an austen-
itizing temperature range was selected to assure that no significant variation
in properties occurs within the normal heat-treat furnace control capability.

PHASE III — DETERMINATION OF MACHINING PARAMETERS FOR AF1410 STEEL

OBJECTIVE

The objective of Phase III was to establish optimum AF1410 steel
machining procedures for the end milling, drilling and reaming machining
processes used in the fabrication of complex airframe hardware.

APPROACH

AF1410 steel specimen blanks were prepared and given either the selec-
ted pre-machine heat treatment or the selected pre and post machining com-
bination heat treatment. Both conditions were machined by end milling
with the full hard material only used for drilling and reaming studies.
Slot and semislot end milling, drilling, and reaming were selected for

203

evaluation in this program because they represent high-cost/high-usage processes in airframe fabrication. A range of feeds and speeds were used to establish cutter tool life at a landwear of 0.008 inch. The results were used to calculate the values of the constants in a tool life equation. This equation was used in combination with machining cost equations (Table 41) to establish the costs for machining the three AF1410 steel test part configuration, and to establish minimum-cost operating speeds (Table 42). The results of these calculations were analyzed in conjunction with observations of cutter performance relative to chipping, overheating, and machined surface integrity to establish optimum machining parameters for AF1410 steel.

RESULTS AND DISCUSSION

End Milling

Premachine Heat-Treat Condition

The results of the end milling tests with Cobalt HSS and carbide cutters on AF1410 steel in the premachine heat-treat condition are presented in Tables 43 through 44, and Figures 105 and 106. Examination of the results in Table 43 indicates that the tool life of cutters with 11-degree primary and 22-degree secondary angles was significantly better (by about 100 percent on the average) than for cutters with 7-degree primary and 14-degree secondary angles. Based on early indications of better tool life at higher chip loads and higher metal removal rates, the six-flute cutter was selected for completion of the machining studies. The data in Table 43 indicates that a metal removal rate of approximately 77 cubic inches per hour and a tool life of about 290 inches of travel can be achieved with six-flute, high-speed steel cutters at a chip load of 0.00292 inch and a speed of 66 SFM. This result is markedly superior to that obtained in the limited studies on the four-flute cutters.

Careful attention to machining practice was required to achieve optimum tool performance. For example, severe flute cracking (Figure 107) resulted from chip entrapment due to improper cutting fluid application. This factor, and machining speed and chip load are especially important in providing good surface integrity. However, since rough machining operations are usually followed by heat treatment and finish machining operations, surface integrity requirements for a rough machined surface are usually not of concern.

Although not anticipated to be cost effective for rough machining AF1410 steel, several carbide end milling cutters were nevertheless tested for this application (Tables 45 and 46). The performance in all cases was poor because of excessive chipping (Figure 108), and testing of carbide cutters for rough end milling was discontinued.

204

TABLE 41

GENERALIZED MACHINING COST EQUATIONS

Milling

$$C = M\left[\frac{D(L+e)}{3.82f_t v} + \frac{R}{r} + t_i + \frac{Lt_d}{2T_t} + \frac{1}{2T_t} + \frac{C_p}{(k_1+1)} + Gt_s + \frac{Gt_b}{k_2} + \frac{2C_c}{k_3} + C_w + Gt_p\right]$$

Drilling or reaming

$$C = M\left[\frac{D(L+e)}{3.82f_r v} + \frac{R}{r} + t_i + \frac{Lt_d}{T_t} + \frac{1}{T_t} + \frac{C_p}{(k_1+1)} + Gt_s + Gt_p\right]$$

Tapping

$$C = M\left[\frac{mD(L+e)}{1.91v} + \frac{R}{r} + t_i + \frac{Lt_d}{T_t} + \frac{1}{T_t} + \frac{C_p}{(k_1+1)} + Gt_s + Gt_p\right]$$

$\dfrac{\$}{Min}$ — Feeding time — Rapid traverse time — Load & unload load time — Setup time — Cutter Index time — Dull tool replacement time — Tool depreciation cost — Tool resharpening cost — Rebrazing or blade reset cost — Insert or blade cost — Grinding wheel cost — Tool presetting cost

From reference 5

TABLE 42

OPTIMIZED MACHINING EQUATIONS

Optimized Cutting Speed Equations

for milling

$$v_{min.\ cost} = \left[\frac{nMD(L+e)}{3.82f_t L \left(Mt_d + \frac{C_p}{k_1+1} + Gt_s + \frac{Gt_b}{k_2} + \frac{2C_c}{k_3} + C_w + Gt_p\right)}\right]^{\frac{n}{n+1}} (S_t)^{\frac{1}{n+1}}$$

$$v_{max.\ prod.} = \left[\frac{nD(L+e)}{3.82f_t L t_d}\right]^{\frac{n}{n+1}} (S_t)^{\frac{1}{n+1}}$$

for drilling or reaming

$$v_{min.\ cost} = \left[\frac{nMD(L+e)}{3.82f_r L \left(Mt_d + \frac{C_p}{k_1+1} + Gt_s + Gt_p\right)}\right]^{\frac{n}{n+1}} (S_t)^{\frac{1}{n+1}}$$

$$v_{max.\ prod.} = \left[\frac{nD(L+e)}{3.82f_r L t_d}\right]^{\frac{n}{n+1}} (S_t)^{\frac{1}{n+1}}$$

Optimized Tool Life Equations

for milling, drilling, reaming, or tapping

$$t_t\ min.\ cost = \left[\frac{S_t}{v_{min.\ cost}}\right]^{\frac{1}{n}}$$

$$t_t\ max.\ prod. = \left[\frac{S_t}{v_{max.\ prod.}}\right]^{\frac{1}{n}}$$

Equations for Operation Time per piece and production rate

Milling

$$t_m = \frac{D(L+e)}{3.82f_t v} + \frac{R}{r} + t_i + \frac{Lt_d}{2t_t}$$

Drilling and reaming

$$t_m = \frac{D(L+e)}{3.82f_r v} + \frac{R}{r} + t_i + \frac{Lt_d}{t_t}$$

Equation for production rate

$$P = \frac{60}{\left(\Sigma t_m + t_L + \frac{t_o}{N_L}\right)}$$

From reference **5**.

206

TABLE 43

RESULTS OF END MILLING TESTS WITH COBALT HSS STEEL CUTTERS ON AF1410 STEEL IN PREMACHINE HEAT-TREAT CONDITION

Cutter No.[a]	Cutter geometry					Machining conditions									At 0.008 scarland					Surface finish	
						Cut geometry			Cutter				Metal removal rate (in.³/hr)								
	Dia (inch)	No. of flutes	Helix angle (deg)	Primary angle (deg)	Secondary angle (deg)	Depth (inch)	Width (inch)	Length (inch)	RPM	Speed (SFM)	Chip load (mils)	Feed (IPM)		No. of passes	Metal removed (in.³)	Time (min)	Travel of work (inch)	Chipping	Start (RHR)	End (RHR)
1CC	1.000	6	28	6	14	0.387	0.725	8.687	213	56	0.00127	1.625	28.91	19.98	51.47	106.81	173.57	None	90	150
1BB-R1	0.996	6	28	7	14	0.391	0.742	8.687	256	67	0.00116	2.250	31.24	26.37	69.97	101.81	229.08	Light	75	80
1BB	1.000	6	28	6	14	0.406	0.729	8.500	176	48	0.00154	1.625	30.69	11.60	31.20	60.99	99.11	V.light	90	90
1AA	1.000	6	28	6	15	0.406	0.729	8.500	160	42	0.00210	2.000	37.98	10.75	28.92	45.69	91.38	Med	100	115
2CC-R2	0.985	6	28	10	20	0.375	0.733	8.687	326	84	0.00131	2.625	45.87	18.57	46.47	60.79	159.58	None	75	75
2CC-R1	0.992	6	28	10	20	0.430	0.733	8.687	304	103[b]	0.00137	3.250	65.70	10.60	31.02	28.33	92.08	None	60	60
2BB-R1	0.996	6	28	10	22	0.386	0.722	8.718	256	67	0.00146	2.250	30.09	28.75	67.01	111.40	250.61	Light	100	100
2CC	1.000	6	28	11	22	0.386	0.725	8.687	213	56	0.00147	1.875	35.39	32.71	84.55	151.55	284.15	None	90	125
2BB	1.000	6	28	10	22	0.375	0.727	8.562	176	48	0.00154	1.625	27.94	43.90	107.87	231.62	376.39	Light	65	250
2BB-R3	0.985	6	28	10	20	0.375	0.733	8.687	326	84[c]	0.00166	3.250	55.19	24.63	60.55	65.83	213.90	None	100	125
2CC-R5	0.935	6	28	10	21	0.375	0.708	8.937	148	36	0.00183	1.625	27.00	37.28	94.35	205.03	333.17	Light	100	125
2CC-R3	0.979	6	28	10	20	0.375	0.746	8.843	250	60	0.00210	3.250	57.50	31.43	82.01	85.57	278.11	None	60	75
2CC-R4	0.985	6	28	10	20	0.375	0.739	8.687	250	65	0.00241	5.750	64.87	20.24	65.72	60.79	227.95	Light	80	75
2BB-R5	0.965	6	28	9	20	0.375	0.739	8.687	256	65	0.00292	4.500	78.79	33.27	84.54	64.23	289.02	Light	180	130
1CC2-R1	0.992	6	28	11	23	0.375	0.706	8.685	250	67	0.00292	1.500	73.84	34.15	83.51	65.91	296.59	None	150	100
1BB2-R2	0.985	6	28	12	21	0.375	0.706	8.685	250	66	0.00341	5.250	88.57	6.71	16.46	11.15	58.54	Light	–	–
3CC	1.000	4	28	–	15	0.356	0.722	8.718	326	85	0.00143	1.875	30.39	15.16	35.70	70.49	152.16	Light	–	125
3BB-R1	0.992	4	28	–	14	0.391	0.742	8.687	250	67	0.00158	1.625	29.82	32.04	85.13	171.28	278.33	None	75	100
3BB	1.000	4	28	6	15	0.375	0.720	8.562	176	46	0.00250	1.625	28.38	22.21	55.35	117.02	190.16	Med	125	100
3AA	1.000	4	28	–	14	0.406	0.720	8.500	148	39	0.00250	1.625	30.91	10.42	28.08	51.50	88.57	Med	120	130
4CC	1.000	4	28	11	20	0.356	0.722	8.500	326	85	0.00144	1.875	30.38	22.91	53.93	106.52	199.73	None	60	100
4BB	1.000	4	28	11	22	0.375	0.727	8.562	176	46	0.00250	1.625	28.19	24.71	61.18	130.20	213.57	Light	70	60
4AA	1.000	4	28	11	21	0.406	0.729	8.500	148	39	0.00250	1.625	30.31	16.78	39.05	77.31	125.63	Med	135	155

a "R" suffix indicates number of times cutter was reground.

b Deep-blue chips. Flutes very discolored.

c Gold to blue chips.

TABLE 44

COBALT HSS CUTTER END MILLING DATA IN THE FORMAT OF THE MACHINING DATA HANDBOOK

MATERIAL	CONDITION AND MICROSTRUCTURE	BHN	TRADE NAME	INDUSTRY GRADE	CUTTER TYPE	DIA. inch	NO. TEETH	FLUTE LENGTH inch	UP OR DOWN MILLING	HELIX ANGLE°	RR°	CORNER RADIUS inch	ECEA°	END REL° PERIPH REL°	CUTTING FLUID CODE	DEPTH OF CUT inch	WIDTH OF CUT inch	FEED ipt	TOOL LIFE END POINT inch	SPEED feet/minute
AF1410	Pre-Machine Heat Treat	340	-	Cobalt HSS M42	SOLID	1	6	2	DOWN	28	7	.060	1.5	7/14	4	.400	.730	.0013	.008	174/56
			-																	229/67
			-															.0015	.008	99/48
			-															.0021	.008	91/42*
AF1410	Pre-Machine Heat Treat	340	-	Cobalt HSS M42	SOLID	1	6	2	DOWN	28	11	.060	1.5	11/22	4	.375	.725	.0014	.008	92/103
			-																	250/67
			-															.0015	.008	284/56
			-															.0017	.008	214/84
			-															.0018	.008	333/36
			-															.0021	.008	278/66
			-																	298/67
			-															.0021	.008	289/65
			-															.0029	.008	59/66
AF1410	Pre-Machine Heat Treat	340	-	Cobalt HSS M42	SOLID	1	4	2	DOWN	28	7	.060	1.5	7/14	4	.380	.730	.0034	.008	132/85
			-															.0014	.008	278/67
			-															.0016	.008	190/46*
			-															.0023	.008	89/39*
AF1410	Pre-Machine Heat Treat	340	-	Cobalt HSS M42	SOLID	1	4	2	DOWN	28	11	.060	1.5	11/22	4	.380	.725	.0027	.008	200/85
			-															.0014	.008	212/46
			-															.0023	.008	126/39*
			-															.0027	.008	

*Chipping

208

Figure 105. Cobalt HSS cutter tool life for end milling
AF1410 steel in premachine heat-treat condition.

209
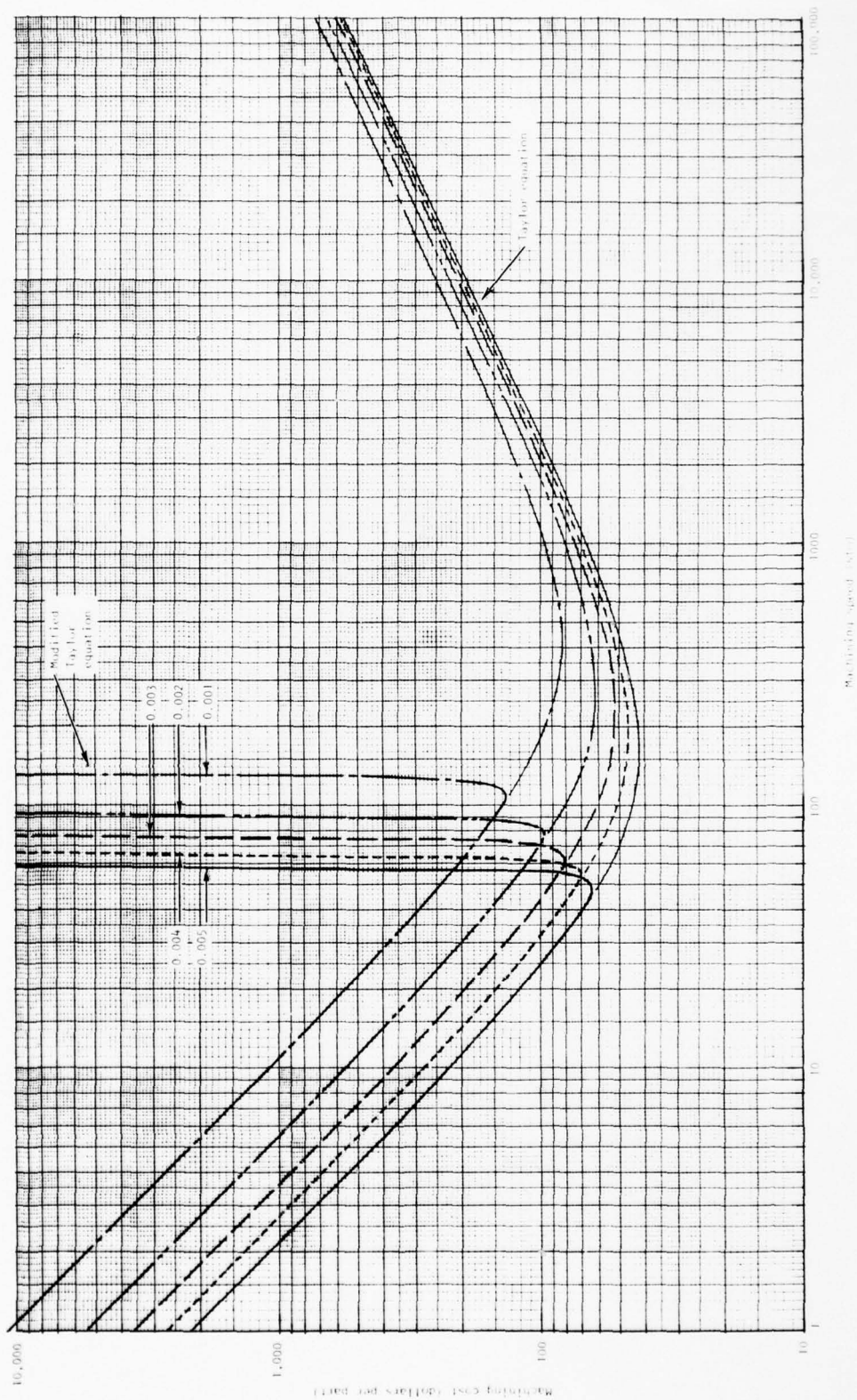
Figure 106. Cost of end mill machining AF1410 steel test part in premachine heat-treat condition.

210
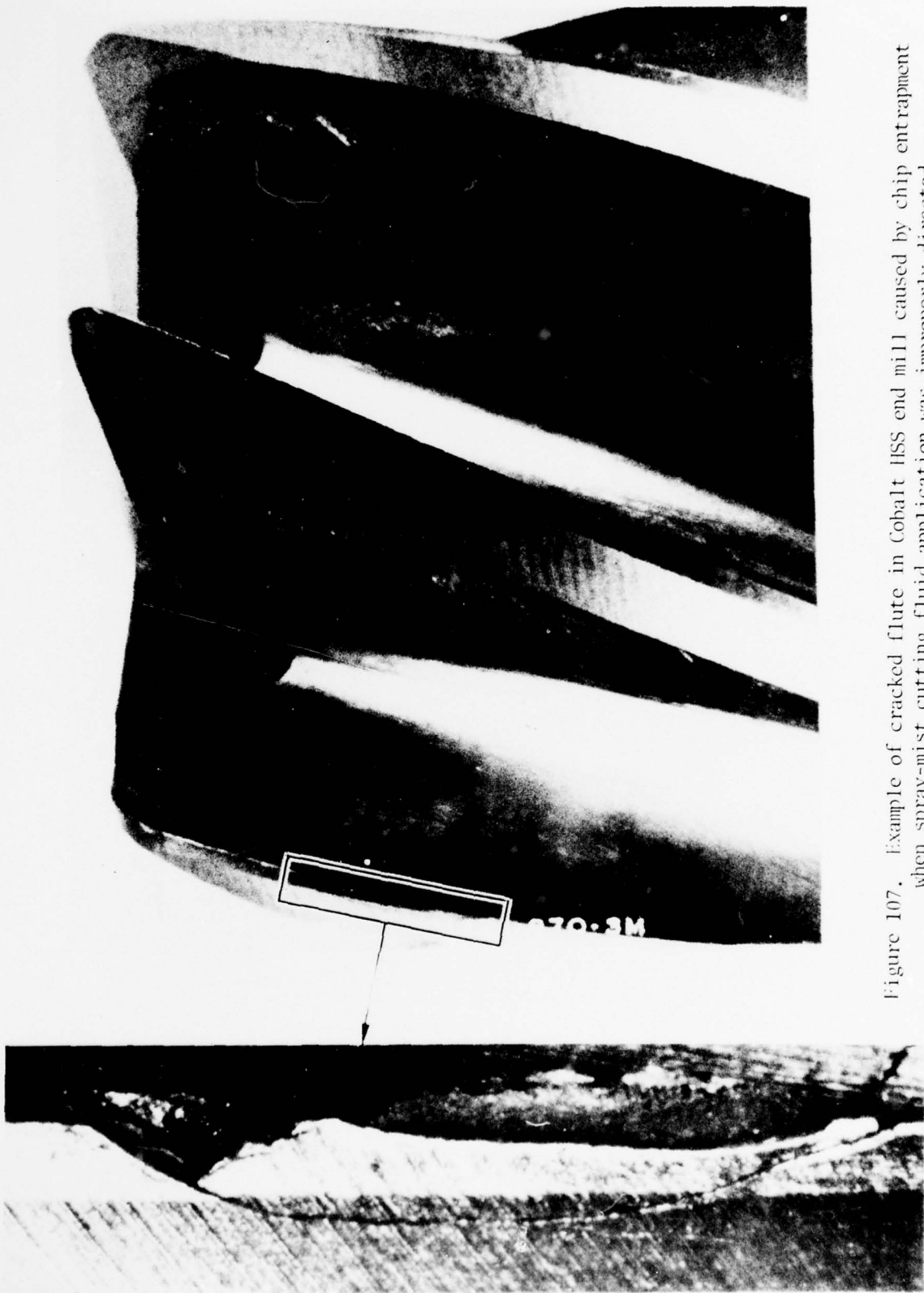
Figure 107. Example of cracked flute in Cobalt HSS end mill caused by chip entrapment when spray-mist cutting fluid application was improperly directed.

211

TABLE 45

RESULTS OF END MILLING TESTS WITH CARBIDE CUTTERS ON AF1410 STEEL IN PREMACHINE HEAT-TREAT CONDITION

| Cutter | | | Cutter geometry | | | | Machining conditions | | | | | | | | At end of test[a] | | | | | Surface finish | |
No.	Carbide	Dia (inch)	No. of flutes	Helix angle (deg)	Primary angle (deg)	Secondary angle (deg)	Cut geometry Depth (inch)	Width (inch)	Length (inch)	Cutter RPM	Speed (SFM)	Chip load (mils)	feed (IPM)	Metal removal rate (in³/hr)	No. of Passes	Metal removed (in³)	Time (min)	Travel of work (inch)	Landwear (inch)	Start (RHR)	End (RHR)
13	C5	0.998	4	28	4	11	0.375	0.661	8.687	394	105	0.00166	2.625	35.50	2	3.92	6.62	17.37	-	-	-
23	C5	0.998	4	28	6	16	0.375	0.746	8.845	394	105	0.00166	2.625	44.06	5	7.42	10.11	26.53	0.0055	-	-
33	AV107	0.999	4	20	8	19	0.375	0.746	8.845	177	125	0.00118	2.250	37.77	4	9.90	15.72	35.37	0.0105	-	-
43	AV107	0.999	4	20	9	15	0.375	0.746	8.845	394	105	0.00250	3.750	62.94	1	2.47	2.36	8.84	b	-	-

[a]All tests stopped because of excessive chipping on flutes

[b]Heavy chipping

212

TABLE 46

CARBIDE CUTTER END MILLING DATA IN THE FORMAT OF THE MACHINING DATA HANDBOOK

| Material | Condition and microstructure | BHN | Tool material | | Cutter type | Dia (in.) | No. teeth | Flute length (in.) | Up or down mill ing | Helix angle (deg) | RR (deg) | Tool geometry | | | fluid code | cut ting fluid code | Depth of cut (in.) | Width of cut (in.) | Feed (ipt) | Tool life end point (in.) | Tool life/cutter (inches work travel) versus |
			Trade name	Indus try grade								Corner radius	ECA (deg)	End rel periph rel (deg)							Speed (feet/minute)
4340	Premachine heat treat	340		C5 carbide	Solid	1	4	1.75	Down	28	5	0.060	1.5	$\frac{5}{10}$		1	0.375	0.001	0.0017	*	$\frac{5}{105}$
			Walmet	BWC carbide						28	-			$\frac{7}{12}$			.375	.76	.0017	.006*	$\frac{26}{105}$
			Walmet	BWC carbide	Solid	1	4	1.75	Down	20	8	.060	1.5	$\frac{8}{10}$		1	.375	.76	.0012	.011*	$\frac{55}{125}$
			Walmet							20	-			$\frac{-}{12}$			.375	.76	.0024	*	$\frac{9}{105}$

*Test stopped because of chipping on flutes.

213

A. Typical 0.008-inch wear
on corner radius
Co HSS
6 flute
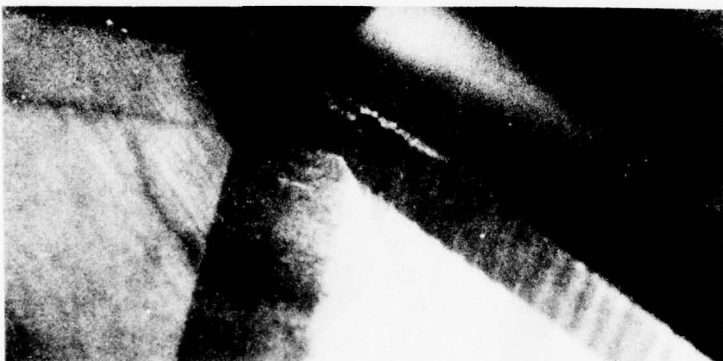
B. Chipping on corner radius
Co HSS
6 flute
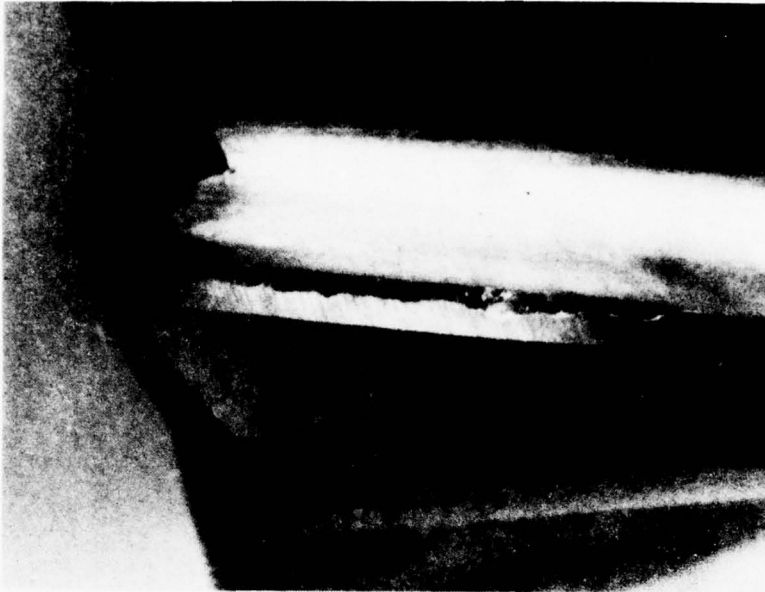
C. Heavy chipping on flute
WA 107 carbide
6 flute

Figure 108. Examples of milling cutter wear and chipping encountered during machining tests on AF1410 steel.

214

Taylor Equation Modification

Initially, the Taylor tool life equation was used for determining the optimum feed and speed for machining AF1410 (Reference 5). The results as presented in Figure 105 show that the observed tool wear accelerates at a faster rate than is taken into account by the Taylor equation. As a consequence, optimum values for machining AF1410 could be in error if calculated on the basis of the Taylor equation.

In an effort to correct this situation, an empirical modification of the Taylor equation was made as follows:

$$VT^n f^a = KZ^n$$

where

V = machining speed

T = tool life

f = feed (chip load)

Z = modification factor = $\exp B [1 + V f) - V f]^r$

n,a,k,B,r = constants

It is readily apparent that if Z is set equal to 1, the modified equation reduces directly to the Taylor equation. Further, it is emphasized that the modified equation was developed specifically to fit the end milling data for AF1410, as reported herein. Additional modification would undoubtedly be required for more general application.

The least square fit of the modified equation to the end milling data is shown in Figure 105 in comparison to the Taylor equation fit. The better fit of the modified equation can be seen. The sharp dropoff in tool life coincides with the appearance of oxidized chips, evidenced by gold to blue coloration, signifying excessive heat generation.

The Taylor equation and the described modification were used with the cost equation for end milling (Table 41) to obtain the comparative costs of rough machining a part (Figure 106). The results, as plotted in Figure 106, show the Taylor equation minimum costs to occur at machining speeds of 150 to 400 SFM, depending on chip load. These speeds are well in excess of the Co HSS cutter capability in this application, as is evident from Figure 105, and are therefore, unrealistic. In comparison, the machining speeds for minimum costs obtained with the modified equation are in good agreement with the experimental results. The minimum cost speed and minimum cost per part results are presented in Table 47. Although the cost appears to decrease with

215

TABLE 47

MINIMUM COST SPEED AND MINIMUM COST PER PART FOR VARIOUS MACHINING OPERATIONS ON AF1410 STEEL

Machining operation*	Minimum cost** speed (SFM) at following chip loads***					Minimum cost** per part ($) at following chip loads				
	0.001	0.002	0.003	0.004	0.005	0.001	0.002	0.003	0.004	0.005
Rough end milling in premachining HT condition (163.625-in.³ metal removed per part)	109	77	63	54	48	133.50	96.68	80.17	70.25	63.45
Finish end milling in full hard condition (86.5-in² surface area per pass, and 4.3 in.³ metal removed per part)	113	87	73	65	58	36.89	21.43	16.09	13.28	11.52
Drilling - 1.1-inch deep x 23/64-inch diam holes in full hard condition (15.9475-in.³ metal removed in reaming 125 holes per part)	-		30	-	-	-	-	87.92	-	-
Reaming - 1.1-inch deep x 23/64-inch diam holes to 3/8-inch diam holes in full hard condition (1.23875-in.³ metal removed in reaming 125 holes per part)	81	44	31	24	19	166.31	153.93	147.15	142.50	138.97

*All with Co HSS cutters; 1-inch diameter for end milling, 23/64-inch diameter for drilling, and 3/8-inch diameter for reaming

**Excluding surface integrity considerations

***IPT for end milling, IPR for drilling and reaming

216

chip load, the desirable tool wear pattern (Figure 108a) can be expected to give way to chipping of the cutting edges (Figure 108b), and thereby limit the chip load at some point. The results of this program did not provide a precise value for this limit, but it is estimated to be between 0.0035 and 0.004 inch.

Full-Hard Condition

The results of end-milling tests on AF1410 in the full-hard, heat-treat condition are presented in Tables 48 and 49, and in Figures 109 through 111. Six-flute Cobalt HSS cutters with a 28-degree helix angle, a 7-degree primary angle, and a 15-degree secondary angle were used in the tests. This cutter geometry was selected as being typical of that used for finish machining of full-hard, high-strength steels.

As with the results for end milling AF1410 in the premachine heat-treat condition, both the Taylor equation and the modified Taylor equation were fit to the tool life test results, as shown in Figure 109. In this case, however, both curves seem to fit that data reasonably well. This can be attributed to the fact that no sharp dropoff in tool life was observed within the range of speeds and feeds tested. The maximum oxidation observed on the chips was a dark-brown color. This indicates that the maximum temperature reached was lower than that reached in the premachine heat-treat tests, and suggests that entry into a sharp dropoff region had not progressed as far as in the premachining heat-treat tests. Thus, the prediction of a sharp dropoff in tool life suggested by the fit of the modified equation to the data from the full-hard tests (Figure 109) may be true.

Of interest is the fact that the tool life on machining air-cooled or oil-quenched, full-hard AF1410 steel is nearly three times that obtained when machining water-quenched, full-hard material based on the results in Table 49. The reason for this was not evident.

The finish end-milling costs for full-hard AF1410 are shown graphically in Figure 109 as obtained using both the Taylor equation and the modified equation. The modified equation predicts only slightly higher costs than the Taylor equation. However, the Taylor equation minimum cost speeds for the higher chip loads appear overly optimistic, while the modified equation speeds are considered to be very realistic. Therefore, the modified equation was used to determine the minimum cost speed and minimum cost per part results presented in Table 47.

Surface integrity of the full-hard AF1410 steel after end milling at near minimum cost conditions of 85 SFM speed and 0.00192 IPT feed is shown in Figure 111b. Light plastic deformation and very light tearing are evident.

217

TABLE 48

RESULTS OF END MILLING TESTS WITH COBALT HSS CUTTERS ON AF1410 IN FULL-HARD CONDITION

Cutter No.	Quenching Medium	Dia (in.)	No. of Flutes	Helix angle (deg)	Primary angle (deg)	Secondary angle (deg)	Depth (in.)	Width (in.)	Length (in.)	RPM	Speed (sfm)	Chip load (ipt)	Feed (ipm)	rate (in.3/hr)	No. of passes	removed (in.3)	Time (min)	of work (in.)	Chipping	Start (BHN)	End (BHN)
3AVBI	Air	0.995	6	28	7	15	0.050	0.770	17.875 196.63	301	105	0.00158	3.750	8.06	8.28	5.69	39.38	17.69	Medium	90	60
6BB	Oil	1.000	6	28	5	15	0.050	0.770	17.875 267.30	326	85	0.00192	3.750	8.06	12.17	8.36	57.89	27.08	Light	60	60
6AV	Oil	1.000	6	28	5	15	0.050	0.770	17.875 535.11	256	67	0.00212	3.250	7.31	23.00	17.17	157.21	115.98	Light	60	70
5AV	Oil	1.000	6	28	7	15	0.050	0.770	17.875 621.30	256	67	0.00212	3.250	7.31	24.05	16.52	151.99	128.98	Medium	70	80
3BB	Oil	1.000	6	28	7	15	0.050	0.770	17.875 535.11	176	46	0.00215	2.250	5.20	38.75	26.61	307.21	691.22	None	60	70
3AVB2	Water	.980	6	28	7	15	0.050	0.770	16.30 189.00	250	66	0.00292	1.500	10.10	15.18	6.11	33.15	159.13	Medium		60
6AVBI	Air	.991	6	28	8	15	0.050	0.770	17.875 551.15	256	67	0.00292	1.500	10.11	23.95	17.80	105.08	165.87	None	70	75

218

TABLE 49

RESULTS OF END MILLING TESTS ON FULL-HARD AF1410 STEEL IN THE FORMAT OF THE MANUFACTURING DATA HANDBOOK

MATERIAL	CONDITION AND MICRO-STRUCTURE	BHN	TOOL MATL. TRADE NAME	INDUS-TRY GRADE	CUTTER TYPE	DIA. inch	NO. TEETH	FLUTE LENGTH inch	UP OR DOWN MILL-ING	HELIX ANGLE°	RR°	CORNER RADIUS	ECEA°	END REL°/PERIPH REL°	CUT-TING FLUID CODE	DEPTH OF CUT inch	WIDTH OF CUT inch	FEED ipt	TOOL LIFE END POINT inch	TOOL LIFE/CUTTER inches work travel vs SPEED-feet/minute
AF1410	Full Hard (Oil Quench)	460		Cobalt HSS M42	Solid	1	6	2	Down	28	6	.250	1.5	6/15	6	.050	.770	.0019	.008	217/85 429/67 691/46
	Full Hard (Air Quench)																	.0021		446/67
																				148/103
	Full Hard (Water Quench)																	.0016		464/67
																		.0029		159/66
AF1410	Full Hard (Air Quench)	460		C-6 Carbide	Solid	1	6	2	Down	13.5	9	.250	1.5	9/17	6	.050	.770	.0014	•	<18*/103

*Corner radius chipped on first pass

219
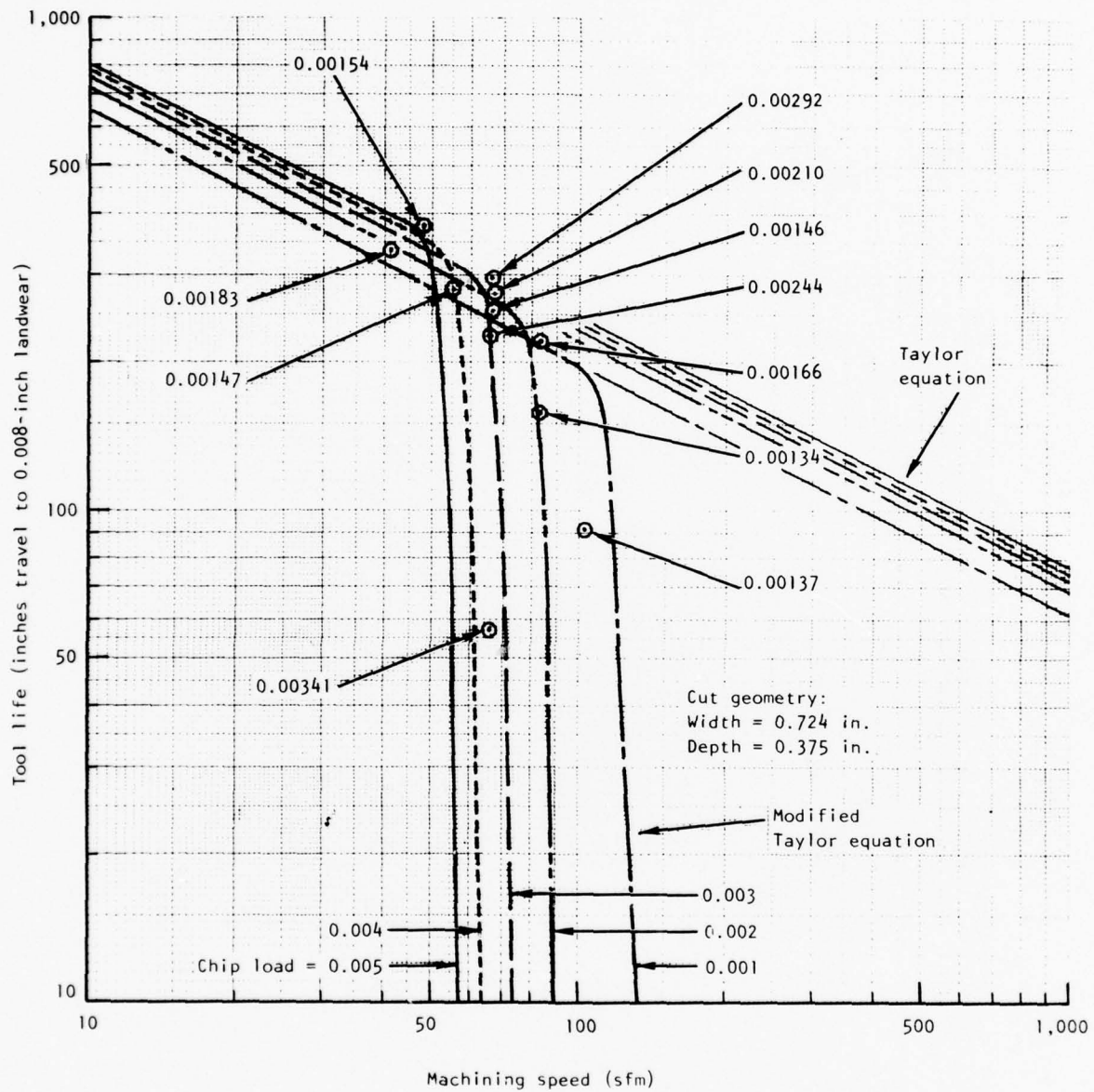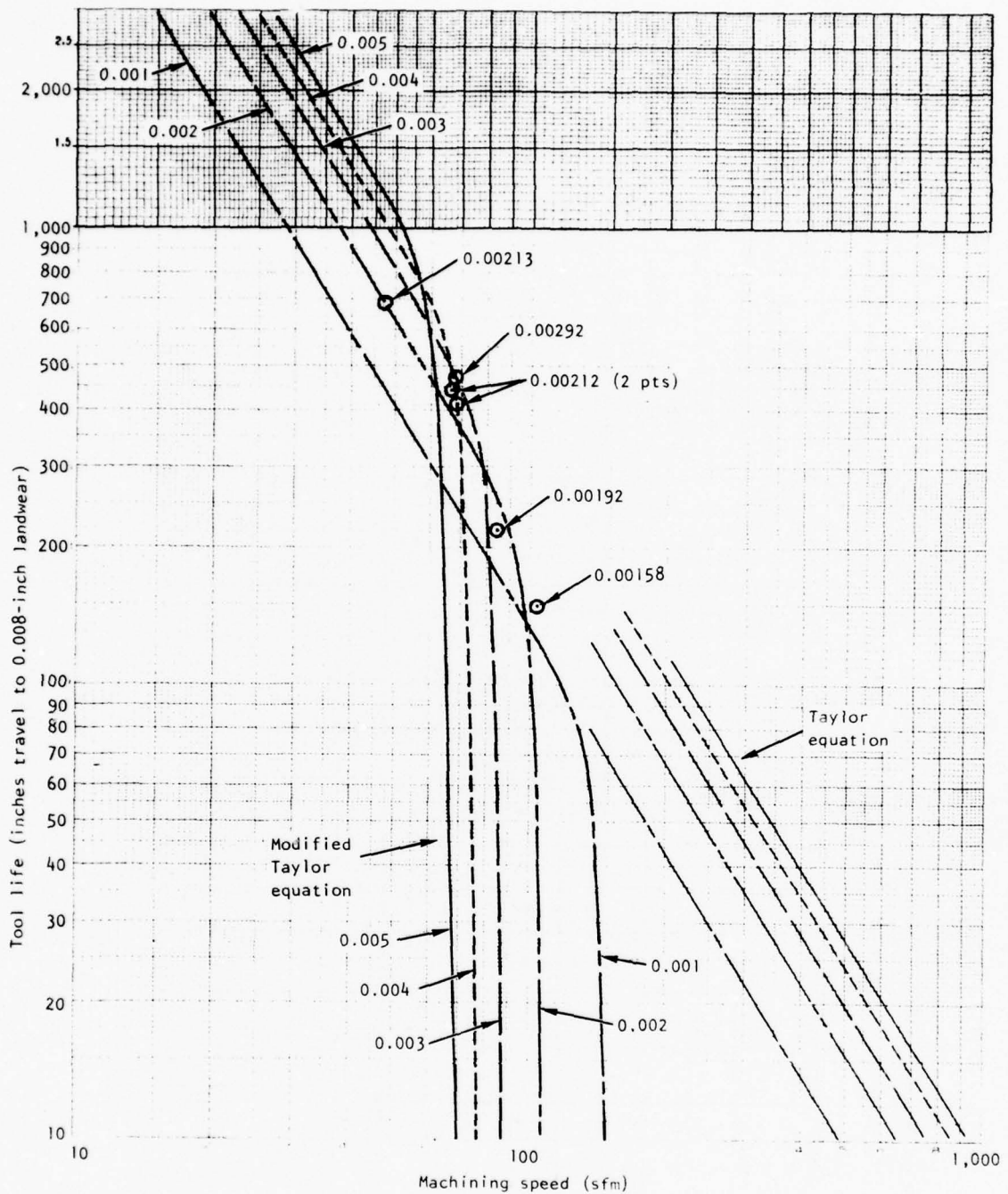
Figure 109. Cobalt HSS cutter tool life for end milling AF1410 steel in full-hard condition.
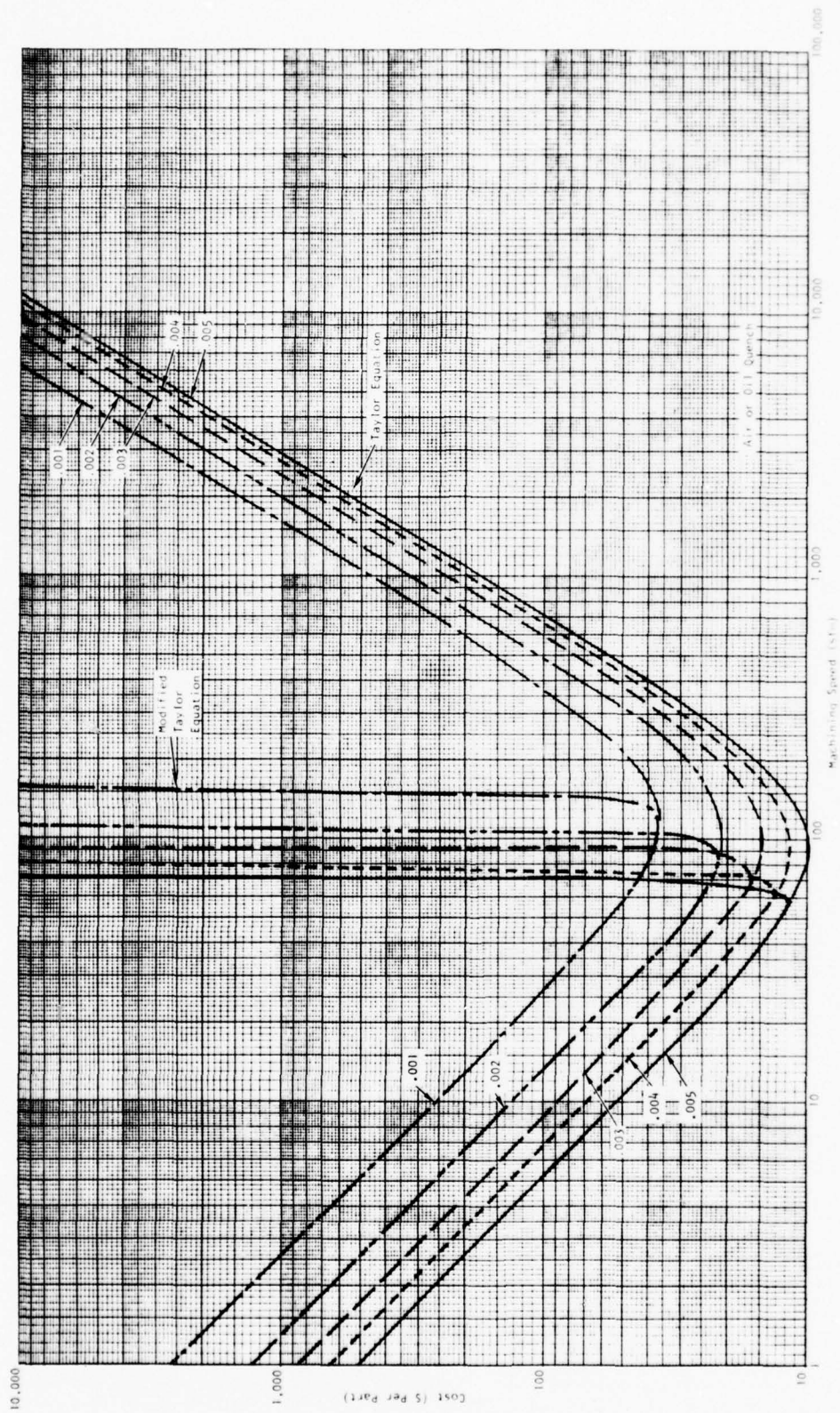
Figure 110. Cost of end mill slotting AF1410 test part in full-hard condition.

(a) 67 SFM
0.00212 IPT
(500x)
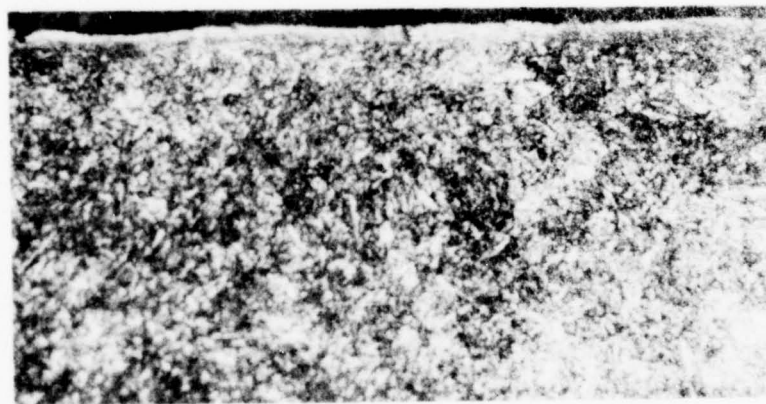
(b) 85 SPM
0.00192 IPT
(500x)

Figure 111. Sections through surfaces of full-hard AF1410 steel
after finish end milling with Cobalt HSS cutters.

222

A reduction in speed to 67 SPM eliminated these features yielding excellent surface integrity (figure 111a). Consequently, depending on the degree of surface integrity quality required, full-hard AF1410 end-milling cutter speed may have to be reduced from that for minimum machining cost by up to 25 percent.

Attempts were made to finish end-mill, full-hard AF1410 steel with a solid C6 carbide cutter having a 20-degree helix angle, a 6-degree primary angle, and a 13-degree secondary angle. When tested at a speed of 103 SFM, a feed of 0.00137 IPT, a depth of 0.050 inch, and a width of 0.725 inch, severe corner radius chipping occurred within a travel of 18 inches (Table 49). The chips were oxidized to a blue color. As a result of this performance, further testing of carbide cutters for end-milling full-hard AF1410 steel was discontinued.

Drilling

The results of the drill tests on 1.1-inch-thick, full (air quenched) AF1410 steel blanks are presented in Tables 50 and 51. The data presented was obtained using Cobalt M42 drills with standard split-point (SP) geometry, and, for comparative purposes, using some drills with a special SK point ground with an Omark Winslomatic spiral drill pointer machine per Rockwell drawing SK207-100. Typical land wear on a Cobalt HSS M42 drill is shown in Figure 112. As with the end-mill tests, tools made of carbide performed poorly compared to those made of Co HSS. Consequently, testing was concentrated on the use of Co HSS drills.

The use of the SK drill-point geometry results in improved selfcentering which might be expected to result in increased tool life. However, although the average number of holes drilled with the SK point was about 30 percent greater than with the SP point, a statistical "t" test, which takes into account the scatter and the difference in average values, yields a "t" value of only 1.8. This is indicative that the difference in averages observed with the present data is not significant.

The drill life results are presented graphically in Figure 113 as a function of speed and feed. Despite the rather large scatter in the data, there is an apparent trend, reflected by the least square fit of the Taylor equation to the data, of increasing tool life with increasing speed and feed. A possible explanation for this was sought in the variations observed in the drill geometry (e.g., the lip relief angle ranged from 7 to 14 degrees about a specified 10 +1 degree); however, no correlations with landwear were found. This anomalous result remains unexplained at this time and would require additional tests, conducted on a statistical basis, to confirm or deny the positive slope, and to determine the upper limit of the apparent increasing trend. The latter would be determined by the occurrence.

223

TABLE 50

RESULTS OF DRILLING TESTS WITH COBALT HSS DRILLS ON AF1410 STEEL IN FULL-HARD CONDITION (AIR OR OIL QUENCH)

Drill no.	Drill geometry						Drilling conditions					Total		At 0.008 in landwear			
	Dia (inch)	Type of point	Helix angle (deg)	Lip relief angle (deg)	Secondary cutting edge angle (deg)	Included angle (deg)	Depth of hole (inch)	RPM	Speed (SFM)	IPR	IPM	No. of holes	Landwear (inch)	No. of holes	Travel (inch)	Time (min)	Chipping
8	0.3595	SP-VG	28	12	130	132	1.032	150	14	0.001	0.150	40	0.0085	36.8	37.95	253.04	None
9	0.3595	SP-VG	26	11	132	132	1.032	190	19	0.001	0.190	22	0.009	19.9	20.56	108.21	None
11	0.3590	SP-VG	28	-	127	130	1.090	150	14	0.001	0.150	54	0.018	36.4	39.65	264.18	None
22	0.3594	SP-VG	28	7	135	132	1.125	150	14	0.0015	0.225	54	0.012	24.8	27.93	124.12	None
23	0.3595	SP-VG	28	7	130	132	1.125	150	14	0.0015	0.225	72	0.020	39.9	44.86	199.40	Light
25	0.3595	SP-VG	28	7	132	132	1.062	265	25	0.0015	0.397	65	0.012	47.5	50.47	127.14	Light
27	0.3592	SP-VG	28	10	135	132	1.080	110	10	0.002	0.220	35	0.010	27.4	29.64	134.73	Light
14-R1	0.3591	SK-B1	28	10	128	136	1.080	190	19	0.002	0.285	40	0.008	39.4	42.57	149.36	None
28	0.3592	SP-VG	28	9	133	132	1.075	265	25	0.002	0.530	50	0.010	41.3	44.45	83.87	Slight
29	0.3591	SP-VG	28	15	134	132	1.075	345	32.5	0.002	0.690	40	0.007	44.4	47.73	69.18	None
30	0.3594	SP-VG	28	10	132	132	1.100	265	25	0.0032	0.848	41	0.010	34.3	37.72	44.48	None
32	0.3594	SP-VG	28	10	135	132	1.100	345	32.5	0.0032	1.10	40	0.0085	57.4	41.18	57.44	Slight
22-R1	0.3592	SK-B1	28	9	136	132	1.100	345	32.5	0.0032	1.10	45	0.005	55.0	60.54	55.04	None
23-R1	0.3595	SK-B1	28	11	133	136	1.100	345	32.5	0.0032	1.10	40	0.007	42.2	46.36	42.15	None
25-R1	0.3595	SK-B1	28	12	134	136	1.100	345	32.5	0.0032	1.10	40	0.006	46.3	50.95	46.30	None
34	0.3595	SP-VG	28	10	134	132	1.100	345	32.5	0.0032	1.10	35	0.007	36.4	40.05	36.39	None

TABLE 51

COBALT HSS DRILLING DATA IN FORMAT OF MACHINING DATA HANDBOOK

Material	Condition and microstructure	BHN	Drill matl		Type drill	Drill size			Drill geometry				Cutting fluid code	Depth of hole (inch)	Feed (ipr)	Drill life end point (inch)	Drill life no. of holes versus speed (feet/minute)
			Trade name	Industry grade		Dia (inch)	Length (inch)	Flute Length (inch)	Type point	Helix angle°	Point angle°	Lip relief°					
AF1410 steel	Full hard (air quench)	460		M42 cobalt	Twist	0.3594	4.875	3.5	Split point	28	132	12	4	1.032 thru	0.0010	0.008	36.8 / 14
AF1410 steel	Full hard (air quench)	460		M42 cobalt	Twist	0.3594	4.875	3.5	Split point	26	132	11	4	1.032 thru	0.0010	0.008	19.9 / 19
AF1410 steel	Full hard (air quench)	460		M42 cobalt	Twist	0.3594	4.875	3.5	Split point	28	130	11	4	1.090 thru	0.0010	0.008	36.4 / 14
AF1410 steel	Full hard (air quench)	460		M42 cobalt	Twist	0.3594	4.875	3.5	Split point	28	132	7	4	1.125 thru	0.0015	0.008	24.8 / 14
AF1410 steel	Full hard (air quench)	460		M42 cobalt	Twist	0.3594	4.875	3.5	Split point	28	132	7	4	1.125 thru	0.0015	0.008	39.9 / 14
AF1410 steel	Full hard (air quench)	460		M42 cobalt	Twist	0.3594	4.875	3.5	Split point	28	132	7	4	1.062 thru	0.0015	0.008	47.5 / 25
AF1410 steel	Full hard (air quench)	460		M42 cobalt	Twist	0.3594	4.875	3.5	Split point	28	132	10	4	1.080 thru	0.002	0.008	22.4 / 10
AF1410 steel	Full hard (air quench)	460		M42 cobalt	Twist	0.3594	4.875	3.5	Split point	28	132	9	4	1.075 thru	0.002	0.008	41.3 / 25
AF1410 steel	Full hard (air quench)	460		M42 cobalt	Twist	0.3594	4.875	3.5	Split point	28	132	15	4	1.075 thru	0.002	0.008	44.4 / 32.5
AF1410 steel	Full hard (air quench)	460		M42 cobalt	Twist	0.3594	4.875	3.5	Split point	25	132	10	4	1.100 thru	0.0032	0.008	34.3 / 25
AF1410 steel	Full hard (air quench)	460		M42 cobalt	Twist	0.3594	4.875	3.5	SK[a]	28	132	10	4	1.100 thru	0.0032	0.008	37.4 / 32.5 36.4 / 32.5
AF1410 steel	Full hard (air quench)	460		M42 cobalt	Twist	0.3594	4.875	3.5	SK[a]	28	136	10	4	1.080 thru	0.0020	0.008	39.4 / 19
AF1410 steel	Full hard (air quench)	460		M42 cobalt	Twist	0.3594	4.875	3.5	SK[a]	28	132	9	4	1.100 thru	0.0032	0.008	55.0 / 32.5
AF1410 steel	Full hard (air quench)	460		M42 cobalt	Twist	0.3594	4.875	3.5	SK[a]	28	136	14	4	1.100 thru	0.0032	0.008	42.2 / 32.5
AF1410 steel	Full hard (air quench)	460		M42 cobalt	Twist	0.3594	4.875	3.5	SK[a]	28	136	12	4	1.100 thru	0.0032	0.008	46.3 / 32.5

(a) Rockwell grind - Tool 207-110

225

0.008 inch

(20X)

0.008 inch
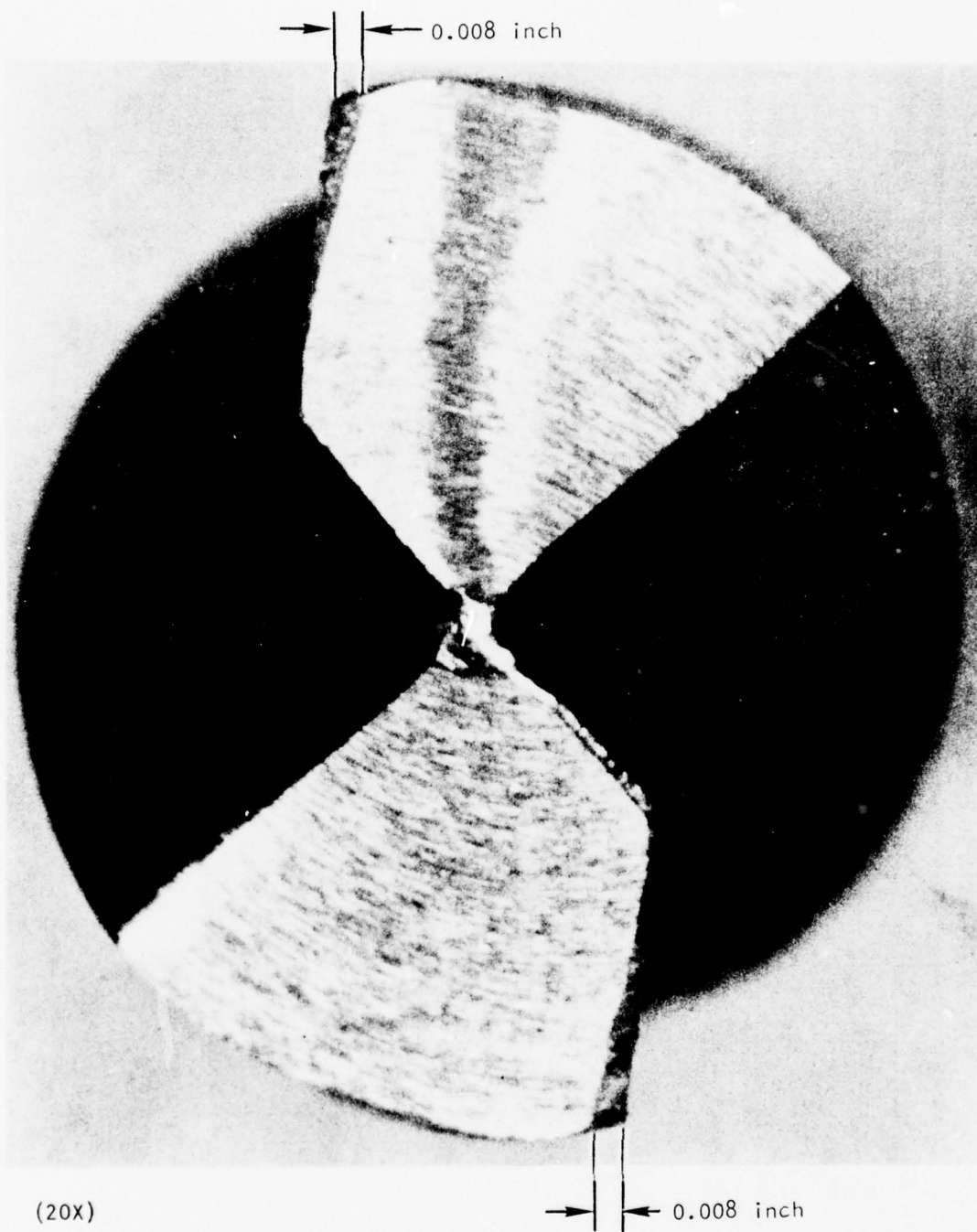
Figure 112. Typical landwear on 23/64-inch-diameter Cobalt HSS M-42 drill used in tests.

226
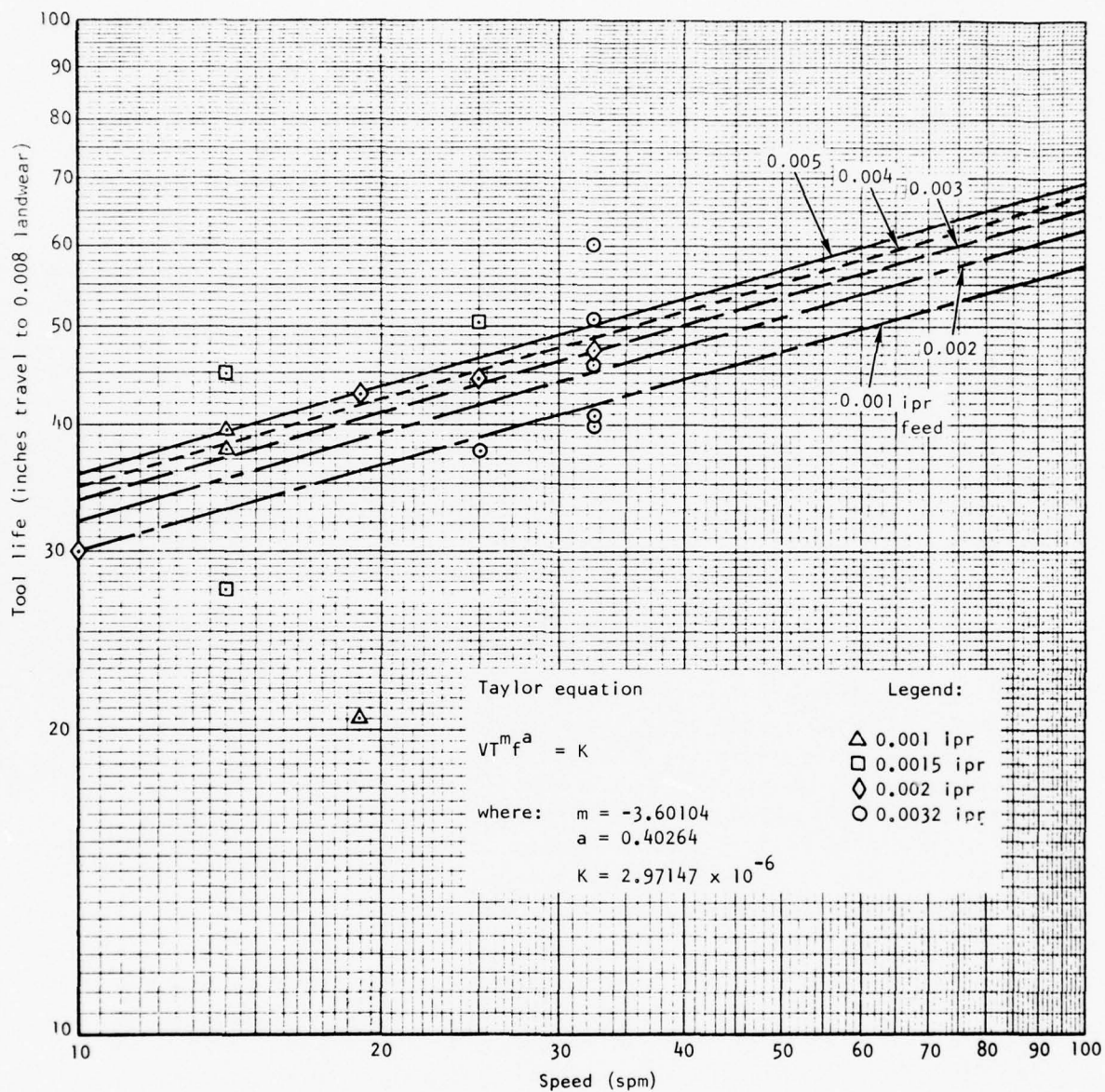
Figure 113. Cobalt HSS drill life in drilling 23/64-inch-diameter holes in 1.1-inch-thick, full-hard AF1410 steel.

227

of accelerated tool wear because of overheating. Judging by the extent of discoloration observed on the drills used at a speed of 32.5 SFM, it is estimated that accelerated wear because of overheating should be encountered between 30 and 40 SFM using the 0.003 IPR feed.

Based on the drilling test results, the optimum drilling speed and feed should be near 30 SFM and 0.003 IPR, respectively. Under these conditions, a 1-inch-deep, 23/64-inch-diameter hole can be drilled in about 1 minute. This compares with typical drill times of 2 and 5 minutes for full-hard HP-9Ni-4Co and full-hard D6AC steels, respectively (Reference 5, pages 237 and 238). Corresponding tool life data were not directly available. However, data available (Reference 5, page 86) for drilling 4340 steel, heat treated to 514 Bhn, shows that a 1/4-inch-diameter drill can travel a distance of about 7 inches at a cutting speed of 30 SFM and a feed of 0.002 IPR before developing a landwear of 0.015 inch. This compares with about 44 inches of travel under approximately similar conditions in full-hard (460 Bhn) AF1410 as estimated by the least-square-fit Taylor equation for 0.008-inch landwear.

Drilling 0.375-inch-diameter holes through 1-inch-thick Ti-6Al-4V with Cobalt HSS drills is typically accomplished in 2 minutes with a tool life of 20 inches. These values are only about half as good as those for AF1410 (as previously described) indicating that the drilling machinability of AF1410 is superior to that of Ti-6Al-4V.

It is apparent from Figure 114 that a feed of 0.0032 IPR combined with a speed of 32.5 SFM does not drill holes with good surface integrity. However, the drilled surfaces are nevertheless satisfactory for holes that are to be subsequently reamed since this operation will more than remove the affected surface metal. Consequently, when drilling is to be followed by reaming, the optimum drilling speed and feed should be near 30 SFM and 0.003 IPR, respectively, as indicated previously from tool wear considerations. If reaming is not to be performed, and good surface integrity is required, then the use of lower drilling feeds and speeds, such as 0.001 IPR and 14 SFM, is indicated.

Some improvement should also be expected from the use of flood cooling which should be more effective than spray mist cooling, especially for holes with high-depth-to-diameter ratios, such as the drill test holes in this program. In such holes, it is difficult to get spray mist to penetrate to the deeper areas.

A minimum cost estimate for drilling 23/64-inch-diameter by 1.1-inch-deep holes in full-hard AF1410 steel plate is presented in Table 47. This estimate was made on the assumption that the drilled holes are to be subsequently reamed, making any surface integrity discrepancies introduced by the drilling inconsequential.
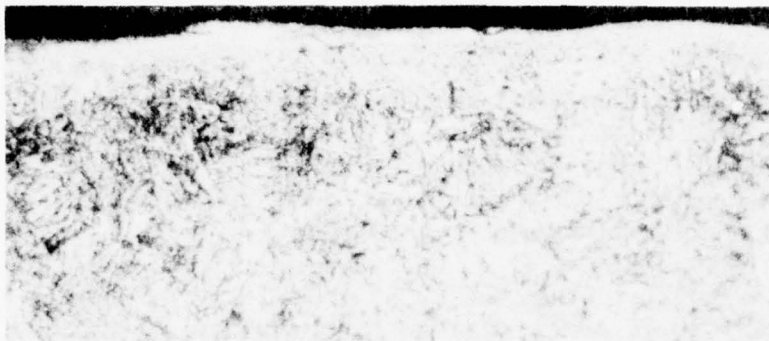
Top of hole
shows plastic
deformation

0.0032 FPR, 32.5 SFM.
Drilled hole
no. 11, part 9.
(Co HSS drill siezed
on drilling 11th hole)
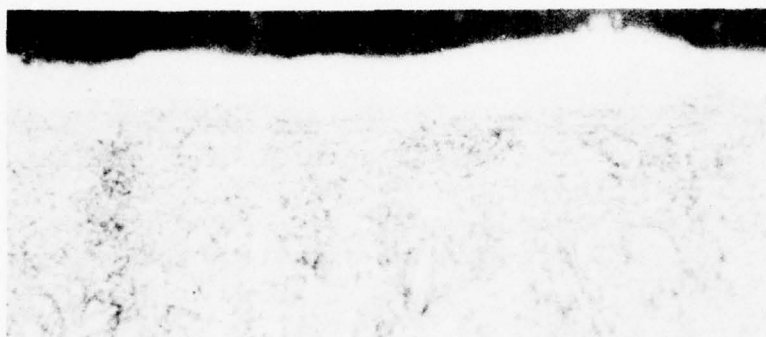
Bottom of hole
shows reverted
austenite

0.0032 IPR, 32.5 SFM.
Drilled hole
no. 95, part 8.
(Co HSS drill
with SK point;
120 RHR, excessive
reverted austenite,
and laps; 13th hole
with this drill)

Figure 114.   Sections through surfaces of 23/64-inch-diameter
holes drilled in full hard AF1410 steel plate (500x).

Reaming

The results of the reaming test on 23/64-inch holes drilled in 1.1-inch thick, full-hard AF1410 steel plate are presented in Tables 52 and 53 for Cobalt HSS reamers and in Tables 54 and 55 for carbide insert reamers. The tool life results are presented graphically in Figures 115 and 116 for the Cobalt HSS and carbide insert reamers, respectively.

The fit of the Taylor equation to the Cobalt HSS reaming data is seen to be rather poor with a correlation coefficient of only 0.424. An attempt to fit the modified Taylor equation to the data yielded an improved correlation coefficient of 0.628, but the resulting curve extrapolated in the wrong direction so that it was not suitable for use in determining optimum machining parameters. This situation no doubt results from the wide scatter in the results and lack of data at high speeds where, according to the end-milling results, wear is accelerated beyond that indicated by the Taylor equation.

The minimum cost results presented in Table 47 show that cost decreases with increasing feed. However, cutter edge chipping at higher feed rates as well as poor surface integrity will no doubt limit the feed rate. Judging from the surface integrity quality shown in Figure 117, the limiting values of feed and speed feed and speed for Cobalt HSS reamers should be near 0.003 IPR and 15 SFM, respectively.

The use of carbide insert reamers for reaming was somewhat more successful than the use of carbide cutters in end milling and drilling. However, the results, as shown in Figure 116, are still disappointing. The tool life is well below that for the Cobalt HSS reamers. The fit of the Taylor equation made by excluding the four low tool life points still indicates the presence of considerable scatter in the data. Use of the resulting tool life equation to determine minimum cost speeds results in values of 85,800 SFM at 0.001 IPR, and 342,000 SFM at 0.004 IPR. These values are obviously far beyond the capability of the test equipment. Further, as shown in Figure 117, the surface integrity of the carbide tool reamed holes is not good. Consequently, the use of carbide reamers in machining AF1410 steel is not considered to be practical, especially in view of the far better performance of the much lower cost Cobalt HSS reamers. The poor performance of the carbide reamers relative to the Cobalt HSS reamers may be because of excessive heat generation (steam was observed in using the carbide reamers). No noticeable heat was generated with the Cobalt HSS reamers.

Results Tabulated in Handbook Format

The machining test results are presented in Tables 44, 46, 49, 50, 53, and 54 in the format used by the Machining Data Handbook (Reference 5)

TABLE 52

RESULTS OF REAMING TESTS WITH COBALT HSS REAMERS ON AF1410 STEEL IN FULL-HARD CONDITION
(AIR OR OIL QUENCH)

Sheet No.	Cutter No.	Dia (inch)	No. of flutes	Helix angle (deg)	Primary relief angle (deg)	Secondary clearance angle (deg)	Chamfer angle	Radial rake angle	Margin width (inch)	Depth of hole (inch)	RPM	Speed (SFM)	IPR 10R	Feed 10R	Feed IPT	No. of holes	Time (min)	Travel of work (in.)	Chipping	Start (RHR)	End (RHR)
1	13	3/8	6	Straight	18		15	4	0.009	1.100	100	18	0.003s	0.084	0.0006	18.1	29.55	20.21	None	55	55 [a]
3	18	3/8	6	Straight	18.5		15	4	0.0105	1.100	315	34	0.003s	1.21	0.0006	5 [b]	4.09	6.19	Medium	—	—
5	16	3/8	6	Straight	19.5		18.5	0	0.0095	1.100	150	15	0.003s	0.540	0.0006	55	68.7	37.12	None	69	55
7	20	3/8	6	Straight	20		12.0	0	0.0135	1.100	110	11	0.003s	0.536	0.0006	20.2	5.250	22.7	None	69	65
13	13 BI	3/8	6	Straight	18		15.0	4	0.004	1.100	100	12	0.003s	0.084	0.0006	19.3	26.2	17.38	None	65	58
17	18 BI	3/8	6	Straight	17.5		15	0	0.0005	1.075	100	13	0.003s	0.084	0.0006	10.3	1.15	11.75	None	70	60
35	16	3/8	6	Straight	22		16	5	0.021	1.125	205	26	0.003s	1.11	0.0006	19.0	19.80	22.06	None	60	65
31	18	3/8	6	Straight	25		15	5	0.011	1.06	150	19	0.003s	0.855	0.0006	15.0	16.85	14.46	None	80	60
29	21	3/8	6	Straight	20		16	5	0.015	1.100	150	11	0.0015	0.675	0.0006	17.0	31.35	18.04	None	60	70
2	25	3/8	6	6.5	18.5		15	0	0.0075	1.100	100	13	0.003s	1.084	0.0006	17.0	28.85	19.72	None	40	58
4	28	3/8	6	6	18.5		18.5	5	0.016	1.100	315	31	0.003s	1.21	0.0006	5.0	4.09	6.19	Medium	—	—
8	30	3/8	6	6	17		17	5	0.013	1.100	110	15	0.003s	0.536	0.0006	20.2	19.50	20.13	None	60	50
16	29 BI	3/8	6	7	18		14	5	0.0015	1.100	110	15	0.003s	0.681	0.0006	17.50	24.84	16.08	None	50	25
36	26	3/8	6	6	18		15	5	0.031	1.075	205	26	0.003s	1.11	0.0006	15.3	22.83	25.56	None	60	50
38	31	3/8	6	6	18		16	5	0.015	1.06	100	13	0.0045	0.855	0.0006 [c]	22.3	22.03	18.81	None	60	70
52	27	3/8	6	6	18		16	0	0.011	1.06	150	13	0.0045	0.625	0.0006 [c]	18.1	24.49	19.25	None	55	65

[a] Poor next pass
[b] No inspection manuscript, estimate only.

TABLE 53

COBALT HSS REAMING DATA IN FORMAT OF THE MACHINING DATA HANDBOOK

Material	Condition and microstructure	BHN	Reamer description					Tool geometry			Cutting fluid code	Stock allow. on dia (inch)	Length of hole (inch)	feed (ipr)	Tool life end point (inch)	Reamer life no. of holes versus speed (feet/minute)				
			Tool matl		Dia (inch)	No. of flutes	Style	Helix & hand	Chamfer	Rel°										
			Trade name	Industry grade																
AF1410	full hard (air quench)	460		M42 cobalt	0.375	6	Chucking	1 RH	15 x 0.060	18	1	0.015	1.100 thru	0.0050	0.008	$\frac{20.7}{11}$	$\frac{33.7}{15}$	$\frac{18.4}{19}$	$\frac{16.3}{19}$	$\frac{10.9}{19}$
AF1410	full hard (air quench)	460		M42 cobalt	0.375	6	Chucking	1 RH	15 x 0.060	18	1	0.015	1.100 thru	0.0050	0.008	$\frac{19.6}{26}$	$\frac{5.6}{31}$			
AF1410	full hard (air quench)	460		M42 cobalt	0.375	6	Chucking	1 RH	15 x 0.060	18	1	0.015	1.100 thru	0.0045	0.008	$\frac{17.0}{11}$	$\frac{15.6}{19}$	$\frac{17.9}{19}$	$\frac{15.8}{19}$	
AF1410	full hard (air quench)	460		M42 cobalt	0.375	6	Chucking	6 RH	15 x 0.060	18	1	0.015	1.100 thru	0.0050	0.008	$\frac{17.9}{11}$	$\frac{26.3}{15}$			
AF1410	full hard (air quench)	460		M42 cobalt	0.375	6	Chucking	6 RH	15 x 0.060	18	1	0.015	1.100 thru	0.0050	0.008	$\frac{5.6}{31}$				
AF1410	full hard (air quench)	460		M42 cobalt	0.375	6	Chucking	6 RH	15 x 0.060	18	1	0.015	1.100 thru	0.0045	0.008	$\frac{18.1}{11}$	$\frac{17.8}{19}$			$\frac{22.5}{26}$

232

TABLE 54

RESULTS OF REAMING TESTS WITH CARBIDE INSERT REAMERS ON AF1410 STEEL IN FULL-HARD CONDITION
(AIR OR OIL QUENCH)

Series No.	Cutter No.	Size (inch)	No. of flutes	Reamer geometry						Depth of hole (inch)	Machining parameters					At 0.008 in. landwear			Chipping	Surface finish	
				Helix angle (deg)	Primary relief angle (deg)	Secondary clearance angle (deg)	Chamfer angle	Radial rake angle	Margin width (inch)		RPM	Speed (SFM)	IPR	IPM	IPT	No. of holes	Time (min)	Travel of work (in.)		Start (RHR)	End (RHR)
13		5/8	4	Straight	15	25	45	0	0.0015	1.100	345	54	0.0015	0.518	0.000375	1[a]	2.1[b]	1.1[b]	None	–	–
14		5/8	4	Straight	20	25	45	0	0.002	1.100	345	54	0.002	0.690	0.0005	9.4	15.01	10.40	None	20	20
15		5/8	4	Straight	15	25	45	0	0.0005	1.100	345	54	0.002	0.690	0.0005	2.1	5.31	2.28	None	–	–
16		5/8	4	Straight	18	30	45	0	0.0015	1.075	110	18	0.0036	0.396	0.0009	11.8	31.97	12.66	None	20	22
17		5/8	4	Straight	18	25	45	0	0.002	1.075	110	18	0.0036	0.396	0.0009	4.1	11.14	4.41	None	20	–
18		5/8	4	Straight	15	30	45	0	0.0015	1.075	190	18	0.0036	0.684	0.0009	9.1	14.37	9.83	None	–	–
																No. after 3 holes					
33		5/8	4	Straight	18	25	45	0	0.0015	1.125	265	20	0.0036	0.954	0.0009	8.0	9.47	9.03	None	25	25
26		5/8	4	Straight	20	25	45	1	0.0005	1.100	110	11	0.0015	0.198	0.000375	3.5	7.16	3.54	None	–	–
12		5/8	4	8.5	25	30	45	0	0.0015	1.100	265	26	0.0015	0.398	0.000575	5.6[a]	15.82	5.50	None	20	–
27		5/8	4	10.5	15	30	45	0	0.0015	1.100	345	34	0.0015	0.518	0.000575	8.6[a]	11.90	6.19	None	25	32
20		5/8	4	8	18	30	45	0	0.001	1.075	345	11	0.0036	0.518	0.0009	9.2	11.21	7.36	None	32	25
21		5/8	4	8	15	30	45	0	0.0036	1.075	150	11	0.0036	0.540	0.0009	8.7	18.51	9.89	Medium	–	–
31		5/8	4	8.5	18	30	45	0	0.0036	1.125	265	26	0.0036	0.954	0.0009	7.1	17.28	9.33	None	22	50
32		5/8	4	16	15	30	45	0	0.0005	1.00	85	8	0.0045	0.385	0.001125	9.9	8.40	8.01	Medium	22	22
22		5/8	4	23.5	25	45	0	0.001	1.00	85	8	0.0045	0.383	0.001125	11.6	27.33	10.47	None	20	25
24		5/8	4	8.5	18	31	45	0	0.0005	1.075	110	11	0.0045	0.198	0.001125	7.3	32.05	12.27	None	25	20
25		5/8	4	8.5	16	30	45	0	0.0005	1.00	110	11	0.0045	0.198	0.001125	11.5	15.76	7.80	None	22	22
																	24.72	12.24	Medium	20	22

[a] No inspection performed

[b] One hole only; no value reported

233

TABLE 55

CARBIDE INSERT REAMING DATA IN FORMAT OF THE MACHINING DATA HANDBOOK

Material	Condition and microstructure	BHN	Reamer description					Tool geometry[a]			Cutting fluid code	Stock allow. on dia (inch)	length of hole (inch)	feed (ipr)	tool life—end point (inch)	Reamer life no. of holes versus speed (feet/minute)
			Tool matl		Dia (inch)	No. of flutes	Style	Helix % hand	Cham-ter	Rel°						
			Trade name	Indus-try grade												
AISI410	Full hard (air quench)	400		C-2 carbide	0.375	1	chuck-ing	0 RH	15 x 0.060	18	1	0.015	1.100	0.002	0.008	$\frac{9.4}{34}$
AISI410	Full hard (air quench)	400		C-2 carbide	0.375	1	chuck-ing	0 RH	15 x 0.060	18	1	0.015	1.100	0.0050	0.008	$\frac{11.8}{17}$ $\frac{9.1}{19}$
AISI410	Full hard (air quench)	400		C-5 carbide	0.375	1	chuck-ing	0 RH	15 x 0.060	18	1	0.015	1.100	0.0015	0.008	$\frac{1}{34}$
AISI410	Full hard (air quench)	400		C-5 carbide	0.375	1	chuck-ing	0 RH	15 x 0.060	18	1	0.015	1.100	0.002	0.008	$\frac{2.1}{34}$
AISI410	Full hard (air quench)	400		C-5 carbide	0.375	1	chuck-ing	0 RH	15 x 0.060	18	1	0.015	1.100	0.0050	0.008	$\frac{4.1}{17}$ $\frac{8.0}{24}$
AISI410	Full hard (air quench)	400		C-5 carbide	0.375	1	chuck-ing	0 RH	15 x 0.060	18	1	0.015	1.100	0.0045	0.008	$\frac{5.5}{17}$
AISI410	Full hard (air quench)	400		C-2 carbide	0.375	1	chuck-ing	9	15 x 0.060	20	1	0.015	1.100	0.0015	0.008	$\frac{5.0}{34}$ $\frac{9.2}{34}$
AISI410	Full hard (air quench)	400		C-2 carbide	0.375	1	chuck-ing	9	15 x 0.060	20	1	0.015	1.100	0.0050	0.008	$\frac{9.2}{17}$
AISI410	Full hard (air quench)	400		C-2 carbide	0.375	1	chuck-ing	9	15 x 0.060	20	1	0.015	1.100	0.0015	0.008	$\frac{9.9}{8}$ $\frac{7.3}{17}$
AISI410	Full hard (air quench)	400		C-5 carbide	0.375	1	chuck-ing	9	15 x 0.060	20	1	0.015	1.100	0.0015	0.008	$\frac{5.0}{26}$
AISI410	Full hard (air quench)	400		C-5 carbide	0.375	1	chuck-ing	9	15 x 0.060	20	1	0.015	1.100	0.0050	0.008	$\frac{8.7}{17}$ $\frac{7.1}{26}$
AISI410	Full hard (air quench)	400		C-5 carbide	0.375	1	chuck-ing	9	15 x 0.060	20	1	0.015	1.100	0.0015	0.008	$\frac{11.0}{8}$ $\frac{11.5}{17}$

[a] 30° secondary clearance angle.

234

Figure 115.   Cobalt HSS tool life for reaming 3/8-inch-diameter by
1.1-inch-deep holes in full-hard AF1410 steel.

235

$VT^n f^a = K$
n = 9.99961
a = -3.13399
K = 5.06443 × 10^18
Correlation coefficient = 0.70
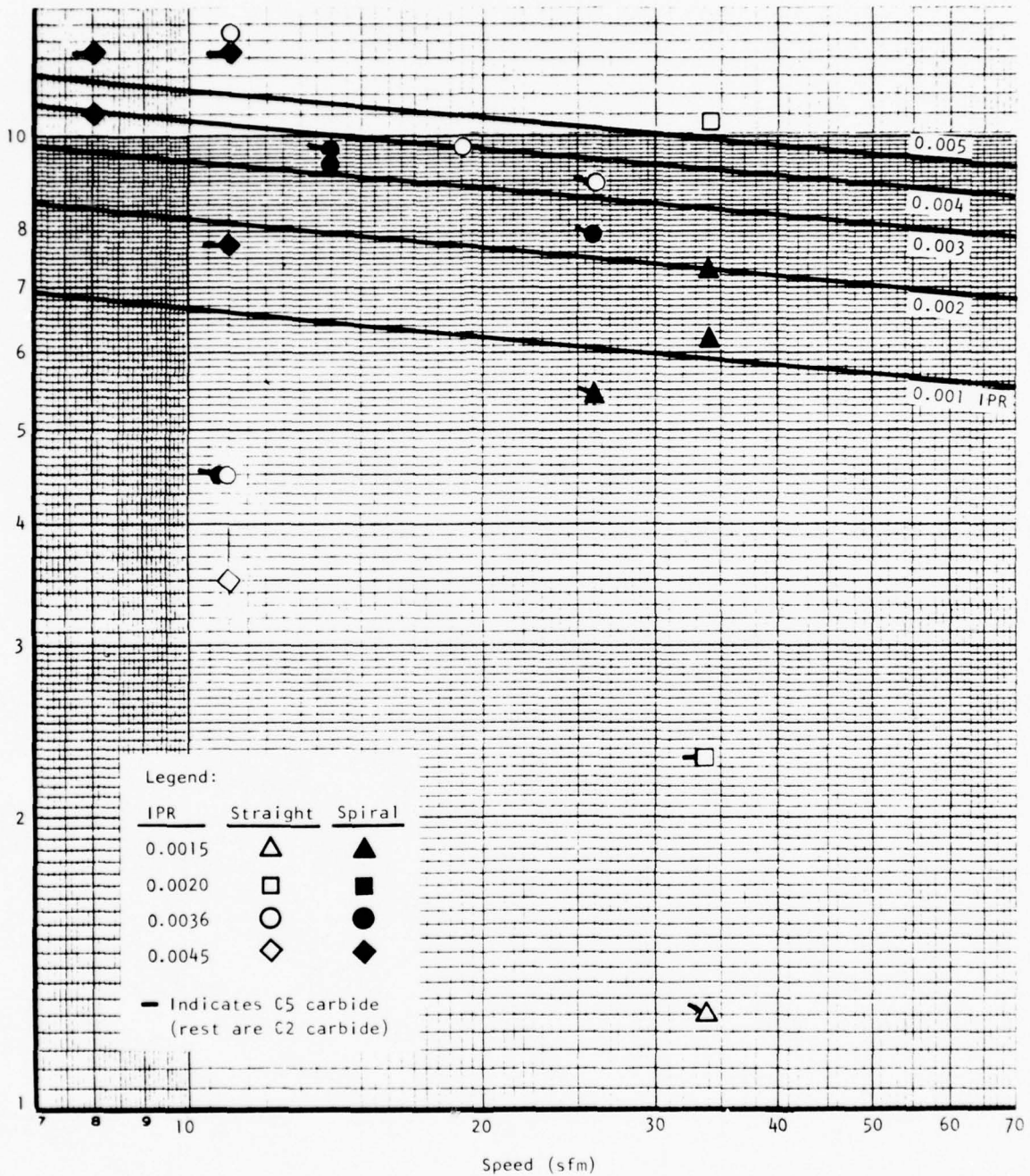
Figure 116. Carbide reamer life in reaming 3/8-inch-diameter
by 1.1-inch-deep holes in full-hard AF1410 steel.

236
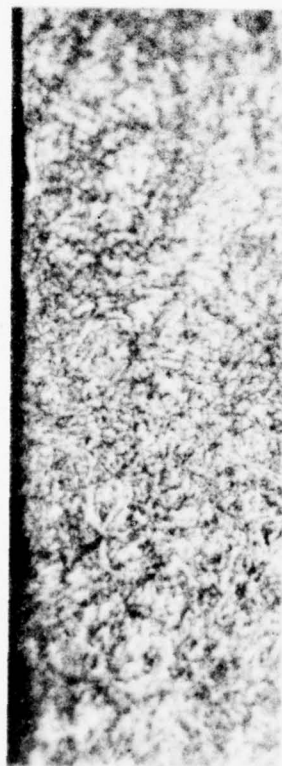
(Top) 0.0036 IPR, 15 SFM, reamed hole no. 5, part 8 (Center)
(Co HSS spiral reamer; 50 RHR, minor austenite reversion; 20th hole with reamer 2C)

0.0015 IPR, 34 SFM, reamed hole no. 108, part 8
(C2 carbide spiral reamer, 32 RHR, thin layer of reverted austenite with some plastic deformation under it; 8th hole with reamers C2-4AR1)
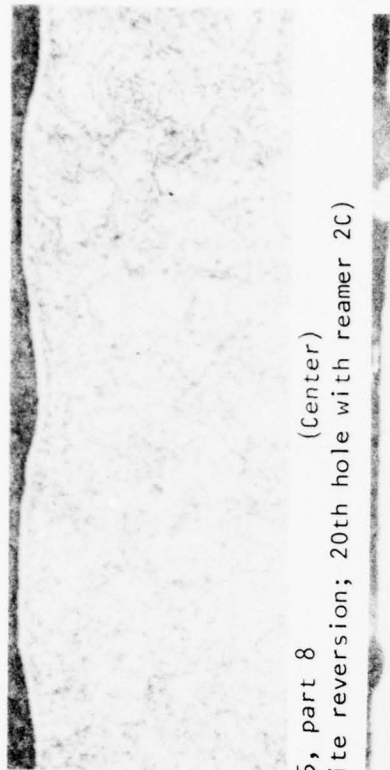
0.0036 IPR, 15 SFM, reamed hole no. 20, part 8
(Co HSS spiral reamer siezed in hole; reverted austenite; 35th hole with reamer 2C)
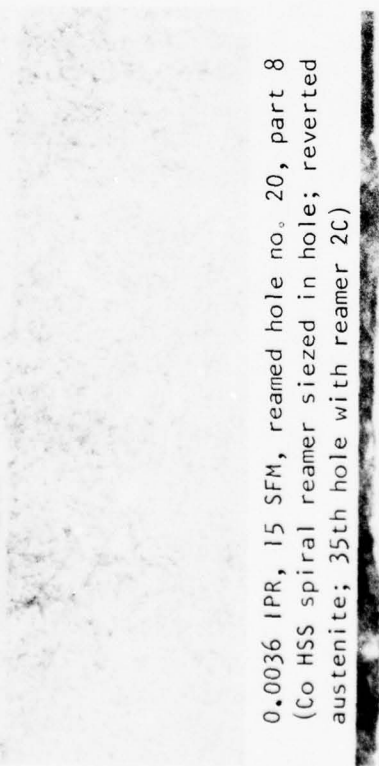
.0020 IPR, 34 SFM, reamed hole no. 76, part 9
(C2 carbide straight reamer, 20 RHR, intermittent austenite reversion; 1st hole with reamer C2-3A)

Figure 117. Sections through surfaces of 3/8-inch-diameter holes as reamed in full-hard AF1410 steel plate (500x).

237

in order to facilitate comparison of the AF1410 machining results of this program with existing results on various materials of interest.

Optimum Machining Parameters and Costs

The optimum machining parameters, as estimated from the results of this program, are summarized in Table 56. The corresponding machining costs are summarized in Table 57. It is apparent, on the basis of work or tool travel, that drilling and reaming are significantly more costly operations than end milling for AF1410 steel. The cost of drilling a hole is about one-half of that for reaming it. However, if the hole is to be left in the as-drilled condition, wherein surface integrity is required, then the cost of drilling the hole is about five times greater because of the slower drilling speed, resulting in higher cost than the combination of drilling and reaming.

Machining Comparisons

Metal removal rates and tool life obtained in the AF1410 steel machining tests in this effort and those reported (Reference 5 and various aerospace firms) for titanium and D6AC and HP9-4-20 steel alloys are presented in Tables 58 through 61. The results, as summarized in Table 62, show that the rough machinability of AF1410 steel in the premachine heat-treat condition is 33.7 percent better than the best value for annealed titanium, 120 percent better than the value for AF1410 in the as-received mill condition, 450 percent better than the value for HP9-4-.20 steel, and 240 percent better than the value for D6AC steel. These results indicate achievement of the goal of improving the rough machinability of AF1410 to enhance its ability to be substituted for titanium on a cost basis.

Machinability of AF1410 in the full-hard condition is somewhat variable when compared to the best values for titanium in the annealed condition. It is 23 percent easier to end mill, 32 percent more difficult to drill, and 5 percent more difficult to ream. Although no attempt was made to modify the machinability of the full-hard AF1410 steel, a significant (190 percent) improvement in end-mill cutter life is indicated for AF1410 steel that is air cooled instead of water quenched (Table 48) during the full-hard heat treatment.

Chemical Milling

Two fully heat-treated AF1410 specimens, approximately 1 by 2 by 5 inches, were submitted to Aerochem, Inc, Orange, California, for chemical milling tests. The specimens were masked to expose 1-inch-wide strips for

238

TABLE 56

OPTIMUM MACHINING PARAMETERS AS ESTIMATED FROM TEST RESULTS OF VARIOUS MACHINING OPERATIONS ON AF1410 STEEL

| Machining operation | Condition of AF1410 steel | Cutter | | | Feed (**) | Speed (SFM) | Expected tool life (inches of travel) |
		Material	Diam (inch)	Geometry			
Rough end milling***	Premachine heat treat	Co HSS	1	11-deg primary 22-deg secondary	0.003	63	270.41
Finish end milling***	Full hard	Co HSS	1	7-deg primary 15-deg secondary	.002*	67*	582.19
Drilling	Full hard	Co HSS	23/64	9-deg lip relief 134-deg secondary SK point	.003 .001*	30 14*	46.02 35.59
Reaming	Full hard	Co HSS	3/8	19-deg primary 44-deg chamfer 0-deg rake	.003*	15*	25.33

*Optimized taking into account surface integrity
**IPT for end milling, IPR for drilling and reaming
***Slotting and semislotting

239

TABLE 57

ESTIMATED MACHINING COSTS USING OPTIMUM MACHINING PARAMETERS

| Machining operation (all with Co HSS tools) | Per part* ($) | Machining costs per program test conditions | | Per unit of work or tool travel* ($/M) |
| | | Per unit of metal removed | | |
		($/ cu in.)	($/ lb)	
Rough end milling	80.17	0.4900	1.7192	0.1636
Finish end milling**	47.56	11.0605	38.8086	0.1998
Drilling	87.92 462.96***	6.3036 33.1930***	22.1180 116.4879***	0.6394 3.36698***
Reaming	182.43	147.2666	516.7250	1.3267

* As machined in this program for indicated machining operation

** Two passes assumed

*** At reduced speed and feed to obtain good surface integrity

240

TABLE 58

ROUGH END MILLING MACHINABILITY OF PREMACHINE HEAT TREATED AF1410 STEEL AND VARIOUS OTHER MATERIALS

	COMP. A*** ANNEALED TITANIUM	COMP. B*** ANNEALED TITANIUM	METCUT**** ANNEALED TITANIUM	ROCKWELL ANNEALED TITANIUM	ROCKWELL WING PIVOT AF1410**	LOCOSST 325-375 BHN AF1410	COMP. C*** 300-350 BHN D6AC	METCUT**** 325-375 BHN HP9-4-20
TYPE OF CUTTER	HSS COBALT	HSS COBALT	HSS COBALT	HSS COBALT	HSS COBALT	HSS COBALT	HSS COBALT	HSS COBALT
DIA OF CUTTER	1.00	1.00	1.00	1.00	1.00	1.00	1.00	1.00
NO. OF FLUTES	4	4	4	4	4	6	4	4
SFM	50	30	55	47	42	67	65	40
RPM	191	114	210	180	160	256	248	153
IPT	.004	.005	.005	.007	.0048	.003	.003	.002
IPM	3.05	2.28	4.2	5.04	3.07	4.500	3.00	1.22
DEPTH OF CUT	.250	.250	.250	.250	.250	.375	.250	.250
WIDTH OF CUT	.765*	.765*	.765*	.765*	.765*	.765	.500	.765*
METAL REMOVAL CUBIC INCH/HR	35.00	26.16	48.20	57.83	35.23	77.45	22.5	14.05
CONDITION OF CUTTER	AV.WEAR .012 INCH	AV.WEAR .012 INCH	AV.WEAR .012 INCH	WEAR MAX. .004 INCH	WEAR MAX. .005 INCH	AV.WEAR .008 INCH	RUN CUTTER TO 140 LINEAR INCH	AV.WEAR .012 INCH
TOOL LIFE	APPROX. 1 HR +	APPROX. 1 HR +	APPROX. 1 HR +	CHIPPED RAD.	CHIPPED O.D.	APPROX. 1 HR +	47 MINUTES	APPROX. 1 HR +

*ASSUMED WIDTH

**NA-75-555 (F33615-75-C-3145)

***AEROSPACE COMPANIES

****REFERENCE 5

241

TABLE 59

FINISH END MILLING MACHINABILITY OF FULL-HARD AF1410 STEEL AND VARIOUS OTHER MATERIALS

	METCUT**** ANNEALED TITANIUM	ROCKWELL** WING PIVOT AF 1410	LOCOSST H.T. 47-50 RC AF 1410	ROCKWELL H.T. 40-45 RC HP9Ni-4Co	METCUT H.T. 43-48 RC HP9Ni-4Co	COMP. B*** H.T. UP TO 49 RC HP9Ni-4Co	METCUT**** H.T. 43-48 RC D6AC
TYPE OF CUTTER	HSS COBALT	HSS COBALT	HSS COBALT	HSS COBALT	HSS COBALT	HSS COBALT	HSS COBALT
DIA OF CUTTER	1.00	1.00	1.00	1.00	1.00	1.00	1.00
NO. OF FLUTES	4	4	6	4	4	4	4
SFM	60	25	67	40	20	30	25
RPM	229	96	256	153	76	114	96
IPT	.004	.0039	.003	.002	.001	.003	.0015
IPM	3.66	1.50	4.500	1.224	.304	1.368	.576
DEPTH OF CUT	.050	.050	.050	.050	.050	.050	.050
WIDTH OF CUT	.770*	.770*	.770	.770*	.770*	.770*	.770*
METAL REMOVAL CUBIC INCH/HR	8.454	3.465	10.395	2.827	.702	3.16	1.331
CONDITION OF CUTTER	AV. WEAR .012 INCH	WEAR MAX. .006 INCH	AV. WEAR .008 INCH	WEAR MAX. .008 INCH	AV. WEAR .012 INCH	AV. WEAR .012 INCH	AV. WEAR .012 INCH
TOOL LIFE	APPROX. 1 HR +	CHIPPED O.D.	APPROX. 1 HR +	APPROX. 1 HR +	APPROX. 1 HR +	APPROX. 1 HR +	APPROX. 1 HR +

*ASSUMED WIDTH

**NA-75-555 (F33615-75-C-3145)

***AEROSPACE COMPANY

****REFERENCE 5

242

TABLE 60

DRILLING MACHINABILITY OF FULL-HARD AF1410 STEEL AND VARIOUS OTHER MATERIALS

	COMP. A** ANNEALED TITANIUM	COMP. B** ANNEALED TITANIUM	METCUT*** ANNEALED TITANIUM	ROCKWELL ANNEALED TITANIUM	LOCOSST H.T. 47-50 RC AF1410	COMP. B** H.T. UP TO 49RC HP9Ni-4Co	METCUT*** 43-48 RC HP9Ni-4Co	METCUT*** 48-50 RC D6AC
TYPE OF DRILL	M42 HSS	M42 HSS	M42 HSS	M42 HSS	M42 HSS	M42 HSS	M42 HSS	M42 HSS
DIA OF DRILL	.3594	.3594	.3594	.3594	.3594	.3594	.3594	.3594
SFM	16	20	35	35	32.5	25	15	10
RPM	170	212	372	372	345	265	159	106
IPR	.005	.004	.004	.002	.0032	.002	.003	.002
IPM	.850	.848	1.488	.75	1.10	.530	.477	.212
DEPTH OF HOLE	1.062*	1.062*	1.062*	1.062*	1.062	1.062*	1.062*	1.062*
CUTTING TIME, MINUTES/INCH	1.18	1.18	.67	1.33	.91	1.89	2.10	4.72

*ASSUMED DEPTH
**AEROSPACE COMPANIES
***REFERENCE 5

TABLE 61

REAMING MACHINABILITY OF FULL-HARD AF1410 STEEL AND VARIOUS OTHER MATERIALS

	COMP. A** ANNEALED TITANIUM	COMP. B** ANNEALED TITANIUM	METCUT*** ANNEALED TITANIUM	ROCKWELL ANNEALED TITANIUM	LOCOSST H.T. 47-50 RC AF 1410	COMP. B** H.T. UP TO 49RC HP9Ni-4Co	METCUT*** 48-50 RC D6AC	
TYPE OF REAMER	M42 HSS	M42 HSS	M42 HSS	M42 HSS	M42 HSS	M42 HSS	M42 HSS	C-2
DIA OF REAMER	.375	.375	.375	.375	.375	.375	.375	.375
NO. OF FLUTES	6	6	6	6	6	6	6	4
SFM	25	15	65	18	26	20	15	65
RPM	255	152	662	180	265	204	153	662
IPR	.005	.006	.008	.006	.0036	.0036	.001	.001
IPT		.002		.001	.0006	.0006		
IPM	1.275	.912	5.30	1.08	.954	.734	.153	.662
DEPTH OF HOLE	1.062*	1.062*	1.062*	1.062*	1.062	1.062*	1.062*	1.062*
CUTTING TIME, MINUTES/INCH	.78	1.10	.19	.93	1.05	1.36	6.54	1.51

*ASSUMED DEPTH
**AEROSPACE COMPANIES
***REFERENCE 5

244

TABLE 62

SUMMARY COMPARISON OF MACHINABILITY OF AF1410 STEEL WITH VARIOUS OTHER MATERIALS

Operation	AF1410		Highest Comparable Removal rate for: units		
	Condition	Removal Rate in.³/hour	Titanium (Annealed)	HP9 - 4 -0.20	D6ac
Rough end milling (slotting)	Premachine heat treat	77.3 in.³/hour	57.83 +33.7%	14.05 +450%	22.5 +240
Rough end milling (slotting)	As received from mill	35.23 in.³/hour	57.83 -39%	14.05 +150	22.5 +56%
Finish end milling	Full hard[1]	10.4 in.³/hour	8.45 +23%	5.16 +229	1.33 +229
Drilling	Full hard[1]	0.91 min/inch	1.33 -32%	2.10 -57%	4.72 -80%
Reaming	Full hard[1]	1.05 min/inch	1.10 -5%	1.36 -23%	6.54 -84%

[1] Air or oil quenched

NOTE: % = difference of AF1410 steel valve.

245

etching in the short transverse and longitudinal directions. This allowed
testing of several chemical milling solutions on one specimen on surfaces
with two different grain orientations. The results, presented in Fig-
ures 118 and 119 and in Table 63, show that none of the tested chemical
milling solutions were entirely satisfactory. Solution 35, normally used
for nickel alloys, produced the highest etch rate, but also gave a poor
surface finish with extensive ripples. The best solution of the group, 37,
is normally used for Cobalt base alloys. It gave a surface finish that was
smooth except for moderate pitting, which would preclude its use on fatigue
sensitive parts. However, it would be a good starting point for development
of an etching solution specifically for AF1410. Such effort was beyond the
scope of this program.
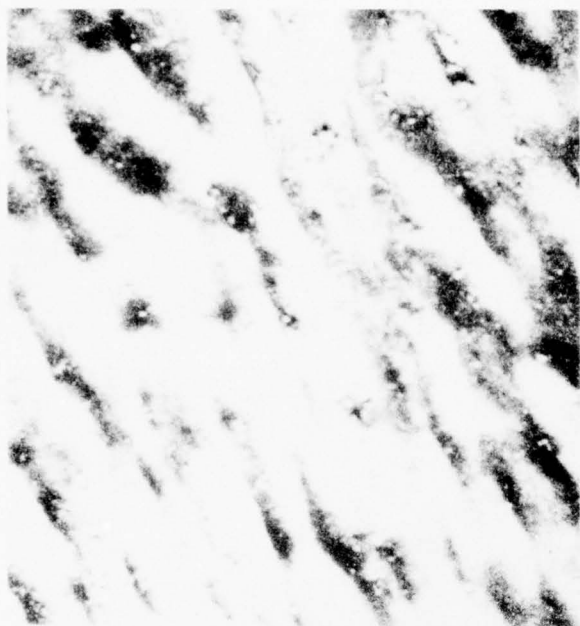
Short transverse surface   Longitudinal surface

Solution 33 (for nickel alloys)
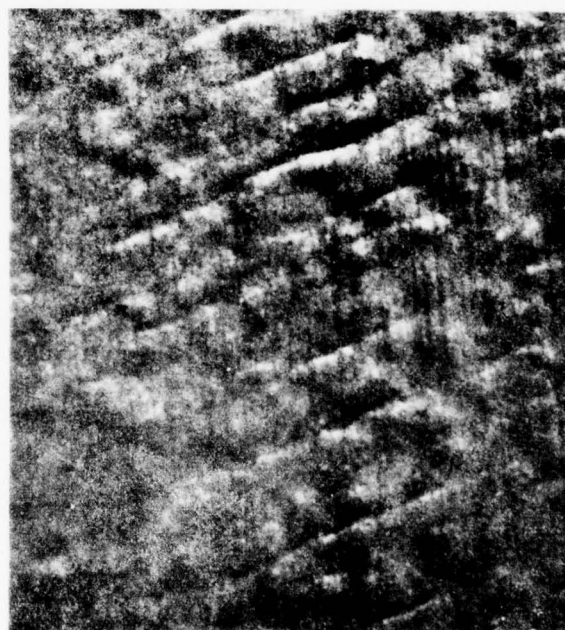
Short transverse surface   Longitudinal surface

Solution 35 (for Cres 300 series)

Figure 118.   Appearances of AF1410 steel surfaces after chemical-milling tests (20X).
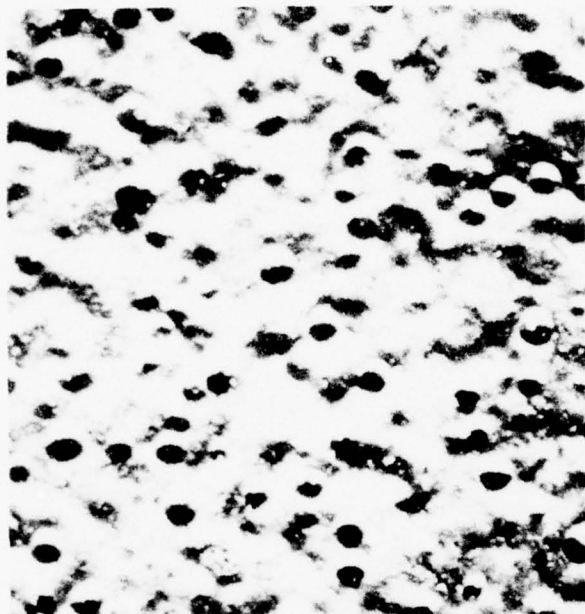
Short transverse surface   Longitudinal surface

Solution 36 (for Rene 41, Hast alloy, and Haynes 188)
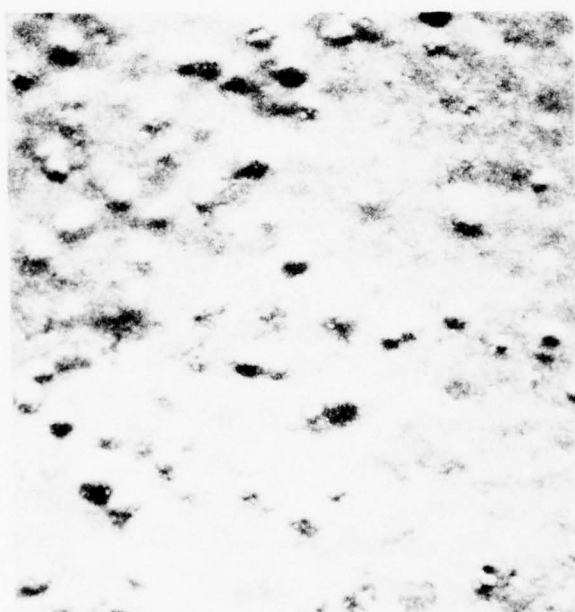
Short transverse surface   Longitudinal surface

Solution 37 (for Cobalt base alloys; e.g., Haynes 25)

Figure 119.   Appearances of AF1410 steel surfaces after chemical-milling
tests (20X).

TABLE 63

AF1410 CHEMICAL MILLING TEST RESULTS

Chemical milling solution		Depth of etch in 30-40 min (in.)	Remarks**
Number*	Normal application		
32	Low alloy steels, e.g., 4340, 8620, Hy tough	<.001	Etch rate far too low
33	Nickel alloys, e.g. Inco 718	.032	Extensive surface rippling
35	CRES 300 series and precipitation hardened steel	.008	Extensive surface roughness (raised areas)
36	Rene 41, Hastalloy, Haynes 188	.017	Extensive, pitting (round hole cratering)
37	Cobalt base alloys, e.g., L605, Haynes 25	.008	Moderate pitting (round hole cratering) otherwise smooth surface. Best of group tested.

* Aerochem, Inc., Orange, California

** Etched in short transverse direction. Effects noted are less pronounced in longitudinal direction.

Section V

TEST COMPONENT FABRICATION

The underlying theme of the fabrication plan was one of minimum cost. To accomplish the fabrication with this in mind, a fabrication sequence was selected based on performing the maximum amount of machining prior to heat treatment (when the machinability is at its best), and the use of an air cool rather a warpage-inducing water quench, which had been used in all prior work with the alloy. The knowledge gained in the machinability studies was applied to the machining operations, all of which were performed on a production machine with production operators. Innovative approaches, such as finish machining the majority of the fitting prior to heat treatment, were adopted to achieve a minimum fabrication-cost sequence. The details of the fabrication sequence used to manufacture the test component are presented in this section.

Forging Procedure and Properties

The closed die forging used for the manufacture of the test component was furnished by the Air Force and was produced as part of the Production Melting and Thermomechanical Processing of AF1410 steel program being conducted concurrently by Universal-Cyclops Specialty Steel Division of Cyclops Corporation. The as-received forging is shown being dimensionally checked at Rockwell in Figure 120 Weight of the forging prior to any machining operation was 600 pounds.

Actual forging of the component was accomplished by Alcoa-Cleveland under subcontract to Universal-Cyclops. The details of the forging are contained in Reference 8. Four closed die forgings were fabricated in the 50,000-ton press, using 28,000 tons. Three blocking operations were used, and the preheat temperature for the final forging operation was 1,800° F. No difficulty was experienced with the forgeability of the alloy.

The four forgings were subjected to the premachining heat treatment (normalized 1,650° F, air cool, overaged for 8 hours at 1,250° F, air cooled) and subsequently ultrasonically inspected. All four met the class A requirement of MIL-I-8950.

One of the forgings was destructively tested for mechanical properties by Universal Cyclops. Eight areas exhibiting the lowest design margins were selected for test, and the property(s) of most concern in each area was measured. These eight areas were excised from the forging, machined to the thickness to be present in each respective area at time of the hardening
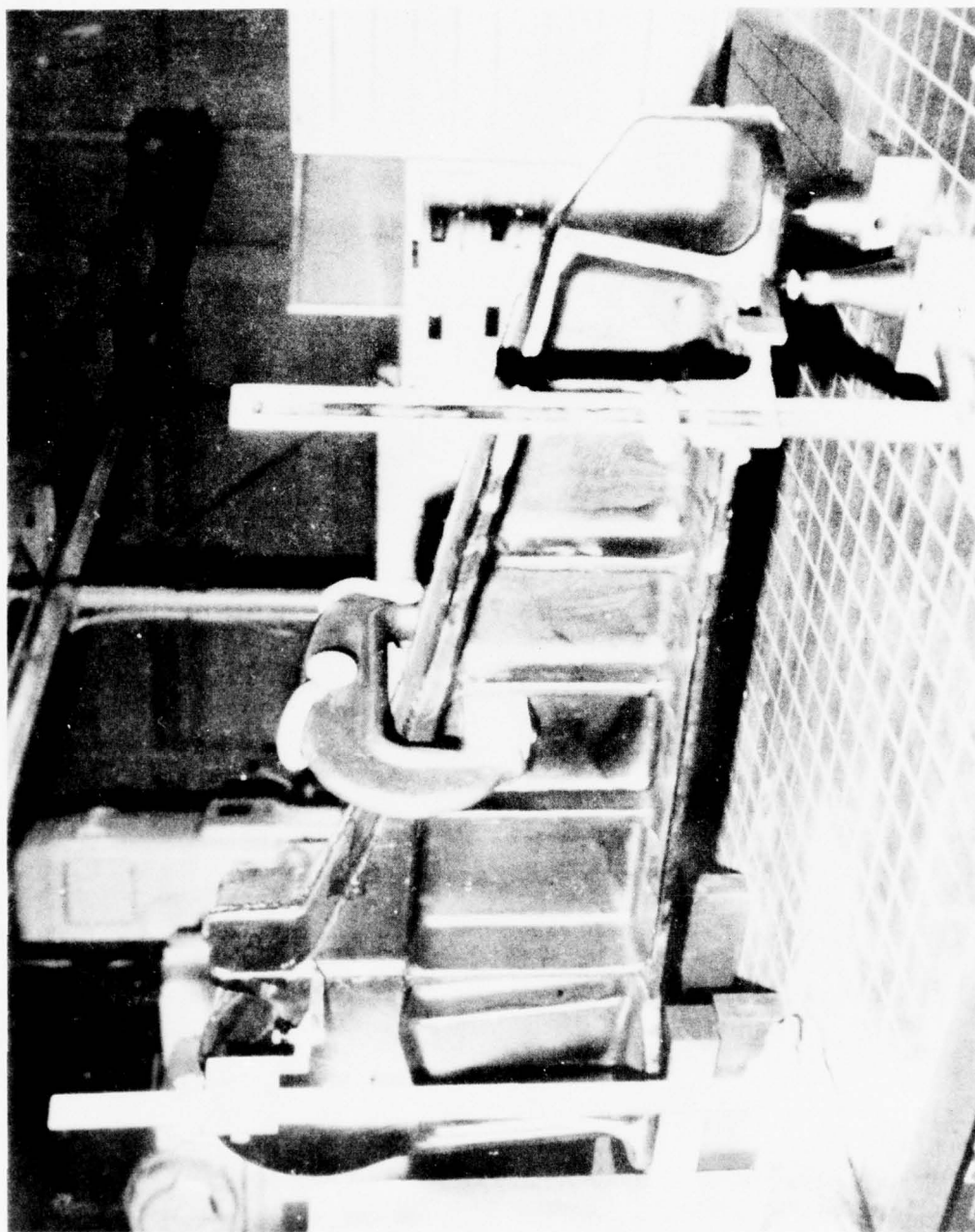
Figure 120. Closed die forging prior to initial machining.

heat treatment, and subsequently heat treated by the procedure planned for the machined test component:

1,500° F for 1 hour, air cool

-100° F for 1 hour, air warm

950° F for 5 hours, air cool

Specimens were then machined from the heat-treated sections and tested. The results, shown in Table 64 together with the design minimums, confirmed the desired properties could be met in the fitting using the air cool rather than the water quench from the austenitizing treatment. Test area 2 displayed FTU and FTY values 1 ksi lower than the design minimum; however, the design margin in this area was substantial, and these properties were therefore judged acceptable.

FABRICATION PLAN

The plan for the manufacture of the test component is shown in the manufacturing sequence chart of Figure 121. The Wilson profile mill was used to machine the pockets and webs, as well as the peripheral surfaces. A power mill was employed to accomplish the machining of the clevis end of component. Prior to the hardening heat treatment, all surfaces were machined to finish dimensions except the lower cap and clevis surface; these two areas were machined to a plus 0.125 inch to allow for correction of heat-treatment warpage.

The component was copper plated to protect the finished surfaces, heat treated, copper plate removed, and the clevis and lower cap surfaces machined to final dimension. The completed component was subsequently Ti-cad plated, primed, and white epoxy top-coated to complete the fabrication sequence.

FABRICATION OF TEST COMPONENT

The initial machining was accomplished on a Wilson profile mill, Figure 122. This machine uses a wooden pattern (to the right in the photo) to guide a stylus which controls the position of the cutting spindel. The part to be machined is fastened to the bed under the cutting spindel. The machine pictured has three cutting positions; only one was used. A view of the forging fastened to the bed of the machine prior to the initial cut is shown in Figure 123. A view of the forging being milled by the profiler is shown in Figure 124. Note the operator guiding the stylus along the pattern contours. Cutting of the clevis area with the power mill is pictured in Figure 125. A spray mist was used on the power mill for cooling; flood

TABLE 64

MECHANICAL PROPERTIES OF WING SWEEP ACTUATOR FORGING OBTAINED WITH SELECTED HEAT TREATMENT

TEST AREA	THICKNESS WHEN AUSTENITIZED	FTU (KSI)	FTY (KSI)	% ELONG.	& R.A.	CVN (FT-LBS)
1	1.75	256	237	17	68	50
2	0.50	229	214	16	67	53
3	0.55	233	218	17	68	56
4	0.15	231	217	16	66	-
5	1.75	252	233	17	66	50
6	0.40	235	218	16	67	-
7	0.55	230	217	16	68	-
8	0.30	253	232	15	63	51
AVER.	-	240	223	16	67	52
DESIGN MINIMUMS	-	230	215	-	-	40

DIMENSIONAL LAYOUT

LOWER CAP & CLEVIS SURFACES 1/8 OVER FINISH

LOWER CAP & CLEVIS SURFACES TO FINISH DIMEN.

CLOSED-DIE FORGING → PROFILE & POWER MILL → HEAT TREAT TO 230 KSI → FINISH MACHINE → Ti-CAD PLATE & PAINT

NORMALIZED & TEMPERED FOR MACHINABILITY

ALL SURFACES EXCEPT LOWER CAP & CLEVIS TO FINISH DIMENSIONS

BORE LOADING-PIN HOLE & DRILL ATTACH HOLES
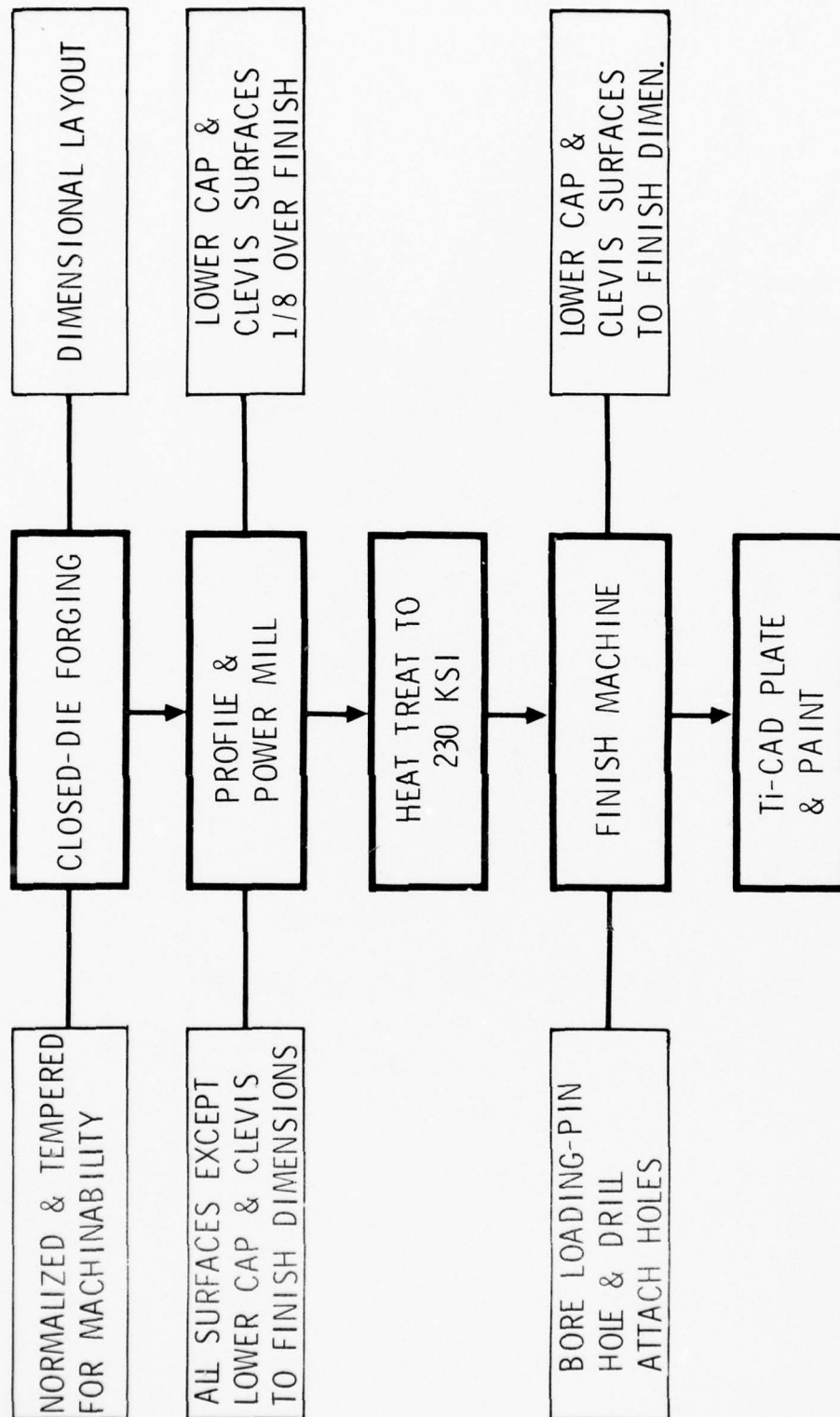
Figure 121. Manufacturing sequence.

254
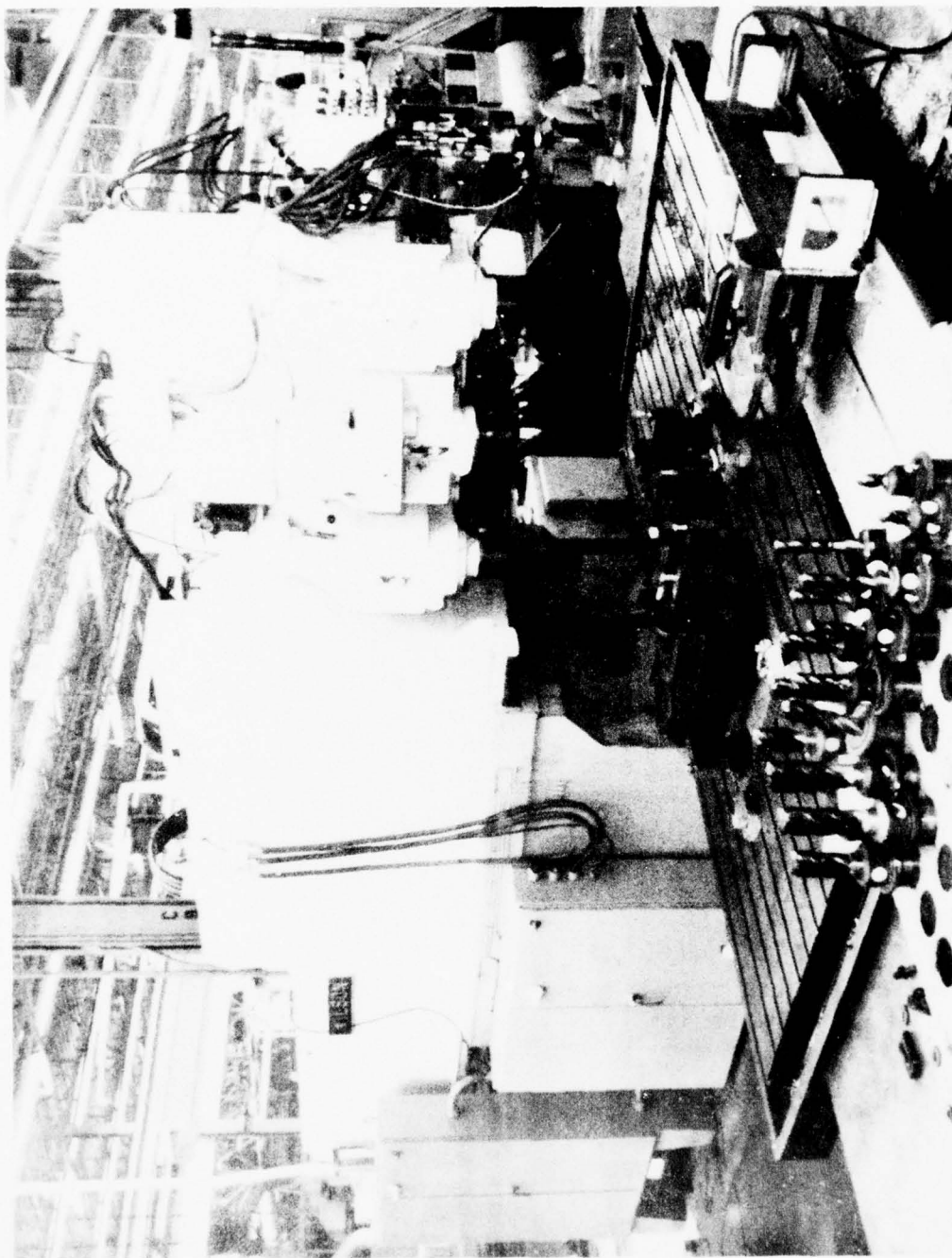
Figure 122. Wilson profile milling machine.
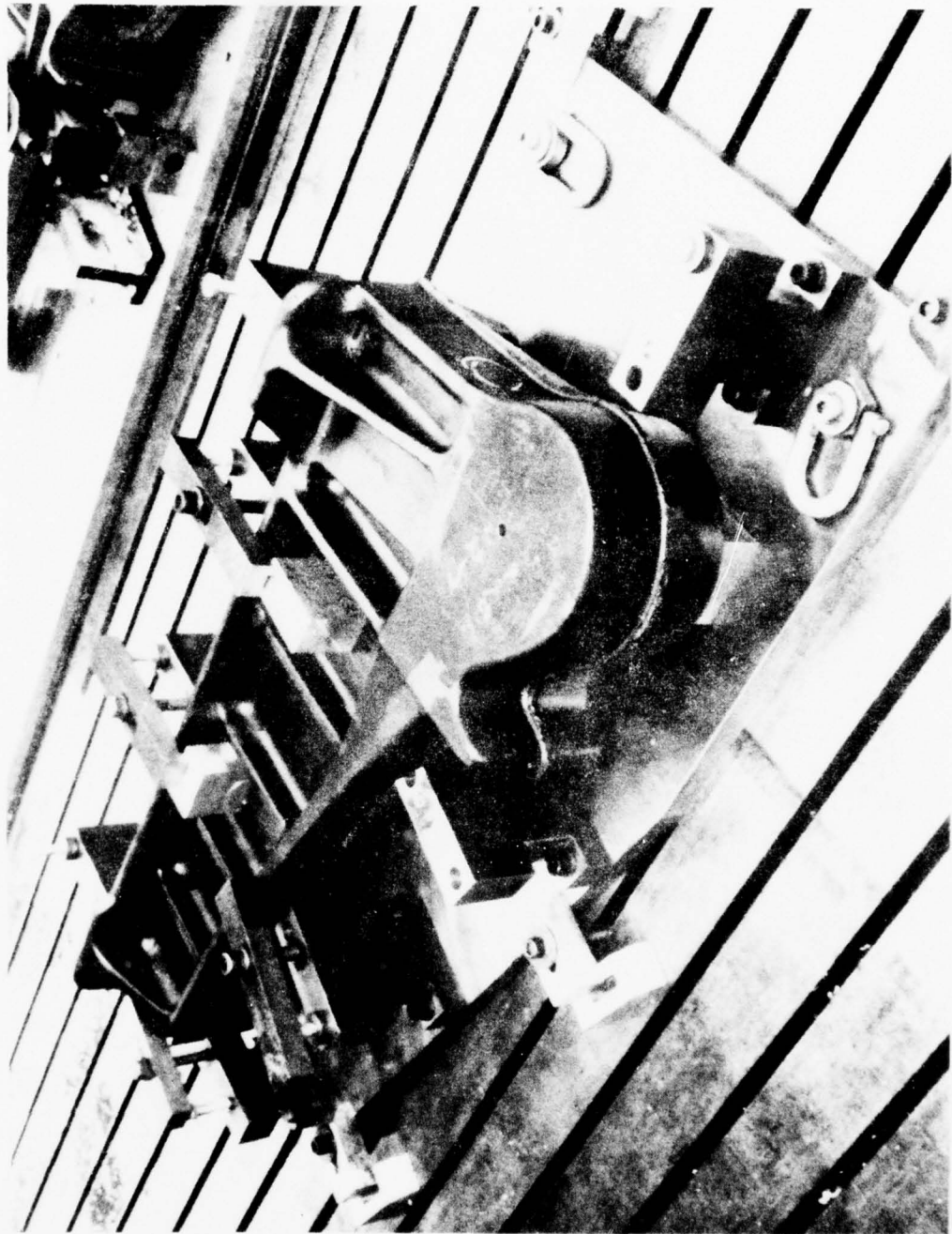
Figure 125. Forging on profile mill ready for initial machining.
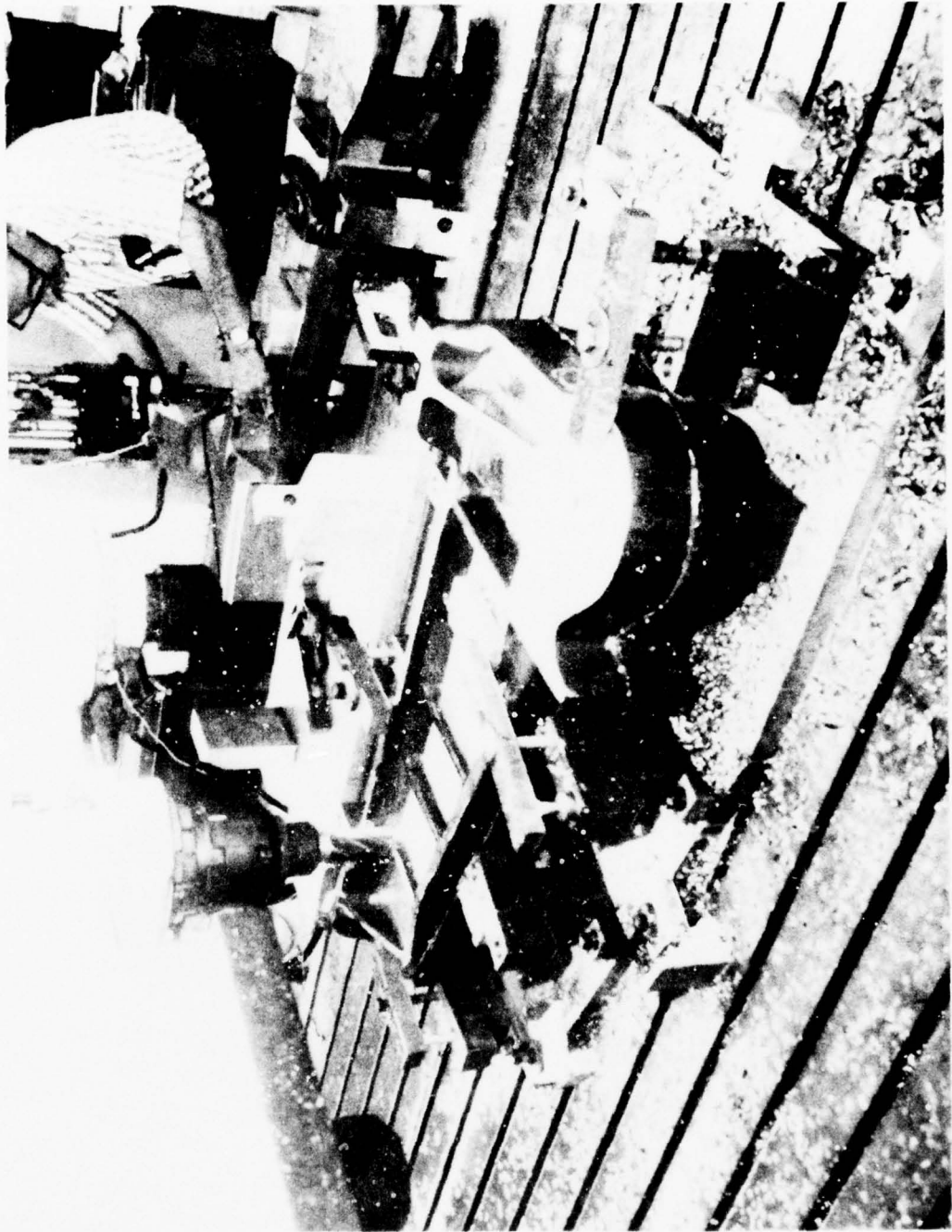
Figure 124. Profile milling.
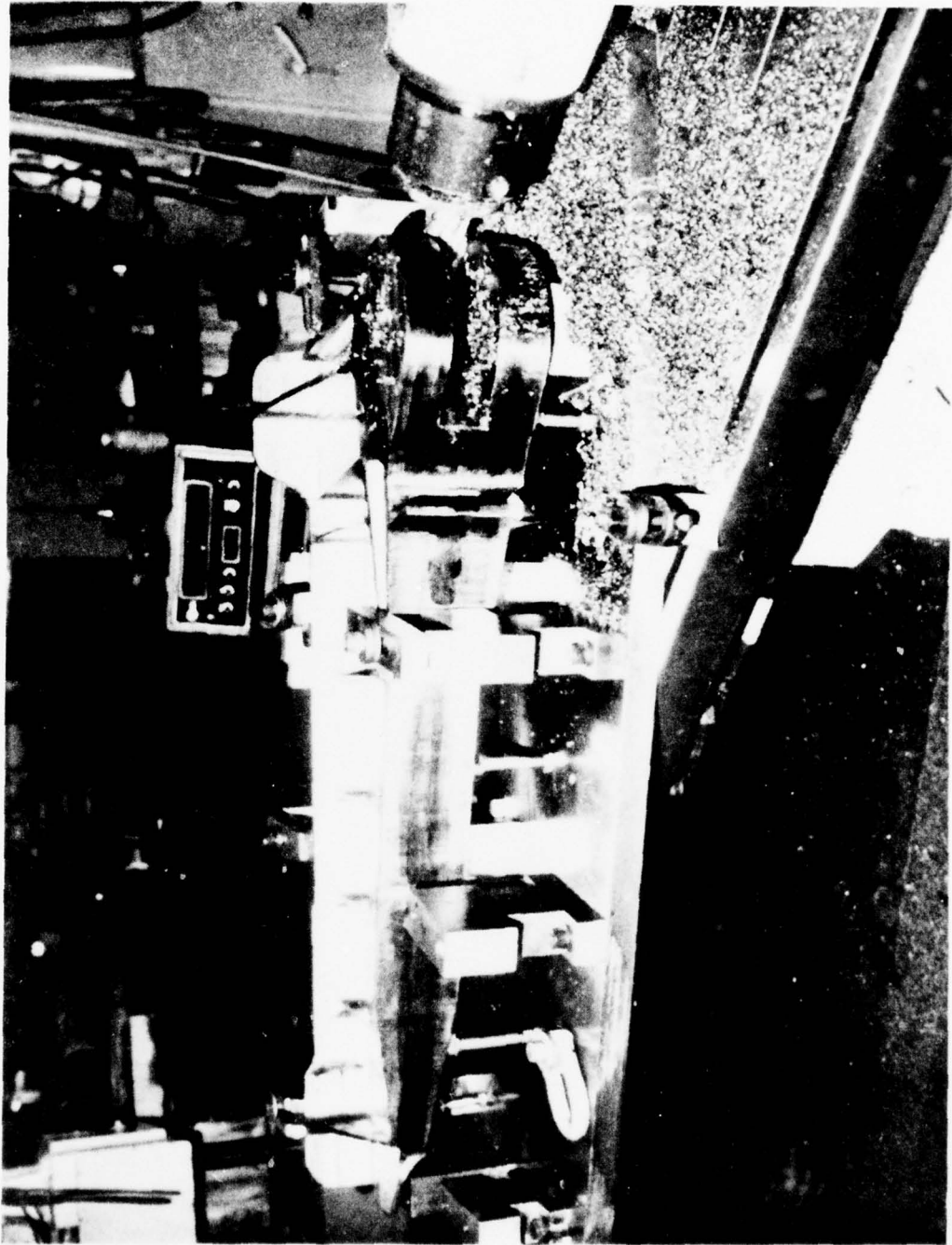
Figure 125. Power mill cutting of clevis area.

coolant was employed on the profiler. The machined component prior to heat treatment is shown in Figure 126. All surfaces at this stage of the manufacture were to finish dimensions except the top and bottom surfaces of the lower cap (upon which the component is sitting) and the four parallel surfaces comprising the clevis on the left of the part as pictured. As mentioned earlier, 0.125 inch was added to each of these surfaces to accommodate any heat-treatment warpage which might be encountered.

Heat treatment to harden the component was performed in the Gantry furnace pictured in Figure 127. This furnace is part of the heat-treatment facilities of Cal-Doran Metallurgical Services of Los Angeles. Prior to heating, the component was given a 0.002-inch-thick copper plating to protect the surfaces which were to finish dimension. A thermocouple was attached to the thickest portion, and the component was placed in a preheat oven operating at 1,000° F. When the attached thermocouple indicated 1,000° F had been achieved (115 minutes), the component was transferred to the Gantry furnace, operating at 1,525° F. Endothermic atmosphere was employed to prevent the copper from being oxidized and destroying its effectiveness. A period of 3 hours and 10 minutes was required to raise the temperature to 1,500° F. The long heat-up time was because of the highly reflective copper surface. The component was then allowed to soak between 1,500° to 1,525° F for 1 hour, after which it was lowered into the air-quench pit in the floor. This pit has a fan at the bottom to provide forced air cooling. A view of the part showing the method of supporting during heat treatment is shown in Figure 128. The component was supported, heavy end down, by a pin through a tooling prolongation. Steel wool was packed into the thin web areas in an effort toward equalizing the temperature during heat-up and cool-down. Upon cooling to room temperature, the steel wool was removed and the component subjected to a -100° F bath for 1 hour. Following that, a 950° F age for 5 hours was accomplished, completing the heat treatment. Results of the furnace control coupons which accompanied the fitting are tabulated in Table 65 and indicate the proper temperatures had been achieved.

The copper plating was removed, revealing a bright, shining part (Figure 129). Warpage was minor. The lower cap bowed upward (as viewed in the photograph) approximately 0.060 inch, which is probably the result of different volume changes occurring between the upper and lower caps because of their relative differences in thickness. The clevis closed approximately 0.030 inch, a condition which could easily be prevented by employing a spacer in this area during heat treatment. Warpage in both of these areas was well under the 0.125-inch allowance. All other surfaces remained within drawing tolerance except the web of the largest pocket (the fifth pocket from the left in Figure 129). This web, which was machined finished to 0.120-inch thick, is approximately 1-foot square. A dimensional check performed subsequent to the -100° F treatment and prior to the age revealed a "can" in this web with a height of 0.130 inch. Two steel plates 1-inch thick were machined to fit
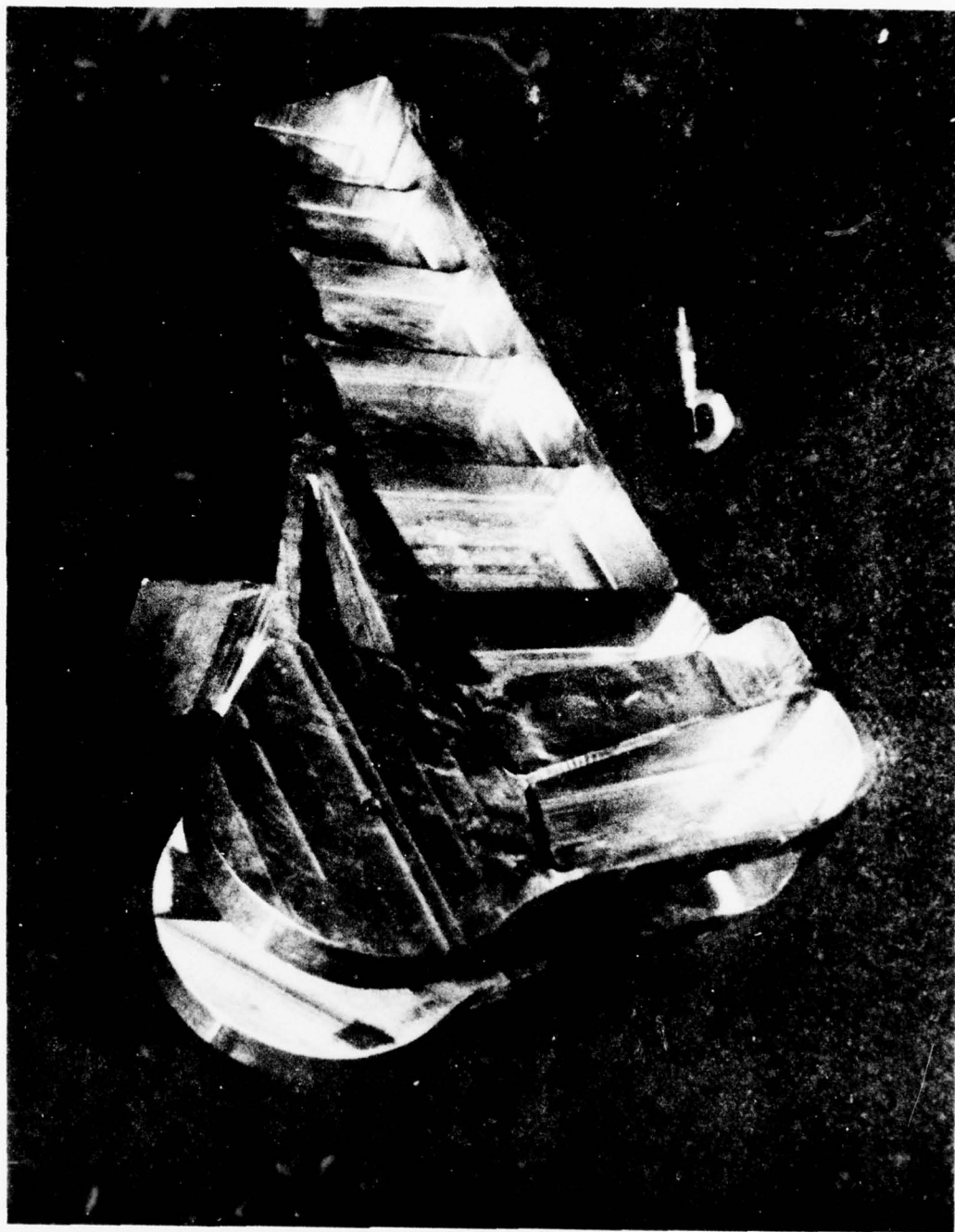
Figure 126. Fitting prior to heat treatment.
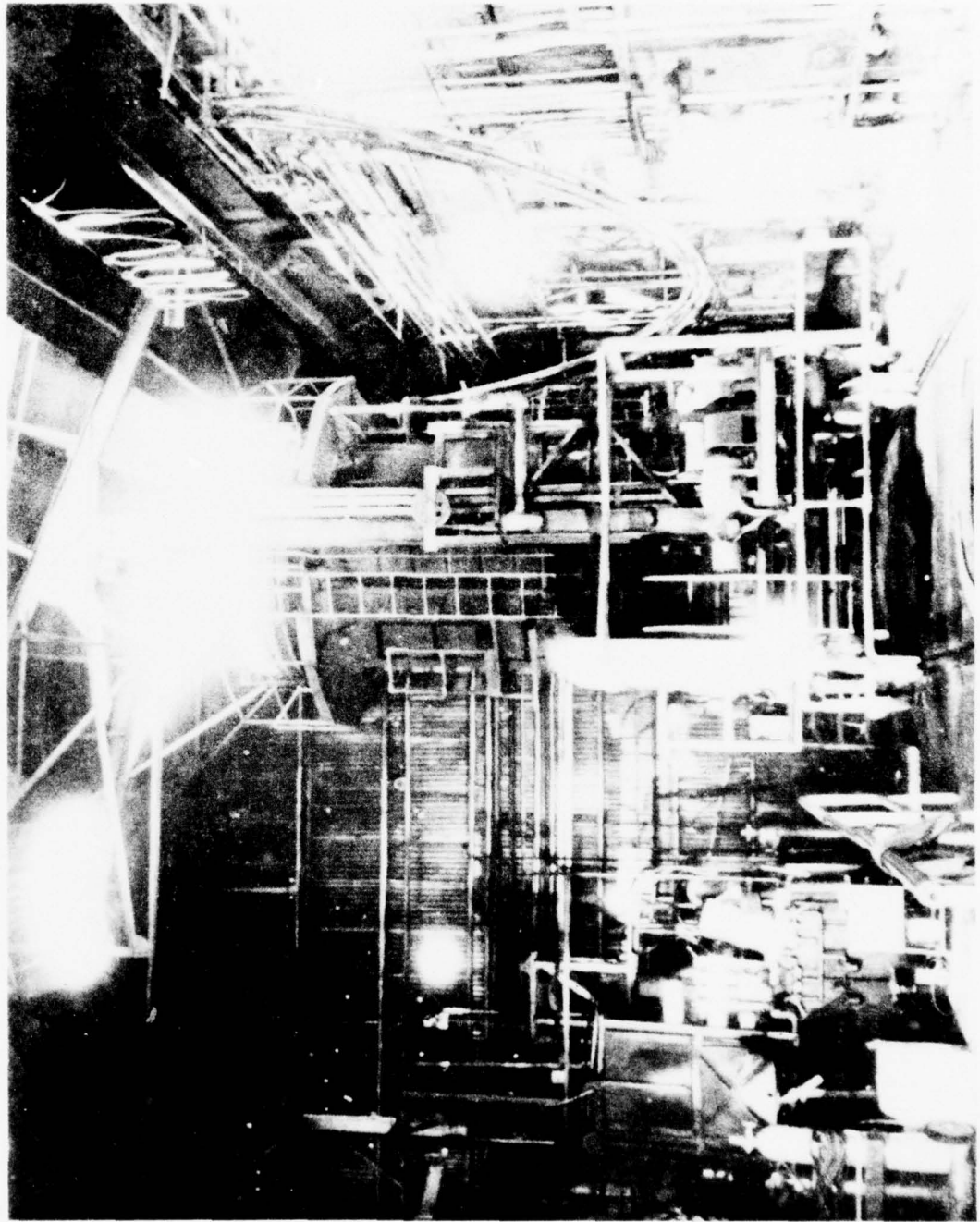
Figure 127. Gantry heat-treatment furnance.
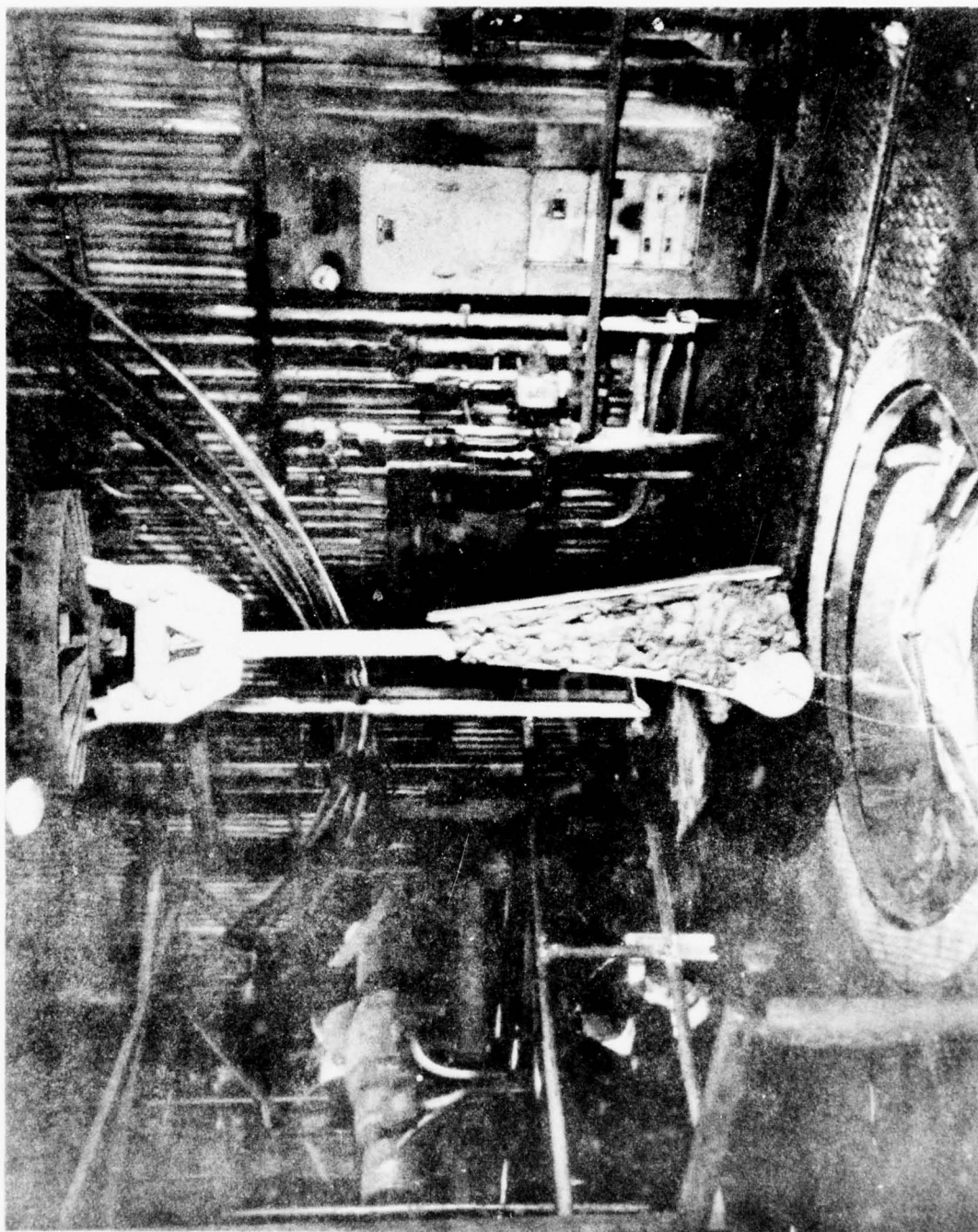
TABLE 65

PROPERTIES OF HEAT TREAT CONTROL COUPONS

SPECIMEN IDENT.	FTU (KSI)	FTY (KSI)	% R.A.	% ELONG.
1	241	226	71	17
2	242	228	69	15
3	244	227	70	16
AVERAGE	242	227	70	16

263
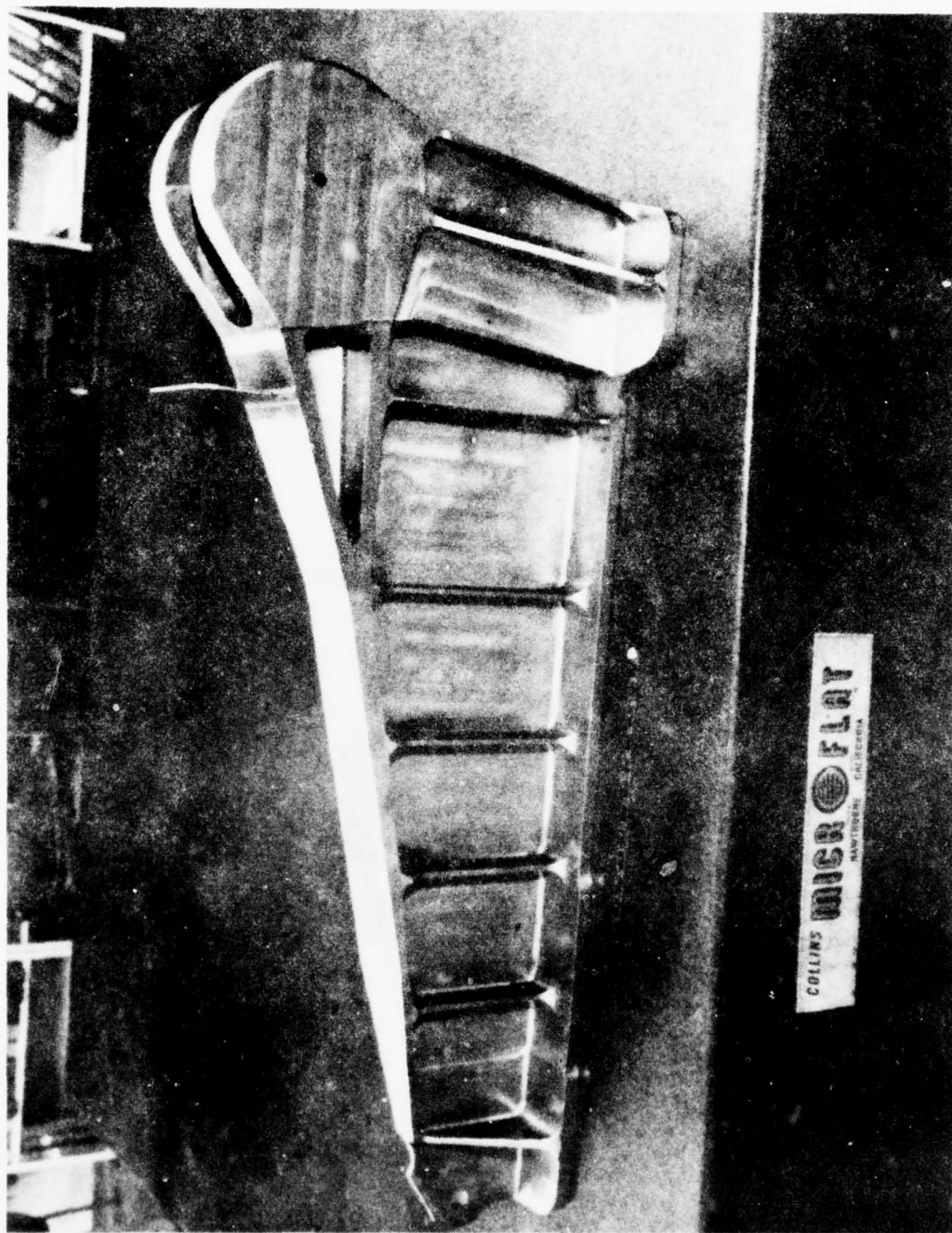
Figure 129. Appearance of fitting after heat treatment.

this pocket, clamped into place with a wedge clamp to flatten the web, and the component aged with the plates installed. Subsequently, the plates were removed, the component again dimensionally checked, and the can in the web was reduced from 0.130 inch to 0.030 inch by this age-straightening procedure. Although this amount of out-of-flatness was outside the drawing requirement, a check of the stress analysis for this area indicated the component should function satisfactorily, and no further effort was made to eliminate the can.

To complete the machining of the component, the attachment holes along the lower cap were drilled with the aid of a drill jig on a radial arm drill press. No difficulties were encountered in drilling the hardened steel. The final operation was machining the hole in the clevis on a jig bore machine, pictured in Figure 130. Note the curl-type chip obtained in the boring operation. Although no boring operations were included in the machinability studies previously discussed, application of the machinability knowledge gained in these studies to the boring operation proved successful in avoiding any difficulties during this operation.

A view of the completed inboard wing sweep actuator attach fitting is presented in Figure 131. Press-fit bushings have been installed in the clevis area to accept the bearing loads to be applied by the large loading pin; up to 150 tons will be loaded into the part by this pin. This was the configuration of the fitting at the beginning of the four-lifetime testing.
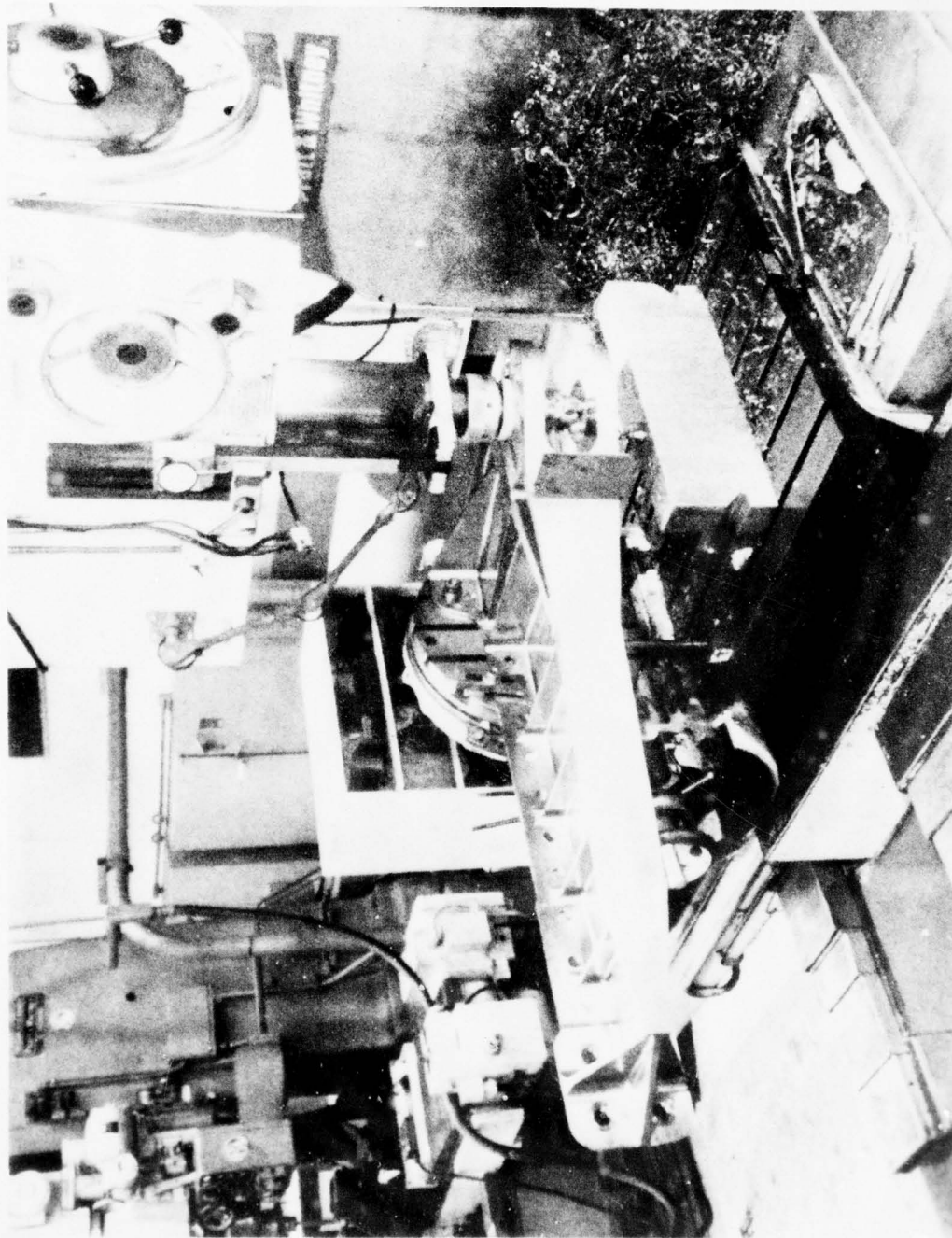
Figure 130. Machining of clevis on boring mill.

266
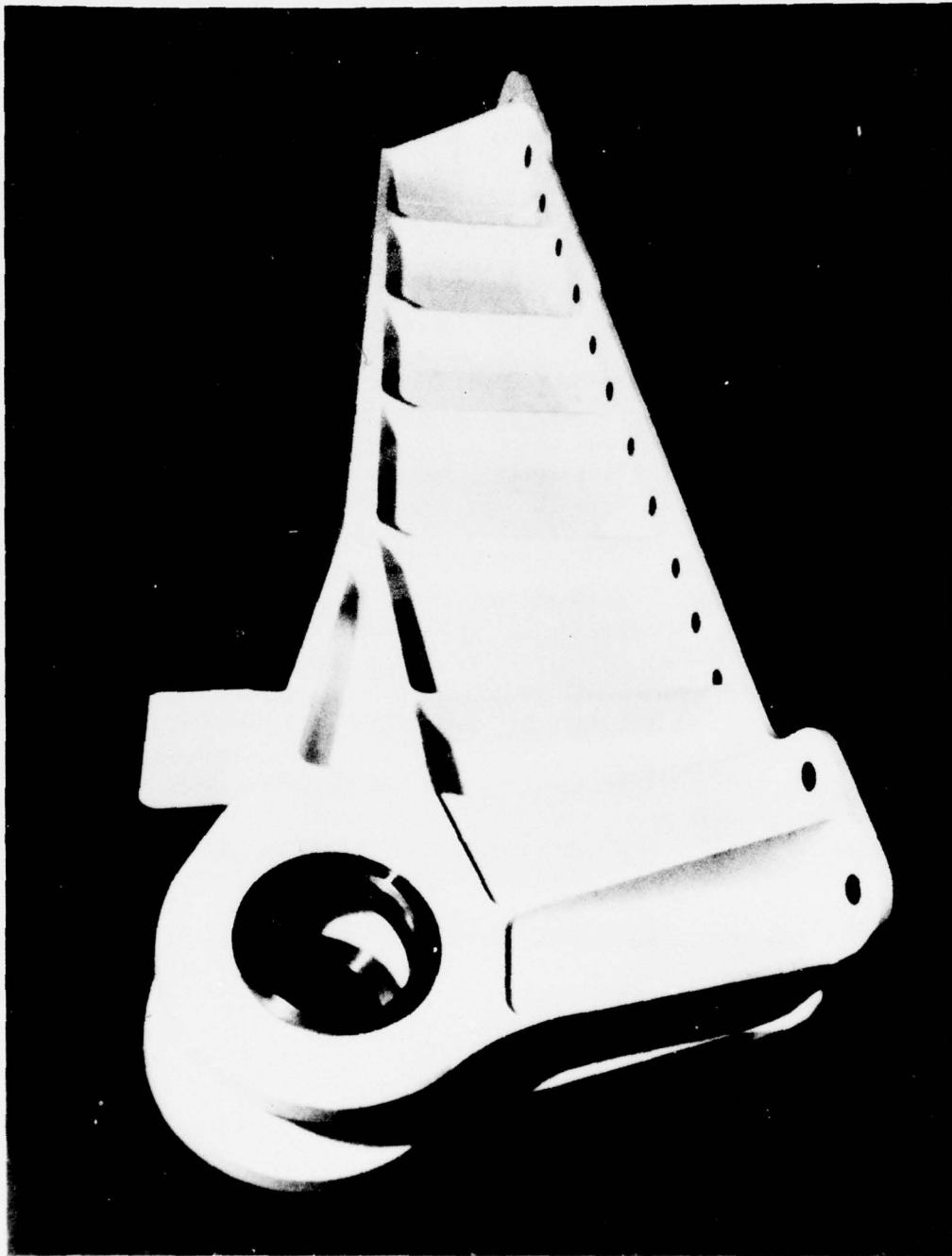
Figure 131. Completed fitting ready for testing.

267

Section VI

COMPONENT TEST

To validate the design and sizing of the AF1410 test component for comparison of weight, cost, structural characteristics, and service life with the titanium component being replaced, a full-scale component test was conducted. A single test component was subjected to two lifetimes of fatigue, two lifetimes of damage-tolerance cycling, and finally a static residual strength test. The details of this test program, together with the results obtained, are presented in this section.

TEST PLAN AND EQUIPMENT

The test component was instrumented with 15 axial strain gages, three shear gages, and one deflectomer. The locations of the gages are indicated in Figure 132. The deflectomer was installed adjacent to shear gage 14 to monitor the "can" which was present in this web as a result of the heat treatment. Data were acquired from the gages with the aid of a digital data acquisition system.

The test component was mounted in the test fixture pictured in Figure 133. The bolts used were PH13-8-M steel at 220 ksi strength level, the same as used for this part in the four B-1 flight test aircraft. Two cylinders were employed to apply negative and positive loads at four angles to the base of the fixture. A schematic of the load angles applied and their relationships to the wing sweep angles is shown in Figure 134. By simultaneously applying negative or positive hydraulic pressure in the two cylinders with the aid of the computer-actuated servo load control system, the desired resultant angle and magnitude was achieved. The test spectrum employed in the testing is contained in Appendix E. Four tests were conducted in the following sequence:

1. Static tests to maximum spectrum load

2. Fatigue test

3. Damage-tolerance test

4. Static residual strength test, limit load, and failure

INITIAL STATIC TEST

The static test to maximum spectrum load was conducted to obtain a survey of all strain gages to insure linear behavior of the test component was being experienced. Two tests were conducted. The first involved a load of

Figure 132. Strain gage locations.

269

Figure 132. Strain gage locations. (concluded)

270
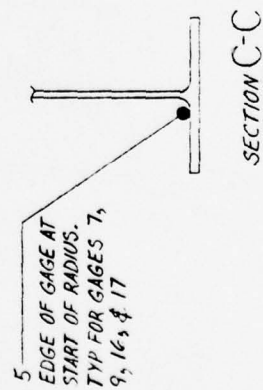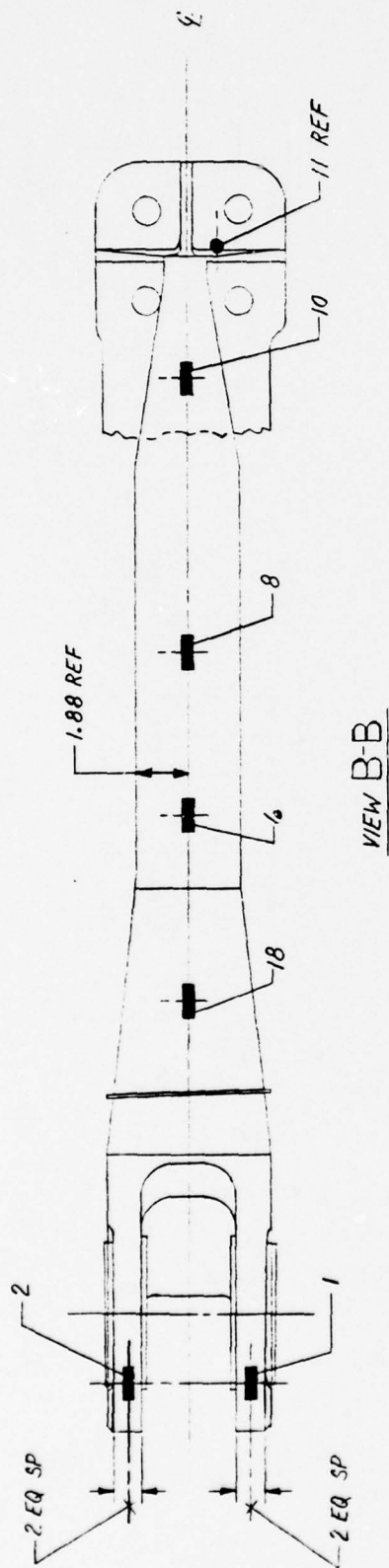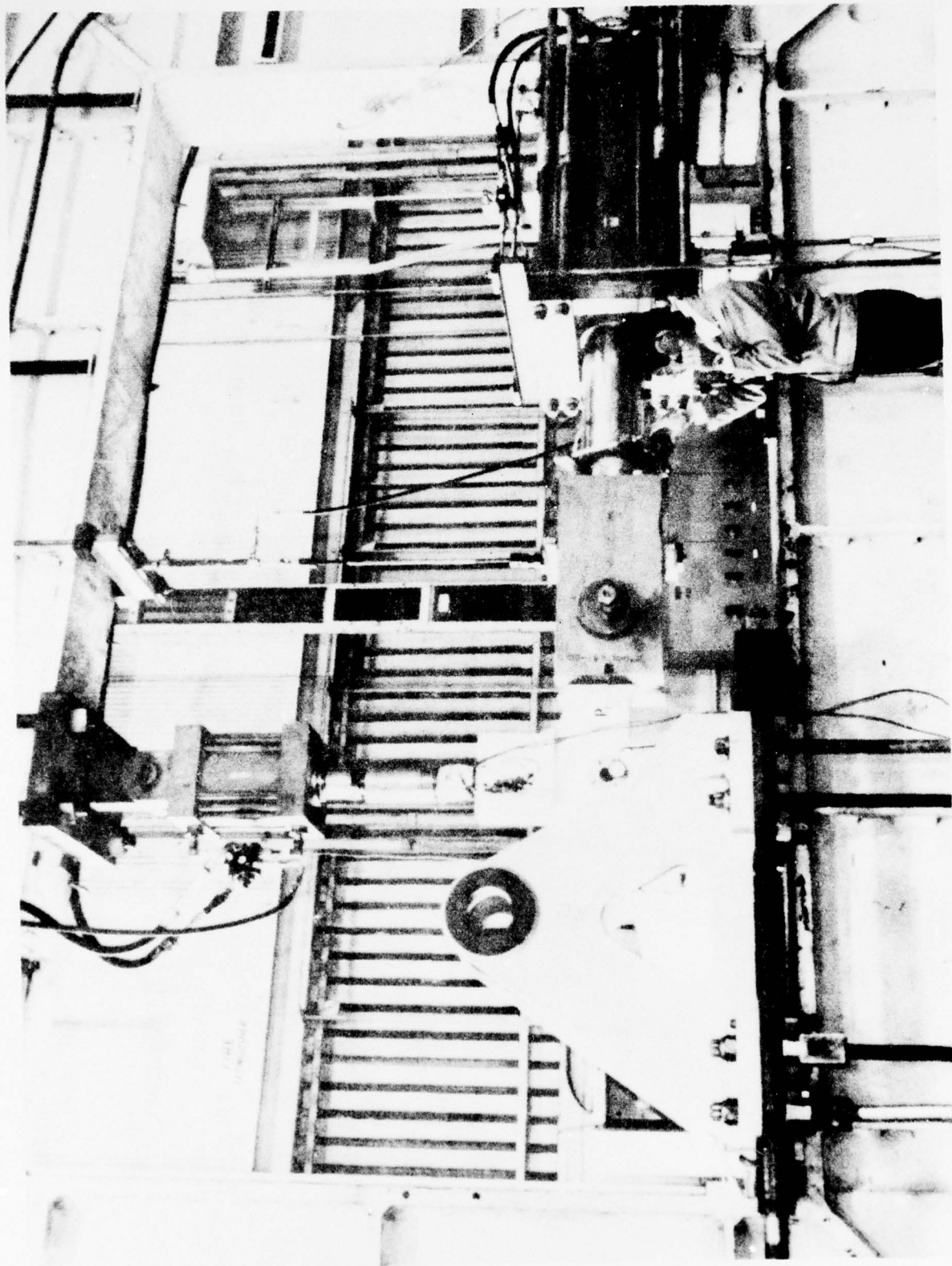
Figure 133. Fatigue test apparatus.

271

Wing Angle vs Load Angle

15°	6°
25°	12°
55°	29°
67.5°	36°
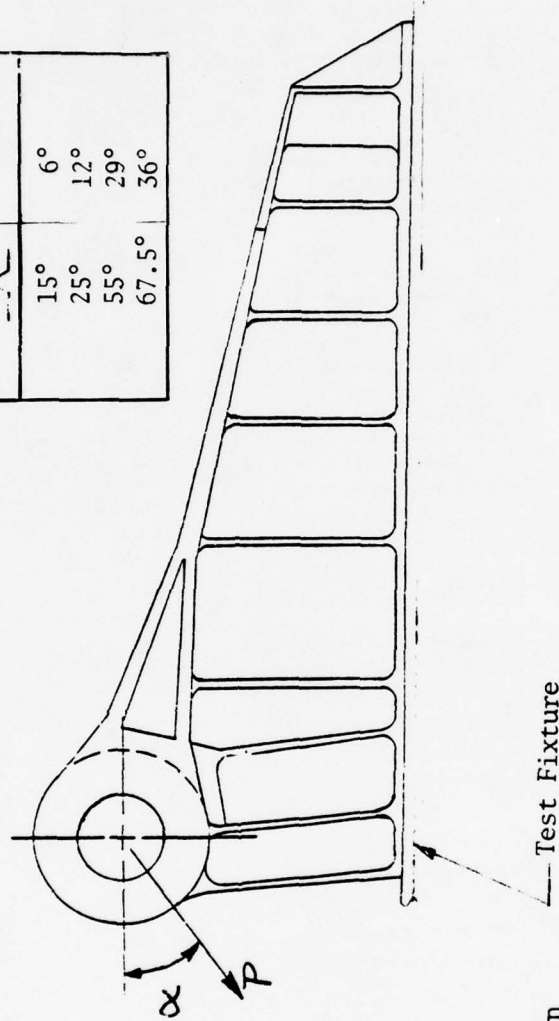
Load P is Positive
in the direction shown

Figure 134. Load Application sketch.

272

-280,000 pounds at an angle of 36 degrees to the base of the component (step 57 of the spectrum). This is the highest load imposed on the component in this direction in the fatigue spectrum and occurs only once every 100 missions. The load was applied in 20-percent increments, recording the strain gage output at each load increment, until the maximum was achieved. Then the load was decreased to zero in 20-percent increments with strain-gage data taken at each increment. In a similar fashion, a load of +305,000 pounds at 36 degrees to the base was applied at 20-percent increments, obtaining strain-gage data at each increment. These data were then analyzed for linearity and compared with the predicted stresses from the stress analysis. The strain at all gages was linear with the load (strain-gage data are contained in Appendix D), and the measured values agree well with the predicted (Table 66). The test component and fixture where examined for evidence of any damage; none was observed. The test component was then committed to the two-lifetime fatigue test, and the cycling per the spectrum in Appendix E was begun.

THE TWO-LIFETIME FATIGUE TEST

One lifetime was composed of 1,280 missions. Rate of testing was approximately 5 minutes per mission. As part of the test plan, the test was interrupted at one-half, one, 1-1/4, 1-1/2, and 1-3/4 lifetimes for bolthole inspection. Five bolts were selected at random and removed to permit visual inspection of the holes with a borescope. No cracks were observed in any of these inspections. Additionally, a strain-gage survey was conducted at the completion of the first and second lifetimes. The same loads were used as in the initial survey, and no change in any gage output was observed.

During the first lifetime, at mission 876, a crack was observed in the fitting. It was on the forward return flange, beneath the clevis (the left end of the component as viewed in Figure 131) at the radius where the vertical flange fairs into the lower cap. A view of the crack in this area is shown in Figure 135, looking down onto the top surface of the lower cap (the forward end of the component is at the left). The crack occurred at the tangent point of the radius to the vertical flange. A small geometric discontinuity resulting from machining (a slight undercut) was also present in this same area. Another view of this same crack, observed from the front surface of the component, is pictured in Figure 136. The slight undercut can be observed in this photo running approximately parallel to the bottom face through the No. 5 on the scale. A pie-shaped section was cut to remove one-half of the fracture surface for examination. The fracture is pictured in Figure 137 and clearly shows the fracture mode as fatigue. Fatigue striations were visible entirely across the area excised for examination. The three pronounced striations result from the higher loading which occurs each 100 missions and, in effect, mark the extent of the crack at the end of 100 missions. Three such lines are shown in this photo, indicating that 300 missions were required to grow the crack to the length pictured. The entire crack was not excised (about one-half is shown in the photograph), so it was not possible to perform a striation

TABLE 66

COMPARISON OF PREDICTED VERSUS MEASURED STRESS

Location[a]	-280K lb		+305K lb	
	Predicted	Measured	Predicted	Measured
1	9.7	6.1 ksi	10.5	17.7 ksi
2	9.7	9.3	10.5	17.0
3	47.1	29.0	-51.3	-26.8
4	47.1	34.2	-51.3	-27.0
5	0.8	3.4	-0.9	-0.2
6	-44.6	-49.5	48.5	45.5
7	0.8	-0.5	-0.9	-0.2
8	-43.8	-45.7	47.7	42.1
9	11.1	-1.0	-12.0	-1.9
10	-32.3	-32.0	35.0	28.4
11	-12.0	-7.0	13.1	7.2
12	-34.3	-29.6	37.3	26.9
13	32.0	36.5	-34.9	-34.8
14	24.1	21.2	-26.2	-29.7
15	13.6	24.6	-14.8	-6.6
16	2.9	1.0	-3.1	-7.0
17	-0.1	-2.3	0.1	0.5
18	-41.4	-47.0	45.1	43.2

[a] See Figure 130

274
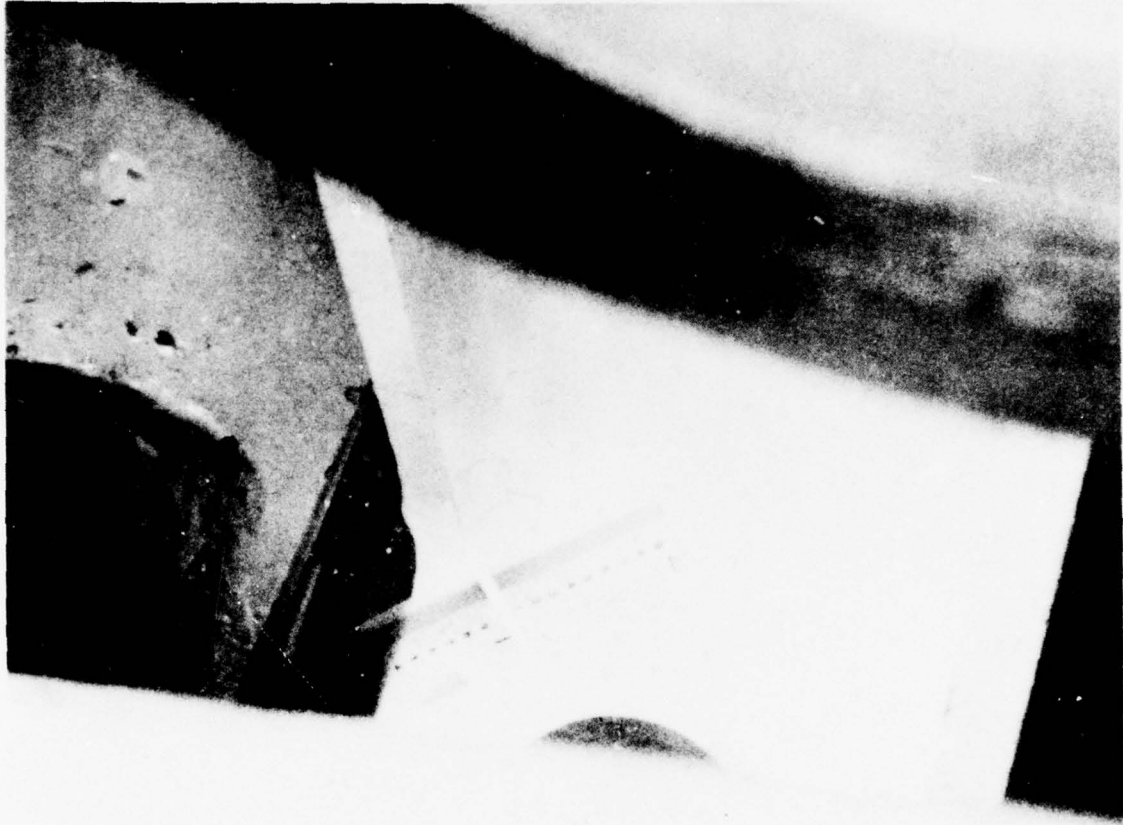
Figure 135. Crack at bottom of forward flange, north side.

Figure 136. North side flange crack shown in previous figure as viewed from front end of test component.

Figure 137. Fracture surface; origin is at lower right corner (10X).

277

count on the fracture to ascertain the number of missions required to cause the crack to form. It was estimated that the crack probably initiated after 300 to 400 missions. The origin of the fracture is shown in the lower right corner of Figure 137, and it is at the corner marked by the arrow in Figure 135.

The fracture origin was examined metallurgically to determine if there were any anomalies at the origin; none were observed. The microstructure was normal, no inclusions were observed, and the hardness was the expected R_c 48. Several photomicrographs were sent to Universal-Cyclops Specialty Steel Division for study by personnel in the research laboratory, and they concurred with the conclusion that the microstructure at the fracture origin was normal.

A decision was made to remove the crack and to repair by welding. It was recognized that the fatigue life of the weld deposit would be inferior to that of the parent metal which it would replace, but it was believed that the manufacturing anomaly present at this location probably resulted in a significant increase in stress, and that the removal of this geometric anomaly would significantly lower the stress at this point. The crack was removed by grinding to the extent shown in Figure 138. Another view of this same grindout is presented in Figure 139. To assist the reader in orienting to locations to be described subsequently, it would be well for the reader to refer back to Figure 133. The side of the component facing the camera in this photo will be referred to as the "south" side; that facing the wall will be termed the "north" side. The end of the fitting nearest the notation "P" on the fixture will be identified as the "front" or "forward" end. Hence, the crack which has just been described occurred on the north side at the front end of the test component.

Welding was accomplished using AF1410 filler wire, and a series of small cross-section passes were deposited by the GTAW process. The interpass temperature was maintained below 300° F. The weld deposit was built up to a minimum of 0.050 above the height desired to provide for removal of the last pass. This was done so that only weld deposits which had seen some refinement by the heat of subsequent weld passes would be present in the completed repair. After welding, the area was blended to the desired geometry by the use of rotary files and emery discs. Radiographic inspection was performed to insure a sound weld. The component was subsequently reinstalled on the test apparatus, and the fatigue test resumed.

One lifetime (1,280 missions) was achieved without any further incident. At this point, some bolts were removed to permit inspection of the holes, and a strain-gage survey was conducted and compared with data obtained on the initial survey. No damage was observed in the holes, and no change was observed in the strain readings.

Shortly after the second lifetime testing was begun, at mission 1,526, the weld repair was observed to be cracked. A photo of this crack is shown in

Figure 138. Extent of grind-out for weld repair, viewed from
front of component.

279
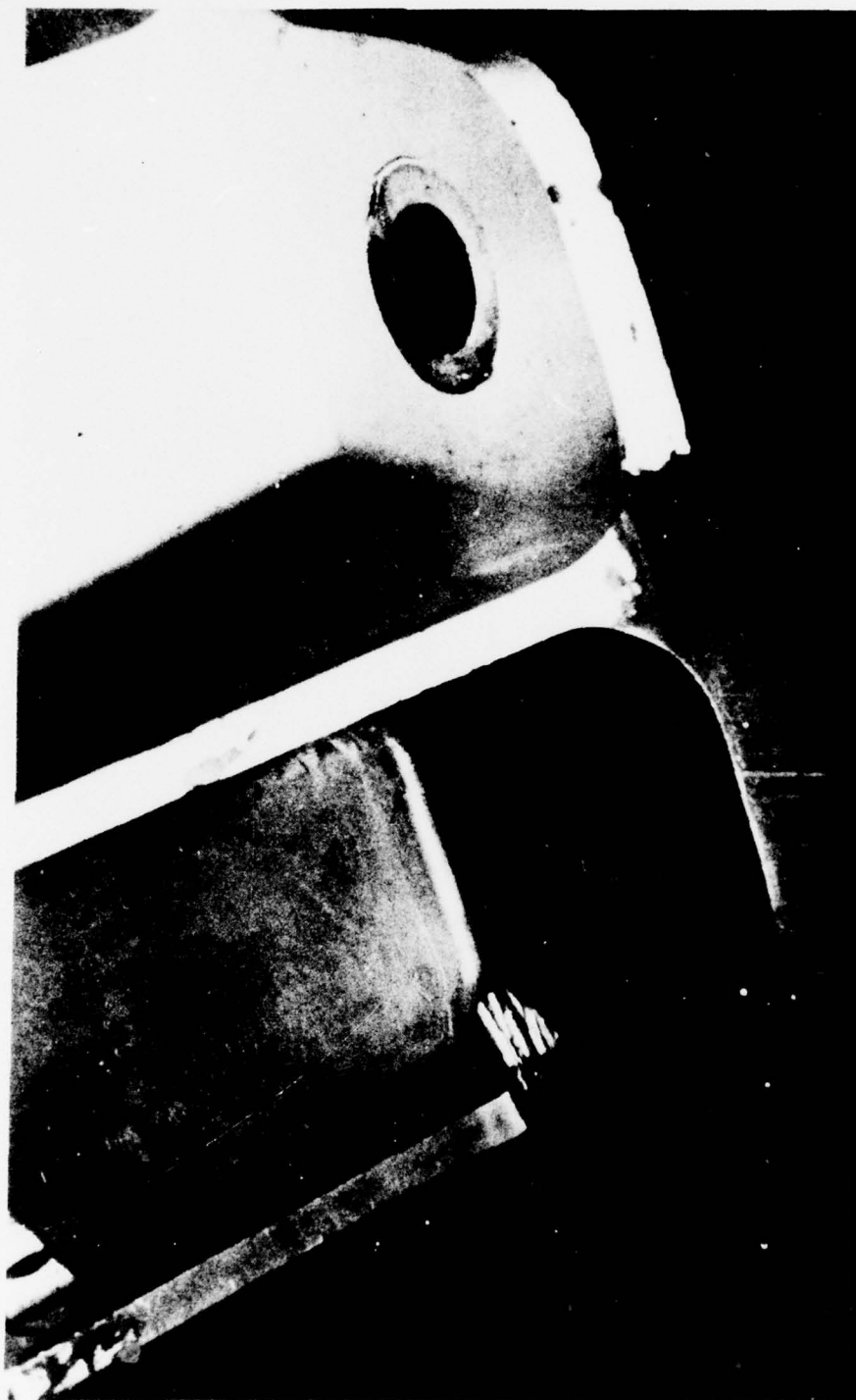
Figure 139. Grind-out as viewed from north side.

Figure 140. Comparing this photo with the previous photos showing the extent of the grindout before welding, it appears the crack occurred along the bottom edge of the weld, or perhaps in the heat-affected zone immediately adjacent to the fusion line. It also became apparent that the stiffness in this area of the component was inadequate, allowing excessive deformations to occur and resulting in high stresses in this local area. To reduce the deflections and thereby lower the stresses in this area, a 0.300-inch thick gusset was welded in place as shown in Figure 141. The same welding technique was used as in the previous weld; i.e., GTAW, AF1410 filler metal, small weld beads, and no postweld thermal treatment. Inasmuch as the component is roughly symmetrical about the centerline, consideration was given to also welding a gusset on the south side to reduce deflection on that side also. However, the decision was made to continue testing without it since no crack had yet appeared in the parent metal, and, perhaps more importantly, it would have been necessary to remove the component from the test fixture to accomplish the south-side gusset weld (the north-side gusset was welded with the component in place; access was impaired on the south side).

Cycling was resumed at mission 1,526. At mission 2,059, a crack appeared at the bottom of the forward flange on the south side, virtually identical to the one in this area on the north side. The location of the crack is indicated by the arrow in Figure 142. The component was removed from the test fixture, a gusset was welded in place as previously described, and the component was reinstalled in the test apparatus. Since the component had to be removed for welding, both welds were radiographically inspected, and some repairs were made to the initial gusset welding on the north side to bring this weld up to radiographic standards.

The component with the new front-end geometry is shown in Figure 143. Four areas were designated as "areas of concern" for close monitoring during the remainder of the cyclic testing. These areas are at the ends of the welds, experiencing stress levels intended only for parent metal. Inasmuch as the fatigue life of the weld deposit is significantly lower than the parent metal, it was anticipated that cracking may develop in any or all of these areas during the two lifetimes of cycling yet to be accomplished. By inspecting these areas frequently while under a high load (highest imposed by the test spectrum), it was anticipated any crack which developed would be detected while it was still small and amenable to a simple in-place weld repair.

The component was reinstalled, testing was resumed, and two lifetimes (2,560 missions) were accomplished without further incident. This completed the planned two-lifetime fatigue test.

THE TWO-LIFETIME DAMAGE-TOLERANCE TEST

To prepare the component for the damage-tolerance test, it was removed from the test apparatus to permit machining of four crack-starter notches at

Figure 140. Crack at weld repair, view looking down along front face.

282

0.040
(±0.010,
0.000)

45°

Weld edge preparation

9 in.

t = 0.30

Ref 0.50

2 in.

Ref 0.40
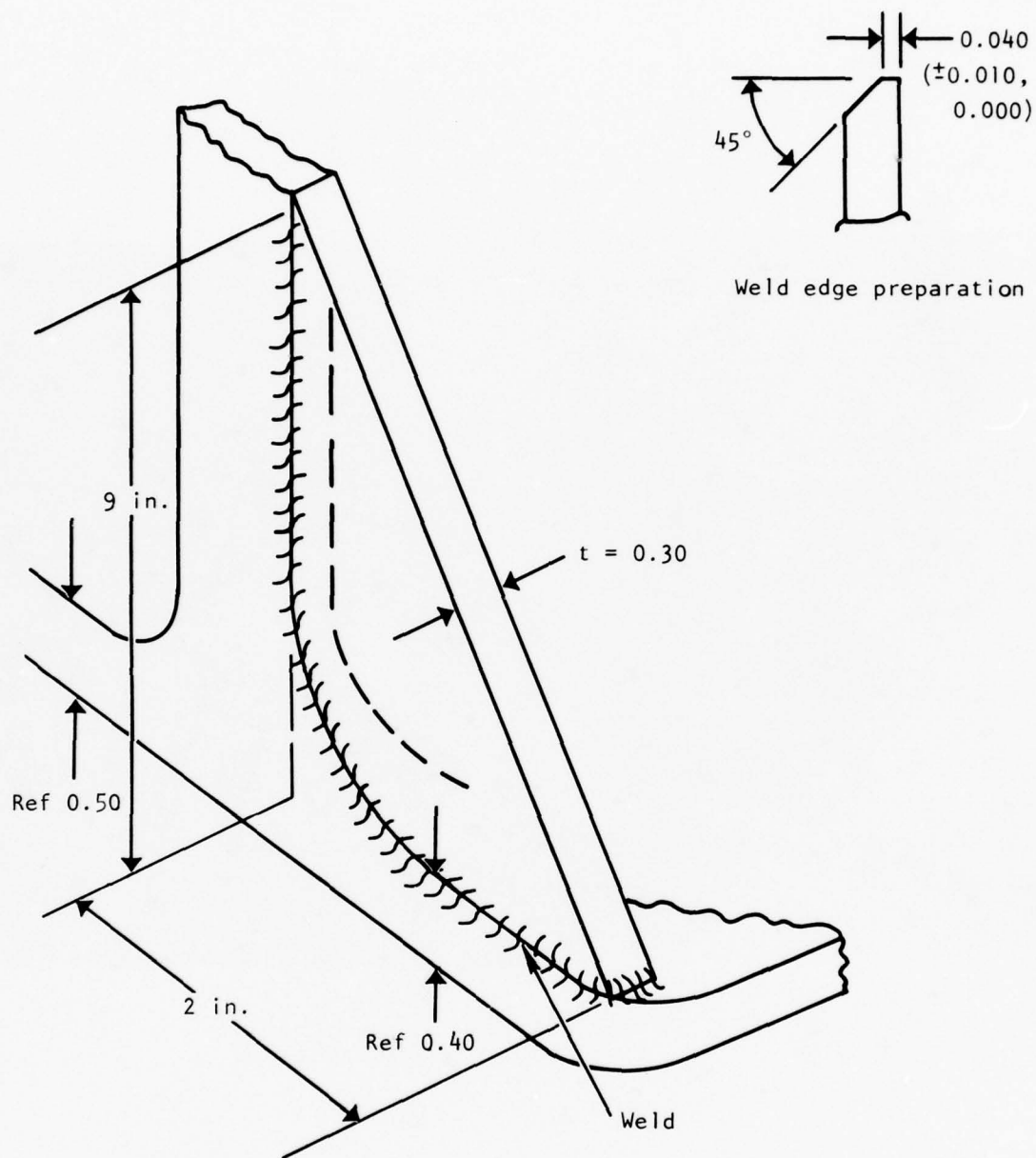
Weld

Figure 141. Sketch of welded gusset.

283

Figure 142. Crack at bottom of forward flange, south side.

284
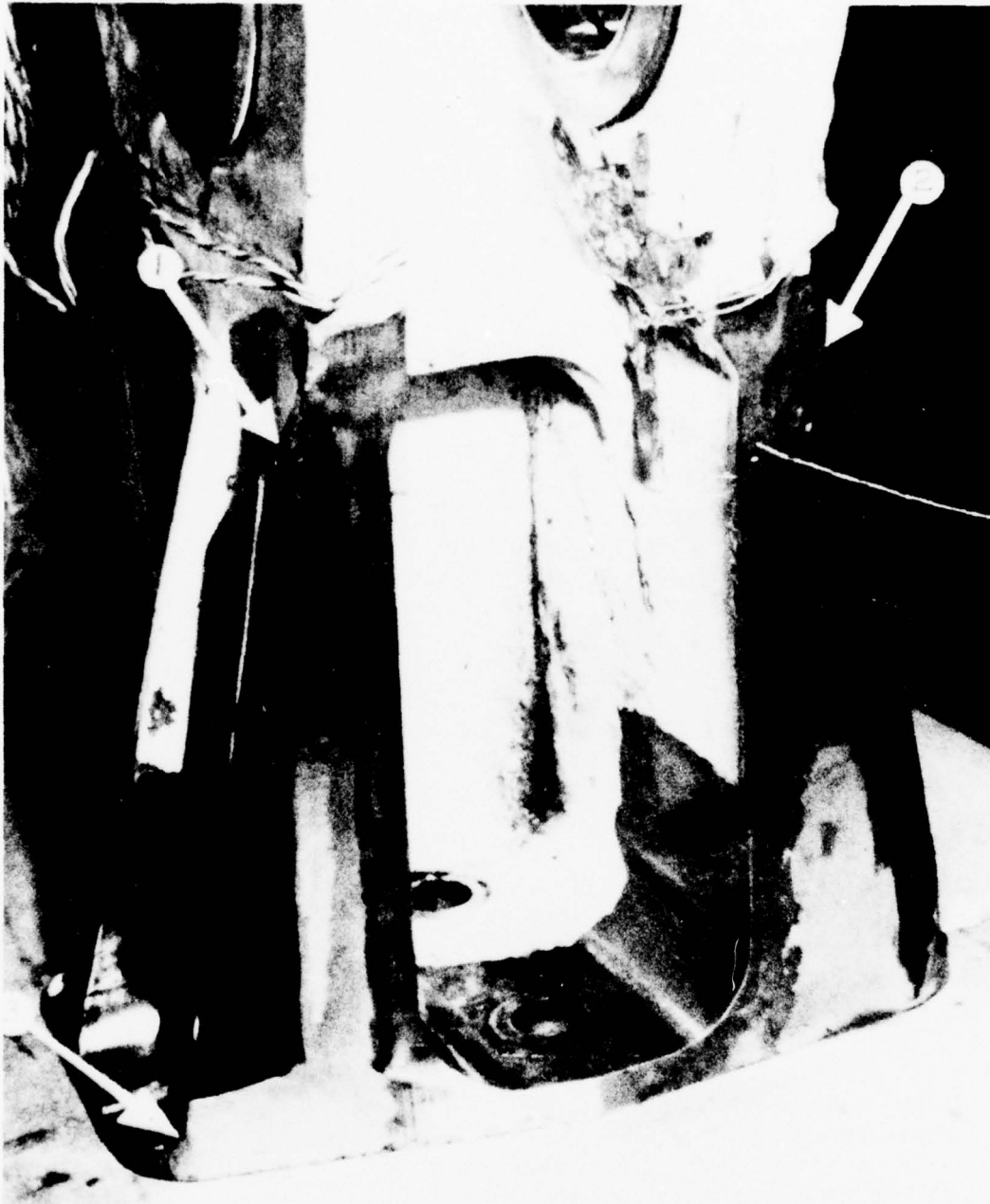
Figure 143. Front end of component after gusset installations
(arrows indicate "areas of concern" at ends of welds).

285

locations shown in Figure 144. The notches were machined to the dimensions shown by electrical-discharge machining (EDM); all were 0.015 to 0.020 inch wide. The boltholes were examined and found to be free of damage, and the fitting was reinstalled. A strain-gage survey was again conducted and compared with the original survey; no changes were observed. Subsequently, the two lifetimes of damage-tolerance testing was commenced at mission 2,560. Throughout the duration of the test, periodic inspections were made of the EDM notches to detect initiation of cracks.

During the two-lifetime damage-tolerance testing, cracking occurred in the welds at three locations, areas 1, 2, and 3 noted in Figure 143. Areas 1 and 2 were repaired after 3,495 missions, and area three was repaired at 3,770 mission. A second repair of area 1 was accomplished at mission 4,842. No cracks appeared in area 4 at any time. Two lifetimes of damage-tolerance testing were achieved without any further incidents, thus completing the planned four-lifetime, 5,120-mission fatigue test. A summary of the cracking incidents and when they occurred throughout the four-lifetime test is presented in Figure 145.

Natural cracks did not form at any of the four EDM notches after two lifetimes of spectrum loading. Although the notches in themselves represent a significant stress concentration, the severity was insufficient to cause cracking in a material as tough as AF1410. In the case of a complex fitting such as the chosen test component, it is not practical to precrack each EDM flaw by individual load application. Nor is it feasible to precrack them all simultaneously, as each location has its own operating stress which negates simultaneous cracking at the four flaw locations.

FINITE-ELEMENT ANALYSIS

To gain a better understanding of the magnitude of the stresses in the forward end of the fitting where cracking occurred, a NASTRAN finite-element analysis was performed. The NASTRAN analysis consisted of the development of NASTRAN models which included a coarse-grid idealization and a refined-grid idealization of the lower flange.

Prior to the test of the wing sweep actuator fitting, a coarse-grid NASTRAN finite-element model was developed as a demonstration aid in the use of a new interactive graphic display system. Figure 146 shows the isometric node idealization of the wing sweep support fitting. The original intention of the model was to check stress levels with the test strain gages located as shown in the test plan, and to demonstrate the Rockwell International finite-element modeler (RIFEM) NASTRAN interactive graphic display capability. Because of the coarse-grid distribution of the model, it was not intended to be used to obtain a satisfactory stress definition for detailed analysis in the lower flange-web region.

286
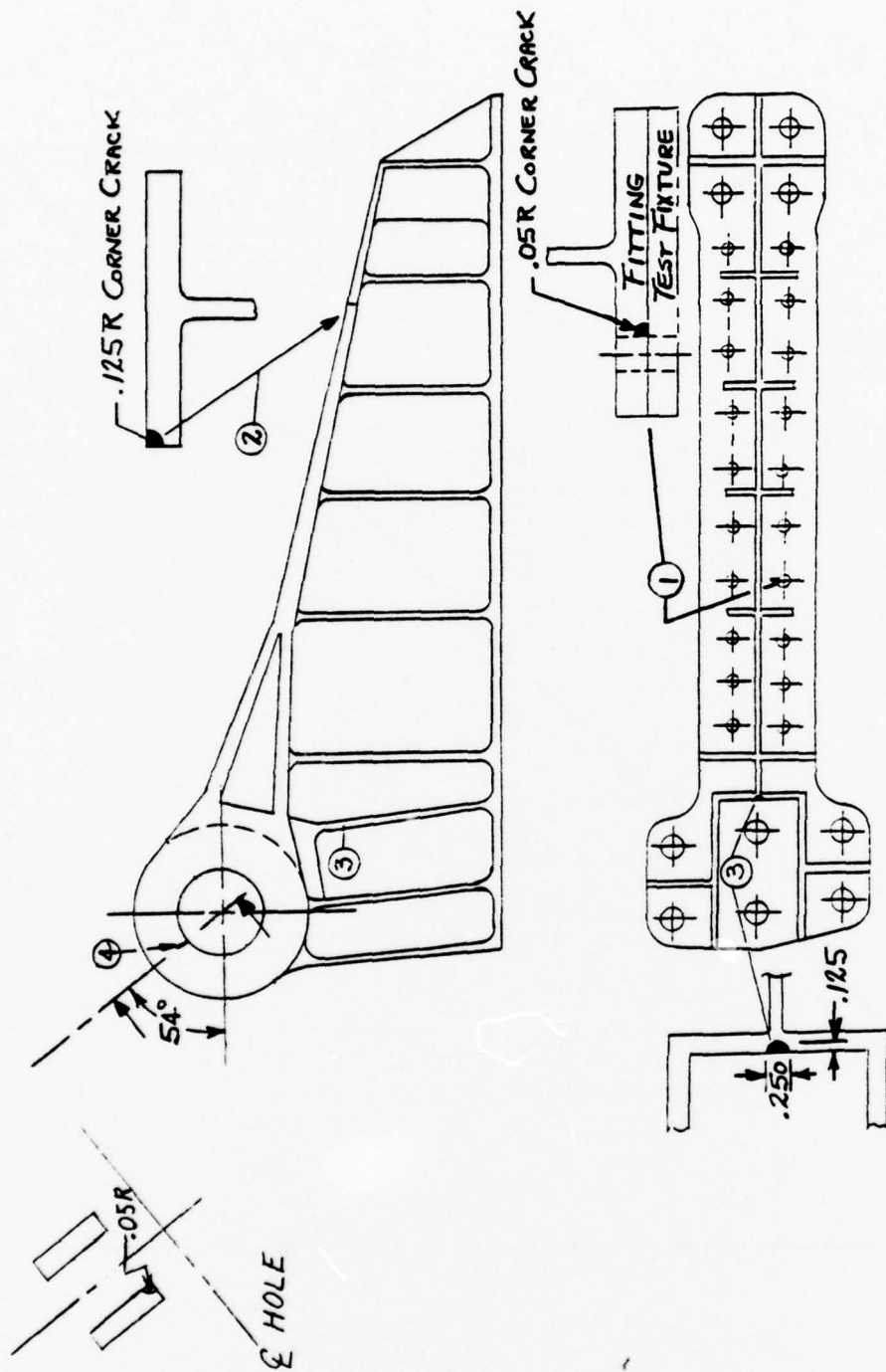
Figure 144. Location of the four EDM notches.
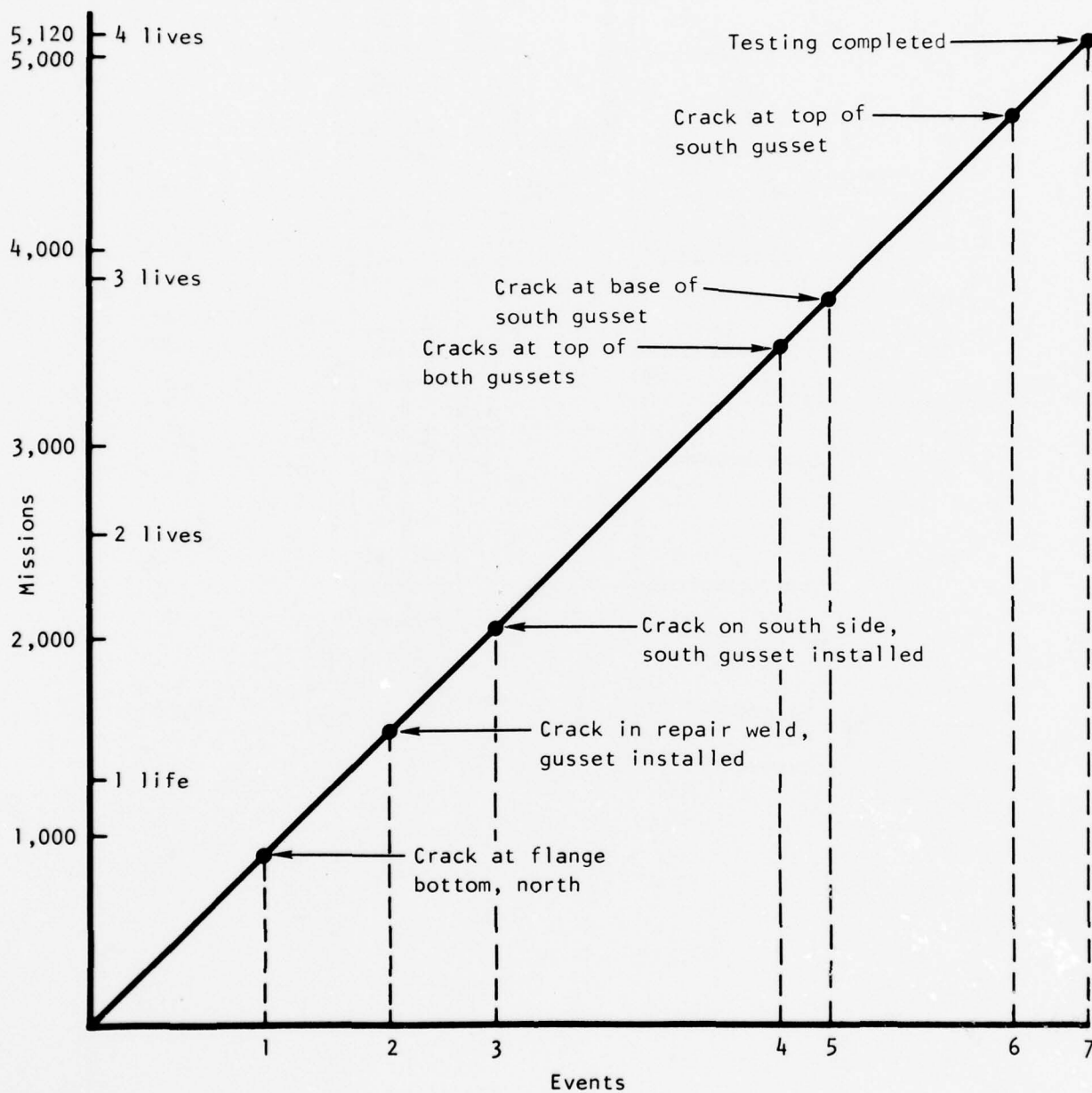
Figure 145. Summary of significant events
during spectrum testing.

288

ROTATION ANGLES
X : 0.0
Y : 45.0
Z : 45.0

DISTORTION
HORZ. 1.00
VERT. 1.00

SIGHT DISTANCE
1.00000E+06

MODEL
DATE : 05/18/77
TIME : 16:26:47
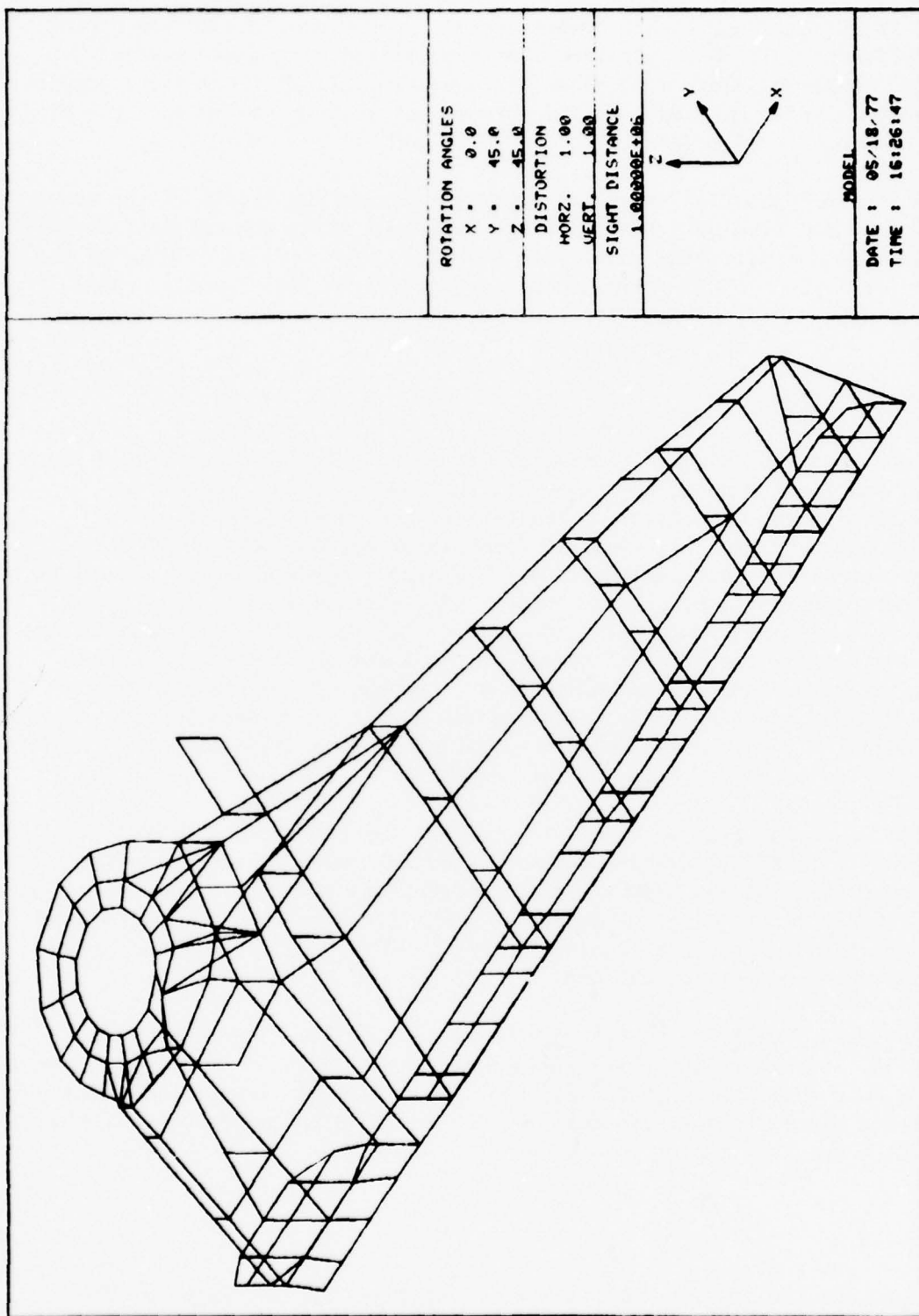
Figure 146. Coarse NASTRAN model node idealization of wing sweep actuator support fitting developed for NASTRAN/RIFEM interactive display.

During the fatigue test, a crack developed in the region where the forward shear web attaches to the lower flange. From visual inspection during load application, it was determined that the fatigue damage was induced by localized upward bending on the lower flange. To nullify the fatigue problem, additional material was added to the forward vertical web to relieve the high upward bending stress concentration.

To obtain a detailed stress distribution map in the region of the cracking, an expanded five-grid FEA model was developed using the original Rockwell NASTRAN/RIFEM demonstration model as a baseline. The refined-grid model was expanded from 186- to 353- grid nodes and from 173 to 389 elements. An isometric node idealization of the refined FEA model is shown in Figure 147.

MODEL IDEALIZATION

The wing sweep actuator fitting was idealized using rod, membrane, plate bending, and axial bending elements. In the idealization, symmetry was assumed through the centerline of the fitting, and only one-half of the structure was modeled. All flange and web intersections were modeled assuming normal-to-plane intersections, and bend fillets were not considered. In the node idealization, grid refinement was determined on the basis of detecting local stress concentrations which could precipitate fatigue damage. Figure 148 details the grid refinement in the lower forward flange region. Further refinement was not deemed necessary because of the elastic solution mode of NASTRAN and the simple bending plate idealization used in this model. A more detailed idealization would need to incorporate solid elements and be representative of intersection fillet bends.

The lug, upper flange, shear webs (except for the forward lower flange transition (Figure 149)), and associated stiffners were represented using CQDMEM quadrilateral and CTRMEN triangular membrane elements. The lower flange which attaches to the wing structure was idealized with CQUAD2 quadrilateral and CTRIA2 triangular plate bending elements. CONROD and CBAR elements were used to stabilize the vertical webs.

An expanded view of the fitting lug region idealization is shown in Figure 150. Simulated lug bearing loads were applied in the model by use of a cosine load distribution. Single point and multipoint lower flange boundry constraints simulated the actuator-fitting-to-wing-attachment bolt pattern and reacted out applied lug loads.

FEA RESULTS

A plot of the major principal bending stresses for the forward lower flange is shown in Figures 151 and 152. The maximum bending stress (239 ksi) occurs at the intersection of the forward web and the lower flange and is in
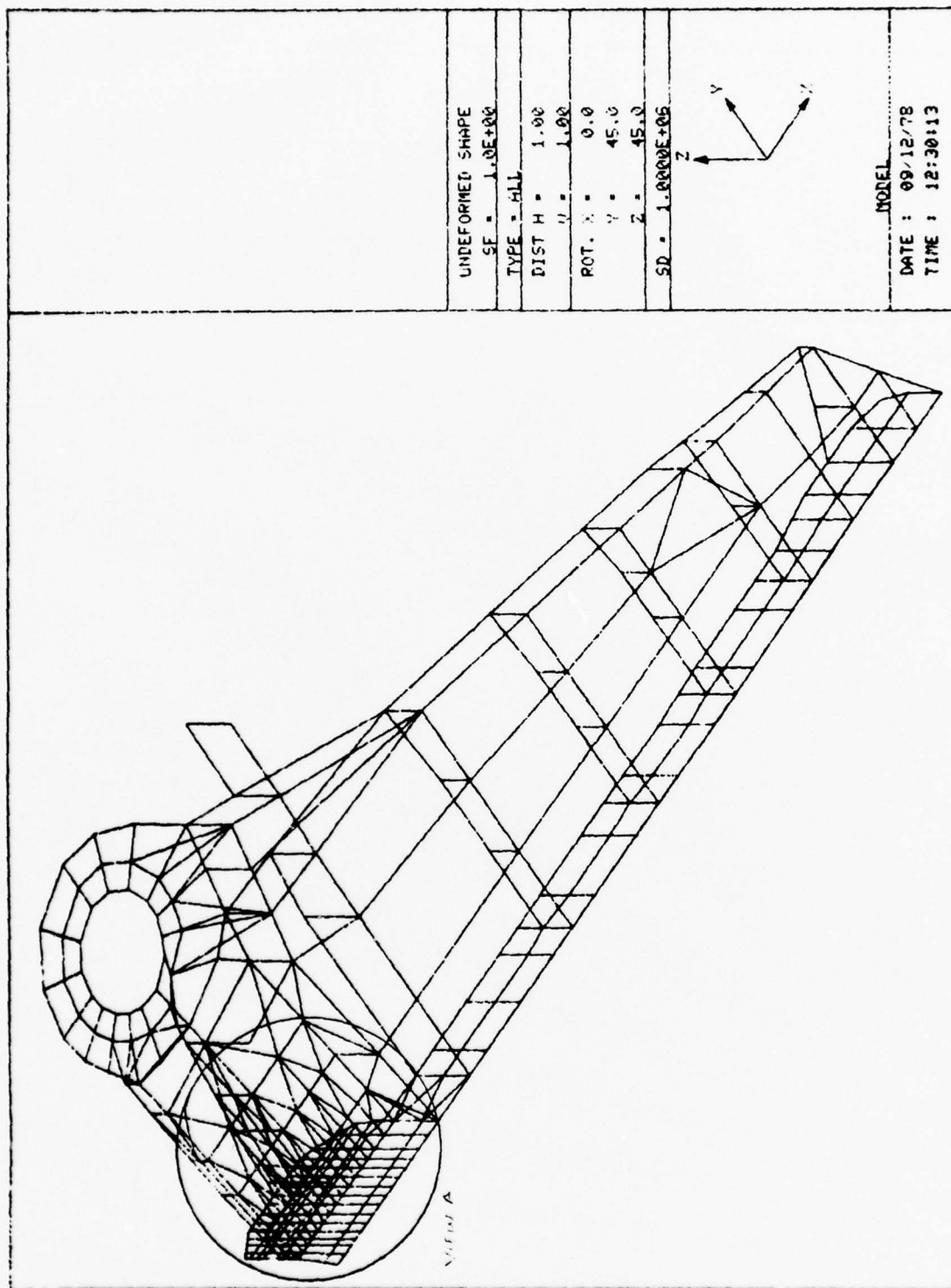
Figure 147. Refined NASTRAN model node idealization - wing sweep actuator support fitting.

UNDEFORMED SHAPE
SF = 1.0E+00
TYPE = ALL
DIST H = 1.00
V = 1.00
ROT. X = 0.0
Y = 45.0
Z = 45.0
SD = 1.0000E+05

MODEL

DATE : 09/12/78
TIME : 12:20:19

CENTER WEB

FORWARD WEB

BOTTOM FLANGE
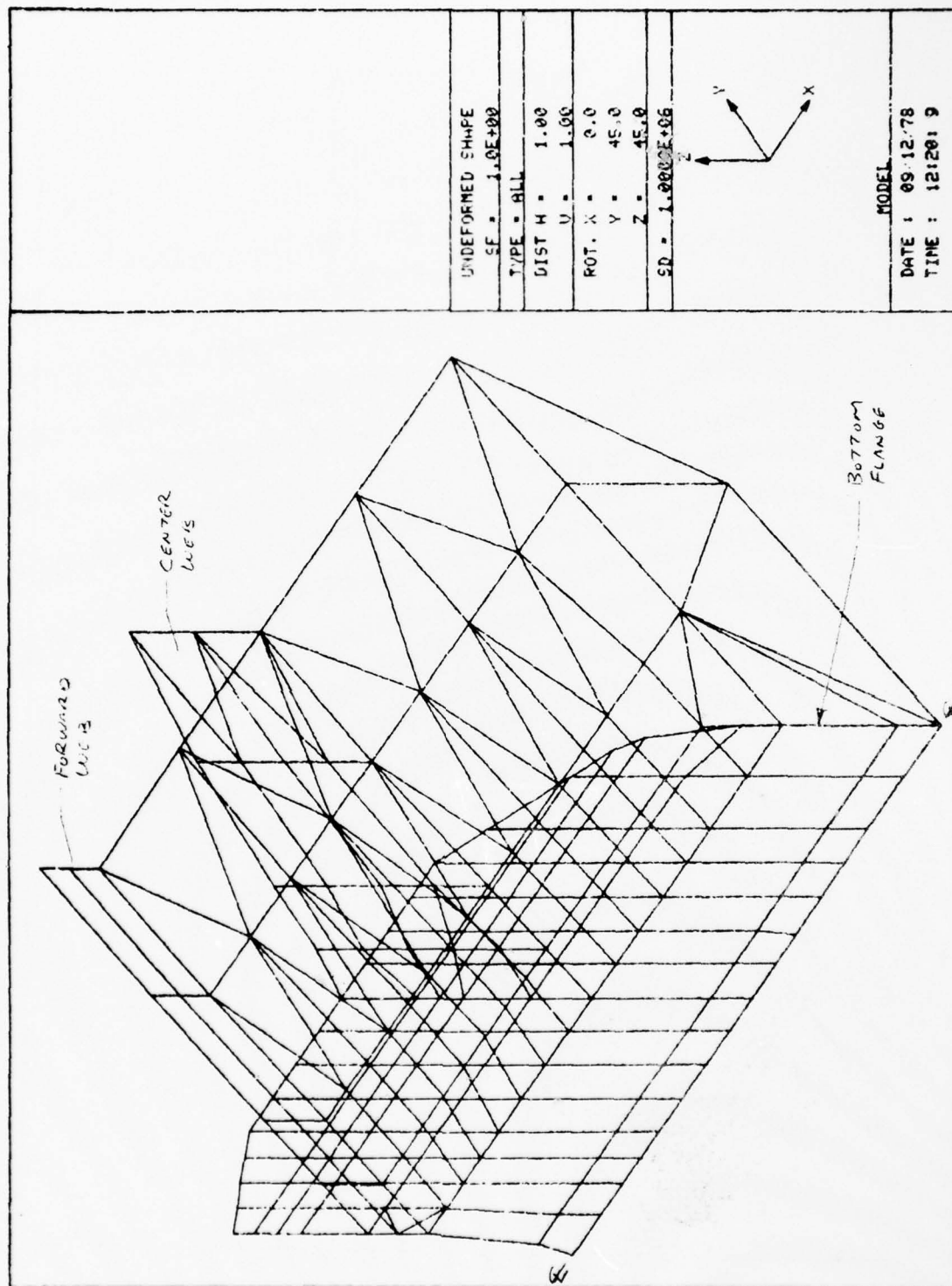
Figure 148. View A - NASTRAN node idealization of lower forward flange region.
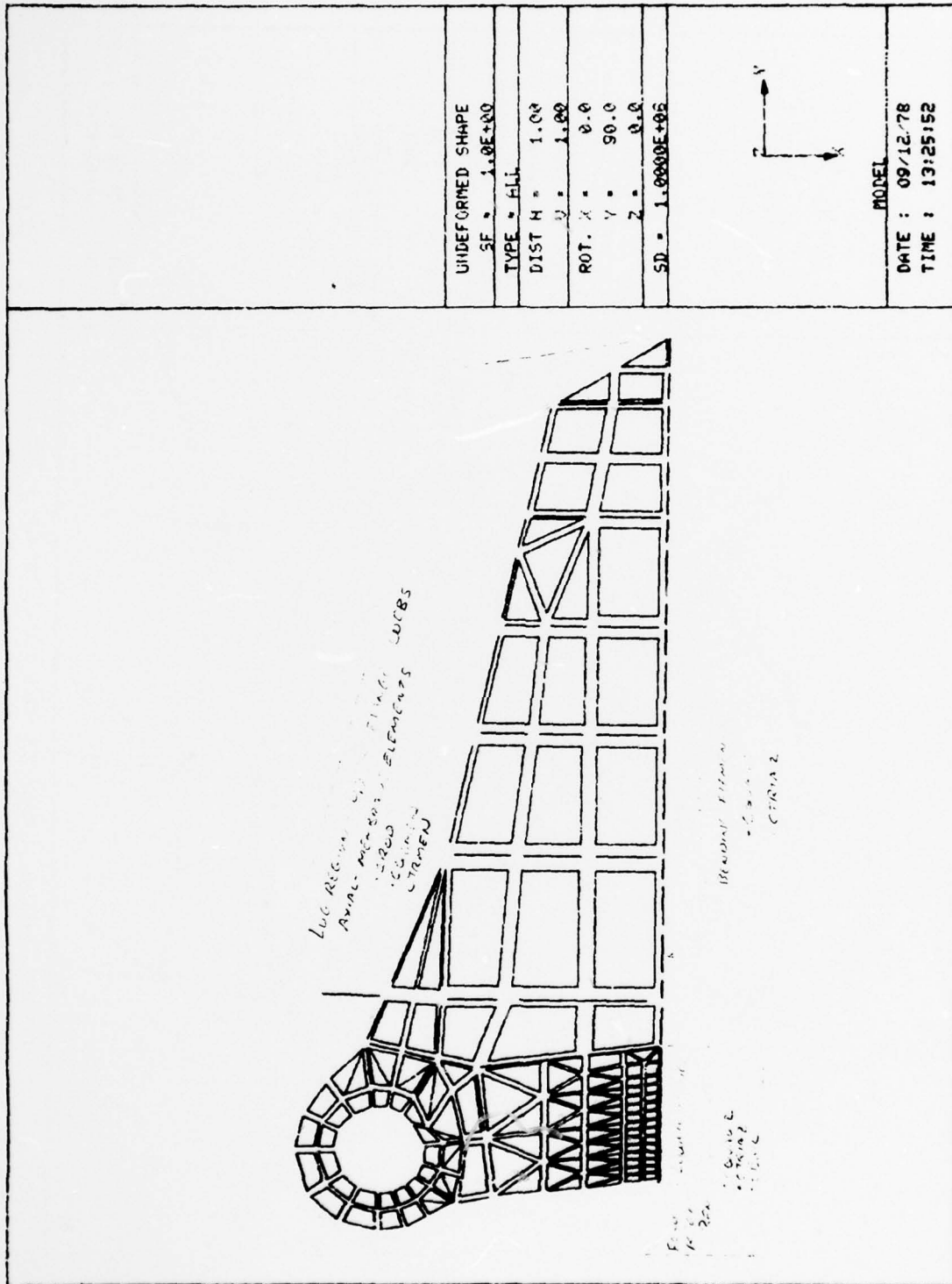
Figure 149. NASTRAN element idealization - wing sweep actuator support fitting.
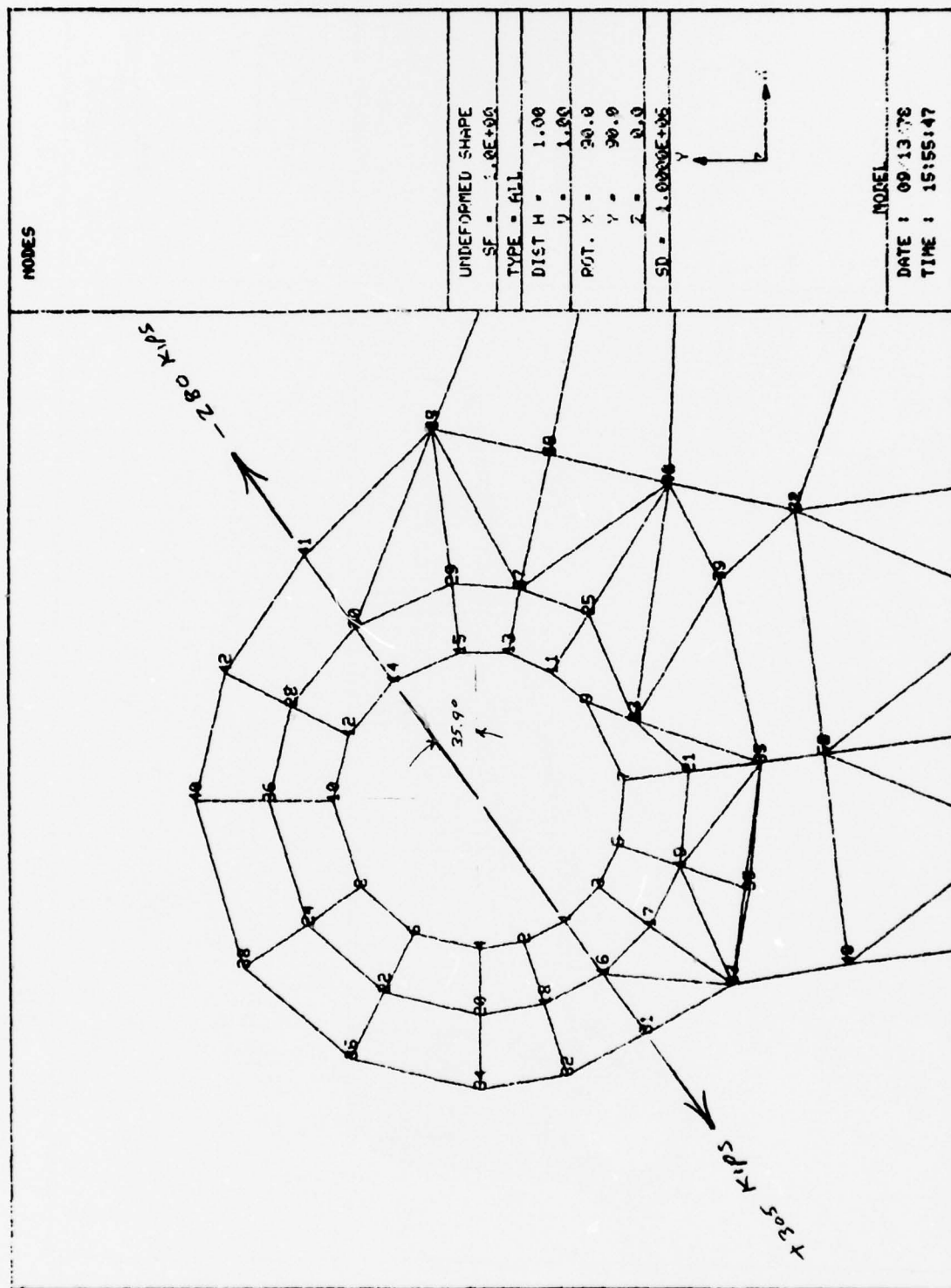
Figure 150. NASTRAN node idealization - lug region.
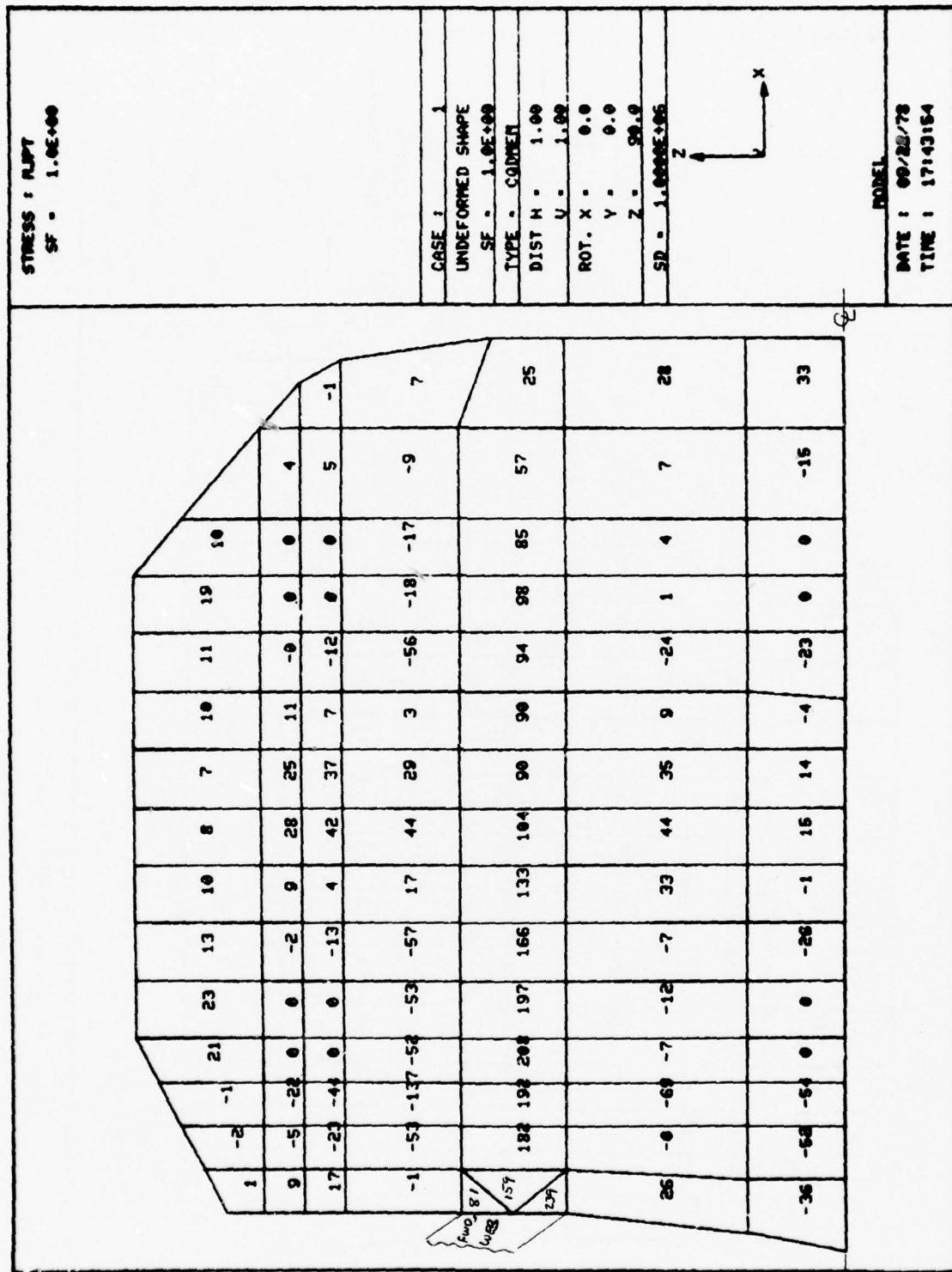
Figure 151. Lower flange major principal bending stress (10^3 psi) top plate surface $(P = 280^K)$.
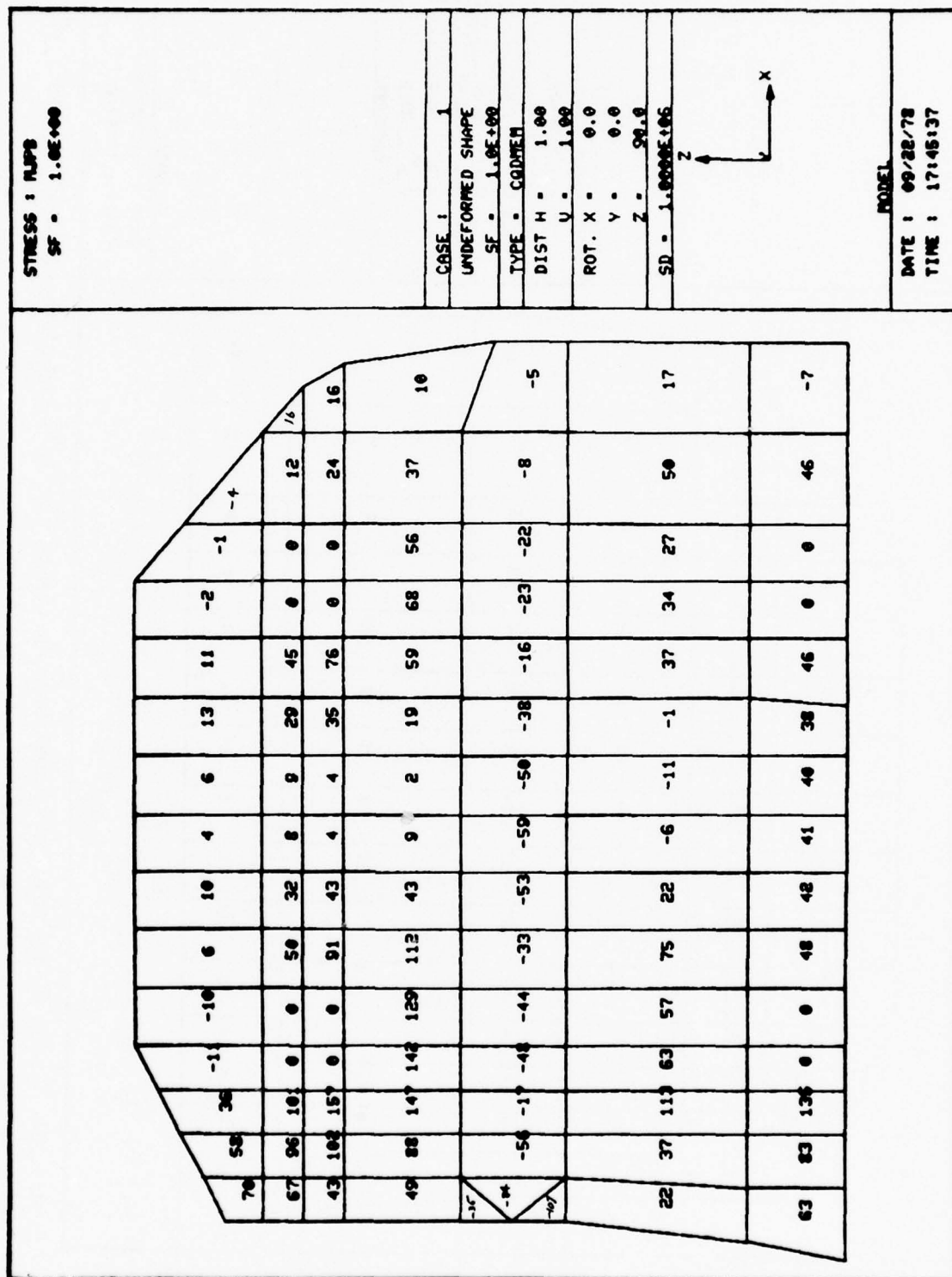
Figure 152. Lower flange major principal bending stress (10^3 psi) bottom plate surface (P = 280^K).

the same identical region as the fatigue crack which occurred during testing. The indicated maximum stress level is significantly above the fatigue-critical level for AF1410 steel.

A distorted displacement plot of the lower flange is shown in Figure 153. Maximum lower flange displacement (0.030 inch) occurs at the free-edge boundry where the forward vertical web intersects the lower attachment flange. This displacement appears to be in good agreement with the values (0.030 to 0.040 inch) visually estimated during the fatigue test.

The overall FEA results show that significant upward bending occurred during the maximum negative fatigue condition (-280 kips) on the lower flange - principally at the intersection of the forward flange. Because of local yielding, the chance of static failure is negligible, but the model results clearly show that this area is fatigue critical.

A cursory analysis of the forward area with the added (welded) flange area was conducted which showed a significant reduction in deflection and the absence of the high stress gradient which existed prior to the addition of the "gussets."

STATIC RESIDUAL STRENGTH TEST

The static residual strength test was comprised of three steps: (1) a limit load of -448,000 pounds, (2) a limit load of 615,000 pounds (see Figure 134 for loading direction), and (3) loading until failure occurs. The first step, the -448,000-pound load, was accomplished with the test component installed in the same fixture used to conduct the spectrum loading tests. The load was applied at a uniform rate until the level of -448,000 pounds was achieved (approximately 1-1/2 minutes to load). Then after a brief hold, data were taken from the strain gages, followed by a slow unloading. These data, presented in Appendix D, showed no evidence of nonlinearity with the gage readings taken periodically throughout the four-lifetime spectrum tests, and all operating gages returned to zero (within experimental error) after the load was released. It should be noted that gages 5, 7, 9, 13, 15, and 16 were not operational during this limit load test. No audible sounds were emitted by the test component/fixture during the loading and unloading. Post-inspection of the test component revealed no evidence of damage to the component resulting from the -448,000-pound limit load.

The test component, together with the triangular-shaped fixture to which it was bolted (Figure 133), was removed from the spectrum-loading apparatus and installed in a 2,000,000-pound capacity MTS universal testing machine for the remaining two portions of the static residual strength test. A photograph of the installation is shown in Figure 154.

297

CASE : 1

DEFORMED SHAPE

SF = 1.0E+06

TYPE = ALL

DIST H = 1.00
V = 1.00

ROT. X = 0.0
Y = 0.0
Z = 92.0

SD = 1.0000E+06

MODEL

DATE : 10/26/78
TIME : 14:56:57
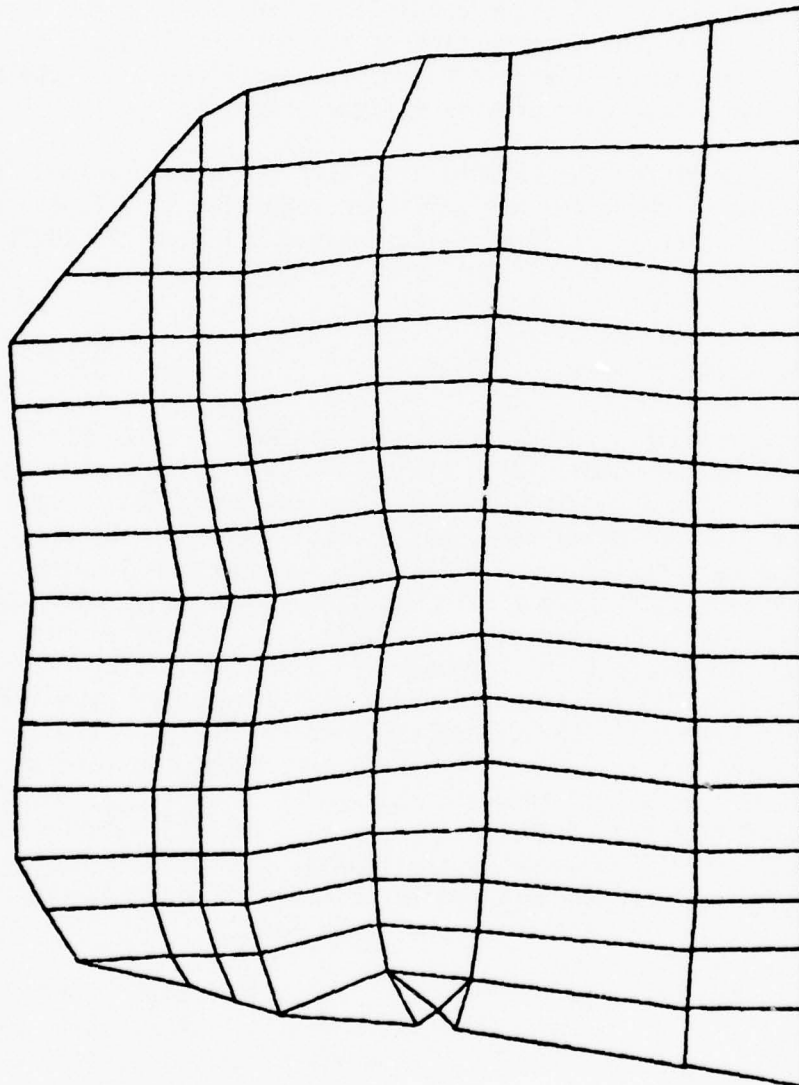
Note: Distortions of grid lines represent a quantitative
indication of lower surface strain distortion.

Figure 153.   Distorted displacement plot of lower flange.
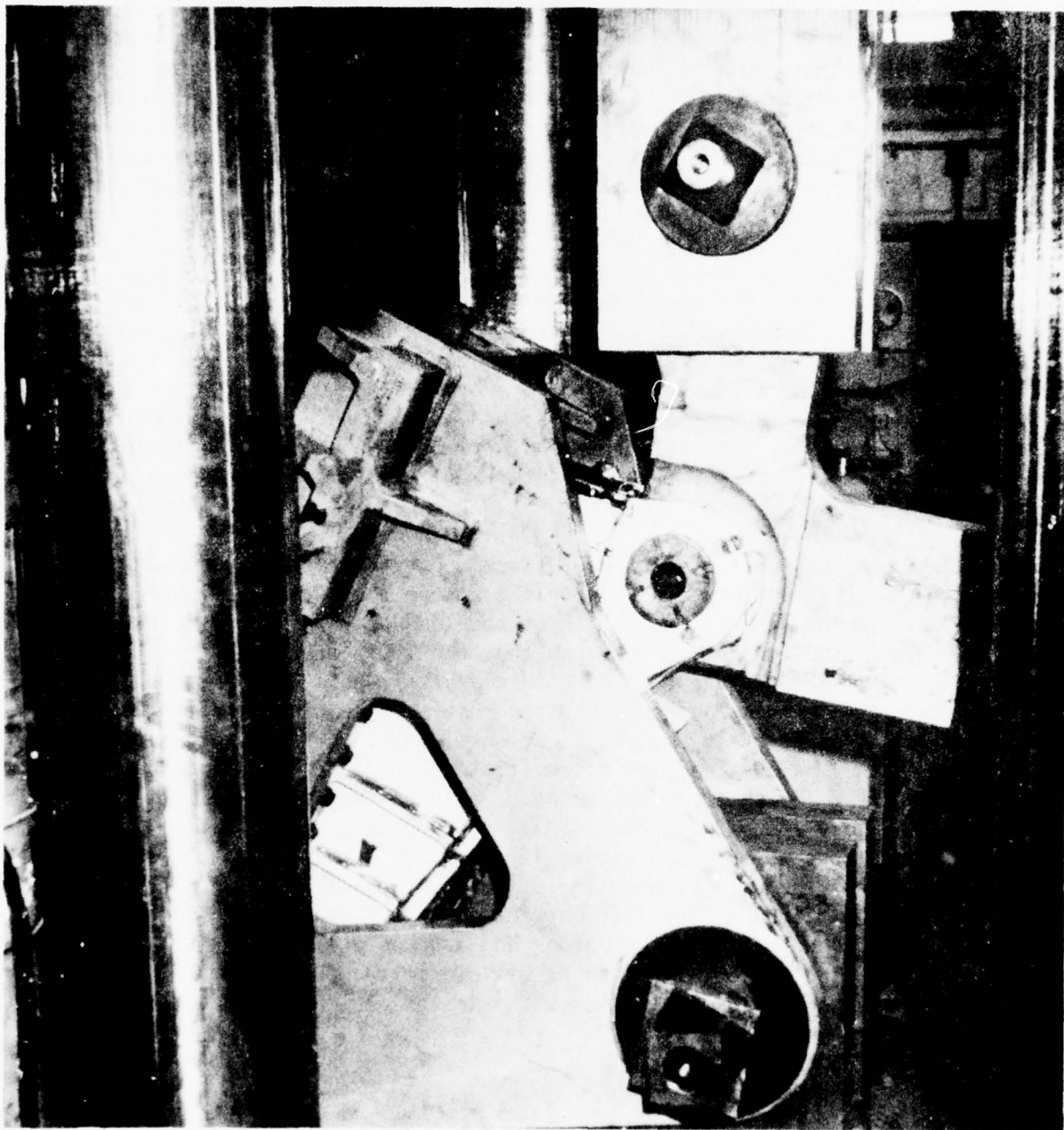
Figure 154. Test component installed in MTS testing machine.

The six gages which were not operational during the -448,000-pound limit load test were repaired; all 19 gages were functioning for the positive limit and ultimate load tests.

The limit load of 615,000 pounds was applied, and the strain gage outputs were obtained; then, the load was gradually released. The gages were again read to observe any zero-shifts which might have occurred due to yielding. All gages indicated strain predicted for the 615,000-pound limit load, and no significant zero shift was observed. The strain gage data are presented in Appendix D. At this point in the residual strength testing, the test component was visually inspected for evidence of damage; none was apparent.

The load was then reapplied, increasing gradually until the design ultimate load of 922,000 pounds was obtained. This load was reached without any audible emissions or other indications of impending failure (the test component was visually monitored during loading with a closed-circuit television camera). The load was held for a short period to permit recording of strain-gage outputs (approximately 30-second hold) and then increased until gross yielding became apparent at a load of 1,370,000 pounds. At this point, the load was lowered to zero and the output of the strain gages again was recorded.

Subsequent examination of the test component and fixture revealed the large hole in the test fixture which picks up the load from the lower clevis of the MTS machine (the lower portion of the load train as shown in Figure 154) had elongated five-sixteenths inch and that the limit of the test fixture had been reached. The strain-gage data obtained after the 1,370,000-pound load had been released (Appendix D) showed clearly that permanent deformation of the test component occurred in several locations. However, the deformation which occurred at the maximum load was not sufficient to result in a buckling or crippling failure of the test component. Posttest examination of the component revealed no gross amount of deformation. A photograph of the fitting showing its "intact" state is shown in Figure 155 (compare with the photo before testing (Figure 131)). A slight buckling of the vertical flange directly below the clevis (the flange at the left between the first and second boltholes) was apparent; both the left and right sides had assumed a slight S-shape. The degree of buckling is too slight to be visible in the photograph. The test component withstood a load 1-1/2 times the design ultimate load without failing.
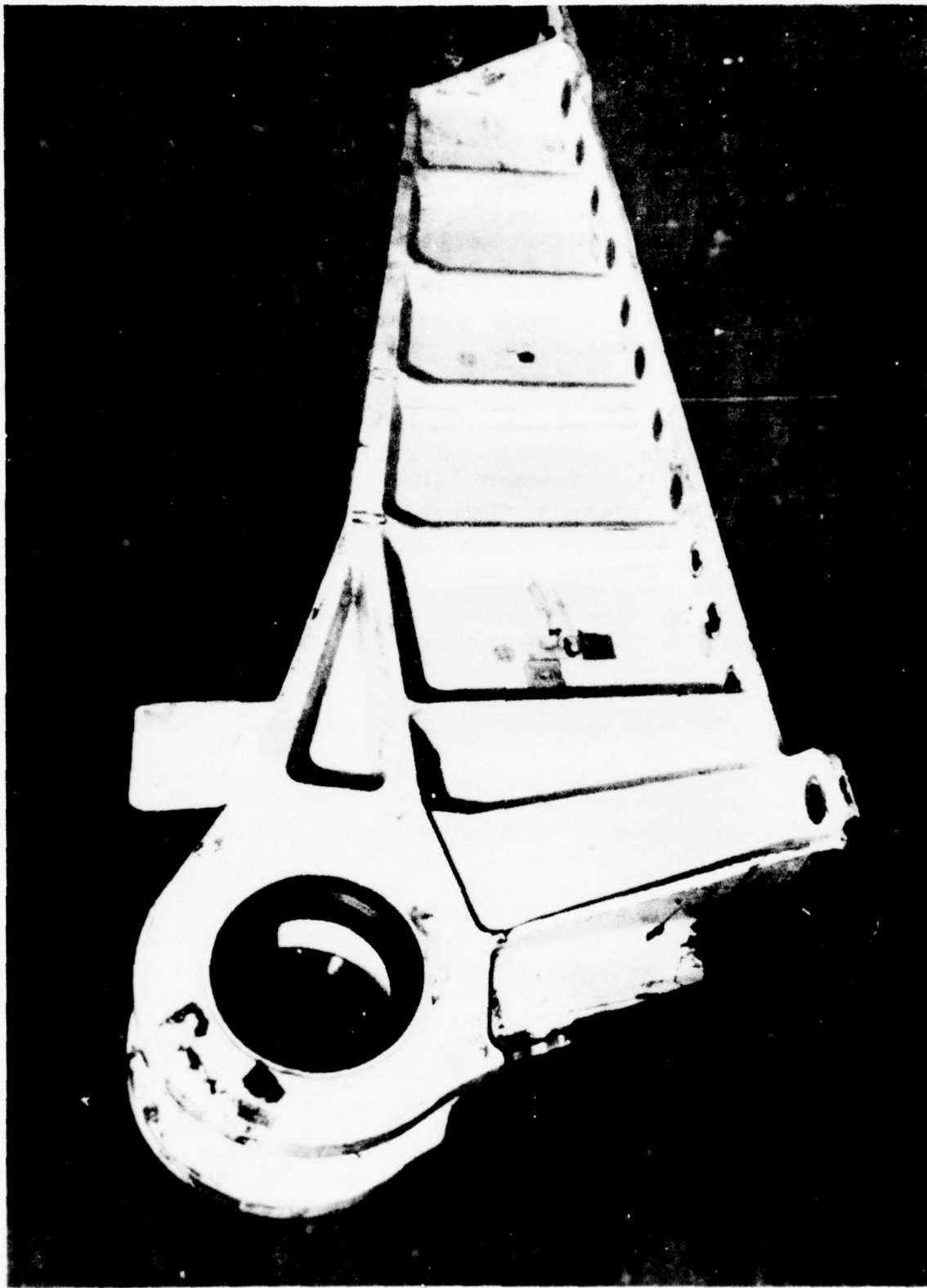
Figure 155. AF1410 test component after the residual strength tests.

Section VII

COST AND WEIGHT ANALYSIS

COST ANALYSIS

Baseline costs for the "as-designed" B-1 6A1-4V titanium wing sweep actuator attach fitting and its AF1410 modified nickel steel counterpart were generated for cost comparison using the data outlined in Table 67.

The titanium forging was procured at a weight of 568 pounds and machined to a finish weight of 175 pounds, with chip removal equal to 393 pounds and a buy-to-fly ratio of 3.2. The forged billet was procured at an estimated cost of $13.70 per pound.

The AF1410 steel forging was procured at a weight of 600 pounds and machined to a finish weight of 158 pounds, with chip removal equal to 442 pounds for a buy-to-fly ratio of 3.8. This forged billet was procured at an estimated cost of $8.88 per pound.

Based upon machinability data obtained from the Engineering laboratory and highlighted in Section IV of this report, the rough and finish machining rates for metal removal of the AF1410 steel have been estimated to be, respectively, 160 and 124 percent greater than the established titanium metal removal rates for these same operations. The estimate for the manufacturing man-hours of the AF1410 steel was based upon these data.

The cost estimate for one unit and the cost projections for a quantity of 300 units are shown in Figure 156 and Table 68. Cost data are reflected in 1977 dollars and are consistent with the data provided by the forged billet suppliers.

The material costs for the 6A1-4V titanium and the AF1410 modified nickel steel were based upon the average cost of two quotes (one for each material) received from two forging suppliers. Normal material procurement cost (NPC) and material mortality were applied to the supplier-furnished costs. For the production quantity (300 units), the costs were run down a Crawford cost-reduction curve (CRC) to reflect the anticipated material cost reduction in quantitative buying.

The labor costs for the two concepts were estimated as in-house fabrication. As indicated previously, the titanium concept was established as the baseline, while the AF1410 steel estimate was factored as a percentage of the titanium estimated machine run time based upon the relative machinability of the two metals and the required amount of metal removal. The decision to air-cool the AF1410 steel during the hardening heat treatment allows the fitting to be machined virtually in its entirety prior to heat treatment and while still in a highly machinable condition.

TABLE 67

DATA USED IN COST COMPARISON

	Titanium	AF1410
Buy weight	568 lb	600 lb
Fly weight	175 lb	158 lb
Forging cost		
Per unit	$7,784	$5,329
Per pound	$13.70	$8.88/lb
Buy/fly	3.2	3.8
Machining rate		
Roughing	48 cu in./hr	77 cu in./hr
Finishing	8.4 cu in./hr	10.4 cu in./hr
Chip weight	393 lb	442 lb

TABLE 68

SUMMARY - WING SWEEP ACTUATOR ATTACH FITTING 1977 DOLLARS

	6A1-4V titanium die forging		AF1410 modified nickel steel die forging	
	1st unit	300 cum avg	1st unit	300 cum avg
Mat1	$ 11,319	$ 9,210	$ 7,163	$ 5,828
Fab	23,319	4,576	17,935	3,560
Tlg	169,195	814	162,059	790
	$203,833	$14,600	$187,157	$10,178
		% of savings	8.18	30.28

303
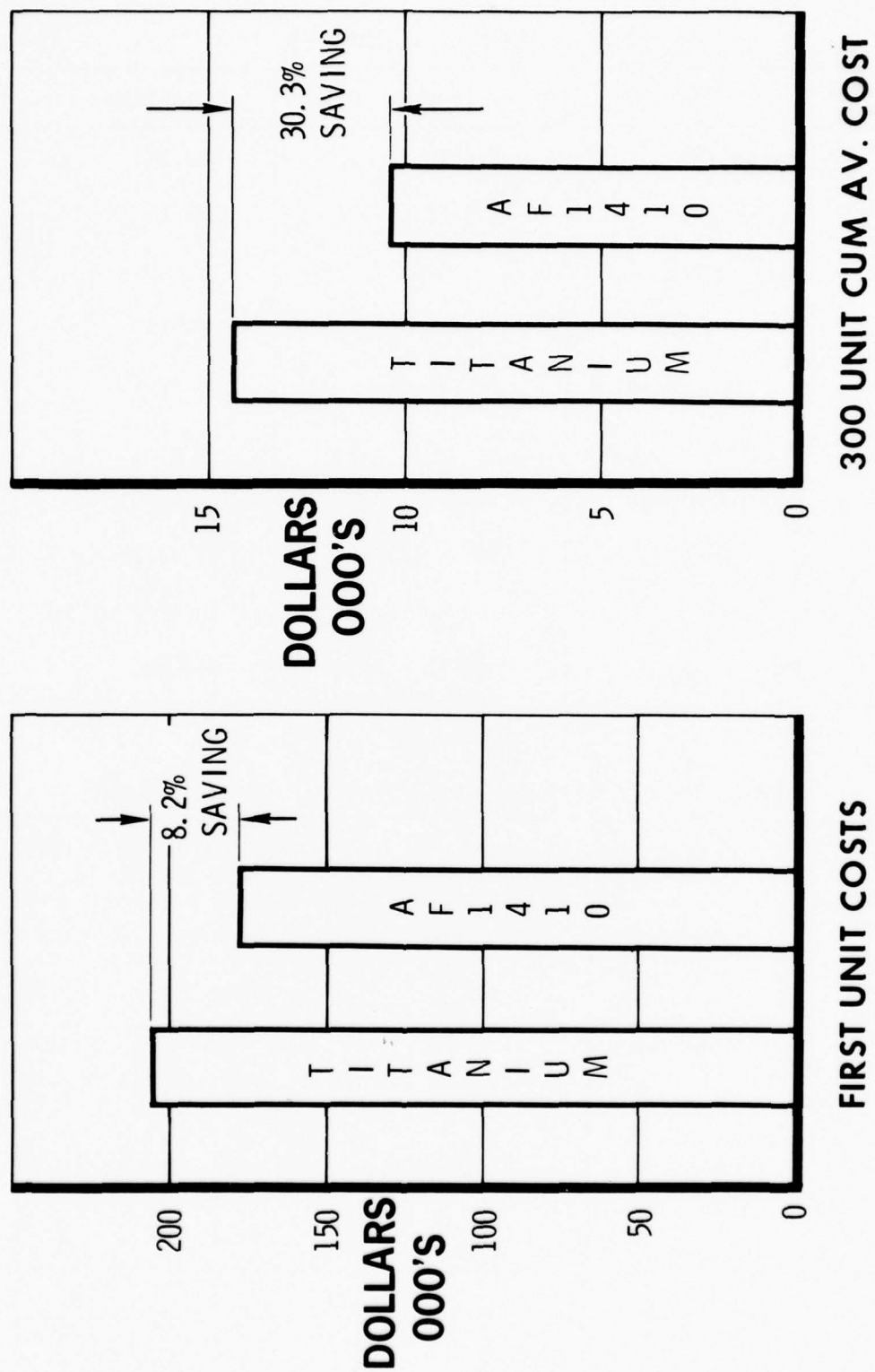
Figure 156. Wing sweep actuator cost comparison.

The tooling cost is broken into two categories: (1) the in-house tooling required to assist in the machining of the forged billet to the required finished drawing dimensions, and (2) the tooling required by the forging suppliers to stamp out a forged billet. The in-house tooling was estimated internally, while the forging tooling was based upon the average of two quotes (one each for the titanium and AF1410 steel) received from the forged billet suppliers.

The cost comparison of the 6Al-4V titanium and the AF1410 modified nickel steel reflects a cost savings of 8.2 and 30.3 percent, respectively, for the first and the 300th average unit, favoring the AF1410 steel over the titanium. The variance in percentage of the stated quantities is answered in the following paragraph.

The percentages of savings for the three cost categories (material, fabrication, and tooling), although essentially the same for the first and the 300th units (i.e., fabrication (37 percent), material 22-23 percent), and tooling 3-4 percent)), do not have the same weighted value effect at these different quantities. For example, the tooling cost at the first unit for both concepts is approximately 85 percent of the total cost, while at a quantity of 300 units, the tooling is approximately 7 percent of the total cost. When weighted against the material cost and the fabrication cost at the first unit, the 85-percent tooling cost carries a substantial influence in reducing the projected savings. When weighted against the production quantity of 300 units, the tooling cost at 7 percent of the total cost becomes relatively insignificant when compared to the material and fabrication cost, thus resulting in an increased projected percentage of savings. The reduction in tooling cost at the larger quantity is due to amortization of the tooling cost over the entire production buy.

The cost comparison of the two concepts projects a savings of $4,422 per fitting at a quantity of 600 fittings (two per aircraft), favoring the AF1410 modified nickel steel concept over the 6Al-4V titanium concept during the acquisition phase.

LIFE CYCLE COSTS

The delta cost savings for the AF1410 steel during the acquisition phase is:

300 aircraft x 2 fittings per A/C x $4,422 = $2,653,200

In addition to the previously outlined projected cost savings, there is also a substantial weight savings (Figure 157) afforded the AF1410 steel fitting when compared to the 6Al-4V titanium fitting. Based upon two fittings

305
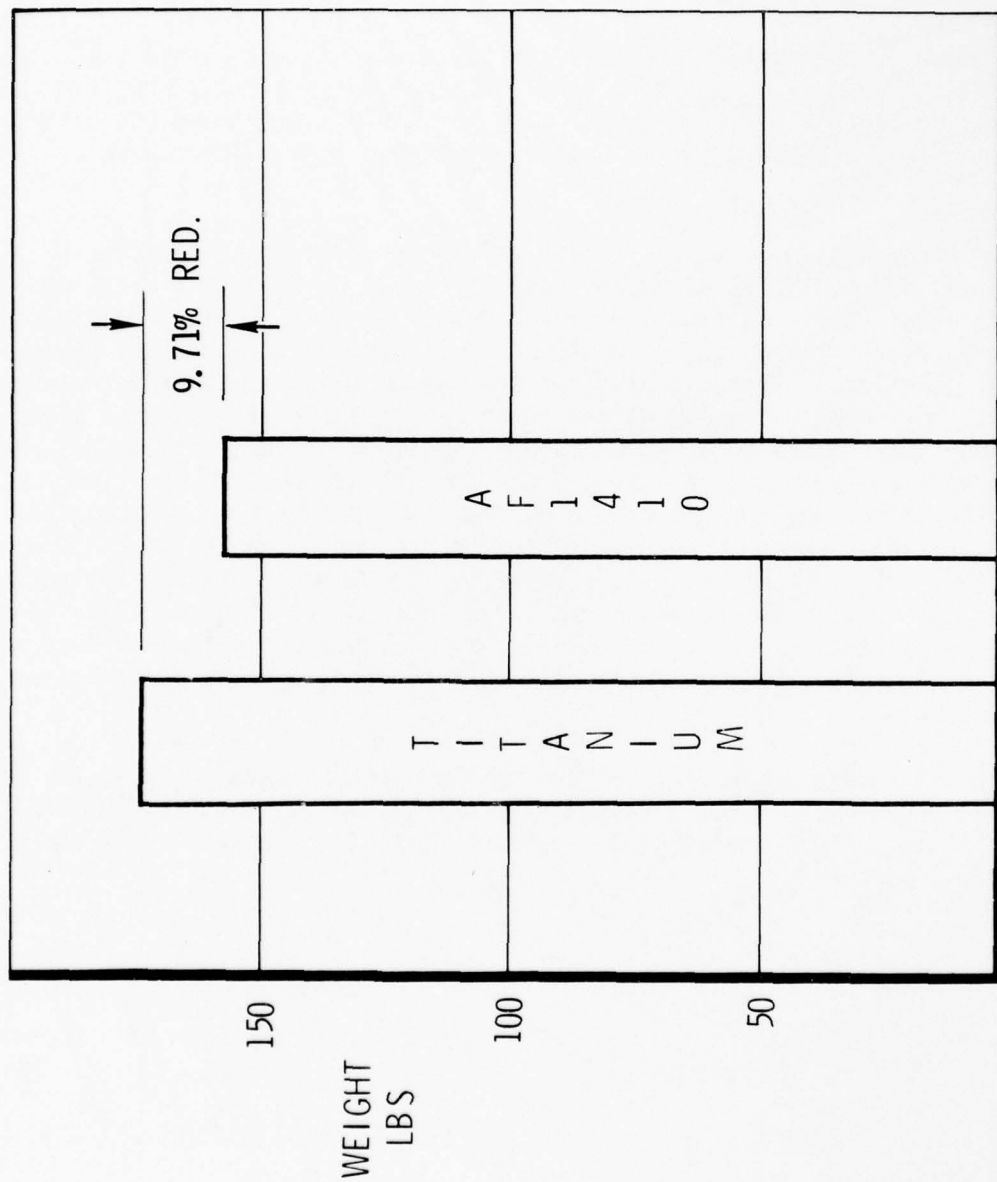
Figure 157. Wing sweep actuator weight comparison.

306

per aircraft, total weight savings is 34 pounds per aircraft. The cost impact of weight savings to the B-1 aircraft can be divided into the following categories.

B-1 AIRCRAFT

Lower weight of the B-1 with constant target coverage can reduce the number of B-1's needed to meet mission requirements, since some fuel weight can be converted to weapons.

FUEL SAVINGS

Lower weight per aircraft means less specific fuel consumption for any given peacetime flying mission.

TANKER FUEL/MAINTENANCE

Lower weight coupled with constant takeoff gross weight of the B-1 and excess fuel capacity means that fewer tankers can meet alert status requirements for wartime missions.

The net dollar savings of the preceding categories is approximately $260 per pound per aircraft in constant 1977 dollars. This is based upon the preceding cost-effectiveness categories for 10 years of peacetime flying.

The cost calculation is as follows:

Savings = 34 (lb) at $260/lb x 300 aircraft = $2,652,000 (1977 dollars)

Total savings (excluding consideration for design, test, and development costs):

$2,652,000 (weight savings) (O&S)
 2,653,200 (acquisition)
$5,305,200 (cost savings in 1977 dollars)

Section VIII

SUMMARY AND CONCLUSIONS

The mechanical properties of the three production heats of AF1410 were found to be uniform from heat to heat. Plate final thickness exhibited no effect on properties, and no anisotropy was observed in any of the material tested on the program. The products of the three production heats all met the target minimum properties, and on an equal density basis exhibited properties equal or superior to annealed Ti-6Al-4V.

For section thicknesses less than 1 inch, air cooling from austenitizing temperature was shown to be equivalent to warpage-inducing water quenching in developing mechanical properties. Air cooling can be used up to 2 inches with only a slight (7 percent) reduction in static properties. The use of air cooling, with the attendant absence of warpage, permits the maximum use of the excellent machinability of AF1410 in the normalized and over-aged condition. It was demonstrated that components of complex geometry can be finish machined prior to heat treatment without suffering heat-treatment warpage.

Machining parameters were developed which markedly increased the machinability of AF1410. Use of these parameters in the fabrication of the test component from a 600-pound, closed die forging has demonstrated the excellent fabricability of the steel. Based on the machining experience attained in the fabrication of the test component, together with forging cost data from two forging suppliers, it was estimated that a cost saving of 30.3 percent could be realized for the B-1 inboard wing sweep actuator attach fitting by the substitution of AF1410 steel for annealed Ti-6Al-4V.

Forgeability of the steel was judged to be good, and a closed die forging with a buy/fly of 3.8/1 was produced without difficulty. Mechanical properties of the die forging in eight preselected areas all met the minimum design allowables used in design of the test component.

During the first lifetime of fatigue testing, a fatigue crack developed in one area of the fitting. The cracking resulted from excessive deflections, and was corrected by welding stiffening webs onto the test component. The weld repairs were made without any subsequent heat treatment, and the success of the weld repairs demonstrates the field repairability of this steel. A finite-element analysis conducted subsequent to the fatigue test of the component verified that higher than anticipated stresses existed in the area of fatigue cracking, and that the welded-in webs lowered these stresses substantially.

Two lifetimes of spectrum loading were conducted to assess the damage tolerance of the fitting. EDM notches were machined in four locations, and it was anticipated cracks would develop at these notches and permit observation of crack-growth rates. Even though the notches were as sharp as possible to produce by the EDM process, no cracks developed.

Subsequent to the four-lifetimes of spectrum-load fatigue testing, the test component was subjected to a static test designed to determine the residual strength. The fitting withstood 1.5 times the ultimate design stress without failure, the test being terminated because of limitations of the test fixture. No cracking occurred in any areas of the test component, which attests to the excellent toughness/strength properties of the steel.

Based on the results of the tests and analyses conducted during the course of this program, it is concluded that AF1410 is a lower-cost, higher-strength, higher-toughness, lighter-weight substitute for annealed Ti-6Al-4V airframe structural components.

Section IX

REFERENCES

1. Little, D. C., and Machmeier, P. M., "Development of a Weladable High Strength Steel," AFML-TR-75-148, Septmeber 1975

2. Routh, W. E., et al, "Lower Cost by Substituting Steel for Titanium," Interim Technical Report AFFDL-TR-77-73, June 1977

3. "B-1 Structures Manual," NA-72-1, Rockwell International, September 1973

4. "Structures Manual," NA-52-400, Rockwell International, March 1952, revised April 1962

5. Machining Data Handbook, Second Edition, Metcut Research Associates, Incorporated, Cincinnati, Ohio

6. Snide, J. A., "Some Aspects of the Physical Metallurgy and Weldability of 10 Nickel Modified Steel," Ph. D. Dissertation, Ohio State University, 1975

7. Erard, A. R., "Technique of Measuring Low Percentages of Retained Austenite Using Filtered X-Ray Radiation and an X-Ray Diffractometer," Advances in X-Ray Analyses, 1973, Vol. 7, pp 256-264

8. Shiring, R. R., Milavec, J. L., and Black, H. L., "Production Melting and Theromechanical Processing of AF1410 Steel," Technical Report IR-160-6 (VII), 15 October 1977

APPENDIX A

INBOARD SHEAR FITTING AF 1410 VERSION

PRELIMINARY STRESS ANALYSIS

DISCUSSION

THE INBD SHEAR FITTING WAS ANALYZED USING THE MATERIAL PROPERTIES TABLE $\overline{IV}$ AND STRUCTURAL ANALYSIS CURVES PROVIDED IN THE "STRUCTURAL ANALYSIS PROPERTIES" SECTION, (FIGS. 17 THRU 25)

THE APPLIED DESIGN LOADS ARE THE SAME AS those USED FOR THE TITANIUM BASELINE COMPONENT.

CONVENTIONAL STRESS ANALYSIS PROCEDURES PER REFERENCES (1) & (2) WERE USED.
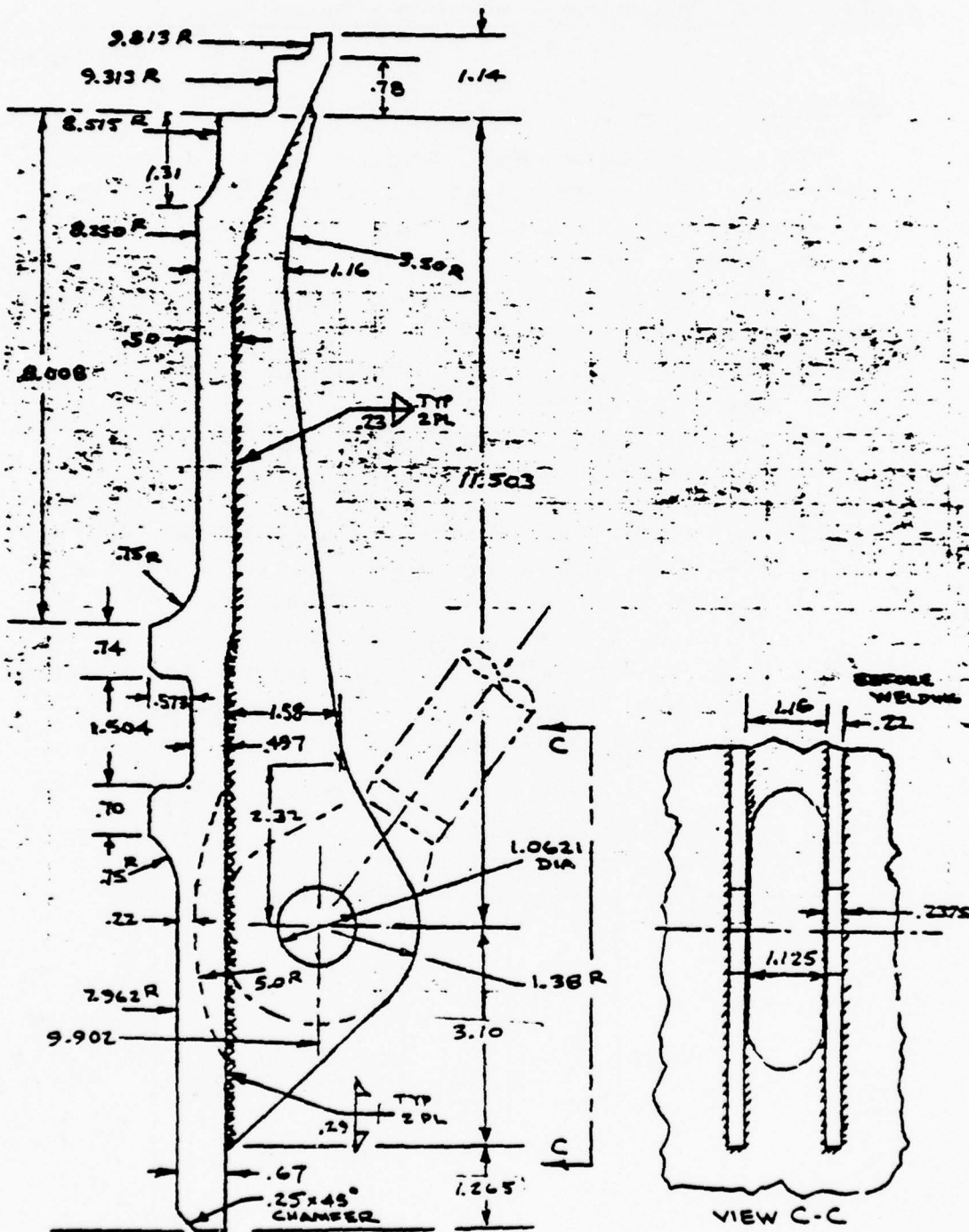
FIGURE   INBOARD SHEAR FITTING - GEOMETRY

PREPARED BY: TM	INBD SHEAR FITTING -	
DATE: Nov 10, 1975	PIVOT PIN - AF 1410 VERSION	MODEL NO.

DWG # 2109-100000

LOADS

THE LOADS USED FOR PRELIM. SIZING OF THE
FITTING ARE THE SAME AS USED BY THE B-1
STRESS GROUP TO SIZE THE TITANIUM BASELINE
COMPONENT.

THREE PRIMARY CONDITIONS GOVERN THE LOADS
ON THE SHEAR FITTING:

① STRUT ATTACH. LOAD - TRANSFER SHEAR TO
INBD RIB AT STA. 119.

② THRUST LOAD ON FITTING DUE TO $\overset{OUTER\ WING\ PIVOT}{\wedge\ LUG-HALF}$
FAILURE (UPPER OR LOWER OUTBD)

③ LUG LOAD COMPONENTS TRANSFERRED BY PIN
VIA THE "NOTCH AND LAND" DESIGN OF THE
SHEAR FITTING - PIN SYSTEM.

THE LUG-HALF FAILURE CONDITION IS CONSIDERED
AN ULTIMATE LOAD CASE ON THE SHEAR
FITTING WHEN USING THE LIMIT LOAD VALUE.

(ULTIMATE DESIGN LOADS)

COND	P_T	$P_L = P_3$	P_{U_1}	P_{U_2}	DESCRIP
	(KIPS)	(KIPS)	(KIPS)	(KIPS)	
① A	27.85				1 g - TERR. FOLLOW
① B	-107.94			4.77	L.LEV. PENET.
② A		318.05			FAIL. PIVOT LUG HALF
② B			64.1	3.18	" " "
③				36.08	2 g - FLAP DN.
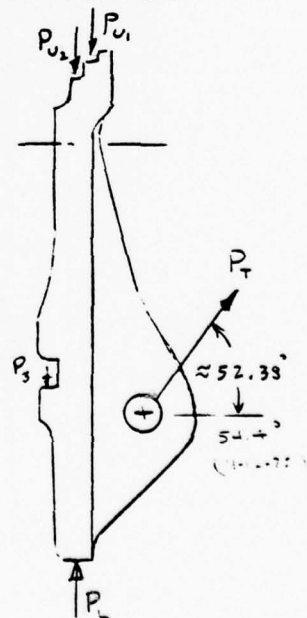
P_{U_2} | P_{U_1}
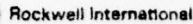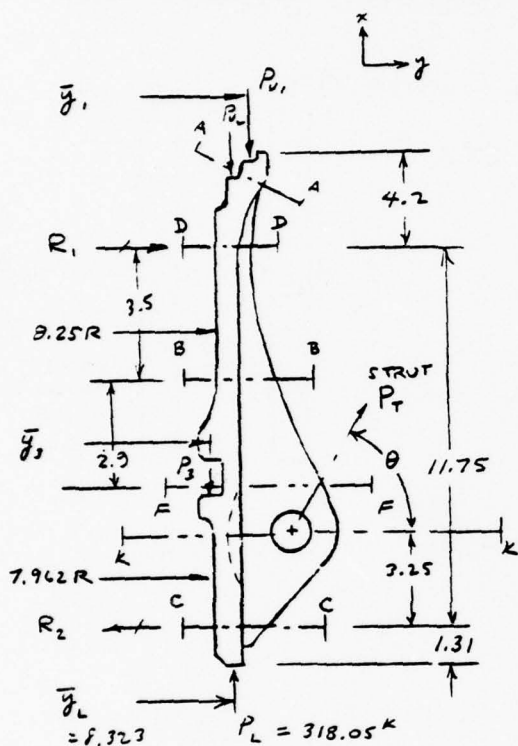
P_T

P_3

$\approx 52.33°$

54 ± °

P_L

PAGE NO A 4

314

LOADS DEVEL. | ULTIMATE |

$P_{U_1} = 64.1^K$, COND ② B

$\bar{y}_1 = 9.471$ $(R_1 = 9.5)$

$P_{U_2} = 3.2^K$ $(R_{U_2} = 8.849)$

$M_{AA} = P_{U_1} \cdot e = 64.1 \times .02$

$= 1.282$ K-IN

COND ② B

$R_1 = 18.08^K = -R_2$

$M_{DD} = P_{U_1} \times e_1 + P_{U_2} e_2$

$= 64.1 \times .893 + 3.2 \times .247$ COND ② B

$= 58.35$ IN-KIP

$M_{BB} = R_1 \times 3.5 = 18.03 \times 3.5 = 63.28$ IN-KIP

COND ① A

$P_T = +27.85^K$, COND ① A

$= -107.94^K$, COND ① B

$\theta = 54.4°$

$P_3 = 318.05^K$ COND ① A

$\bar{y}_3 = 7.655$ $(R_3 = 7.8385)$

$M_{FF} = R_1 \times (3.5 + 2.9)$

$= 18.03 \times 6.4 = 115.712$ IN-KIP

COND ② A

$M_{FF} = 27.85 \times \cos 54.4°^2 \times 11.75 \times .25$

$= 47.61$ IN-KIP COND ① A

$M_{KK} = R_2 \times 3.25 + P_L \times e$

$= 18.03 \times 3.25 = 58.76$ K-IN $+ P_L \times e$ COND ② A

MATERIAL

    AF1410 STEEL

(LUG ANALYSIS) COND ①

$P_c = -107.94^k$ ① B

$P_T = 27.85^k$ ① A

52.38

1.38R

1.062 DIA

t_1 $t_1 = (.375)$ TITANIUM

= .21" STEEL

1.12"   .03 × 45° CHAMFER
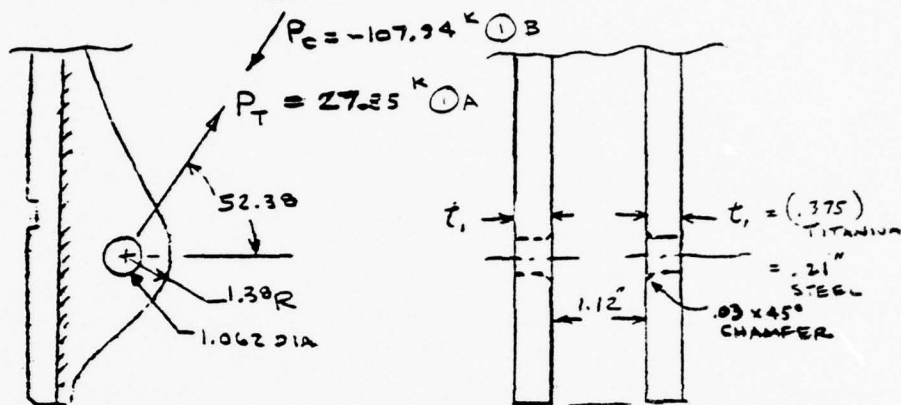
ASSUME 60-40% LOAD DISTRIB. TO EACH LUG

$$e/_D = \frac{1.38}{1.062} = 1.30$$

$$W/_D = \frac{2 \times 1.38}{1.062} = 2.6$$

$$D/_t = 1.062/_{.21} = 5.06 \qquad (\text{LET } t = .21")$$

$$A_{br} = 1.062 \times (.21 - .03) = .191 \ \text{IN}^2/\text{LUG}$$

$$A_t = (2 \times 1.38 - 1.062)(.21) = .356 \ \text{IN}^2/\text{LUG}$$

<u>SHEAR BEARING</u> - COND ① A

$$K_{br} = 1.2 \qquad (NASZ - 900 \qquad PG \ 6.90.30.1)$$

$$P_{bru} = A_{br} \ K_{br} \ F_{tu} = .191 \times 1.2 \times 230.000 = 52.7 \ K$$

APPLIED LOAD $\quad P_1 = .60 \times P_T = .60 \times 27.85 = 16.7 \ K$

$$M.S. = \frac{P_{bru}}{P_1} - 1 = \frac{52.7}{16.7} - 1 = \boxed{(SHR \cdot BRG)} \quad +2.16$$

TENSILE - LUG $W/D = 2.6$ - COND ① A

$\quad k_t = 0.9$ ($NAS2-400$ A_S $6-40-30-S$) curve ③

$P_{tu} = k_t F_{tu} A_t$ $\quad = 0.9 \times 230 \times .356 = 73.7$ k

M.S. $= \dfrac{P_{tu}}{P_1} - 1 = \dfrac{73.7}{16.7} - 1 = $ $(LUG + TEN) = + 3.41$

SHEAR - OUT   - COND ① A

$\quad A_S \approx 2 \times .9 \times .21 = .378^{in^2}$ ($40°$ SHR·OUT AREA)

$\quad f_s = \dfrac{P_1}{A_s} = \dfrac{16.7}{.378} = 44.2$ ksi

M.S. $= \dfrac{F^{su}}{f_s} - 1 = \dfrac{147}{44.2} - 1 = $ $(SHEAR·OUT) = + 2.32$

MAXIMUM BEARING - COND ① B

$P_c = -107.94$ k $P_1 = .6 \times P_c = 64.8$ k

$f_{br} = \dfrac{P_1}{A_{br}} = \dfrac{64.8}{.191} = 339.$ ksi

$F^{bru} = 446.$ ksi   (with an e/D ratio > 2.0) $\overset{FOR\ LOAD}{P_c}\ _{DIRECTION}$

MS $= \dfrac{F^{bru}}{F_{br}} - 1 = \dfrac{446}{339} - 1 = $ $(BEARING) = +0.31$

CROSS-SECTION CHECKS
(SECTION A-A)

9.813R

$P_{u_1} = 64.1^k$

9.5R

9.313R

36

$P_{u_2} = 3.2^k$

.78

8.843R

A

8.515R

A

8.23R

3.06

D   D

.50
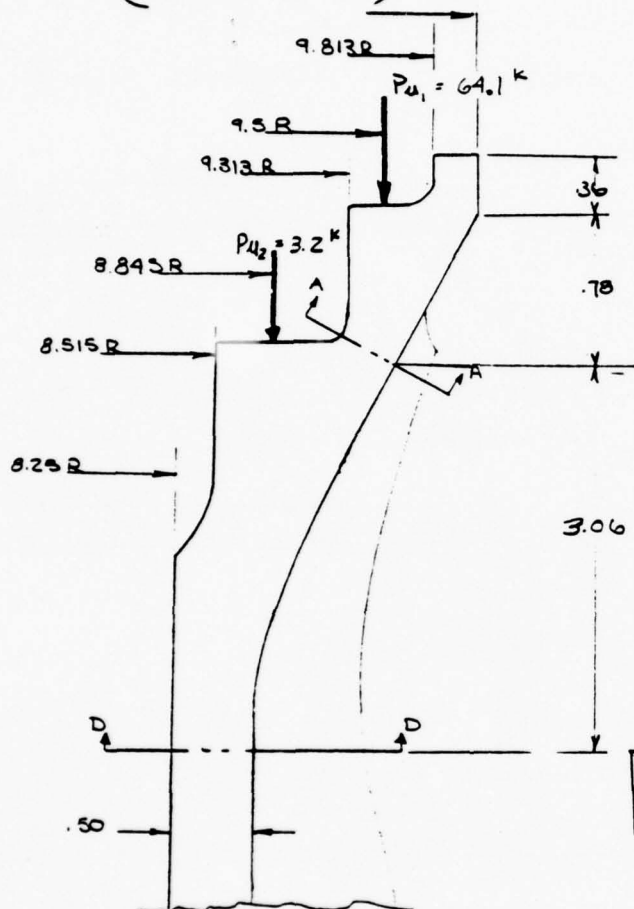
LOAD COND ②B

To Check   Sec A-A
$t \approx .40^{in}$
let $b = 2^{in}$

$M = P_{u_1} e$
$= 64.1 \times (9.5 - 9.52)$
$= 1.282^{k-in}$ (COND ② B)

$f_c = \dfrac{M}{cI} + \dfrac{P_{u_1}}{bt}$ and $I = \dfrac{bt^3}{12}$
$c = t/2$

$= \dfrac{6 \times 1.282}{2 \times .40^2} + \dfrac{64.1}{.40 \times 2}$

$= 104^{KSI}$

(compression)

THE MARGIN of SAFTEY IS

$M.S. = \dfrac{F^{cy}}{f_c} - 1 = \dfrac{226}{104} - 1 = + 1.173$

(SECTION D-D)

$\bar{y} = \dfrac{\Sigma Ay}{\Sigma A}$

*ASSUME RECTANGULAR SECTIONS

1.14

.70

RA

.22

≈.50

effect. b = 3"

DIM	A	Y	AY	AV²	$I_o = \frac{bh^3}{12}$
.22 × .70	.164	.85	.0639	.01286	.00629
.22 × .70	.164	.25	.0639	.01286	.00629
5 × .50	1.500	.25	.375	.09375	.03125
Σ	1.208	$\bar{y} = 1.418$	.2672	.13147	.04383

$I_x = I_o + \Sigma A y^2 - \bar{y} \Sigma A y = .13581$ $\dfrac{I}{c} = .16015$

PAGE NO A-8   REV.

(SECTION D-D) (CONT.)

$R_3 = 8.25 + .50 - .1478 = 8.602$

$M = P_{U_1}(9.5 - 8.602) + P_{V_2}(8.849 - 8.602)$

$= 64.1 \times (.898) + 3.2(.247) = 58.35$ IN-K)

$f_b = \dfrac{Mc}{I} = \dfrac{58.35 \times .848}{.13581} = 364.3$ KSI $\leftarrow$ TOO HIGH

$f_c = \dfrac{P}{A} = \dfrac{67.3}{1.808} = 37.2$ KSI

ASSUME EFFECTIVE $b = 5.4"$ $t = .50$, NEGLECT LUGS

$M = P_{U_1}(9.5 - 8.5) + P_{U_2}(8.849 - 8.5)$

$= 64.1(1.0) + 3.2(.349) = 65.12$ IN-KIP

$f_b = \dfrac{6M}{bt^2} = \dfrac{6 \times 65.12}{5.4 \times .5^2} = 289$ KSI

$f_c = \dfrac{P_{U_1} + P_{U_2}}{A} = \dfrac{67.3}{5.4 \times .5} = 24.9$ KSI

$R_c = \dfrac{f_c}{F_{cy}} = \dfrac{24.9}{226} = .1101$ Q.H

$R_b = \dfrac{f_b}{F_{cy}(1.5)} = .853$

$M.S = \dfrac{2}{R_b + \sqrt{R_b^2 + 4R_c^2}} - 1 = $ | (AXIAL + BENDING) = +0.15 |

CONSIDER LUGS AS PART OF SECTION D-D

$\Sigma A = 2 \times .154 + 5.4 \times .50 = 3.008$

$\Sigma Ay = 2 \times .0539 + 5.4 \times .50 \times (.25) = -.5072$, $\bar{y} = -.1385$

$-\bar{y}\Sigma Ay = -.10692$

$\Sigma Ay^2 = 2 \times .01834 + 5.4 \times .50 \times .25^2 = .20647$

$\Sigma I = 2 \times .00629 + 5.4 \times .5^3/12 = .06883$

$I = .20647 + .06883 - .10692 = .16838$

$c = .70 + .1885 = .8885$, $I/c = .18951$

Rockwell International

PREPARED BY: TM

DATE: 11-24-75

REV. 7/30/76 R.H.

MODEL NO.

EWG #6109-100000

(SEC D-D) (CONT.)

$$M = P_M (9.5 - 8.561) + P_{VL} (8.845 - 8.561)$$
$$= 64.1 (.939) + 3.2 (.284) = 61.11 \text{ in-k} \qquad \text{COND ② B}$$

$$f_b = \frac{Mc}{I} = \frac{61.11 \times .8885}{.16838} = 322 \text{ ksi}$$

$$f_c = \frac{P}{A} = \frac{67.3}{3.008} = 22.4 \text{ ksi}$$

$$R_c = \frac{f_c}{F_{cy}} = \frac{224}{226} = .099 \qquad \qquad R.H.$$

$$R_b = \frac{f_b}{1.5 F_{cy}} = \frac{322}{339} = .949$$

$$M.S. = \frac{2}{R_b + \sqrt{R_b^2 + 4R_c^2}} - 1 = \overline{(\text{AXIAL} + \text{BENDING})} = + 0.04$$

WE NOW CHECK SECTION D-D, TREATING
IT AS A CURVED SECTION

(SEC D-D)

RECHECK FOR $\bar{y}$ CURVED SECTION

$(R_{u_1} = 9.5) \leftarrow 2\alpha = \dfrac{2.88}{9.5}$ $w = 2.88''$

$\alpha = 8.69°$

$\bar{y}_1 = \dfrac{R \sin \alpha}{\alpha} = \dfrac{9.5 \times \sin 8.69°}{\alpha} = 9.471''$

$\bar{y}_0 = \dfrac{R \sin \alpha}{\alpha}$ (SEE BELOW)

$R_0 = 8.75$, $R_i = 8.25$, $R = 8.50$
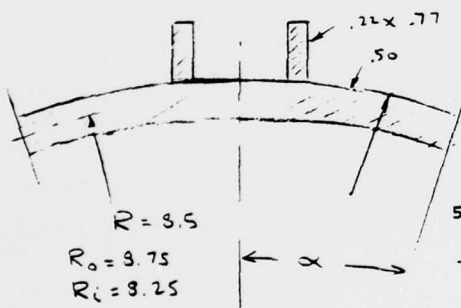
	A	y	Ay	Ay^2	I_0
2×.22 ×.77	.3388	.385	.1304	.0502	.0167
5.4×.5	2.7	−.40	−1.080	.4320	.0563
Σ	3.0388	−.312	−.9496	.4822	.0720

$2\alpha = \dfrac{5.4}{8.5} = .6353$

$\alpha = .3176 = 18.2°$

$\sin \alpha = .312$

$\bar{y} = \dfrac{R \sin \alpha}{\alpha} = 8.350$

$y = R_0 - \bar{y} = 0.40$

$I = .4822 + .0720 - .312 \times .9496 = .2579$

$\dfrac{I}{c} = \dfrac{.2579}{\dfrac{(.77 + .312)}{1.082}} = .2384$

$R_D = 8.75 - .312 = 8.438$

$\bar{y}_0 = \dfrac{8.438 \times .312}{.3176} = 8.289$

$e_1 = \bar{y}_1 - \bar{y}_0 = 9.471 - 8.289 = 1.182$

$e_2 = \bar{y}_2 - \bar{y}_0 = 8.822 - 8.289 = .533$

Rockwell International

PREPARED BY:

DATE: 12 - 1 - 75

REV. 7/30/76   R.H.

MODEL NO.

DWG# 8109-100000

(SEC D-D) (CONT)

$$M = P_{U_1} (1.182) + P_{U_2} (.533)$$

$$= 64.1 (1.182) + 3.2 (.533) = 77.47 \; KIN-IN$$

$$P = P_{U_1} + P_{U_2} = 67.3 \; K$$

$$f_c = \frac{P}{A} = \frac{67.3}{3.039} = 22.1 \; KSI$$

$$f_b = \frac{M}{(I/c)} = \frac{77.47}{.2334} = 325 \; KSI$$

$$R_c = \frac{f_c}{F_{cy}} = \frac{22}{226} = .097$$

$$R_b = \frac{f_b}{1.5 F_{cy}} = \frac{325}{339} = .959$$

$$M.S = \frac{2}{R_b + \sqrt{R_b^2 + 4 R_c^2}} - 1 = \boxed{(AXIAL + BENDING) = +0.03}$$

(SECTION B-B)

$M_{BB} = R_1 \times 3.5 = 18.08 \times 3.5 = 63.3 \text{ KIP-IN}$ } COND ② A

$P = 0$

$M_{BB} = P_{U_1} e_1 + P_{U_2} e_2 - R_1 \times 3.5$ } COND ② B

$P = P_{U_1} + P_{U_2} = 64.1 + 3.2 = 67.3^K$

$R = 8.25 , \quad t = .49 , \quad b = 6.0$

DIM	A	y	Ay	Ay²	I₀
.22 × 1.13	.248	.56	.1389	.0778	.0264
.22 × 1.13	.248	.56	.1389	.0778	.0264
6 × .49	2.940	-.409	-1.2025	.4918	.0533
Σ	3.436	-.2691	-.9247	.6474	.1116

$\bar{y}' = \frac{R' \sin\alpha}{\alpha} = \frac{8.50 \times .346}{.353} = 8.331$

$2\alpha = \frac{b}{R} = \frac{6}{8.50} = .706$

$\alpha = .353 = 20.22$

$y = 8.74 - 8.331 = .409$

$c = 1.13 + .2691 = 1.399$

$I_x = \Sigma I_0 + \Sigma Ay^2 - \bar{y} \Sigma Ay = .7590 - .2488$
$\qquad\qquad = .5102$

$\frac{I_x}{c} = \frac{.5102}{1.399} = .3647$

$\bar{y}_{BB} = 8.74 - .2691 = 8.4709$

$f_b = \frac{M_{BB}}{(I/c)} = \frac{63.3}{.3647} = 173.6 \text{ KSI}, \quad \text{COND} ② A$

$e_1 = 9.5 - 8.471 = 1.029''$

$e_2 = 8.849 - 8.471 = 0.378$

$P_{BB} = P_{U_1} + P_{U_2} = 67.3^K$

$M_{BB} = P_{U_1} \times e_1 + P_{U_2} \times e_2 - R_1 \times 3.5$
$\qquad = 64.1 \times 1.029 + 3.2 \times .378 - 9.907 \times 3.5$
$\qquad = 65.96 + 1.2096 - 34.67 = 32.50 \text{ IN-KIP}$

$f_b = M_{BB} / (I/c) = \frac{32.5}{.3647} = 89.1 \text{ KSI}$ } COND ② B

$f_c = P_{BB} / A = \frac{67.3}{3.436} = 19.59 \text{ KSI}$

$(\text{SECTION B-B})(\text{CONT})$

$$b/t = \frac{1.13}{.22} = 5.136 \qquad F_{cc} = 206 \text{ KSI (ONE EDGE FREE)}$$

$$M.S. = \frac{F_{cc}}{f_b} - 1 = \frac{206}{173.6} - 1 = \boxed{\begin{pmatrix} \text{LUG} \\ \text{CRIPPLING} \end{pmatrix} + .19}$$

$$\text{COND ①A}$$

(SECTION F-F)

LUG $t = .22$
LUG $b = 1.70$
WALL $t = .497$
WALL $b = 6.00$

		A	y	Ay	Ay²	I₀
$2 \times .22 \times 1.70$		.748	.35	.6358	.5404	.1801
$6 \times .497$		2.982	-.431	-1.2852	.5539	.0614
	Σ	3.730	-.1741	-.6494	1.0943	.2415

$R_i = 7.562 + .573 = 8.135''$

$R' = 8.135 + .249 = 8.384''$

$C = 1.70 + .174 = 1.874$

$2\alpha = \frac{6}{8.384} = .7156$

$\alpha = .3578 = 20.5°$

$I_x = \Sigma I_0 + \Sigma Ay^2 - \bar{y}\Sigma Ay$

$= 1.3358 - .1131 = 1.2227$

$\bar{y}' = \frac{R'\sin\alpha}{\alpha} = \frac{8.384 \times .35}{.3578} = 8.201$

$R_0 - \bar{y}' = 8.632 - 8.201 = -.431$

$\left(\frac{I}{C}\right) = \frac{1.2227}{1.874} = .652$

$M_{FF} = 115.72 \text{ IN-KIP} \quad \text{COND ②A} \quad (\text{REF. PG A-5})$

$$f_b = \frac{M_{FF}}{\left(\frac{I}{C}\right)} = \frac{115.72}{.652} = 177.5 \text{ KSI}$$

$$b/t = 1.70/.22 = 7.73, \quad F_{cc} = 180 \text{ KSI}$$

$$M.S. = \frac{F_{cc}}{f_b} - 1 = \frac{180}{177.5} - 1 = \boxed{(\text{CRIPPLING}) + .014}$$

Rockwell International

PREPARED BY: TM | INBD SHR FITTING - PIVOT |
DATE: Nov 25, 1975 | PIN - AF1412 VERSION | MODEL NO.

(BEARING CHECK)
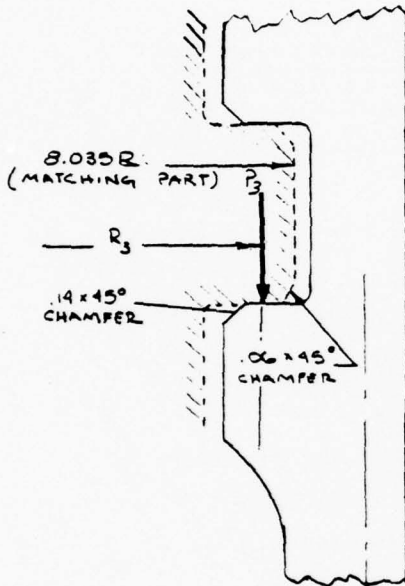
ASSUME R_3 ACTS AT MIDPOINT OF CONTACT BETWEEN PARTS:

$$R_3 = .5 \left(7.562 + .14 + 8.035 - .06 \right)$$

$$= 7.8385$$

CONTACT WIDTH $= (8.035 - .06) -$
$$(7.562 + .14)$$
$$= 0.273$$

$$A_{br} = 6.5 \times 0.273 = 1.774 \text{ in}^2$$

$$P_3 = P_L = 318.05^K$$

CONSERV. INCLUDE VERTIC. COMPONENT

OF $P_T = $ SINE $52.38° \times 27.846^K$
$$= 22.06$$

$$P_3' = 318.05 + 22.06 = 340.11^K$$

$$f_{br} = \frac{P_3'}{A_{br}} = \frac{340.1}{1.774} = 191.7^{ksi}$$

$F_{bru} = 330$ ksi (CONSERV.)

$$M.S. = \frac{330}{192} - 1 = (\text{BEARING}) + \underline{.72}$$
$$\text{COND} \textcircled{2} A$$

(DETERMINATION OF LOAD PATH FOR R_L, P_3)
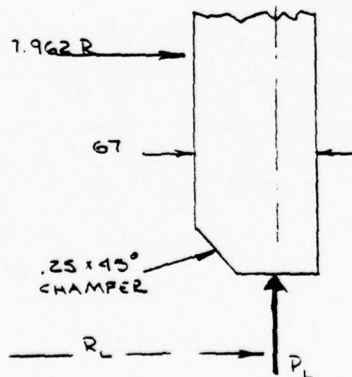
$$R_L = (7.962 + .25 + 7.962 + .67) \times .5$$
$$= 8.422 \text{ IN.}$$

AT P_L, $2\alpha = 30.38°$, $\alpha = 15.19°$

$R_L = 8.422$
$s = 4.460$

$$\bar{y}_L = \frac{R_L \sin \alpha}{\alpha}$$

$$= \frac{8.422 \times \sin 15.19°}{15.19 \cdot \frac{\pi}{180}} = 8.323$$

8.035 R (MATCHING PART) P_3

R_3

$.14 \times 45°$ CHAMFER

$\alpha \times 45°$ CHAMFER

7.962 R

67

$.25 \times 45°$ CHAMFER

R_L P_L
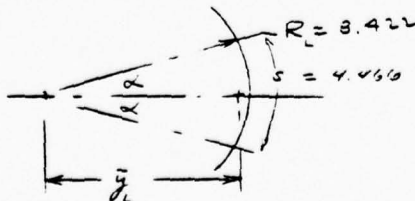
Rockwell International

PREPARED BY: TM | INBD SHR FITTING - PIVOT |
DATE: 11-25-75 | PIN — AF 1417 VE | MODEL NO.

(DETERM. OF LOAD PATH FOR R_L, P_3) (CONT)

AT P_3, $2\alpha = 44°$, $\alpha = 22°$, $s = 6.020$

$R_3 = 7.8335$
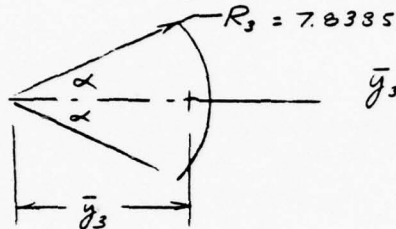
$$\bar{y}_3 = R_3 \frac{\sin \alpha}{\alpha} = \frac{7.8335 \times \sin 22°}{22 \times \pi/180}$$

$$= \frac{7.8335 \times .375 \times 180}{22 \times \pi} = 7.655 \text{ "}$$

$$a = \bar{y}_L - \bar{y}_3 = 8.323 - 7.655 = 0.668 \text{ "}$$

(REACTION R_1, R_2 FROM LOWER RACE LOAD P_L)

$$R_1 = -R_2 = \frac{P_L \times a}{11.75} = \frac{318.052 \times .668}{11.75}$$

$$= 18.08 \text{ KIPS}$$
$$\text{COND } ② \text{ A}$$

(LOAD PATH FOR UPPER BEARING RACE LOAD P_{U_1})

AT P_{U_1}, $2\alpha = 17.37°$, $\alpha = 9.69°$, $S = 2.88 \text{ "}$

$$\bar{y}_1 = R \frac{\sin \alpha}{\alpha} = \frac{9.5 \times \sin 8.69°}{8.69 \times \pi/180} = 9.471$$

FOR P_3, ASSUME $\bar{y}_3 = 7.655 \text{ "}$

$$a = \bar{y}_1 - \bar{y}_3 = 9.471 - 7.655 = 1.816$$

REACTION, $R_1 = -R_2 = \frac{P_{U_1} \times a}{11.75} = \frac{64.1 \times 1.816}{11.75} = 9.907 \text{ K}$

$$\text{COND } ② \text{ 3}$$

(SEC K-K) (REF DRAWING PG. P-4)
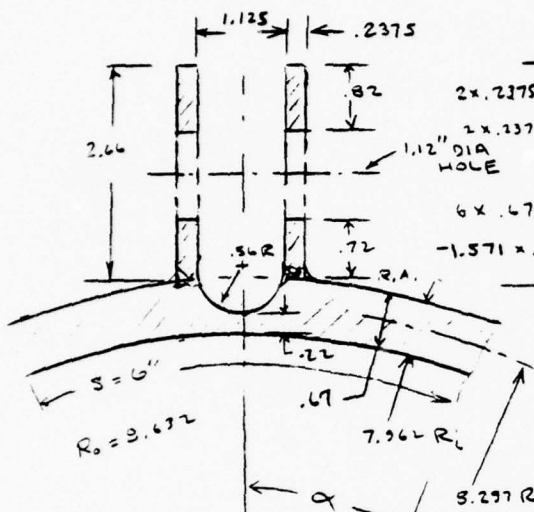
	A	y	Ay	Ay²	I₀
2 x .2375 x .82	.3895	2.25	.8764	1.9719	.0218
2 x .2375 x .72	.3420	.36	.1231	.0443	.0143
6 x .67	4.02	-.509	-2.0462	1.0415	.1504
-1.571 x .56²	-0.493	-.237	+.1168	-.0277	-.0138
Σ	4.2585	-.7134	-.9299	3.0299	.1762

$$C = 2.66 + .218 = 2.878$$

$$I = \Sigma I_0 + \Sigma Ay^2 - \bar{y} \Sigma Ay$$

$$I = .1762 + 3.0299 - .2031 = 3.003 \text{ in}^4$$

$$I/c = 3.003/2.878 = 1.0434$$

$$2\alpha = \frac{6}{8.297} = .72315$$

WALL $A = (R_o^2 - R_i^2)\alpha = 4.0202$

$$\alpha = .3616 = 20.72°$$

WALL $I_0 = \frac{\alpha}{4}(R_o^4 - R_i^4)(1 + \frac{\sin\alpha \cos\alpha}{\alpha}) - A\bar{y}^2$

$$\sin\alpha = .354$$

WALL $\bar{y} = \frac{2\sin\alpha (R_o^3 - R_i^3)}{3A} = \frac{2 \times .354 \times 138.44}{3 \times 4.0202} = 8.127$

$$\bar{y}' = \frac{R'\sin\alpha}{\alpha} = \frac{3.297 \times .354}{.3616} = 8.123$$

$$y = 7.962 + .67 - 8.123 = .509 \quad \text{WALL}$$

SEMICIRCLE = $y = .4244 R = .4244 \times .56$
$$= .237$$

SEMICIRCLE $I_0 = .1097 R^4 = .0138$

WALL $I_0 = \frac{.3616}{4}(8.672^4 - 7.962^4)(1 + \frac{.354 \times .935}{.3616}) - 4.0202 \times 8.127^2$

$$I_0 = .0904 \times 1533.229 \times 1.9153 - 265.527 = -.0.0 \text{ N.G.}$$
$$\text{USE APPROX EQ}$$

$$P_{KK} = P_L = 318^K \quad \text{COND ②A}$$

$$M_{KK} = R_2 \times 3.25 + P_L \times e = 18.09 \times 3.25 + 318 \times (8.032 - .218 - 3.323)$$

$$f_b = \frac{M_{KK}}{(I/c)} = \frac{587 + 28.9}{1.0434} = 94. KSI , \quad f_c = \frac{P}{A} = \frac{318}{4.26} = 75 KSI$$

$$b/t = \frac{2.66}{.2375} = 11.2 , \quad F_{cc} = 130 KSI \quad \text{ONE EDGE FREE} \quad (REF. NA 52-400 APP. A)$$

PREPARED BY: TM | INBD SHEAR FITTING -

DATE 11-26-75 | PIVOT PIN - AFICIO VERSION MODEL NO.

Revised 3/2/76 R.H.

(SEC. K-K) (CONT.)

$$R_c \cdot \frac{f_c}{F_{cy}} = \frac{75}{226} = .332$$

$$R_b = \frac{f_b}{F_{cc}} = \frac{94}{.130} = .696 \quad (conserv.) \quad (F_{cc} \; ref \; Fig. 25)$$

$$M.S. = \frac{2}{R_b + \sqrt{R_b^2 + 4R_c^2}} - 1 = \boxed{(AXIAL + BENDING) = + 0.27}$$

(SEC. C-C) $R_i = 7.962$, $R_o = 8.632$, $R = 8.297$

                                                                $t = .67$

$P_c = P_L = 318^K$ COND ① A

$M_c = P_L (\bar{y}_L - \bar{y})$ $\bar{y}_L = 8.323$

LET $w = 4.56$

$2\alpha = \frac{w}{R} = \frac{4.56}{8.297} = .5496$

$\alpha = .275 = 15.74°$

$sine \; \alpha = .2715$

$\bar{y} = \frac{R \; sine \; \alpha}{\alpha} = \frac{8.297 \times .2715}{.275} = 8.191$

$M_c = 318 (8.323 - 8.191) = 42 \; IN-KIP$

$A = 4.56 \times .67 = 3.05$

$I_c = \frac{bt^2}{6} = \frac{4.56 \times .67^2}{6} = .341$

$f_c = \frac{P_c}{A} = \frac{318}{3.05} = 104 \; KSI$

$f_b = \frac{M_c}{I_c} = \frac{42}{.341} = 123 \; KSI$

$R_c \cdot \frac{f_c}{F_{cy}} = \frac{104}{226} = .460$

$R_b = \frac{f_b}{F_{cy}} = \frac{123}{226} = .544 \quad (conserv.)$

$M.S. = \frac{2}{R_b + \sqrt{R_b^2 + 4R_c^2}} - 1 = \boxed{+ .240 \quad (AXIAL + BEND)}$

DWG # 3109-10XXXX

(WELD CHECK   SEC. D-D)
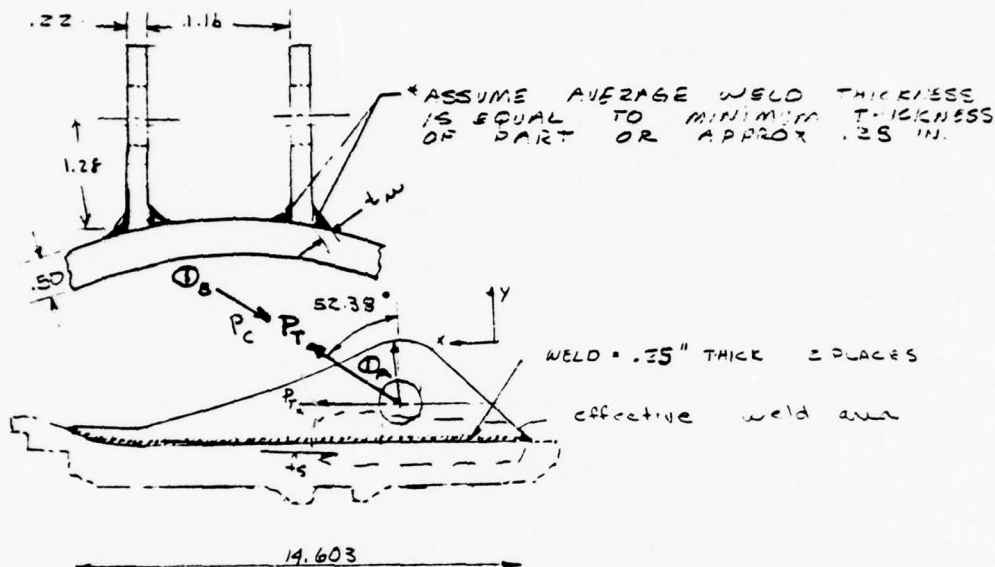
LOAD COND ①$_A$ $P_T = 27.85^k$

①$_B$ $P_C = -107.04^k$

COND. ①$_B$ -   ASSUME LOAD IS DIST EQUALLY ON EACH LUG

$P_C = -107.04$ $P_X = \dfrac{P_C (\cos 37.62)}{2} = \dfrac{85.49^k}{2} = 42.74^k$

$P_Y = \dfrac{P_C (\cos 52.38)}{2} = 32.95^k$

Assume effective weld length ≈ 40% of TOTAL WELD
LENGTH $L_w = .40 (14.6) = 5.84''$

$f_s = \dfrac{P_X}{L_w \, t_w} = \dfrac{42.74}{5.84(2)(.25)} = 14.64^{KSI}$

$f_c = \dfrac{P_Y}{L_w \, t_w} = \dfrac{32.95}{5.84(2)(.25)} = 11.28^{KSI}$

PEEL $f_b = \dfrac{P_X \cdot 1.28 \times 6}{.250 \times 2 \times 5.84^2} = \dfrac{42.74 \times 1.28 \times -}{.50 \times 5.84^2} = \pm 19.25$ ksi

PAGE NO. A - 15   REV.

$$R_S = \frac{f_S}{F_{Su}} = \frac{14.64}{125} = .117$$

$$R_C = \frac{f_c + f_b}{F_{CY}} = \frac{11.28 + 19.25}{192} = .159 \qquad .2.5?$$

$$M.S. = \frac{1}{\sqrt{R_S^2 + R_C^2}} - 1 = \boxed{+ (WELD \ SHEAR + COMP)} = \underline{\underline{HIGH}}$$

$P = 27.85^K \ (T)$

$P_X = 27.85 (cos. 37.62) = 22.06^K /2 = 11.03^K$

$P_Y = 27.85 (cos 52.33) = 17.00^K /2 = 8.5^K$

$Lw = 6.00''$

$tw = .25''$

$$f_S = \frac{11.03}{6.00(2)(.25)} = 3.68^{KSI} \qquad f_t = \frac{8.5}{6.00(2)(.25)} = 2.33^{SI}$$

$$R_S = \frac{f_S}{F_{Su}} = \frac{3.68}{125} = .0294$$

$$R_T = \frac{f_t}{F_{tu}} = \frac{2.33}{196} = .014$$

$$M.S. = \frac{1}{\sqrt{R_S^2 + R_t^2}} - 1 = (WELD \ SHEAR - TENSION)$$

$$= \underline{\underline{HIGH}}$$

Rockwell International

PREPARED BY: R H

DATE: 8/7/76

MODEL NO.

(SEC. W-W   WELD   CHECK)

consider lines as
part of section
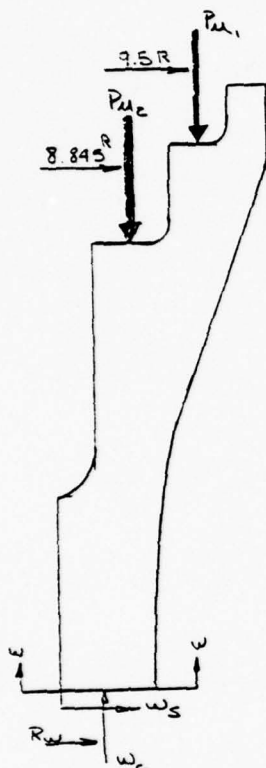
COND. 2B $P_{M_1} = 64.1^k$
            $P_{M_2} = 3.18^k$

$R_W = 8.561$ (see Pg P-11)

$W_c = 67.3^k$

$\Sigma M_{P_{M_2}} = 0 \quad +\circlearrowleft$

$0 = (64.1)(9.5 - 8.561) + 67.3(8.845 - 8.561) -$
   $W_s(6.11)$

$W_s = 12.46^{kk}$

$f_s = \dfrac{12.46}{A}$ A: 3.008

$\quad = \dfrac{12.46}{3.008} = 4.143^{ksi}$

$f_c = \dfrac{67.3}{3.008} = 22.397^{ksi}$

$R_s = \dfrac{4.143}{125} = .033$

$R_c = \dfrac{22.397}{196} = .1143$

$M.S. = \dfrac{1}{\sqrt{R_s^2 + R_c^2}} - 1 = (shear - comp) \ \underline{HIGH}$

APPENDIX B

WING SWEEP ACTUATOR

FITTING - FORGING

PRELIMINARY STRESS ANALYSIS

APPENDIX

INBD WING SWEEP ACTUATOR

SUPPORT FITTING

MODEL NO.

DWG. 3109-100001

DWG. 3109-100003

AF 1410 VERSIONS

DISCUSSION

THE INBD SWEEP ACTUATOR SUPPORT
FITTING (TRUSS DESIGN #3109-100001 & STIFFENED
WEB DESIGN · MACHINED FORGING #3109-100003) WERE
STRESS ANALYZED USING THE PROPERTIES AND
ALLOWABLE CURVES PROVIDED IN THE
"STRUCTURAL ANALYSIS PROPERTIES" SECTION
(TABLE IV , FIGURES 17 THROUGH 25)

THE APPLIED DESIGN LOADS ARE THE
SAME AS THOSE USED FOR THE TITANIUM
BASELINE COMPONENT

CONVENTIONAL STRESS ANALYSIS
PROCEDURES WERE USED PER REFERENCES

INBD WING SWEEP ACTUATOR SUPPORT FITTINGS
DESIGN CONCEPTS
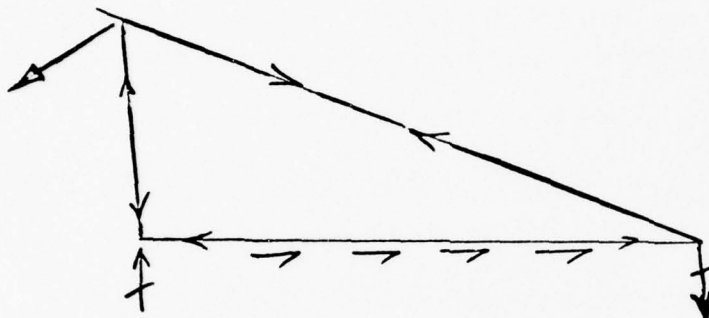
TRUSS DESIGN

(MACHINED- WELDED)
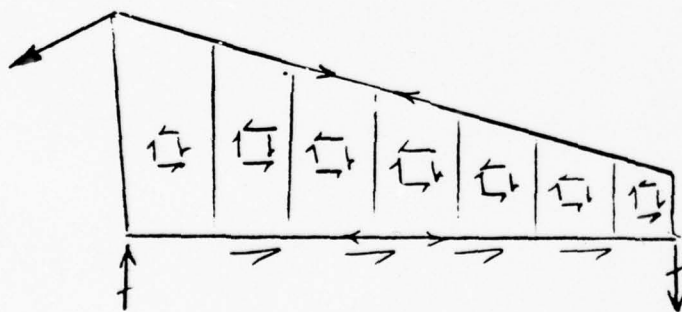
STIFFENED WEB DESIGN
(MACHINED FORGING)

PREPARED BY: TRUSS DESIGN — INBD SWEEP

DATE: ACTUATOR SUPPORT FITTING

MODEL NO.

#3109-100001

REFERENCE:
DRAWING No. 3109-100001

LOCOSST INBOARD SWEEP ACTUATOR SUPPORT FITTING
TRUSS DESIGN OF AFAIO VERSION

DIAGONAL TRUSS MEM. AB
$P_C = (636^k)$ (COMP.) COND II
$P_T = 914^k$ (TEN.) COND I

LOADS

ULTIMATE

COND I — $P_{ACT} = 922^k$ $\left(\begin{array}{l}\text{B-1}\\ \text{LOAD CASE 160316}\end{array}\right)$
COND II — $P_{ACT} = -642^k$

$(-642^k) P_{ACT}$

X_F 126.75

Y_F 9.17   35.92°

P_{ACT} .922 K

19.35

$P = 85^k$ (C)
CHORDWISE MEMBER AC

(NO WEB)

$+914^k$
$(=636^k)$

X_F 121.75

$R_1 = 851^k$ (539 K) ₵
$X_F \approx 121.0$

1.88

Y_F 991.₵

3

$\widehat{A}$

28.3

3

$R_3 = 747^k$ (520^k)
(SPANWISE TRUSS MEMBER BC)   37.9

B

REF.
Y_F 932 BKHD

$R_2 = 310^k$ (216^k)₳
X_F 83.1′

SUMMARY — LOADS & GEOMETRY DETAILS

LOADS DEVELOPMENT

(DIAGONAL LOAD) $\overline{AB}$

$$P_T = R_2 \times \frac{42.29}{14.35} = 914^k \, (T)$$

$$P_C = \frac{-642}{922} \times 914 = -636^k \, (C)$$

HORIZ. COMPON. $P_{ACT}^X = \overleftarrow{747}^k$ $\Big\}$ $P_{ACT} = 922^k$, $\dfrac{(COND\,\,II)}{(-642^k)}$ COND I

VERT. COMPON. $P_{ACT}^Y = 541^k \downarrow$

(ATTACHMENT LOADS)

$$R_1 = P_{ACT}^X \times \frac{14.35}{37.9} + P_{ACT}^Y \times \frac{39.78}{37.9} =$$

$$= 747 \times .3786 + 541 \times 1.0496 = 851.^k \uparrow$$

$$R_2 = P_{ACT}^Y - R_1 = 541 - 851 = 310^k \downarrow$$

R_3 = ASSUME X COMPONENT OF $P_{ACT} = 747^k$

     IS REACTED BY FASTENERS IN SHEAR

ASSUMPTION ① — PROPORTION R_3, $\frac{1}{3}$ AT $X = 83$,

           $\frac{1}{3}$ AT X_F 121 REGION, $\frac{1}{3}$ BETWEEN

           X_F 121 — X_F 83

ASSUMPTION ② — PROPORTION R_3 IN TERMS OF
           SHEAR ALLOWABLES

$P^{SU} = 98^k$ (1" DIA) $\Big\}$
$P^{SU} = 75^k$ ($\frac{7}{8}$" DIA)
$P^{SU} = 55^k$ ($\frac{3}{4}$" DIA)

TOTAL ALLOW = $4 \times 98 = 392$
           $12 \times 55 = 660$
           $2 \times 98 + 4 \times 75 = 496$
           $\Sigma = 1548$ k

PAGE NO. **B.5**   REV. 3-25-76

Rockwell International

PREPARED BY: TM	IN3D WING SWEEP	
DATE: 12-17-75	ACTUATOR SUPPORT FITTING	MODEL NO.
REV: 3-29-76		DWG# 3109-100001

(<u>LOWER TRUSS MEMBER LOADS</u>)

$$P_3 = P_T \times \frac{39.78}{42.29} = 914 \times .941 = 860^k \leftarrow \Big\} \begin{array}{l} 748^k \\ \text{COND I} \end{array}$$
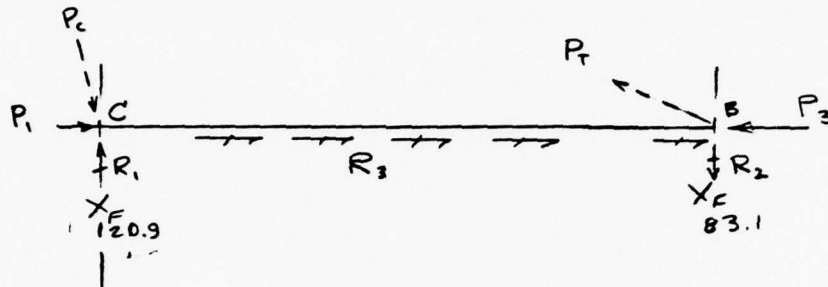
$$P_1 = R_1 \times \frac{1.88}{14.35} = 851 \times .131 = 112^k \rightarrow$$

X_F	Δ BOLT ALLOW	$\frac{\Delta \text{ALLOW}}{\text{TOT. ALLOW.}}$	ΔP^*	LOAD
82.2	0	0		860^k (c)
83.1	TWO 1" DIA = 196^{k**}	.1266	95	-
85.8	TWO 1" DIA = 196	.1266	95	765^k
89.9$^+$	TWO 3/4" DIA = 110	.0711	53	670^k
93.9$^+$	TWO 3/4" DIA = 110		53	617
99.6$^+$	TWO 3/4" DIA = 110		53	564
103.4$^+$	TWO 3/4" DIA = 110		53	511
109.1$^+$	TWO 3/4" DIA = 110		53	458
113.$^+$	TWO 3/4 DIA = 110	.0711	53	405
117.	0	0	0	352
118.8$^+$	ONE 1" DIA + TWO 7/8" = 248^k	.1602	120	352
120.9	0	0	$P_1 = 112^k$	232
123.$^-$	ONE 1" DIA + TW. 7/8" = 248^k	.1602	120	120^k (c)
				0

TOT. ALLOW = 1548^k

$* \quad \Delta P = \frac{\Delta \text{ALLOW}}{\text{TOT ALLOW}} \times 748$

$**$ ASSUME LOAD REACTED IN PROPORTION TO FASTENER VALUES

@ X_F 83.1 — (4) 1" DIA = 98^k/BOLT ALLOW

@ X_F 85.8 — X_F 117 (12) ~ 3/4" DIA = 55^k/BOLT ALLOW

@ X_F 120.9 — (2) 1" DIA + (4) 7/8" DIA = 98^k/BOLT & 75^k/BOLT

PAGE NO. <u>B-6</u>   REV. 3-29-76

337

Rockwell International

PREPARED BY: TM	INBD SWEEP ACTUATOR	
DATE: 12-16-75	SUPPORT FITTING	MODEL NO.
REV. 3-29-76		DWG# 8109·100001

(ATTACHMENT CHECK)

AT X_F 84 REGION ASSUME BOLT $F^{su} = 125$ KSI

$F^{tu} = 220$ KSI

FOUR (4) ONE INCH DIA. BOLTS IN $t = .50$

ALLOW $P^{su} = F^{su} \frac{\pi}{4} D^2 = 125 \times .785 \times 1^2 = 98^k/\text{BOLT}$

LET APPLIED $P_s = \frac{1}{3} \times$ HORIZ. COMPONENT OF DIAG. LOAD

$= \frac{1}{3} \times 747 = 249^k$ ON 1" DIA FASTENERS

ALLOW. $P^{tu} = F^{tu} \times A_{MINOR} =$

$= 220 \times .64156 = 141^k/\text{BOLT}$ (1" DIA)

APPLIED $P_T = 100\%$ VERT. COMPONENT ON 1" DIA FASTENERS

$= 1.00 \times R_2$

$R_s = .P_s/P^{su} = \frac{249}{4 \times 98} = .635$

$R_T = P_T/P^{tu} = \frac{310}{4 \times 141} = .550$

USING CIRCULAR INTERACTION

$$M.S. = \frac{1}{\sqrt{R_s^2 + R_T^2}} - 1 = \frac{1}{.840} - 1 = \boxed{\left(\begin{array}{c} \text{COMBINED} \\ \text{BOLT} \\ \text{TEN & SHL} \end{array}\right) +.19} \quad \text{COND I}$$

(ATTACH. CHECK) (CONT.)

AT X_F 121 REGION (220 HT BOLT)

(2) TWO 1" DIA. BOLTS + (4) FOUR $\frac{7}{8}$" DIA BOLTS

$P^{su} = 98^k / \text{BOLT}$ $\qquad$ $P^{su} = 75^k / \text{BOLT}$

$P^{Tu} = 141^k / \text{BOLT}$ $\qquad$ $P^{Tu} = 108^k / \text{BOLT}$

LET APPLIED $P_T = R_1 (c) = \frac{642}{922} \times 851 = 593^k \downarrow$

APPLIED $P_s = \frac{1}{3} \times R_1 (c) = \frac{1}{3} \times \frac{642}{922} \times 747 = 174^k$

$$R_s = \frac{P_s}{\text{TOT } P^{su}} = \frac{174}{\underset{496}{(2 \times 98 + 4 \times 75)}} = .351$$

$$R_T = \frac{P_T}{\text{TOT } P^{tu}} = \frac{593}{\underset{714}{(2 \times 141 + 4 \times 108)}} = .831$$

$$M.S. = \frac{1}{\sqrt{R_s^2 + R_T^2}} - 1 = \frac{1}{.902} - 1 = \boxed{\begin{pmatrix} \text{COMBINED} \\ \text{TEN.} \\ + \text{SHEAR} \\ \text{BOLT} \end{pmatrix} + .108}$$ COND II

LET $P_s = \frac{1}{3} \times R_3 (T) = \frac{1}{3} \times 747 = 249^k$

TOT $P_{su} = 2 \times 98 + 4 \times 75 = 496^k$

$$M.S. = \frac{P^{su}}{P_s} - 1 = \boxed{\begin{pmatrix} \text{BOLT} \\ \text{SHEAR} \end{pmatrix} + .99}$$ COND I

AT X_F 121 — X_F 84 (12) $\frac{3}{4}$" BOLTS $P^{su} = 55^k / \text{BOLT}$

TOT $P^{su} = 12 \times 55 = 660^k$

APPLIED $P_s = \frac{1}{3} \times R_3 = 249^k$ ← ASSUMP. ①

$\qquad = \frac{660}{1548} \times 747 = 318^k$ ← ASSUMP ② ← USE COND I

$$M.S. = \frac{660}{318} - 1 = \boxed{\begin{pmatrix} \text{BOLT} \\ \text{SHEAR} \end{pmatrix} + 1.07}$$

Rockwell International

PREPARED BY: TM

DATE: 12-5-75   ACTUATOR SUPPORT FITTING   MODEL NO.

REVISED 3-25-76 TTM

DWG REF. 3109-100001 (DATED 12-4-75)
REVISED 3-24-76 · MARKED UP

MATERIAL : AF 1410 STEEL — REFER TO TABLE IV
FOR PROPERTIES

DISCUSSION   THIS CONFIGURATION HAS BEEN
REVISED FROM EARLIER CONCEPTUAL
VERSIONS. THE BASIC APPLIED
LOADS HAVE NOT CHANGED TO DATE.
HOWEVER, INTERNAL LOADS WILL CHANGE

DIAGONAL TRUSS MEMBER AB

(DIAGONAL LOAD)
$P_c = 636^k$ COMP. COND II
$P_T = 914^k$ TEN. COND I

35.92° -642^k $+922^k$
$+914^k$ (-636^k)
$12.86''$ 11 23.3
14.35 (WAS 15.96)
C
1.88 37.9
$R_1 = 851^k$ (593^k)
$X_F \approx 121.0$
$R_2 = 310^k$ (216^k)
$X_F = 89.7$
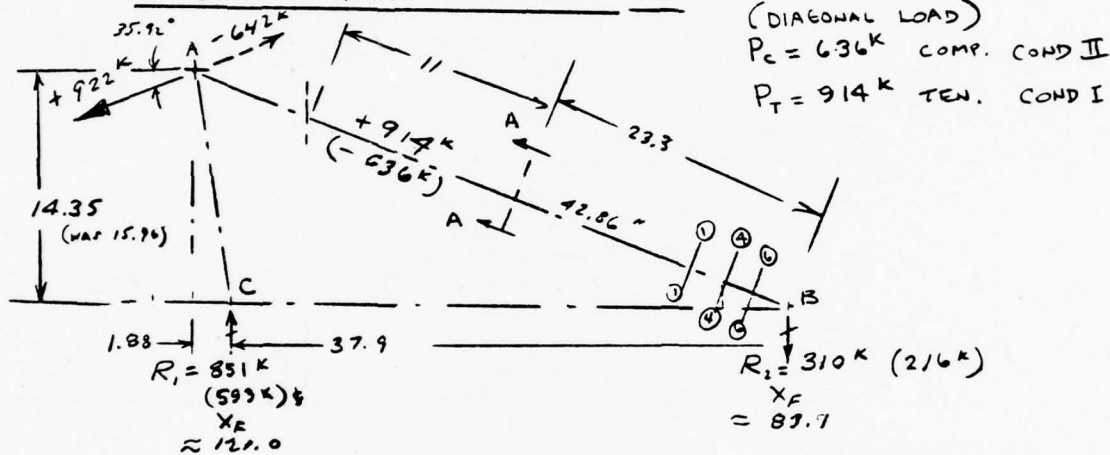
(SEC A-A) (WAS $T_{WEB} = .19$) NOW $T_{WEB} = .25$ FLG $t = .30$ (WAS .38)

DIMEN.	A	x	Ax	Ax²	I_{o_z}
2.90 x .25 x 2	1.45	0	0	0	.0075
1.0 x .50 x 2	1.0	+1.25	1.25	1.5625	.0208
1.0 x .50 x 2	1.0	-1.25	-1.25	1.5625	.0208
.30 x 2.0 x 2	1.20	0	0	0	.4000
Σ	4.65	0	0	3.1250	0.4491

$I_z = \Sigma I_{o_z} + \Sigma A x^2 - \bar{x}\Sigma A x = 3.574 \text{ IN}^4$

$\rho_z = \sqrt{\dfrac{I_z}{A}} = .8767 \text{ IN.}$

PAGE NO. B-9   REV. 3-25-76

340

(SEC. A-A) (CONT)

DIMEN.	A	z	Az	Az²	I_{o_x}
25 5.33	1.45				4.0478
		0	0	0	
.50 x 1.0 x 4	2.0	±2.7	±2.7	14.58	.1666
2.0 x .30 x 2	1.20	±3.0	3.6	10.8	.0045
Σ	4.65	$\overline{0}$	0	25.38	4.236

$$I_x = \Sigma I_{o_x} + \Sigma Az^2 - \overline{z}\ \Sigma Az = 29.61 \text{ in}^4$$

$$\rho_x = \sqrt{\frac{I_x}{A}} = 2.53 \leftarrow \text{NOT CRITICAL}$$

(COLUMN CHECK)   USE $\rho_z = 0.877$

ASSUME COLUMN LENGTH $L' = 22''$

$$\frac{L'}{\rho_z} = \frac{22}{.877} = 25.1$$

$$F_{co} = 202. \text{ KSI} \qquad (\text{REF. FIGURE 22})$$

$$f_c = \frac{P_c}{A} = \frac{636}{4.65} = 137. \text{ KSI} \quad \text{COND II}$$

$$M.S = \frac{F_{co}}{f_c} - 1 = \frac{202}{137} - 1 = \boxed{(\text{COLUMN STABIL.}) + .47}$$

(WEB. CRIPPLING)   - COND II

$$\frac{b}{t} = \frac{5.8}{.25} = 23.2$$

$$F_{cc} = 140. \text{ KSI} \quad (\text{REF. FIG. 25})$$

$$M.S. = \frac{F_{cc}}{f_c} - 1 = \frac{140}{137} - 1 = \boxed{(\text{CRIPPLING}) + .02}$$

(TENSION CHECK) $f_T = \dfrac{P_T}{A} = \dfrac{914}{4.65} = +197 \text{ KSI}$ COND I

LET $F^{tu} = 230 \text{ KSI}$

$$M.S. = \frac{F^{tu}}{f_T} - 1 = \frac{230}{197} - 1 = \boxed{(\text{TENSION}) + .17}$$

Rockwell International

PREPARED BY: TTM | INBD SWEEP ACTUATOR
DATE: 3-25-76 | SUPPORT FITTING | MODEL NO.

DWG# 8109-100001

(LOCAL AXIAL + BENDING CHECK)

SECTION ① ① (DWG 3109-100001 DATED 12-4-75
MARKED UP REVISED 3-24-76)

ASSUME EFFECTIVE SECTION
AS SHOWN:

ITEM	A	x	Ax	Ax²	I_{o_z}
①	.500	1.25	.625	.7813	.0104
②	.590	0	0	0	.0031
③	.813	-.07	-.0569	.0039	.3103
④	.360	-1.39	-.5004	.6955	.0075
			.0677		
Σ	2.263	.0299		1.4807	.3313
ΣΣ	4.526		.1354	2.9614	.6626
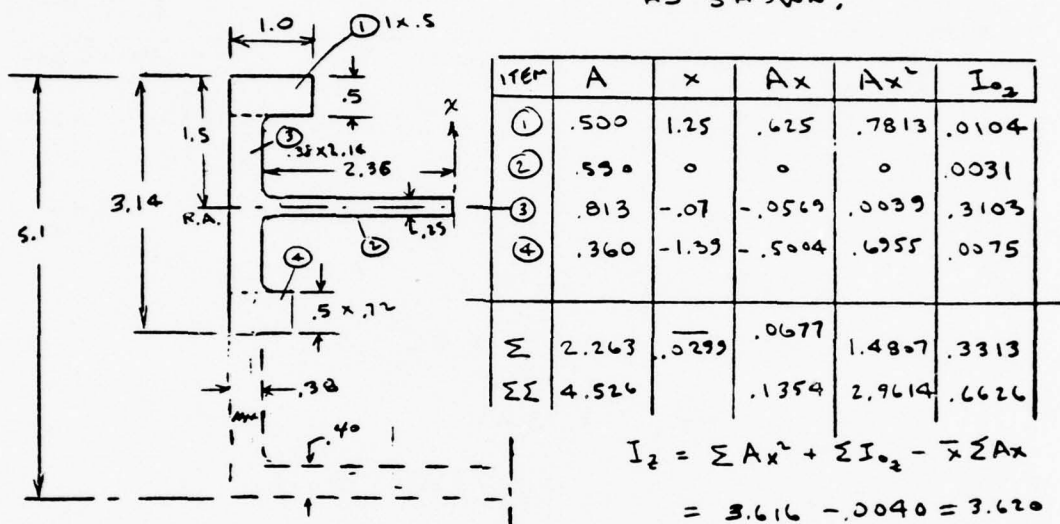
$$I_z = \Sigma A x^2 + \Sigma I_{o_z} - \bar{x} \Sigma A x$$

$$= 3.616 - .0040 = 3.620$$

$$\frac{I}{c_1} = \frac{3.62}{1.5 - .03} = 2.463 \quad , \quad \frac{I}{c_2} = \frac{3.62}{1.67} = 2.168$$

$$e = .0299$$

$$\sigma_t = \frac{P}{A} = \frac{914}{4.526} = 202 \text{ KSI}$$

$$\sigma_b = \frac{Pe}{I/c_2} = \frac{914 \times .0299}{2.168} = 12.6 \text{ KSI}$$

$$\sigma_{TOT} = 215 \text{ KSI}$$

$$F_{tu} = 230 \text{ KSI}$$

$$M.S. = \frac{F_{tu}}{\sigma_{TOT}} - 1 = \frac{230}{215} - 1 \boxed{= \left(\frac{-EJ}{+BEND}\right) + .07}$$

(LOCAL AXIAL & BENDING CHECK)

SECTION ①① (CONT.)

$$P_c = 636^k$$

$$\sigma_c = \frac{P_c}{A} = \frac{636}{4.526} = 140.5 \text{ KSI}$$

$$\sigma_b = \frac{Pe}{I/c_2} = \frac{636 \times .0295}{2.168} = 8.8 \text{ KSI}$$

$$\sigma_{TOT} = \sigma_c + \sigma_b = \qquad 149.3 \text{ KSI}$$

$$F_{cy} = 226 \text{ KSI} \quad (\text{REF. TABLE } \underline{\text{IV}})$$

$$M.S. = \frac{F_{cy}}{\sigma_{TOT}} - 1 = \frac{226}{149.3} - 1 = \boxed{\left(\begin{array}{c}\text{COMP.}\\ +\text{BEND}\end{array}\right) + .51}$$

$$b/t \text{ OF WEB. ITEM} ① = 2.36/.25 = 9.44$$

$$F_{cc} \text{ (ONE EDGE FREE)} = 153. \text{ KSI} \quad (\text{REF Pg. M-13})$$

$$M.S. = \frac{F_{cc}}{\sigma_c} - 1 = \frac{153}{140.5} - 1 = \boxed{(\text{CRIPPLING}) + 09}$$

(LOCAL AXIAL + BENDING CHECK) (CONT)

SECTION ④④ (DWG 3109-100001 MARKED UP)
REVISED 3-24-76
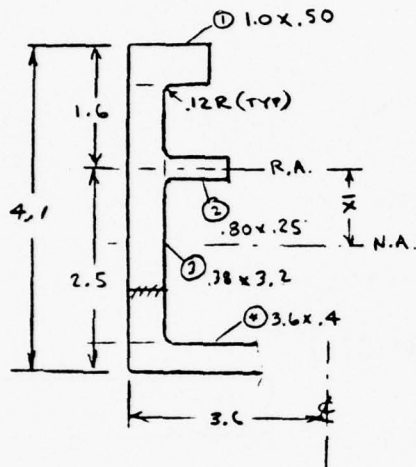
	A	x	Ax	Ax^2	I_{0z}
①	.500	1.35	.675	.9111	.0104
②	.200	0	0	0	.0010
③	1.216	-.50	-.608	.3040	1.0376
④	1.440	-2.30	-3.312	7.6176	.0192
Σ	3.356	-.967	-3.245	8.8327	1.0682
ΣΣ	6.712	-.967	-6.490	17.6654	2.1364

$$I_z = \Sigma A x^2 + \Sigma I_{0z} - \bar{x} \Sigma A_x$$
$$= 19.8018 - 6.2758 = 13.526$$

$C_1 = 1.6 + \bar{x} = 2.567$

$C_2 = 2.5 - \bar{x} = 1.533$

$$I/C_1 = \frac{13.526}{2.567} = 5.269$$

$$\sigma_t = \frac{P}{A} = \frac{914}{6.712} = 136.2 \text{ KSI}$$

$$\sigma_b = \frac{P \bar{x}}{I/c_1} = \frac{914 \times .967}{5.269} = 167.7 \text{ KSI}$$

$$\sigma_{TOT} = \sigma_t + \sigma_b = 303.9 \text{ KSI} \leftarrow \text{TOO HIGH TRY INTERACTION}$$
$$\underline{\underline{M.S. = -.24}}$$
NG.

$$R_t = \frac{\sigma_t}{F_{tu}} = \frac{136.2}{230} = .592$$

$$R_b = \frac{\sigma_b}{F_{tu}} = \frac{167.7}{230} = .729$$

$$MS = \frac{2}{R_b + \sqrt{R_b^2 + 4R_t^2}} - 1 = \frac{2}{.729 + \sqrt{.729^2 + 4 \times .59^2}} - 1 = -\underline{.056}$$
$$\text{(TEN + BEND.)}$$

REVISE SECTION ASSUMPTION - SEE NEXT PAGE

PAGE NO. B-13   REV. _____

344

(LOCAL AXIAL + BENDING CHECK)

SECTION ④④ (CONT.)

ASSUME ONLY EFFECTIVE AREA SUCH THAT
$\bar{x} = 0$ ABOUT REF. AXIS (R.A.)

ITEM	DIM.	A	X	Ax
①	.50 × 1.00	.500	1.35	..675
②	.80 × .25	.200	0	.0
③	b × .38	.33b	x_3	-.675
Σ			$\overline{0}$	0
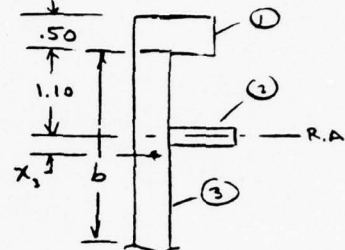
$.38b \times x_3 = -.675$, $x_3 = -\left(\frac{b}{2} - 1.10\right)$

$A_3 x_3 = .38 b \left(\frac{b}{2} - 1.10\right) = .675$

$.19 b^2 - .418 b - .675 = 0$

$b = \dfrac{+.418 + \sqrt{(.418)^2 + 4 \times .675 \times .19}}{2 \times .19} = 3.231$

USE $b = 3.28$ $x_3 = 1.64 - 1.10 = .54$

CHECK $3.28 \times .38 = A_3 = 1.2464$

$A_3 x = 1.2464 \times .54 = 0.6731$

$A_{TOT} = 2 \times (.500 + .200 + 1.2464) =$

2×1.964 $= 3.928$ IN

$\sigma_t = \dfrac{P}{A} = \dfrac{914^k}{3.928} = 232.7$ KSI

M.S. $= \dfrac{F^{tu}}{\sigma_t} - 1 = \dfrac{230}{233} - 1 = \boxed{\left(\frac{LY/LY}{-IN}\right) -.01}$

REV. ITEM ① → $t = .60$ $^3/_8$ OK, SEE NEXT
                                      PAGE –
                                      SEC. ⑥⑥

DWG# 3109-100001

(LOCAL AXIAL + BENDING)

SECTION $\overline{6}$ $\overline{6}$ (REF. MARKED UP DWG 3109-100001)
REVISED 3-24-76

ITEM	A	X	Ax	Ax²	I₀
①	.500	1.35	.675	.9113	.0104
②	.050	0	0	0	—
③	.912	-.10	-.0912	.0091	.4378
Σ	1.462		.5838		
④	.40 b	x₄	-.5838		
Σ	1.8512				
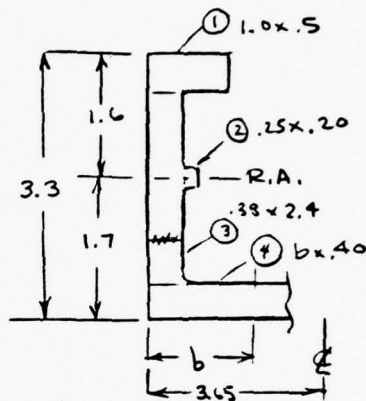
ASSUME SECTION SUCH THAT $\bar{x} = 0$ $\therefore A_4 x_4 = -.5838$

$\therefore .40 b \cdot x_4 = -.5838$ $x_4 = -(1.7 - .20) = -1.5$

$$.40 b (-1.5) = -.5838$$
$$b = .5838 / (.40 \times 1.5) = 0.973$$

CHECK $.40 \times .573 \times 1.5 = .3892 \times (-1.5) = -.5838$ ✓
$$A_4 = .3892$$
$$A_{TOT} = 2 (1.462 + .3852) = 1.8512 \text{ IN}^2 \times 2 = 3.7024 \text{ IN}^2$$

$$\sigma_t = \frac{P_T}{A_{TOT}} = \frac{914^k}{3.7024} = 247 \text{ KSI} \quad \text{N.G.}$$

$$M.S. = \frac{F^{tu}}{\sigma_t} - 1 = \frac{230}{247} - 1 = \text{(TEN)} \quad -\underline{\underline{.07}}$$

INCREASE ITEM ① TO $t = .70$ (~ .50) $A_1 = .70$
$$A_1 x = .70 \times 1 \times 1.45 = 1.015 \quad ; \quad Ax = 1.015 - .0912 = .924$$
$$b = .924 / (.40 \times 1.5) = 1.54 \quad A_4 = 1.54 \times .4 = .616$$
$$A_{TOT} = 2 \times (1.015 + .05 + .912 + .616) = 5.186$$
$$\sigma_t = 914 / 5.186 = 177 \text{ KSI}$$
$$M.S. = \frac{230}{177} - 1 = \boxed{\text{(TEN)} \qquad +.30}$$

PAGE NO. B-15   REV. _____

LOWER TRUSS MEMBER BC

$(X_F 93. \bar{\ })$ $\overset{\text{COND I}}{P = 617^k (c)}$ (REF. PAGE B-4)
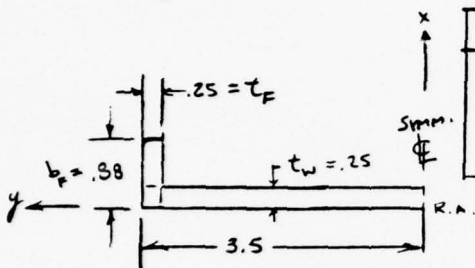
DIM.	A	x	Ax	Ax²	I₀
.25 × .83 × 2	.44	.44	.1936	.08513	.02839
3.25 × .25 × 2	1.625	.125	.2031	.02539	.00846
Σ	2.065	.1921	.3967	0.11157	.03685

$.25 = t_F$

$b_F = .88$

$t_w = .25$

3.5

$\Sigma I_o + \Sigma A x^2 - \bar{x} \Sigma A x = .14842 - .07621$

$I_y = .07221$

$I/c_1 = .07221/(.88 - .192) = .1108$
     .688

$f_c = \dfrac{608^k}{2.065} = \underline{294.5^{ksi}}$! ← TOO HIGH INCREASE AREA

$s/t = \dfrac{\text{SPACING}}{\text{THICK.}} = \dfrac{4}{.25} = 16$, $F_{cc} = 183$ ksi (NA 52-400) $F_{cy} = 204$ MTL

$b/t_w = \dfrac{3.5 \times 2}{.25} = 28$, $F_{cc} = 140$ ksi $\begin{pmatrix} \text{REF.} \\ NA 52-400 \\ F_{cy} = 204 \\ \text{MATERIAL} \end{pmatrix}$

TRY INCREASE $t_w = \dfrac{294}{220 \times .85} \times .25 = .392 = .40$ (WAS .25)

INCREASE $t_F = .40$,   INCREASE $b_F = 1.0$

REV. $A = (3.5 \times .40 + .60 \times .40) \times 2 = 3.28 \, \square''$

$b/t = \dfrac{3.5 \times 2}{.40} = 17.5$, $F_{cc} = 206$ ksi $\begin{pmatrix} C_e = .735 \\ F_{cy} = 206 \\ \text{prelim} \end{pmatrix}$

$f_c = \dfrac{P}{A} = \dfrac{617}{3.28} = 188$ ksi, $\begin{array}{l} F_{cc} = 226 \, (C_e = .315) \\ F_{cc} = 172 \text{ ksi} (C_e = .540) \\ \text{pg n.10} \\ F_{cc} = 183 \text{ ksi (AVG)} \end{array}$

$F_{cc} = 22.$
$b/t = 2.5$

$F_{cc} = 172$
$b/t = 17.5$

M.S. $= \dfrac{F'_{cc}}{f_c} - 1 = \boxed{\text{(CRIPPLING)} \quad +.05}$
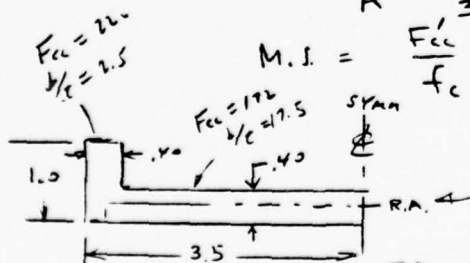
$\Sigma I_o = .40 \times 1^3/12 + 3.1 \times 2 \times .40^3/12 = .0667 - .0331 = .0998$

REVISED ½A = 1 × .4 + 3.1 × .4 = 1.64, $\sigma_c = \dfrac{617}{3.28} = 133$ ksi

REVISED SECTION - USE $t = .40$

AVG $F'_{cc} = \dfrac{172 \times 3.5 + .6 \times 226}{4.1} = 180$ ksi

$\Sigma A x = 1 \times .4 \times .3 = .12 \times 2$ $\bar{x} = .12/1.64 = .073$

$I_z = \Sigma I_o + \Sigma A x^2 - \bar{x} \Sigma A x = .0998 + .072 - .0175 = .1718$; $I/c = \dfrac{.1718}{.273} = .629$

1.0   .40   .40   3.5

PAGE NO. B-16   REV. 3-29-76

LOWER TRUSS MEMBER BC

$(X_F \, 93)$

(COMP + BEND. CHECK)

$$f_c = \frac{P}{A} = \frac{617}{3.28} = 188 \text{ KSI}$$

$$f_b = \frac{Pe}{I/c} = \frac{617 \times .073}{.629} = 72 \text{ KSI}$$

$$f_c + f_b = \qquad 260 \text{ KSI}$$

$$\text{LET } F_b = f_u + f_y (1-k)$$
$$= 226 + 226 \left(1 - \frac{2 \Phi}{I/c}\right) = 226 + 226 \left(1 - \frac{.173 \times 3.5 \times 1 \times .173}{.629}\right)$$
$$= 226 + 226 \,(.170) = \qquad 264 \text{ KSI}$$

$$M.S. = \frac{F_b}{f_{Tot}} - 1 = \frac{264}{260} - 1 = \left| \left(\begin{array}{c} \text{COMP +} \\ \text{BEND.} \end{array}\right) +.015 \right.$$

Rockwell International

PREPARED BY: TM | INBD WING SWEEP
DATE: 3-29-7- | ACTUATOR SUPPORT FITTING | MODEL NO.

DWG# 8109·100001

LOWER TRUSS MEMBER BC

$(x_F \leq 6)$ COND I $\quad P = 564^K$ (C)

$A = .40 \times 1.0 + (3.4 - .4) \times .4 = .40 + 1.2 = 1.6 \times 2 = 3.2$

$Ax = .40 \times (0.50 - .20) = .12$; $\bar{x} = \frac{.12}{1.6} = .075$

$Ax^2 = 2 \times .40 \times .3 \times .3 = .072$

$I_o = 2 \times .40 \times 1^3/12 + 6.0 \times .4^3/12 = .06667 + .0320$
$\qquad\qquad = .09867 \, in^4$

$I_z = \Sigma I_o + \Sigma Ax^2 - \bar{x} \Sigma Ax = .17067 - .005 = .1617 \, in^4$

$I/c_1 = .1617 / (.80 - .075) = 0.2230 \, in^3$; $I/c_2 = \frac{.1617}{.215} = .588$

$\rho_r = \sqrt{.0505} = .2245$

$f_c = \frac{P}{A} = \frac{564}{3.2} = 176 \, ksi \, (C)$

$f_{b_2} = \frac{Pe}{I/c_2} = \frac{564 \times .075}{.588} = 71.9 \, ksi^{(C)} \quad f_{b_1} = \frac{Pe}{I/c_1} = 189.7^{(T)}$

$b/t = \frac{3.4 \times 2}{.4} = 17$, $\quad F_{cc} = 177 \quad\quad C_c = .55$ ⑥
$\qquad\qquad = 226 \, ksi \quad\quad C_c = .312$ ①

$F_{cc \, AVG} = \frac{.40 \times 226 + 1.2 \times 177}{1.6} =$

$\qquad\qquad = 189. \, ksi$

$M.S. = F_{cc}/f_c - 1 = \frac{189}{176} - 1 = \boxed{(\text{CRIPPLING}) +.07}$

(COMP + BENDING CHECK)

TOT $f_b = f_c + f_b = 176 + 72 = 248 \, ksi$ ← TOO HIGH
USE BENDING MODULUS

LET $F_b = f_u + f_o (1-k)$; $K = \frac{2Q}{I_z} = \frac{2 \times .2571}{.588} = .875$
$\qquad = 226 + 226 \left(1 - \frac{2Q}{I/c}\right) =$
$\qquad = 226 + 226 (1 - .875) = 226 + 28 = 254 \, ksi$

$M.S. = \frac{F_b}{f_{TOT}} - 1 = \frac{254}{248} - 1 = \boxed{\left(\begin{array}{c}\text{AXIAL} + \\ \text{BENDING}\end{array}\right) +.02}$

DWG# 3109-100001

LOWER TRUSS MEMBER BC

$(X_F 102)$
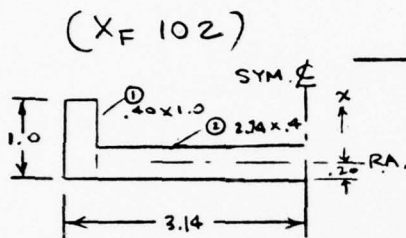
ITEM	A	x	Ax	Ax²	I₀
①	.400	.30	.120	.0360	.0333
②	1.096	0	0	0	.0146
Σ	1.456	.0802	.120	.0360	.0475
ΣΣ	2.992	.0802	.240	.0720	.0958

$I_y = \Sigma I_o + \Sigma Ax^2 - \bar{x}\,\Sigma Ax$

$\quad = .0958 + .0720 - .0802 \times .240 = .06835 \text{ in}^4$

$I/c = \dfrac{.06835}{(1.0 - .2802)} = .09495 \text{ in}^3$

$\rho_r = \sqrt{I/A} = \sqrt{\dfrac{.06835}{2.992}} = \sqrt{.022844} = .1511$

$L'/\rho_r = \dfrac{X_F 107.08 - X_F 95.55}{(\sqrt{4})(.1511)} = \dfrac{11.53}{2 \times .1511} = \dfrac{76.3}{2} = 38.15$

$F_{co} = 172. \text{ ksi} \quad (\text{REF. FIG. 22})$

$f_c = \dfrac{P}{A} = \dfrac{511^k}{2.992} \quad (\text{REF. pg 8-6}) = 170.8 \text{ ksi}$

✳ $M.S. = \dfrac{F_{co}}{f_c} - 1 = \dfrac{172}{170.8} - 1 = \boxed{(\text{COLUMN}) + .01}$

✳ NEGLECTS STABILIZING EFFECT OF SUPPORT STRUCTURE
    (Y_F 932 BKHD WEB)

MEMBER AC

$$P_c = 856^k \, (c) \quad (\text{WAS } 837^k) \quad \text{COND I}$$

$$(\text{SECTION @ } Y_F \, 923.4) \qquad \text{NOTE: OTHER HALF EQUAL AREA}$$

$$A = (1.2 \times .5 + 2.32 \times .2) \times 2$$
$$+ .35 \times 2$$
$$= 2.828 \, \text{in}^2 \, (\text{ONE SIDE})$$

$$\text{TOTAL } A = 2 \times 2.828 = 5.656 \, \text{in}^2$$
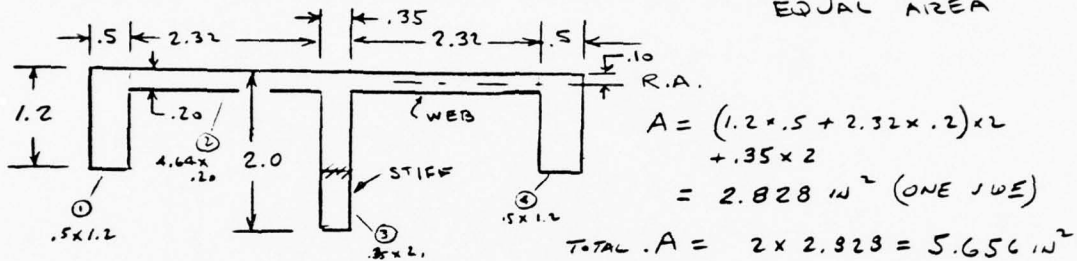
$$f_c = \frac{P_c}{A} = \frac{856}{5.656} = 151 \, \text{KSI} \quad (\text{WAS } 157)$$

$$\text{WEB } \frac{b}{t} = \frac{2.32 + .25 + .175}{.20} = 13.7, \quad F_{cc} = 208 \, \text{KSI} \left\} \begin{array}{c} \text{REF} \\ (\text{FIG. } 25) \end{array} \right.$$

$$\text{STIFF } \frac{b}{t} = \frac{2.0}{.35} = 5.7, \quad F_{cc} = 215 \, \text{KSI} \left\} \quad (\text{WAS } 200) \right.$$

$$M.S. = \frac{F_{cc}}{f_c} - 1 = \frac{208}{151} - 1 = \underline{\underline{(\text{CRIPPLING}) + .37}}$$
$$(\text{WAS } +.27)$$

	A	x	Ax	Ax²	I₀
①	.600	.50	.300	.150	.0720
②	.928	0	0	0	.0031
③	.700	.90	.630	.567	.2333
④	.600	.50	.300	.150	.0720
Σ	2.828	.435	1.230	.867	.3304

$$I_y = .867 + .3304 - .435 \times 1.230 = .7133$$

$$\rho_r = \sqrt{.7133/2.828} = .502$$

$$\frac{L'}{\rho_r} = 10/.502 = 20$$

$$F_{co} = 210 \, \text{KSI} \qquad M.S. = \frac{F_{co}}{f_c} - 1 = \frac{210}{151} - 1 = \underline{\underline{(\text{COLUMN}) + .39}}$$

LUG ANALYSIS

THE LUG WILL BE CHECKED FOR

SHEAROUT, SHEAR-BEARING, NET TENSION, & BENDING

4.38 R
(WAS 4.5*)R

* ANALYSE AS 4.38 R

35.9°

P

X_F 122.75

D = 4.5 (BUSHING)
PIN DIA = 4.125

Y_F 917

1.2 — | 3.44 | ← 1.2
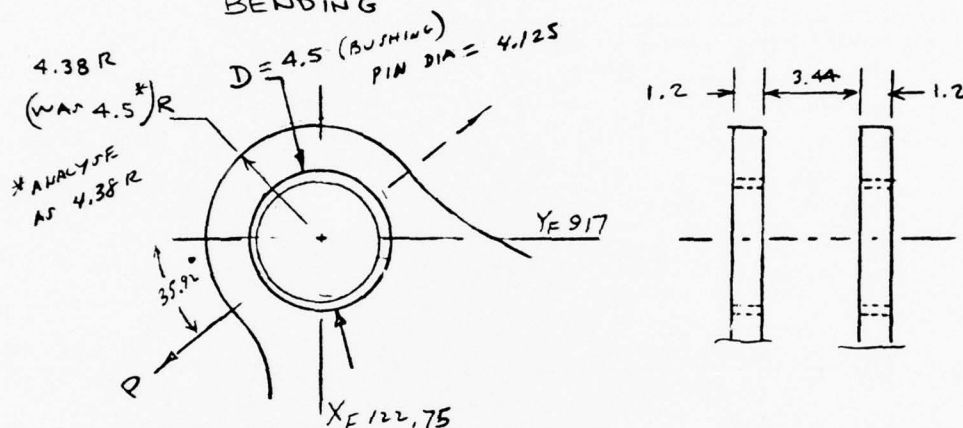
CHECK WITH $D = 4.5$, $t = 1.20$, $R = 4.38$

(SHEAR OUT) LET $F_{su} = 147$ KSI & 60/40 LOAD DISTRIB.
OF $P = 922^k$

$$P^{so} = F^{su}\left(R - \frac{D}{2}\right) 2t$$

$$= 147 \times (4.38 - 2.25) \, 2 \times 1.2 = 750^k / LUG$$

$$P_{LUG} = .60 \times P = .60 \times 922^k = 553^k$$

$$M.S. = \frac{P^{so}}{P_{LUG}} - 1 = \frac{750}{553} - 1 = \boxed{(SHR-OUT) + .36}$$

LUG ANALYSIS (CONT.)

(SHEAR-BRG)

$$D/t = \frac{4.5}{1.2} = 3.75 \; ; \; e/D = \frac{4.38}{4.5} = .973$$

$$K_{br} = .76 \quad (\text{REF. NA 52-400, PG. 6-40.30-4})$$
$$\text{NA 72-1, PG. 24-2.16}$$

$$P_{bru} = K_{br} F_{tu} A_{br}$$

$$= .76 \times 230 \times 4.5 \times 1.2 = 945 \text{ K/LUG}$$

$$P_{LUG} = .60 \times P = 553^k$$

$$M.S. = \frac{P_{bru}}{P_{LUG}} - 1 = \frac{945}{553} - 1 = \boxed{\text{(SHR-BRG)} \quad + .71}$$

USING PIN $A_{br} = 4.125 \times 1.2 = 4.96$

$$P'_{bru} = .76 \times 230 \times 4.96 = 866 \text{ K/LUG}$$

$$M.S. = \frac{P'_{bru}}{P_{LUG}} - 1 = \frac{866}{553} - 1 = \boxed{\text{(SHR BRG)} \quad + .57}$$

(NET TENSION)

LET $W/D = \frac{2 \times 4.38}{4.5} = 1.947$

$$K_t = .94 \quad (\text{REF. NA·52-400, PG. 6.40.30.5})$$

$$P_{tu} = K_t F_{tu} A_t$$
$$= .94 \times 230 \times (4.38 - 2.25) 2 \times 1.2$$

$$= 1106 \text{ K/LUG}$$

$$P_{LUG} = .60 \times P = .60 \times 922 = 553^k$$

$$M.S. = \frac{P_{tu}}{P_{LUG}} - 1 = \frac{1106}{553} - 1 = \boxed{\text{(NET TENSION)} \quad + 1.00}$$

Rockwell International

PREPARED BY: TM	INBD SWEEP ACTUATOR	
DATE: 12-19-75	SUPPORT FITTING	MODEL NO.
REV 4-5-76		DWG# 8109-100001

(LUG ANALYSIS)

(BENDING)

$D = 4.5$

$b = 1.2$

$t = 4.38 - 2.25$
$\quad = 2.13''$
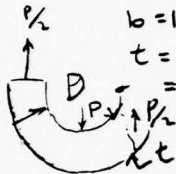
$M = \dfrac{PD}{2 \times 4} = \dfrac{922 \times 4.5}{2 \times 4} = \dfrac{529}{2}$ IN-KIP/LUG

$f_b = \dfrac{6M}{bt^2} = \dfrac{6 \times 529/2}{1.2 \times 2.13^2} = 291$ KSI

$F_b = 1.5 \times F_{ty} = 1.5 \times 215 = 322$ KSI *

$M.S. = \dfrac{F_b}{f_b} - 1 = \dfrac{322}{291} - 1 = \boxed{(\text{BENDING}) \quad +.11}$
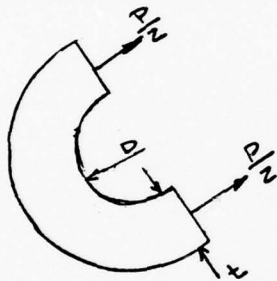
* LATEST PROP $F^{ty} = 215$ PARENT METAL   (WAS $F_{cy} = 220 = F_{ty}$)
(REF TABLE IV)

LUG ANALYSIS (CONT.)

(TRANSV. LOAD CHECK)
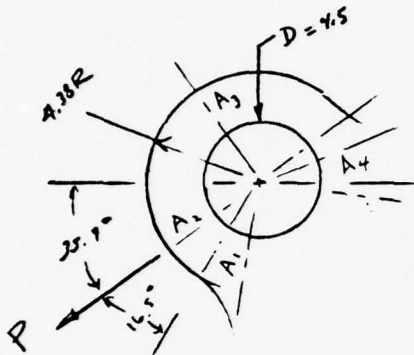
$A_{br} = D t = 4.5 \times 1.2 = 5.4$ IN.^{2}

LET $A_4 = A_1 = (4.5 - 2.25) 1.2 = 2.7$ IN^2

$A_2 = A_3 = (4.38 - 2.25) 1.2 = 2.556$

$A_{AVG} = \dfrac{6}{(3/A_1) + (1/A_2) + (1/A_3) + (1/A_4)}$

$= \dfrac{6}{\dfrac{3}{2.7} + \dfrac{1}{2.556} + \dfrac{1}{2.556} + \dfrac{1}{2.7}}$

$= \dfrac{6}{2.263} = 2.651$ IN^2

$A_{AVG}/A_{br} = {}^{2.651}/_{5.4} = .491$

$K_{tru} = .69$ (NA-72-1, PG. 2Y-2.YY)

$K_{try} = .64$ (" ")

$P'_{tru} = K_{tru} A_{br} F_{tu_x} = .69 \times 5.4 \times 230 = 857. k$

$P'_{try} = K_{try} A_{br} F_{ty_x} = .64 \times 5.9 \times 215 = 743. k$ NOT CRIT

LUG P $= 922^k \times .6 = 553^k$ ULT LOAD/LUG

M.S. $= \dfrac{P'_{tru}}{P} - 1 = \dfrac{857}{553} - 1$ $\boxed{= \left(\begin{array}{c} \text{TRANSV.} \\ \text{LOAD} \\ \text{LUG} \\ \text{SHR-BRG.} \end{array} \right) + .55}$

SEC P-P   WELD CHECK
(see Pg F-14)

$P = 922^k$ assume 50/50 load distribution

$P_S = 922(\cos 35.92) = 746.67^k$

$P_c = 922(\sin 35.92) = 540.896^k$

$A_w = t_w \cdot l_w = .148(5) + .198(2.32)2 + .375(1.20)2 + .375(1.20-.2-.148)2$
$+ .375(.5)2 + .262(3.8-.148)2 = 5.25$

$f_s = \dfrac{746.67}{2(5.25)} = 71.11 \text{ ksi}$ $f_c = \dfrac{540.29}{2(5.25)} = 51.5 \text{ ksi}$

$R_s = \dfrac{71.11}{125} = .589$ $R_c = \dfrac{51.5}{192} = .267$

$$M.S. = \dfrac{1}{\sqrt{R_s^2 + R_c^2}} - 1 = \boxed{(\text{SHEAR} + \text{COMPRESSION}) = \underline{+0.589}}$$

PREPARED BY _____ INBD SWEEP ACTUATOR

DATE _____ SUPPORT FITTING _____ MODEL NO. _____

$P = 642^k$

DWG# 3109-10000 1

$P_S = 642 (\cos 35.92) = 519.92^k$

$P_T = 642 (\sin 35.92) = 376.63^k$

* ASSUME 60/40 LOAD DISTRIBUTION

$\dfrac{P_S}{2} = 259.96^k$ $\qquad$ $\dfrac{P_T}{2} = 188.32^k$ $\qquad\qquad$ $A_W = 5.25$

$f_S = \dfrac{259.96}{5.25} = 49.52^{ksi}$

$f_T = \dfrac{188.32}{5.25} = 35.87^{ksi}$

$R_S = \dfrac{49.52}{125} = .396$

$R_T = \dfrac{35.87}{196} = .183$

$M.S. = \dfrac{1}{\sqrt{R_S^2 + R_T^2}} - 1 \quad \Big|$ = (SHEAR + TENSION)

$= +1.29$

REV. _____

SEC W'-W'

$\ell_w \approx .40"$
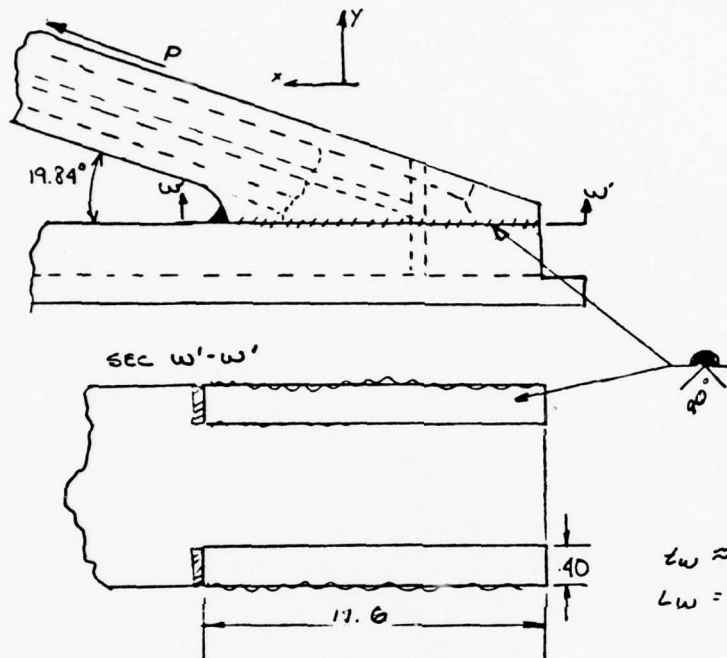
$L_w = 11.6 / SIDE \; 5"$

$P = 914^K \; (T)$

$P_x = 914 (\cos 19.84) = 859.77^K$

$P_y = 919 (\cos 19.84) = 310.197^K$

$\dfrac{P_x}{2} = 430^K$ $\dfrac{P_y}{2} = 155^K$

50/50 LOAD DIST. TO EACH HALF.

$A_w = 11.6 \times (.4) = 4.64 \; IN^2$

$f_x = \dfrac{430}{4.64} = 93 \; KSI = f_s$

$f_y = \dfrac{155}{4.64} = 33 \; KSI = f_t$

$R_s = f_s / F_{su} = {}^{93}/_{125} = .744$; $R_T = {}^{33}/_{196} = .168$

$M.S. = \dfrac{1}{\sqrt{R_s^2 + R_T^2}} - 1 =$ (WELD SHR+TEN) $\boxed{+ .31}$

DWG.# 3109-100003

INBOARD WING SWEEP ACTUATOR
FITTING - MACHINED FORGING
STIFFENED WEB DESIGN

PREPARED BY: TM | INBD WING SWEEP
REV 4-23-76
DATE: 4-6-76 | ACTUATOR FITTING | LOCOSST

MACHINED FORGING | MODEL NO. 3105-100003 - DATED 4-17-76

LOADS DEVELOPMENT

3109-100001-1
REV 4-12-76

(REACTIONS)

COND ① $P_{ACT} = +922^k$ $\qquad P_{ACT}^Y = 541^k$, $P_{ACT}^X = 747$

$R_2 = 922 \times \left(\sin 35.917° \times 1.88/36.82 + \cos 35.917° \times 14.35/36.82\right)$

$\qquad = 541 \times 1.88/36.82 \downarrow + 747 \times 14.35/36.82^\leftarrow = 27.6 + 292$

$\qquad\qquad = 320. \quad^k \downarrow$

$R_1 = 541 \times 38.7/36.82^\uparrow + 747 \times 14.35/36.82^\uparrow = 568 + 292$

$\qquad\qquad = 860. \quad^k \uparrow$

$R_3 = 922 \times \cos 35.917° = 746.9 = 747^k \longrightarrow$

COND ② $P_{ACT} = -642^k$

$\qquad R_2 = \left(642/922\right) \times 320 = 223.^k \uparrow$

$\qquad R_1 = \left(642/922\right) \times 860 = 600.^k \downarrow$

$\qquad R_3 = \left(642/922\right) \times 747 = 520.^k \leftarrow$

$\qquad COND Ⓑ/COND Ⓐ = .697$

Rockwell International

PREPARED BY: TM | INBD WING SWEEP | LOCOSST
DATE: 4.23.76 | ACTUATOR FITTING | MODEL NO.
3109-150003-4-27-76
3109-150001-1
REV. 4-12-76

LOADS DEVELOPMENT

(CAP AREAS, WEB HEIGHTS & FASTENER SIZES)

COND I - $P_{ACT} = 922^k$ ULT.

A_C = UPPER CAP AREA

X_F 122.75

$R_3 = 747^k$

$R_1 = 860^k$

$R_3 = 747^k$

$320^k = R_2$

X_F 82.05

A_B = LOWER CAP AREA
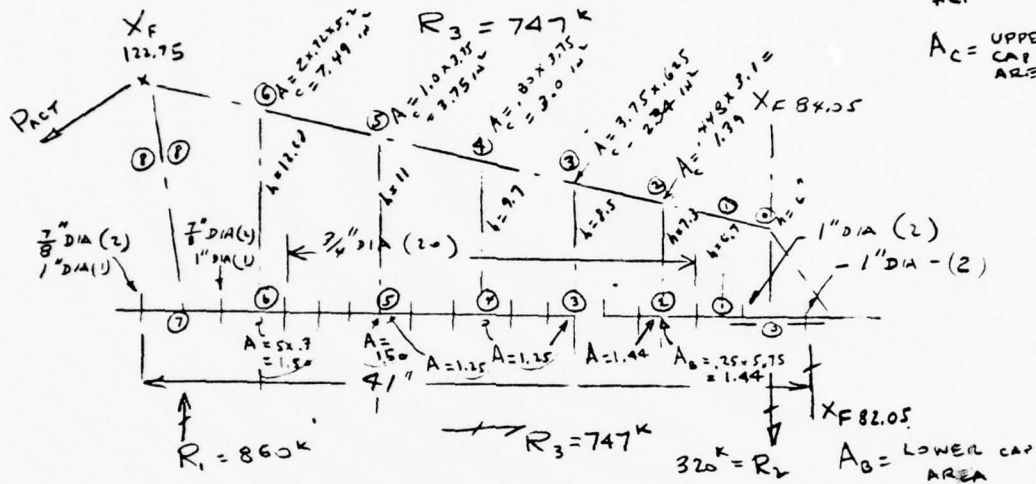
CASE (A) - LET R_3 BE DISTRIB. PROPORTIONAL TO FASTENER AREAS OR ALLOWABLES

CASE (B) - LET R_3 BE REACTED BY UNIFORM SHEAR FLOW OVER $L = 41"$

$$q = \frac{R_3}{L} = \frac{747}{41} = 18.22^{k/IN}$$

(CAP LOADS, WEB SHEARS)

	⑦	⑥	⑤	④	③	②	①	⓪	⓪'	
P'_U (k)	864^k	799^k	693^k	577^k	445^k	272^k	159^k	0		
P_U (k)	845	730	678	564	435	265	155	0		← HORIZ COMPONENT
P_L	-195	-223	-245	-214	-168	-77	-3	+73.5		← CASE (A)
P_L	-135	-180	-216	-216	-188	-118	-59	+36		← CASE (B)
q (k/in)	9.9	12.0	16.3	20.4	26.6	36.0	42.3	53.3		WEB
X_F	120.87	115	101.4	101.2	95.6	90.1	87.3	84.05		

PREPARED BY: T M | INBD WING SWEEP |
4-22-76
DATE: 4-6.76 | ACTUATOR FITTING | LOCOSST
MODEL NO.

3109 - 100003
3109 - 100001 - 1
REV. 4-12-76
DATED 4-27-76

LOADS DEVELOPMENT
(ATTACHMENT LOADS)

CASE Ⓐ ASSUME SHEAR R_3 REACTED PROPORTIONAL TO ALLOWABLES OR SHEAR AREA OF FASTENERS

P^{su} = DIA $\frac{3}{4}$" ALLOW = 55^k ; $\frac{7}{8}$" = 75^k ; 1" = 98^k

X_F	120.57$^{\pm}$	111.3	104.3	98.5	93	88.7	84.05$^{\pm}$
FASTEN.	(4) $\frac{7}{8}$" +(2) 1"	(6) $\frac{3}{4}$"	(4) $\frac{3}{4}$"	(4) $\frac{3}{4}$"	(4) $\frac{3}{4}$"	(2) $\frac{3}{4}$"	(4) 1"
SHR ALLOW	436^k	330^k	220^k	220^k	220^k	110^k	392^k
t	.40	.30	.25	.25	.25	.25	.40
MIN. BRG t_{REQ}^*	.24/.275	.207	.207	.207	.207	.207	.275

Σ ALLOW = 1933 K

PROPORTION = .249 | .166 | .111 | .111 | 111 | .0553 | .197

* BRG $t_{REQ} = \dfrac{P^{su}}{D \times F^{brg}} = \dfrac{P^{su}}{D \times 357}$; $R_3 = 747^k$

| $\Delta R_3'$ | 186^k | 124^k | 83^k | 83^k | 83^k | 41^k | 147^k |

CASE Ⓑ ASSUME UNIFORM SHEAR DISTRIB. FOR R_3 OVER L = 41

$q = 747/41 = 18.22$ K/IN

| $\Delta R_3'$ | 149^k (8.2) | 135^k (7.4) | 114^k (6.15) | 101^k (5.5) | 102^k (5.6) | 51^k (2.8) | 95^k (5.2) |

(ATTACH. CHECK AT X_F 84.05)

(4) 1" DIA FASTENERS $P^{su} = 98$ K , $P^{tu} = 141$ K

$R_2 = 320^k$ TEN.

$R_3' = 147^k$ SHEAR - CASE Ⓐ

$R_T = 320./141 \times 4 = .568$

$R_S = 147/98 \times 4 = .376$

ASSUME CIRCULAR INTERACTION

$M.S. = \dfrac{1}{\sqrt{R_T^2 + R_S^2}} - 1 = \dfrac{1}{.682} - 1 = \boxed{\begin{pmatrix} \text{ATTACH.} \\ \text{SHR} \& \\ \text{TEN.} \end{pmatrix} + .46}$

(OTHER FASTENERS NOT AS CRITICAL BY INSPECTION)

PAGE NO. B-31

REV. 4-22-76

Rockwell International

PREPARED BY: TM   INBD WING SWEEP

DATE: 4-23-76   ACTUATOR FITTING

LOCOSST
MODEL NO.
3109-100003
3109-100001-1
REV 4-12-76

SECTION CHECK AT X_F 84.05 & X_F 87.3 ① ①

(WEB CHECK)

$$q = \frac{R_L}{h} = \frac{320}{6} = 53.3 \text{ k/in}$$

$$f_s = \frac{q}{t} = \frac{53.3}{.40} = 133. \text{ ksi}$$

(REF FIG 24) LET $b/t = 6.7/.40 = 16.8$, $F_{s,cr} = F_{su} = 147$ ksi

$$M.S. = F_{su}/f_s - 1 = \frac{147}{133} - 1 = \boxed{\begin{array}{c}\text{WEB}\\(\text{SHEAR})\end{array} + .10}$$
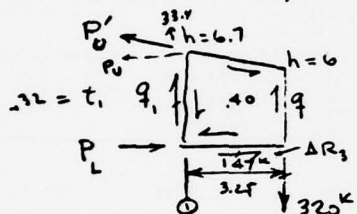
$$P_u = \frac{3.25 \times 320}{6.7} = 155.2^k$$

$$P_u' = \frac{3.25 + .7}{3.25} \times 155.2 = 158.8^k \text{ (T)}$$

$$P_L = -P_u + \Delta R_3 = -155.2 + 147 = -8.2^k \text{ (C)} \quad \text{CASE Ⓐ}$$

$$q_1 = \frac{320 - 155.2 \times \frac{.7}{3.25}}{6.7} = \frac{320 - 33.4}{6.7} = 42.8 \text{ k/in}$$

$$f_{s_1} = \frac{q_1}{t_1} = \frac{42.8}{.32} = 133.75 \text{ ksi}$$

LET $b_1/t_1 = \frac{(7.3 + 6.7).5}{.32} = 21.9 \checkmark$ OR $\frac{3.25 + 2.8}{.32} = 18.90$

$$F_{s,cr} = 141 \text{ ksi} \quad (\text{REF. FIG. 24})$$

$$M.S. = F_{s,cr}/f_{s_1} - 1 = \frac{141}{133.8} - 1 = \boxed{\begin{array}{c}\text{WEB}\\(\text{SHEAR}\\\text{BUCKLING})\end{array} + .05}$$

SECTION CHECK AT X_F 90.1 ② ②

$$P_u = \frac{2.8 \times (236.6 + 33.4) + 155.2 \times 6.7}{7.3}$$

$$= 122.7 + 142.4 = 265.1$$
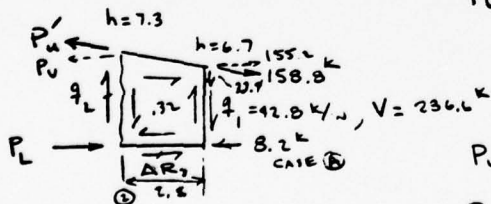
$$P_u' = \frac{2.8 + .6}{2.8} \times 265.1 = 271.1^k \text{ (T)}$$

$$P_L = -P_u + \Delta R_1 - P_{Lu} + P_{uu}$$
$$= -265.1 + 41 - 3.2 + 155.2$$
$$= -77.1^k \text{ (C)} \quad \text{CASE Ⓐ}$$

Rockwell International

PREPARED BY: TM	INBD SWEEP ACTUATOR	
DATE: 4-27-76	SUPPORT FITTING	LOCOSST
		MODEL NO.
		3109-100003
		3109-100001-1
		REV 4-12-76

SECTION CHECK AT X_F 90.1 ②① (CONT.)

$$h_2 q_2 = q_1 \times 6.7 + 155.2 \times \frac{6}{2.8} \quad , \quad -P_U \times \frac{6}{2.8}$$

$$q_2 = \frac{1}{7.3} \left(320 - 265.1 \times \frac{6}{2.8} \right) = \frac{263}{7.3} = 36 \, {}^K/_{IN}$$

$$f_{s_2} = q/t = {}^{36}/.32 = 112.3 \, KSI \qquad OK$$

(UPPER CAP CHECK AT ②) $f_T = \frac{P_U'}{A_c} = \frac{271.1}{.448 \times 3.10} = \frac{271.}{1.39} = 195 \, KSI$

$$b_F/t_F = \frac{1.55}{.448} = 3.46 \, , \quad F_{cc} = F_{cy} = 226 \, KSI \, , \quad F^{tu} = 230 \, KSI$$

$$M.S. = \frac{F_{tu}}{f_t} - 1 = \frac{230}{195} - 1 = \boxed{\begin{array}{c}(\text{TENSION} \\ \text{FLANGE}) + .18 \\ \text{UPPER}\end{array}}$$

(LOWER CAP CHECK AT ①) $f_c = \frac{P_L}{A_D} = \frac{72.1}{1.51} = 51 \, KSI \qquad \text{CASE Ⓐ}$

CASE Ⓑ UNIFORM & REACTION $P_L = 265 - 18.22 \times 8.05 = 265 - 147 = 118^K, \, f_c = 78 \, KSI$

$$\frac{b}{t} = \frac{6.04}{2 \times .25} = 12.1 \, , \quad F_{cc} = 120 \, KSI \, (\text{ONE EDGE FREE}) \, (\text{REF. FIG. 25})$$

$$M.S. = \frac{F_{cc}}{f_c} - 1 = \frac{120}{78} - 1 = \boxed{\begin{array}{c}(\text{CRIPLING}) + .46 \\ \text{CONSERV. OMIT}\end{array}}$$

$$s/t = \frac{2.9}{.25} = 11.6 \, , \quad F_{cr}^{IR} = 210 \, KSI \, (\text{REF. FIG. 23})$$

$$M.S. = \frac{F^{IR}}{f_c} - 1 = \frac{210}{78} - 1 = \boxed{\begin{array}{c}(\text{INTER RIVET}) + 1.69 \\ \text{BUCKLING}\end{array}}$$

SECTION CHECK - X_F 95.63 ②③
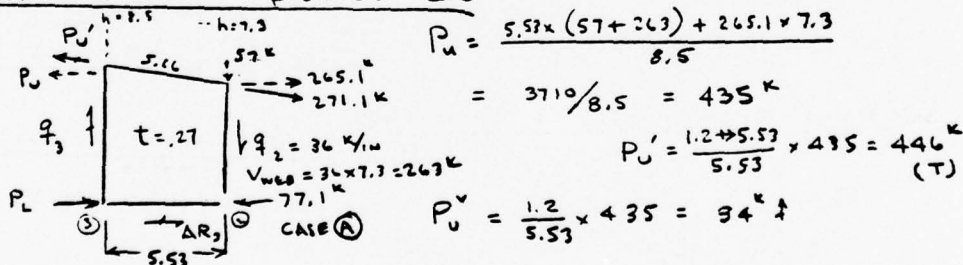
$$P_U = \frac{5.53 \times (57 + 263) + 265.1 \times 7.3}{8.5}$$

$$= 3710/8.5 = 435^K$$

$$P_U' = \frac{1.2 \leftrightarrow 5.53}{5.53} \times 435 = 446^K \quad (T)$$

$$P_U^V = \frac{1.2}{5.53} \times 435 = 94^K \uparrow$$

$$V_{WEB} ③ = 57 + 263 - 94 = 320 - 94 = 226^K$$

$$q_3 = {}^{226}/_{8.5} = 26.6 \, {}^K/_{IN}$$

CASE Ⓐ $P_L = -P_U - 77.1 + 265 + \Delta R_3 = -439 - 77 + 265 + 83 = 168^K \, (\cup)$

CASE Ⓑ $P_L = -P_U + 18.22 (95.63 - 82.35) = -435 + 247 = -188^K \, (C)$
$$\underset{13.56}{}$$

Rockwell International

PREPARED BY: TM
DATE: 4-28-76

INBD SWEEP ACTUATOR
SUPPORT FITTING

MODEL NO.
3109-100003
DATED 4-27-76

SECTION CHECK - X_F 95.63 ③③ (CONT)

(WEB CHECK) $t = .27$ $b/t = {}^{5.6}/.27 = 20.8$

$F_{s,cr} = 140$ KSI   (REF. FIG. 24)

$f_{s_{AVG}} = \dfrac{(q_3 + q_2).5}{t} = \dfrac{(26.6 + 30)}{2} \times \dfrac{1}{.27} = 116$ KSI, NG

$f_{s_{MAX}} = \dfrac{q_2}{t} = \dfrac{36}{.27} = 133$ KSI   CASE Ⓐ

M.S. $= \dfrac{F_{s,cr}}{f_s} - 1 = \dfrac{140}{133} - 1 = \boxed{\genfrac{}{}{0pt}{}{\text{(SHR.}}{\text{BUCKLING)}} + .05}$

(UPPER CAP) $f_t = \dfrac{P'_U}{A_c} = \dfrac{446}{2.34} = 191.$ KSI $F^{tu} = 230$ KSI

$b/t = \dfrac{3.75}{2 \times .625} = 3.,$ $F_{cc} = 226$ KSI   (REF. FIG 25)

$f_c = .697 f_t = 134$ KSI

M.S. $= \dfrac{F_{tu}}{f_t} - 1 = \dfrac{230}{191} - 1 = \boxed{\text{(TENSION)} + .20}$

(LOWER CAP) $f_c = \dfrac{P_L}{A_{MIN}} = \dfrac{188.}{1.29} = 146$ KSI (C),   CASE Ⓑ $P_L = 164^K$ CASE Ⓐ $f_c = 128$ KSI
$X_F 95.63+$

$b/t = \dfrac{5.16}{2 \times .25} = 10.3,$ $F_{cc} = 138$ KSI (REF. FIG. 25)

M.S. $= \dfrac{138}{146} - 1 = $ (CRIPPLING) $- .05$ ← CONSERV. CHECK INTER-RIVET BUCKLING

TRY $t = .3$ $b/t = \dfrac{5}{2 \times .30} = 8.3,$ $F_{cc} = 160$ KSI

$f_c = \dfrac{188}{5 \times .3} = 125$ KSI,   OK.

$s/t = {}^{2.9}/.25 = 11.6,$ $F^{IR}_{cr} = 210$ KSI   (REF. FIG 24)

M.S. $= \dfrac{F^{IR}}{f_c} - 1 = \dfrac{210}{146} - 1 = \boxed{\genfrac{}{}{0pt}{}{\text{(INTER-RIVET}}{\text{BUCKLING)}} + .43}$

CASE Ⓑ

CWG #   3109·100003

SECTION CHECK. X_F 101.15 ④④
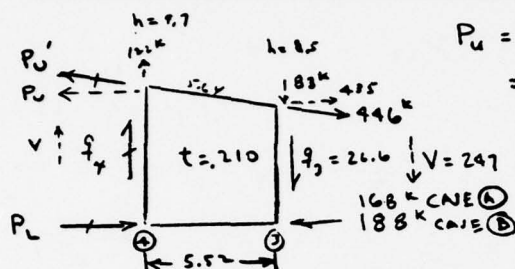
$$P_u = \left[5.52(83+247) + 435 \times 8.5\right] \div 9.7$$
$$= 5460/9.7 = 564^k$$

$$P_u' = \frac{1.2 + 5.52}{5.52} \times 564 = \underline{577^k}$$

$$P_u^v = \frac{1.2}{5.52} \times 564 = 122^k$$

$$V = 247 + 83 - 122 = 198^k$$

$$q_4 = \frac{V}{9.7} = \frac{198}{9.7} = \underline{20.4}\ ^{k/in}$$

$$P_L = 435 - 564 - 168 + 83^k = \qquad -214^k \text{ CASE } Ⓐ$$

$$P_L = -564 + 18.22(X_F 101.15 - X_F 82.05) = \qquad -216^k \text{ CASE } Ⓑ$$

(WEB CHECK) $t = .210$ $f_s = \frac{q_{AVG}}{.210} = \frac{(20.4 + 26.6)}{2 \times .210} = 112$ KSI

$f_{s \, MAX} = q_3/.210 = 266/.210 = 126.6$ KSI

$$b/t = \frac{5.52}{.210} = 26.3, \quad F_{s,cr} = 135 \text{ (REF FIG. 24)}$$

$$M.S. \text{ (SHR. BUCKLING)} = \frac{F_{scr}}{f_s} - 1 = \boxed{+ .07}$$

(UPPER CAP) $A = .80 \times 3.75 = 3.0$ IN²

$$f_t = P_u''/A = 577/3 = 193 \text{ KSI}, \quad F^{tu} = 230 \text{ KSI}$$

$$f_c = \frac{642}{922} \times f_t = -134 \text{ KSI}$$

$$b/t = \frac{3.75}{2 \times .8} = 2.34, \quad F_{cc} = F_{cy} = 226 \text{ KSI}$$

$$M.S. \text{ (CAP. TENSION)} = \frac{F^{tu}}{f_t} - 1 = \frac{230}{193} - 1 \boxed{+.19}$$

(LOWER CAP) $A' = 5.14 \times .25 = 1.29$ ▢" ,

$$f_c = P_L/A' = 216/1.29 = 167 \text{ KSI}; \text{ CASE } Ⓑ$$

$$b/t = \frac{5.14}{2 \times .25} = 10.3, \quad F_{cc} = 139 \text{ KSI}; \quad s/t = 11.6, \quad F_{cr}^{IR} = 210 \text{ KSI}$$

M.S. (CRIPPLING) = $\underline{-.17}$ ← CONSERV. CHECK → $\boxed{M.S. = \frac{210}{167} - 1 = \binom{\text{INTER}}{\text{RIVET}}_{\text{BUCKLING}} +.26}$

DWG# 2109-100003

SECTION CHECK - X_F 107.4 ③⑤ h = 11.0
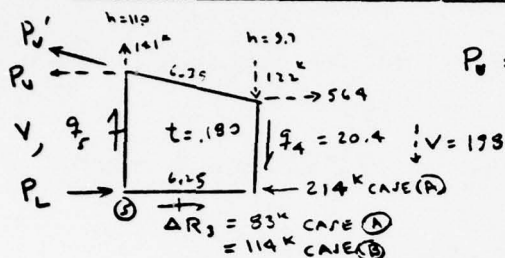
$$P_u = [6.25(122+198)+564 \times 9.7] \div 11.0$$
$$= 7460/11.0 = \underline{678^k}$$

$$P_u' = \frac{(1.3+6.25)}{6.25} \times 678 = \underline{695^k}$$

$$P_u^v = \frac{1.3}{6.25} \times 678 = 141^k$$

$$V = 198 + 122 - 141 = 175^k; \quad q_s = \frac{179}{11.0} = \underline{16.3 \text{ K/IN}}$$

$$P_L = -678 + 564 - 214 + 83 = -245^k \text{ CASE } Ⓐ$$

$$P_L = -678 + 18.22 (X_F 107.4 - X_F 82.05) = -216^k \text{ CASE } Ⓑ$$

(WEB CHECK) $t = .180$, $b/t = 6.25/.180 = 34.7$

$$F_{scr} = 122 \text{ KSI} \quad (\text{REF. FIG. 24})$$

$$f_s = \frac{q_a}{t} = \frac{20.4}{.180} = 113. \text{KSI}$$

$$M.S. = \frac{F_{scr}}{f_s} - 1 = \frac{122}{113} - 1 = \boxed{\binom{\text{WEB}}{\text{SHEAR}} + .08}$$

(UPPER CAP) $A = 1.0 \times 3.75 = 3.75 \text{ IN.}^2$

$$f_T = P_u'/A = 693/3.75 = 185. \text{KSI}$$

$$F^{tu} = 230. \text{KSI}$$

$$M.S. = \frac{F^{tu}}{f_T} - 1 = \frac{230}{185} - 1 = \boxed{(\text{TENSION}) + .24}$$

(LOWER CAP) $\qquad A = 5.16 \times .25 = 1.29 \text{ IN}^2$

$$f_c = P_L/A = 245/1.29 = 190. \text{KSI CASE } Ⓐ$$

$\left(\frac{b}{t} = \frac{5.16}{2 \times .25} = 10.3\right)$ $F_{cc} = 138 \text{ KSI} \leftarrow \text{CONSERV. CHK.} \boxed{(\text{CRIPPING}) - .27}$

$\qquad\qquad\qquad\qquad$ CHECK INTER FASTENER BUCKLING

$\left(\frac{s}{t} = \frac{2.9}{.25} = 11.6\right)$ $\bar{F}_{cr}^{ir} = 210 \text{ KSI} \quad (\text{REF. FIG. 23})$

$$M.S. = \frac{F_{cc}^{ir}}{f_c} - 1 = \frac{210}{190} - 1 = \boxed{\binom{\text{INTER}}{\text{RIVET}}_{\text{BUCKLING}} + .10}$$

CWF# 3109-100003
REV. A

SECTION CHECK - X_F 115. ⒶⒷ h = 12.68"

$P_U = \left[7.4(141 + 179) + 678 \times 11.0 \right] \div 12.68$

$= 780$

$P_U' = \frac{12.68 + 7.4}{7.4} \times 780 = 798^k$

$P_U^v = \frac{1.68}{7.4} \times 780 = 177^k$
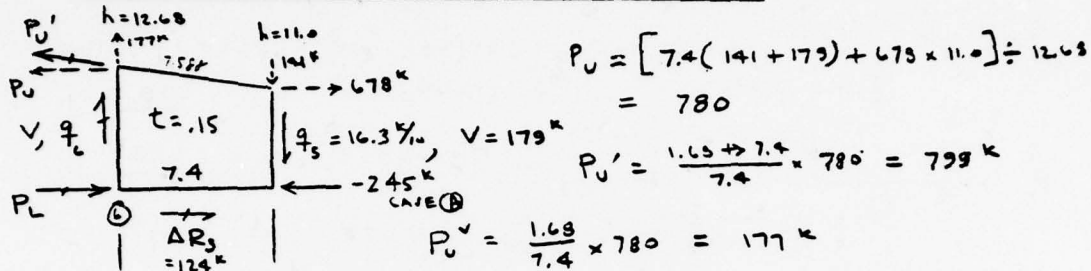
$V = 141 + 179 - 177 = 143^k$; $q_c = \frac{V}{12.68} = 11.28 \,^k/in$

$P_L = -780 + 678 - 245 + 124^k = -223^k$ CASE Ⓐ

$P_L = -780 + 18.24 (X_F 115 - X_F 82.05) = -180$ CASE Ⓑ

(WEB CHECK) $t = .15$, $b/t = 7.4/.15 = 49.3$

$F_{s,cr} = 77.5 \, ksi$ ←

MAX $f_s = q_s/t = {}^{16.3}/.15 = 109 \, ksi$ ← NG.

AVG $f_s = 13.79/.15 = 91.3 \, ksi$.

TRY $t = .17$, $b/t = 7.4/.17 = 43.5$

$f_s = \frac{16.3}{.17} = 96. \, ksi$, $F_{scr} = 99 \, ksi$ (REF. FIG. 24)

$M.S. = \frac{F_{scr}}{f_s} - 1 = \frac{99}{96.} - 1 = \boxed{\begin{array}{c}(SHR.\\BUCKLING)\end{array} +.03}$

USE $t = .17$

(UPPER CAP) $A = 2 \times .72 \times 5.2 = 7.43 \, in^2$

$f_T = P_U'/A = 798/7.43 = 106.5 \, ksi$

$F^{tu} = 230 \, ksi$

$M.S. = \frac{F^{tu}}{f_T} - 1 = \frac{230}{106.5} - 1 = \boxed{(TEN.) \quad 1.16}$

(LOWER CAP) $A' = 5 \times .30 = 1.50 \; (t = .30)$; $A = 5.16 \times .3 = 1.548 \, in^2$

$f_c = P_L/A' = 223/1.5 = 149. \, ksi$ CASE Ⓐ

$b'/t = \frac{5}{2 \times .3} = 8.33$, $F_{cc} = 160. \, ksi$ (CRIPPLING) $+.07$ ← CONSERV.

$s/t = \frac{2.9}{.3} = 9.67$, $F_{cr}^{ir} = 217 \, ksi$

$M.S. = \frac{F_{cc}^{ir}}{f_c} - 1 = \frac{217}{149} - 1 = \boxed{\begin{array}{c}(INTER.\\RIVET\\BUCKLING)\end{array} +.45}$

PAGE NO. B-37   REV.

SECTION CHECK AT Y_F 923.35 ⑧ⓕ
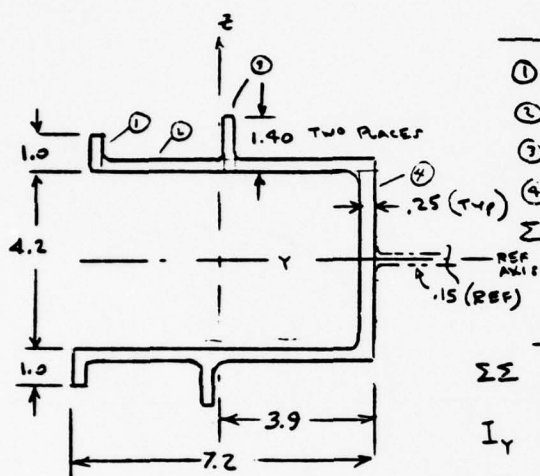
	A	z	Az	Az²	I₀
①	.250	2.6	.650	1.690	.0208
②	1.675	2.22	3.720	8.250	.0087
③	.350	2.8	.980	2.740	.0572
④	.525	1.05	.551	.579	.1925
Σ	2.800	/	5.901	13.259	.2792
	2.800		-5.901	13.259	.2792
ΣΣ	5.60	—	0	26.519	.5584

$$I_Y = 26.519 + .5584 = 27.076 \text{ IN}^4$$

$$A = 5.60 \qquad \rho_r = \sqrt{I/A} = 2.2$$

$$P = R_1 \frac{1.88 + 14.35}{14.35} = \frac{14.473}{14.35} \times 860 = 867^k$$

$$P_s = \frac{1.88}{14.35} \times 860 = 113^k$$

$$f_c = P/A = \frac{867}{5.6} = 155 \text{ KSI}$$

$$b/t = 1.40/.25 = 5.6 \text{ (ONE EDGE FREE)}, \quad F_{cc} = 220 \text{ KSI}$$

$$b/t = 4.7/.25 = 18.8 \text{ (NO EDGE FREE)}, \quad F_{cc} = 163 \text{ KSI}$$

$$\text{M.S. (CRIPPLING)} = \frac{F_{cc}}{f_c} - 1 = \frac{163}{155} - 1 = \boxed{+.05}$$

Rockwell International

PREPARED BY: TM | INBD SWEEP ACTUATOR |
DATE: 5.4.76 | SUPPORT FITTING | LOCOSST
MODEL NO.

3109-100003
DATED 4-27-76

LUG ANALYSIS
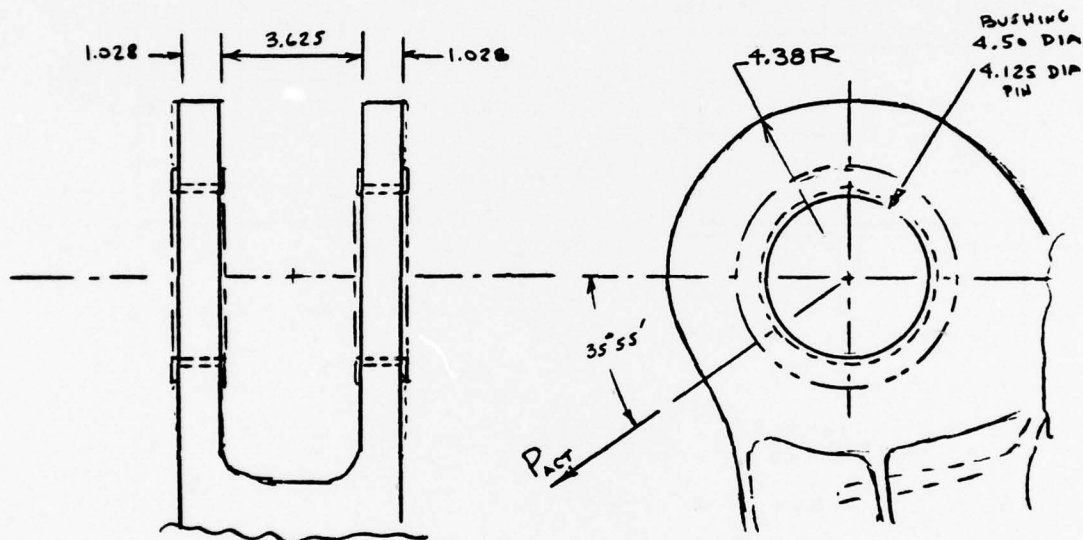
COND I

$P_{ACT} = 922^k$, $D = 4.5$, $t = 1.028$, $R = 4.38$

(SHEAROUT) LET $F_{su} = 147$ KSI (REF. TABLE Ⅳ -)
& 60/40 DISTRIB. OF $P_{ACT} = 922^k$

$P^{so} = F^{su} \left(R - \frac{D}{2} \right) 2t$

$= 147 \left(4.38 - \frac{4.50}{2} \right) 2 \times 1.028 = 644^{k}/LUG$

APPLIED $P_{LUG} = .60 \times 922 = 553^k$

$M.S. = \dfrac{P^{so}}{P_{LUG}} - 1 = \dfrac{644}{553} - 1 = \boxed{(SHR\text{-}OUT) \ +.16}$

Rockwell International

PREPARED BY: TM   INBD SWEEP ACTUATOR

DATE: 5-4-76   SUPPORT FITTING

MODEL NO.
.3109-100003
DATED 4-27-76

LUG ANALYSIS (CONT.)

(SHEAR-BRG)

$$D/t = 4.5/1.026 = 4.39 \quad ; \quad e/D = \frac{4.38}{4.5} = .973$$

$$K_{br} = .73 \quad (\text{REF. NA 72-1, PG. 24-2.16})$$

$$P_{bru} = K_{br} F_{tu} A_{br} = .73 \times 230 \times 4.5 \times 1.026 = 775 \, ^k/\text{LUG}$$

$$P_{LUG} = .60 \times P = 553^k$$

$$M.S. = \frac{P_{bru}}{P_{LUG}} - 1 = \frac{775}{553} - 1 = \boxed{\left(\begin{array}{c}\text{SHR-}\\\text{BRG}\end{array}\right) \quad +.40}$$

(NET TENSION)

$$\text{LET } W/D = \frac{2 \times 4.38}{4.5} = 1.947$$

$$K_t = .97 \quad (\text{REF NA 72-1, PG. 24-2.17})$$

$$P_{tu} = K_t F_{tu} A_t = .97 \times 230 \times (4.38 - 2.25) 2 \times 1.026$$
$$= 975. \, ^k/\text{LUG}$$

$$P'_{LUG} = .60 \times P = 553^k$$

$$M.S. = \frac{P_{tu}}{P_{LUG}} - 1 = \frac{975}{553} - 1 = \left(\begin{array}{c}\text{NET}\\\text{TEN}\end{array}\right) \quad + .76$$

(SHEAR-BRG)

WING PIN DIA. 4.125

$$P'_{bru} = .73 \times 230 \times 4.125 \times 1.026 = 712^k$$

$$P_{LUG} = 553^k$$

$$M.S. = \frac{P'_{bru}}{P_{LUG}} - 1 = \frac{712}{553} - 1 = \boxed{\left(\begin{array}{c}\text{SHR-}\\\text{BRG}\end{array}\right) \quad + .29}$$
$$\text{CONSERV.}$$

PAGE NO. B-40   REV. ____

LUG ANALYSIS (CONT.)

(TRANSVERSE LOAD CHECK)
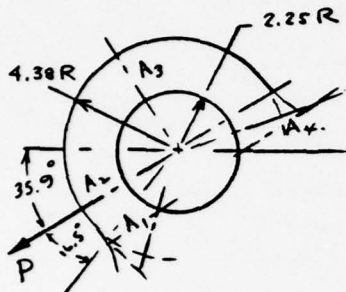
$A_{br} = Dt = 4.5 \times 1.026 = 4.61 \, \text{IN}^2$

LET $A_4 = A_1 = 2.6 \times 1.026 = 2.66 \, \text{IN}^2$

$A_2 = A_3 = \dfrac{(4.38 - 2.25)}{2.13} \, 1.026 = 2.18 \, \text{IN}^2$

$A_{AVG} = \dfrac{6}{\left[\left(\frac{3}{A_1} + \frac{1}{A_2} + \frac{1}{A_3} + \frac{1}{A_4} \right) \right]}$

$= \dfrac{6}{\left[1.127 + .459 + .459 + .376 \right]}$

$= 6/2.421 = 2.48 \, \text{IN}^2$

$A_{AVG}/A_{br} = 2.48/4.61 = .539$

$K_{tru} = .76$
$K_{try} = .68$ } NA 72-1, PG 24-2.44

$P'_{tru} = K_{tru} A_{br} F_{tux} = .76 \times 4.61 \times 230 = 805. \, \text{K}$

$P'_{try} = K_{try} A_{br} F_{tyx} = .68 \times 4.61 \times 215 = 674 \, \text{K}$ NOT CRIT.

$P_{LUG} = .6 \times P'_{TOT} = .6 \times 922 = 553^K / \text{LUG}$ (ULT)

$M.S. = \dfrac{P'_{tru}}{P_{LUG}} - 1 = \dfrac{805}{553} - 1 = \boxed{\left(\begin{matrix} \text{TRANSV.} \\ \text{SHR-BRG} \end{matrix} \right) \; + \underline{.45}}$

APPENDIX C

NACELLE SUPPORT BEAM

AF1410 VERSION

BUILT-UP WELDED DESIGN

Rockwell International

PREPARED BY: TM | NACELLE SUPPORT BEAM |
DATE: 11-11-76 | AF 1410 VERSION | MODEL NO.

DWG. 3109-100002

DISCUSSION

THE NACELLE SUPPORT BEAM — WELDED
BUILT-UP DESIGN VERSION WAS ANALYZED
USING THE MATERIAL PROPERTIES AND
ANALYSIS CURVES PROVIDED IN THE
"STRUCTURAL ANALYSIS PROPERTIES" SECTION.

THE APPLIED DESIGN LOADS ARE THOSE
PROVIDED BY THE B-1 STRESS GROUP AND
ARE THE SAME AS THOSE USED FOR THE
TITANIUM MACHINED FORGING BASELINE
COMPONENT.

CONVENTIONAL STRESS ANALYSIS
METHODS PER REFERENCES   &
WERE USED.

LOADS (Y_F 1250) & TOTAL BOX BEAM

FWD FRAME Y_F 1244
AFT FRAME Y_F 1256

ULTIMATE

X_F 75.9

MAX $P_C = 232.1$ K
COND 360312

+ OUTBD
x ←

X_F 139.535 X_F 130.511

X_F 158.084

(SIDE VIEW)

P_6^z

P_4^x P_6^x

FRP

P

$+P_2^z$ P_5^z

X_F 114.657

V

M

COND 360312
$V = +66333$
$M = +6.395 \times 10^6$

COND 360313
$V = 64877$
$M = 6.297 \times 10^6$ + FWD

$+P_4^Y$ P_5^Y P_6^Y

x ←

$-P_2^Y$

(PLAN VIEW)
LOOKING DOWN

P_6
DRAG
STRUT

COND 360392
$V = -29576$
$M = -1.732 \times 10^6$
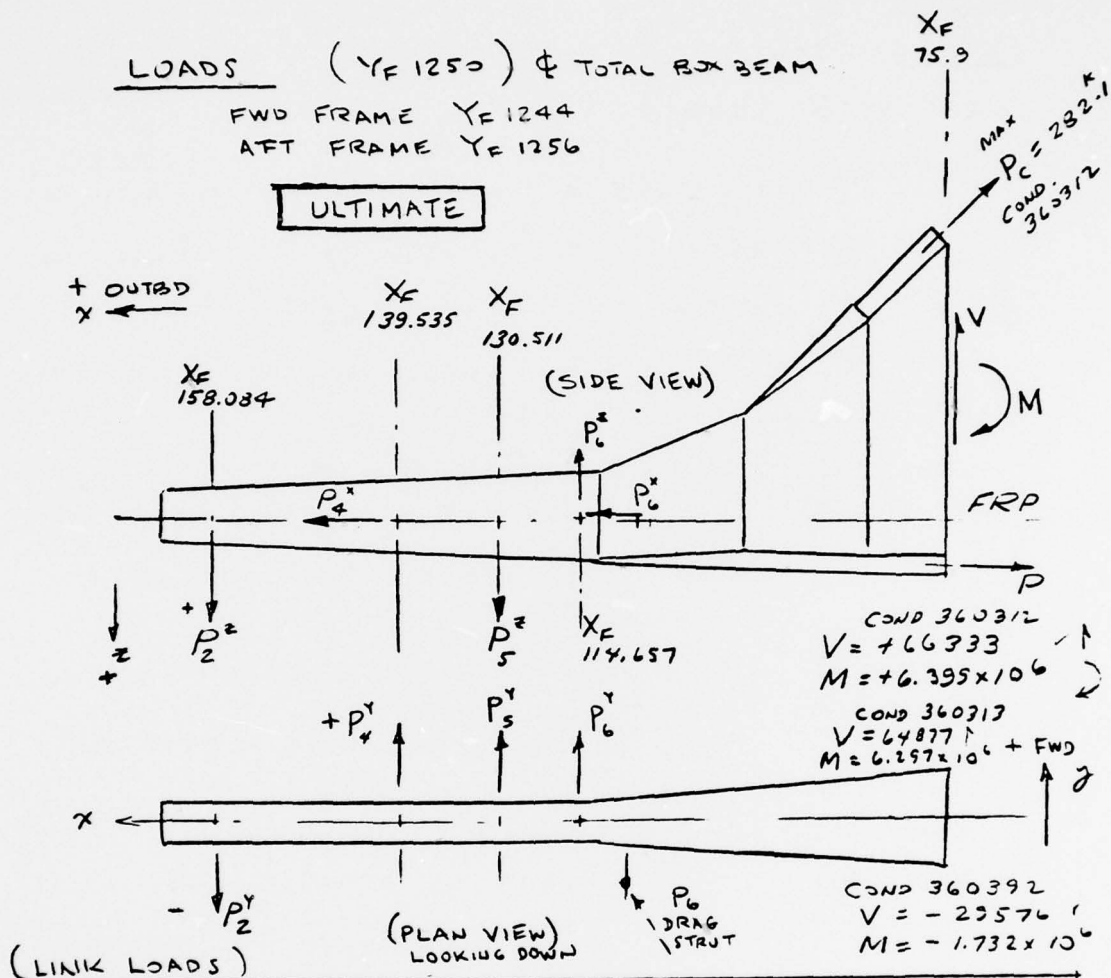
(LINK LOADS)

COND	VERT.	INBD-OUTBD	VERT.	FORE & AFT		
	P_2^z	P_4^x	P_5^z	P_2^Y	P_4^Y	P_5^Y
	(LBS)	(LBS)	(LBS)	(LBS)	(LBS)	(LBS)
360313	+97392.	-39825.	-32236.	-9770.	+1983	+3219.
360315		-37143	-34122.			
360316		+18728				
360312						
360392	-72827		+43251			
161422			+99261			

Rockwell International

PREPARED BY: TM | NACELLE SUPPORT BEAM
DATE: NOV 12, 1975 | AF 1410 VERSION | MODEL NO.

RWG# 3109-100002

LOADS (CONT.)

(DRAG STRUT LOADS)

COND 360313 $\qquad$ COND 360312

$$P_6^x = 7642 \times 1.5 = +11463. \text{ LB} \leftarrow \quad \leftarrow 46609. \text{LB}$$

$$P_6^Y = 8858 \times 1.5 = 13287. \text{ LB} \uparrow \quad \uparrow 40210. \text{LB}$$

$$P_6^z = 519 \times 1.5 = -779. \text{ LB} \hat{\uparrow} \quad \cdots$$

$$P_6 = \qquad = 17566. \text{ LB.} \qquad P_6 = 61617. \text{LB}$$

(DIFF. BEND. LOADS) - COND 360313

LINK 2:
$(Y_F 158.084)$

$$M_{SC} = 5.039 \, P_2^Y + P_2^z \times .191$$
$$= 45284 \times 1.5 = 67926. \text{ IN-LB}$$

$$P_{2_{DIFF.}} = \frac{M_{SC}}{6.3} = 7188 \times 1.5 = 10782. \text{LB}$$

LINK 4:
$(Y_F 139.535)$

$$M_{SC} = 7.602 \, P_4^Y = 1.5 \times 10050 = 15075. \text{ IN-LB}$$

$$P_{4_{DIFF}} = \frac{M_{SC}}{6.3} = 1.5 \times 1595 = 2392. \text{LB}$$

LINK 5:
$(Y_F 130.511)$

$$M_{SC} = 8.738 \times P_5^Y - P_5^z \times .0494$$
$$= 1.5 \times 17810 = 26715. \text{ IN-LB}$$

$$P_{5_{DIFF}} = \frac{M_{SC}}{6.3} = 1.5 \times 2827 = 4240. \text{LB}$$

$(X_F 149.297)$ (BETWN 158.084 & 139.535)   COND 360313

$$M_{YY}' = P_{2_{DIFF}} \times 8.787 = 1.5 \times 63161 = 94742 \text{ IN-LB/BEAM}$$

$$M_{YY} = P_2^z \frac{(158.084 - 149.297)}{2} =$$

$$= 97892 \times \frac{8.787}{2} = 430089. \text{ IN-LB/BEAM}$$

TOTAL $M_{YY} = 94.742 + 430.089 = 524.831$ KIP-IN/BEAM

DWG # 3109-100002

<u>LOADS</u> (CONT.)

$(X_F \ 139.534)$ COND 360313

$$M'_{YY} = P_{2_{DIFF}} \times 18.55 = 10782 \times 18.55$$

$$= 1.5 \times 133337 = 200006. \ \text{IN-LB/BEAM}$$

$$M_{YY} = P_2^Z \ (158.084 - 139.534)/2$$

$$= 97892 \times \frac{18.550}{2} = 907948. \ \text{IN-LB/BEAM}$$

TOT M_{YY} = 1107.95 KIP-IN/BEAM

$$P_x = P_4^x/2 = -\frac{39825}{2} \ \text{LB} = 19913. \ \text{LB/BEAM}$$

$(X_F \ 130.511)$ COND 360313

$\Sigma M_{YY} = 1624.39$ KIP-IN

$$M'_{YY} = P_{2_{DIFF}} \times 27.573 - P_{4_{DIFF}} \times 9.023$$

$$= 1.5 \times 183803 = 274805. \ \text{IN-LB/BEAM}$$

$$M_{YY} = P_2^Z \ (158.084 - 130.511)/2$$

$$= 97892 \times 27.573/2 = 1349588. \ \text{IN-LB/BEAM}$$

$$P_x = P_4^x/2 = -\frac{39825}{2} \ \text{LB}. = -19913. \ \text{LB/BEAM}$$

$(X_F \ 124.954)$ COND 360313

$\Sigma M_{YY} = 1920.33$ KIP-IN

$$M'_{YY} = P_{2_{DIFF}} \times 33.13 - P_{4_{DIFF}}^x \times 14.59 - P_{5_{DIFF}} \times 5.557$$

$$= 1.5 \times 199174 = 298751. \ \text{IN-LB/BEAM}$$

$$M_{YY} = P_2^Z \ (158.084 - 124.954)/2$$

$$= 97892 \times \frac{33.130}{2} = 1621581. \ \text{IN-LB/BEAM}$$

$$P_x = P_4^x/2 = -\frac{39825}{2}. \ \text{LB} = -19913 \ \text{LB/BEAM}$$

PAGE NO. C-5   REV.

DWG # 3109-100002

LOADS (CONT.)

$(X_F \ 111.874)$ COND 360313

$\begin{cases} M'_{YY} = \left[P_6^z \times (114.657 - 111.874) - P_6' \times (1.6 + .15) \right] \frac{1}{2} \\ \qquad = 1.5 \times \underset{2583}{5965} = \quad 8948 \text{ IN-LB/BEAM} \\ \\ M_{YY} = \left[P_2^z (158.084 - 111.874) - P_5^z (130.511 - 111.874) \right] \frac{1}{2} \\ \qquad = 97892 \times \frac{46.210}{2} - 32236 \times \frac{18.637}{2} \quad = 1961403. \frac{\text{IN-LB}}{\text{BEAM}} \end{cases}$

TOT M_{YY} = 1970.35 KIP-IN

$M'_{zz} = -P_6^Y \times 2.783 - P_5^Y \times 18.637 - P_4^Y \times 27.66 + P_2^Y \times 46.21$

$\qquad = 1.5 \times \underset{95886}{199771} = 299657. \text{ IN-LB}, \quad (S_Y = 8.72^K)$

$P_X^{TOT} = 53.61^K \begin{cases} P_{Mz}^x = M'_{zz} / 7.60 = 1.5 \times 26286 = \pm 39429. \text{ LB/BEAM} \\ \qquad\qquad\qquad\qquad\qquad {}_{13143} \\ P_{Px}^z = \left[-P_4^x + P_6^x \right] / 2 = (-39825 + 11463) \frac{1}{2} = -14181 \text{ LB/BEAM} \end{cases}$

$(X_F \ 96.534)$ COND 360313

TOT M_{YY} = 2461.13 KIP-IN

$\begin{cases} M'_{YY} = \left[P_6^z \times (114.657 - 96.534) - P_6^x \times (1.6) \right] / 2 \\ \qquad = 1.5 \times 1411 = \quad 2117. \text{ IN-LB/BEAM} \\ \\ M_{YY} = 1961403 + (97892 - 32236 - 779)(\underset{64877}{111.874 - 96.534}) \frac{7.67}{2} \\ \qquad = 1961403 + \ 497606 \ = 2459009 \text{ IN-LB/BEAM} \end{cases}$

$M'_{zz} = 299657 - (8720) \times 15.34 = 165892 \text{ IN-LB}$

$P_x = 31.65^K \begin{cases} P_{Mz}^x = \dfrac{M'_{zz}}{9.43} = \dfrac{165892}{9.48} = \pm 17499. \text{ LB} \\ \\ P_{Px}^x = (-P_4^x + P_6^x) / 2 = -14181 \end{cases}$

$S_z = P_4^z + P_5^z + P_6^z = 64.83^K$

CAP LOAD $= \dfrac{M_{yy}}{13.64} = \dfrac{2461.13}{13.64} = \begin{matrix} \pm 180.43^K \\ \pm \ 31.63 \times \frac{1}{2} \end{matrix} \Big\} \ 196.3^K$

$\pm P_{x/2}$

LOADS (CONT)

DWG # 8109-100002

(X$_c$ 75.50)   COND 360313

M_{YY}^{T-T} = 3148.23 KIP-IN

$$M'_{YY} = [P_6^x \times 1.6 - P_6^z \times (114.657-75.50)]/2$$

$$= [11463 \times 1.6 - 779 \times 38.757]/2 = 5926. \text{ IN-LB}$$

11151

$$M_{YY} = \left[P_2^z (158.084 - 75.50) - P_5^z (130.511-75.50)\right] \tfrac{1}{2}$$

$$= (57892 \times 82.184 - 32236 \times 54.611) \tfrac{1}{2} =$$

$$= 6284715 \times \tfrac{1}{2} = 3142357 \text{ IN-LB}$$

82.184

$$M'_{ZZ} = P_2^Y (158.084 - 75.50) - P_4^Y (139.535-75.5) - P_5^Y (130.511-75.5)$$

$$- P_6^Y (114.657-75.50)$$

$$= 9770 \times 82.1 - 1983 \times 63.636 - 3213 \times 54.611$$

$$- 13287 \times 38.757 = -13952$$

$$P_{Mz}^x = \frac{M'_{ZZ}}{12.0} = \frac{13952}{12} = \mp 1163 \text{ LB}$$ $\left.\right\}$ $P_x^{T-V} = -15344$ LB

$$P_{Px}^x = (P_4^x - P_6^x).50 = -14181 \text{ LB}$$ ↑ NEGLECT FOR UPPER CAP

UPPER CAP $$P_{My} = \frac{M_{YY}}{32.359} = \frac{3148.23}{32.359} = +97.29 \text{ k}$$

TOTAL P_{CAP}^x LOWER $= -97.29 - 15.3 \approx 112^k$

NOTE: COND 360312 $M = 6399 \text{ KIP-IN}/2 = 3199.5 \text{ KIP-IN}$

$$V = \frac{66.33^k}{2} = 33.17^k/\text{BEAM}$$

$$P_{CAP} = \frac{3199.5}{32.359} = 98.88^k$$

$$P_c (\text{GIVEN}) = 282.1^k/2 = 141.05^k/\text{BEAM CAP}$$

PAGE NO C-7   REV. 11.9 .76

Rockwell International

LOADS (CONT.)

ULTIMATE

(CAP LOAD DEVELOPMENT)
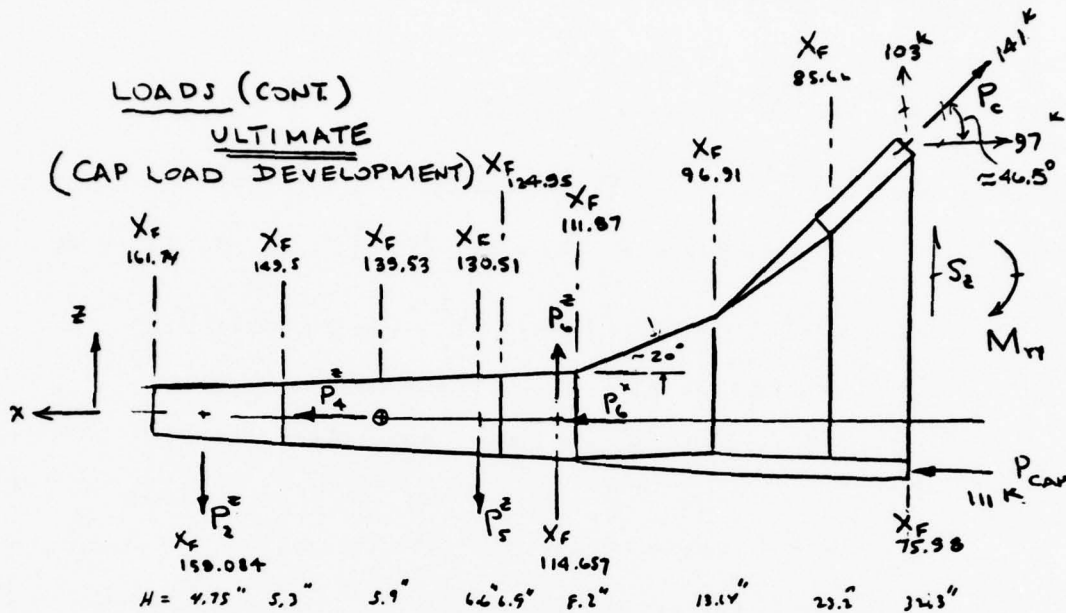
COND 360313
ULTIMATE   LOAD / BEAM

X_F	S_z	S_Y	M_{YY}	M_{ZZ}	P_X	Horizontal $P_{CAP}/BEAM$		
	(KIPS)	(KIPS)	(KIP-IN)	(KIP-IN)	(KIPS)	(K)	(K) LOWER CAP	(K) UPPER CAP
158.08	97.89	0	0	0	0			
149.3	97.89	0	524.83	0	0	99.0	-99.	99
139.53	97.89	-9.77	1107.95	0	-19.91	193 +18	-196 230	188 217
136 130.51	97.89	-7.79	1624.39	*	-19.91	246. +12	-264	246
124.95	65.65	-4.57	1920.33	*	-19.91	273. +18	-296	273
111.87	64.88	+8.72	1970.35	**	-53.61	240.0 +48	-288	240 255
96.53	64.88	+8.72	2461.11	**	-31.68	196.3 +88	-224	196 282
85.66	64.88	+8.72	2805.		-22	121.88	-141	175
75.98	64.88	+8.72	3148.28		-15.34	97.318 ①	-112	141 ①

* DIFF BENDING IN X-Z PLANE   ** REACT. AS COUPLE LOAD
① $99/-4.5 = 141^K$

PAGE NO C-8

380

Rockwell International

PREPARED BY: TM NACELLE SUPPORT BEAM

DATE: NOV 11, 1975

MODEL NO.

CW§ # 8109-100002

SA000003-6012

LOADS

ULTIMATE

(SHEAR FLOW DEVELOPMENT)
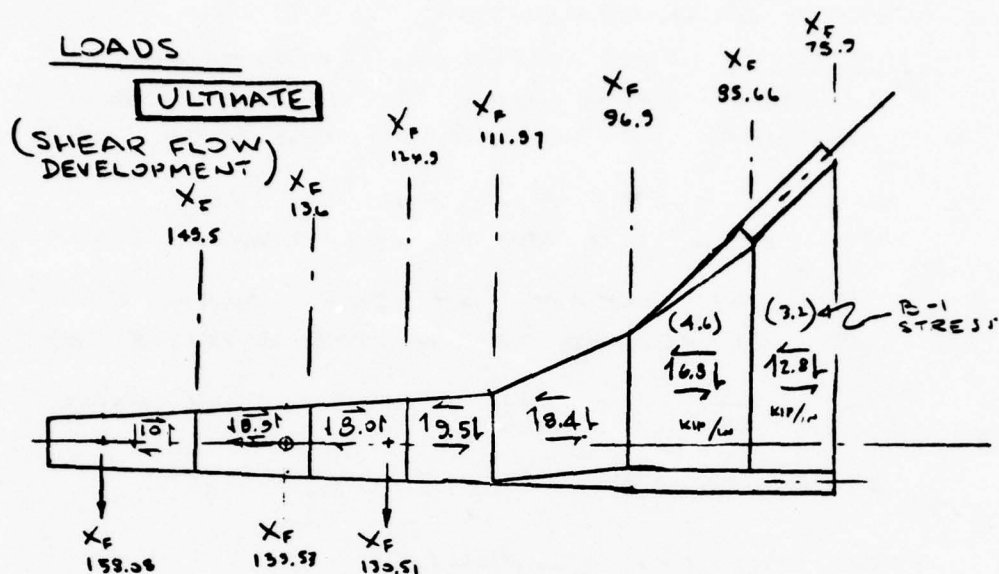
PANEL X_F	L	ΔP	q (KIP/IN)	H	NE-S_z	CHECK q
158 — 149	9	99	10.	5	48.95	9.8
149 — 139	10	89	8.9	5.5	48.95	8.5
139 — 130	9	58	6.5	6.1	48.95	5.0
130 — 125	5	32	6.4	6.75	32.83	4.9
125 — 112	13	−38+KICK −	$\frac{2.92}{+6.5}$ = 9.5	7.5	32.44	4.3
112 — 97	15	−44+KICK −	3+5.4 = 8.4	13.0	32.44	2.99
97 — 86	11	75	6.8 4.575	13	32.44	
86 — 75.5	10	24	2.4 3.15		32.44	2.3

① = q = $\frac{109}{2\times10.}$ = 5.4

* B-1 STRESS GROUP VALUES

② $q = \frac{135}{2\times0}$ = 6.5

PREPARED BY: TM | NACELLE SUPPORT |
DATE: 1-15-76 | BEAM - YE1244, YE1256 | LOCOSST
MODEL NO.

DWG 3109-100002

(STIFFNESS REQUIREMENTS)

DISCUSSION - THE BASELINE TITANIUM NACELLE
SUPPORT BEAM WAS DESIGNED FOR
STIFFNESS AS WELL AS STRENGTH REQMTS.

USING $E = 28.5$ Msi FOR AF1410
& $E = 16.0$ Msi FOR TITANIUM 6-4

THE CAP AREAS OF THE BEAM CAN
BE DECREASED FROM THE BASELINE BY:

$$\frac{E_{Ti}}{E_{STEEL}} = \frac{16.}{28..} = \underline{.57}$$ FOR EQUIV. AXIAL

STIFF. CAPS

WHERE STRENGTH GOVERNS:

$F_{tu} (AF1410) = 230$

$F_{tu} (Ti) = 130$

$$\frac{F_{tu}(Ti)}{F_{tu}(AF1410)} = \frac{130}{230} = .565$$

THEREFORE SINCE STIFF. GOVERNS, CAP AREAS
CAN BE REDUCED BY $100(1.00 - .57) = 43\%$
OR CAP AREAS CAN BE 57% OF THE
TITANIUM BASELINE AREAS.

PAGE NO. C-10   REV. _____

382

Rockwell International

PREPARED BY: TM NACELLE SUPPORT
DATE: 1-15-75 BEAM MODEL NO.

DWG 3109-100002
B REVISION

CAP AREAS & STRESSES

(UPPER CAP)

SECTION X_F	P (k)	AF1410 A_{ST} (10^-)	STEEL f (ksi)	TITANIUM BASELINE A_{Ti} (10^-)		STIFF. CHECK A_{ST}/A_{Ti} (S/B 0.57)	MARGIN (TENSION) F^{tu} = 230 ksi
81.8	158	≈ 2.50	63.2	> 4.45		.56 ✓ OK	HIGH
85.7	175	2.432	70.2	4.45		.56 ✓	HIGH
96.9	282	2.34	120.3	4.18		.56 ✓	+.91
111.9	255	2.195	116.	3.92		.56 ✓	+.98
124.9	278	1.435	186.	2.67		.56 ✓	+.24
136.	217	.907	239 ×	1.62	134	.56 ✓	−.04
145.5	99	.46	215	.82		.561 ✓	+.07
158.1							

(LOWER CAP)

X_F	P (k)	AF1410 A_{ST} (10^-)	f (ksi)	TITANIUM A_{Ti} (10^-)	STIFF. CHECK A_{ST}/A_{Ti} (S/B 0.57) OK	MARGIN (COMP.) F_{cy} = 226 ksi
85.7	−141	1.652	−85.3	2.95	0.56 ✓	(F_{cc}=130) +.52
96.9	−224	1.973	−113.5	3.524	.56 ✓	(F_{cc}=190) +.67
111.9	−288	2.57	−112.	3.37	.763 —	($F_{cc}=F_{cy}$) +1.02
124.9	−296	2.57	−115.	4.59	.56 ✓	+.96
130.5	−264					
136.0	−230	1.596	−144.	2.85	.56 ✓	+.57
149.5	−99	.75	−132.	1.335	.561 ✓	($F_{cc}=F_{cy}$) +.71
158.1						

NACELLE SUPPORT BEAM
DWG #J109-100002
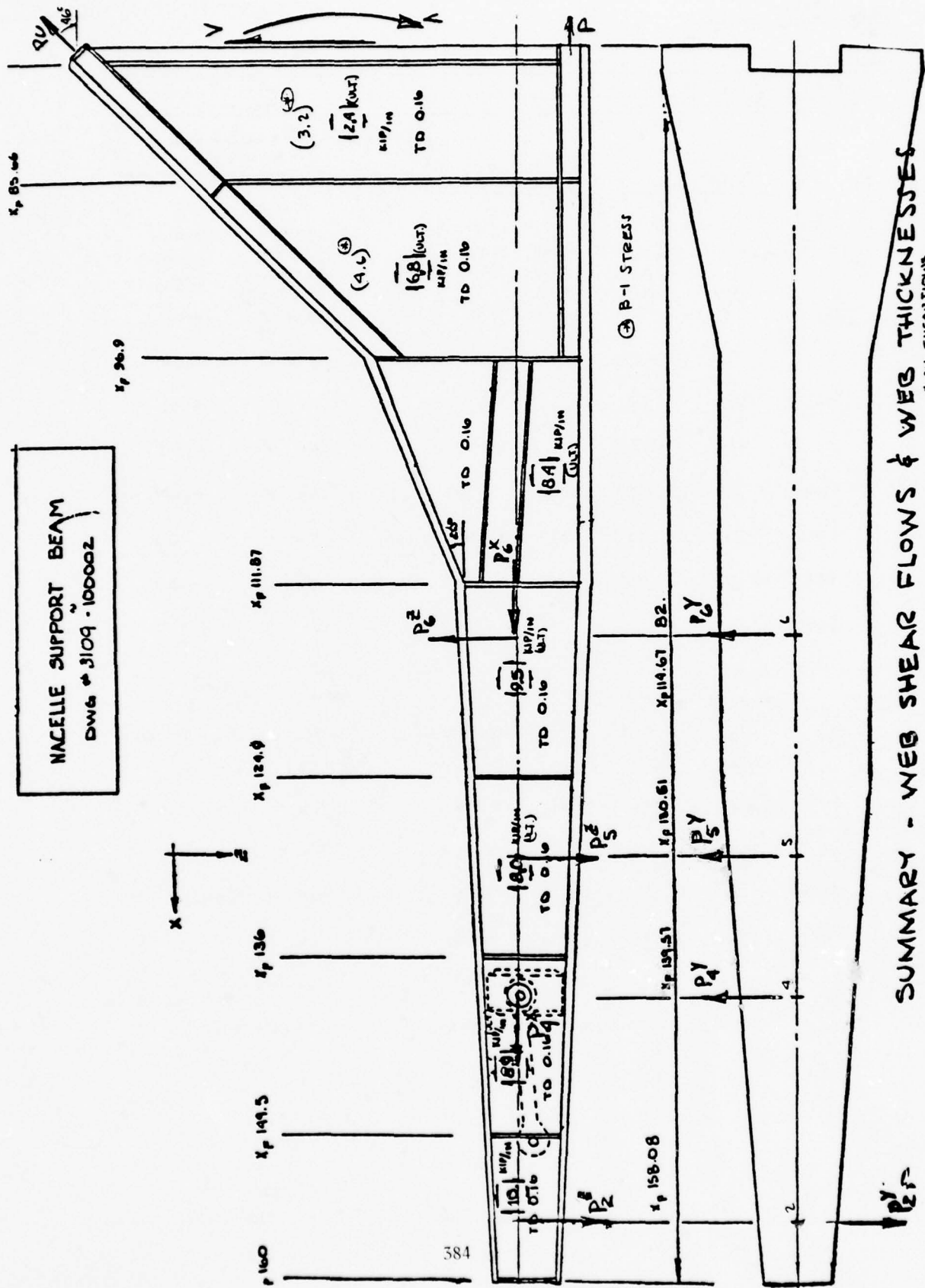
SUMMARY - WEB SHEAR FLOWS & WEB THICKNESSES
* ALL SHEAR FLOWS ARE ULTIMATE

384

Rockwell International

PREPARED BY: TM   NACELLE SUPPORT BEAM

DATE: 1-20-75   MODEL NO.

REV. 11-9-76 TTM

(WEB CHECK - X_F 97 - X_F 86)

$$t = .160 \qquad b = 11 \qquad a = 16 \text{ AVG}$$

$$a/b = \frac{16}{11} = 1.45 \; ; \quad b/t = 68.8$$

$$K_s = 6.6 \quad (S.S.) \qquad \rightarrow \text{NA 72-1}, \text{ PG. 10-8}$$

$$\frac{F_{scr}}{\eta} = K_s \, E / (b/t)^2 = \frac{6.6 \times 28000}{(68.8)^2} = 39. \text{ KSI}$$

$$F_{scr} = 39 \text{ KSI} \qquad (\eta = 1.0)$$

$$q_{(AVG)} = 6.8 \text{ k/in} ; \quad f_s = \frac{6.8}{.16} = 42.5 \text{ KSI} \quad \leftarrow \text{NG. BUCKLES AT ULT. LOAD}$$

$$f_s \, (\text{LIMIT}) = \frac{2}{3} f_s = 28.3 \text{ KSI} \quad \text{OK} < F_{scr} = 39 \text{ KSI}.$$

REVISED CRITERIA (NO BUCKLING AT LIMIT LOAD)

$$F_s \, (\text{ULT}) = 102 \text{ KSI} \; (\overset{\text{SEMI-TENSION FIELD}}{\text{ULT. SHR WEB STRENGTH}})$$

$$F_s \, (\text{NEW}) = .85 \times 102 = 87 \text{ KSI} > f_s = 47.5 \text{ KSI} \quad \text{OK}$$

$$\text{M.S.} = \frac{87}{42.5} - 1 = \left(\text{ULT. SHEAR} \right) = + \underline{\underline{1.04}}$$

$$\text{M.S.} = \frac{F_{scr}}{f_s \, (\text{LIMIT})} - 1 = \frac{39}{28.3} - 1 = \left(\overset{\text{LIMIT LOAD}}{\text{BUCKLING}} \right) = + \underline{\underline{.38}}$$

(WEB CHECK - X_F 86 - X_F 75.98)

$$q = 3.2 \text{ k/in} , \quad f_s = 20 \text{ KSI ULT} = 13.3 \text{ KSI LIMIT}$$

$$t = 0.16" ; \quad b = 10" ; \quad a = 27.7" \text{ AVG}$$

$$a/b = 2.77 ; \quad b/t = 10/.16 = 62.5$$

$$K_{ss} = 5.3 \; (S.S.) \quad \leftarrow \text{REF. NA 72-1}, \text{ PG. 10-8}$$

$$F_{scr} = 5.3 \times 28000 / (62.5)^2 = 38 \text{ KSI} \quad (\text{NOT CRITICAL})$$

$$\text{M.S.} = (38/13.3) - 1 = \left(\overset{\text{LIMIT LOAD}}{\text{BUCKLING}} \right) = + \underline{\underline{1.86}}$$

(WEB CHECK X_F 112 – X_F 125)   DWG# 3109-100002

$a = 13$ $b = 7.1$ $t = 0.16$

$\frac{b}{t} = 44.375$

$F_{s,cr} = 95$ KSi (REF FIG. 24)

$q_{av} = 8.75 \frac{k}{in}$ $f_s = \frac{8.75}{t} = 54.69$ KSI

$f_s(limit) = \frac{2}{3} f_s = 36.46$ KSI $< F_{s,cr} = 95$ o.k.

$F_s(ult) = 102$ KSI $F_s(weld) = 85\% \, F_s = 87$

M.S. $= \frac{F_{s(w)}}{f_s} - 1 = \frac{87}{54.69} - 1 =$ (ultimate SHEAR) $= +0.591$

M.S. $= \frac{F_{s,cr}}{f_s(limit)} - 1 = \frac{95}{36.46} - 1 =$ (limit load buckling) $= +1.61$

(WEB CHECK X_F 125 – X_F 136)

$b = 7$ $t = 0.16$ $\frac{b}{t} = 43.75$

$F_{s,cr} = 100$ KSi $q = 8.45 \frac{k}{in}$

$f_s = \frac{q}{t} = \frac{8.45}{0.16} = 52.81 < 100$ OK. $f_s(limit) = 35.20$ KSI

M.S. $= \frac{F_{s(w)}}{f_s} =$ (ultimate shear) $= +0.647$

M.S. $= \frac{F_{s,cr}}{f_s(limit)} - 1$ (limit load buckling) $= +1.84$

PAGE NO. C-14   REV.

DWG.# 3109-100002

(WEB CHECK $X_F 136 - X_F 149$)

$a = 13$ $b = 6.6$ $t = 0.16$

$\dfrac{b}{t} = 41.25$ $F_{S,cr} = 105$ (REF FIG. 24)

$q = 9.45$ $f_S = \dfrac{9.45}{0.16} = 59.06$ KSI

$f_S < F_{S,cr}$ o.k. f_S(limit) = 39.375 KSI

M.S. $= \dfrac{F_S}{f_S} - 1 = \dfrac{87}{59.06} - 1$ $\boxed{\text{(ultimate Shear)} = + 0.473}$

M.S. $\dfrac{F_{S,cr}}{f_S(\text{limit})} - 1 = \dfrac{105}{39.375} - 1$ $\boxed{\text{(limit load Buckling)} = + 1.667}$

DWG # 3109-100002

XF 96.9 STIFFENER CHECK

$P_{STIFF} = 283 \times SINE\ 46.5 - 213\ SINE\ 25.3°$
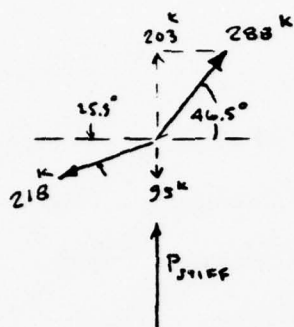
$= 203 - 95 = 108.^k$

$t = .25 \qquad b = 2$

LET $A = 2bt = 2 \times 2 \times .25 = 1.0\ \square''$

$f_T = 108^{KSI}$

COMP $\qquad f_c = 75\%.\ f_T = 81.\ KSI$

$b/t = \frac{2}{.25} = 8.$ (ONE EDGE FREE)

$F_{cc} = C_c [F_{cy} E]^{1/2} (t/b)^{3/4}$

$= .30 [226 \times 28000]^{1/2} [.125]^{.75} =$

$= .30 \times 2.52 \times 10^3 \times .211 = 159\ KSI$

$M.S. = \frac{.85^* F^{tu}}{f_T} - 1 = \frac{.85 \times 230}{108} - 1 = \boxed{+ \underline{.81}\ (TENSION)}$

$M.S. = \frac{.85^* F_{cc}}{f_c} - 1 = \frac{.85 \times 159}{81} - 1 = \boxed{+ \underline{.67}\ (CRIPPLING)}$

*.85 = WELD FACTOR - TRANSV. LOAD

$$\left(WELD\ CHECK\quad X_F\ 149 - X_F\ 159 \right)$$

DWG # 3109-100002

$$t_w \approx .125''\qquad l_w = 10''$$

$$q = 10\frac{k}{in}$$

$$f_s = \frac{10}{.125} = 80\ KSI$$
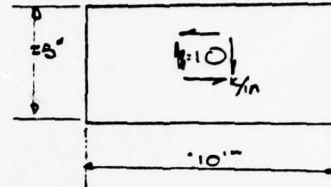
$$M.S = \frac{F_{su}}{f_s} - 1 = \frac{125}{80} - 1 = \boxed{\left(WELD\ ULT.\ SHEAR \right) + .56}$$

(LUG BENDING CHECK)

ASSUME $2°$ MISALIGNMENT $\quad P_z = 61.6 \times \text{SINE } 2°$
$$= 2.16^k$$

$M = 2.16 \times 2 = 4.32 \, k\text{-in}$

$f_b = \dfrac{6M}{2b't^2} = \dfrac{6 \times 4.32}{2 \times 3 \times .224^2} = 86.3 \text{ KSI}$

$f_c = \dfrac{P_Y}{2b't} = \dfrac{46}{2 \times 3 \times .224} = 34.2 \text{ KSI}$

$f_{TOT} = f_b + f_c = 120.5 \text{ KSI}$

$F_b = F_{cy} = 226 \text{ KSI}$

$M.S. = \dfrac{F_b}{f_{TOT}} - 1 = \dfrac{226}{120.5} - 1 = \boxed{(\text{BENDING}) + .87}$

(LUG SHEAROUT)

ASSUME $P = 61.6^k$ IN TENSION DIRECTION

$f^{so} = \dfrac{P \times \frac{1}{2}}{2(1.25 - \frac{1.1}{2})t} = \dfrac{61.6 \times \frac{1}{2}}{2(.70) \times .224} = 99 \text{ KSI}$

$F^{su} = 147 \text{ KSI}$

$M.S. = \dfrac{F^{su}}{f^{so}} - 1 = \dfrac{147}{99} - 1 = \boxed{(\text{SHR-OUT}) + .48}$

(LUG · SHR · BEARING)

$D/t = \dfrac{1.1}{.224} = 4.91 ; \quad e/D = \dfrac{1.25}{1.1} = 1.14$

$K_{br} = 1.05$

$P_{bru} = A_{br} K_{br} F_{tu} = 1.1 \times .224 \times 1.05 \times 230 = 59.5^k$

$P = \frac{1}{2} P_{STRUT} = \frac{1}{2} \times 61.6 = 30.8^k$

$M.S. = \dfrac{P_{bru}}{P} - 1 = \dfrac{59.5}{30.8} - 1 = \boxed{(\text{SHR-BRG}) + .93}$

DWG # 3109-100002

(SIDE STRUT LOAD EFFECT CHECK)

$P = 61.6$ ^{k} $\alpha = 48.3°$ COND
360312

$P_x = 41.0$ ^{k}

$P_y = 46.0$ ^{k}

LUG $t = 224$ (TWO LUGS)

1.5" SPACE BETWEEN LUGS

$D = 1.1"$

$f_{br} = \dfrac{P}{Dt} = \dfrac{61.6^k}{1.1 \times .224 \times 2} = 125$ KSI   OK

$F^{bru} = 331$ KSI

$\updownarrow 41.0 \times 3/15.1 = 8.14^k$

$\uparrow \dfrac{15.1-2.5}{15.1} \times 46.0 = \underline{33.4}$

$\quad\quad\quad\quad\quad 46.5^k$ ✓

$\updownarrow 41.0 \times 3/15.1 = 8.14^k$

$\uparrow \dfrac{2.5}{15.1} \times 46.0 = \underline{7.61^k}$

$\quad\quad\quad\quad\quad .5^k \approx 0$

$2^{\;.}$
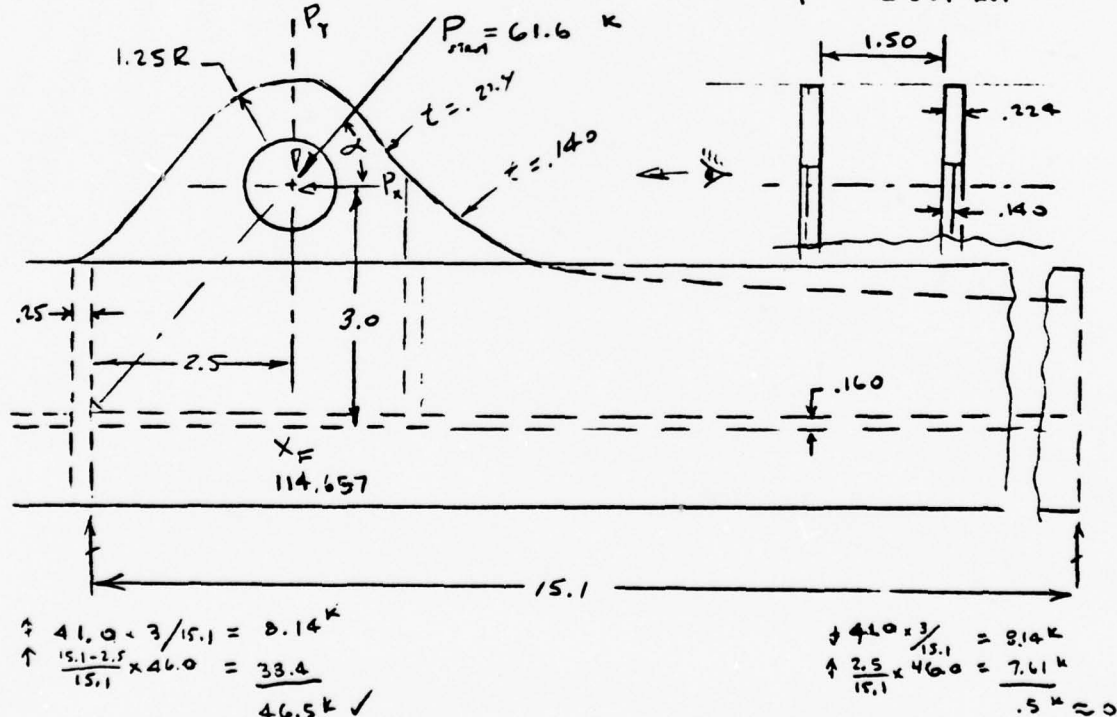
Appendix D

STRAIN-GAGE SURVEYS

STRAIN-GAGE SURVEY PRIOR TO FIRST MISSION

The strains measured on each gage, and the calculated stress, prior to initiation of the fatigue testing are contained in this appendix. Two loads were used, a positive 305,000 pounds and a negative 280,000 pounds. Data were acquired at zero load, 20 percent steps up to the maximum, 20 percent steps down to zero, and at the zero return.
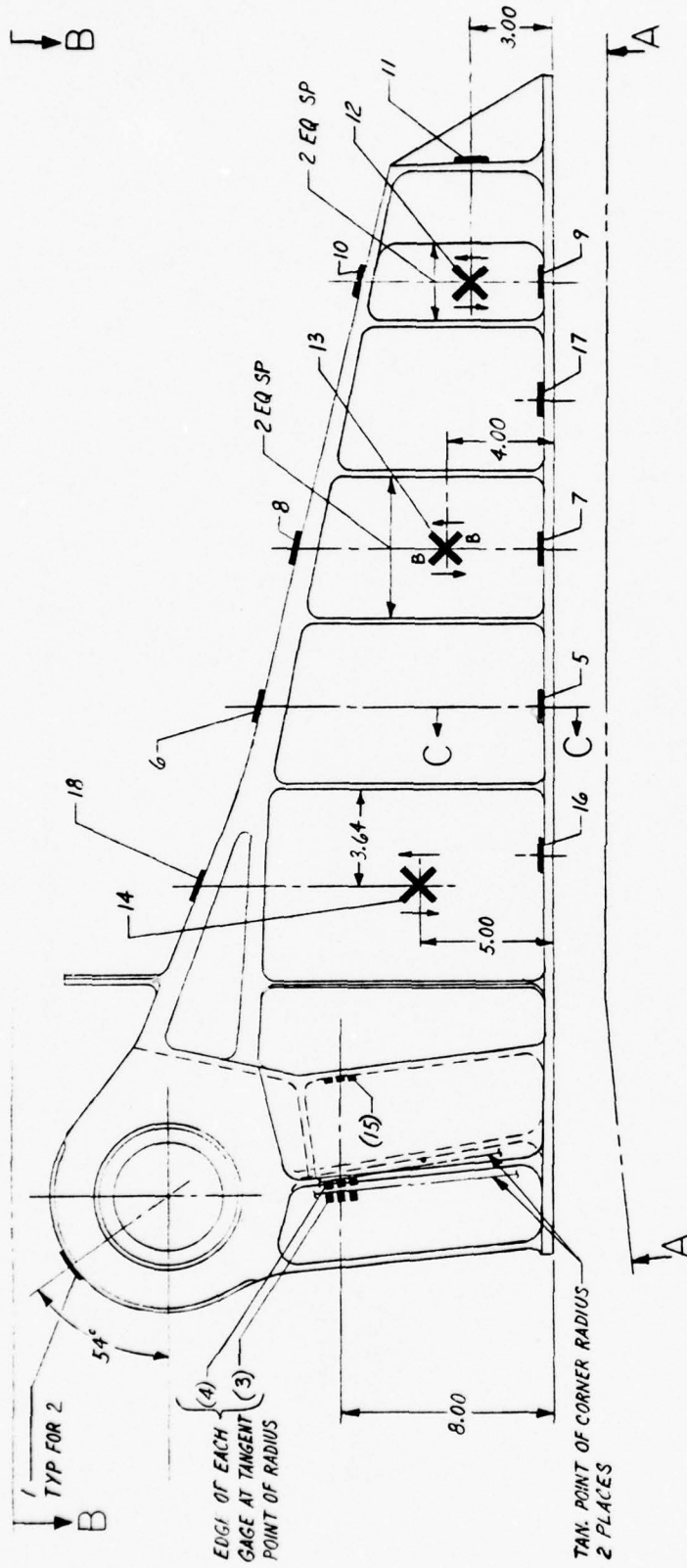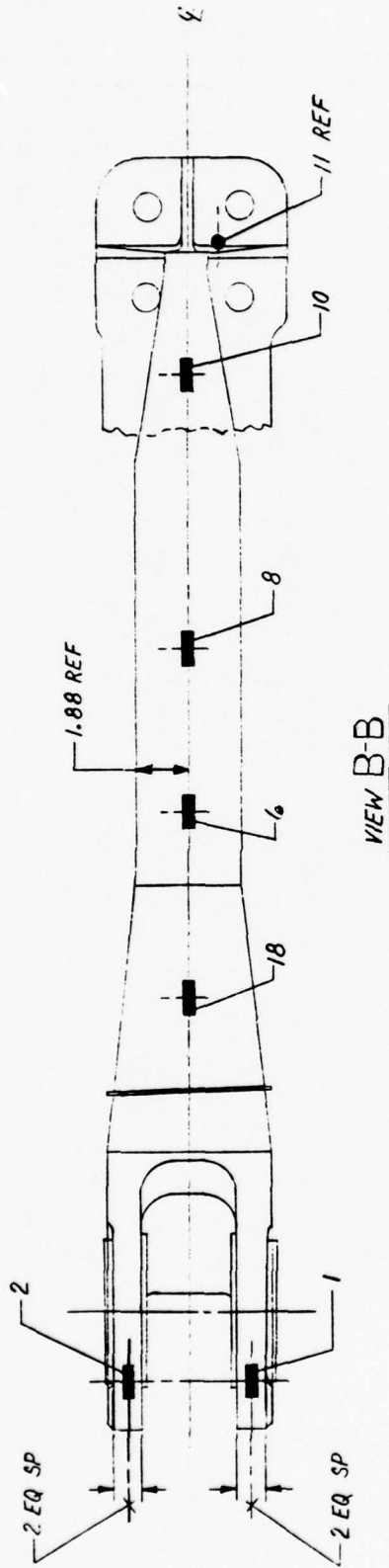
VIEW A-A
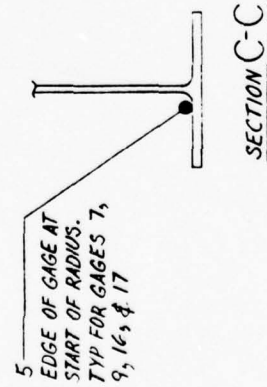
Strain gage locations.

VIEW B-B

SECTION C-C

5
EDGE OF GAGE AT
START OF RADIUS.
TYP FOR GAGES 7,
9, 16, & 17

Strain gage locations. (concluded)

394

STRUCTURES LAB. ROSETTE SOLUTIONS

CONDITION: LOCOSST   STEP 92 MIN (P=305 K)   APR 11,1978

GAGE: 1   TYPE A1-1   MTL CODE S-01

LOAD (%)	READING (U IN/IN)	-SX- (PSI)
0.0	0.	1.
20.0	112.	3137.
40.0	232.	6486.
60.0	358.	10024.
80.0	492.	13776.
100.0	634.	17742.
60.0	400.	11203.
40.0	271.	7585.
20.0	139.	3887.
0.0	9.	242.

* * * * * * * * * *

GAGE: 2   TYPE A1-1   MTL CODE S-01

LOAD (%)	READING (U IN/IN).	-SX- (PSI)
0.0	0.	4.
20.0	98.	2734.
40.0	214.	5999.
60.0	340.	9533.
80.0	471.	13199.
100.0	606.	16973.
60.0	390.	10924.
40.0	261.	7311.
20.0	126.	3537.
0.0	11.	298.

* * * * * * * * * *

GAGE: 3   TYPE A1-1   MTL CODE S-01

LOAD (%)	READING (U IN/IN)	-SX- (PSI)
0.0	1.	31.
20.0	-143.	-4008.
40.0	-357.	-9438.
60.0	-543.	-15216.
80.0	-755.	-21127.
100.0	-959.	-26851.
60.0	-554.	-15510.
40.0	-345.	-9652.
20.0	-134.	-3741.
0.0	60.	1689.

* * * * * * * * * *

GAGE: 4   TYPE A1-1   MTL CODE S-01

LOAD (%)	READING (U IN/IN)	-SX- (PSI)
0.0	0.	4.
20.0	-200.	-5586.
40.0	-393.	-11016.
60.0	-586.	-16419.
80.0	-777.	-21769.
100.0	-966.	-27039.
60.0	-578.	-16179.
40.0	-378.	-10588.
20.0	-181.	-5078.
0.0	6.	165.

* * * * * * * * * *

GAGE: 5   TYPE A1-1   MTL CODE S-01

LOAD (%)	READING (U IN/IN)	-SX- (PSI)
0.0	-1.	-25.
20.0	-52.	-1445.
40.0	-133.	-3722.
60.0	-141.	-3937.
80.0	-169.	-4740.
100.0	-194.	-5437.
60.0	-171.	-4794.
40.0	-145.	-4070.
20.0	-112.	-3133.
0.0	-74.	-2061.

* * * * * * * * * *

GAGE: 6   TYPE A1-1   MTL CODE S-01

LOAD (%)	READING (U IN/IN)	-SX- (PSI)
0.0	0.	1.
20.0	340.	9509.
40.0	660.	18481.
60.0	978.	27373.
80.0	1299.	36372.
100.0	1626.	45531.
60.0	1005.	28150.
40.0	691.	19338.
20.0	370.	10366.
0.0	44.	1233.

* * * * * * * * * *

CONDITION: LOCOSST   STEP 92 MIN (P=305 K)   APR 11,1978

GAGE: 8   TYPE A1-1   MTL CODE S-01

LOAD (%)	READING (U IN/IN)	-SX- (PSI)
0.0	-0.	-0.
20.0	313.	8776.
40.0	609.	17043.
60.0	902.	25257.
80.0	1200.	33605.
100.0	1504.	42113.
60.0	927.	25953.
40.0	633.	17712.
20.0	334.	9364.
0.0	32.	883.

* * * * * * * * * *

GAGE: 10   TYPE A1-1   MTL CODE S-01

LOAD (%)	READING (U IN/IN)	-SX- (PSI)
0.0	-0.	-0.
20.0	207.	5783.
40.0	404.	11298.
60.0	606.	16974.
80.0	810.	22677.
100.0	1015.	28434.
60.0	627.	17563.
40.0	426.	11941.
20.0	223.	6238.
0.0	17.	482.

* * * * * * * * * *

GAGE: 11   TYPE A1-1   MTI CODE S-01

LOAD (%)	READING (U IN/IN)	-SX- (PSI)
0.0	0.	5.
20.0	52.	1453.
40.0	96.	2687.
60.0	146.	4081.
80.0	199.	5583.
100.0	259.	7246.
60.0	144.	4027.
40.0	88.	2472.
20.0	39.	1104.
0.0	-10.	-290.

* * * * * * * * * *

GAGE: 12   TYPE S1-2   MTL CODE S-01

LOAD (%)	READING (U IN/IN)	-SXY- (PSI)
0.0	0.	1.
20.0	526.	5576.
40.0	1003.	10634.
60.0	1504.	15945.
80.0	2020.	21415.
100.0	2538.	26905.
60.0	1562.	16558.
40.0	1062.	11257.
20.0	569.	6030.
0.0	62.	656.

* * * * * * * * * *

GAGE: 13   TYPE S2-2   MTL CODE S-01

LOAD (%)	READING (U IN/IN)	-SXY- (PSI)
0.0	1.	11.
20.0	-689.	-7300.
40.0	-1330.	-14099.
60.0	-1965.	-20834.
80.0	-2616.	-27729.
100.0	-3278.	-34752.
60.0	-1980.	-20983.
40.0	-1334.	-14142.
20.0	-681.	-7215.
0.0	-19.	-203.

* * * * * * * * * *

GAGE: 14   TYPE S1-2   MTL CODE S-01

LOAD (%)	READING (U IN/IN)	-SXY- (PSI)
0.0	0.	2.
20.0	-545.	-5772.
40.0	-1086.	-11514.
60.0	-1635.	-17330.
80.0	-2210.	-23430.
100.0	-2806.	-29740.
60.0	-1631.	-17288.
40.0	-1067.	-11315.
20.0	-535.	-5646.
0.0	-28.	-293.

* * * * * * * * * *

398

GAGE: 15   TYPE A1-1   MTL CODE S-01

LOAD (%)	READING (U IN/IN)	-SX- (PSI)
0.0	1.	31.
20.0	-71.	-1976.
40.0	-115.	-3207.
60.0	-155.	-4331.
80.0	-196.	-5482.
100.0	-236.	-6606.
60.0	-160.	-4492.
40.0	-129.	-3609.
20.0	-89.	-2485.
0.0	-31.	-879.

* * * * * * * * * *

GAGE: 16   TYPE A1-1   MTL CODE S-01

LOAD (%)	READING (U IN/IN)	-SX- (PSI)
0.0	-1.	-26.
20.0	-14.	-401.
40.0	-116.	-3244.
60.0	-165.	-4612.
80.0	-204.	-5712.
100.0	-249.	-6973.
60.0	-210.	-5873.
40.0	-189.	-5283.
20.0	-170.	-4773.
0.0	-171.	-4800.

* * * * * * * * * *

GAGE: 17   TYPE A1-1   MTL CODE S-01

LOAD (%)	READING (U IN/IN)	-SX- (PSI)
0.0	0.	1.
20.0	12.	323.
40.0	20.	564.
60.0	27.	751.
80.0	29.	805.
100.0	19.	537.
60.0	34.	966.
40.0	44.	1233.
20.0	51.	1421.
0.0	53.	1475.

* * * * * * * * * *

CONDITION: LOCOSST   STEP 92 MIN (P=305 K)   APR 11,1978

GAGE: 18   TYPE A1-1   MTL CODE S-01

LOAD (%)	READING (U IN/IN)	-SX- (PSI)
0.0	-1.	-25.
20.0	314.	8779.
40.0	619.	17343.
60.0	922.	25826.
80.0	1230.	34444.
100.0	1542.	43168.
60.0	948.	26549.
40.0	644.	18039.
20.0	341.	9556.
0.0	38.	1072.

* * * * * * * * * *

GAGE: 19   TYPE S1-2   MTL CODE S-01

LOAD (%)	READING (U IN/IN)	-SXY- (PSI)
0.0	0.	0.
20.0	664.	7042.
40.0	1283.	13598.
60.0	1912.	20269.
80.0	2561.	27142.
100.0	3213.	34057.
60.0	1900.	20143.
40.0	1248.	13228.
20.0	609.	6450.
0.0	-21.	-222.

* * * * * * * * * *

DEFL TRANSDUCER: 9001

LOAD (%)	DEFLECTION (INCHES)
0.0	-0.000
20.0	-0.000
40.0	-0.002
60.0	-0.003
80.0	-0.003
100.0	-0.004
60.0	-0.004
40.0	-0.004
20.0	-0.004
0.0	-0.004

* * * * * * * * * *

STRUCTURES LAB ROSETTE SOLUTIONS

CONDITION: LOCOSST   STEP 57 MAX (P= -280 K)   APR 11,1978

GAGE: 1   TYPE A1-1   MTL CODE S-01

LOAD (%)	READING (U IN/IN)	-SX- (PSI)
0.0	0.	2.
20.0	33.	912.
40.0	80.	2251.
60.0	121.	3376.
80.0	172.	4822.
100.0	218.	6108.
60.0	160.	4474.
40.0	122.	3403.
20.0	56.	1555.
0.0	10.	270.

* * * * * * * * * *

GAGE: 2   TYPE A1-1   MTL CODE S-01

LOAD (%)	READING (U IN/IN)	-SX- (PSI)
0.0	0.	7.
20.0	30.	836.
40.0	106.	2977.
60.0	168.	4717.
80.0	254.	7099.
100.0	333.	9320.
60.0	212.	5948.
40.0	128.	3593.
20.0	47.	1318.
0.0	9.	247.

* * * * * * * * * *

GAGE: 3   TYPE A1-1   MTL CODE S-01

LOAD (%)	READING (U IN/IN)	-SX- (PSI)
0.0	9.	248.
20.0	267.	7473.
40.0	506.	14164.
60.0	720.	20158.
80.0	897.	25109.
100.0	1034.	28963.
60.0	586.	16412.
40.0	387.	10845.
20.0	179.	5011.
0.0	-29.	-823.

* * * * * * * * * *

CONDITION: LOCOSST   STEP 57 MAX (P=-208 K)   APR 11,1978

GAGE: 4   TYPE A1-1   MTL CODE S-01

LOAD (%)	READING (U IN/IN)	-SX- (PSI)
0.0	7.	194.
20.0	251.	7017.
40.0	494.	13840.
60.0	726.	20341.
80.0	981.	27458.
100.0	1221.	34174.
60.0	749.	20983.
40.0	510.	14268.
20.0	266.	7445.
0.0	16.	435.

* * * * * * * * * *

GAGE: 5   TYPE A1-1   MTL CODE S-01

LOAD (%)	READING (U IN/IN)	-SX- (PSI)
0.0	1.	29.
20.0	-1.	-25.
40.0	-9.	-266.
60.0	8290.	213690.
80.0	108.	3030.
100.0	122.	3405.
60.0	135.	3780.
40.0	131.	3673.
20.0	106.	2976.
0.0	59.	1663.

* * * * * * * * * *

GAGE: 6   TYPE A1-1   MTL CODE S-01

LOAD (%)	READING (U IN/IN)	-SX- (PSI)
0.0	-2.	-52.
20.0	-308.	-8618.
40.0	-624.	-17479.
60.0	-977.	-27357.
80.0	-1356.	-37958.
100.0	-1767.	-49472.
60.0	-1093.	-30596.
40.0	-729.	-20423.
20.0	-378.	-10572.
0.0	-29.	-801.

* * * * * * * * * *

GAGE: 8   TYPE A1-1   MTL CODE S-01

LOAD (%)	READING (U IN/IN)	-SX- (PSI)
0.0	-2.	-54.
20.0	-284.	-7941.
40.0	-576.	-16123.
60.0	-905.	-25347.
80.0	-1253.	-35080.
100.0	-1631.	-45669.
60.0	-1006.	-28155.
40.0	-668.	-18716.
20.0	-344.	-9626.
0.0	-22.	-615.

* * * * * * * * * *

GAGE: 10   TYPE A1-1   MTL CODE S-01

LOAD (%)	READING (U IN/IN)	-SX- (PSI)
0.0	-1.	-27.
20.0	-193.	-5407.
40.0	-393.	-11002.
60.0	-617.	-17266.
80.0	-869.	-24332.
100.0	-1141.	-31961.
60.0	-694.	-19434.
40.0	-455.	-12742.
20.0	-231.	-6478.
0.0	-15.	-428.

* * * * * * * * * *

GAGE: 11   TYPE A1-1   MTL CODE S-01

LOAD (%)	READING (U IN/IN)	-SX- (PSI)
0.0	-1.	-27.
20.0	-53.	-1476.
40.0	-102.	-2844.
60.0	-151.	-4239.
80.0	-200.	-5607.
100.0	-251.	-7029.
60.0	-141.	-3944.
40.0	-88.	-2468.
20.0	-42.	-1180.
0.0	-0.	-0.

* * * * * * * * * *

403

CONDITION: LOCOSST   STEP 57 MAX (P=-208 K)   APR 11,1978

GAGE: 12   TYPE S1-2   MTL CODE S-01

LOAD (%)	READING (U IN/IN)	-SXY- (PSI)
0.0	-3.	-31.
20.0	-470.	-4985.
40.0	-964.	-10214.
60.0	-1510.	-16002.
80.0	-2128.	-22555.
100.0	-2796.	-29636.
60.0	-1733.	-18369.
40.0	-1155.	-12242.
20.0	-595.	-6305.
0.0	-49.	-517.

* * * * * * * * * *

GAGE: 13   TYPE S2-2   MTL CODE S-01

LOAD (%)	READING (U IN/IN)	-SXY- (PSI)
0.0	2.	21.
20.0	634.	6723.
40.0	1275.	13520.
60.0	1941.	20576.
80.0	2670.	28306.
100.0	3444.	36506.
60.0	2130.	22583.
40.0	1428.	15132.
20.0	736.	7801.
0.0	42.	448.

* * * * * * * * * *

GAGE: 14   TYPE S1-2   MTL CODE S-01

LOAD (%)	READING (U IN/IN)	-SXY- (PSI)
0.0	1.	12.
20.0	443.	4692.
40.0	864.	9163.
60.0	1249.	13244.
80.0	1637.	17357.
100.0	1997.	21168.
60.0	1276.	13528.
40.0	879.	9321.
20.0	455.	4819.
0.0	-8.	-83.

* * * * * * * * * *

404

CONDITION: LOCOSST   STEP 57 MAX (P=-208 K)   APR 11,1978

GAGE: 15   TYPE A1-1   MTL CODE S-01

LOAD (%)	READING (U IN/IN)	-SX- (PSI)
0.0	4.	107.
20.0	134.	3750.
40.0	287.	8035.
60.0	449.	12562.
80.0	660.	18481.
100.0	880.	24642.
60.0	560.	15669.
40.0	380.	10633.
20.0	206.	5759.
0.0	33.	937.

* * * * * * * * * *

GAGE: 16   TYPE A1-1   MTL CODE S-01

LOAD (%)	READING (U IN/IN)	-SX- (PSI)
0.0	1.	27.
20.0	3.	80.
40.0	-9.	-241.
60.0	-24.	-671.
80.0	11.	295.
100.0	35.	993.
60.0	76.	2120.
40.0	91.	2549.
20.0	105.	2952.
0.0	104.	2925.

* * * * * * * * * *

GAGE: 17   TYPE A1-1   MTL CODE S-01

LOAD (%)	READING (U IN/IN)	-SX- (PSI)
0.0	-0.	-0.
20.0	-8.	-214.
40.0	-22.	-616.
60.0	-50.	-1392.
80.0	-71.	-1981.
100.0	-81.	-2276.
60.0	-50.	-1392.
40.0	-37.	-1044.
20.0	-28.	-777.
0.0	-20.	-562.

* * * * * * * * * *

405

GAGE: 18   TYPE A1-1   MTL CODE S-01

LOAD	READING	-SX-
(%)	(U IN/IN)	(PSI)
0.0	-2.	-54.
20.0	-313.	-8776.
40.0	-628.	-17579.
60.0	-954.	-26703.
80.0	-1311.	-36709.
100.0	-1679.	-47013.
60.0	-1035.	-28977.
40.0	-696.	-19478.
20.0	-361.	-10114.
0.0	-21.	-589.

* * * * * * * * *

GAGE: 19   TYPE S1-2   MTL CODE S-01

LOAD	READING	-SXY-
(%)	(U IN/IN)	(PSI)
0.0	1.	11.
20.0	-563.	-5973.
40.0	-1128.	-11956.
60.0	-1670.	-17707.
80.0	-2201.	-23334.
100.0	-2712.	-28750.
60.0	-1625.	-17220.
40.0	-1084.	-11491.
20.0	-531.	-5624.
0.0	45.	476.

* * * * * * * * *

DEFL TRANSDUCER: 9001

LOAD	DEFLECTION
(%)	(INCHES)
0.0	-0.000
20.0	-0.000
40.0	-0.000
60.0	-0.000
80.0	0.000
100.0	0.000
60.0	-0.001
40.0	-0.002
20.0	-0.002
0.0	-0.002

* * * * * * * * *

STRAIN-GAGE SURVEY DURING -448,000-POUND LIMIT LOAD

The strain-gage readings and corresponding calculated stresses obtained during the -448,000 pound limit load test are tabulated in the following pages. Gages 5, 7, 9, 13, 15, and 16 were inoperative and are not reported.

STRUCTURES LAB ROSETTE SOLUTIONS

CONDITION: LOCO3ST (P=-448K) LIMIT LOAD 8/15/78

GAGE: 1   TYPE A1-1   MTL CODE S-01

LOAD (%)	READING (U IN/IN)	-SX- (PSI)
0.0	-1.	-27.
100.0	371.	10379.
0.0	8.	214.

* * * * * * * * * *

GAGE: 2   TYPE A1-1   MTL CODE S-01

LOAD (%)	READING (U IN/IN)	-SX- (PSI)
0.0	1.	27.
100.0	464.	12985.
0.0	15.	428.

* * * * * * * * * *

GAGE: 3   TYPE A1-1   MTL CODE S-01

LOAD (%)	READING (U IN/IN)	-SX- (PSI)
0.0	0.	0.
100.0	1675.	46932.
0.0	7.	187.

* * * * * * * * * *

GAGE: 4   TYPE A1-1   MTL CODE S-01

LOAD (%)	READING (U IN/IN)	-SX- (PSI)
0.0	1.	27.
100.0	1837.	51445.
0.0	19.	535.

* * * * * * * * * *

CONDITION: LOCOSST (P=-448K) LIMIT LOAD   8/15/78

GAGE: 6   TYPE A1-1   MTL CODE S-01

LOAD	READING	-SX-
(%)	(U IN/IN)	(PSI)
0.0	-0.	-0.
100.0	-2465.	-69030.
0.0	6.	160.

* * * * * * * * * *

GAGE: 8   TYPE A1-1   MTL CODE S-01

LOAD	READING	-SX-
(%)	(U IN/IN)	(PSI)
0.0	-1.	-27.
100.0	-2268.	-63504.
0.0	11.	321.

* * * * * * * * * *

GAGE: 10   TYPE A1-1   MTL CODE S-01

LOAD	READING	-SX-
(%)	(U IN/IN)	(PSI)
0.0	-1.	-27.
100.0	-1582.	-44292.
0.0	15.	428.

* * * * * * * * * *

GAGE: 11   TYPE A1-1   MTL CODE S-01

LOAD	READING	-SX-
(%)	(U IN/IN)	(PSI)
0.0	1.	27.
100.0	-374.	-10462.
0.0	11.	322.

* * * * * * * * * *

GAGE: 12   TYPE S1-2   MTL CODE S-01

LOAD	READING	-SXY-
(%)	(U IN/IN)	(PSI)
0.0	-0.	-1.
100.0	-3842.	-40725.
0.0	-3.	-32.

* * * * * * * * * *

CONDITION: LOCOSST (P=-448K) LIMIT LOAD 8/15/78

GAGE: 14   TYPE S1-2   MTL CODE S-01

LOAD (%)	READING (U IN/IN)	-SXY- (PSI)
0.0	-0.	-1.
100.0	2589.	27442.
0.0	36.	377.

* * * * * * * * * *

GAGE: 17   TYPE A1-1   MTL CODE S-01

LOAD (%)	READING (U IN/IN)	-SX- (PSI)
0.0	-0.	-0.
100.0	-105.	-2943.
0.0	-19.	-535.

* * * * * * * * * *

GAGE: 18   TYPE A1-1   MTL CODE S-01

LOAD (%)	READING (U IN/IN)	-SX- (PSI)
0.0	0.	0.
100.0	-2387.	-66835.
0.0	-11.	-294.

* * * * * * * * * *

GAGE: 19   TYPE S1-2   MTL CODE S-01

LOAD (%)	READING (U IN/IN)	-SXY- (PSI)
0.0	-0.	-0.
100.0	-3997.	-42365.
0.0	-27.	-285.

* * * * * * * * * *

DEFL TRANSDUCER: 9001

LOAD (%)	DEFLECTION (INCHES)
0.0	2.041
100.0	2.008
0.0	2.005

* * * * * * * * * *

410

STRUCTURES LAB ROSETTE SOLUTIONS

CONDITION: LOCOSST (P=-448K) LIMIT LOAD 8/15/78

GAGE: 20   TYPE A1-1   MTL CODE S-01

LOAD	READING	-SX-
(%)	(U IN/IN)	(PSI)
0.0	-4961.	-138912.
100.0	-4961.	-138912.
0.0	-4961.	-138912.

* * * * * * * * *

GAGE: 21   TYPE A1-1   MTL CODE S-01

LOAD	READING	-SX-
(%)	(U IN/IN)	(PSI)
0.0	3299.	92372.
100.0	3299.	92372.
0.0	3299.	92372.

* * * * * * * * *

411

Strain-gage readings during the +615,000-pound limit load, at the 922,000-pound ultimate load, and at the maximum load obtained in the residual strength test (1,370,000 pounds).

412

CONDITION: LOCOSST ULT. STATIC +P=615K KIPS   AUG. 29,1978

GAGE: 1   TYPE A1-1   MTL CODE S-01

LOAD (%)	READING (U IN/IN)	-SX- (PSI)
0.0	-2.	-51.
67.0	718.	20107.
0.0	-9.	-238.
100.0	1066.	29851.
0.0	7.	190.

* * * * * * * * * *

(Refer to note)

GAGE: 2   TYPE A1-1   MTL CODF S-01

LOAD (%)	READING (U IN/IN)	-SX- (PSI)
0.0	-1.	-17.
67.0	669.	18728.
0.0	-3.	-98.
100.0	1017.	28475.
0.0	-33.	-928.

* * * * * * * * * *

GAGE: 3   TYPE A1-1   MTL CODE S-01

LOAD (%)	READING (U IN/IN)	-SX- (PSI)
0.0	-1.	-15.
67.0	-2636.	-73805.
0.0	3.	92.
100.0	-3868.	-108314.
0.0	-464.	-12983.

* * * * * * * * * *

GAGE: 4   TYPE A1-1   MTL CODE S-01

LOAD (%)	READING (U IN/IN)	-SX- (PSI)
0.0	-1.	-18.
67.0	-2690.	-75315.
0.0	10.	276.
100.0	-3889.	-108888.
0.0	-862.	-24143.

* * * * * * * * * *

NOTE: ① Zero reading prior to start of test
         ② Reading at limit load of 622,000 pounds
         ③ Zero after release of limit load
         ④ Reading at ultimate load of 922,000 pounds
         ⑤ Reading after release of the max load achieved (1,370,000)

413

STRUCTURES LAB ROSETTE SOLUTIONS

CONDITION: LOCOSST ULT. STATIC +P=615K KIPS   AUG. 29,1978

```
        GAGE:    5      TYPE A1-1     MTL CODE S-01

        LOAD           READING              -SX-
        (%)          (U IN/IN)            (PSI)
        0.0              0.                 3.
       67.0           -196.             -5487.
        0.0            -89.             -2487.
      100.0           -338.             -9450.
        0.0             68.              1905.
     * * * * * * * * * *


        GAGE:    6      TYPE A1-1     MTL CODE S-01

        LOAD           READING              -SX-
        (%)          (U IN/IN)            (PSI)
        0.0             -1.               -25.
       67.0           3106.             86971.
        0.0             90.              2518.
      100.0           4833.            135322.
        0.0            613.             17155.
     * * * * * * * * * *


        GAGE:    7      TYPE A1-1     MTL CODE S-01

        LOAD           READING              -SX-
        (%)          (U IN/IN)            (PSI)
        0.0              0.                 6.
       67.0           -119.             -3338.
        0.0             87.              2440.
      100.0           -317.             -8875.
        0.0           -227.             -6361.
     * * * * * * * * * *


        GAGE:    8      TYPE A1-1     MTL CODE S-01

        LOAD           READING              -SX-
        (%)          (U IN/IN)            (PSI)
        0.0             -1.               -28.
       67.0           2876.             80526.
        0.0             85.              2379.
      100.0           4512.            126335.
        0.0            816.             22837.
     * * * * * * * * * *
```

414

STRUCTURES LAB ROSETTE SOLUTIONS

CONDITION: LOCOSST ULT. STATIC +P=615K KIPS   AUG. 29,1978

GAGE: 9   TYPE A1-1   MTL CODF S-01

LOAD (%)	READING (U IN/IN)	-SX- (PSI)
0.0	0.	1.
67.0	-120.	-3370.
0.0	28.	777.
100.0	-254.	-7116.
0.0	-55.	-1551.

* * * * * * * * * *

GAGE: 10   TYPE A1-1   MTL CODF S-01

LOAD (%)	READING (U IN/IN)	-SX- (PSI)
0.0	-0.	-0.
67.0	1947.	54516.
0.0	73.	2031.
100.0	3054.	85501.
0.0	3903.	109273.

* * * * * * * * * *

GAGE: 11   TYPE A1-1   MTL CODE S-01

LOAD (%)	READING (U IN/IN)	-SX- (PSI)
0.0	-1.	-25.
67.0	607.	16985.
0.0	14.	404.
100.0	958.	26816.
0.0	788.	22075.

* * * * * * * * * *

GAGE: 12   TYPE S1-2   MTL CODF S-01

LOAD (%)	READING (U IN/IN)	-SXY- (PSI)
0.0	-1.	-10.
67.0	4833.	51233.
0.0	135.	1434.
100.0	7501.	79510.
0.0	5036.	53382.

* * * * * * * * * *

415

STRUCTURES LAB ROSETTE SOLUTIONS

CONDITION: LOCOSST ULT. STATIC +P=615K KIPS   AUG. 29.1978

GAGE: 13   TYPE S2-2   MTL CODE S-01

LOAD (%)	READING (U IN/IN)	-SXY- (PSI)
0.0	-1.	-11.
67.0	-6218.	-65913.
0.0	-121.	-1279.
100.0	-9695.	-102763.
0.0	65796.	154012.

* * * * * * * * * *

GAGE: 14   TYPE S1-2   MTL CODE S-01

LOAD (%)	READING (U IN/IN)	-SXY- (PSI)
0.0	-1.	-10.
67.0	-5246.	-55603.
0.0	-47.	-493.
100.0	-8155.	-86448.
0.0	-710.	-7527.

* * * * * * * * * *

GAGE: 15   TYPE A1-1   MTL CODE S-01

LOAD (%)	READING (U IN/IN)	-SX- (PSI)
0.0	0.	2.
67.0	-917.	-25689.
0.0	-54.	-1522.
100.0	-1473.	-41247.
0.0	-185.	-5184.

* * * * * * * * * *

GAGE: 16   TYPE A1-1   MTL CODE S-01

LOAD (%)	READING (U IN/IN)	-SX- (PSI)
0.0	-0.	-0.
67.0	-158.	-4425.
0.0	56.	1555.
100.0	-172.	-4827.
0.0	568.	15902.

* * * * * * * * * *

416

STRUCTURES LAB ROSETTE SOLUTIONS

CONDITION: LOCOSST ULT. STATIC +P=615K KIPS   AUG. 29,1978

GAGE: 17   TYPE A1-1   MTL CODE S-01

LOAD	READING	-SX-
(%)	(U IN/IN)	(PSI)
0.0	0.	1.
67.0	-43.	-1202.
0.0	23.	642.
100.0	-195.	-5452.
0.0	-251.	-7029.

* * * * * * * * * *

GAGE: 18   TYPE A1-1   MTL CODE S-01

LOAD	READING	-SX-
(%)	(U IN/IN)	(PSI)
0.0	0.	0.
67.0	2883.	80719.
0.0	68.	1898.
100.0	4398.	123149.
0.0	1743.	48816.

* * * * * * * * * *

GAGE: 19   TYPE S1-2   MTL CODE S-01

LOAD	READING	-SXY-
(%)	(U IN/IN)	(PSI)
0.0	-1.	-11.
67.0	5734.	60784.
0.0	39.	411.
100.0	8520.	90311.
0.0	65155.	153904.

* * * * * * * * * *

DEFL TRANSDUCER: 9001

LOAD	DEFLECTION
(%)	(INCHES)
0.0	0.000
67.0	-0.017
0.0	-0.004
100.0	-0.025
0.0	-0.070

* * * * * * * * * *

417

APPENDIX E

WING SWEEP ACTUATOR ATTACH FITTING TEST SPECTRUM

418

TABLE E-1

WING SWEEP ACTUATOR ATTACH FITTING TEST SPECTRUM FOR LOCOSST PROGRAM FULL-SCALE TEST

STEP	MISSION SEGMENT	WING ANGLE	LOAD TYPE	LOAD IN KIPS		CYCLES/ MISSION
				MAXIMUM	MINIMUM	
1	GROUND	15	TAXI	0.22	0.07	0.01
2				0.21	0.08	0.10
3				0.20	0.09	1.00
4	POST TAKE OFF	15	MANEUVER	-186.90	125.72	0.01
5				-136.19	79.30	0.10
6				-93.94	43.39	1.00
7	WING SWEEP	15	1G	-105.98	-105.98	1.00
8		25		-94.12	-94.12	1.00
9	SUBSONIC CLIMB	25	MANEUVER	-68.67	18.31	0.01
10				-57.17	6.31	0.10
11				-47.17	-2.18	1.00
12	SUBSONIC CRUISE	25	GUST	-115.99	93.11	0.01
13				-81.55	58.67	0.10
14				-53.26	30.38	1.00
15	WING SWEEP	25	1G	-79.33	-79.33	1.00
16		67.5		-36.07	-36.07	1.00
17	SUPERSONIC CLIMB	67.5	MANEUVER	61.09	37.43	0.01
18				57.42	40.88	0.10
19				54.20	43.42	1.00
20	SUPERSONIC CRUISE	67.5	MANEUVER	77.83	57.09	0.01
21				74.43	59.88	0.10
22				71.19	62.14	1.00
23	SUPERSONIC DESCENT	67.5	MANEUVER	92.31	275.61	0.01
24				120.73	240.81	0.10
25				145.88	229.21	1.00
26				186.85	213.96	1.00
27	WING SWEEP	67.5	1G	133.85	133.85	1.00
28		25		61.48	61.48	1.00
29	SUBSONIC DESCENT	25	MANEUVER	-68.67	18.31	0.01
30				-57.17	6.31	0.10
31				-47.17	-2.18	1.00
32	WING SWEEP	25	1G	-94.12	-94.12	1.00
33		67.5		-196.40	-196.40	1.00
34	TERRAIN FOLLOW .85	67.5	GUST	-171.02	9.29	0.01
35				-151.60	-10.13	0.10
36				-138.35	-25.39	1.00
37				-121.00	-40.55	10.00
38				-111.29	-50.26	10.00

419

WING SWEEP ACTUATOR ATTACH FITTING TEST SPECTRUM FOR LOCOSST
PROGRAM FULL-SCALE TEST (CONT)

STEP	MISSION SEGMENT	WING ANGLE	LOAD TYPE	LOAD IN KIPS		CYCLES/ MISSION
				MAXIMUM	MINIMUM	
39	TERRAIN FOLLOW.85	67.5	GUST	-211.99	-15.04	0.01
40				-191.18	-35.84	0.10
41				-174.54	-52.48	1.00
42				-160.68	-66.36	10.00
43				-146.81	-80.23	10.00
44				-249.37	-69.06	0.01
45				-231.34	-87.09	0.10
46				-216.08	-102.35	1.00
47				-202.36	-116.37	10.00
48				-191.26	-127.46	10.00
49	FLY UP	67.5	3.0G	-244.10	-113.51	1.00
50			2.5G	-211.45	-113.51	1.00
51	TERRAIN FOLLOW .85	67.5	MANEUVER	-190.55	-70.42	1.00
52				-184.03	-73.68	11.00
53				-172.27	-75.64	15.00
54				-159.22	-79.56	10.00
55				-146.27	-85.36	5.00
56				-133.17	-94.53	5.00
57	TERRAIN FOLLOW .95	67.5	GUST	-279.57	93.32	0.01
58				-242.29	56.03	0.10
59				-209.66	23.40	1.00
60				-179.36	-6.90	10.00
61				-158.38	-27.87	10.00
62				-144.40	-41.85	10.00
63			MANEUVER	-144.86	-41.40	0.01
64				-140.88	-46.70	0.10
65				-134.25	-53.34	1.00
66				-124.96	-62.62	3.00
67	WING SWEEP	67.5	1G	-11.79	-11.79	1.00
68		55		37.68	37.68	1.00
69	TERRAIN FOLLOW .55	55	GUST	-96.10	81.29	0.01
70				-76.55	61.75	0.10
71				-58.51	43.71	1.00
72				-129.51	65.92	0.01
73	TERRAIN FOLLOW .55	55	GUST	-108.46	44.87	0.10
74				-88.92	25.33	1.00
75				-73.99	10.23	4.00
76				-64.97	1.21	7.00
77				-151.26	29.14	0.01
78				-130.21	8.09	0.10
79				-112.17	-9.95	1.00

WING SWEEP ACTUATOR ATTACH FITTING TEST SPECTRUM FOR LOCOSST
PROGRAM FULL-SCALE TEST (CONT)

STEP	MISSION SEGMENT	WING ANGLE	LOAD TYPE	LOAD IN KIPS		CYCLE/ MISSION
				MAXIMUM	MINIMUM	
80	TERRAIN FOLLOW	55	GUST	-97.34	-25.16	4.00
81			MANEUVER	-78.62	0.40	1.00
82				-72.28	-2.04	6.00
83				-61.74	-7.40	8.00
84	WING SWEEP	55	1G	37.68	37.68	1.00
85		25		53.54	53.54	1.00
86	SUBSONIC CLIMB	25	MANEUVER	-40.28	19.70	0.01
87				-32.04	14.10	0.10
88				-24.79	9.16	1.00
89	SUBSONIC CRUISE	25	MANEUVER	-47.64	9.62	0.01
90				-40.36	4.65	0.10
91				-33.08	-0.64	1.00
92	SUBSONIC DESCENT	25	MANEUVER	260.62	304.94	0.01
93				266.71	300.80	0.10
94				272.07	297.14	1.00
95	WING SWEEP	25	1G	53.54	53.54	1.00
96		15		150.93	150.93	1.00
97	PRE-LANDING	15	GUST	-34.31	214.17	0.01
98				-0.32	180.18	0.10
99				26.64	153.22	1.00
100				52.43	127.44	10.00
101			MANEUVER	0.47	159.42	0.01
102				24.79	148.13	0.10
103				44.77	135.97	1.00
104				66.48	89.93	1.00
105				89.91	123.80	1.00
106				235.08	89.93	1.00
107	GROUND	15	TAXI	0.31	0.09	0.01
108				0.30	0.11	0.10
109				0.28	0.13	1.00
110	POST TAKE OFF	15	MANEUVER	44.77	135.97	1.00
111	WING SWEEP	15	1G	28.93	28.93	1.00
112		25		-71.48	-71.48	1.00
113	SUBSONIC CLIMB	25	MANEUVER	-24.79	9.16	1.00
114	WING SWEEP	25	1G	53.54	53.54	1.00
115		15		150.93	150.93	1.00
116	PRE-LANDING	15	MANEUVER	44.77	135.97	1.00
117				235.08	89.93	1.00
118	GROUND	15	TAXI	0.28	0.13	1.00
119			TAXI	0.28	0.13	0.10
120	POST TAKE OFF	15	MANEUVER	44.77	135.97	0.10

421

TABLE E-1

WING SWEEP ACTUATOR ATTACH FITTING TEST SPECTRUM FOR LOCOSST
PROGRAM FULL-SCALE TEST (CONCL)

STEP	MISSION SEGMENT	WING ANGLE	LOAD TYPE	LOAD IN KIPS		CYCLES/ MISSION
				MAXIMUM	MINIMUM	
121	WING SWEEP	15		28.93	28.93	0.10
122		25	1G	-71.48	-71.48	0.10
123	SUBSONIC CLIMB	25	MANEUVER	-24.79	9.16	0.10
124	WING SWEEP	25	1G	53.54	53.54	0.10
125		15		150.93	150.93	0.10
126	PRE-LANDING	15	MANEUVER	44.77	135.97	0.10
127				235.08	89.93	0.10
128	GROUND	15	TAXI	0.28	0.13	0.10